Ph.D. Thesis

RELAY-ASSISTED TRANSMISSION

AND

RADIO RESOURCE MANAGEMENT FOR

WIRELESS NETWORKS

Author: **Adrián Agustín de Dios**

Advisor: **Josep Vidal Manzano**

Abstract

THE RELAY-ASSISTED or COOPERATIVE transmission is a relatively new class of spatial diversity technique where a new element comes up in the conventional *source-destination* or point-to-point communication: an assisting relay or cooperating user. The relay assists the source in transmitting a message to the destination and allows dealing with the channel impairments like shadowing, multipath fading, interference and pathloss. Although the seminal works were issued in the 70's by van der Meulen, Cover and El Gamal, it has been during the last years when it has re-gained more attention by the researchers. In fact, the relay-assisted transmission can be seen as a *virtual* MIMO (Multiple Input Multiple Output) with distributed antennas. In contrast to MIMO systems, the transmission requires the use of additional channel resources because of the limitation of the current radio technology: the relay terminal is constrained to work in *half-duplex mode*, which motivates that the transmission must be carried out in two orthogonal phases (*relay-receive* and *relay-transmit phase*), duplexed in time or frequency domains.

This dissertation investigates protocols and strategies for the relay-assisted transmission which improve the spectral efficiency and homogenize the bit rate service in the cellular communication systems with uniformly distributed users. The new element present in the communication, the relay terminal, imposes a redefinition of many techniques and protocols commonly used in the point-to-point and MIMO systems, which are placed at the *physical* and *upper layers*.

First, achievable rates using the relay-assisted transmission are provided which depend on the role of the relay (*amplify-and-forward* or *decode-and-forward*), the type of the transmission (*persistent transmission*, *incremental* or *selective relaying*), the data transmitted by the relays (*repetition* or *unconstrained coding*) and the type of half-duplex protocol. There are up to four protocol definition depending on the activity of the terminals on each phase. An additional aspect addressed is the *resource allocation* for each phase, that is, either it is fixed beforehand (*static*) or it is adjusted dynamically (*dynamic*) as a function of the channel quality. For the single-user relay-assisted transmission the resources can be allocated based on the channel quality of the different links. Moreover, if there is complete channel state information about all channel coefficients (including the carrier phase of the transmitting terminals), source and relay can transmit *synchronously* enhancing the transmission thanks to the (distributed) *eigenvector precoding*.

Two relay-assisted transmission techniques are evaluated when a destination is assisted by multiple relays. Both depend on the messages intended to each assisting relay (*independent* or *common messaging*). The resource allocation for both techniques is shown to be convex.

Additionally, three different scenarios illustrate the multi-user relay-assisted transmission with a single destination and different types of *half-duplex* relays: RMAC (*Relay-assisted Multiple Access Channel*), UC (*User Cooperation*) and MARC (*Multiple Access Relay Channel*). The relay-assisted transmission can be done *synchronously* or *asynchronously*. The sources and relays are power limited and access in each phase of the communication by TDMA (time division multiple access), FDMA (frequency division multiple access) or SC (superposition coding multiple access). For those scenarios the allocation of transmitted power and time resources can be formulated as a convex problem under some circumstances, evaluating the optimal solution.

Afterwards, the relay-assisted transmission duplexed in time is applied to a centralized cellular system based on TDMA in the *downlink*. The reuse of one time slot for the transmissions done from the relays to destinations (relay slot) is proposed to improve the spectral efficiency. This solution produces interference for all the destinations active in that time slot. A *power control algorithm* (at the relays) based on game theory is proposed to combat the generated interference. Under that configuration a scheduler algorithm explores the *multi-user gain* for the relay-assisted transmission, measuring the introduced *overhead*.

Another way of dealing with the interference is by *rate control management*. Under some circumstances it is possible to model the probability density function (*pdf*) of the interfering power. In such a case, the source can tune the transmission rate in order to maximize the throughput. This solution is extended to the case where each destination is assisted by multiple relays. In spite of the interfering power, both proposed solutions are able to provide significant gains over the direct transmission.

Finally, *the dynamic link control* of the relay-assisted transmission is investigated under two different assumptions on the knowledge about the channel: *statistical knowledge of the channel state* and *actual information about the current channel state*. Both types of knowledge lead to different transmission strategies, in terms of selecting the modulation and coding scheme (MCS). Under the first case, the transmission rates are not adapted to the current channel realization and the destination can decode wrongly the messages. The Automatic Repeat reQuest (ARQ) protocols are redefined for the relay-assisted transmission to cope with these events. In this work we specify the (distributed) space-time codes, the coding at the source and relay and the length of the retransmissions. When there is *actual information about the channel state* the MCS can be adapted to the current channel realization. In such a case, the link error prediction for the relay-assisted transmission is investigated, and thus the MCS can be designed for maximizing the information rate for a given probability of packet loss or maximizing the throughput.

Resumen

L A TRANSMISIÓN ASISTIDA POR RELAY O TRANSMISIÓN COOPERATIVA es una *nueva* técnica de diversidad espacial donde aparece un elemento nuevo (un *relay* o un usuario cooperativo) en la tradicional transmisión punto a punto (fuente a destino). Ahora en la comunicación intervienen tres enlaces: fuente-*relay*, *relay*-destino y fuente-destino. El *relay*, además de asistir a la fuente en la transmisión de un mensaje, permite combatir las degradaciones que puede sufrir el canal como el s*hadowing, la atenuación del canal (fading), la interferencia recibida* y el *pathloss*. Aunque esta técnica está basada en el trabajo realizado en los 70 por Van der Meulen, Cover y El Gamal, ha sido en los últimos años cuando se han vuelto a considerar el uso de *relays*. En realidad, la transmisión asistida por un *relay* puede verse como un sistema virtual multi-antena (*virtual* MIMO) donde las antenas están distribuidas en diferentes terminales. Sin embargo, al contrario de los sistemas multi-antena y debido a la limitación de la actual tecnología radio, el *relay* debe trabajar en modo *half-duplex*, ya que no puede transmitir y recibir simultáneamente en la misma banda. Este hecho, motiva que la transmisión deba realizarse en dos fases ortogonales en función del modo del *relay* (recibiendo datos – *relay-receive phase* o transmitiendo datos – *relay-transmit phase*). Estas fases pueden implementarse en el dominio de la frecuencia o el tiempo.

Esta tesis investiga protocolos y estrategias para la transmisión asistida por *relay* para mejorar la eficiencia espectral y homogeneizar el servicio para todos los usuarios uniformemente distribuidos en un sistema de comunicación celular. La introducción del *relay* en la comunicación implica la redefinición de muchas técnicas y protocolos considerados en las comunicaciones punto a punto y en los sistemas multi-antena, situados en la capa física y/o superiores.

En primer lugar se presentan los *achievable rates* obtenidos por la transmisión asistida por *relay* en función del rol del *relay* (amplifica y retransmite o decodifica y retransmite), el tipo de transmisión (siempre transmite, incremental o selectiva), los datos transmitidos por el *relay* (repite los símbolos recibidos o son independientes) y el tipo del protocolo *half-duplex*. En función de los terminales activos en cada fase de la comunicación (fuente, destino o relay), existen hasta cuatro protocolos. Otro aspecto considerado es la asignación de recursos (*resource allocation*) para cada fase de la comunicación, la cual puede estar fijada de antemano o puede ser ajustada dinámicamente en función de los canales de los diferentes enlaces. En el caso de que todos los coeficientes del canal se conocieran perfectamente (incluyendo la fase de portadora de los transmisores), los terminales podrían transmitir síncronamente, mejorando la comunicación gracias a la ganancia debida a técnicas de precodificación con autovectores del canal (con antenas distribuidas).

Además dos técnicas de transmisión asistida por *relay* son evaluadas cuando existen múltiples *relays* por destino. Ambas dependen del tipo de mensajes transmitidos a cada *relay* (mensajes independientes o uno común). La asignación de recursos para ambas técnicas puede verse como un problema convexo.

Tres escenarios resumen diferentes tipos de transmisión asistida por *relay* para múltiples fuentes y un solo destino: RMAC (*Relay-assisted Multiple Access Channel*), UC (*User Cooperation*) and MARC (*Multiple Access Relay Channel*). Su diferencia se basa en el tipo de *relay half-duplex* considerado. La transmisión puede hacerse *síncrona* o *asíncronamente*. Las fuentes y los *relays* están limitados en potencia y el acceso de ellos en cada fase de la comunicación pude hacerse por medio de TDMA (*time division multiple access*), FDMA (*frequency division multiple access*) or SC (*superposition coding multiple access*). La asignación de recursos puede ser formulada como un problema convexo en algunos casos y la solución óptima puede ser encontrada.

Seguidamente la transmisión asistida por *relay* y duplexada en tiempo es aplicada a un sistema celular centralizado basado en TDMA en el *downlink*. Con el objetivo de mejorar la eficiencia espectral se propone el reuso espacial de un *slot* temporal para las transmisiones de los *relays* hacia sus respectivos destinos (*slot* de relay), generando interferencia para todos los restantes destinos activos. Un *algoritmo de control de potencia* basado en la teoría de juegos es propuesto para combatir la interferencia generada. Bajo esa configuración, un algoritmo de *scheduling* investiga las posibles ganancias debidas al *multi-user gain* y mide el *overhead* introducido.

Otra forma de tratar con la interferencia es la de controlar el *rate* de nuestra transmisión (*rate control management*). Bajo ciertas condiciones es posible modelar la función de densidad de probabilidad de la potencia interferente. En ese caso, la fuente ajusta el *rate* para maximizar el *throughput* de la comunicación. Esta solución es extendida para el caso en el que cada destino es asistido por varios *relays*. Las dos soluciones propuestas son capaces de proporcionar mejores resultados que la transmisión directa, a pesar de la interferencia existente en el *slot* de *relay*.

Finalmente, se investiga el control dinámico del enlace para la transmisión asistida por relay con dos diferentes tipos de conocimiento sobre el canal: conocimiento estadístico (*statistical knowledge of the channel state*) o conocimiento del canal instantáneo (*actual information about the current channel state*). Estos dos tipos de conocimiento derivan en diferentes estrategias a utilizar para seleccionar la modulación y el esquema de codificación (MCS). En el primer caso, los *rates* seleccionados no están adaptados al canal actual, por lo que el destino puede recibir erróneamente los mensajes. Los protocolos de retransmisión de mensajes (ARQ – *automatic repeat request*) son los encargados de asegurarse la correcta recepción y son redefinidos para la transmisión asistida por *relay*. En este trabajo, se especifica los códigos espacio-tiempo distribuidos, la codificación en al fuente y el *relay* y la longitud de las retransmisiones. Cuando la fuente conoce algún parámetro del canal instantáneo puede adaptar el MCS para esa realización del canal. En ese caso se investiga la predicción del error en las transmisiones asistidas por *relay*, y con ello es posible diseñar el MCS para que maximice la cantidad de información transmitida para una probabilidad de pérdida de paquete o que maximice el *throughput*.

Resum

L A TRANSMISSIÓ ASSISTIDA PER RELAY O TRANSMISSIÓ COOPERATIVA és una nova tècnica de diversitat espacial on apareix un element nou (un *relay* o un usuari cooperatiu) en la tradicional transmissió punt a punt (font a destí). Ara en la comunicació hi intervenen tres enllaços : font-relay, relay-destí i font-destí. El *relay*, a més a més d'assistir a la font en la transmissió d'un missatge, permet combatre les degradacions que pot patir el canal, com el *shadowing, fading, interferència* i el *pathloss*. Encara que aquesta tècnica està basada en el treball realitzat en els 70 per Van der Meulen, Cover i El Gamal, ha estat els darrers anys quan s'han tornat a considerar l'ús de *relays*. En realitat, la transmissió assistida per un *relay* es pot veure com un sistema *virtual* multi-antena (*virtual* MIMO) on les antenes estan distribuïdes en diferents terminals. No obstant, al contrari dels sistemes multi-antena i a causa de la limitació de l'actual tecnologia ràdio, el relay ha de treballar de manera *half-duplex*, ja que no pot transmetre i rebre simultàniament a la mateixa banda. Aquest fet, motiva que la transmissió hagi de realitzar-se en dues fases ortogonals en funció de la manera del relay (rebent dades - *relay-receive phase* o transmetent dades - *relay-transmit phase*). Aquestes fases es poden implementar en el domini de la freqüència (FDD) o el temps (TDD).

Aquesta tesi investiga protocols i estratègies per la transmissió assistida per *relay* per millorar l'eficiència espectral i homogeneïtzar el servei per a tots els usuaris uniformement distribuïts en un sistema de comunicació cel·lular. La introducció del *relay* en la comunicació implica la redefinició de moltes tècniques i protocols considerats en les comunicacions punt a punt i en els sistemes multi-antena, situats a la capa física i / o superiors.

En primer lloc es presenten els *achievable rates* obtinguts per la transmissió assistida per *relay* en funció del rol de *relay* (amplifica i retransmet o decodifica i retransmet), el tipus de transmissió (sempre transmet, incremental o selectiva), les dades transmeses per *relay* (repeteix els símbols rebuts o són independents) i el tipus del protocol *half-duplex*. En funció dels terminals actius en cada fase de la comunicació (font, destí o *relay*), hi ha fins a quatre protocols. Un altre aspecte considerat és l'assignació de recursos (*resource allocation*) per cada fase de la comunicació, la qual pot estar fixada per endavant o pot ser ajustada dinàmicament en funció dels canals dels diferents enllaços. En el cas que tots els coeficients del canal es coneguessin perfectament (incloent també la fase de portadores dels transmissors), els terminals podrien transmetre síncronament, millorant la comunicació gràcies al guany degut a tècniques precodificació amb autovectors (amb antenes distribuïdes).

A més a més dues tècniques de transmissió assistida per *relay* són avaluades quan existeixen múltiples *relays* per destí. Totes dues depenen del tipus de missatges que es transmeten a cada *relay* (missatges independents o un comuns). L'assignació de recursos per a totes dues tècniques es pot veure com un problema convexe.

Tres escenaris resumeixen diferents tipus de transmissió assistida per *relay* per a múltiples fonts i un sol destí : RMAC (*Relay-assisted Multiple Access Channel*), UC (*User Cooperation*) and MARC (*Multiple Access Relay Channel*). La seva diferència es basa en el tipus de *relay half-duplex* considerat. La transmissió es pot fer síncrona o asíncronamente. Les fonts i els *relays* estan limitats en potència i l'accés d'ells a cada fase de la comunicació es pot fer per mitjà de TDMA (*time division multiple access*), FDMA (*frequency division multiple access*) or SC (*superposition coding multiple access*). L'assignació de recursos pot ser formulada com un problema convexe en alguns casos i la solució òptima pot ser trobada.

Seguidament la transmissió assistida per *relay* i duplexada en temps és aplicada a un sistema cel·lular centralitzat basat en TDMA al *downlink*. Amb l'objectiu de millorar l'eficiència espectral es proposa el reus espacial d'un *slot* temporal per les transmissions de les *relays* cap als seus respectius destins (*slot* de *relay*), generant interferència per a tots els destins actius. Un algoritme de control de potència basat en la teoria de jocs és proposat per combatre la interferència generada. Sota aquesta configuració, un algoritme de *scheduling* investiga els possibles guanys deguts al *multi-user gain*, i mesura el *overhead* introduït.

Una altra manera de tractar amb la interferència és controlar el *rate* de la nostra transmissió (*rate control management*). Sota certes condicions és possible modelar la funció de densitat de probabilitat de la potència interferent. En aquest cas, la font ajusta el *rate* amb vista a maximitzar-ne el *throughput* de la comunicació. Aquesta solució és estesa per al cas en què cada destí és assistit per diversos *relays*. Les dues solucions proposes proporcionen més bons resultats que la transmissió directa, malgrat la interferència existent al *slot* de *relay.*

Finalment, s'investiga el control dinàmic de l'enllaç per a la transmissió assistida per *relay* amb dos diferents tipus de coneixement sobre el canal: coneixement estadístic (*statistical knowledge of the channel state*) o coneixement del canal instantani (*actual information about the current channel state*). Aquests dos tipus de coneixement deriven en diferents estratègies a utilitzar per seleccionar la modulació i l'esquema de codificació (MCS). En el primer cas, els rates seleccionats no estan adaptats al canal actual, i per aquest motiu el destí pot rebre erròniament els missatges. Els protocols de retransmissió de missatges (ARQ - *automatic repeat request*) són els encarregats d'assegurar-se la correcta recepció i son redefinits per la transmissió assistida per *relay*. En aquest treball, s'especifica els codis espai-temps distribuïts, la codificació en al font i la *relay* i la longitud de les retransmissions. Quan, la font coneix algun paràmetre del canal instantani pot adaptar el MCS per a aquesta realització del canal. En aquest cas s'investiga la predicció del error en les transmissions assistides per relay, i amb això és possible dissenyar el MCS per maximitzar la quantitat d'informació que s'ha de transmetre per una probabilitat de pèrdua de paquet o per maximitzar el *throughput*.

Acknowledgments[1]

THERE are a number of people I wish to thank for making my experience as a Ph.D. student one of the most rewarding periods of my life. Foremost, I would like to gratefully thank my advisor and friend Dr. Josep Vidal for his continual support and guidance over all this time. We have been working together almost eight years, taking into account also the two final projects needed to get my Master Degrees in Telecommunications (Electrical) and Electronic engineering. His extraordinary motivation and technical insight has been truly inspirational. Additionally, his great confidence on me and his considerable effort to create the best work-environment have been determinant to make possible this Ph.D.

I am also grateful to Dr. Olga Muñoz with whom I had the pleasure of working in several European projects and joint publications.

I have to thank my current and former office's partners and colleagues at UPC for making these years so enjoyable: Christian Ferran, Miriam Leon, Frank Diehl, Ami Wiesel, Andreu Urruela, Jose Luis Landabaso, Josep Maria Crego, Adrià de Gispert, Marta Casar, Mariella, Vuk Marojevic, Eduard Calvo, Maribel Madueño, Marga Cabrera, Alba Pagès, Meritxell Lamarca, Camilo Chang, Joel Sole and Andreu Alcón. Moreover, special thanks to the members of the futsal team named D4 (Pablo, Roberto, Alex, Txema, Luis, Jordi, Jorge, Ali Nassar and Kike) with whom I had the opportunity of winning the UPC cup in 2007. In addition, I would like to thank my friends at the Multimedia Communications Laboratory of the University of Texas at Dallas, Ali Tajer, Harsh Shah, Negar Bazargani and Ramy Tannious, for their help during my research stage in that laboratory and finally, Aria Nosratinia, who was an excellent mentor.

I would like to thank my parents Gregorio and Antonia, my brother Dani, his girlfriend Marta, my eldest brother Gregor, his wife Toni, their sons Marc and Pablo, and all my extended family, for all the love, support and encouragement they have given me throughout this process. I am particularly indebted to my wife Ana, her love and constant support made possible to overcome all the ups and downs of my studies.

Adrian Agustin de Dios
March 2008

Contents

*3   Radio resource optimization for the synchronous/asynchronous
half-duplex relay multiple access channel* _____ *85*

*4   TDD half-duplex relaying applied to TDMA systems
with reuse of resources*_____ *109*

Acronyms

ACK	Acknowledgment
AF	Amplify and forward
AMC	Adaptive Modulation and Coding
ARQ	Automatic Repeat request
ASEP	Average Symbol Error Probability
AWGN	Additive White Gaussian Noise
BC	Broadcast Channel
BER	Bit Error Rate
BICM	Bit Interleaved Coded Modulation
BLER	BLock Error Rate
BPSK	Binary Phase Shift Keying
CDF	Cumulative Density Function
CDI	Channel Distribution Information
CDIT	CDI at the Transmitter
CF	Compress and forward
CRSC	Circular Recursive Systematic Convolutional
CSI	Channel State Information
CSIR	CSI at the Receiver
CSIT	CSI at the Transmitter
CTC	Convolutional Turbo Codes
DSTC	Distributed – STC
DF	Decode and Forward
DLC	Data Link Control
DM	Dispersion Matrices
DVB	Digital Video Broadcasting
ESM	Effective SIR Mapping
Exp-ESM	Exponential Effective SIR Mapping
FEC	Forward Error Correction
FDD	Frequency Division Duplexing
FDMA	Frequency Division Multiple Access
HARQ	Hybrid ARQ
IFC	Interference Channel
INT	Interleaver
LDC	Linear Dispersion Codes
LDPC	Low Density Parity Check
LESM	Logarithmic ESM
LOS	Line of Sight
MAC	Multiple Access Channel
MACL	Media Access Control Layer

MARC	Multiple Access Relay Channel
MCS	Modulation and Coding Scheme
MIESM	Mutual Information ESM
MIMO	Multiple Input Multiple Output
MISO	Multiple Input Single Output
MMSE	Minimum Mean Square Error
MRC	Maximal Ratio Combining
MSE	Mean Square Error
NLOS	Non-LOS
OFDM	Orthogonal Frequency Division Multiplexing
OFDMA	Orthogonal Frequency Division Multiple Access
OSI	Open Systems Interconnection
PDF	Probability Density Function
PER	Packet Error Rate
PF	Proportional Fair
PTC	Parallel Turbo Code
PUSC	Partial Usage of Sub-Channels
QAM	Quadrature Amplitude Modulation
QOD	Quasi-Orthogonal Design codes
QPSK	Quadrature Phase Shift Keying
QoS	Quality of Service
RC	Repetition coding
RCPTC	Rate Compatible Punctured Turbo Codes
RMAC	Relay Multiple Access Channel
RMSE	Root Mean Square Error
RR	Round Robin
RSC	Recursive Systematic Convolutional
SC	Superposition Coding multiple access
SD	Sphere Decoder
SISO	Single Input Single Output
SIR	Signal to Interference Ratio
SNR	Signal to Noise Ratio
STC	Space-Time Code
TC	Turbo Code
TDD	Time Division Duplexing
TDMA	Time Division Multiple Access
UC	Unconstrained coding
ULA	Uniform Linear Array
UOHL	Urban Outdoor High-to-Low
UOHM	Urban Outdoor High-to-Medium
UOML	Urban Outdoor Medium-to-Low
VBLAST	Vertical Bell Laboratories Layered Space-Time
WIFI	Wireless Fidelity
ZMSW	Zero Mean Spatially White
ZF	Zero Forcing

Chapter 1

Introduction

IN this dissertation the relay-assisted transmission with half-duplex relays is analyzed from different points of view. This study is motivated by the necessity of finding innovative solutions to cope with the requirements of next generation wireless services, and with current radio technology. The use of relayed communications represents a change of paradigm of conventional communications, and requires the definition and evaluation of protocols to be applied to single or multiple-user relay communication. With the twofold goal of enhancing *spectral efficiency* and homogenize the bit rate service in cellular communications with uniformly distributed users, system design is investigated at *physical* (type of transmissions of the relay, decoding mode, etc) and *upper layers* (resource allocation, dynamic link control).

1.1 Motivation

The growth of wireless networks in recent decades is motivated by their ability of providing communications *anywhere and anytime*. Because of the importance of this aspect on the modern society, a high proliferation of wireless services and devices such as mobile communications, WiFi (Wireless Fidelity) or cordless phones has emerged. However, in contrast to the wired networks, the wireless networks present two main drawbacks: the *scarcity of radio spectrum* and *channel impairments*. Therefore, the wireless networks should be designed to exhibit a high spectral efficiency and combat channel impairments (including multipath fading, shadowing, interference and path-loss) for an enhanced homogeneous coverage for uniformly distributed users.

Wireless networks are built around a number of nodes which communicate with each other over a wireless channel, some having a wired backbone with only the last hop being wireless, such as the cellular voice and data networks. However, the provision of high capacity and reliable wireless multimedia communications to carry bursty packet traffic as well as voice and delay constrained traffic continues to be a challenging aspect of modern and future wireless communications networks.

Recently, advances in radio transceiver techniques such as Multiple Input Multiple Output (MIMO) architectures have shown an enhancement in the capacity of the current systems by dealing with the channel multipath fading. This is possible by adding multiple antennas at the transmitter and/or the receiver. Another technique which has recently gained attention is the *cooperative* or *relay-assisted*[1] communication where several distributed terminals cooperate to transmit/receive their intended signals (Laneman, Tse, Wornell, Erkip, Sendonaris, Aazhang, Host-Madsen). In this

---

[1] In many publications it has been considered that both terms refer to the same type of communication. However its definition is based on the type of relay considered. If the relay terminal has information of its own to transmit then the transmission is referenced as *cooperative communication*, otherwise it is named *relay-assisted communication*.

technique based on the seminal works issued in the 70's by van der Meulen, Cover and El Gamal, a new element comes up in the communication, the relay terminal. Figure 1.1 depicts an example of the relay-assisted transmission in a three-terminal network. In that scenario, the source desires to transmit a message to the destination (solid line), but obstacles degrade the source-destination link quality. That message is also received by the relay terminal, which can re-transmit that message to destination (dashed line). The destination may combine the transmissions received by the source and relay in order to decode the message[2]. This architecture exhibits some properties of MIMO systems, in fact it is a *virtual* MIMO system because of the distributed antennas. In contrast to conventional MIMO systems, the relay-assisted transmission is able to combat the channel impairments due to the shadowing and path-loss provided in source-destination and relay-destination links because they are statistically independent. In the example depicted in Figure 1.1, the relay-assisted transmission also benefits of the *path-loss breaking* effect and the shadowing present in the source-destination link is combated by using the transmission through the assisting relay, where there is not any obstacle. We have used the term *path-loss breaking* to point out that the source-relay and relay-destination links in Figure 1.1 present lower pathloss degradation than the source-destination link. The pathloss degradation is approximately proportional to the *n*-th power of distance between two terminals.
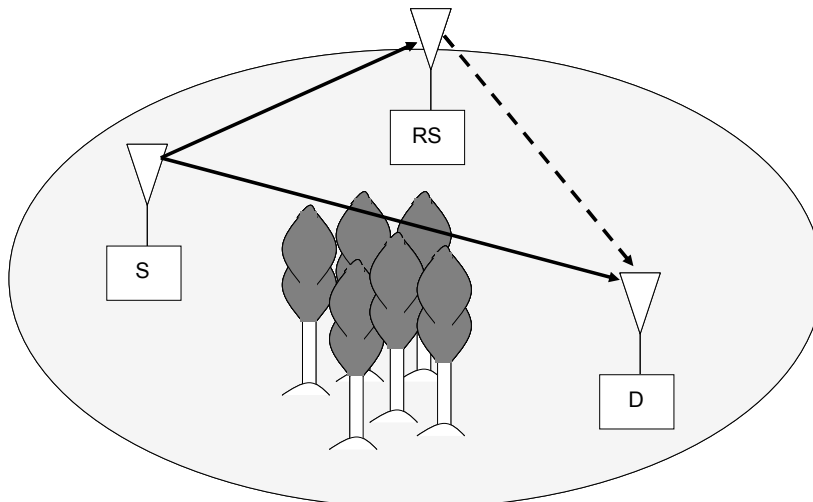
Figure 1.1.- Relay-assisted transmission in a three-terminal network with a source (S), a relay terminal (RS) and a destination (D). Source transmits to the destination (solid line) but the signal is also received by the relay. Afterwards, the relay transmits to the destination (dashed line).

The application of the relay-assisted transmission into practical systems is constrained by the current radio technology, which cannot transmit and receive simultaneously in the same band because of the dynamic range of the incoming and outgoing signals through the same antenna element. Even when different antenna elements are used for transmission and reception the Electromagnetic (EM) coupling is too strong. As a result, the assisting relays must operate in *half-duplex* mode. Therefore the relay-assisted transmission is carried out in two orthogonal phases (duplexed in time or frequency): the *relay-receive* and the *relay-transmit phase*, according to the state of the assisting relay. The *half-duplex* constraint impacts negatively on the theoretical spectral efficiency provided by an ideal *full-duplex* assisting relay. Multiplexing gains are not possible in half-duplex relaying, although significant *additive capacity gains* are still possible.

---

[2] This protocol will be defined in chapter 2 as protocol I.

In this sense, relay-assisted multi-hop networks are expected to play a significant role in 4G wireless communication systems, because of its potentiality to cost-effectively extend the coverage and/or increase the spectral efficiency, and driving the cost of deploying 3G+ and 4G systems lower. To this end the 802.16j Task Group [1] is currently working in the extension of the 802.16e Standard (mobile WiMAX) with multihop transmission. The European Union is funding several projects looking into all the benefits of relay-assisted transmission with joint participation of industry and academia, as for example WINNER [2], MEMBRANE [3], ROMANTIK [4], FIREWORKS [5], ROCKET[3] [6] and COOPCOM [7]. Moreover, the EASY-C project, [8], will build a cellular testbed for testing some relaying techniques.

The introduction of a new terminal in the relay-assisted transmission entails a cross-layer architecture, where a variety of algorithms and procedures placed at different layers of the OSI (Open Systems Interconnection) model have to be jointly designed in order to benefit from this new type of transmission. Therefore a new paradigm in communications appears: *source-relay-destination*. At the *physical layer*, algorithms for encoding and signal processing are required at the source and relay. Additionally, decoding algorithms are also needed at the relay and destination. The decoding role of the relay terminal is grouped in three categories,

- ➢ *Amplify and forward* (AF). The relay amplifies and forwards the signal received during the *relay-receive phase*.

- ➢ *Decode and forward* (DF). The relay decodes the message received in the *relay-receive phase*, re-encodes and transmits in the *relay-transmit phase*.

- ➢ *Compress and forward* (CF). The relay compress the estimated symbols of the signal received during the *relay-receive phase* and transmits in the *relay-transmit phase*.

The use of *half-duplex* relays leads to the definition of several protocols, depending on which terminals (source and/or relay) are transmitting and which are listening (relay and/or destination) in the *relay-receive* or *relay-transmit phase.* Those phases may be duplexed in time (TDD) or in frequency (FDD).

The Radio Resource Management (RRM) and Data Link Control (DLC), both in the *data link layer* also have to be revised. An efficient RRM should consider the allocation of transmitted power and time resources to each phase of the relay-assisted transmission and the scheduling process. Additionally, an appropriate DLC should investigate the Automatic Repeat reQuest (ARQ) procedures and the modulation and coding scheme (MCS) selection. The activity of the relay is connected with the retransmission scheme, where the relay terminal may either always transmit (*persistent transmission*) or do it only when the packet at the destination is received in error (*incremental relaying*). For DF case, the relay may further decide transmit the received packet if it is received correctly at the relay (*selective relaying*).

Likewise, efficiency of the relay-assisted transmission is improved when the techniques of the *data link layer* consider some information available at the *physical layer* (*cross-layer design*), as the knowledge of the wireless medium and the transceiver technique to be used.

---

[3] Part of the results of this work has been considered as UPC's contribution to ROMANTIK and FIREWORKS. Additionally, part of the future work is planned to be investigated under the ROCKET project.

1.2 Outline of dissertation

This dissertation addresses protocols and strategies of the half-duplex relay-assisted transmission for enlarging the spectral efficiency under the single-user (with single and multiple assisting relays) and multiple-user (with single assisting relay) scenarios. It shows how a joint design of the system unveils the benefits of this type transmission and describes guidelines for its forthcoming applicability to the current/future communication systems. Those protocols and strategies consider relays working under *amplify-and-forward* or *decode-and-forward*. *Compress-and-forward* relays increase the complexity of the protocols and they are out of scope of this dissertation.

This dissertation is organized as Figure 1.2 shows. Chapter 1 is devoted for the introduction of the dissertation. Afterwards, chapter 2 describes protocols and strategies for the single half-duplex relay-assisted transmission. The extension for the multiple user case is tackled in chapter 3 and chapter 4. Chapter 3 investigates different scenarios where there are multiple sources, possibly multiple relays and a single destination. The resources are optimized for different access methods. On the other hand, chapter 4 investigates the relay-assisted transmission in a cellular system based on TDMA in the *downlink* (a single source and multiple destinations and relays). A time slot is reused for reducing the spectral efficiency loss due to work under static resource allocation. The interference generated in that time slot is combated by means of a distributed power control or a rate control. Chapter 5 considers the dynamic link control for the relay-assisted transmission under different approaches of knowledge about the channel state. Automatic repeat request procedures and link error prediction methods are considered to maximize the throughput of the system. Finally, chapter 6 presents the conclusions and the future work.
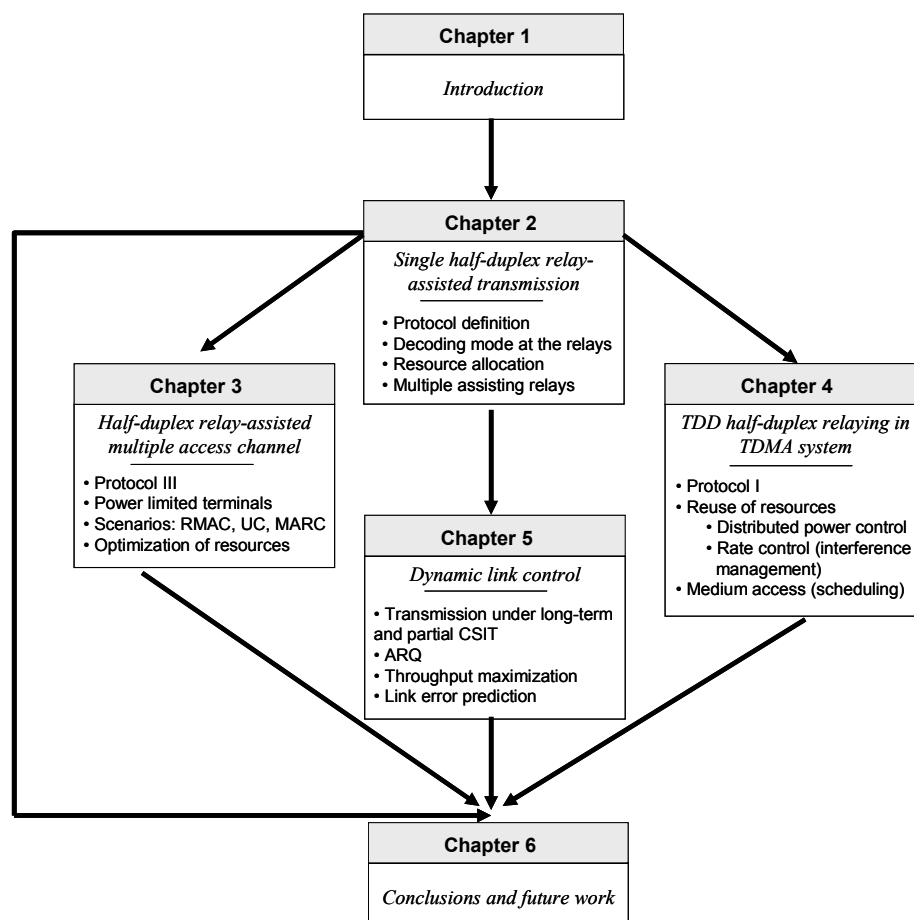

Figure 1.2.- Organization of the dissertation.

The outline of each chapter is as follows.

Chapter 1 describes the motivation and the outline of the work. It also includes the research contributions by the author during the elaboration of his Ph.D. degree.

Chapter 2 presents an overview of the single user cooperative/relay-assisted transmission and provides new results. The achievable rate obtained by the relay-assisted transmission depends on the type of data transmitted by the relay (*repetition* or *unconstrained coding*) when it is working in *decode-and-forward* mode. Additionally, all the protocols considered for the relay-assisted transmission with *half-duplex* relays are detailed, providing their mutual information. The communication is carried out in two orthogonal phases (*relay-receive* and *relay-transmit phase*), leading to the definition of several protocols which depend on the number of terminals active in each phase of the communication. It is shown that the spectral efficiency of the different relay-assisted protocols depends on the optimization of the duration of each phase (*resource allocation*) which can be: *static* or *dynamic*. *Dynamic resource allocation relaying* adapts each phase of the transmission as a function of the quality of the different links.

Additionally, two transmission techniques are evaluated when the destination is assisted by multiple relays. Those techniques differ in the type of messages intended to each assisting relay (*independent* or *common messaging*). The source and relays may have exact channel state information (CSI), thus they can transmit *synchronously*[4] (distributed *eigenvector precoding*) or do not have it, *asynchronous transmission*. The resource allocation for both proposed techniques can be defined as convex problems, evaluating their achievable rates.

Chapter 3 analyzes different cooperative/relay-assisted scenarios for multiple sources and a single destination. Those sources may be assisted by a relay (RMAC, relay-assisted multiple access channel), cooperate between them (UC, user cooperation) or have a powerful single relay (possibly placed as a lamppost) to help simultaneously all the sources (MARC, multiple access relay channel) to transmit to a single destination. Among the relay-assisted protocols analyzed in chapter 2 the one with the largest spectral efficiency is adopted for the cooperative/relay-assisted scenarios tackled in chapter 3. The source and relay terminals are power limited and are able to transmit *synchronously* or *asynchronously*, depending of the CSI available at the different nodes. The relay-assisted transmission is analyzed under time division duplexing (TDD) and frequency division duplexing (FDD) when the multiple sources access to the medium by means of TDMA (time division multiple access), FDMA (frequency division multiple access) or SC (superposition coding multiple access[5]). As the transmission is duplexed in two phases, the sources (and relays) have to access in each phase, generating a large number of combinations. In this work it has been assumed that if the duplexing mode is done in TDD, the access method in each phase can be TDMA or SC (FDMA or SC for FDD). It will be shown that the problem of allocating the transmission resources for the multiple sources is convex in some circumstances.

Chapter 4 addresses the application of the relay-assisted transmission duplexed in time in a centralized cellular system TDMA-based in the *downlink* (i.e. one source and multiple

---

[4] In this dissertation we have used *synchronous transmission* for referencing the case where the source and relays have perfect channel state information (CSI) and additionally they are synchronized in terms of carrier phase (phase alignment). When they do not have CSI the case is referenced as *asynchronous transmission*.
[5] In such a case the multiple sources share the same medium.

destinations). In such systems the source transmits to destinations in equally sized slots without possibility of modifying their duration. If some destination is interested in using the relay-assisted transmission, it is required an additional time slot where the relay will transmit (relay slot). The relaying assistance is performed by terminals not active in the current frame (*user relaying*). In this case the transmission resources cannot be optimized due to the system constraints (*relay-transmit* and *relay-receive* phase are equal sized, 1 time slot, *static resource allocation relaying*) so there is a spectral efficiency loss which is combated by spatial reusing the relay slot. All the assisting relays (associated to different destinations) will transmit simultaneously in the same time slot (relay slot) producing interference between destinations. Likewise, two approaches are considered to deal with that interference: *distributed power control* algorithms and *rate control management*. The first approach considers that all the assisting relays adjust its transmitted power during the relay slot according to a power control algorithm based on game theory where each relay-destination pair maximizes its own utility function (*power control*). On the other hand, the second approach assumes that the relays are transmitting with a constant-in-time power (it may be different for different relays) and the statistics of the interfering power can be accurately modeled. In that case the source designs its transmission rate (*rate control*) to reduce the probability of outage event due to the interference. This chapter gives the statistical model of the interfering power received at each destination when all the terminals are distributed in the cell following a *Poisson* distribution and each destination selects the nearest idle terminal as assisting relay.

A comparison between different types of relays is reported. That study considers the use *infrastructure* relaying (for example a lamppost) and *user relaying* (the relays are other terminals) under cellular system based on TDMA. The *user relaying* uses the proposed method of reusing a time slot for the transmissions from the relays with a distributed power control. Finally, the medium access (traditional scheduling algorithms) under *user relaying* is analyzed in order to study the *multiuser gain* in this type of transmission.

Chapter 5 deals with the *dynamic link control* of the relay-assisted transmission. As it can be seen as a *virtual* MIMO, the system design should extend the MIMO methods for the relay-assisted transmission. Therefore aspects such as the *distributed* space-time coding, modulation and coding and automatic repeat request (ARQ) procedures have to be reviewed. In this regard, when the transmission rate is designed under *statistical knowledge about the channel state*, it is possible that for some channel realization the selected modulation and coding scheme (MCS) will not be supported, producing that the receiver will decode wrongly the message (*outage event*). We have assumed that the transmitters have *long-term* Channel Distribution Information at the transmitter (CDIT), for example the average signal-to-noise ratio (SNR) of each link.

On the other hand, when there is *actual information about the channel state*, the transmitter can adapt the MCS to the current channel realization. The errors in the transmission are due to the *thermal noise* of the channel. This case has been considered for a *multicarrier* relay-assisted transmission when there is *partial* CSIT. Under that configuration the Exponential Effective SIR Mapping (Exp-ESM) provides the *effective SNR* for describing the quality of each link and is useful for the link error prediction given a forward error correction (FEC) code and MCS. In this regard, the link error prediction for relaying transmission is found as an extension of the Exp-ESM. The MCS can be designed in order to maximize the information rate for a given probability of packet loss or to maximize the throughput.

Chapter 6 concludes the dissertation and proposes future lines of work.

1.3 Research contributions

The details of the research contributions in each chapter have been reported in the following publications.

Chapter 2

1. D.P.Palomar, A.Agustín, O.Muñoz, J.Vidal, "Decode and forward protocol for cooperative diversity in multi-Antenna Wireless Networks", in *Proc. IEEE Annual Conference on Information Sciences and Systems* (CISS-2004), Princeton, NJ (USA), Feb. 17–19, 2004.

2. A.Agustin, J.Vidal, "Resource optimization in the decode-and-forward half-duplex multiple relay-assisted channel", *submitted to Proc. 9th IEEE Workshop on Signal Processing Advances in Wireless Communications* (SPAWC-2008), Recife-Pernanbuco, Brazil, July 2008.

Chapter 3

3. A.Agustin, J.Vidal, "Radio resources optimization for the half-duplex relay-assisted multiple access gaussian channel", in *Proc. 8th IEEE Workshop on Signal Processing Advances in Wireless Communications* (SPAWC-2007), Helsinki, Finland, June 2007.

4. A.Agustin, J.Vidal, "Radio resource optimization for the synchronous/asynchronous half-duplex relay multiple access channel", *submitted to IEEE Trans. on Wireless Communications* , December 2007 (TW-Dec-07-1454).

Chapter 4

5. J.Vidal, A.Agustín, O.Muñoz, "Cellular capacity gains of cooperative MIMO transmission in the downlink", in *IEEE Proc. International Zurich Seminar on Communications*, (IZS-2004). Feb. 2004.

6. A.Agustin, O.Muñoz, J.Vidal, "A game theoretic approach for cooperative MIMO systems with cellular reuse of the relay slot"*, in Proc. IEEE International Conference on Acoustics, Speech and Signal Processing* (ICASSP-2004), Montreal, Canada, May 2004.

7. J.Vidal, S.Barbarossa, A.Agustin, Document IEEE 802.11-00/797r0 presented at the Wireless Next Generation Standing Committee de IEEE 802.11 about Cooperative Transmission, as a result of the research done in the ROMANTIK project, Portland, USA, July 13, 2004.

8. A.Agustin, J.Vidal, O.Muñoz, "Multi-user diversity in the cooperative transmissions", in *Proc. IST Mobile and Wireless Communications Summit* (IST-2005), Dresden, Germany, June 2005.

9. A.Agustin, J.Vidal, "TDMA amplifying and forward cooperation under interference-limited spatial reuse of the relay slot", in *Proc. IEEE International Conference on Acoustics, Speech and Signal Processing* (ICASSP-2006), Toulouse, France, May 2006.

10. A.Agustín, J.Vidal, "High spectral efficiency of multiple-relays assisted amplify-and-forward cooperative transmissions under spatial reuse", *in Proc. IEEE Vehicular Technology Conference Fall* (VTC-Fall 2007), Baltimore, USA, Sep. 2007.

11. A.Agustin, J.Vidal, "Amplify-and-forward cooperation under interference-limited spatial reuse of the relay slot", *accepted to IEEE Trans. on Wireless Communications*, December 2007. (TW-Aug-07-0973.R1).

Chapter 5

12. A.Agustín, J.Vidal, E. Calvo, O.Muñoz, "Evaluation of turbo H-ARQ schemes for cooperative MIMO transmission", *in Proc. IEEE International Workshop on Wireless Ad-Hoc Networks* (IWWAN-2004),Oulu, Finland, May 31-June 3, 2004.

13. A.Agustin, E.Calvo, J.Vidal, O.Muñoz, "Evaluation of turbo coded cooperative retransmission schemes", in *Proc. IST Mobile and Wireless Communication Summit* (IST-2004), Lyon, France, June 27-30, 2004.

14. A.Agustin, E.Calvo, J.Vidal, O.Muñoz, M.Lamarca, "Hybrid turbo FEC/ARQ systems and distributed space-time coding for cooperative transmission in the downlink", in *Proc. IEEE Personal Indoor Mobile Radio Communications* (PIMRC-2004), Barcelona, Spain, Sept. 5-8, 2004.

15. A.Agustin, J.Vidal, O.Muñoz, "Hybrid turbo FEC/ARQ systems and distributed space-time coding for cooperative transmission", *International Journal of Wireless Information Networks* (IJWIN), vol. 4, no. 12, pp. 263-280. December 2005.

Other contributions not presented in this dissertation

16. A.Agustín, A.Pagès, J.Vidal*, "*Coordinated MIMO transmission for multi-user interference nulling with simple receiver constraint", in *Proc. IEEE International Conference on Acoustics, Speech and Signal Processing* (ICASSP-2003), Hong Kong, China, April 2003.

17. J.Vidal, A.Agustín, A.Pagès*,* "Coordinated MIMO transmission for Multi-User Interference", *in Proc. IST Mobile and Wireless communication Summit*, Aveiro, Portugal, June 2003.

18. A.Agustín, J.Vidal, A.Pagès, "Linear Dispersion Codes Construction with a defined structure", in *Proc. IEEE Vehicular Technology Conference Fall* (VTC-Fall 2003), Orlando, FL, Oct. 2003.

19. O.Muñoz, J.Vidal, A.Agustin, "Non-regenerative MIMO relaying with channel state information"*,* in *Proc. IEEE International Conference on Acoustics, Speech and Signal Processing* (ICASSP-2005), Philadelphia,USA, March 2005.

20. S. Valentin, H. Lichte, H. Kart, G. Vivier, S. Simoens, J. Vidal, A. Agustin, I Aad, "Cooperative Wireless Networking beyond Store-and-Forward: Perspectives for PHY and MAC Design", *WWRF white paper,* Heidelberg WWRF meeting, November 2006.

21. Stefan Valentin, Herman S. Lichte, Holger Karl, Sebastien Simoens, Guillaume Vivier, Josep Vidal, and Adrian Agustin, "Cooperative wireless networking beyond store-and-forward: Perspectives in PHY and MAC design", *Wireless Personal Communications Journal*, March 2008.

22. A.Agustin, "Cooperative transmission and radio resources management for wireless networks: Achievable rates for the non-degraded Gaussian broadcast relay channel", *Scientific report of the research stage at University of Texas at Dallas with Professor A.Nosratinia* (Sept-Dec 2005). Financed by the scholarship BE (DURSI). Available on: www.recercat.net.

23. O.Muñoz, J.Vidal, A.Agustin, "Linear transceiver design in nonregenerative relays with channel state information", *IEEE Trans. on Signal Processing*, vol. 44, no. 6, pp. 2593-2604, June 2007.

1.4 References

[1] IEEE 802.16j-06/013r1, "Multi-hop relay system evaluation methodology (Channel Model and Performance Metric)", October 2006, http://www.ieee802.org/16/relay/ .

[2] Wireless World Initiative New Radio (WINNER), 6th Framework Program. http://www.ist-winner.org.

[3] Multi-Element Multihop Backhaul Reconfigurable Antenna Networks (MEMBRANE), January 2006 - June 2008, http://www.imperial.ac.uk/membrane.

[4] Resource Management and Advanced Transceiver algorithms for Multihop Networks (ROMANTIK), March 2002 - February 2005. http://www.ist-romantik.org.

[5] Flexible Relay Wireless OFDM-based Networks (FIREWORKS), January 2006 – March 2008, http://www.ist-fireworks.eu.

[6] Reconfigurable OFDMA-based Cooperative Networks Enabled by Agile Spectrum Use (ROCKET), January 2008 – December 2009, http://www.ict-rocket.eu.

[7] Cooperative and Opportunistic Communications in Wireless Networks (COOPCOM), October 2006 – October 2009, http://www.coopcom.eu.org

[8] Enablers of Ambient Services and Systems part C – Wide Area Coverage (EASY-C), http://www.easy-c.org.

Chapter 2

Single user relay-assisted and cooperative communication

THIS chapter is devoted to study the *relay-assisted* and *cooperative* communication in a three-terminal network where the scenario is built upon a source, a single relay and a destination. It presents the prior work developed in the relay-assisted transmission, describing which decoding strategies are possible at the relay. The use of half-duplex relays imposes the definition of two orthogonal phases (*relay-receive* and *relay-transmit phase*) and motivates up to four protocols for implementing the relay-assisted transmission.

First, the benefits of the relay-assisted transmission with half-duplex relays are evaluated when terminals are equipped with multiple antennas and the assumption that there is not complete channel state information of all the links (we reference to this case as *asynchronous transmission*). This chapter investigates the type of message transmitted by the *decode-and-forward* relay (*repetition* or *unconstrained* coding). When the *phases* of the communication are fixed (*static resource allocation relaying*) an adaptive protocol based on *selective relaying* is adopted to deal with source-relay links with bad quality, because they limit the efficiency of the relay-assisted transmission. Moreover, it also explores a dynamic resource allocation for each *phase* of the communication (*dynamic resource allocation relaying*) under different constraints on the transmitting power of the terminal which lead to the evaluation of the relay-assisted transmission duplexed in the time domain (*power limited terminals transmitting with maximum power*), duplexed in the frequency domain (*individual average power constraints*) and the evaluation the spectral efficiency of unit total power (*average sum power constraint*). The gains provided by the relay-assisted transmission are evaluated in terms of *outage mutual information* and *average achievable rate*.

Finally, the relay-assisted transmission with multiple assisting relays is investigated when all terminals have complete channel state information of the different links and the carrier phases of the distributed nodes are synchronized (we reference to this case as *synchronous transmission* and *eigenvector precoding* techniques are assumed) or there is not channel state information at the transmitters (*asynchronous transmission*). Two source transmission strategies are considered depending on the messages intended to each relay (*independent or common messaging*). It will be shown that the resource allocation can be formulated as a convex problem for both strategies, evaluating their achievable rates.

2.1 Background and related work

Communications through wireless channels have motivated new problems in the transmissions over the mobile users due to the time-varying fading channels, interference and the shadowing effect, mainly. The appropriate method to combat these effects is the use of diversity (*diversity gain*). Typically, time and frequency diversity have been considered. In recent years the space diversity [1],[2] by means of multiple antenna system (MIMO – Multiple Input Multiple Output) has received much attention from the research community because it can be combined with the previous forms of diversity and additionally, offers an increase of the total information theoretic capacity (*multiplexing gain*) of the system. The diversity-multiplexing tradeoff exhibited by the multiple antenna channels is shown in [3]. MIMO systems have proven to increase the channel information theoretic capacity linearly with the minimum number of transmitting and receiving antennas. Recently and motivated by the work of [4] and [5], there has been a growing interest in a new space-time method which uses antennas belonging to multiple terminals, the *cooperative diversity*. The cooperative terminals create a virtual array through distributed transmissions [6],[7],[8]. This method is based in the classical relay channel, [9], [10].

In order to detail all the main aspects of the relay channel the literature revision will be structured as follows. Section 2.1.1 describes the *relay channel*. Afterwards, the cooperative transmission is outlined in section 2.1.2. In relay-assisted transmissions with a half-duplex constraint there are four possible protocols which are presented in section 2.1.3. The strategies of the relay-assisted transmission are detailed in section 2.1.4 describing the decoding modes at the relay and the resource allocation for each phase of the communication.

2.1.1 The relay channel

The relay channel is introduced in [9]. It assumes that there is a source that wants to transmit information to a single destination. However, there is a relay terminal that is able to help the destination (*relay-assisted transmission*). Based on the past received symbols, it can transmit and additional message to the destination. Figure 2.1 illustrates the channel model. When the relay terminal presents a better channel conditions than the destination, this scheme is able to improve the source-destination transmission. In general it is assumed that the relay works in *full-duplex mode*, i.e. receiving and transmitting simultaneously. Inner bounds of the information theoretic capacity (capacity in the following) of a discrete memoryless channel are given by [9] based on a timesharing approach. Afterwards, the capacity for the special case of degraded relay channels by the use of superposition block Markov encoding is found in [10]. For other type of channels the capacity is upper-bounded (*max-flow-min-cut* theorem [11]) by the minimum of mutual information obtained by the broadcast channel (transmission from the source to relay and destination, [11]) and the multiple access channel (independent and simultaneous transmission from the source and relay to the destination, [11]).
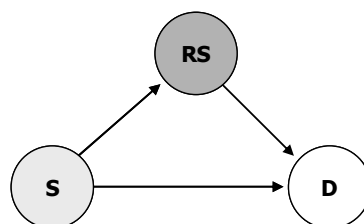

Figure 2.1.- The relay channel. Source (S), Relay (RS) and Destination (D).

Capacity bounds and power allocation for wireless relay channels are given in [12] for *half-duplex* relay and single-antenna terminals. Additionally, algorithms to compute the capacity bounds for the multi-antenna terminals are presented in [13]. In some conditions the upper bound meets the lower bound characterizing the capacity of the MIMO relay channel.

2.1.2 Cooperative communication

Cooperative communication is based on the relay channel model, Figure 2.1, however, the principal difference between the *relay-assisted* and the *cooperative transmission* is the type of terminals involved in the communication. In the *relay-assisted transmission* the relay terminal is an additional terminal which helps to the source (it does not have its own information to transmit), while in the *cooperative communication* there are two sources which have to help one to each other and both have information to transmit.

The cooperative diversity[1] is introduced in [4] using the scenario depicted in Figure 2.1 but with the relay terminal being another source. Both sources (associated partners) are also responsible of transmitting the information of their partners. It is assumed that the sources are working in full-duplex mode, so that both sources are transmitting to the destination and receiving a noisy version of the partner's transmission. Results in terms of ergodic achievable rate regions and outage probability of the cooperative and non-cooperative transmission show the benefits of this scheme.

The cooperative diversity for the *ad hoc* four-node network presented in Figure 2.2 and made up of two sources and two destinations is analyzed in [14]-[16], providing some upper and lower bounds of the capacity offered by that network. Each source wants to send a message to a different receiver. Basically, two types of cooperation can be found: *receiver* and *transmitter* cooperation, depending which nodes are relaying each other's messages. It is assumed that all the nodes work on the full-duplex mode. Although this four-node network is quite similar to a MIMO system (it will be equal if both sources/destinations have prior information about the transmitted/received data by the other node) there is no *multiplexing gain* for either transmitter or receiver cooperation, but there is an *additive gain* over the direct transmission, [14].
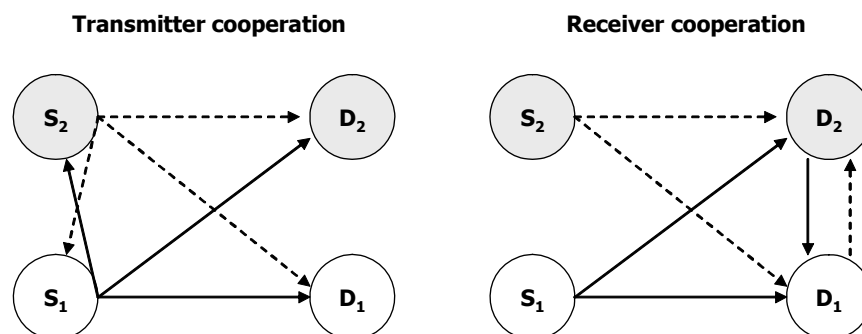

Figure 2.2.- Cooperative diversity network. 2 sources (S$_1$, S$_2$) and 2 destinations (D$_1$,D$_2$).

---

[1] This term is defined as *user cooperation* in [4].

2.1.3 Half-duplex relay protocol overview

Full duplex terminals are currently unrealistic in practical systems, hence the relays are forced to work under half-duplex mode, i.e. there will be an orthogonal duplexing (in time or frequency) between the relay is receiving (*relay-receive phase*) and the relay is transmitting (*relay-transmit phase*), see chapter 1. This phase separation allows defining several half-duplex relay protocols with various degrees of broadcasting and receiving collision in each *relay-receive* and *relay-transmit phase* among the three terminals (source, destination and relay). The number of options leads to the four protocol definition[2] [27], [28] presented in Figure 2.3 and named in this dissertation protocol I, II and III, and in Figure 2.4 and named forwarding.
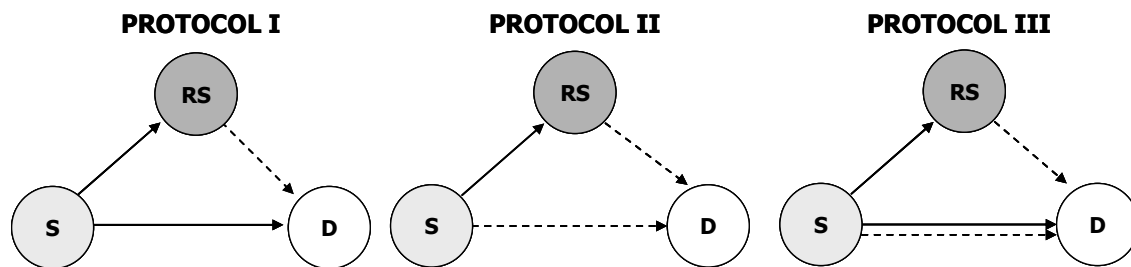
Figure 2.3.- Half-duplex relay protocols. S, RS and D refer to the source, relay and destination, respectively. Solid lines correspond to the transmission during the *relay-receive phase* and dashed line for the transmission during the *relay-transmit phase*.

In protocol I the source communicates with the relay and destination during the *relay-receive phase* (solid lines in Figure 2.3). Afterwards, in the *relay-transmit phase*, the relay terminal communicates with the destination (dashed line in Figure 2.3). This protocol shows the same structure as the Broadcast Channel (BC) during the *relay-receive phase*. For example this protocol is used by the cooperative transmission defined in [5] and [23] and also in the relay-assisted transmission described in [21].

On the other hand, in protocol II during the *relay-receive phase* the source only transmits to the relay (solid line in Figure 2.3). It is assumed that the destination is not able of receiving the message from the source in that phase. In the *relay-transmit phase* source and relay transmit simultaneously to the destination (dashed lines in Figure 2.3). Hence in the *relay-transmit phase* the channel becomes a multiple access channel (MAC).

Protocol III can be seen as a combination of protocols I and II. The source transmits to the relay and the destination (solid lines in Figure 2.3) in the *relay-receive phase*. Then, in the *relay-transmit phase*, the source and the relay transmit to the destination (dashed lines in Figure 2.3). Notice that the relay is transmitting during the second phase, so that it cannot be aware of the signal transmitted by the source in the second phase. This protocol can achieve a better spectral efficiency than previous ones. For example this protocol is considered for obtaining the achievable rates of the relay channel in [12]. Moreover, the cooperation scheme defined in [4] is akin to protocol III because the destination is considering the signal received in both phases to decode the message transmitted by the source.

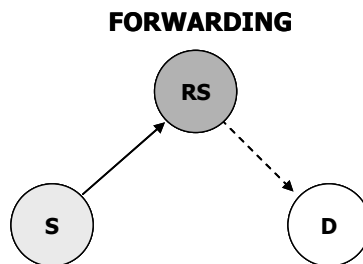[2] The current enumeration differs from the one used in [27].

FORWARDING

Figure 2.4.- Half-duplex forwarding protocol. S, RS and D refer to the source, relay and destination, respectively. Solid lines correspond to the transmission during the *relay-receive phase* and dashed line for the transmission during the *relay-transmit phase*.

Finally, the traditional forwarding protocol consists in a transmission from the source to the relay during the *relay-receive phase* and a transmission from the relay to the destination in the *relay-transmit phase*, see Figure 2.4. It should be emphasized that the half-duplex relay protocols defined in Figure 2.3 make good use of the source-destination link in contrast to the forwarding protocol. Likewise, if that link presents a very bad quality compared with the source-relay and relay-destination link, the performance obtained by protocols I, II and III converges to the forwarding one.

2.1.4 Strategies of the relay-assisted transmission

The paradigm of the conventional source-destination communication is now changed to *source-relay-destination*, and the role played by the relay can be selected over different modes of operation influencing the total achievable rate of the system. Additionally, when there is a half-duplex relay the resources allocated for each phase of the relay-assisted transmission also has an important impact on the achievable rate. Therefore, the strategies of the relay-assisted transmission have to consider the decoding mode at the relay and the resource allocation.

Decoding at the relay

Basically there are three decoding modes analyzed in the literature are: *amplify-and-forward* (AF), *decode-and-forward* (DF) and *compress-and-forward* (CF).

A. Amplify-and-forward (AF)

This is the simplest strategy that can be used at the relay because it acts as a *dummy* with a constraint on the maximum power. The relay amplifies the received signal from the source and transmits it to the destination without doing any decision. The main drawback of this strategy is that the relay terminal is also amplifying the received noise to the destination. When this strategy is applied to the cooperative communication, it is able to obtain a better uncoded bit error rate (BER) than direct transmission [5]. Additionally, the outage probability of the cooperative communication is also derived, demonstrating that a diversity order of two is obtained for two cooperative users. When the relay is equipped with multiple antennas and there is channel state information (CSI) of the source-relay and relay-destination links, the AF strategy can attain significant gains over the direct transmission by means of optimum linear filtering the data to be forwarded by the relay [18],[19].

B. Decode-and-forward (DF)

The complexity at the receiver increases in comparison to the AF strategy. Now the relay terminal has to estimate the message received from the source and the total performance

will depend on the success of decoding correctly the message. Depending on the type of symbols retransmitted the strategy at the relay is *repetition coding* (RC) or *unconstrained coding*[3] (UC). In the RC, the relay retransmits the same symbols previously estimated, while in the UC the symbols transmitted are not the same to the received ones, but related to the same information sent by the source (source and relay are using different codebooks). An example for UC is the following. Let us assume that the source is going to transmit a coded codeword using a forward error correction (FEC) code, where there are *systematic* and *parity* bits. Once the relay has decoded the signal received in the *relay-receive phase*, it re-encodes the message, selecting new *parity* bits and transmits them to the destination in *the relay-transmit phase*.

Two sources that cooperate for transmitting to a common destination are investigated in [4],[17]. Basically, the transmission is done over three intervals of time. The first one is devoted to transmit directly to the destination (without cooperation) and the remaining two are used for cooperation. In the second period each source transmits new information to the destination which is estimated by the other source (partner). Afterwards, both sources transmit a linear combination of its own bits transmitted in the previous interval of time and the estimated ones belonging to the other source to the destination. The relay, in this case the other source, is working with DF-RC. The *decode-and-forward* scheme defined in [5] also works under DF-RC.

Upper and lower bounds for the *unconstrained coding*[4] (UC) in a cooperative scenario where each source can cooperate with m terminals in orthogonal mode are shown in [20]. The destination must combine the signals received in two orthogonal periods of time which come from the source and from those cooperative users who were able to decode the message transmitted by the source in the first period of time (protocol I). The total mutual information is the same as two parallel channels [11]. Unconstrained coding is superior to repetition coding in terms of diversity for larger spectral efficiencies.

A practical implementation of *unconstrained coding* (UC) for protocol I can be found in [21], [22] and chapter 5, where the relay terminal instead of transmitting the same symbols, it uses a different part of a rate compatible turbo code, (TC), as in the example given at the beginning of this section. In that case it is assumed that the source transmits a message to the relay and destination in one time interval. Afterwards, the relay transmits to the destination in an orthogonal period of time. The destination must combine both transmissions in order to decode the message and observes total coded codeword with more protection (*incremental redundancy*). This idea is applied to the *cooperative transmission* in [23]-[25] and is named *coded cooperation*.

C. Compress-and-forward (CF)

In this strategy the relay does not decode the data and use the Wyner-Ziv lossy source coding [26] on the estimated symbols of the received signal. Then, the compressed signal is transmitted to the destination by the relay. Depending on the channel gains of the different links CF can be superior to the DF strategy. This strategy is suggested in [10] (Theorem 6). However it adds more complexity to the system and for that reason will not be considered in this dissertation.

---

[3] This term has been defined in [30] and is introduced in section 2.2.1.
[4] It is referenced as space-time-coded cooperative diversity in section IV of [20].

Resource allocation in half-duplex relays

The half duplex protocols presented in section 2.1.3 assume that the relay-assisted transmission is done in orthogonal phases, the *relay-receive* and *relay-transmit phase*. The achievable rate of the system depends on the duration of each phase. Two strategies are possible for defining the duration of each phase: *static* or *dynamic resource allocation relaying*. The adoption of one of those strategies may depend on the kind of channel state information at the source and/or the type of system where the relay-assisted transmission is implemented.

Static resource allocation relaying is defined when the duration of each phase is previously assigned. This can be found when the cooperative transmission is implemented in a centralized cellular system based on Time Division Multiple Access (TDMA) as it is done in chapter 4. The transmission from the source to destinations is done over time slots with fixed duration. In that case the relay-assisted transmission needs two time slots (*relay-receive* and *relay-transmit phase*). Another possible scenario for *static relaying* is when there is only statistical information about the channel model and resources cannot be allocated based on the quality of the different links involved in the relay-assisted transmission. Despite not using an optimal resource allocation, there are several retransmission strategies at the relay to enhance the spectral efficiency of the relay-assisted transmission:

- *Persistent transmission*

- *Incremental relaying*

- *Selective relaying*

The previous decoding modes at the relay terminal can be adopted all the time (*persistent transmission*) or adapt it to the current channel state by exploiting limited feedback from the destination and/or the relay. Source and relay can have knowledge about the success of the transmission at the relay and destination thanks to the existing feedback logical channels in the modern communication systems. Two different options are analyzed in [5]: *selective* and *incremental* relaying. The *selective relaying* is applied to the DF because the performance is constrained by the success on the transmissions from the source to the relay. When the relay receives wrongly or the source measures that the current channel state of the source-relay link is below a threshold, then the relay remains silent and the source transmits again (using repetition or more powerful codes). For *incremental relaying* the relay should be aware of the success or not of the direct transmission during the *relay-receive phase* at the destination. The relay only transmits when the direct transmission (source-destination) is wrongly decoded by the destination. Using this option it is possible to obtain an improvement of the spectral efficiency over the *persistent* and *selective* transmission.

Protocols	Persistent transmission	Selective relaying	Incremental relaying
forwarding	√	×	×
protocol I	√	√	√
protocol II	√	√	×
protocol III	√	√	√

Table 2.1.- Types of retransmission at the relay for different protocols.

Table 2.1 depicts the available types of relay transmission (*persistent*, *selective relaying* or *incremental relaying*) for the different half-duplex protocols. For the forwarding protocol it is required that relay always transmit because the destination is considering only the data received during the *relay-transmit phase*. For protocol I all types of transmission are possible. For protocol II *incremental relaying* is not implementable because the relay is transmitting simultaneously with the source in the *relay-transmit phase* and the destination is considering only the data received in that phase. When the relay is working under *selective relaying* and the relay remains silent because it has not been able to decode the message from the source, the equivalent system is the same as the direct transmission using only the *relay-transmit phase*. For protocol III under *selective relaying* the source is transmitting in both phases and the destination considers the data received in both phases. Additionally, *incremental relaying* is also possible because the message transmitted by the relay in the *relay-transmit phase* is connected with the transmission done by the source in the *relay-receive phase* (as in protocol I), so the destination might inform the relay about the success in decoding the message in that phase and the relay terminal will remain silent in the *relay-transmit phase*. It is worth noticing that under *selective relaying* in protocol I when the relay terminal remains silent, the source transmits during the *relay-transmit phase*, while for protocol II and III the source is already transmitting during that phase by definition. Section 2.2.1 investigates the achievable rates obtained by protocol I using *repetition coding* (RC) or *unconstrained coding* (UC) for *static relaying* and the benefits of using an adaptive relay working under *selective relaying*.

Dynamic resource allocation relaying is assumed when the source has knowledge of the quality of all the links (source-destination, source-relay and relay-destination). Under that circumstance the spectral efficiency of the relay-assisted transmission is maximized by adapting the resource allocation of each phase in function of the quality of the different links. Otherwise, the retransmission strategies considered for the *static relaying* should be considered also here. In this regard section 2.3 investigates the achievable rates of the all half-duplex protocols presented in section 2.1.3.

Finally, Figure 2.5 presents a classification of the possible strategies for relay-assisted transmission, differentiating between the decoding mode at the relay and the resource allocation for each orthogonal phase (half-duplex relays).
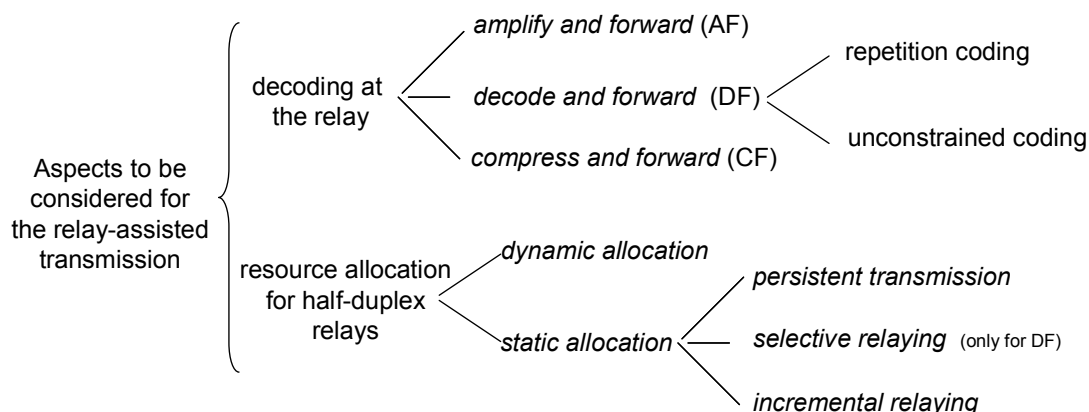

Figure 2.5.- Aspects to be considered for the relay-assisted transmission.

2.2 Static resource allocation relaying

This section investigates the half-duplex relay protocols when there is a *static resource allocation*. Section 2.2.1 considers protocol I with a *decode-and-forward* relay. The type of message transmitted by the relay and the benefits of *selective relaying* will be investigated. The *additive capacity gain* [12] available by protocol I is measured for different antenna configurations. Afterwards, section 2.2.2 presents the performance of all the half-duplex protocols with DF relay and working under *repetition coding*. Finally, section 2.2.3 presents the half-duplex protocols when the relay works in *amplify-and-forward* mode.

2.2.1 DF-Protocol I

This section studies the half-duplex relay protocol I (section 2.1.3) under the *decode-and-forward* transmission, the same as the one considered in [5]. The relay-assisted transmission is duplexed in time (TDD – Time Division Duplexing). It is extended to the multi-antenna scenario and an arbitrary code at the relay instead of the repetition code is used. Such a communication system can be interpreted as a compound channel [31],[32], which allows a simple analysis based on the many existing results on compound channels. We will give expressions for the mutual information[5] of protocol I when the channel state information at the transmitter (CSIT) is assumed at all terminals and for the no CSIT case. That mutual information is obtained by means of Gaussian codebooks. The channel state information at the receiver is always assumed. Those expressions consider the fixed channel case (instantaneous mutual information). However results presented in this section only tackle the no CSI case. Moreover, the *selective relaying* is also analyzed. The following work has been presented in [30]. Finally, the *additive capacity gain* obtained by this protocol is evaluated.

2.2.1.1 Signal model

In the three-terminal network depicted in Figure 2.3 consisting in a source, a TDD half-duplex relay and a single destination, the relay-assisted transmission under protocol I is done during N symbols in the time domain. It is assumed that *relay-receive* and *relay-transmit phase* present the same size, i.e. $N/2$ symbols. Moreover, the source, relay and destination are equipped with n_s, n_r and n_d antennas, respectively.

During the *relay-receive phase*, the source transmits the signal $\mathbf{x}_s$. Afterwards during the *relay-transmit phase* the relay terminal transmits the signal $\mathbf{x}_r$. The signals received by the relay $\mathbf{y}_r$ and by the destination $\mathbf{y}_d$ during all the transmission are given by,

$$\mathbf{y}_r(t) = \mathbf{H}_1\mathbf{x}_s(t) + \mathbf{w}_r(t) \qquad 1 \le t \le N/2$$

$$\mathbf{y}_d(t) = \begin{cases} \mathbf{H}_0\mathbf{x}_s(t) + \mathbf{w}_d(t) & 1 \le t \le N/2 \\ \mathbf{H}_2\mathbf{x}_r(t) + \mathbf{w}_d(t) & N/2 \le t \le N \end{cases} \qquad (2.1)$$

where $\mathbf{H}_1$, $\mathbf{H}_2$ and $\mathbf{H}_0$ denotes the $n_r{\times}n_s$, $n_d{\times}n_r$ and $n_d{\times}n_s$ channel matrices between the source-relay, relay-destination and the source-destination, respectively. The terms $\mathbf{w}_r$ and $\mathbf{w}_d$

---

[5] In general the capacity of the relay channel is not known (only the degraded case with full-duplex relay [10]). Therefore the different protocols with different decoding strategies provide lower bounds of the capacity of that channel. The capacity of a channel is defined as the maximum mutual information between the transmitted and received signals. However, the maximum mutual information of each protocol with different decoding strategies will not be capacity of the relay channel because we are enforcing a predefined signaling which might not be optimal.

denote Gaussian noise with zero mean and covariance matrices $\mathbf{R}_{w_r}$ and $\mathbf{R}_{w_d}$ We will assume that $\mathbf{x}_s$ and $\mathbf{x}_r$ to be circularly symmetric complex Gaussian vectors with zero mean and transmit covariance matrix $\mathbf{Q}_s = E\{\mathbf{x}_s(t)\mathbf{x}_s^H(t)\}$ and $\mathbf{Q}_r = E\{\mathbf{x}_r(t)\mathbf{x}_r^H(t)\}$, respectively. The source and the relay are constrained in their average transmit power by P_s and P_r, respectively, which is conveniently expressed as a trace constraint on the transmit covariance matrices. These matrices are variables to be designed under the CSIT case. On the contrary, for no CSIT case we will assume $\mathbf{Q}_s = P_s/n_s \mathbf{I}_{n_s}$ and $\mathbf{Q}_r = P_r/n_r \mathbf{I}_{n_r}$. We know that equal average power transmission per antenna solution obtains the ergodic capacity in MIMO systems [1] with Rayleigh fading (source to destination) and it becomes a robust solution under channel uncertainty [33].

In the following the signal received by the destination will be rewritten in a more compact way for the direct transmission and for two implementations of the *decode-and-forward* (DF): *unconstrained coding* (UC) and *repetition coding* (RC). In the single-antenna case, the same signal model is still valid, but all the terms become scalars as in [5].

Direct Transmission

The source is transmitting to the destination using the *N* symbols,

$$\mathbf{y}_d(t) = \mathbf{H}_0 \mathbf{x}_s(t) + \mathbf{w}_d(t) \quad 1 \leq t \leq N \tag{2.2}$$

where the transmitted signal is constrained by $Tr(\mathbf{Q}_s) \leq P_{direct}$, $Tr(.)$ is the trace operator and $\mathbf{Q}_s$ the covariance matrix of the transmitted signal.

DF with unconstrained coding (UC)

The unconstrained coding (UC) has been defined for the case when the signal transmitted by the relay during the *relay-transmit phase* $\mathbf{x}_r$ is not correlated with the signal transmitted by the source $\mathbf{x}_s$. The signal model at the destination during the *relay-transmit phase* is given by,

$$\begin{bmatrix} \mathbf{y}_d(t) \\ \mathbf{y}_d(t+N/2) \end{bmatrix} = \begin{bmatrix} \mathbf{H}_0 & \mathbf{0} \\ \mathbf{0} & \mathbf{H}_2 \end{bmatrix} \begin{bmatrix} \mathbf{x}_s(t) \\ \mathbf{x}_r(t+N/2) \end{bmatrix} + \begin{bmatrix} \mathbf{w}_d(t) \\ \mathbf{w}_d(t+N/2) \end{bmatrix} \quad 1 \leq t \leq N/2 \tag{2.3}$$

where the transmitted signals are constrained by $Tr(\mathbf{Q}_s) \leq P_s$ and $Tr(\mathbf{Q}_r) \leq P_r$ subject to $P_s/2 + P_r/2 = P_{direct}$ to keep the total average transmitted power equal to the direct transmission scheme for a fair comparison.

DF with repetition coding

A particular case arises when the relay retransmits the same signal transmitted by the source during the *relay-receive phase*, in a nutshell when $\mathbf{x}_r(n+N/2) = \varphi \mathbf{x}_s(n)$ as in [5]. This technique can be used when the number of antennas at the source and the relay are equal ($n_r=n_s$). In such a case, the signal model at the destination during the *relay-receive phase* reduces to,

$$\begin{bmatrix} \mathbf{y}_d(t) \\ \mathbf{y}_d(t+N/2) \end{bmatrix} = \begin{bmatrix} \mathbf{H}_0 \\ \varphi \mathbf{H}_2 \end{bmatrix} \mathbf{x}_s(t) + \begin{bmatrix} \mathbf{w}_d(t) \\ \mathbf{w}_d(t+N/2) \end{bmatrix} \quad \varphi = \sqrt{\frac{P_r}{P_s}} \quad 1 \leq t \leq N/2 \tag{2.4}$$

where the transmitted signal is constrained by $Tr(\mathbf{Q}_s) \leq P_s$.

2.2.1.2   Maximum mutual information of protocol I

To analyze the performance of protocol I in *decode-and-forward* mode, we first obtain a general result related to *compound channels* and then show that the proposed transmission technique, for both unconstrained and repetition coding, can be seen a specific case of a *compound channel* [31]. Figure 2.6 presents a scheme for the *compound channel* where a source is transmitting a single message W in N symbols that must be successfully received by two destinations. However, the first destination only receives a part of the total transmitted signal, while the other destination receives the entire transmitted signal. The transmitted signal is given by,

$$x(t) = \begin{cases} x_a(t) & 1 \le t \le \varphi \\ x_b(t) & 1 \le t \le N \end{cases}$$

where φ defines the number of symbols where the first destination is listening. The received symbols at each destination $\mathbf{y}_1$ and $\mathbf{y}_2$ drawn according to the conditional probability distribution $p_1(\mathbf{y}_1 \mid \mathbf{x}_a)$ and $p_2(\mathbf{y}_2 \mid \mathbf{x})$, where the effect of the noise has been considered.
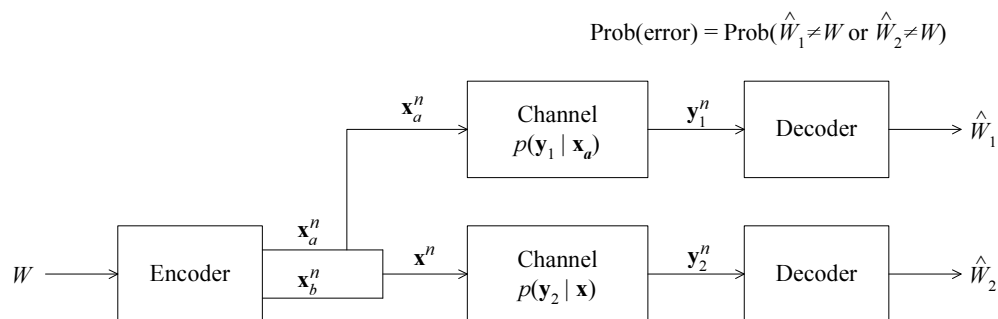
Figure 2.6.- Scheme of the compound channel with two receivers.

Proposition 1: Consider a channel where the transmitted signal $\mathbf{x}$, which can be structured as $x=(x_a, x_b)$, is received as $\mathbf{y}_1$ and $\mathbf{y}_2$ by two receivers with channel transition probabilities given by $p_1(\mathbf{y}_1 \mid \mathbf{x}_a)$ and $p_2(\mathbf{y}_2 \mid \mathbf{x})$, respectively (see Figure 2.6). Then the capacity[6] of the compound channel is given by

$$C = \sup_{p(x)} \min\left(I(\mathbf{x}_a, \mathbf{y}_1), I(\mathbf{x}, \mathbf{y}_2)\right) \tag{2.5}$$

where the supremum is over all $p(x)$ that satisfy the system specifications. It has been assumed that no error happens only when both receivers decode the transmitted message without error.
Proof. See Appendix A. Proof of proposition 1.

We now particularize the previous general result to the Gaussian case in the following corollary.

Corollary 1: Consider a vector Gaussian channel where the transmitted signal vector $\mathbf{x}$, which can be structured as $\mathbf{x}^T = \left[\mathbf{x}_a^T, \mathbf{x}_b^T\right]$ is received as

---

[6] It should be pointed out that protocol I under DF describes a compound channel, where the capacity for that channel is known. However, that value is not the capacity of the relay channel and for that reason it will be referenced as maximum mutual information of protocol I in the following.

$$\mathbf{y}_a = \mathbf{H}_a \mathbf{x}_a + \mathbf{w}_a$$
$$\mathbf{y} = \mathbf{H}\mathbf{x} + \mathbf{w}$$

by two receivers where $\mathbf{H}_a$ and $\mathbf{H}$ represent a linear transformation on the transmitted signal and both $\mathbf{w}_a$ and $\mathbf{w}$ are Gaussian distributed with zero mean and covariance matrices $\mathbf{R}_{w_a}$ and $\mathbf{R}_w$. Then the capacity of the compound channel under CSI is given by[7],

$$C = \sup_{\mathbf{Q}, \mathbf{Q}_a} \min\left(I_a, I_{ab}\right)$$
$$I_a = \log\det\left(\mathbf{I} + \mathbf{R}_{w_a}^{-1}\mathbf{H}_a\mathbf{Q}_a\mathbf{H}_a^H\right) \quad I_{ab} = \log\det\left(\mathbf{I} + \mathbf{R}_w^{-1}\mathbf{H}\mathbf{Q}\mathbf{H}^H\right)$$

(2.6)

with $\mathbf{Q} = E\left\{\mathbf{x}\mathbf{x}^H\right\}$ and $\mathbf{Q}_a = E\left\{\mathbf{x}_a\mathbf{x}_a^H\right\}$ being the transmit covariance matrix of $\mathbf{x}$ and $\mathbf{x}_a$. The supremum is over all $\mathbf{Q}$ and $\mathbf{Q}_a$ that satisfy the system specifications. The capacity is achieved when $\mathbf{x}$ is Gaussian distributed with zero mean and covariance matrix $\mathbf{Q}$.

Proof.- The proof is straightforward from *Proposition 1* and taking into account that $\mathbf{w}_a$ and $\mathbf{w}$ are Gaussian distributed, [11]. □

We now analyze the performance of the *decode-and-forward* transmission scheme along with the direct transmission in terms of the capacity and achievable rate.

Direct transmission

The capacity of the direct transmission with CSIT (fixed channel case with system model in (2.2)) is well known [1],[11] and given by

$$C_{DT}^{CSIT} = \sup_{\mathbf{Q}_s} \log\det\left(\mathbf{I}_{n_d} + \mathbf{R}_{w_d}^{-1}\mathbf{H}_0\mathbf{Q}_s\mathbf{H}_0^H\right)$$

(2.7)

In the single-antenna case, the capacity expression simplifies to,

$$C_{DT}^{CSIT} = \log\left(1 + \frac{P_{direct}}{\sigma_{w_d}^2}\left|h_0\right|^2\right)$$

(2.8)

Under no CSIT and equal average power transmission the capacity of the fixed channel is given by,

$$C_{DT} = \log\det\left(\mathbf{I}_{n_d} + \frac{P_{direct}}{n_s}\mathbf{R}_{w_d}^{-1}\mathbf{H}_0\mathbf{H}_0^H\right)$$

(2.9)

Notice that for the single-antenna case the capacity with and without CSIT coincides.

DF with unconstrained coding

In this case we have to particularize the result of *Corollary 1* with the signal model defined in (2.1). In this regard $\mathbf{H}_1$ (source-relay link) and the equivalent $\mathbf{H}$ of (2.3) stands for the matrices

---

[7] All the *log* functions considered in this work without specify the base are in base 2.

$\mathbf{H}_a$ and $\mathbf{H}$ defined in *Corollary 1*. The maximum mutual information of protocol I with DF and UC is given by,

$$I_{DF-UC}^{CSIT} = \frac{1}{2}\sup_{\mathbf{Q},\mathbf{Q}_s}\min\left(I_a, I_{ab}\right)$$

$$I_a = \log\det\left(\mathbf{I}_{n_r} + \mathbf{R}_{w_r}^{-1}\mathbf{H}_1\mathbf{Q}_s\mathbf{H}_1^H\right) \quad I_{ab} = \log\det\left(\mathbf{I}_{2n_d} + \mathbf{R}_w^{-1}\mathbf{H}\mathbf{Q}\mathbf{H}^H\right) \tag{2.10}$$

$$\mathbf{H} = \begin{bmatrix} \mathbf{H}_0 & \mathbf{0} \\ \mathbf{0} & \mathbf{H}_2 \end{bmatrix}, \quad \mathbf{R}_w = \begin{bmatrix} \mathbf{R}_{w_d} & \mathbf{0} \\ \mathbf{0} & \mathbf{R}_{w_d} \end{bmatrix} \quad \mathbf{Q} = E\left\{\begin{bmatrix} \mathbf{x}_s\mathbf{x}_s^T & \mathbf{x}_s\mathbf{x}_r^T \\ \mathbf{x}_r\mathbf{x}_s^T & \mathbf{x}_r\mathbf{x}_r^T \end{bmatrix}\right\} \quad \mathbf{Q}_s = E\left\{\mathbf{x}_s\mathbf{x}_s^T\right\}$$

where the 1/2 factor comes from the fact that the vector signal is actually transmitted in two time instances so the efficiency drops by a half. Moreover, using the Hadamard's inequality it follows that the optimal $\mathbf{Q}$ is block diagonal. In the single-antenna case, the capacity expression simplifies to

$$I_{DF-UC} = \frac{1}{2}\min\left\{\log\left(1 + \frac{P_s}{\sigma_{w_r}^2}|h_1|^2\right), \log\left(1 + \frac{P_s}{\sigma_{w_d}^2}|h_0|^2\right) + \log\left(1 + \frac{P_r}{\sigma_{w_d}^2}|h_2|^2\right)\right\} \tag{2.11}$$

For the case with no CSIT and equal average power transmission per antenna at the source and relay the maximum mutual information is given by,

$$I_{DF-UC} = \frac{1}{2}\min\left(C_a, C_{ab}\right)$$

$$C_a = \log\det\left(\mathbf{I}_{n_r} + \frac{P_s}{n_s}\mathbf{R}_{w_r}^{-1}\mathbf{H}_1\mathbf{H}_1^H\right) \tag{2.12}$$

$$C_{ab} = \log\det\left(\mathbf{I}_{n_d} + \frac{P_s}{n_s}\mathbf{R}_{w_d}^{-1}\mathbf{H}_0\mathbf{H}_0^H\right) + \log\det\left(\mathbf{I}_{n_d} + \frac{P_r}{n_r}\mathbf{R}_{w_d}^{-1}\mathbf{H}_2\mathbf{H}_2^H\right)$$

Notice that the maximum mutual information of the DF-UC under no CSIT can be written as a function of the capacity of the different links (under no CSIT).

DF with repetition coding

Applying *Corollary 1* for the repetition coding is done by considering the signal model of (2.1) and identifying $\mathbf{H}_1$ (source-relay link) and the equivalent $\mathbf{H}$ of (2.4) stands for matrices $\mathbf{H}_a$ and $\mathbf{H}$ of *Corollary 1*. Therefore, the maximum mutual information for DF with RC is defined by,

$$I_{DF-RC}^{CSIT} = \frac{1}{2}\sup_{\mathbf{Q}_s}\min\left(I_a, I_{ab}\right)$$

$$I_a = \log\det\left(\mathbf{I}_{n_r} + \mathbf{R}_{w_r}^{-1}\mathbf{H}_1\mathbf{Q}_s\mathbf{H}_1^H\right) \quad I_{ab} = \log\det\left(\mathbf{I}_{2n_d} + \mathbf{R}_w^{-1}\mathbf{H}\mathbf{Q}_s\mathbf{H}^H\right) \tag{2.13}$$

$$\mathbf{H} = \begin{bmatrix} \mathbf{H}_0 \\ \varphi\mathbf{H}_2 \end{bmatrix} \quad \mathbf{R}_w = \begin{bmatrix} \mathbf{R}_{w_d} & \mathbf{0} \\ \mathbf{0} & \mathbf{R}_{w_d} \end{bmatrix} \quad \varphi = \sqrt{\frac{P_r}{P_s}\frac{n_s}{n_r}}$$

Notice that the principal difference between RC and UC lies in the definition of matrix $\mathbf{H}$ at (2.10) and (2.13), with dimensions $2n_d\times(n_s+n_r)$ and $2n_d\times n_s$, respectively, leading to different results. In the single-antenna case the capacity expression simplifies to,

$$I_{DF-RC} = \frac{1}{2}\min\left\{\log\left(1+\frac{P_s}{\sigma_{n_r}^2}|h_1|^2\right),\log\left(1+\frac{P_s}{\sigma_{n_d}^2}|h_0|^2+\frac{P_r}{\sigma_{n_d}^2}|h_2|^2\right)\right\} \qquad (2.14)$$

For the case with no CSIT and considering equal average power transmission per antenna the maximum mutual information is given by[8],

$$I_{DF-RC} = \frac{1}{2}\min\left(C_a, C_{ab}\right)$$

$$C_a = \log\det\left(\mathbf{I}_{n_r} + \frac{P_s}{n_s}\mathbf{H}_1\mathbf{R}_{w_r}^{-1}\mathbf{H}_1^H\right) \quad C_{ab} = \log\det\left(\mathbf{I}_{n_s} + \frac{P_s}{n_s}\mathbf{H}_0^H\mathbf{R}_{w_d}^{-1}\mathbf{H}_0 + \frac{P_r}{n_r}\mathbf{H}_2^H\mathbf{R}_{w_d}^{-1}\mathbf{H}_2\right) \qquad (2.15)$$

Note that unconstrained coding always outperforms the repetition coding.

2.2.1.3 Retransmission strategies

A relay participating in the relay-assisted transmission under decode-and-forward (*unconstrained* or *repetition coding*) may always transmit to the destination (*persistent transmission*) or just when it is able to decode the message from the source (*selective transmission*), as it was described in section 2.1.4, see Figure 2.5. Hence, following the guidelines of [5], we will describe a protocol that avoids bottlenecks in the source-relay link by switching to a direct transmission during the *relay-transmit phase*. In this case, the source is transmitting in both phases and it plays the same role as the relay (*repetition* or *unconstrained coding*). In a nutshell, in the RC the source transmits the same signal in both phases, while in UC, they are uncorrelated. Additionally, it will be assumed equal average power transmission by the source and relay because there is no CSIT. Notice that under no CSIT, the maximum mutual information of protocol I can be written as a function of the capacity of the individual links, also defined under no CSIT.

The capacity of source-relay link under no CSIT with a fixed channel is given by

$$C_1 = \frac{1}{2}\log\det\left(\mathbf{I}_{n_r} + \frac{P_s}{n_s}\mathbf{R}_{w_r}^{-1}\mathbf{H}_1\mathbf{H}_1^H\right) \qquad (2.16)$$

The main objective is that the relay-assisted transmission will not become limited by the source-relay link, (2.16). Therefore, the source transmits in the *relay-transmit phase* (remaining the assisting relay terminal silent) wherever,

$$C_1 \in S = \left\{x \in \Re \quad | \quad x \le I_0 \le I_{ab}\right\} \qquad (2.17)$$

where I_{ab} and I_0 are defined by,

---

[8] Using $\det\left(\mathbf{I}_k + \mathbf{AB}\right) = \det\left(\mathbf{I}_m + \mathbf{BA}\right)$ where $\mathbf{A}$ and $\mathbf{B}$ are matrices with dimensions ($k \times m$) and ($m \times k$) respectively.

$$
I_{ab} = \begin{cases} \dfrac{1}{2}\log\det\left(\mathbf{I}_{n_d} + \dfrac{P_s}{n_s}\mathbf{R}_{w_d}^{-1}\mathbf{H}_0\mathbf{H}_0^H\right) + \log\det\left(\mathbf{I}_{n_d} + \dfrac{P_r}{n_r}\mathbf{R}_{w_d}^{-1}\mathbf{H}_2\mathbf{H}_2^H\right) & if \quad UC \\[4mm] \dfrac{1}{2}\log\det\left(\mathbf{I}_{n_s} + \dfrac{P_s}{n_s}\mathbf{H}_0^H\mathbf{R}_{w_d}^{-1}\mathbf{H}_0 + \dfrac{P_r}{n_r}\mathbf{H}_2^H\mathbf{R}_{w_d}^{-1}\mathbf{H}_2\right) & if \quad RC \end{cases}
$$

$$
I_0 = \begin{cases} C_{DT} & if \quad UC \\[2mm] \dfrac{1}{2}\log\det\left(\mathbf{I}_{n_s} + \dfrac{2P_s}{n_s}\mathbf{H}_0^H\mathbf{R}_{w_d}^{-1}\mathbf{H}_0\right) & if \quad RC \end{cases} \tag{2.18}
$$

where I_{ab} stands for the mutual information due to the transmissions from the source and relay to destination for the UC (2.12) and RC (2.15) and I_0 represents the mutual information obtained through the source-destination link when the source is transmitting in both phases and it is using the UC (in such a case it is the capacity of the source-destination link under no CSIT) or RC mode during the *relay-transmit phase*.

The final expressions for the mutual information of the UC and RC will be modified because of the additional transmission from the source. The adaptive unconstrained coding (UC-A) will be given by,

$$
I_{UC-A} = \begin{cases} I_{DF-UC} & if \quad C_1 \in S \\[2mm] C_{DT} & otherwise \end{cases} \tag{2.19}
$$

with C_1 defined in (2.16), C_{DT} defined in (2.9) and S given in (2.17). When the source transmits during the *relay-receive* and *relay-transmit phase* using unconstrained coding, the capacity of the source-destination link under no CSIT is obtained.

For the repetition coding the adaptive protocol (RC-A) is defined by

$$
I_{RC-A} = \begin{cases} I_{DF-RC} & if \quad C_1 \in S \\[3mm] \dfrac{1}{2}\log\det\left(\mathbf{I}_{n_d} + \dfrac{2P_s}{n_s}\mathbf{R}_{w_d}^{-1}\mathbf{H}_0\mathbf{H}_0^H\right) & otherwise \end{cases} \tag{2.20}
$$

where C_1 and S are defined in (2.16) and (2.17) respectively. In this regard, when the source transmits during both phases because the relay is not able to decode the message, the mutual information obtained is lower than the direct transmission in contrast to the UC-A, (2.19). The reason is due to the repeated message in both phases using the same symbols, the received signal power increases twice (2.20), at the expenses of using more resources, motivating the 1/2 factor in (2.20). Hence, the performance in such a case is worse than direct transmission (2.9).

2.2.1.4 Results

The different protocols presented at (2.12) (DF-UC), (2.15) (DF-RC), (2.19) (UC-A) and (2.20) (UC-R) will be evaluated under a scenario with multiple-antennas at the terminals and non-frequency selective Rayleigh channels on each link. Those protocols will be compared with the direct transmission (2.9) (DT). The relay-assisted transmission is performed in intervals of time

named frames (with *relay-receive* and *relay-transmit phase*) where it is assumed that the channel coefficients remain constant, changing from frame to frame. Different average SNR values are considered to account for the quality of the links including pathloss and slow fading. The scenario considered assumes that $P_s=P_r=P_{direct}$ and results are presented in terms of:

- *Average achievable rate*

- *Outage mutual information*

Definition 2.1.- The *average achievable rate* is measured by averaging all the code rates selected in different frames. It is assumed that the source is able to select a code rate for the transmission in each frame depending on the quality of the different links (i.e. the capacity of each link). Hence, after *k* frames *k* different code rates are selected.

Definition 2.2.- In this scenario the source is not able to adapt its code rate in each frame. We define the *outage mutual information* at p_{out} [1] as the code rate that is below the mutual information with a probability (1-p_{out}),

$$I^{out} = \arg\max_{R} \Pr\left(I \geq R\right)$$
$$\text{subject to } \Pr\left(I \geq R\right) \geq \left(1 - p_{out}\right)$$

(2.21)

where I^{out} is the outage mutual information, I denotes the mutual information and p_{out} is the outage probability. In contrast to the scenario given by *definition 2*.1, now, a single code rate is maintained over the *k* frames.

Figure 2.7[9] shows the outage mutual information (at an outage probability of p_{out}=5%) for different values on the quality of the source-relay link, given SNR$_0$=SNR$_2$=15 dB and $n_s=n_r=n_d$=1 antenna where SNR$_0$ and SNR$_2$ stand for the mean signal to noise ratio (SNR) in the source-destination and relay-destination link respectively. For low values of SNR$_1$ (source-relay link) the UC and RC schemes have an unacceptable performance because the mutual information is limited by the source-relay link. On the other hand, the adaptive methods achieve better results because they switch to a direct transmission when source-relay presents bad quality. At SNR$_1$= 5 dB, see Table 2.2, the UC-A and RC-A use the direct transmission 97% and 95% of the time, whereas at SNR$_1$= 25 dB, it is used 60% and 15% of the time, respectively. The differences of the percentage of time with direct transmission between both adaptive protocols are due to the mutual information obtained by each protocol, (2.18). For the RC-A the mutual information conditions defined for a transmission of the source in the *relay-transmit phase* are smaller than for the UC-A. Hence, in the RC-A the source will transmit in both phases in a smaller percentage of the time than UC-A. Although, when the source-relay link presents a bad link quality compared with other links (low SNR$_1$ in Table 2.2), both adaptive protocols tend to use the direct transmission in both phases. When the source-relay link quality is good, adaptive and fixed schemes achieve the same performance because the adaptive schemes do not switch to direct transmission, see Table 2.2 at SNR$_1$=50 dB. Note that relay-assisted transmission can improve the direct transmission with RC and UC, where UC-A gets the best performance, achieving at SNR$_1$=30 dB the maximum value, 2.22 bits/s/Hz and getting a steady value of 2.20 bits/s/Hz for SNR$_1 \geq$40 dB. The reason of this maximum value is discussed in the context of Figure 2.8.

---

[9] We will henceforth assume ideal sampling and filtering. Therefore, the mutual information will be the same measured in *bits/channel* use as in *bits/s/Hz.*
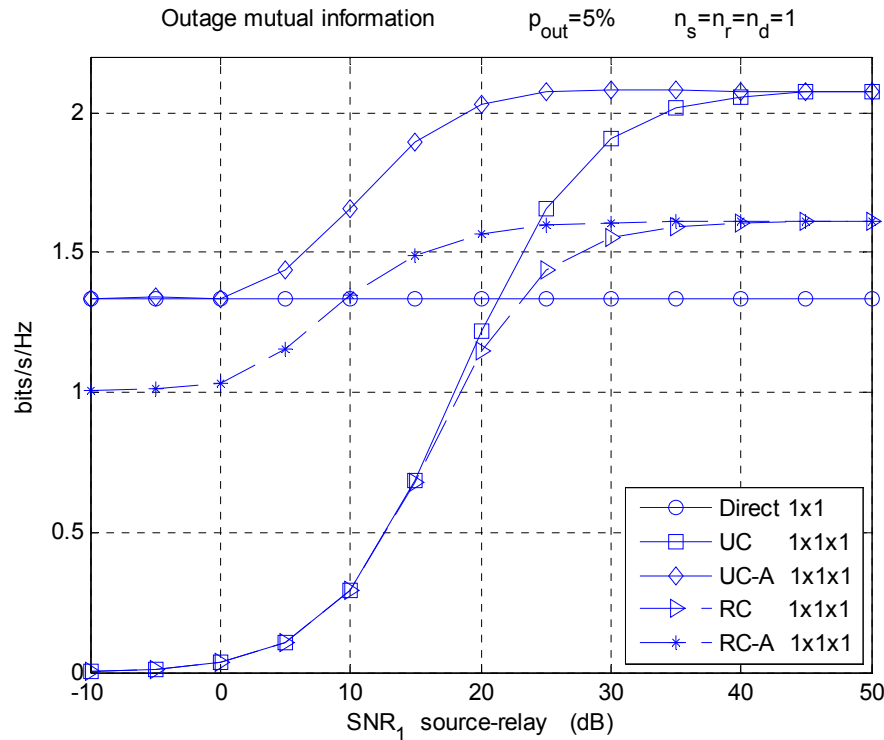
Figure 2.7.- Outage mutual information (p_{out}=5%) for the different relay schemes with SNR$_0$ (source-destination) =SNR$_2$ (relay-destination) = 15 dB and different SNR$_1$ (source-relay) values (single antenna).

Percentage of time that the source transmits in both phases										
SNR$_1$ (dB)	*5*	*10*	*15*	*20*	*25*	*30*	*35*	*40*	*45*	*50*
RC-A	95%	86%	65%	37%	16%	6%	2%	1%	0.2%	0.1%
UC-A	97%	94%	87%	77%	62%	44%	26%	13%	5%	2%

Table 2.2.- Percentage of time that the source is transmitting in both phases for UC and RC adaptive protocols at different values of SNR$_1$. SNR$_0$=SNR$_2$=15 dB. n_s=n_r=n_d=1.

The average achievable rate for n_s=n_r=n_d=1 for SNR$_0$=SNR$_2$=15 dB is presented in Figure 2.8 as a function of the SNR$_1$. In this case the RC is always worse than the direct transmission (also the adaptive protocol RC-A). The gains of the UC and UC-A over the direct transmission are 0.2 bits/s/Hz at SNR$_1$=50 dB. Moreover, it is worth noticing that UC-A gets the maximum gain over the direct transmission at SNR$_1$=30 dB (around 0.3 bits/s/Hz). This performance is due to the possibility to change to direct transmission when the source-relay link satisfies equation (2.19). However, for SNR$_1$>30 dB the percentage of the time that the source is transmitting in both phases decreases (source-relay link becomes good) and the mutual information (2.18) depends only on the source-destination and relay-destination link, both with the same average SNR in our scenario. Then, in some frames, the cooperative transmission may force a code rate smaller than the direct transmission, but UC-A cannot change to direct transmission because source-relay link satisfies equation (2.19). This motivates the decrease of the gain, reaching the steady average achievable rate gain of 0.2 bits/s/Hz. For SNR$_1$<30 dB those events are alleviated by the bad source-relay link, switching to direct transmission.
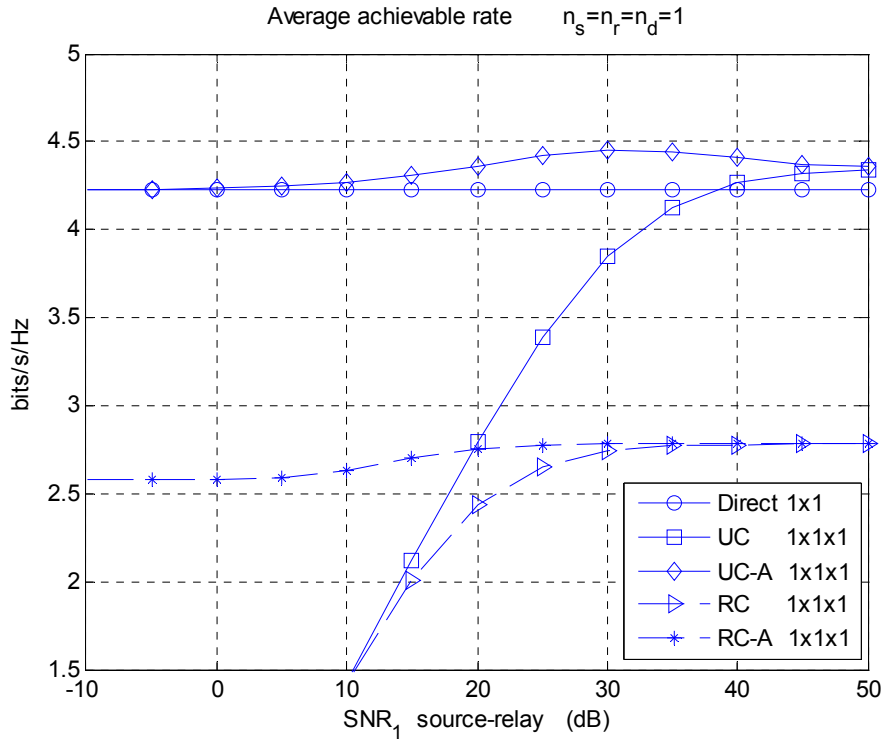
Figure 2.8.- Average achievable rate for the different relay schemes with SNR$_0$ (source-destination)=SNR$_2$ (relay-destination)= 15 dB and different SNR$_1$ (source-relay) values (single antenna).

In the following the *additive capacity gain* [12] of the outage mutual information over the direct transmission will be investigated. It will be defined as,

$$a = I^{out} - I_{DT}^{out} \qquad bits/s/Hz \qquad (2.22)$$

where I_{DT}^{out} is the outage mutual information of the direct transmission and I^{out} denotes the outage mutual information of the {UC, UC-A, RC, RC-A}, using the definition of (2.21). It will be considered a scenario where the SNR$_0$=SNR$_2$=SNR and SNR$_1$=2×SNR (dB). This configuration particularized at SNR=15 dB has shown the best results for the UC-A in terms of outage mutual information in Figure 2.7 and average achievable rate at Figure 2.8. Figure 2.9 shows the *additive capacity gain* of the outage mutual information at p_{out}=5% for n_s=n_r=n_d=1 and -5≤SNR≤40 dB. It can be seen that RC and RC-A only can get a positive *additive capacity gain* for SNR≤20 dB. However, for the UC and UC-A, there is always a positive *additive capacity gain* and for SNR≥20 the *additive capacity gain* is steady respect the SNR. This result confirms that under our scenario there is not multiplexing gain for the relay-assisted transmission because this gain does not increases logarithmically with SNR. Finally, in Figure 2.10 it is depicted the *additive gain* of the outage mutual information at p_{out}=5% over the direct transmission, (2.22) for the UC-A when the terminals are equipped with multiple antennas. It can be seen that the additive gain is always positive and get similar values for the different antenna configuration, around 1.3 bits/s/Hz. The difference is based at which SNR the performance becomes steady, for example for n_s=n_r=n_d=1 it is at SNR≥20, n_s=n_r=n_d=2 it is at SNR≥30, n_s=n_r=n_d=3 it is at SNR≥35 and n_s=n_r=n_d=4 it is at SNR≥40. It is important to remark that although there is an *additive capacity gain* by the relay-assisted transmission, depending on the antenna configuration and the SNR, this gain can be neglected when is compared with the outage

mutual information of the direct transmission, for example at high SNR the increase of 1 bits/s/Hz will not have a great impact on the total performance.

Figure 2.9.- Additive gain of the outage mutual information (p_{out}=5%) over the direct transmission for the different relay schemes with SNR_0=SNR_2=SNR and SNR_1=2×SNR (dB). n_s=n_r=n_d=1.

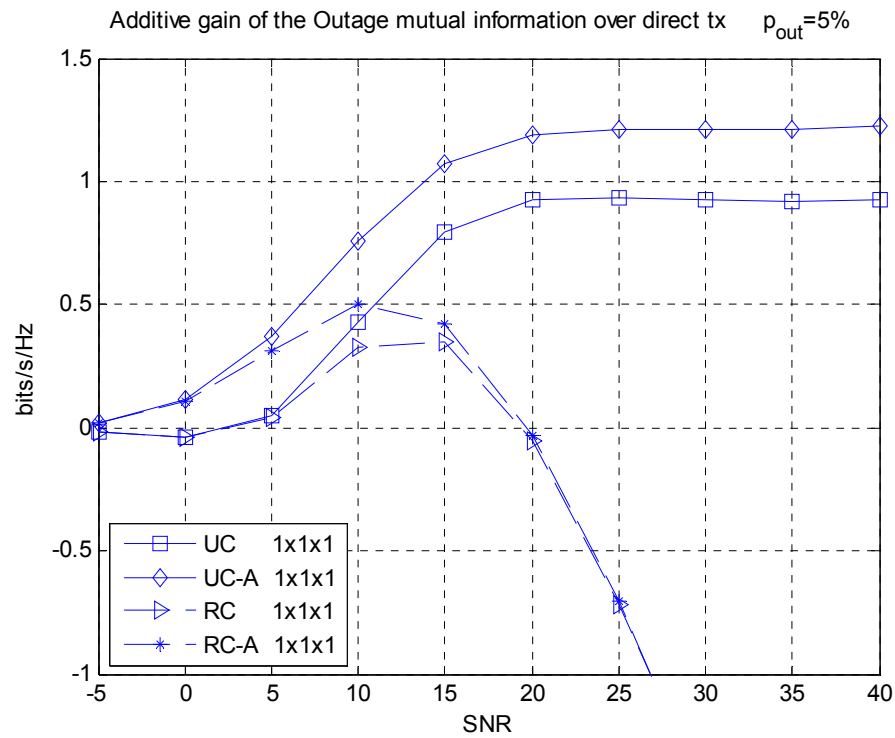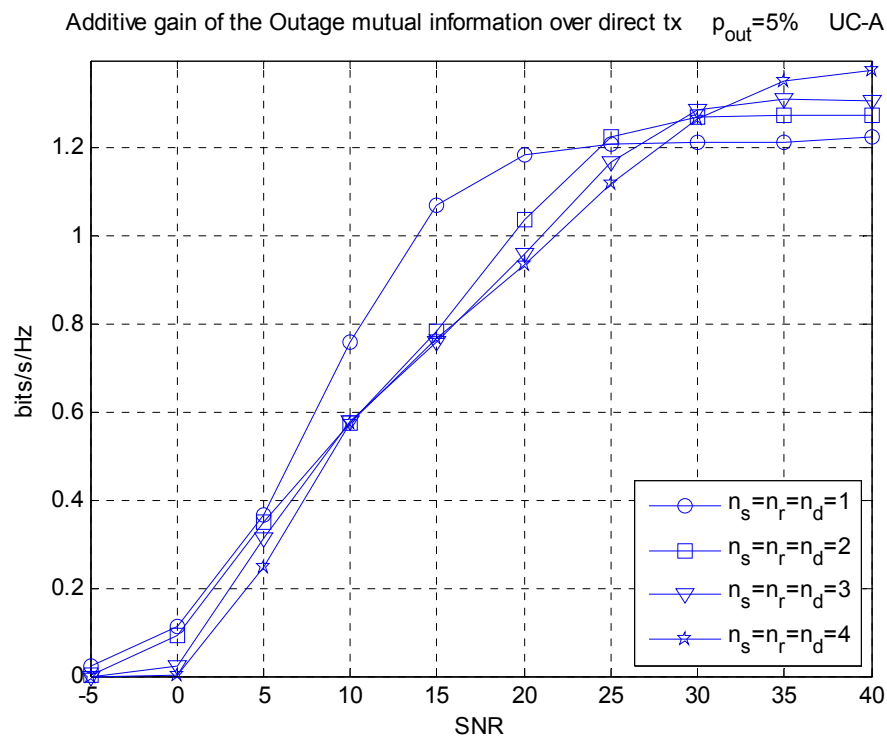**Figure 2.10.- Additive gain of the outage mutual information (p_{out}=5%) over the direct transmission for the different relay schemes with SNR_0=SNR_2=SNR and SNR_1=2×SNR (dB). n_s=n_r=n_d={1,2,3}.**

2.2.2 DF-Protocols with Repetition Coding

Hereinafter, the forwarding, protocol II and protocol III will be analyzed when half-duplex relays are operating in repetition coding mode. Hence, it is assumed that the relay and/or the source use the same codewords and both are equipped with the same number of antennas, $n_s = n_r$. The transmissions are done during N symbols in the time domain. The variables[10] $\mathbf{x}_s^1$ and $\mathbf{x}_s^2$ will denote the signals transmitted by the source during the *relay-receive* and *relay-transmit phase* respectively, depending on the selected protocol, $\mathbf{x}_r$ the signal transmitted by the relay terminal in the *relay-transmit phase.* All these signals are Gaussians with zero mean and covariance given by,

$$\mathbf{Q}_s^1 = E\left\{\mathbf{x}_s^1 \mathbf{x}_s^{1H}\right\} = \frac{P_s}{n_s}\mathbf{I}_{n_s} \quad \mathbf{Q}_s^2 = E\left\{\mathbf{x}_s^2 \mathbf{x}_s^{2H}\right\} = \frac{P_s}{n_s}\mathbf{I}_{n_s} \quad \mathbf{Q}_r = E\left\{\mathbf{x}_r \mathbf{x}_r^H\right\} = \frac{P_r}{n_r}\mathbf{I}_{n_r}$$

$$Tr\left(\mathbf{Q}_s^1\right) = P_s \qquad\qquad Tr\left(\mathbf{Q}_s^2\right) = P_s \qquad\qquad Tr\left(\mathbf{Q}_r\right) = P_r \tag{2.23}$$

The capacity of the source-relay link (fixed channel case) under no CSIT and equal average power transmission per antenna will be common for all the protocols and will be defined by,

$$C_a = \log\det\left(\mathbf{I}_{n_r} + \frac{P_s}{n_s \sigma_{w_s}^2}\mathbf{H}_1\mathbf{H}_1^H\right) \tag{2.24}$$

with n_r and n_s the number of antennas at the relay and source, respectively.

RC Forwarding

The signal model can be written as,

$$\mathbf{y}_r(t) = \mathbf{H}_1\mathbf{x}_s^1(t) + \mathbf{w}_r(t) \qquad\qquad 1 \le t \le N/2$$

$$\mathbf{y}_d(t) = \begin{cases} 0 & 1 \le t \le N/2 \\ \mathbf{H}_2\mathbf{x}_r(t - N/2) + \mathbf{w}_d(t) & N/2 + 1 \le t \le N \end{cases} \tag{2.25}$$

The destination only takes into account the signal received during the *relay-transmit phase*. Hence the obtained mutual information is,

$$I_{FW}^{RC} = \frac{1}{2}\min\left(C_a, C_b\right)$$

$$C_b = \log\det\left(\mathbf{I}_{n_d} + \frac{P_r}{n_r \sigma_{w_r}^2}\mathbf{H}_2\mathbf{H}_2^H\right) \tag{2.26}$$

with C_a defined in (2.24).

RC Protocol II

In this case the source is transmitting during the *relay-receive phase*, while in the *relay-transmit phase*, source and relay are transmitting to the destination. The destination only is aware about the signal received in the second phase. The signal model is,

---

[10] A variable that is used in both phases of the relay-assisted transmission will use the super-index 1 for denoting the *relay-receive phase* and super-index 2 for the *relay-transmit phase*.

$$\mathbf{y}_r(t) = \mathbf{H}_1 \mathbf{x}_s^1(t) + \mathbf{w}_r(t) \qquad\qquad 1 \le t \le N/2$$

$$\mathbf{y}_d(t) = \begin{cases} 0 & 1 \le t \le N/2 \\ \begin{bmatrix} \mathbf{H}_2 & \mathbf{H}_0 \end{bmatrix} \begin{bmatrix} \mathbf{x}_r(t-N/2) \\ \mathbf{x}_s^2(t-N/2) \end{bmatrix} + \mathbf{w}_d(t) & N/2+1 \le t \le N \end{cases} \qquad (2.27)$$

When we assume that source and relay are transmitting the same codeword in the *relay-transmit phase*, it is implicit that both know the same message. Hence, total mutual information of the protocol is constrained by the mutual information of the source-relay link (*relay-receive phase*) which is the capacity under no CSIT and equal average power transmission per antenna. Protocol II with repetition coding is defined when $\mathbf{x}_r = \varphi \mathbf{x}_s^1$. The mutual information is,

$$I_{p-IIA}^{RC} = \frac{1}{2} \min \left(C_a, C_b \right)$$

$$C_b = \log \det \left(\mathbf{I}_{n_d} + \frac{P_s}{n_s} \mathbf{R}_w^{-1} \mathbf{H}_{eq} \mathbf{H}_{eq}^H \right) \quad \mathbf{H}_{eq} = \begin{bmatrix} \mathbf{H}_0 & \varphi \mathbf{H}_2 \end{bmatrix} \quad \varphi = \sqrt{\frac{P_r}{P_s} \frac{n_s}{n_r}} \quad \mathbf{R}_w = \sigma_{w_d}^2 \mathbf{I} \qquad (2.28)$$

Note that the difference between protocol I and protocol II is based on the definition of matrix $\mathbf{H}_{eq}$, see (2.13) and (2.28).

RC Protocol III

This protocol was originally defined in [27][11]. The main idea is to combine the signals at the physical layer thanks to both phases of the relay-assisted transmission being equal. The source transmits a Gaussian signal during the *relay-receive phase* $\mathbf{x}_s^1$ of rate R_r which is received at the relay and destination. The relay decodes the data received and transmits the signal $\mathbf{x}_r$ to the destination (*repetition coding*) while the source transmits a Gaussian signal related to another message, $\mathbf{x}_s^2$ of rate R_s. The signal model is given by,

$$\mathbf{y}_r(t) = \mathbf{H}_1 \mathbf{x}_s^1(t) + \mathbf{w}_r(t) \qquad\qquad 1 \le t \le N/2$$

$$\mathbf{y}_d(t) = \begin{cases} \mathbf{H}_0 \mathbf{x}_s^1(t) + \mathbf{w}_d(t) & 1 \le t \le N/2 \\ \begin{bmatrix} \mathbf{H}_2 & \mathbf{H}_0 \end{bmatrix} \begin{bmatrix} \mathbf{x}_r(t-N/2) \\ \mathbf{x}_s^2(t-N/2) \end{bmatrix} + \mathbf{w}_d(t) & N/2+1 \le t \le N \end{cases} \qquad (2.29)$$

The definition of repetition coding establishes that $\mathbf{x}_r = \varphi \mathbf{x}_s^1$. Therefore, the received signal at the destination during both phases can be rewritten in the following way,

$$\mathbf{y}_d = \mathbf{H}_{eq} \mathbf{x} + \mathbf{w}$$

$$\mathbf{H}_{eq} = \begin{bmatrix} \mathbf{H}_0 & \mathbf{0} \\ \varphi \mathbf{H}_2 & \mathbf{H}_0 \end{bmatrix} \quad \varphi = \sqrt{\frac{P_r}{P_s} \frac{n_s}{n_r}} \quad \mathbf{x} = \begin{bmatrix} \mathbf{x}_s^1 \\ \mathbf{x}_s^2 \end{bmatrix} \quad \mathbf{w} = \begin{bmatrix} \mathbf{w}_{d,1} \\ \mathbf{w}_{d,2} \end{bmatrix} \qquad (2.30)$$

where $\mathbf{w}$ defines the received noise vector at the destination during the *relay-receive* and *relay-transmit phase* ($\mathbf{w}_{d,1}$ and $\mathbf{w}_{d,2}$, respectively). This protocol obtains good performance results in terms of diversity and ergodic capacity gains [27]. The relay must be able to decode the first

---

[11] It was defined as protocol I.

message, $\mathbf{x}_s^1$, while the destination has to decode the messages $\mathbf{x}_r$ and $\mathbf{x}_s^2$ (*successive decoding*). During the *relay-transmit phase* the equivalent channel can be modeled as the conventional MAC channel, [11]. Therefore, the achievable rate region G for this protocol can be written as,

$$G = \begin{cases} R_r \leq \dfrac{1}{2}C_a \\[2mm] R_r \leq \dfrac{1}{2}C_s \\[2mm] R_s \leq \dfrac{1}{2}C_0 \\[2mm] R_r + R_s \leq \dfrac{1}{2}C_b \end{cases} \tag{2.31}$$

with C_a, C_s, C_0 and C_b being the capacity of the source-relay, joint (source,relay)-destination, source-destination and equivalent system with two simultaneous transmissions given by (2.30), all of them under no CSIT and equal average power transmission per antenna. They are defined as,

$$C_a = \log\det\left(\mathbf{I}_{n_r} + \frac{P_s}{n_s\,\sigma_{w_r}^2}\mathbf{H}_1\mathbf{H}_1^H \right) \quad C_s = \log\det\left(\mathbf{I}_{n_d} + \frac{P_r}{n_r\,\sigma_{w_d}^2}\mathbf{H}_2\mathbf{H}_2^H + \frac{P_s}{n_s\,\sigma_{w_d}^2}\mathbf{H}_0\mathbf{H}_0^H \right)$$

$$C_0 = \log\det\left(\mathbf{I}_{n_d} + \frac{P_s}{n_s\,\sigma_{w_s}^2}\mathbf{H}_0\mathbf{H}_0^H \right) \quad C_b = \log\det\left(\mathbf{I}_{2n_d} + \frac{P_s}{n_r\,\sigma_{w_d}^2}\mathbf{H}_{eq}\mathbf{H}_{eq}^H \right) \tag{2.32}$$

with $\mathbf{H}_{eq}$ defined in (2.30).

The achievable rate region G obtained by protocol III with repetition coding presents a pentagonal shape with the constraints of (2.31). Because we are interested in the sum-rate, the achievable rate can be defined as

$$I_{p-III}^{RC} = \begin{cases} \dfrac{1}{2}C_b & if \quad C_a \geq \left(C_b - C_0 \right) \\[3mm] \dfrac{1}{2}\left(C_a + C_0 \right) & otherwise \end{cases} \tag{2.33}$$

with C_a, C_0 and C_s defined in (2.32).

Comparison of static DF-RC protocols

In Table 2.3 it is provided a summary of the achievable rates obtained by the different repetition and coding protocols. These protocols are affected by the factor 1/2 due to work with an equally sized *relay-receive* and *relay-transmit phase*, the source-relay capacity and C_b, which definition depends on the matrix $\mathbf{H}_{eq}$ different for each protocol and describing an equivalent system. Those equivalent systems are $(n_d \times n_r)$, $(2n_d \times n_r)$, similar to $(n_d \times (n_s + n_r))$ and akin to $(2n_d \times (n_s + n_r))$ MIMO systems for the forwarding, protocol I, protocol II and protocol III, respectively. The differences between protocols II and III and MIMO schemes lies in the power used through the distributed antennas and the equivalent channel $\mathbf{H}_{eq}$ considered for protocol III. For example in

protocol II there are n_s+n_r antennas, but the antennas at the source and the relays transmits with an average power equal to P_s/n_s and P_r/n_r, while in a MIMO system all the antennas should use $P/(n_s+n_r)$.

When the relay-assisted transmission is not limited by the source-relay link, then the performance of DF-RC protocol I and II depends on the antenna configuration (see Appendix C in section 2.8),

$$
\begin{cases}
I_{p-II}^{RC} \leq I_{p-I}^{RC} & if \quad n_s = n_r > n_d \\
I_{p-II}^{RC} = I_{p-I}^{RC} & if \quad n_s = n_r = n_d \\
I_{p-II}^{RC} \geq I_{p-I}^{RC} & if \quad n_s = n_r < n_d
\end{cases}
\tag{2.34}
$$

Hence, the relation between the repetition coding protocols is given by,

$$
I_{FW}^{RC} \leq
\begin{cases}
I_{p-II}^{RC} \leq I_{p-I}^{RC} \\
or \\
I_{p-I}^{RC} \leq I_{p-II}^{RC}
\end{cases}
\leq I_{p-III}^{RC}
\tag{2.35}
$$

where the dependence protocol II and I is defined in (2.34).

DF-RC protocols	Achievable rate	$\mathbf{H}_{eq}$ (used in C_b)
forwarding	$\dfrac{1}{2}\min(C_a, C_b)$	$\mathbf{H}_2$
protocol I	$\dfrac{1}{2}\min(C_a, C_b)$	$\begin{bmatrix} \mathbf{H}_0 \\ \varphi\mathbf{H}_2 \end{bmatrix}$
protocol II	$\dfrac{1}{2}\min(C_a, C_b)$	$\begin{bmatrix} \mathbf{H}_0 & \varphi\mathbf{H}_2 \end{bmatrix}$
protocol III	$\begin{cases} \dfrac{1}{2}C_b & C_a \geq C_b - C_0 \\ \dfrac{1}{2}(C_a + C_0) & otherwise \end{cases}$	$\begin{bmatrix} \mathbf{H}_0 & \mathbf{0} \\ \varphi\mathbf{H}_2 & \mathbf{H}_0 \end{bmatrix}$

Table 2.3.- Achievable rates of the different static DF-RC protocols.

Figure 2.11 presents the scenario considered for evaluating the half-duplex protocols. The source and the destination are separated at normalized distance equal to 1 and the relay terminal is placed at normalized distance d from the source. The signal to noise ratio in the source-relay and relay-destination depends on the inverse of d^2 and $(1-d)^2$ respectively. The noise power σ^2 has been assumed equal at the relay and destination terminals. With this simple scenario it is possible to set up the SNR of the source-relay and relay-destination links by defining the SNR_0 (source-destination link). In the following the half-duplex protocols will be compared in an additive white Gaussian noise (AWGN) channel when all terminals are equipped with a single antenna ($n_s=n_r=n_d=1$) and in a multiple antenna with Rayleigh fading channel. Basically the performance of the different protocols will be investigated at $SNR_0=0$ (*low SNR*) and SNR=10 dB (*medium SNR*).

$$SNR_1 = \frac{P}{\sigma^2}\frac{1}{d^2} \quad SNR_2 = \frac{P}{\sigma^2}\frac{1}{(1-d)^2} \quad SNR_0 = \frac{P}{\sigma^2}$$
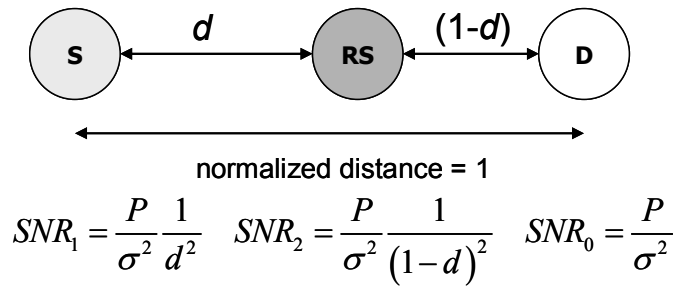
Figure 2.11.-Scenario for the evaluation of the half-duplex protocols. SNR_0, SNR_1 and SNR_2 stand for the SNR in the source-destination, source-relay and relay-destination link.

Additive white Gaussian noise (AWGN) channel

In the following the half-duplex protocols with RC will be compared in an AWGN channel with $n_s=n_r=n_d=1$ and the scenario presented in Figure 2.11 for *low SNR* (SNR_0=0 dB) and *medium SNR* (SNR_0=10 dB). Figure 2.12 shows the performance at low SNR. Forwarding and protocols I and II obtain the same result for $d{\geq}0.5$ because the achievable rate is limited by the source-relay link (C_a), Table 2.3. The relation between protocol I and II follows (2.35). Protocol III is the best protocol in terms of achievable rate. Additionally, Figure 2.13 depicts the results when the SNR_0=10 dB. In that case, only protocol III with RC is able to provide better performance than the direct transmission. It should be remarked that the source in protocol III is transmitting independent messages during the *relay-receive* and *relay-transmit phase*, while the relay *repeats* the received signal. When the relay-assisted transmission is limited by the source-relay link, the achievable rate of protocol III gets $I_{p-III}^{RC} = 0.5(C_a + C_0)$ while the other protocols only obtain $I^{RC} = 0.5 C_a$.
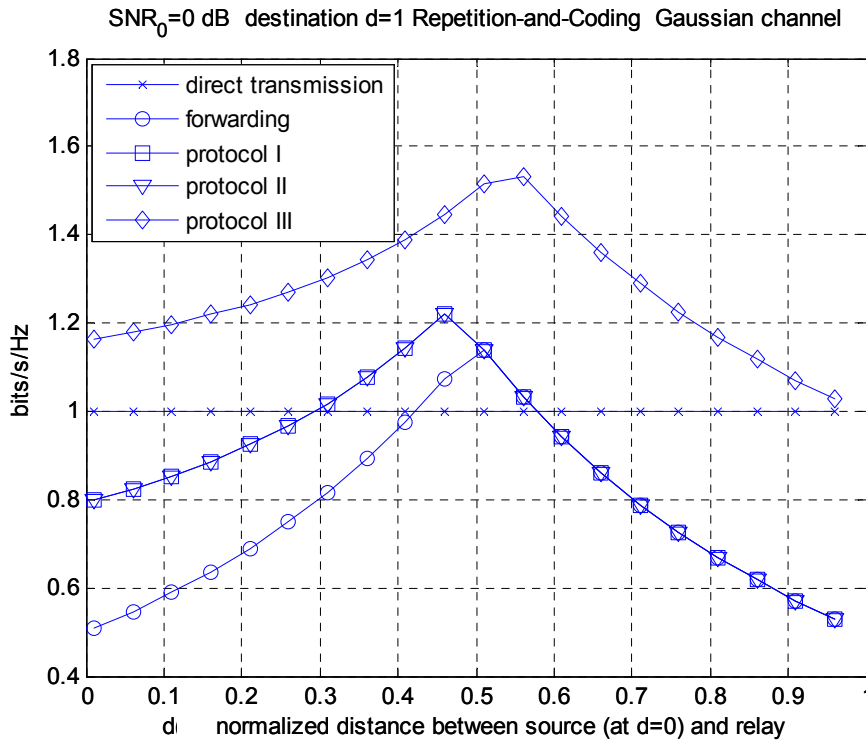
Figure 2.12.- Maximum achievable rate vs. distance between the source and relay. Gaussian channel. Destination with SNR_0= 0 dB. Repetition and Coding. Time domain.

Figure 2.13.- Maximum achievable rate vs. distance between the source and relay. Gaussian channel. Destination with SNR_0= 10 dB. Repetition and coding. Time domain.

Multiple antenna and Rayleigh fading

The multiple antenna case will be evaluated under Rayleigh fading channels whose channel coefficients are constant over a frame where the relay-assisted transmission is carried out. The scenario considered will be the same presented in Figure 2.11. Res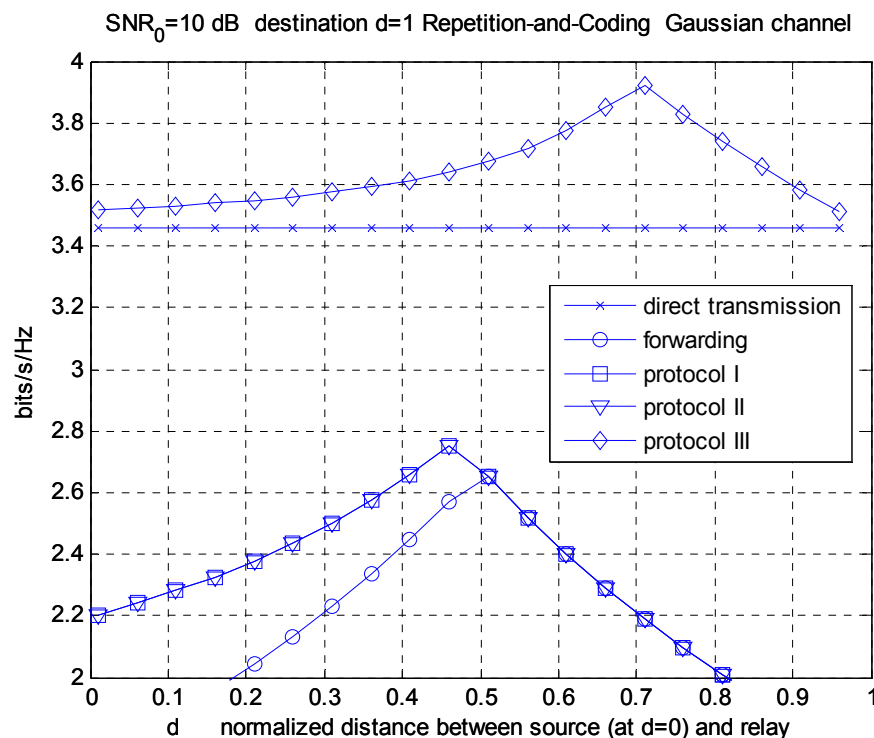ults will consider the following combination of antennas (n_s, n_r, n_d): (1,1,1),(1,1,2), (2,1,1) and (2,2,2) at *low SNR* (SNR_0=0 dB).

Figure 2.14-(top-left) depicts the performance of the RC protocols for n_s=n_r=n_d=1 in terms of average achievable rate (see definition 2.1 in section 2.2.1.4). It can be seen that protocol III is the only one which outperforms the direct transmission, obtaining a maximum gain of 29% over the direct transmission when the relay is at *d*=0.4, see Table 2.4. Additionally, the performance of protocol I and II is the same due to n_r=n_s, as was derived in Appendix C in section 2.8. When the antennas at the destination are increased, n_s=n_r=1, n_d=2 in Figure 2.14-(top-right), the maximums of the average achievable rate are attained in places where the relay is close to the source. On the other hand, when the number of antennas at the source and relay are larger than in the destination, n_s=n_r=2, n_d=1 in Figure 2.14-(bottom-left), the position of the relay where the average achievable rate is maximum is moved to the destination. In this case, all protocols can get better performance than the direct transmission. It is worth noticing that all protocols get the maximum gains over the direct transmission for this antenna configuration, Table 2.4, where protocol III gets a gain of 78% over the 2×1 MIMO system with a single antenna at the destination. Moreover, the relation between protocol I and II when (n_s=n_r=2,n_d=1) and (n_s=n_r=1,n_d=2) follows (2.35). Finally, for n_s=n_r=n_d=2 in Figure 2.14-(bottom-right) the maximum average achievable rates are obtained with the relay placed in similar positions as in the case n_s=n_r=n_d=1, although the maximum gains of the relay-assisted transmission are better, see Table 2.4.
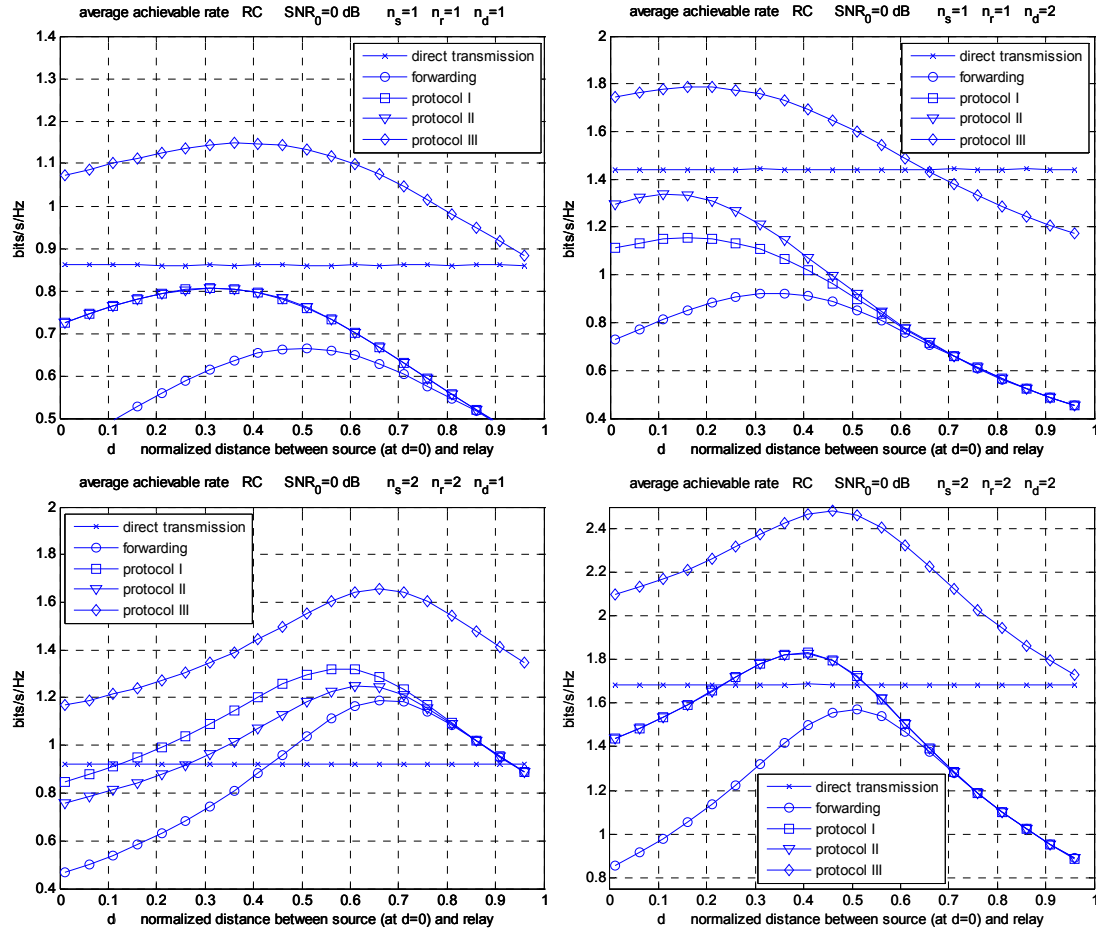
Figure 2.14.- Average achievable rate vs. distance between the source and relay. Rayleigh fading. Destination with SNR$_0$=0 dB. (top-left) n_s=1,n_r=1, n_d=1, (top-right) n_s=1, n_r=1, n_d=2, (bottom-left) n_s=2, n_r=2, n_d=1, (bottom-right) n_s=2, n_r=2,n_d=2. Repetition-and-Coding (RC).

SNR$_0$=0 dB	Maximum average achievable rate gain over direct transmission			
	n_s=1, n_r=1, n_d=1	n_s =1, n_r=1, n_d=2	n_s =2, n_r=2, n_d=1	n_s =2, n_r=2, n_d=2
forwarding	-25%	-35%	30%	-7%
protocol I	-10%	-17%	35%	6%
protocol II	-10%	-3%	43%	6%
protocol III	29%	25%	78%	47%

Table 2.4.- Maximum average achievable rate gain over the direct transmission under Rayleigh fading with multiple antenna: n_s (source), n_r (relay), n_d (destination). SNR$_0$=0 dB. RC.

2.2.3 AF-Protocols

Here, we will consider the case when the relay just *amplify and forward* the received signal. Hence, the resources allocated to both phases of the *relay-assisted transmission* must be the same. In general we will assume that the relay uses the following amplifying gain factor taking into account that the CSI is not known,

$$\mathbf{G} = \mathbf{I}_{n_r} g \qquad g = \sqrt{\frac{P_r}{Tr\left(\mathbf{H}_1 \mathbf{H}_1^H\right)\frac{P_s}{n_s} + n_r \sigma_{w_r}^2}} \qquad (2.36)$$

where P_r and P_s are the power at the relay and the source, respectively, n_r and n_s denote the number of antennas at the relay and the source, $\sigma_{w_r}^2$ is the noise power at the relay and $\mathbf{H}_1$ stands for the channel between the source and the relay, with dimensions $n_r \times n_s$.

The source transmits the zero-mean Gaussian signals $\mathbf{x}_s^1$ and $\mathbf{x}_s^2$ during the *relay-receive* and *relay-transmit phase*. The transmitters do not have CSIT (fixed channel realization), so then, the covariance signal matrices will be defined by,

$$\mathbf{Q}_s^1 = E\left\{\mathbf{x}_s^1 \mathbf{x}_s^{1H}\right\} = \frac{P_s}{n_s}\mathbf{I}_{n_s} \qquad \mathbf{Q}_s^2 = E\left\{\mathbf{x}_s^2 \mathbf{x}_s^{2H}\right\} = \frac{P_s}{n_s}\mathbf{I}_{n_s}$$

$$Tr\left(\mathbf{Q}_s^1\right) = P_s \qquad\qquad\qquad Tr\left(\mathbf{Q}_s^2\right) = P_s$$

(2.37)

AF Forwarding

The received signal at the relay and destination terminal are defined by,

$$\mathbf{y}_r(t) = \mathbf{H}_1 \mathbf{x}_s^1(t) + \mathbf{w}_r(t) \qquad\qquad 1 \le t \le N/2$$

$$\mathbf{y}_d(t) = \begin{cases} 0 & 1 \le t \le N/2 \\ \mathbf{H}_2 \mathbf{G} \mathbf{H}_1 \mathbf{x}_s^1(t - N/2) + \mathbf{w}_d(t) & N/2 + 1 \le t \le N \end{cases}$$

(2.38)

The mutual information of this protocol can be written as,

$$I_{FW}^{AF} = \frac{1}{2} I_b$$

$$I_b = \log\det\left(\mathbf{I}_{n_d} + \mathbf{R}_w^{-1} \mathbf{H}_{AF} \mathbf{Q} \mathbf{H}_{AF}^H\right)$$

$$\mathbf{H}_{AF} = \begin{bmatrix} \mathbf{H}_2 \mathbf{G} \mathbf{H}_1 \end{bmatrix} \quad \mathbf{Q} = \mathbf{Q}_s^1 \quad \mathbf{R}_w = \sigma_{w_d}^2 \mathbf{I}_{n_d} + \sigma_{w_r}^2 \mathbf{H}_2 \mathbf{G} \mathbf{G}^H \mathbf{H}_2^H$$

(2.39)

In a SISO system with $\sigma_{w_s}^2 = \sigma_{w_r}^2$, the mutual information can be written as,

$$I_{FW}^{AF} = \frac{1}{2}\log\left(1 + \frac{\rho_2 \rho_1}{1 + \rho_1 + \rho_2}\right) \quad \rho_1 = \frac{|h_1|^2 P_s}{\sigma_{w_r}^2} \quad \rho_2 = \frac{|h_2|^2 P_r}{\sigma_{w_d}^2}$$

AF Protocol I

For the protocol I, the source and relay transmit in orthogonal phases,

$$\mathbf{y}_r(t) = \mathbf{H}_1 \mathbf{x}_s^1(t) + \mathbf{w}_r(t) \qquad\qquad 1 \le t \le N/2$$

$$\mathbf{y}_d(t) = \begin{cases} \mathbf{H}_0 \mathbf{x}_s^1(t) + \mathbf{w}_d(t) & 1 \le t \le N/2 \\ \mathbf{H}_2 \mathbf{G} \mathbf{H}_1 \mathbf{x}_s^1(t - N/2) + \mathbf{w}_d(t) & N/2 + 1 \le t \le N \end{cases}$$

(2.40)

The resulting mutual information using this protocol is

$$I_{p-I}^{AF} = \frac{1}{2} I_b$$

$$I_b = \log \det \left(\mathbf{I}_{2n_d} + \mathbf{R}_w^{-1} \mathbf{H}_{AF} \mathbf{Q} \mathbf{H}_{AF}^H \right) \tag{2.41}$$

$$\mathbf{H}_{AF} = \begin{bmatrix} \mathbf{H}_0 \\ \mathbf{H}_2 \mathbf{G} \mathbf{H}_1 \end{bmatrix} \quad \mathbf{Q} = \mathbf{Q}_s^1 \quad R_w = \begin{bmatrix} \sigma_{w_d}^2 \mathbf{I}_{n_d} & \mathbf{0} \\ \mathbf{0} & \sigma_{w_d}^2 \mathbf{I}_{n_s} + \sigma_{w_r}^2 \mathbf{H}_2 \mathbf{G} \mathbf{G}^H \mathbf{H}_2^H \end{bmatrix}$$

If the system present the following antenna configuration, $n_d=n_r=1$ and $n_s \geq 1$, the previous expression can be re-written in a simpler way [42] (and in chapter 4),

$$I_{p-I}^{AF} = \frac{1}{2} C_0 + \frac{1}{2} \log \left(1 + \frac{\rho_1 \rho_2 \Theta}{\rho_2 + \rho_1 + 1} \right) \tag{2.42}$$

$$\Theta = \frac{1 + \rho_0 (1 - \xi)}{1 + \rho_0} \qquad \xi = \frac{\left| \mathbf{h}_1^H \mathbf{h}_0 \right|^2}{\mathbf{h}_0^H \mathbf{h}_0 \mathbf{h}_1^H \mathbf{h}_1} = \cos^2 (\phi) \qquad C_0 = \log \left(1 + \rho_0 \right)$$

$$\rho_0 = \frac{P_s \mathbf{h}_0^H \mathbf{h}_0}{\sigma_{w_d}^2 L_0 n_s} \qquad \rho_2 = \frac{P_r h_2 h_2^*}{\sigma_{w_d}^2 L_2 n_r} \qquad \rho_1 = \frac{P_s \mathbf{h}_1^H \mathbf{h}_1}{\sigma_{w_r}^2 L_1 n_s}$$

where ξ depends on the product of the channels between the source and relay ($\mathbf{h}_1$) and source and destination ($\mathbf{h}_0$). L_0, L_1 and L_2 are variables connected to the path-loss in the different links. When the channels present Rayleigh distribution, this variable is random and follows a Beta distribution (see details in chapter 4, section 4.6.3). When the number of antennas at the source n_s increases, the random variable ξ tends to zero, improving mutual information. On the other hand, for the SISO case $n_d=n_r=n_s=1$, $\xi=1$ and hence,

$$I_{p-I}^{AF} = \frac{1}{2} C_0 + \frac{1}{2} \log_2 \left(1 + \frac{\rho_1 \rho_2}{(1 + \rho_0)(\rho_2 + \rho_1 + 1)} \right)$$

AF Protocol II

In protocol II the source transmits in both phases using $\mathbf{x}_s^1$ and $\mathbf{x}_s^2$, the received signal at the relay and destination is,

$$\mathbf{y}_r(t) = \mathbf{H}_1 \mathbf{x}_s^1(t) + \mathbf{w}_r(t) \qquad\qquad 1 \leq t \leq N/2$$

$$\mathbf{y}_d(t) = \begin{cases} 0 & 1 \leq t \leq N/2 \\ \begin{bmatrix} \mathbf{H}_2 \mathbf{G} \mathbf{H}_1 & \mathbf{H}_0 \end{bmatrix} \begin{bmatrix} \mathbf{x}_s^2(t - N/2) \\ \mathbf{x}_s^1(t - N/2) \end{bmatrix} + \mathbf{w}_d(t) & N/2 + 1 \leq t \leq N \end{cases} \tag{2.43}$$

The mutual information of this protocol is

$$I_{p-II}^{AF} = \frac{1}{2} I_b$$

$$I_b = \log \det \left(\mathbf{I}_{n_d} + \mathbf{R}_w^{-1} \mathbf{H}_{AF} \mathbf{Q} \mathbf{H}_{AF}^H \right) \tag{2.44}$$

$$\mathbf{H}_{AF} = \begin{bmatrix} \mathbf{H}_0 & \mathbf{H}_2 \mathbf{G} \mathbf{H}_1 \end{bmatrix} \quad \mathbf{Q} = \mathbf{I}_{2n_s} \frac{P_s}{n_s} \quad \mathbf{R}_w = \mathbf{I}_{n_d} \sigma_{w_s}^2 + \sigma_{w_r}^2 \mathbf{H}_2 \mathbf{G} \mathbf{G}^H \mathbf{H}_2^H$$

In a SISO system with $\sigma_{w_d}^2 = \sigma_{w_r}^2$, the mutual information for a fixed channel realization can be written as,

$$I_{p-II}^{AF} = \frac{1}{2}\log_2\left(1 + \frac{\rho_0(1+\rho_1) + \rho_2\rho_1}{1+\rho_1+\rho_2}\right) \quad \rho_0 = \frac{|h_0|^2 P_s}{\sigma_{w_d}^2} \quad \rho_1 = \frac{|h_1|^2 P_s}{\sigma_{w_r}^2} \quad \rho_2 = \frac{|h_2|^2 P_r}{\sigma_{w_d}^2}$$

AF Protocol III

In protocol III the source and the destination are transmitting and receiving in both phases, respectively. The signal model is,

$$
\begin{aligned}
\mathbf{y}_r(t) = \quad & \mathbf{H}_1\mathbf{x}_s^1(t) + \mathbf{w}_r(t) && 1 \le t \le N/2 \\
\mathbf{y}_d(t) = & \begin{cases} \mathbf{H}_0\mathbf{x}_s^1(t) + \mathbf{w}_d(t) & 1 \le t \le N/2 \\ \begin{bmatrix} \mathbf{H}_2\mathbf{G}\mathbf{H}_1 & \mathbf{H}_0 \end{bmatrix}\begin{bmatrix} \mathbf{x}_s^1(t-N/2) \\ \mathbf{x}_s^2(t-N/2) \end{bmatrix} + \mathbf{w}_d(t) & N/2+1 \le t \le N \end{cases}
\end{aligned}
$$
(2.45)

With that definition the mutual information of the protocol III is written as,

$$
\begin{aligned}
& I_{p-III}^{AF} = \frac{1}{2}I_b \\
& I_b = \log\det\left(\mathbf{I}_{2n_d} + \mathbf{R}_w^{-1}\mathbf{H}_{AF}\mathbf{Q}\mathbf{H}_{AF}^H\right) \\
& \mathbf{H}_{AF} = \begin{bmatrix} \mathbf{H}_0 & \mathbf{0} \\ \mathbf{H}_2\mathbf{G}\mathbf{H}_1 & \mathbf{H}_0 \end{bmatrix} \quad \mathbf{Q} = \mathbf{I}_{2n_s}\frac{P_s}{n_s} \quad \mathbf{R}_w = \begin{bmatrix} \sigma_{w_d}^2\mathbf{I}_{n_d} & \mathbf{0} \\ \mathbf{0} & \sigma_{w_d}^2\mathbf{I}_{n_d} + \sigma_{w_r}^2\mathbf{H}_2\mathbf{G}\mathbf{G}^H\mathbf{H}_2^H \end{bmatrix}
\end{aligned}
$$
(2.46)

In a SISO system with $\sigma_{n_d}^2 = \sigma_{n_r}^2$, the achievable rate can be written as,

$$I_{p-III}^{AF} = \frac{1}{2}\log_2\left((1+\rho_0)\left(1 + \frac{\rho_0(1+\rho_1)+\rho_2\rho_1}{1+\rho_1+\rho_2}\right) - \frac{\rho_0\rho_1\rho_2}{1+\rho_1+\rho_2}\right)$$

$$\rho_0 = \frac{|h_0|^2 P_s}{\sigma_{w_d}^2} \quad SNR_1 = \frac{|h_1|^2 P_s}{\sigma_{w_d}^2} \quad SNR_2 = \frac{|h_2|^2 P_r}{\sigma_{w_d}^2}$$

Comparison between the AF protocols

Table 2.5 presents the equivalent channel matrix $\mathbf{H}_{AF}$ and the noise covariance matrix to be used by the different protocols in the *amplify-and-forward*, (2.39), (2.41), (2.44) and (2.46). The spectral efficiency of AF protocols is affected by the factor 1/2 and the noise retransmitted by the relays $\sigma_{w_r}^2\mathbf{H}_2\mathbf{G}\mathbf{G}^H\mathbf{H}_2^H$. The equivalent system is similar to ($n_d \times n_s$), ($2n_d \times n_s$), ($n_d \times 2n_s$) and ($2n_d \times 2n_s$) MIMO systems for the forwarding, protocol I, protocol II and protocol III. The number of virtual antennas at the destination is increased in protocol I, protocol II increases the virtual antennas at the source and protocol III increases both.

AF protocols	Noise covariance matrix $\mathbf{R}_w$	$\mathbf{H}_{AF}$ (used in C_b)
forwarding	$\left[\sigma_{w_s}^2 + \sigma_{w_r}^2 \mathbf{H}_2 \mathbf{G} \mathbf{G}^H \mathbf{H}_2^H\right]$	$\mathbf{H}_2 \mathbf{G} \mathbf{H}_1$
protocol I	$\begin{bmatrix} \sigma_{w_d}^2 \mathbf{I} & \mathbf{0} \\ \mathbf{0} & \sigma_{w_d}^2 \mathbf{I} + \sigma_{w_r}^2 \mathbf{H}_2 \mathbf{G} \mathbf{G}^H \mathbf{H}_2^H \end{bmatrix}$	$\begin{bmatrix} \mathbf{H}_0 \\ \mathbf{H}_2 \mathbf{G} \mathbf{H}_1 \end{bmatrix}$
protocol II	$\left[\sigma_{w_s}^2 + \sigma_{w_r}^2 \mathbf{H}_2 \mathbf{G} \mathbf{G}^H \mathbf{H}_2^H\right]$	$\begin{bmatrix} \mathbf{H}_0 & \mathbf{H}_2 \mathbf{G} \mathbf{H}_1 \end{bmatrix}$
protocol III	$\begin{bmatrix} \sigma_{w_d}^2 \mathbf{I} & \mathbf{0} \\ \mathbf{0} & \sigma_{w_d}^2 \mathbf{I} + \sigma_{w_r}^2 \mathbf{H}_2 \mathbf{G} \mathbf{G}^H \mathbf{H}_2^H \end{bmatrix}$	$\begin{bmatrix} \mathbf{H}_0 & \mathbf{0} \\ \mathbf{H}_2 \mathbf{G} \mathbf{H}_1 & \mathbf{H}_0 \end{bmatrix}$

Table 2.5.- Achievable rates of the different non-dynamic AF protocols.

Additive white Gaussian noise (AWGN) channel

Figure 2.15 depicts the different protocols with AF under a Gaussian channel with $n_s=n_r=n_d=1$ and the scenario presented in Figure 2.11 for *low SNR* (SNR$_0$=0 dB). It is shown that protocol III is the only protocol that can provide better results than the direct transmission ($0 \leq d \leq 0.7$). From experimental results the performance of the AF protocols is ordered in the following way,

$$I_{FW}^{AF} \leq I_{p-II}^{AF} \leq I_{p-I}^{AF} \leq I_{p-III}^{AF} \qquad (2.47)$$
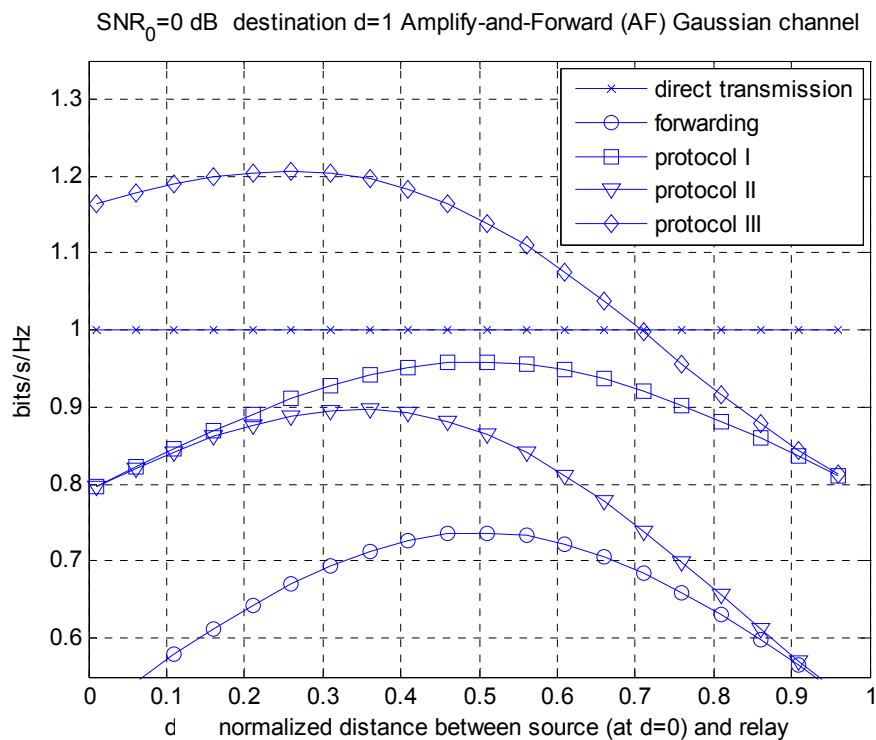
Figure 2.15.- Maximum achievable rate vs. distance between the source and relay. Gaussian channel. Destination with SNR$_0$= 0 dB. Amplify and forward. Time domain.

Multiple antenna and Rayleigh fading

The AF protocols will be evaluated under non-frequency selective Rayleigh channels and the terminals will be equipped with multiple antennas. The channel coefficients are constant during the relay-assisted transmission. Because in the AF mode, the relay only retransmits the signal

received in the *relay-received phase* and additionally it is not considered any signal processing at the relay, only the source and destination will feature more than one antenna. Therefore, assuming the scenario considered of Figure 2.11, results will be presented in terms of average achievable rate (see *definition 2.1* in section 2.2.1.4) with the following combination of antennas (n_s, n_r, n_d): (1,1,1),(2,1,1), (4,1,1) and (4,1,2) at *low SNR* (SNR_0=0 dB). Figure 2.16-(top-left) depicts the average achievable rate of the AF protocols for n_s=1, n_r=1, n_d=1 where only protocol III can get better performance than the direct transmission for $d \leq 0.75$. In Figure 2.16-(top-right) and Figure 2.16-(bottom-left) the number of antennas at the source is n_s=2 and n_s=4, respectively. It should be remarked that protocol I experiments an important improvement with n_s and n_r=n_d=1 as was predicted by (2.42). For example, in Table 2.6, which presents the maximum gains of the relay-assisted transmission over the direct transmission, it can be seen that protocol I can get a maximum gain up to 4% for n_s=4, while the gain for n_s=1 is -14%. However, for the configuration n_s=4, n_r=1, n_d=2 presented Figure 2.16-(bottom-right), protocol I gets a worse performance than direct transmission (maximum gain of -10%, see Table 2.6). Protocol III obtains the best performance with steady maximum gain over the direct transmission for $n_s \geq 2$, n_r=1, $n_d \geq 1$ (around 30%, see Table 2.6).
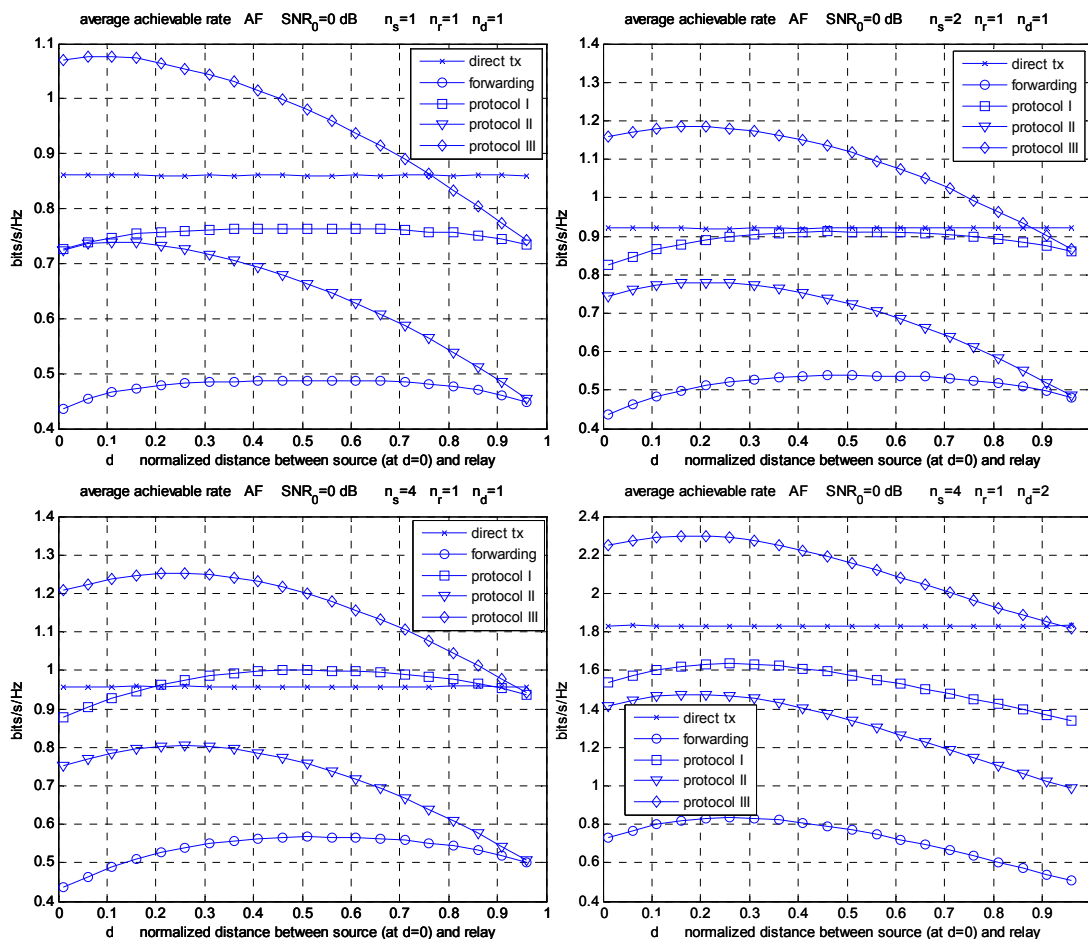

Figure 2.16.- Average achievable rate vs. distance between the source and relay. Rayleigh fading is assumed in all links. Destination with SNR$_0$=0 dB. (top-left) n_s=1,n_r=1,n_d=1, (top-right) n_s=2,n_r=1,n_d=1, (bottom-left) n_s=4,n_r=1,n_d=1, (bottom-right) n_s=4,n_r=1,n_d=2. Amplify-and-Forward.

SNR$_0$=0 dB	Maximum average achievable rate gain over direct transmission			
	n_s=1, n_r=1, n_d=1	n_s=2, n_r=1, n_d=1	n_s=4, n_r=1, n_d=1	n_s=4, n_r=1, n_d=2
forwarding	-46%	-43%	-39%	-54%
protocol I	-14%	-1%	4%	-10%
protocol II	-17%	-15%	-16%	-20%
protocol III	21%	30%	30%	27%

Table 2.6.- Maximum average achievable rate gain over the direct transmission under Rayleigh fading with multiple antenna: n_s (source), n_r (relay), n_d (destination). SNR$_0$=0 dB. AF.

2.3 Dynamic resource allocation relaying

In section 2.1.3 the different half-duplex protocols were described: forwarding, protocol I, II and III. Mainly, the literature of relay and cooperative transmission have proposed different schemes based on those protocols where the *relay-receive* and *relay-transmit phase* present the same size (in time or frequency domain), as in [27],[28] with protocols I, II and III. Nevertheless, when there is some CSI about the different links it is possible to optimize the duration of each phase (*resource optimization* or *dynamic resource allocation*) based on that knowledge and thus improve the spectral efficiency of the relay-assisted transmission. In such a case, the resources are allocated to each phase depending on the quality of the links. For example, consider the protocol I described in section 2.2.1, where the source-relay link becomes a bottleneck when it presents a bad quality. However, by increasing the *relay-receive phase* duration, the mutual information (in terms of number of bits) in the source-relay link also increases and the bottleneck may be avoided. Clearly, this implies a reduction of the *relay-transmit phase* duration. Forwarding protocol is considered in [29] and protocol III is studied in [12] and [34] (named as dynamic DF protocol and analyzed from the diversity-multiplexing tradeoff point of view). Regarding protocol I, references [35] and [36] investigate the resource optimization. Additionally, the resource allocation optimization based on the outage probability in each link for protocol I is tackled in [37].

This section investigates the achievable rate of the half-duplex protocols when three average power constraints are imposed to the terminals during the phases of the relay-assisted transmission:

- Source and relay terminals transmit with *maximum power* during each phase. This situation is typically found when the relay-assisted transmission is duplexed in the *time domain* (TDD[12]) with *power limited terminals*. It is investigated in section 2.3.1.

- Source and relay terminals transmit with *individual average power constraint*. Under this constraint the relay-assisted transmission duplexed in time (TDD) or frequency (FDD) get the same achievable rate, [7],[11]. Moreover, this type of constraint is also met for *power limited terminals* transmitting with *maximum power* under the relay-assisted transmission duplexed in the frequency domain. The FDD case is studied in section 2.3.2.

- Source and relay terminal transmit with a *sum average power constraint*. In this regard, the *spectral efficiency per unit total power* of the relay-assisted transmission can be compared, i.e. the obtained mutual information under the same average power inserted in the three-terminal network. It is tackled in section 2.3.3.

---

[12] For the FDD case this type of constraint can also be seen as an *individual average power constraint*.

The average power transmitted by the terminals depends on the type of power constraint considered. For example, when terminals have *individual average power constraint*, the average transmitted power in the three-terminal network is larger than the case where source and relay transmit with *maximum power* in each phase. In all cases the source and relay do not have exact channel state information, hence *eigenvector precoding* solutions are not considered[13] in this section and both terminals transmit with equal average power transmission per antenna.

2.3.1 Time domain duplexing (TDD)

The relay-assisted transmission in the time domain will be carried out during a frame of N symbols. The *relay-receive* and *relay-transmit phase* present a size of αN and $(1-\alpha)N$, respectively, as Figure 2.17 depicts. The α parameter will be optimized for the different protocols in order to provide the maximum mutual information. The protocol considered in section 2.2.1 and those in [5] assumed a *static resource allocation* relaying when $\alpha = 0.5$.
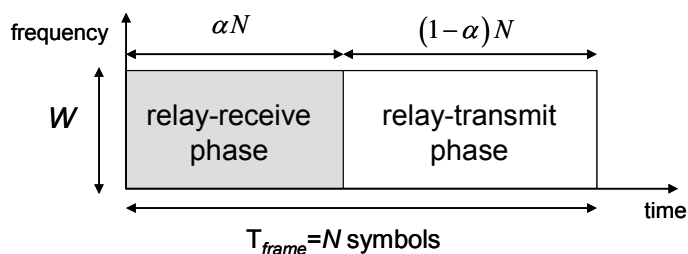

Figure 2.17.- Duration of the *relay-receive* and *relay-transmit phase* in the time domain.

The received signals in each terminal during the *relay-receive* and *relay-transmit phase* depend on the protocol selected and will be detailed in future sections. However, the following definitions are used for all the protocols. The variables n_s, n_r and n_d denote the number of antennas at the source, relay and destination, P_s and P_r are the power used by the source and the relay respectively. The channel matrices are defined by $\mathbf{H}_1 \, (n_r \times n_s)$, $\mathbf{H}_2 \, (n_d \times n_r)$ and $\mathbf{H}_0 \, (n_d \times n_s)$ for the source-relay, relay-destination and source-destination link, respectively. The channel coefficients remain constant during all the transmission. The noise at the destination and the relay terminals is assumed to be Gaussian with zero mean and covariance matrices $\mathbf{R}_{w_d} = \sigma_{w_d}^2 \mathbf{I}$ and $\mathbf{R}_{w_r} = \sigma_{w_r}^2 \mathbf{I}$ when the transmitted bandwidth is W. Moreover, the source may transmit the signals $\mathbf{x}_s^1$ and $\mathbf{x}_s^2$ during the *relay-receive* and *relay-transmit phase* respectively, depending on the selected protocol. The relay terminal transmits the signal $\mathbf{x}_r$ during the *relay-transmit phase*. All these signals are Gaussian with zero mean and diagonal covariance matrices which *trace* (sum of the diagonal elements) must be equal to the maximum power used at each terminal, P_s and P_r, respectively. Therefore, the covariance matrix of the signals transmitted by the terminals with no CSIT, [33], will be defined by,

$$\mathbf{Q}_s^1 = E\left\{\mathbf{x}_s^1 \mathbf{x}_s^{1H}\right\} = \frac{P_s}{n_s} \mathbf{I}_{n_s} \quad \mathbf{Q}_s^2 = E\left\{\mathbf{x}_s^2 \mathbf{x}_s^{2H}\right\} = \frac{P_s}{n_s} \mathbf{I}_{n_s} \quad \mathbf{Q}_r = E\left\{\mathbf{x}_r \mathbf{x}_r^{H}\right\} = \frac{P_r}{n_r} \mathbf{I}_{n_r}$$
$$Tr\left(\mathbf{Q}_s^1\right) = P_s \qquad\qquad Tr\left(\mathbf{Q}_s^2\right) = P_s \qquad\qquad Tr\left(\mathbf{Q}_r\right) = P_r$$

$$(2.48)$$

The mutual information of the different protocols will be written as a function of the capacities of the different links under no CSIT and equal average power transmission per antenna.

---

[13] *Asynchronous transmission* is considered in this section following the definition of [12].

2.3.1.1 DF-Forwarding

In this protocol (see Figure 2.3) the source transmits a message to the relay during the *relay-receive phase*, $\mathbf{x}_s^1$. The relay decodes the message, re-encodes and transmits $\mathbf{x}_r$ to the destination in the *relay-transmit phase*. The signals received at the relay and the destination are defined by

$$
\begin{aligned}
\mathbf{y}_r(t) &= \mathbf{H}_1 \mathbf{x}_s^1(t) + \mathbf{w}_r(t) && 1 \le t \le \lfloor \alpha N \rfloor \\
\mathbf{y}_d(t) &= \begin{cases} 0 & 1 \le t \le \lfloor \alpha N \rfloor \\ \mathbf{H}_2 \mathbf{x}_r\big(t - \lfloor \alpha N \rfloor\big) + \mathbf{w}_d(t) & \lfloor \alpha N \rfloor + 1 \le t \le N \end{cases}
\end{aligned} \tag{2.49}
$$

where $\mathbf{x}_s^1$ and $\mathbf{x}_r$ denote the Gaussian signals transmitted from the source and relay respectively, with covariance matrices given by (2.48). Notice that in the forwarding protocol the destination only receives data during the *relay-transmit phase* and the source only transmits during the *relay-receive phase*.

The duration of each phase (selection of α) is computed according the maximization of the mutual information,

$$
I_{FW} = \max_{0 \le \alpha \le 1} \min\big(\alpha C_a, (1-\alpha) C_b \big)
$$

$$
C_a = \log \det\left(\mathbf{I}_{n_r} + \frac{P_s}{n_s \, \sigma_{w_r}^2} \mathbf{H}_1 \mathbf{H}_1^H \right) \qquad C_b = \log \det\left(\mathbf{I}_{n_d} + \frac{P_r}{n_r \, \sigma_{w_d}^2} \mathbf{H}_2 \mathbf{H}_2^H \right) \tag{2.50}
$$

where C_a and C_b stand for the capacity of the source-relay and relay-destination link, respectively. The optimum value, α^*, is obtained after equating the two arguments of the $\min()$ function, hence the optimal value and the mutual information for the forwarding protocol reduces to,

$$
\alpha^* = \frac{C_b}{C_a + C_b} \qquad I_{FW}^* = \frac{C_a C_b}{C_a + C_b} \tag{2.51}
$$

where C_a and C_b are defined in (2.50).

2.3.1.2 DF-Protocol I

This protocol has already been described in section 2.2.1 when *relay-receive* and *relay-transmit phase* present the same size (α=1/2). Here, it has been assumed that the relay works with *unconstrained coding* (UC). Basically, the source transmits a message which is received by the relay and destination during the *relay-receive phase*, $\mathbf{x}_s^1$. Afterwards, the relay decodes, re-encodes and transmits $\mathbf{x}_r$ to the destination. This message does not be necessary equal to the original transmitted by the source. The destination considers the signal received during both phases to decode the original message. The signal model is,

$$\mathbf{y}_r(t) = \mathbf{H}_1\mathbf{x}_s^1(t) + \mathbf{w}_r(t) \qquad 1 \leq t \leq \lfloor \alpha N \rfloor$$

$$\mathbf{y}_d(t) = \begin{cases} \mathbf{H}_0\mathbf{x}_s^1(t) + \mathbf{w}_d(t) & 1 \leq t \leq \lfloor \alpha N \rfloor \\ \mathbf{H}_2\mathbf{x}_r(t - \lfloor \alpha N \rfloor) + \mathbf{w}_d(t) & \lfloor \alpha N \rfloor + 1 \leq t \leq N \end{cases} \qquad (2.52)$$

where $\mathbf{x}_s^1$ and $\mathbf{x}_r$ are the Gaussian signals transmitted from the source and relay, respectively, of zero mean and covariance matrices defined in (2.48). Now the destination is receiving both signals orthogonally during the entire frame and the source only transmits during the *relay-receive phase*.

The optimization of the resources is done in order to maximize the mutual information,

$$I_{p-I} = \max_{0 \leq \alpha \leq 1} \min\left(\alpha C_a, (1-\alpha)C_b + \alpha C_0\right)$$

$$C_a = \log \det\left(\mathbf{I}_{n_r} + \frac{P_s}{n_s \sigma_{w_r}^2}\mathbf{H}_1\mathbf{H}_1^H\right) \qquad C_b = \log \det\left(\mathbf{I}_{n_d} + \frac{P_r}{n_r \sigma_{w_d}^2}\mathbf{H}_2\mathbf{H}_2^H\right) \qquad (2.53)$$

$$C_0 = \log \det\left(\mathbf{I}_{n_d} + \frac{P_s}{n_s \sigma_{w_d}^2}\mathbf{H}_0\mathbf{H}_0^H\right)$$

where C_a, C_b and C_0 stand for the capacity of the source-relay, relay-destination and source-destination link, respectively. The optimum α can equate the two terms of the $\min()$ function only if $C_a \geq C_0$ as is depicted in Figure 2.18, otherwise the mutual information will be constrained by the source-relay link obtaining results lower that the direct transmission. Clearly, in such a case, we should avoid the use of protocol I (and the relay) and consider only the direct transmission.
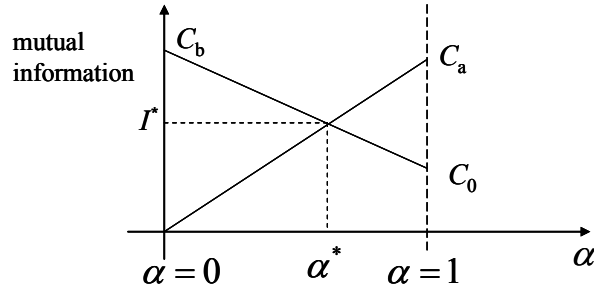
Figure 2.18.- Optimum value of α in protocol I.

As a result the optimum α and the mutual information obtained by protocol I is,

$$\alpha^* = \begin{cases} \dfrac{C_b}{C_a + C_b - C_0} & if \quad C_a \geq C_0 \\ 1 & otherwise \end{cases} \qquad I_{p-I}^* = \begin{cases} \dfrac{C_b C_a}{C_a + C_b - C_0} & if \quad C_a \geq C_0 \\ C_a & otherwise \end{cases} \qquad (2.54)$$

with C_a, C_b and C_0 being defined in (2.53). It can be seen from equation (2.54) that the use of equal sized *relay-receive* and *relay-transmit phase* is only optimal when $C_a = C_b + C_0$, i.e. when the capacity of the source-relay link is equal to the sum of mutual information of the relay-destination and source-destination links.

2.3.1.3 DF-Protocol II

Protocol II (Figure 2.3 in section 2.1.3) assumes that the source transmits to the relay during the *relay-receive phase*, $\mathbf{x}_s^1$ and both source and relay transmit simultaneously to destination in the *relay-transmit phase*, $\mathbf{x}_s^2$ and $\mathbf{x}_r$. The destination only considers the signal received in the second phase for decoding the message. However, depending on the type of messages transmitted by the source and relay, two different implementations are possible: protocol IIA and protocol IIB. The former assumes that the relay is able to decode all the data transmitted by the relay network. On the contrary, the second one assumes that the relay can decode only a part of the total data delivered to the destination (*partial decoding*).

Protocol IIA

This case is similar to the forwarding protocol described in section 2.3.1.1, but now during the *relay-transmit phase* both the source and relay are transmitting to the destination. Hence the signal model can be written as,

$$
\begin{aligned}
\mathbf{y}_r(t) &= \mathbf{H}_1 \mathbf{x}_s^1(t) + \mathbf{n}_r(t) & 1 \le t \le \lfloor \alpha N \rfloor \\
\mathbf{y}_d(t) &= \begin{cases} 0 & 1 \le t \le \lfloor \alpha N \rfloor \\ \begin{bmatrix} \mathbf{H}_2 & \mathbf{H}_0 \end{bmatrix} \begin{bmatrix} \mathbf{x}_r(t - \lfloor \alpha N \rfloor) \\ \mathbf{x}_s^2(t - \lfloor \alpha N \rfloor) \end{bmatrix} + \mathbf{n}_d(t) & \lfloor \alpha N \rfloor + 1 \le t \le N \end{cases}
\end{aligned}
\tag{2.55}
$$

where $\mathbf{x}_s^1$ denotes the Gaussian signal transmitted by the source in the *relay-receive phase* and $\mathbf{x}_s^2$, $\mathbf{x}_r$ are the Gaussian signals transmitted by the source and relay during the *relay-transmit phase* covariance matrices of (2.48).

All these signals are related to a common message. For this reason the relay must be able to decode the whole message from the signal received in the *relay-receive phase*. Notice that the equivalent MIMO system during the *relay-transmit phase* can use space-time codes with distributed antennas, [7]. Space-time codes transmit linear combinations of symbols in space (antennas) and time, but all the antennas must have access to all the symbols to be transmitted, [38], as it happens in this protocol.

The optimization of the resources will be found by maximizing the mutual information,

$$
\begin{aligned}
I_{p-IIA} &= \max_{0 \le \alpha \le 1} \min \left(\alpha C_a, (1-\alpha) C_b \right) \\
C_a &= \log \det \left(\mathbf{I}_{n_r} + \frac{P_s}{n_s \sigma_{w_r}^2} \mathbf{H}_1 \mathbf{H}_1^H \right) \\
C_b &= \log \det \left(\mathbf{I}_{n_d} + \frac{P_r}{n_r \sigma_{w_d}^2} \mathbf{H}_2 \mathbf{H}_2^H + \frac{P_s}{n_s \sigma_{w_d}^2} \mathbf{H}_0 \mathbf{H}_0^H \right)
\end{aligned}
\tag{2.56}
$$

where C_a and C_b stand for the capacity of the source-relay and joint (source,relay)-destination link, respectively, see (2.55). The optimal values are given by

$$
\alpha^* = \frac{C_b}{C_a + C_b} \qquad I_{p-IIA}^* = \frac{C_a C_b}{C_a + C_b}
\tag{2.57}
$$

This result presents the same structure as for the forwarding protocol (2.51), but now the definition of C_b is different, compare (2.56) with (2.51).

Protocol IIB

In protocol IIB the relay only decodes part of the total message transmitted from the source to the destination (*partial decoding*). As this protocol is less restrictive than protocol IIA, it is expected larger mutual information values. The signal model is the same as protocol IIA, defined in (2.55), but now since the signals transmitted by the terminals are related to two independent messages, the *relay-transmit phase* resembles the traditional Multiple Access Channel (MAC) [11] with two virtual users. The complexity of the receiver increases because two simultaneous and independent messages are received, requiring a *successive cancellation* scheme. One virtual user is made up of the relay during the *relay-transmit phase*, which transmits a message of rate R_r (using the signals $\mathbf{x}_s^1$ and $\mathbf{x}_r$ in (2.55)). The other virtual user is the source during the *relay-transmit phase* transmitting a new message of rate R_s through the signal $\mathbf{x}_s^2$. The achievable rate region $B(\alpha)$ in terms of (R_s,R_r) depends also on the constraints of R_r during the *relay-receive phase* and constraints of the MAC channel [11] during the *relay-transmit phase*, which reduces to

$$B(\alpha) = \begin{cases} R_r \leq \alpha C_a \\ R_r \leq (1-\alpha)C_2 \\ R_s \leq (1-\alpha)C_0 \\ R_r + R_s \leq (1-\alpha)C_b \end{cases} \tag{2.58}$$

where $\alpha \in [0,1]$ and C_a, C_2, C_0 and C_b denote the capacity of the source-relay, relay-destination, source-destination and joint (source,relay)-destination and defined by,

$$C_a = \log \det\left(\mathbf{I}_{n_r} + \frac{P_s}{n_s \sigma_{w_r}^2}\mathbf{H}_1\mathbf{H}_1^H\right) \quad C_b = \log \det\left(\mathbf{I}_{n_d} + \frac{P_r}{n_r \sigma_{w_d}^2}\mathbf{H}_2\mathbf{H}_2^H + \frac{P_s}{n_s \sigma_{w_d}^2}\mathbf{H}_0\mathbf{H}_0^H\right)$$
$$C_0 = \log \det\left(\mathbf{I}_{n_d} + \frac{P_s}{n_s \sigma_{w_s}^2}\mathbf{H}_0\mathbf{H}_0^H\right) \quad C_2 = \log \det\left(\mathbf{I}_{n_d} + \frac{P_r}{n_r \sigma_{w_d}^2}\mathbf{H}_2\mathbf{H}_2^H\right) \tag{2.59}$$

The achievable rate region $B(\alpha)$ of (2.58) is presented in Figure 2.19. It is a pentagon where we have taken into account the fact $C_b \leq C_0 + C_2$. The total mutual information $(R_r + R_s)$ for a given value of α is defined by the following piecewise function,

$$\lambda(\alpha) = \begin{cases} \lambda_1(\alpha) = (1-\alpha)C_b & \text{if } \alpha C_a \geq (1-\alpha)(C_b - C_0) \\ \lambda_2(\alpha) = \min(\alpha C_a, (1-\alpha)C_2) + (1-\alpha)C_0 & \text{otherwise} \end{cases} \tag{2.60}$$

with $\lambda_1(\alpha)$ and $\lambda_2(\alpha)$ being the achievable rate dominated by the sum-rate and the direct transmission constraint, respectively.
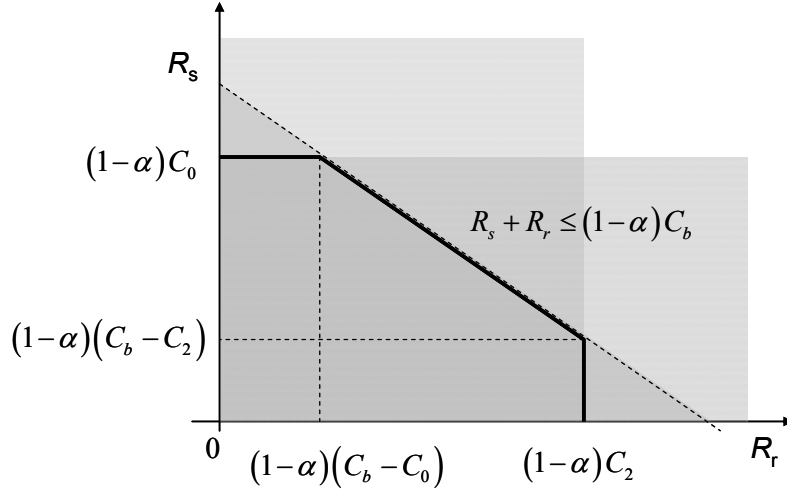
Figure 2.19.- Achievable rate region B(α) for protocol IIB.

We are interested in working in the sum-rate region $\lambda_1(\alpha)$ because it offers a larger rate. However, when (2.60) is maximized over the variable α we must consider the value at α=0, where $\lambda(\alpha) = C_0$ (given by $\lambda_2(\alpha)$). For that reason the optimization is done in both regions, selecting the maximum of both,

$$
\begin{aligned}
I_{p-IIB} &= \max\left(\lambda_1^{max}, \lambda_2(0)\right) \\
\lambda_1^{max} &= \max_{0 \leq \alpha \leq 1} \lambda_1(\alpha), \qquad \lambda_2(0) = C_0
\end{aligned}
\tag{2.61}
$$

where α is a variable to perform the maximizations of $\lambda_1(\alpha)$. The mutual information of this protocol is given by,

$$
\alpha_1^* = \begin{cases} \dfrac{C_b - C_0}{C_b + C_a - C_0} & \text{if} \quad C_a \geq C_0 \\ 0 & \text{otherwise} \end{cases}
\qquad
I_{p-IIB}^* = \begin{cases} \dfrac{C_a C_b}{C_b + C_a - C_0} & \text{if} \quad C_a \geq C_0 \\ C_0 & \text{otherwise} \end{cases}
\tag{2.62}
$$

with C_a, C_0 and C_b being defined in (2.59). Interestingly, from previous equations it can be seen that either the relay-destination link or the source-relay link presents a bad quality, $C_b \approx C_0$ or $C_a \approx 0$, the optimal α tends to 0 which means this protocol is transformed to the direct transmission avoiding the use of the relay.

2.3.1.4 DF-Protocol III

Protocol III (Figure 2.3) can be seen as a combination of protocol I and protocol II. The destination is receiving data during both relay phases. This section assumes that the relay decodes a part of the total message ($\mathbf{x}_s^1$ as in protocol IIB). The destination will receive two simultaneous independent messages requiring of a successive cancellation scheme, $\mathbf{x}_s^2$ and $\mathbf{x}_r$. This protocol is studied in [12]. The signal model is defined by,

$$\mathbf{y}_r(t) = \mathbf{H}_1 \mathbf{x}_s^1(t) + \mathbf{n}_r(t) \qquad\qquad 1 \le t \le \lfloor \alpha N \rfloor$$

$$\mathbf{y}_d(t) = \mathbf{H}_0 \mathbf{x}_s^1(t) + \mathbf{n}_d(t) \qquad\qquad 1 \le t \le \lfloor \alpha N \rfloor \qquad (2.63)$$

$$\mathbf{y}_d(t) = \begin{bmatrix} \mathbf{H}_2 & \mathbf{H}_0 \end{bmatrix} \begin{bmatrix} \mathbf{x}_r(t - \lfloor \alpha N \rfloor) \\ \mathbf{x}_s^2(t - \lfloor \alpha N \rfloor) \end{bmatrix} + \mathbf{n}_d(t) \qquad \lfloor \alpha N \rfloor + 1 \le t \le N$$

where $\mathbf{x}_s^1$ and $\mathbf{x}_r$ stand for the Gaussian signals transmitted by the source and the relay during the *relay-receive* and *relay-transmit phase* respectively, both related to the same message of rate R_r, and $\mathbf{x}_s^2$ is the Gaussian signal transmitted by the source during the *relay-transmit phase* of rate R_s.

The achievable rate of this protocol can be obtained using the same techniques that have been considered in [12]. Additionally, it will be shown that the achievable rate from a point of view similar than protocol IIB. This latter point of view will be useful to obtain the optimum solution when this protocol is duplexed in FDD and/or there are multiple users [39] to be shown in section 2.3.2 and chapter 3, respectively.

Following the same guidelines of [12] the achievable rate is given by,

$$I_{p-III} = \max_{0 \le \alpha \le 1} \min(I_1, I_2)$$

$$I_1 = \alpha C_a + (1 - \alpha) C_0 \qquad I_2 = \alpha C_0 + (1 - \alpha) C_b \qquad (2.64)$$

with I_1 and I_2 being the mutual information delivered in the *relay-receive* and *relay-transmit phase*, and C_a, C_b, C_0 taking into account the signal model (2.63) and defined as,

$$C_a = \log\det\left(\mathbf{I}_{n_r} + \frac{P_s}{n_s \sigma_{w_r}^2} \mathbf{H}_1 \mathbf{H}_1^H \right) \quad C_b = \log\det\left(\mathbf{I}_{n_d} + \frac{P_r}{n_r \sigma_{w_d}^2} \mathbf{H}_2 \mathbf{H}_2^H + \frac{P_s}{n_s \sigma_{w_d}^2} \mathbf{H}_0 \mathbf{H}_0^H \right)$$

$$C_0 = \log\det\left(\mathbf{I}_{n_d} + \frac{P_s}{n_s \sigma_{w_s}^2} \mathbf{H}_0 \mathbf{H}_0^H \right) \qquad\qquad (2.65)$$

The variables C_a, C_b, C_0 are the capacities of the source-relay, source-destination, joint (source,relay)-destination and equivalent system with two simultaneous transmissions (2.63). Note that C_b is always greater than C_0. The optimum achievable rate of (2.64) is obtained when both terms inside of the min() function are equal, for example Figure 2.20 presents the different possibilities.
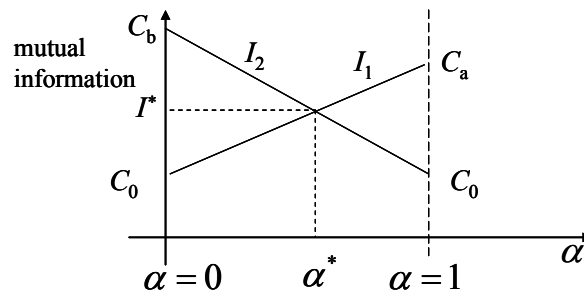

Figure 2.20.- Optimum value of α for protocol III.

Therefore, the optimum values are,

$$\alpha^* = \begin{cases} \dfrac{C_b - C_0}{C_a + C_b - 2C_0} & \text{if } C_a \geq C_0 \\[2mm] 0 & \text{otherwise} \end{cases} \qquad I_{p-III}^* = \begin{cases} \dfrac{C_b C_a - (C_0)^2}{C_a + C_b - 2C_0} & \text{if } C_a \geq C_0 \\[2mm] C_0 & \text{otherwise} \end{cases} \qquad (2.66)$$

with C_a, C_b, C_0 being defined in (2.65). This protocol converges to the direct transmission either when the source-relay link is in worse conditions than the source-destination link, $C_a < C_0$, or when the relay-destination link presents a poor quality, so $C_b \approx C_0$, and $\alpha^* = 0$.

On the other hand the scheme defined in (2.63) is similar to a MAC channel with 2 virtual users. One virtual user (*source-relay virtual user*) transmits a message with rate R_r. The other virtual user (*source-only virtual user*) is the source in the *relay-transmit phase* transmits a message of rate R_s. Both messages are independent. The achievable rate region in terms of (R_s, R_r) in the time domain, named $B_{tdd}(\alpha)$, is given by (see appendix B in section 2.7)

$$B_{tdd}(\alpha) = \begin{cases} R_r \leq \alpha C_0 + (1-\alpha) C_2 \\ R_r \leq \alpha C_a \\ R_s \leq (1-\alpha) C_0 \\ R_r + R_s \leq \alpha C_0 + (1-\alpha) C_b \end{cases} \qquad (2.67)$$

where C_0, C_b and C_a are the capacity of the source-destination, joint (source,relay)-destination and source-relay links (2.65) and C_2 the capacity of the relay-destination link (2.63) defined as,

$$C_2 = \log \det \left(\mathbf{I}_{n_d} + \frac{P_r}{n_r \, \sigma_{w_d}^2} \mathbf{H}_2 \mathbf{H}_2^H \right) \qquad (2.68)$$

The region defined by $B_{tdd}(\alpha)$ given a fixed vector α is a polyhedron with a rectangular or pentagonal shape, depending on the capacity of the links. This region satisfies the properties to be a *polymatroid* (*definition 3.1* in [40]), and hence any vertex of that region can be achieved by *successive decoding*. The achievable rate region will be given by the convex hull of the union of all the regions $B_{tdd}(\alpha)$ defined by all possible α. Its boundary can be found as those rates which are solution of (*lemma 3.2* of [40]),

$$\max_{\alpha, R_r, R_s} \mu_r R_r + \mu_s R_s \quad s.t. (R_r, R_s) \in B_{tdd}(\alpha) \qquad (2.69)$$

for some positive μ_r, $\mu_s \in \Re_+$. The maximum is attained at some vertex of $B_{tdd}(\alpha)$ such that $\mu_r \geq \mu_s$. Equation (2.69) can be solved by linear program or convex optimization [41].

2.3.1.5 Comparison of dynamic DF protocols

Table 2.7 presents the optimum ratio between the *relay-receive* and *relay-transmit phase* (α) and the achievable rates for the different protocols using the definitions of (2.70). It can be seen that protocol IIB and III are able to switch to direct transmission when the source-relay link is worse than the source-destination link. In that situation, protocols I, IIA and forwarding get a

worse achievable rate that direct transmission. Additionally, both pairs of protocols, forwarding and protocol IIA, and protocol I and IIB (when $C_a \geq C_0$) present the same expressions for the achievable rate and α, but the variable C_b (2.70) differs in each case due to the variable Δ.

$$C_a = \log \det \left(\mathbf{I}_{n_r} + \frac{P_s}{n_s \sigma_{w_r}^2} \mathbf{H}_1 \mathbf{H}_1^H \right) \qquad C_b = \log \det \left(\mathbf{I}_{n_d} + \frac{P_r}{n_r \sigma_{w_d}^2} \mathbf{H}_2 \mathbf{H}_2^H + \Delta \right)$$

$$C_0 = \log \det \left(\mathbf{I}_{n_d} + \frac{P_s}{n_s \sigma_{w_s}^2} \mathbf{H}_0 \mathbf{H}_0^H \right)$$

(2.70)

protocol	α^*	Achievable rate	Δ (defined in C_b)
forwarding	$\dfrac{C_b}{C_b + C_a}$	$\dfrac{C_b C_a}{C_b + C_a}$	0
protocol I	$\begin{cases} \dfrac{C_b}{C_a + C_b - C_0} & if \quad C_a \geq C_0 \\ 1 & otherwise \end{cases}$	$\begin{cases} \dfrac{C_b C_a}{C_a + C_b - C_0} & if \quad C_a \geq C_0 \\ C_a & otherwise \end{cases}$	0
protocol IIA	$\dfrac{C_b}{C_b + C_a}$	$\dfrac{C_b C_a}{C_b + C_a}$	$\dfrac{P_s}{n_s \sigma_{w_d}^2} \mathbf{H}_0 \mathbf{H}_0^H$
protocol IIB	$\begin{cases} \dfrac{C_b - C_0}{C_b + C_a - C_0} & if \; C_a \geq C_0 \\ 0 & otherwise \end{cases}$	$\begin{cases} \dfrac{C_b C_a}{C_a + C_b - C_0} & if \quad C_a \geq C_0 \\ C_0 & otherwise \end{cases}$	$\dfrac{P_s}{n_s \sigma_{w_d}^2} \mathbf{H}_0 \mathbf{H}_0^H$
protocol III	$\begin{cases} \dfrac{C_b - C_0}{C_a + C_b - 2C_0} & if \; C_a \geq C_0 \\ 0 & otherwise \end{cases}$	$\begin{cases} \dfrac{C_b C_a - (C_0)^2}{C_a + C_b - 2C_0} & if \; C_a \geq C_0 \\ C_0 & otherwise \end{cases}$	$\dfrac{P_s}{n_s \sigma_{w_d}^2} \mathbf{H}_0 \mathbf{H}_0^H$

Table 2.7.- Optimum resource allocation of the *relay-receive* and *relay-transmit phase* (α) and achievable rates of the different dynamic DF protocols.

When protocol IIA and protocol I are compared (assuming $C_a > C_0$) the mutual information of one protocol is better than the other depending on the value of C_a.

$$\begin{cases} I_{p-IIA} \geq I_{p-I} & C_a > \dfrac{C_b^{IIA} C_0}{C_b^{IIA} - C_b^I} \\ I_{p-IIA} < I_{p-I} & otherwise \end{cases}$$

(2.71)

where C_b^{IIA} and C_b^I follow the definition of C_b (2.70) (see Table 2.7 for protocol IIA and I, respectively). When the source-relay link (C_a) is very good, protocol IIA obtains a better achievable rate than using protocol I. In this regard the mutual information of the different protocols satisfies the following order,

$$I_{FW} \leq \begin{cases} I_{p-IIA} \leq I_{p-I} \\ or \\ I_{p-I} \leq I_{p-IIA} \end{cases} \leq I_{p-IIB} \leq I_{p-III}$$

(2.72)

where protocols III and IIB get the best achievable rate at the cost of a more complex receiver at the destination. In those cases *successive decoding* is required because two independent messages are received simultaneously, see sections 2.3.1.3 and 2.3.1.4.

Figure 2.21 presents how the different protocols are connected as a function of the parameter α^* and on the activity of the terminals on each relay phase. For example, from protocol I we can change either to forwarding protocol when the destination is not listening the data in the *relay-receive phase* or to direct transmission when α^*=1 and assuming that the mutual information of the source-relay link is superior to the source-destination link, see definition in Table 2.7. Protocol III leads to direct transmission when α^*=0 and to protocol II when destination is not listening in the *relay-receive phase*. Finally, protocol II is transformed to direct transmission when α^*=0 (only for protocol IIB see Table 2.7).
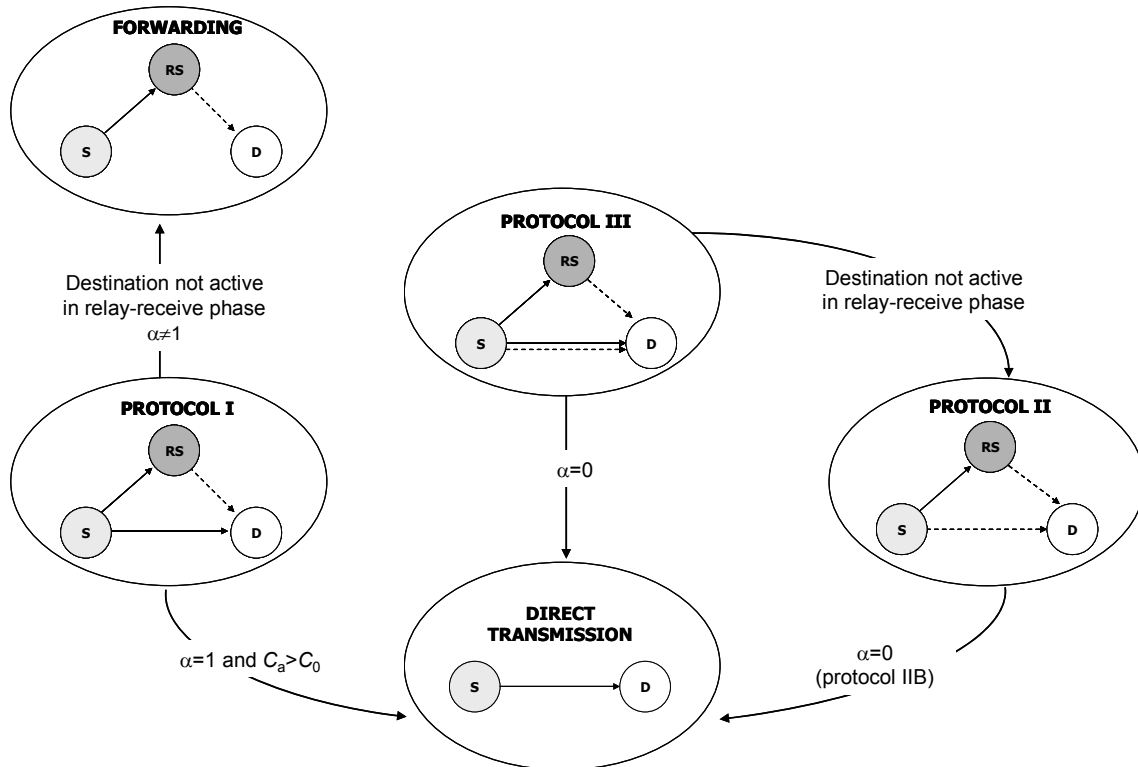
Figure 2.21.- Transition between protocols. Solid lines stands for the transmission in the *relay-receive phase* and dashed lines for the transmissions in the *relay-transmit phase*.

Additive white Gaussian noise (AWGN) channel

Figure 2.22 presents the achievable rate of the half-duplex protocols when the destination has a SNR_0=0 dB with the scenario defined in Figure 2.11 in an AWGN channel. For *low SNR* values the forwarding can get better performance than direct transmission in $0.1 \leq d \leq 0.9$. Protocol IIA is better than forwarding, but for $d \geq 0.7$ both protocols get the same results. In that case both achievable rate expressions are limited by the value of C_a (source-relay link, it decreases as d increases to 1), see Table 2.7. Protocol I is able to get better results than protocol IIA for $d \geq 0.24$, otherwise protocol IIA is better than protocol I as was derived in (2.71). Protocol IIB and III get better results than previous protocols, with protocol III the best one, following (2.72).

Figure 2.23 shows the performance of the different protocols when the SNR_0 is increased up to 10 dB. Now, forwarding and protocol IIA (except for d close to 0) get a worse performance result than direct transmission. The remaining protocols are able to provide better results than direct transmission, with protocol III being the best one. Moreover it should be remarked that under

this scenario $C_a(d=1)=C_0$ (variables defined in (2.70)), so that protocol IIB, III and I at d=1 get the same values because the mutual information is limited by the source-relay link, C_a, see Table 2.7.

Figure 2.22.- Maximum achievable rate vs. distance between the source and relay. Gaussian channel. Destination with SNR$_0$=0 dB. Time domain.
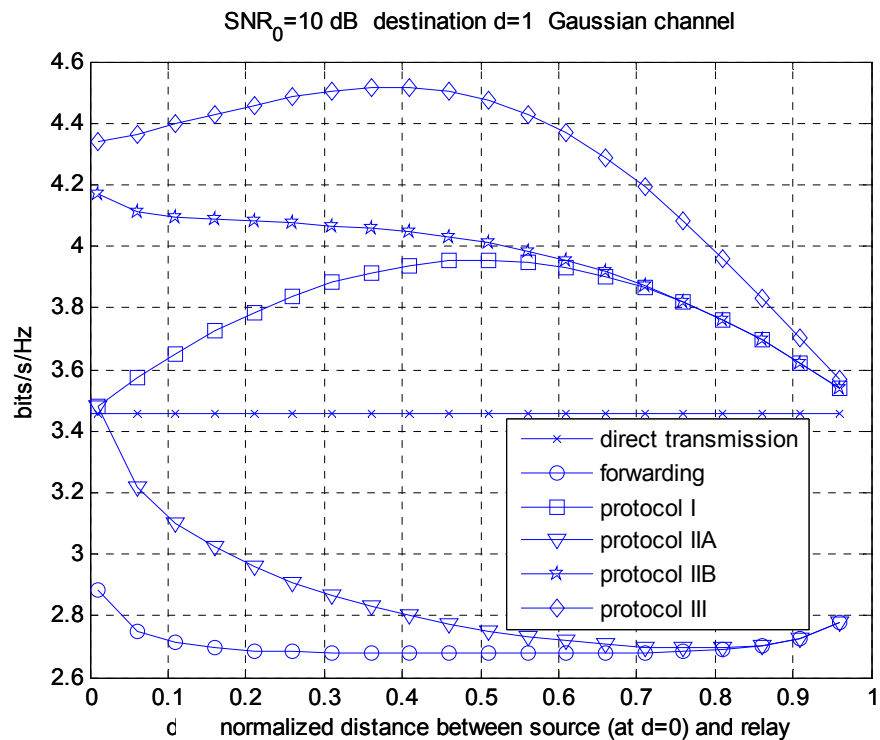
Figure 2.23.- Maximum achievable rate vs. distance between the source and relay. Gaussian channel. Destination with SNR$_0$= 10 dB. Time domain.

Multiple antenna and Rayleigh fading

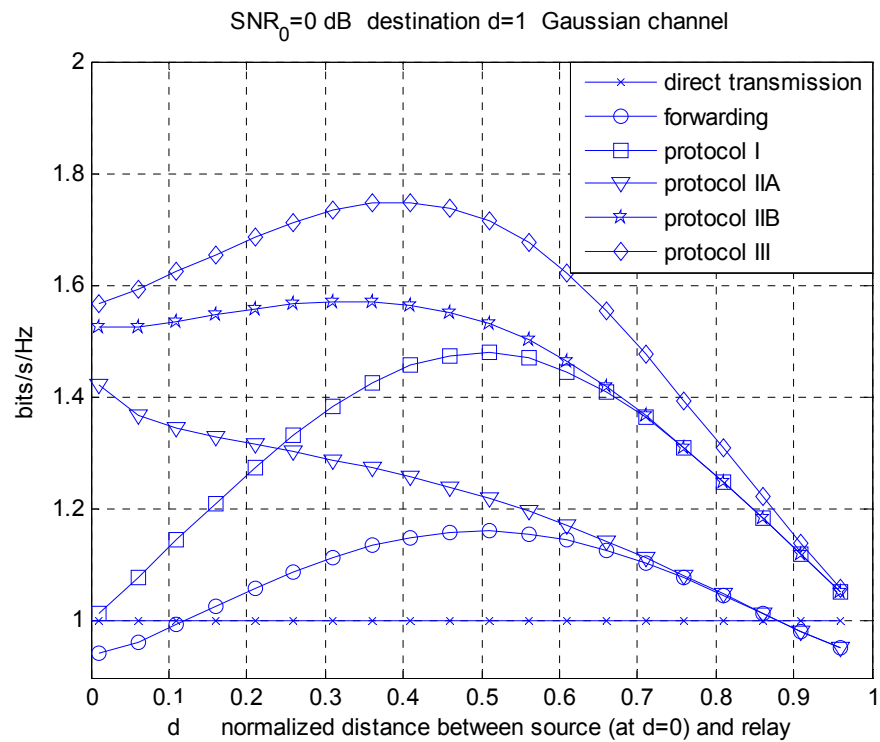In order to evaluate the half-duplex protocols in the time domain with multiple antennas we have assumed that the channel coefficients involved in the relay-assisted transmission are *Rayleigh* random variables which remain constant over the transmission interval of time (one frame). However the relay-assisted transmission can be adapted to each frame (see *definition 2.1* in section 2.2.1.4). Because the achievable rate will vary from frame to frame, results will be presented in terms of average achievable rate. The scenario considered will be the same as in Figure 2.11. Results assume the following combination of antennas (n_s, n_r, n_d): (1,1,1),(1,1,2), (2,1,1) and (2,2,2) at SNR_0=0 dB.
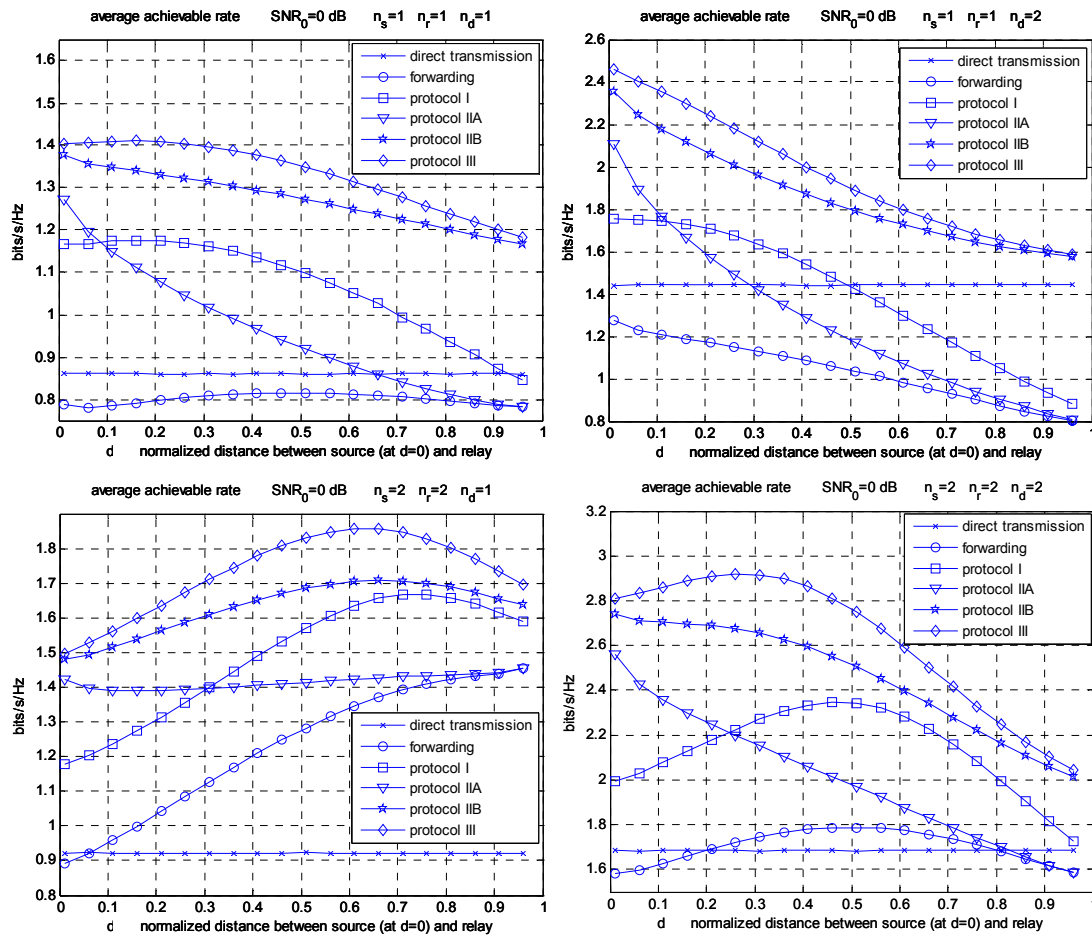
Figure 2.24.- Average achievable rate vs. distance between the source and relay. Rayleigh fading. Destination with SNR$_0$=0 dB. (top-left) n_s=1, n_r=1, n_d=1, **(top-right)** n_s=1, n_r=1, n_d=2, **(bottom-left)** n_s=2, n_r=2, n_d=1, **(bottom-right)** n_s=2, n_r=2, n_d=2.

Figure 2.24-(top-left) presents the average achievable rate of the different protocols under a Rayleigh channel with n_s=1, n_r=1 and n_d=1. Now, the Rayleigh fading produces that the forwarding protocol get worse values than direct transmission, in contrast to the Gaussian channel case, Figure 2.22. Additionally, the performance of protocol IIB and III when the relay is close to destination is better than average achievable rate of the direct transmission. Moreover, if the receiving antennas are increased up n_d=2 (with n_s=n_r=1), Figure 2.24-(top-right) shows that the maximums of the average achievable rates are obtained in positions d where the relay is close to the source. On the other hand, if we increase the number of antennas at the source and relay, n_s=n_r=2 (with n_d=1), Figure 2.24-(bottom-left) the maximums of the average

achievable rates move to positions *d* where the relay is close to destination. In that case, protocol IIA offers a steady average achievable rate independent of the position of the relay. Finally, increasing all the antennas of the terminals, $n_s=n_r=n_d=2$, Figure 2.24-(bottom-right) the maximum of the average achievable rates are obtained when the relay is placed in similar positions as the case $n_s=n_r=n_d=1$ (except for protocol I). Moreover, the forwarding protocol when all terminals feature two antennas obtains an average achievable rate better than the direct transmission when the relay is placed in $0.2 \leq d \leq 0.8$.

Additionally, Table 2.8 reports the maximum average achievable rate gain of the different half duplex protocols over the direct transmission in Rayleigh fading with multiple antenna terminals at $SNR_0=0$ dB. These gains are observed in Figure 2.24 where the best position of the relay depends on each protocol and antenna configuration. The largest gains are obtained when all protocols feature $n_s=n_r=2$, $n_d=1$. In that case, protocol III can double the average achievable rate of the direct transmission (2×1 MIMO) with a single antenna at the destination when the relay is placed at $d=0.65$ (Figure 2.24-(bottom-left)).

SNR₀=0 dB	Maximum average achievable rate gain over direct transmission			
	$n_s=1, n_r=1, n_d=1$	$n_s=1, n_r=1, n_d=2$	$n_s=2, n_r=2, n_d=1$	$n_s=2, n_r=2, n_d=2$
forwarding	-9%	-8%	57%	5%
protocol I	33%	25%	82%	40%
protocol IIA	45%	51%	57%	51%
protocol IIB	56%	67%	84%	63%
protocol III	57%	71%	102%	70%

Table 2.8.- Maximum average achievable rate gain over the direct transmission under Rayleigh fading with multiple antenna: n_s (source), n_r (relay), n_d (destination). SNR₀=0 dB.

2.3.2 Frequency domain duplexing (FDD)

This section adopts the dynamic relaying with frequency division duplexing (FDD) as Figure 2.25 depicts. The *relay-receive* and *relay-transmit phase* use orthogonal frequency bands, but both using the same frame time duration, i.e. the counterpart of relay transmission in the time domain described in section 2.3.1. Hence the signal models considered in section 2.3.1 are still valid but exchanging time by frequency (*N* by *W*).
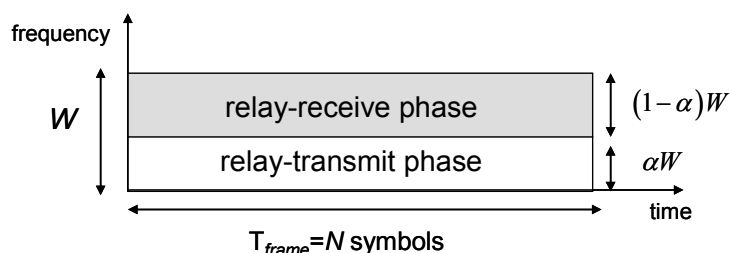
Figure 2.25.- *Relay-receive* and *relay-transmit phase* duplexed in frequency.

There are two differences with respect to the relay transmission duplexed in the *time domain* with *power limited terminals*. First, now in the frequency domain when the source transmits in both phases (protocol II and III) the amount of power assigned and the bandwidth allocated in each phase can also be also optimized. The terminals are constrained by *individual average power*. The other difference is that varying the allocated bandwidth of each phase, the noise power received at the different terminals also changes.

The relay will be receiving and transmitting simultaneously but in different frequencies. In order to have a causal system the relay will not able to transmit the estimated packet after it has decoded it, see Figure 2.26. When the source is transmitting the m_j packet, the relay is receiving that packet in the *relay-receive phase*, while in the *relay-transmit phase* (other frequency band) it is transmitting the estimated (and re-encoded) $\hat{m}_{j-1}$ packet. This implies an overhead which can be reduced by transmitting a large number of packets.
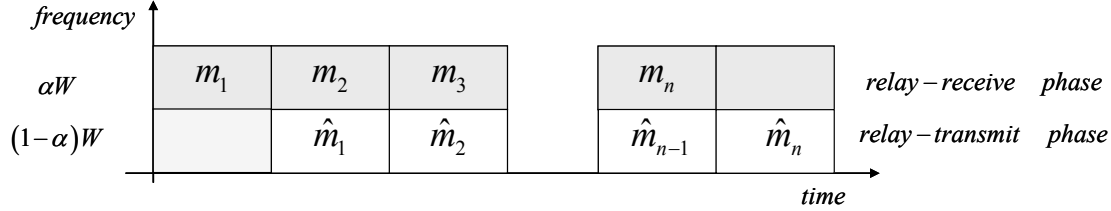
Figure 2.26.-Reception and transmission at the relay working in DF and in the frequency domain. m_j **is a packet transmitted by the source in the relay-receive phase and** $\hat{m}_j$ **is the estimated packet by the relay terminal, re-encoded and transmitted to destination.**

In the following it will be assumed that the source transmits the signals $\mathbf{x}_s^1$, $\mathbf{x}_s^2$ during the *relay-receive* and *relay-transmit phase*, respectively, while the relay is transmitting the signal $\mathbf{x}_r$ during the *relay-transmit phase*. All these signals are Gaussian with the following covariance matrices,

$$\mathbf{Q}_s^1 = E\left\{\mathbf{x}_s^1\mathbf{x}_s^{1H}\right\} = \frac{\beta_1 P_s}{n_s}\mathbf{I}_{n_s} \quad \mathbf{Q}_s^2 = E\left\{\mathbf{x}_s^2\mathbf{x}_s^{2H}\right\} = \frac{\beta_2 P_s}{n_s}\mathbf{I}_{n_s} \quad \mathbf{Q}_r = E\left\{\mathbf{x}_r\mathbf{x}_r^H\right\} = \frac{P_r}{n_r}\mathbf{I}_{n_r}$$

$$Tr\left(\mathbf{Q}_s^1\right) = \beta_1 P_s \quad Tr\left(\mathbf{Q}_s^2\right) = \beta_2 P_s \quad Tr\left(\mathbf{Q}_r\right) = P_r \quad \beta_1 + \beta_2 = 1 \tag{2.73}$$

where $\beta_1, \beta_2 \in [0,1]$. The variables β_1, β_2 distribute the power at the source when it is allowed by the corresponding protocol (protocol IIA, IIB and III). Protocols I and forwarding operate with $\beta_1 = 1$, because the source only transmits in the *relay-receive phase*.

DF-Forwarding

Assuming the signal model of (2.49) applied to the frequency domain and considering that this protocol works with $\beta_1 = 1$ (2.73), the optimization of the resources for the forwarding protocol reduces to,

$$I_{FW} = \max_{0 \leq \alpha \leq 1} \min\left(\alpha C_a(\alpha), (1-\alpha)C_b(1-\alpha)\right)$$

$$C_a(\delta) = \log\det\left(\mathbf{I}_{n_r} + \frac{P_s}{\delta n_s \sigma_{w_r}^2}\mathbf{H}_1\mathbf{H}_1^H\right) C_b(\delta) = \log\det\left(\mathbf{I}_{n_d} + \frac{P_r}{\delta n_r \sigma_{w_d}^2}\mathbf{H}_2\mathbf{H}_2^H\right) \tag{2.74}$$

where C_a and C_b stand for the capacity of the source-relay and relay-destination link, respectively, under no CSIT, equal average power transmission per antenna and parameter δ. Note that $\sigma_{w_d}^2$ is the noise power assuming all the bandwidth *W*. Moreover, in contrast to the time domain case with power limited terminals (section 2.3.1), it is not possible to find a closed-form solution for mutual information.

DF-Protocol I

The mutual information of protocol I in the frequency domain with the signal model given in (2.52) and using β=1, (2.73), is defined by.

$$I_{p-I} = \max_{0 \leq \alpha \leq 1} \min\left(\alpha C_a(\alpha), (1-\alpha)C_b(1-\alpha) + \alpha C_0(\alpha)\right)$$

$$C_0(\delta) = \log\det\left(\mathbf{I}_{n_d} + \frac{P_s}{\delta n_s \sigma_{w_d}^2}\mathbf{H}_0\mathbf{H}_0^H\right)$$

(2.75)

with C_a, C_b defined in (2.74) and C_0 related to the capacity in the source-destination link.

Protocol II

The signal model for protocol II in the frequency domain is the counterpart of the one defined in (2.55). Two implementations are possible, protocol IIA and IIB. Because the source is transmitting in both phases and it can optimize the power allocated to each one. In protocol IIA the resource optimization lead us to,

$$I_{p-IIA} = \max_{0 \leq \alpha \leq 1, 0 \leq \beta \leq 1} \min\left(\alpha C_a(\alpha, \beta_1), (1-\alpha)C_b(1-\alpha, \beta_2)\right)$$

$$C_a(\delta, \chi) = \log\det\left(\mathbf{I}_{n_r} + \frac{\chi P_s}{\delta n_s \sigma_{w_r}^2}\mathbf{H}_1\mathbf{H}_1^H\right)$$

(2.76)

$$C_b(\delta, \chi) = \log\det\left(\mathbf{I}_{n_d} + \frac{P_r}{\delta n_r \sigma_{w_d}^2}\mathbf{H}_2\mathbf{H}_2^H + \frac{\chi P_s}{\delta n_s \sigma_{w_d}^2}\mathbf{H}_0\mathbf{H}_0^H\right)$$

where C_a and C_b stand for the capacity of the source-relay and joint (source,relay)-destination link (in terms of parameters δ, χ), and β_1 is the fraction of power allocated to the *relay-receive phase* (β_2 to the *relay-transmit phase*), (2.73).

The same arguments used in the time domain, section 2.3.1.3, apply to protocol IIB in the frequency domain. Therefore, the achievable rate region defined by the two independent messages of rate R_r and R_s is defined by,

$$B_{fdd}(\alpha, \boldsymbol{\beta}) = \begin{cases} R_r \leq \alpha C_a(\alpha, \beta_1) \\ R_r \leq (1-\alpha)C_2(1-\alpha) \\ R_s \leq (1-\alpha)C_0(1-\alpha, \beta_2) \\ R_r + R_s \leq (1-\alpha)C_b(1-\alpha, \beta_2) \end{cases}$$

(2.77)

with $\alpha, \beta_1, \beta_2 \in [0,1]$ and C_a, C_b defined in (2.76) and C_2, C_0 given by

$$C_0(\delta, \chi) = \log\det\left(\mathbf{I}_{n_d} + \frac{\chi P_s}{\delta n_s \sigma_{w_d}^2}\mathbf{H}_0\mathbf{H}_0^H\right) \quad C_2(\delta) = \log\det\left(\mathbf{I}_{n_d} + \frac{P_r}{\delta n_r \sigma_{w_r}^2}\mathbf{H}_2\mathbf{H}_2^H\right) \quad (2.78)$$

Because the rate region defined by (2.77) is a polyhedron and following similar steps as in protocol III in the time domain (2.67), [39], the boundary of the achievable rate region can be found as,

$$\max_{\alpha,\boldsymbol{\beta},R_r,R_s} \mu_r R_r + \mu_s R_s \quad s.t. \left(R_r, R_s\right) \in B_{fdd}\left(\alpha, \boldsymbol{\beta}\right) \tag{2.79}$$

for some positive μ_r, $\mu_s \in \mathfrak{R}_+$. The maximum is attained at some vertex of $B_{fdd}(\alpha,\boldsymbol{\beta})$ such that $\mu_r \geq \mu_s$. Equation (2.79) can be solved by convex optimization [41].

Protocol III

For protocol III in the frequency domain, the size and the power allocated to each phase at the source is optimized, (2.73). The following achievable rate region can be defined by the two messages of rate R_s and R_r, (2.63),

$$G_{fdd}\left(\alpha, \boldsymbol{\beta}\right) = \begin{cases} R_r \leq \alpha C_0\left(\alpha, \beta_1\right) + \left(1-\alpha\right) C_2\left(\alpha\right) \\ R_r \leq \alpha C_a\left(\alpha, \beta_1\right) \\ R_s \leq \left(1-\alpha\right) C_0\left(1-\alpha, \beta_2\right) \\ R_r + R_s \leq \alpha C_0\left(\alpha, \beta_1\right) + \left(1-\alpha\right) C_b\left(1-\alpha, \beta_2\right) \end{cases} \tag{2.80}$$

with $\alpha \in [0,1]$ and $\boldsymbol{\beta}$ defined in (2.73), C_a, C_b defined in (2.76) and C_2, C_0 defined in (2.78). In [39] it is shown that the boundary of the achievable rate region can be attained by maximizing,

$$\max_{\alpha,\boldsymbol{\beta},R_r,R_s} \mu_r R_r + \mu_s R_s \quad s.t. \left(R_r, R_s\right) \in G_{fdd}\left(\alpha, \boldsymbol{\beta}\right) \tag{2.81}$$

which is a convex problem and exists an optimal solution.

Comparison of dynamic DF protocols

The comparison of half-duplex protocols duplexed in frequency will be done using the simple scenario defined in Figure 2.11.

Additive white Gaussian noise (AWGN) channel

It will be assumed Gaussian channels and all the terminals equipped with a single antenna. Figure 2.27 presents the achievable rates at $SNR_0 = 0$ dB. It can be seen that protocol I and III obtain almost the same performance and protocol I is also better than forwarding and protocols IIA and IIB. When $SNR_0 = 10$ dB, Figure 2.28, forwarding and protocol IIA get a worse performance than direct transmission and protocol III is the best one (closely followed by protocol I). It is worth noticing that the performance obtained in the frequency domain is different of the one obtained in the time domain (Figure 2.22 and Figure 2.23) in terms of achievable rate and relation between protocols. For example, in the frequency domain protocol I is always superior to protocol IIA and IIB. The reason is due to the assumption of *power limited terminals*. In the time domain, the average transmitted power at the source depends of the protocol selected while in the frequency domain is kept constant. For protocol II the source is transmitting in the *relay-receive* and *relay-transmit phase* while protocol I only is using the first

phase, with maximum power. Therefore, in the time domain, protocol II can get better achievable rate at the cost of more required average power at the source. However, when the average power is kept constant at the source, protocol I outperforms protocol IIA and IIB.

SNR_0=0 dB destination d=1 Gaussian channel Frequency domain

Figure 2.27.- Maximum achievable rate vs. distance between the source and relay. Gaussian channel. Destination with SNR_0=0 dB. Frequency duplexing.

SNR_0=10 dB destination d=1 Gaussian channel Frequency domain
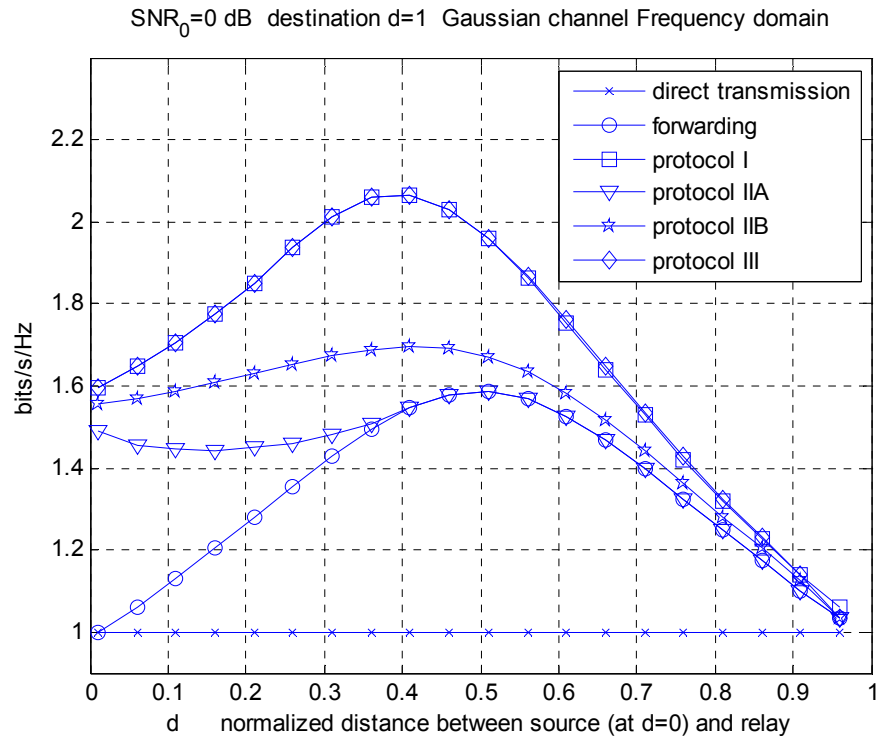

Figure 2.28.- Maximum achievable rate vs. distance between the source and relay. Gaussian channel. Destination with SNR_0= 10 dB. Frequency duplexing.

Multiple antenna and Rayleigh fading

Rayleigh fading channels will be assumed to evaluate the performance of the different half-duplex protocols with multiple antennas. The scenario considered will be that presented in Figure 2.11. Results are obtained in terms of average achievable rate (see *definition 2.1* in section 2.2.1.4) for the following combination of antennas (n_s, n_r, n_d): (1,1,1),(1,1,2), (2,1,1) and (2,2,2) at *low SNR* (SNR_0=0 dB).
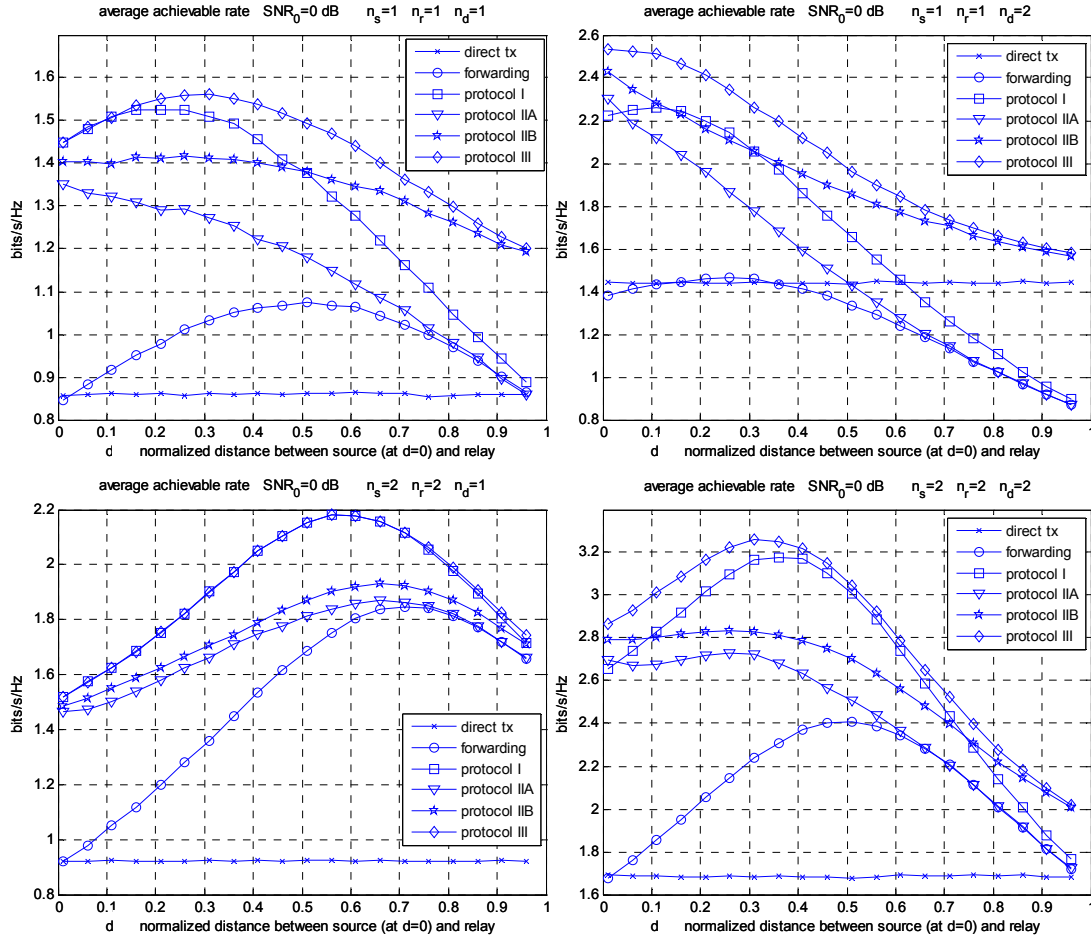
Figure 2.29.- Average achievable rate vs. distance between the source and relay. Rayleigh fading. Destination with SNR$_0$=0 dB. (top-left) n_s=1, n_r=1,n_d=1, **(top-right)** n_s=1, n_r=1, n_d=2, **(bottom-left)** n_s=2, n_r=2, n_d=1, **(bottom-right)** n_s=2, n_r=2, n_d=2.

Figure 2.29-(top-left) presents the case where the antenna configuration is n_s=n_r=n_d=1. It can be seen that protocol III is the best one. Protocol I and IIB also get a good performance depending on position of the relay, for d≤0.5 protocol I outperforms protocol IIB and for d≥0.5 the situation is the other way round. When the antennas at the destination (n_s=n_r=1 n_d=2 in Figure 2.29-(top-right)) or at the source (n_s=n_r=2 n_d=1 in Figure 2.29-(bottom-left)) are increased, the positions of the relay which produce the maximum gains of the protocols are moved to the source or destination, respectively. In the latest case, protocol I obtains almost the same performance of protocol III Figure 2.29-(bottom-left). When n_s=n_r=n_d=2 (Figure 2.29-(bottom-right)) the performance among protocols is similar to the single-antenna case, but now protocol I get better results than protocol IIB for a wider rage of relay positions.

2.3.3 Spectral efficiency with total power constraints

In this section we look into the efficiency of the relay-assisted transmission when there is a constraint on the average sum power of the three-terminal network, i.e the mutual information for a given amount of power used by the relay-assisted transmission (*spectral efficiency per unit total power*). The source is also transmitting the signals $\mathbf{x}_s^1$, $\mathbf{x}_s^2$ during the *relay-receive* and *relay-transmit phase*, respectively, and the relay is using $\mathbf{x}_r$ during the *relay-transmit phase*. All these signals are Gaussian with the following covariance matrices to keep an average sum-power (total) constraint,

$$\mathbf{Q}_s^1 = E\left\{\mathbf{x}_s^1 \mathbf{x}_s^{1H}\right\} = \frac{\beta_1 P}{n_s}\mathbf{I}_{n_s} \quad \mathbf{Q}_s^2 = E\left\{\mathbf{x}_s^2 \mathbf{x}_s^{2H}\right\} = \frac{\beta_2 P}{n_s}\mathbf{I}_{n_s} \quad \mathbf{Q}_r = E\left\{\mathbf{x}_r \mathbf{x}_r^{H}\right\} = \frac{\beta_3 P}{n_r}\mathbf{I}_{n_r}$$

$$Tr\left(\mathbf{Q}_s^1\right) = \beta_1 P \qquad Tr\left(\mathbf{Q}_s^2\right) = \beta_2 P \qquad Tr\left(\mathbf{Q}_r\right) = \beta_3 P \quad \beta_1 + \beta_2 + \beta_3 = 1$$

(2.82)

Since the transmission is done in orthogonal phases of total duration D, the source may transmit with power $\beta_1 P/\alpha D$ and $\beta_2 P/(1-\alpha)D$ in the *relay-receive* and *relay-transmit phase*, while the relay can use $\beta_3 P/(1-\alpha)D$ in the *relay-transmit phase*. This scheme can be analyzed in a similar way as the relay-assisted transmission in the frequency domain, but using the covariance matrices defined in (2.82).

Figure 2.30.- Maximum achievable rate vs. distance between the source and relay. Gaussian channel. Destination with $SNR_0=0$ dB. Average sum-power constraint.
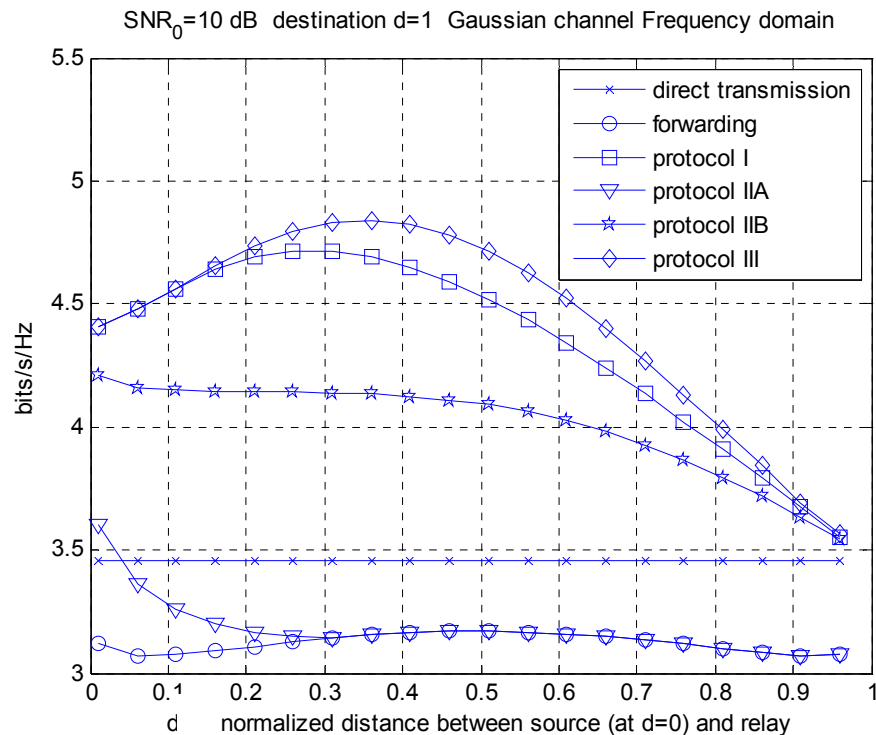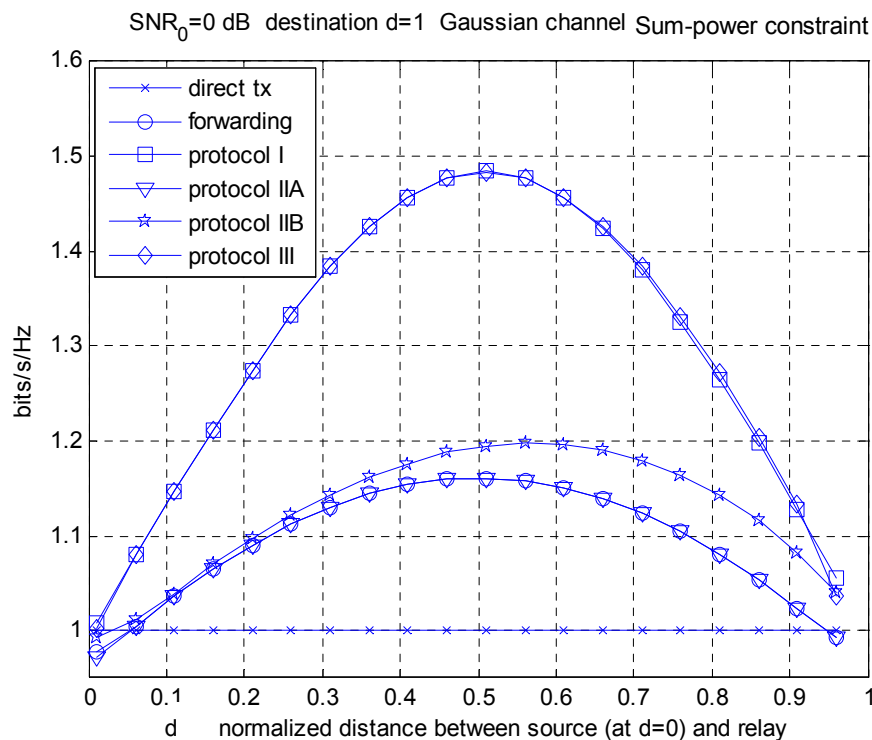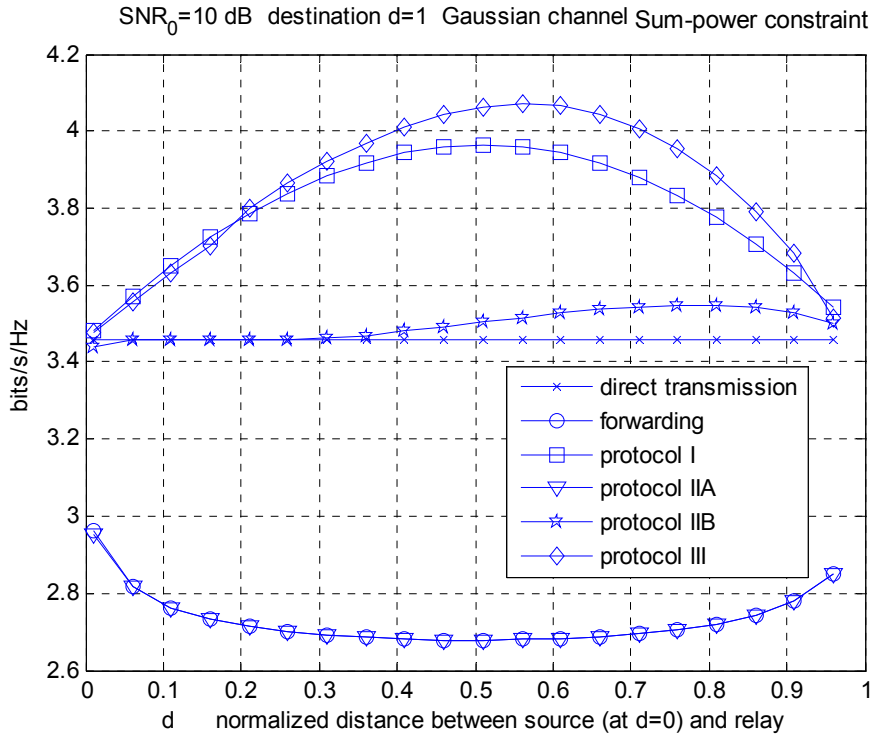
Figure 2.31.- Maximum achievable rate vs. distance between the source and relay. Gaussian channel. Destination with SNR_0= 10 dB. Average sum-power constraint.

Additive white Gaussian noise (AWGN) channel

Figure 2.30 and Figure 2.31 present the achievable rates of the half-duplex protocols when the efficiency of the transmission is considered at *low SNR* (SNR_0=0 dB) and *medium SNR* (SNR_0=10 dB), under the scenario depicted in Figure 2.11 with Gaussian channels and single-antenna terminals. In such a case, forwarding and protocol IIA get the same performance. For both SNR_0 values, protocol I obtains similar performance as protocol III, which is the best. Those protocols improve the direct transmission at *low* and *medium SNR*. On the other hand, the remaining protocols only are able to improve the direct transmission at SNR_0=0 dB (protocol IIB at SNR_0=10 dB get a slight improvement over the direct transmission).

Multiple antenna and Rayleigh fading

In the following the half-duplex protocols under Rayleigh fading and terminals equipped with multiple antennas are evaluated in the scenario presented in Figure 2.11. Results in terms of average achievable rate (see *definition 2.1* in section 2.2.1.4) consider the following combination of antennas (n_s, n_r, n_d): (1,1,1),(1,1,2), (2,1,1) and (2,2,2) at *low SNR* (SNR_0=0 dB).

In contrast to the Gaussian case, for the single antenna case n_s=n_r=n_d=1 and Rayleigh fading, Figure 2.32-(top-left), protocol I is outperformed by protocol IIB, which gets a steady performance independent of the position of the relay. Additionally, protocol IIA and forwarding are different, due to the independent channel coefficients in the relay-destination and source-destination link. When the antennas at the destinations increases, n_s=n_r=1 n_d=2, Figure 2.32-(top-right), the position of the relay for which the protocols get the maximum value is moved to the source. On the contrary, when the antennas at the source and relay are increased, n_s=n_r=2 n_d=1, Figure 2.32-(bottom-left), that relay positions are moved to the destination. In this case, protocol I can get a similar performance as the protocol III. Finally, when all the antennas are

increased $n_s=n_r=n_d=2$ Figure 2.32-(bottom-right), results are akin to the single antenna case, but now protocol I outperforms protocol IIB.
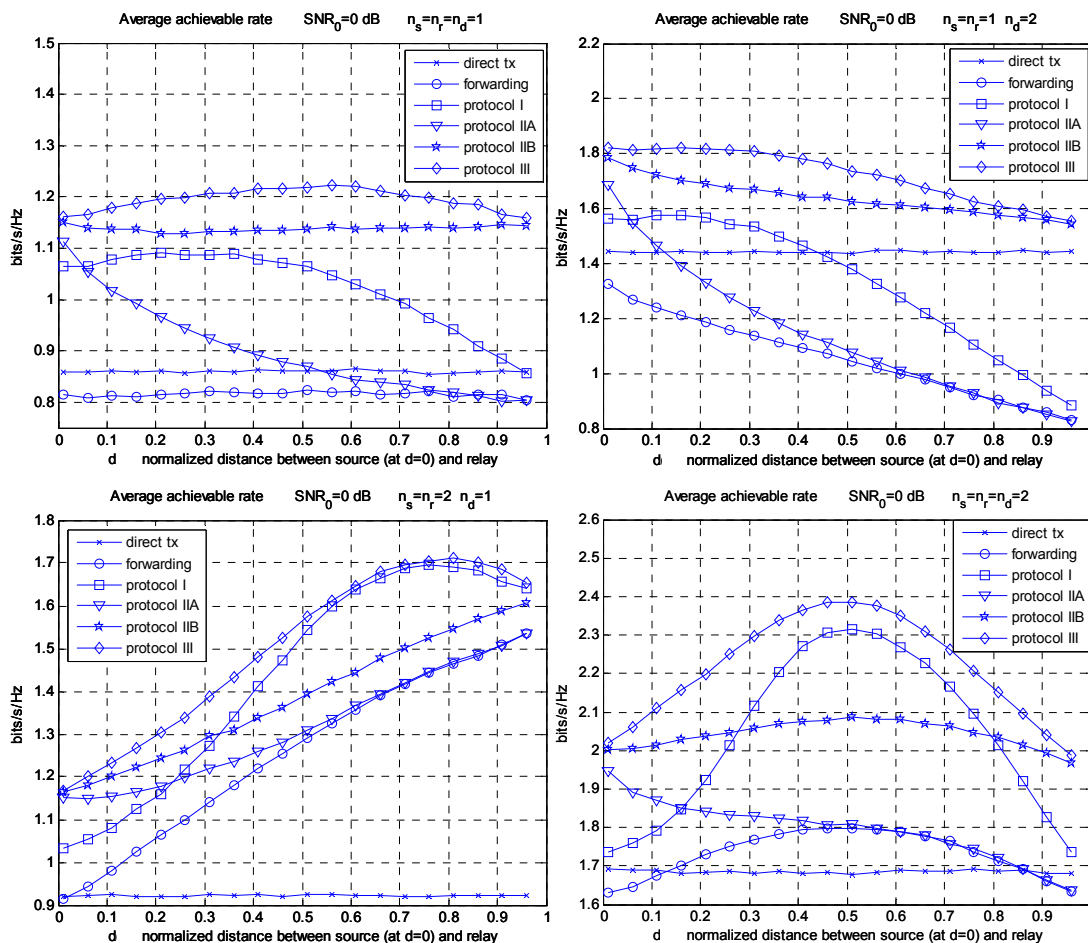
Figure 2.32.- Average achievable rate vs. distance between the source and relay. Rayleigh fading. Destination with SNR$_0$=0 dB. (top-left) n_s=1,n_r=1, n_d=1, (top-right) n_s =1, n_r=1, n_d=2, (bottom-left) n_s=2, n_r=2, n_d=1, (bottom-right) n_s=2, n_r=2,n_d=2. Average sum-power constraint.

Additive capacity gain of the relay-assisted transmission

Figure 2.33 shows the *additive gain* of the different protocols with *dynamic relaying* over the direct transmission in terms of outage mutual information (2.22), (see *definition 2.2* in section 2.2.1.4) with p_{out}=5% and Rayleigh fading channels. Our configuration assumes an average SNR$_0$=SNR$_2$=SNR in the source-destination and relay-destination link, and SNR$_1$=2×SNR (dB) in the source-relay link, the same configuration as the protocol I with *static relaying* (Figure 2.10). For single antenna terminals ($n_s=n_r=n_d$=1) protocol I and III get similar results when the *additive capacity gain* becomes steady (1.7 bits/s/Hz), enhancing protocol II. Additionally, protocol I with *dynamic relaying* is superior to the implementation with *static relaying* and *selective relaying*, (1.2 bits/s/Hz in Figure 2.10). When all terminals are equipped with 2 antennas, protocol III is able to get 3 bits/s/Hz.

Figure 2.34 sketches the outage mutual information with p_{out}=5% of the direct transmission as a function of the SNR of the source-destination link when $n_s=n_d$=1 and $n_s=n_d$=2. When the relay-assisted transmission gets a *steady additive capacity gain* of 1.7 bits/s/Hz for protocol III with $n_s=n_r=n_d$=1 (Figure 2.33) at SNR=20 dB, the direct transmission obtains 2.6 bits/s/Hz, so there is an improvement around 65% of the outage mutual information. But the improvement at

SNR=30 dB (where the direct transmission obtains an outage mutual information of 5.71 bits/s/Hz with $n_s=n_d=1$) is just around 30%. Under the configuration $n_s=n_r=n_d=2$ protocol III gets an improvement over the direct transmission at SNR=30 dB around 21%. For higher SNR values this improvement tends to decrease. Therefore, the impact of these *additive capacity gains* in the *high* SNR can be neglected.

Additive gain of the Outage mutual information over direct tx $p_{out}=5\%$

Figure 2.33.- Additive capacity gain of the outage mutual information (p_{out}=5%) over the direct transmission for protocol {I, II, III}, with SNR$_0$=SNR$_2$=SNR and SNR$_1$=2×SNR (dB).

outage mutual information $p_{out}=5\%$ direct transmission

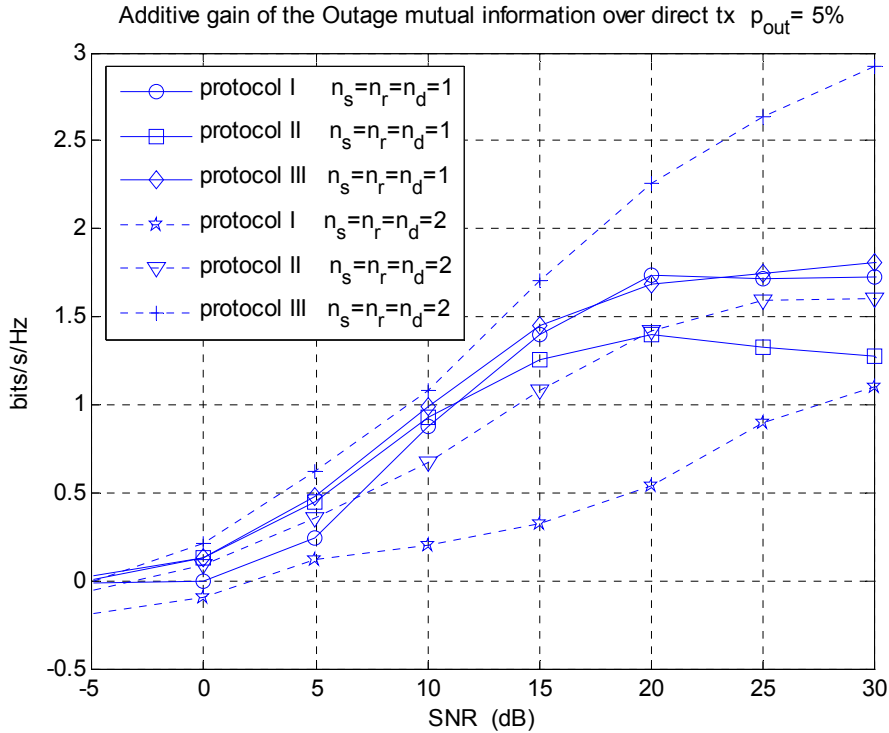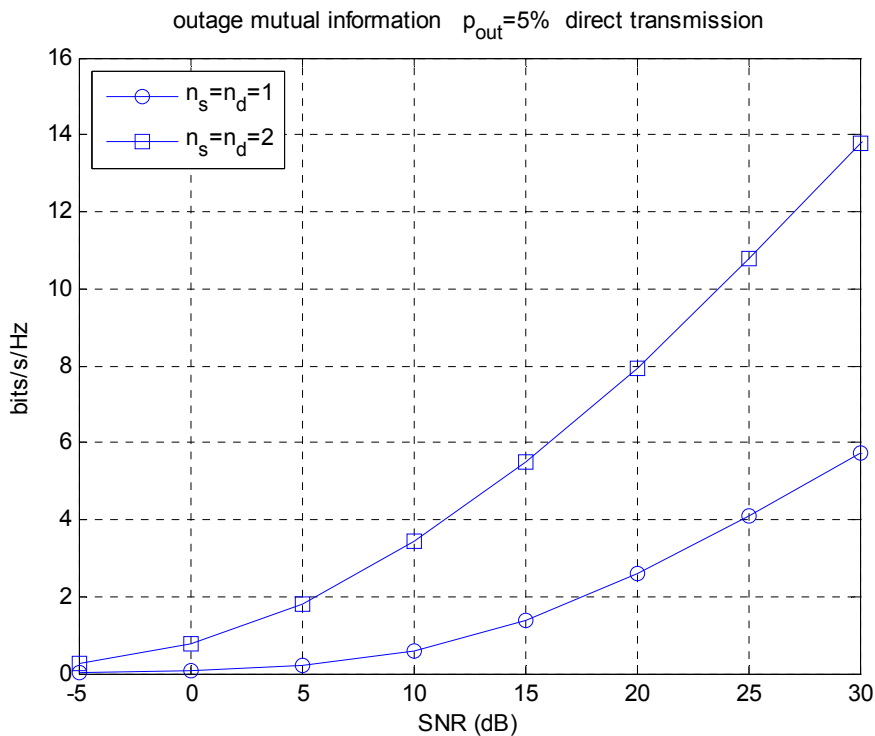**Figure 2.34.- Outage mutual information (p_{out}=5%) for the direct transmission. $n_s=n_r$={1,2}.**

2.4 Dynamic resource allocation relaying with multiple assisting relays

In this section we investigate the achievable rates when multiple *half-duplex* relay assist a single destination, see Figure 2.35. This scenario has been considered in [43] and [44] when the relays operate in *full-duplex* mode. In this work, we concentrate on the *half-duplex relays* and the proper resource allocation for the two phases of the transmission. Moreover, the relays only assist to the destination, i.e. they cannot assist among them. The *half-duplex* constraint at the relays generates a few difficulties when trying to adopt the schemes defined in [43] as how the transmission time between the two phases is selected, how the power is assigned, the optimum messaging or the coordination between relays. One possibility of using two assisting relays is described in [45][46] where both relays receive and transmit alternatively. On the contrary, here we assume that both relays are receiving or transmitting simultaneously.

The relay protocol is defined as follows: the source sends a signal to the relays and destination during the *relay-receive phase* (solid lines in Figure 2.35). In a subsequent phase, and after the relays have decoded and re-encoded the received messages, the source and relays simultaneously transmit during the *relay-transmit phase*, (dashed lines in Figure 2.35). This protocol is similar to protocol III defined in section 2.1.3 for single assisting relay. Two source transmission strategies are considered: either the relays receive *independent messages*, or both receive a *single common message*. In both cases we consider that either the transmitting terminals have a complete (and perfect) CSI of all links (*synchronous case*[14]) so distributed *eigenvector precoding* techniques can be considered or they do not have it (*asynchronous case*). This perspective has been presented in [47].

The optimum duration of each phase of the transmission and power allocation at the source and relays is obtained by maximizing the achievable rate. We formulate the problem for the case where the relays are receiving independent messages with CSI. Some other cases of practical interest (including the single relay-assisted transmission and the no-CSI case) can be seen as particularizations of that problem.

Figure 2.35.- Multiple half-duplex relay-assisted transmission.

[14] We adopt the definition from [12], where the distributed terminals have CSIT and additionally they have the carrier phase aligned (synchronized).

2.4.1 Signal model

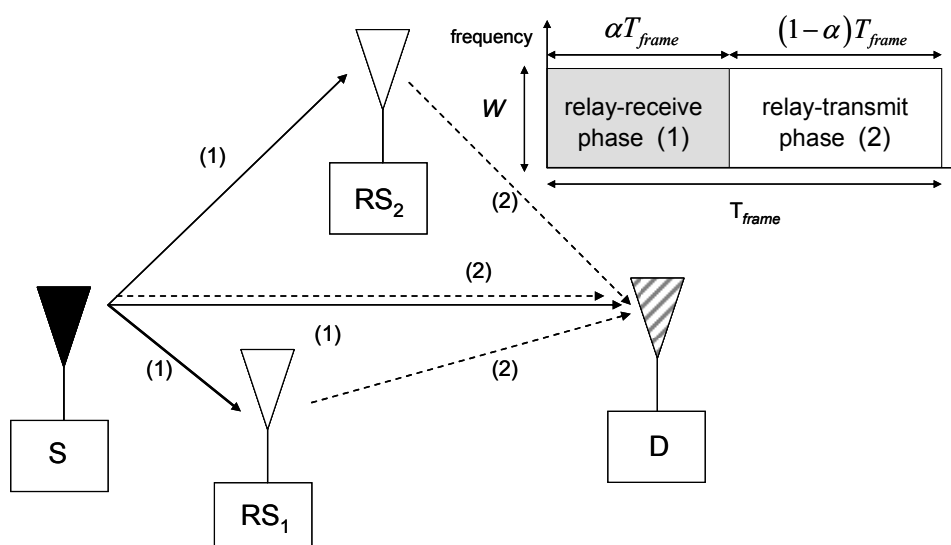It is assumed that all the terminals are equipped with a single antenna. In the following ρ_0 denotes the signal to noise (SNR) ratio in the source-destination link, $\rho_{1,i}$ and $\rho_{2,i}$ the SNR in the link between the source and the *i*-th relay (RS$_i$) and *i*-th relay and destination, respectively. All these values have been measured using power P at each terminal. The transmission is carried out in frames of length T_{frame} (s) and bandwidth *BW* (Hz) (both parameters will be normalized to one). The relays operate in *half-duplex* mode with a duration αT_{frame} and $(1-\alpha)T_{frame}$ for the *relay-receive* and *relay-transmit phase*, respectively. We will assume an *average sum power constraint* for all the terminals. An extension to the MIMO case should consider the achievable rate of the BC (Broadcast channel) with common information introduced in [48].

The signals received at the relays and destination during the *relay-receive phase* are ($0 \leq t \leq \alpha T_{frame}$),

$$y_{RS_1}(t) = \sqrt{\rho_{1,1}}\, e^{j\theta_{1,1}} x_0(t) + n_{RS_1}(t)$$
$$y_{RS_2}(t) = \sqrt{\rho_{1,2}}\, e^{j\theta_{1,2}} x_0(t) + n_{RS_2}(t) \tag{2.83}$$
$$y_D^{(1)}(t) = \sqrt{\rho_0}\, e^{j\theta_0} x_0(t) + n_D(t)$$

where n_D, n_{RS_1} and n_{RS_2} are the white Gaussian noise of unitary power at the different terminals. The channel gains are expressed in terms of amplitude (square root of the SNR of each link when the noise power is unitary) and the complex phase: θ_0, $\theta_{1,1}$ and $\theta_{1,2}$ for the source-destination, source-RS$_1$ and source-RS$_2$ links, respectively. Finally, x_0 is the signal transmitted by the source in this phase. On the other hand, the signal received during the *relay-transmit phase* at the destination is ($\alpha T_{frame} < t \leq T_{frame}$)

$$y_D^{(2)}(t) = \sqrt{\rho_0}\, e^{j\theta_0} x_3(t) + \sqrt{\rho_{2,1}}\, e^{j\theta_{2,1}} x_1(t) + \sqrt{\rho_{2,2}}\, e^{j\theta_{2,2}} x_2(t) + n_D(t) \tag{2.84}$$

where θ_0, $\theta_{2,1}$ and $\theta_{2,2}$ are the complex phases for the source-destination, RS$_1$-destination and RS$_2$-destination links, respectively. In this phase the assisting relays transmit the signals x_1 and x_2, while the source transmits x_3.

2.4.2 Independent messaging

In the scenario depicted in Figure 2.35 we will assume that the relay-assisted transmission sends independent messages to the relays. The transmission consists in three messages W_1, W_2 and W_3, at rates R_1, R_2 and R_3 respectively. The first two messages use the help of the relays and the third message is sent by the source only in the *relay-transmit phase*. The messages have associated different Gaussian codebooks. Table 2.9 depicts how the messages, terminals and codewords are connected along with the fractions of total power P used by each terminal. There, $\gamma_{0,i}$ with *i*={1,2,3} stands for the fraction of total power used by the source for transmitting the codewords $m_1^{(1)}, m_2^{(1)}, m_3^{(2)}$. The assisting relays which have decoded the messages W_1 and W_2, only transmit $m_1^{(2)}, m_2^{(2)}$ along with the source. The variable $\varphi_{j,i}$ with *j*={0,1,2} and *i*={1,2} defines the fraction of power allocated by the *j*-th terminal (*j*=0 corresponds to the source) to the *i*-th codeword. This is a general description, where some of the variables could be set directly to zero depending on the scenario definition, i.e. if RS$_1$ is able to decode both messages and RS$_2$ just the second one, then $\varphi_{2,1}$ will be zero.

Messages	W_1		W_2		W_3	
Phase	RR	RT	RR	RT	RR	RT
codewords	$m_1^{(1)}$	$m_1^{(2)}$	$m_2^{(1)}$	$m_2^{(2)}$	×	$m_3^{(2)}$
S	$\gamma_{0,1}$	$\varphi_{0,1}$	$\gamma_{0,2}$	$\varphi_{0,2}$	×	$\gamma_{0,3}$
RS_1	×	$\varphi_{1,1}$	×	$\varphi_{1,2}$	×	×
RS_2	×	$\varphi_{2,1}$	×	$\varphi_{2,2}$	×	×

Table 2.9.- Fraction of power P allocated by each terminal to each codeword used in each phase (RR for relay-receive and RT for relay-transmit phase).

2.4.2.1 Messages and codewords

During the *relay-receive phase* only the source is active and is broadcasting the messages W_1 and W_2 to the relays RS$_1$ and RS$_2$ using Gaussian signals of power $\gamma_{0,1}P$ and $\gamma_{0,2}P$, respectively, where $\gamma_{0,1}$ and $\gamma_{0,2}$ are fractions of total power P (see Table 2.9). Therefore the signal transmitted by the source x_0 in this period of time, see (2.83), can be written as,

$$x_0 = \sqrt{\gamma_{0,1}}\,m_1^{(1)} + \sqrt{\gamma_{0,2}}\,m_2^{(1)} \tag{2.85}$$

where $m_1^{(1)}, m_2^{(1)}$ are the Gaussian codewords of powers P associated to messages W_1 and W_2. In our single antenna scenario, we may assume that the *relay-receive phase* is a degraded channel [11], so one of the relays will be able to decode both messages, while the other relay will only decode one. During the *relay-transmit phase* the former relay can transmit to destination signals connected to both messages. For example, if RS$_1$ decodes both messages, then it might transmit two Gaussian signals with power $\varphi_{1,1}P$ and $\varphi_{1,2}P$ conveying message W_1 and W_2 respectively, while RS$_2$ will transmit a signal of power $\varphi_{2,2}P$ connected to the message W_2 and $\varphi_{2,1}$ in Table 2.9 will be zero. In the limiting case where the channel state from the source to both relays is equal, only one message is transmitted.

Afterwards, during the *relay-transmit phase* the source transmits two Gaussian signals with power $\varphi_{0,1}P$ and $\varphi_{0,2}P$ (see Table 2.9) devoted to help the transmission from the relays, as well as a new Gaussian signal of power $\gamma_{0,3}P$ connected to message W_3. The Gaussian signals transmitted from the different terminals in (2.84) are,

$$\begin{aligned}
x_1 &= \sqrt{\varphi_{1,1}}\,m_1^{(2)} + \sqrt{\varphi_{1,2}}\,m_2^{(2)} \\
x_2 &= \sqrt{\varphi_{2,1}}\,m_1^{(2)} + \sqrt{\varphi_{2,2}}\,m_2^{(2)} \\
x_3 &= \sqrt{\varphi_{0,1}}\,m_1^{(2)} + \sqrt{\varphi_{0,2}}\,m_2^{(2)} + \sqrt{\gamma_{0,3}}\,m_3^{(2)}
\end{aligned} \tag{2.86}$$

where $m_1^{(2)}, m_2^{(2)}, m_3^{(2)}$ denote the Gaussian codewords of power P associated to W_1, W_2 and W_3. It is worth noticing that equation (2.86) describes the general case. However, for the degraded channel where RS$_1$ is better than RS$_2$, then $\varphi_{2,1}$=0 because it cannot decode the message W_1. If RS$_2$ is better than RS$_1$, then $\varphi_{1,2}$=0 because it cannot decode the message W_2.

In order to obtain the spectral efficiency per unit total power, the fraction of power allocated to each of the different Gaussian codewords in (2.85) and (2.86) must satisfy the *average sum power constraint* considered here,

$$\sum_{j=1}^{3} \gamma_{0,j} + \sum_{j=1}^{2} \left(\varphi_{0,j} + \varphi_{1,j} + \varphi_{2,j} \right) = 1 \tag{2.87}$$

in which we are considering that at the source (relay) terminal the transmitted power is inversely proportional to the fraction of time allocated to the first (second) phase. In this regard, the different transmission schemes use the same total power. Other power constraints can be considered, for example an individual power constraint at the source and a sum-power constraint for all the relays. Their evaluation will be considered as a future work.

2.4.2.2 Achievable rate region

The achievable rate region described here depends on the maximum decodable rates of messages W_1 and W_2 at the relays during the *relay-receive phase* (denoted by the rate region $\mathcal{R}_{RS}$), as well as the decodable rates of messages W_1, W_2 and W_3 at the destination during both phases of the transmission (denoted by the rate region $\mathcal{R}_D$). In the first case, the rates of the messages W_1 and W_2 are defined by the degraded broadcast channel (BC) [11] to RS$_1$ and RS$_2$ transmitting the Gaussian codewords $m_1^{(1)}$ and $m_2^{(1)}$. Assuming that $\rho_{1,1} \geq \rho_{1,2}$ the data rates are given by

$$\mathcal{R}_{RS} = \begin{cases} R_1 \leq \alpha \log_2 \left(1 + \dfrac{\rho_{1,1}\gamma_{0,1}}{\alpha} \right) \\[4mm] R_2 \leq \alpha \log_2 \left(1 + \dfrac{\rho_{1,2}\gamma_{0,2}}{\alpha\left(1 + \rho_{1,2}\gamma_{0,1}\right)} \right) \end{cases} \tag{2.88}$$

where α is the duration of the *relay-receive phase*. Notice that in this case, RS$_1$ is able to decode both messages while RS$_2$ only can decode message W_2. The decodable rates of the different messages (using the codewords $m_1^{(2)}$, $m_2^{(2)}$ and $m_3^{(2)}$) can be seen as Multiple Access Channel (MAC) with three terminals [11] taking into consideration the signal received during the *relay-receive phase* at the destination. The achievable rate region is given by,

$$\mathcal{R}_D = \begin{cases} R_1 \leq f\left(\gamma_{0,1}\rho_0\right) + g\left(\kappa_1\right) \\ R_2 \leq f\left(\gamma_{0,2}\rho_0\right) + g\left(\kappa_2\right) \\ R_3 \leq g\left(\gamma_{0,3}\rho_0\right) \\ R_1 + R_2 \leq f\left(\left(\gamma_{0,1} + \gamma_{0,2}\right)\rho_0\right) + g\left(\kappa_1 + \kappa_2\right) \\ R_1 + R_3 \leq f\left(\gamma_{0,1}\rho_0\right) + g\left(\kappa_1 + \gamma_{0,3}\rho_0\right) \\ R_2 + R_3 \leq f\left(\gamma_{0,2}\rho_0\right) + g\left(\kappa_2 + \gamma_{0,3}\rho_0\right) \\ \displaystyle\sum_{j=1}^{3} R_j \leq f\left(\left(\gamma_{0,1} + \gamma_{0,2}\right)\rho_0\right) + g\left(\kappa_1 + \kappa_2 + \gamma_{0,3}\rho_0\right) \end{cases} \tag{2.89}$$

with the following definitions

$$f(x) = \alpha \log_2 \left(1 + \frac{x}{\alpha} \right) \quad g(x) = (1 - \alpha) \log_2 \left(1 + \frac{x}{1 - \alpha} \right) \tag{2.90}$$

$$\kappa_1 = \left(\sqrt{\varphi_{1,1}\rho_{2,1}} + \sqrt{\varphi_{0,1}\rho_0}\right)^2 \quad \kappa_2 = \left(\sqrt{\varphi_{2,2}\rho_{2,2}} + \sqrt{\varphi_{1,2}\rho_{2,1}} + \sqrt{\varphi_{0,2}\rho_0}\right)^2 \tag{2.91}$$

where κ_1 and κ_2 are the signal power of the Gaussian codewords $m_1^{(2)}$ and $m_2^{(2)}$ obtained from the assumption of *synchronous* transmission of the terminals (distributed *eigenvector precoding*). Moreover, it has been considered that $\varphi_{2,1}=0$ because RS$_2$ is not able to decode message W_1. Otherwise, the roles of RS$_1$ and RS$_2$ are exchanged.

2.4.2.3   Optimizing the resource allocation

The destination must be able to decode the messages W_1, W_2 and W_3 transmitted by the source and relays, so the resource allocation (which involves the duration of each phase α, and the power of the different codewords at the different terminals) can be obtained as the result of the following optimization problem,

$$\max_{\mathbf{z},R_1,R_2,R_3} R_1 + R_2 + R_3 \quad s.t. \quad (R_1,R_2,R_3) \in B_{ind}(\mathbf{z}) = \{\mathcal{R}_{RS} \cap \mathcal{R}_D\}$$

$$\mathbf{z} = \left[\alpha, \gamma_{0,1}, \gamma_{0,2}, \gamma_{0,3}, \varphi_{0,1}, \varphi_{0,2}, \varphi_{1,1}, \varphi_{1,2}, \varphi_{2,1}, \varphi_{2,2}\right] \tag{2.92}$$

$$\alpha \in [0,1] \quad \sum_{j=1}^{3}\gamma_{0,j} + \sum_{j=1}^{2}\left(\varphi_{0,j} + \varphi_{1,j} + \varphi_{2,j}\right) = 1$$

where B_{ind} is the rate region defined by the inequalities (2.88) and (2.89). This problem is not convex [41] due to the inequalities of $\mathcal{R}_{RS}$ in (2.88) which correspond to the achievable rate region of a degraded broadcast channel (in that case the capacity region). However, we can use the duality BC-MAC [49] to define the achievable rate region at the relays as,

$$\mathcal{R}_{RS} = \begin{cases} R_1 + R_2 \leq \alpha \log_2\left(1 + \dfrac{\lambda_1\rho_{1,1}}{\alpha} + \dfrac{\lambda_2\rho_{1,2}}{\alpha}\right) \\ s.t. \quad \lambda_1 + \lambda_2 = \gamma_{0,1} + \gamma_{0,2} \end{cases} \tag{2.93}$$

where the optimization is done over the variables λ_1 and λ_2. Those variables are related to $\gamma_{0,1}$ and $\gamma_{0,2}$ in the following way

$$\gamma_{0,1} = \lambda_1\frac{1}{1 + \rho_{1,2}\lambda_2} \qquad \gamma_{0,2} = \lambda_2\left(1 + \frac{\rho_{1,2}\lambda_1}{1 + \rho_{1,2}\lambda_2}\right) \tag{2.94}$$

Finally, the optimization problem given by (2.92) with B_{ind} defined by (2.93), (2.94) and (2.89) is convex.

2.4.3 Other transmission strategies

The transmission scheme presented above requires the use of successive cancellation receivers at the relay and destination terminals, as well as the knowledge of the channel state for all links, which may lead to some practical implementation problems in terms of complexity and information feedback. In the following some simplified strategies are detailed, which can be seen as particular cases of the transmission schemes defined in section 2.4.2.

2.4.3.1 Asynchronous transmission

When there is no CSI the terminals should transmit *asynchronously*. This implies the following changes,

$$\varphi_{0,1} = \varphi_{0,2} = 0, \quad \kappa_2 = \varphi_{2,2}\rho_{2,2} + \varphi_{1,2}\rho_{1,2} \tag{2.95}$$

2.4.3.2 Relays receiving a common message

The use of simple receivers implies forcing all the assisting relays to receive (and hence transmit) a common message, and hence no resources are allocated to the transmission of message W_1. Now the achievable rates at the relays are given by

$$\mathcal{R}_{RS} = \begin{cases} R_2 \leq f\left(\rho_{1,1}\gamma_{0,2}\right) \\ R_2 \leq f\left(\rho_{1,2}\gamma_{0,2}\right) \end{cases} \tag{2.96}$$

Additionally, the modifications to be considered for the *synchronous* and *asynchronous* transmission are,

$$Sync \begin{cases} \gamma_{0,1} = 0, \quad \kappa_1 = 0, \quad R_1 = 0, \quad \varphi_{0,1} = \varphi_{2,1} = \varphi_{1,1} = 0 \\ \kappa_2 = \left(\sqrt{\varphi_{0,2}\rho_0} + \sqrt{\varphi_{1,2}\rho_{2,1}} + \sqrt{\varphi_{2,2}\rho_{2,2}}\right)^2 \end{cases}$$

$$Async \begin{cases} \gamma_{0,1} = 0, \quad \kappa_1 = 0, \quad R_1 = 0, \\ \varphi_{0,1} = \varphi_{0,2} = \varphi_{2,1} = \varphi_{1,1} = 0, \kappa_2 = \varphi_{1,2}\rho_{2,1} + \varphi_{2,2}\rho_{2,2} \end{cases} \tag{2.97}$$

2.4.3.3 Single relay

The achievable rates for the single relay case are easily found by considering one assisting relay (e. g. RS$_1$). The particularizations for *synchronous* and *asynchronous* cases are,

$$Sync \begin{cases} \gamma_{0,2} = 0, \quad \kappa_2 = 0, \quad R_2 = 0, \quad \varphi_{0,2} = \varphi_{2,1} = \varphi_{2,2} = 0 \\ \varphi_{1,2} = 0, \quad \kappa_1 = \left(\sqrt{\varphi_{0,1}\rho_0} + \sqrt{\varphi_{1,1}\rho_{2,1}}\right)^2 \end{cases}$$

$$Async \begin{cases} \gamma_{0,2} = 0, \quad \kappa_2 = 0, \quad R_2 = 0, \quad \varphi_{1,2} = 0 \\ \varphi_{0,1} = \varphi_{0,2} = \varphi_{2,1} = \varphi_{2,2} = 0, \quad \kappa_1 = \varphi_{1,1}\rho_{2,1} \end{cases} \tag{2.98}$$

2.4.4 Results

The relay-assisted protocols defined previously are evaluated in a Gaussian scenario where the source-destination distance is normalized to 1. The RS$_1$ and RS$_2$ are placed at distance d_1 and d_2 from the source, and $(1-d_1)$ and $(1-d_2)$ from the destination. The path-loss of each link is proportional to the square of the distance between the terminals. The SNR of the different links is given by defining the ρ_0 (source-destination link),

$$\rho_{1,i} = \frac{P}{\sigma^2}\frac{1}{d_i^2} \quad \rho_{2,i} = \frac{P}{\sigma^2}\frac{1}{\left(1-d_i\right)^2} \quad \rho_0 = \frac{P}{\sigma^2} \quad i = \{1,2\} \tag{2.99}$$

The signal model defined in (2.83) and (2.84) will be assumed with the previous SNR definition. In our scenario the complex phases of the channels are equal to zero, (θ_0, $\theta_{1,1}$, $\theta_{1,2}$, $\theta_{2,1}$, and $\theta_{2,2}$) but this value only is known at the transmitters under CSI.
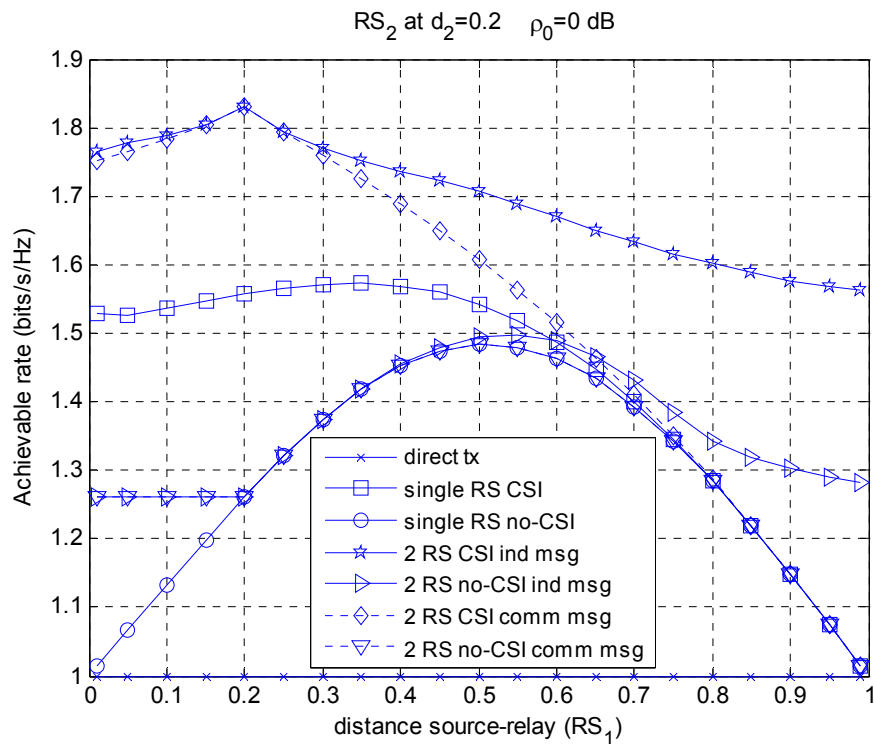

Figure 2.36.- Achievable rate for the single and 2-relays with/without CSI vs distance between source-RS$_1$, RS$_2$ at d_2=0.2. ρ_0=0 dB.
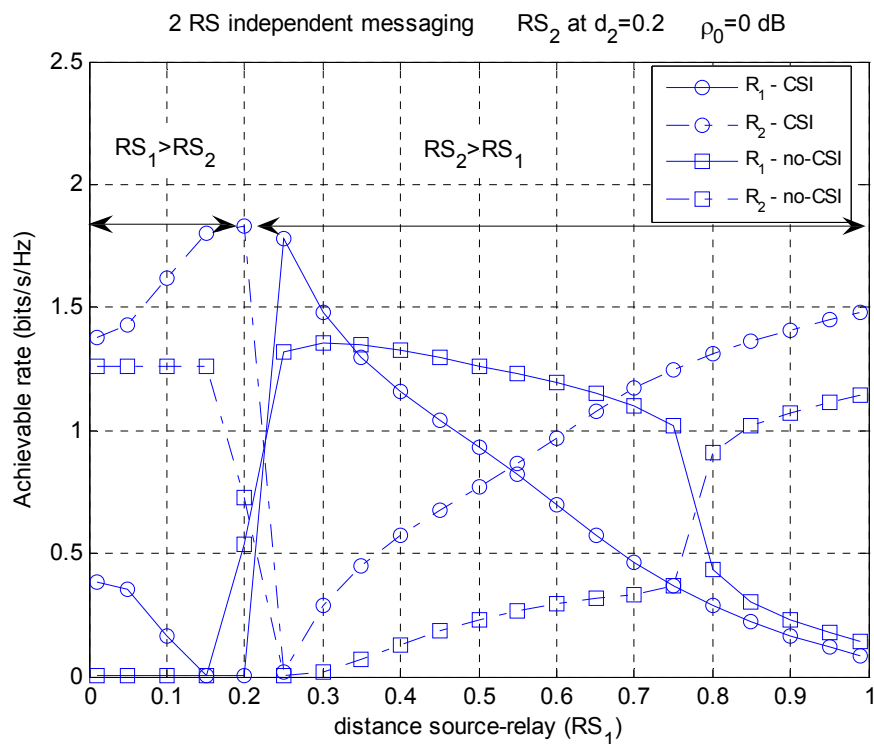

Figure 2.37.- Achievable rate of the messages for 2-relays with/without CSI *vs* distance between source-RS$_1$, RS$_2$ at d_2=0.2. ρ_0=0 dB. R_3=0.

Figure 2.36 presents the achievable rate for the transmission using a single relay placed at different positions when CSI is available (square-line) or not (circle-line). Notice that when the relay is close to the destination the source-relay link limits the communication and the performance obtained with and without CSI becomes the same. In fact, the CSI is helpful to deal with the case where relay-destination link limits the communication. Those rates are compared with *synchronous* and *asynchronous* transmission of *independent* or *common messaging* with two relays, being RS_2 placed at d_2=0.2. The best performance is obtained by the *synchronous* transmission of *independent messages*. When both relays are at the same distance d_1=d_2=0.2, *independent* and *common messaging* coincide. However, in certain configurations the adoption of a *common messaging* strategy provides no rate gains compared to the use of a single relay case, even when CSI is considered. The main drawback of *common messaging* is that the achievable rate is dominated by the relay with the worst channel quality. For the CSI case, there is a rate gain over a single relay case for $0 \leq d_1 \leq 0.65$. In that region, the relay-destination link limits the communication but thanks to the *synchronous* transmission of the two relays the equivalent link is improved. The source-relay channel limits the performance when RS_1 is close to the source and then RS_2 is not helpful. For the *asynchronous* transmission, *common messaging* does not offer any rate gain[15] for $0.2 \leq d_1 \leq 1$. However, for those positions of RS_1, *independent messaging* under *asynchronous* transmission improves the single relay case because the position of RS_1 does not limit the total transmission.

In order to analyze in more detail what happen with the *independent messaging*, Figure 2.37 sketches the rate of the different codewords as a function of the position of RS_1, being RS_2 placed at d_2=0.2. The codeword rate of message W_3 is zero for both cases for this scenario and it has not been included in Figure 2.37. R_1 and R_2 stand for the codeword rate through RS_1 and RS_2, respectively. When $0 \leq d_1 \leq 0.2$, RS_1 is able to decode the message intended to RS_2. Under the CSI case (*synchronous*), R_2 increases with d_1, while R_1 converges to zero at d_1=0.2. In such a case, a single message is transmitted to the relay with the worst channel link quality. Hence the performance of common and independent messaging is the same (see Figure 2.36). A similar conclusion can be obtained for no-CSI case (asynchronous), where R_1 is set to 0. When $0.2 < d_1 \leq 1$ the role of RS_2 and RS_1 are exchanged, explaining the discontinuity of the codeword rates at d_1=0.2. The codeword rates are adapted as a function of d_1.

Figure 2.38 and Figure 2.39 present results of *independent messaging* with ρ_0=10 dB and the RS_2 placed at d_2=0.2 and d_2=0.5 respectively. In all cases *independent messaging* with CSI exhibits a performance which is almost independent of the position of RS_1, and superior to the single relay case. Additionally, even if CSI is not considered, the use of an additional relay outperforms single relay transmission when RS_1 is close to the destination. In such a case, the achievable rate for the single relay case is limited by the source-relay link. However, the use of two relays (one near of the source and other close to destination) together with the optimization of allocated power and duration of the relay-transmission phases may deal with that drawback. On the other hand, in Figure 2.39 the RS_2 is placed at d_2=0.5 and in that case the *asynchronous* transmission obtains a performance almost equal for the different positions of the RS_1. The *synchronous* transmission (CSI) has worse performance than when RS_2 is placed at d_2=0.2 (Figure 2.38). For positions of RS_1 close to destination *synchronous* and *asynchronous* transmission with independent messaging have similar performance.

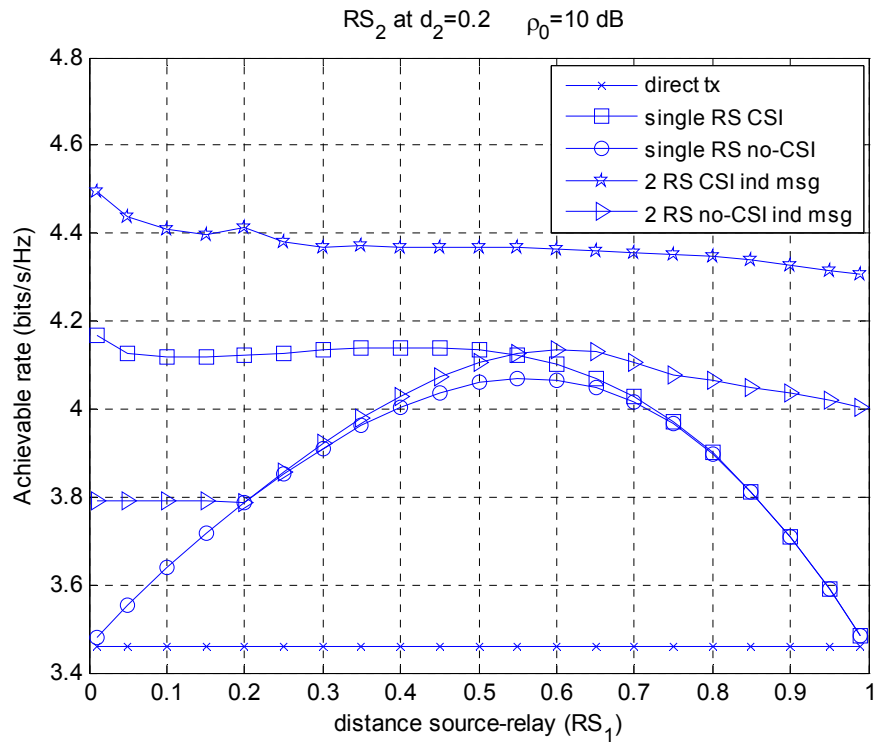[15] When the channel phases are random (as in fading channels), outage capacity gains are observed.

Figure 2.38.- Achievable rate for the single and 2-relays with/without CSI vs distance between source-RS$_1$, RS$_2$ at d_2=0.2. ρ_0=10 dB.
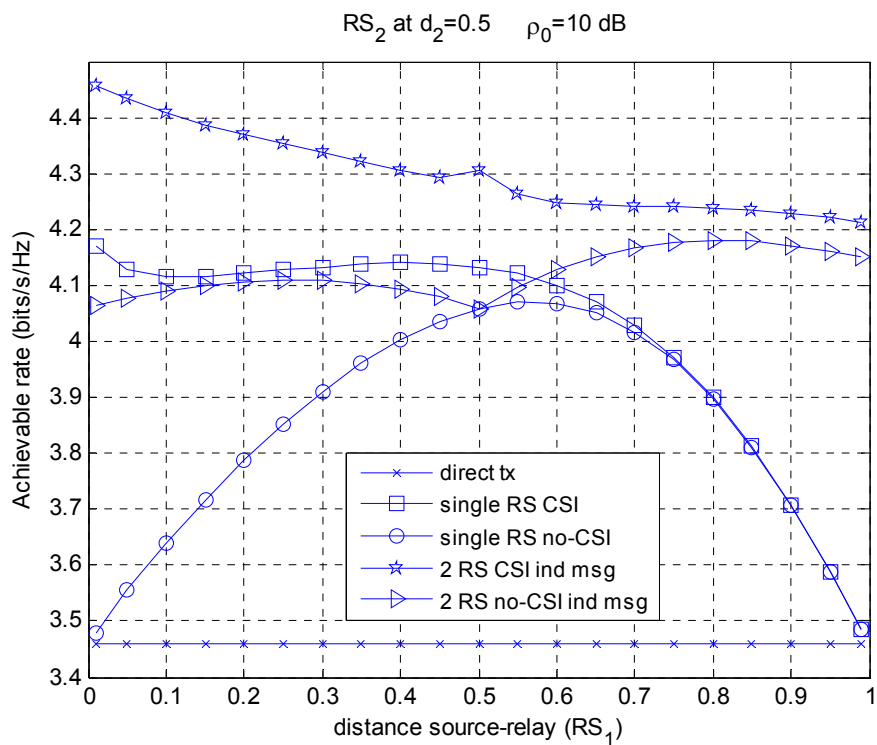

Figure 2.39.- Achievable rate for the single and 2-relays with/without CSI vs distance between source-RS$_1$, RS$_2$ at d_2=0.5. ρ_0=10 dB.

2.5 Chapter summary and conclusions

This chapter has looked into the *relay-assisted transmission* and *cooperative communication*, presenting an overview of the current state-of-art and providing new results. It has been shown that when *half-duplex* relays are employed, the resources are split in a *relay-receive* and *relay-transmit phase* which motivates that several protocols come up (*forwarding, protocol I, protocol II and protocol III*), Figure 2.3 and Figure 2.4. Moreover, the strategy of the relay-assisted transmission must consider the decoding operation at the relay (AF or DF) and either the resource allocation is fixed (*static resource allocation relaying*) or can be dynamically adjusted as a function of the channel quality of the different links (*dynamic resource allocation relaying*).

Section 2.2 has presented the performance of the half-duplex protocols with *static resource allocation relaying*. For DF-protocol I, the type of message transmitted by the relay has been investigated (*repetition* (RC) or *unconstrained coding* (UC)). It has shown that RC only is able to improve the direct transmission in terms of outage mutual information (see *definition 2.2* in section 2.2.1.4), while UC provides better gain than RC in terms of outage mutual information and a slight gain over the direct transmission in terms of average achievable rate (see *definition 2.1* in section 2.2.1.4). The *static resource allocation* does not consider the current quality of the different links and hence cannot adapt the amount of resources allocated to each phase. In order to improve the spectral efficiency for protocol I, an adaptive protocol (*selective relaying*) is analyzed. It exploits a limited feedback from the relay terminal for combating the events where the source-relay link presents a bad quality, in such a case, the source transmits again and the relay remains silent. Additionally, all the half-duplex protocols based on DF relays (with *repetition coding*) and AF are evaluated considering multiple antenna terminals and Rayleigh fading.

Dynamic resource allocation relaying has been investigated in section 2.3. The resource allocation for each phase of the relay-assisted transmission adapts to the current channel state in order to maximize the achievable rate of the half-duplex protocols. In this work the resource optimization has been done using three different constraints on the *average power* which account for the analysis of the relay-assisted transmission under different point of views:

- Source and relay transmit with *maximum power* on each phase (for relay-assisted transmission under TDD).

- Source and relay transmit with *individual average power* constraint.

- Source and relay transmit with *sum average power* constraint.

The first case can be found when the relay-assisted transmission is duplexed in the time-domain using *power limited terminals*. In that case the performance of the different protocols follows (2.72), see Table 2.7. The second case, *individual average power*, allows obtaining the same achievable rates when the relay-assisted transmission is duplexed in the frequency or time domain. The performance between protocols differs from the time domain with *power limited terminals*. First and second cases differ in the average power used by the three-terminal network. Finally, the *sum average power* constraint is considered to evaluate the half-duplex protocols in terms of efficiency per unit total power, i.e. comparing the direct and the relay-assisted transmission with the same average power. Results have shown that,

- Protocol III gets the largest gains for *low* and *medium SNR* under the three power constraints.

- Protocol I obtains similar performance to protocol III for *low* and *medium SNR* under the *individual average* and *sum-average power* constraints.

- Protocol IIB is able to improve the direct transmission for *low SNR* and the three types of power constraints and for *medium SNR* under *maximum* and *individual power* constraint.

- Forwarding and protocol IIA only can get better results than direct transmission for *low SNR.*

All half-duplex protocols with DF relay and multiple antennas under Rayleigh fading attain the maximum average achievable rate gains for $n_s, n_r \geq n_d$. Moreover, for the AF case, only it is required to increase the antennas at the source to improve the relay-assisted transmission, n_s.

Additionally, the *additive capacity gain* provided by the relay-assisted transmission over the direct transmission in terms of outage mutual information has been investigated for *static* and *dynamic resource allocation*. The *additive capacity gain* obtained in the second case is superior to the ones obtained by *static relaying*. This type of gain depends on the quality of the different links, but it becomes steady for some channel configuration where the SNR of the different links present medium to high values. The impact of the relay-assisted transmission is significant for *low* and *medium SNR* values, but at high SNR values, in spite of the additive gain the benefits of the relay-assisted transmission tend to decrease.

Finally, the achievable rate gains of multiple relay transmission schemes based on decode-and-forward and dynamic relaying, under different conditions of CSI and complexity of decoding has been investigated in section 2.4. When there is complete CSI the source and relay can transmit *synchronously* the same message (*eigenvector precoding*). Otherwise, the transmission is *asynchronous*. Two techniques are evaluated for transmitting messages intended to each relay, *independent* or *common messaging*. Moreover, the single-relay case can be seen as a particularization of those techniques. The resource allocation problem based on rate optimization is shown to be convex for both techniques. It is found that for the Gaussian channel the use of multiple relays outperforms the single relay case when *synchronous* transmissions are possible, due to the *eigenvector precoding*. Additionally, when one of the relays is placed near the source, independent messaging with *synchronous* transmission allows a quasi constant achievable rate irrespective of the position of the other relay. If one of the relays is placed half way between the source and destination, then *asynchronous* transmission get a performance not dependant of the position of the second relay.

2.6   Appendix A. Proof of proposition 1

Proof of proposition 1: It suffices to realize that this particular channel is in fact a compound channel [31],[32] where the set of possible probabilities is by $p_1(\mathbf{y}_1 \mid \mathbf{x}_a)$ and $p_2(\mathbf{y}_2 \mid \mathbf{x})$, as is depicted in Figure 2.6. We consider that no error happens only when both receivers decode the transmitted message W without error,

$$\Pr(\text{no error}) = \Pr\left(\hat{W}_1 = W \text{ and } \hat{W}_2 = W\right)$$

where $\hat{W}_1$ and $\hat{W}_2$ are the messages decode by both receivers. Hence, the corresponding model is a compound channel with an uninformed transmitter of the channel transition probability and the capacity expression given by (2.6) follows.

This result can be alternatively proved in a direct way without referring to compound channels, following the ideas in [11] for the case of a known transition probability.

2.7   Appendix B. Achievable rate region of protocol III

We derive here the achievable rate region of equation (2.67). Although the achievable sum-rate for the decode and forward relay channel is known [12], we require the definition of the region so as to be able to extend the relay transmission to the multiple user case with half-duplex relays.

Let us assume the conventional MAC channel [11], two nodes transmitting independent messages of length *n* symbols, $X_{1,1}, X_{1,2}, \ldots X_{1,n}$ and $X_{2,1}, X_{2,2}, \ldots X_{2,n}$ with rate R_r and R_s, respectively. Both are transmitting to a common destination which is receiving the message $Y_1, Y_2, \ldots Y_n$ corrupted by Gaussian noise,

$$Y_k = X_{1,k} + X_{2,k} + N_k \qquad k = 1 \ldots n \tag{2.100}$$

This channel is the MAC channel with capacity region is given by,

$$\begin{cases} nR_r \leq \displaystyle\sum_{k=1}^{n} I\left(X_{1,k}; Y_k \mid X_{2,k}\right) \qquad nR_s \leq \displaystyle\sum_{k=1}^{n} I\left(X_{2,k}; Y_k \mid X_{1,k}\right) \\[4mm] n\left(R_s + R_r\right) \leq \displaystyle\sum_{k=1}^{n} I\left(X_{1,k}, X_{2,k}; Y_k\right) \end{cases} \tag{2.101}$$

In the following it will be shown that the half-duplex relay channel with decode and forward at the relay can be seen as MAC channel. There are two orthogonal phases, see the signal model in (2.63), (*relay-receive* and *relay-transmit phase*). Furthermore, the relay only is able to help the destination during *relay-transmit phase* using the data received in *relay-receive phase* from the source. The destination is receiving in both periods. In this scenario we can identify two *virtual* users: the first, named *source-relay virtual user*, is transmitting in two parallel channels from the source (in *relay-receive phase* with αn symbols) and the relay (in *relay-transmit phase* with $(1-\alpha)n$ symbols); the second one (*source-only virtual user*) is the source transmitting in

relay-transmit phase ((1-α)*n* symbols). Both virtual users are transmitting independent messages, $X_{1,1}, X_{1,2}, \ldots X_{1,n}$ and $X_{2,1}, X_{2,2}, \ldots X_{2,n}$, respectively. The message of the *source-relay virtual user* is given by,

$$X_{1,k} = \begin{cases} X_{a,k} & k = 1 \ldots \lfloor \alpha n \rfloor \\ X_{b,k} & k = \lfloor \alpha n \rfloor + 1 \ldots n \end{cases} \tag{2.102}$$

where $X_{a,k}$ and $X_{b,k}$ denote the messages transmitted from the source and relay terminal. Therefore the equation defined in (2.101) will be modified in the following way. The achievable rate of the *source-relay virtual user* using decode and forward at the relay is given by the two constraints of the conventional relay channel [11],

$$\begin{cases} nR_r \le \sum_{k=1}^n I\left(X_{a,k}; \tilde{Y}_k \mid X_{b,k}, X_{2,k}\right) = \sum_{k=1}^{\lfloor \alpha n \rfloor} I\left(X_{a,k}; \tilde{Y}_k \mid X_{2,k}\right) \\ nR_r \le \sum_{k=1}^n I\left(X_{a,k}, X_{b,k}; Y_k \mid X_{2,k}\right) = \\ \qquad \sum_{k=1}^{\lfloor \alpha n \rfloor} I\left(X_{a,k}; Y_k \mid X_{2,k}\right) + \sum_{k=\lfloor \alpha n \rfloor + 1}^n I\left(X_{b,k}; Y_k \mid X_{2,k}\right) \end{cases} \tag{2.103}$$

with $\tilde{Y}_k$ being the signal received at the relay corrupted with Gaussian noise. The rate for the *source-only virtual user*, transmitting only in the *relay-transmit* phase, is given by,

$$nR_s \le \sum_{k=1}^n I\left(X_{2,k}; Y_k \mid X_{1,k}\right) = \sum_{k=\lfloor \alpha n \rfloor + 1}^n I\left(X_{2,k}; Y_k \mid X_{1,k}\right) \tag{2.104}$$

Finally, the constraint over the sum of the rates is given by

$$n\left(R_s + R_r\right) \le \sum_{k=1}^{\lfloor \alpha n \rfloor} I\left(X_{a,k}; Y_k\right) + \sum_{k=\lfloor \alpha n \rfloor + 1}^n I\left(X_{b,k}, X_{2,k}; Y_k\right) \tag{2.105}$$

2.8 Appendix C. Relation between protocol I and II in repetition coding

The expressions for the mutual information of protocol I and protocol II (assuming that source-relay link is not limiting the total expressions) depend on,

$$C_b^I = \log \det \left(\mathbf{I}_{2n_d} + \frac{P_s}{\sigma^2 n_s} \begin{bmatrix} \mathbf{H}_0 \\ \varphi \mathbf{H}_2 \end{bmatrix} \begin{bmatrix} \mathbf{H}_0^H & \varphi \mathbf{H}_2^H \end{bmatrix} \right) \tag{2.106}$$

$$C_b^{II} = \log \det \left(\mathbf{I}_{n_d} + \frac{P_s}{\sigma^2 n_s} \begin{bmatrix} \mathbf{H}_0 & \varphi \mathbf{H}_2 \end{bmatrix} \begin{bmatrix} \mathbf{H}_0^H \\ \varphi \mathbf{H}_2^H \end{bmatrix} \right) = \log \det \left(\mathbf{I}_{n_d} + \frac{P_s}{\sigma^2 n_s} \left(\mathbf{H}_0 \mathbf{H}_0^H + \varphi^2 \mathbf{H}_2 \mathbf{H}_2^H \right) \right) \tag{2.107}$$

with $\mathbf{H}_0$ and $\mathbf{H}_2$ of dimensions $n_d \times n_s$ and $n_d \times n_r$, respectively, and σ^2 the noise power. Because we are considering repetition coding, $n_s = n_r$ by definition in section 2.2.2. The motivation of this

section is obtain the conditions when protocol I is better than protocol II. The following determinant property will be considered,

$$\det\left(\mathbf{I}_n + \mathbf{AB}\right) = \det\left(\mathbf{I}_m + \mathbf{BA}\right) \tag{2.108}$$

where $\mathbf{A}$ and $\mathbf{B}$ are matrices of dimensions $n{\times}m$ and $m{\times}n$, respectively.

Applying the determinant property (2.108) to the expression for protocol I, (2.106), it can be rewritten as,

$$C_b^I = \log\det\left(\mathbf{I}_{n_s} + \frac{P_s}{\sigma^2 n_s}\left[\mathbf{H}_0^H \quad \varphi\mathbf{H}_2^H\right]\begin{bmatrix}\mathbf{H}_0 \\ \varphi\mathbf{H}_2\end{bmatrix}\right) = \log\det\left(\mathbf{I}_{n_s} + \frac{P_s}{\sigma^2 n_s}\left(\mathbf{H}_0^H\mathbf{H}_0 + \varphi^2\mathbf{H}_2^H\mathbf{H}_2\right)\right) \tag{2.109}$$

✚ If $n_s = n_d$,

For this configuration, the eigenvalues of $\mathbf{H}_0\mathbf{H}_0^H$ and $\mathbf{H}_2\mathbf{H}_2^H$ are the same as the eigenvalues of $\mathbf{H}_0^H\mathbf{H}_0$ and $\mathbf{H}_2^H\mathbf{H}_2$, respectively. Therefore, equations (2.107) and (2.109) are equal, $C_b^I = C_b^{II}$

✚ If $n_s < n_d$

In this case, the mutual information for protocol II (2.107) can be written in the following way by using the property (2.108),

$$C_b^{II} = \log\det\left(\mathbf{I}_{2n_s} + \frac{P_s}{\sigma^2 n_s}\begin{bmatrix}\mathbf{H}_0^H\mathbf{H}_0 & \varphi\mathbf{H}_0^H\mathbf{H}_2 \\ \varphi\mathbf{H}_2^H\mathbf{H}_0 & \varphi^2\mathbf{H}_2^H\mathbf{H}_2\end{bmatrix}\right) \tag{2.110}$$

For $n_s{=}1$ and $n_d{>}1$, the previous equation is given by,

$$C_b^{II} = \log\det\left(\mathbf{I}_2 + \frac{P_s}{\sigma^2 n_s}\begin{bmatrix}\mathbf{h}_0^H\mathbf{h}_0 & \varphi\mathbf{h}_0^H\mathbf{h}_2 \\ \varphi\mathbf{h}_2^H\mathbf{h}_0 & \varphi^2\mathbf{h}_2^H\mathbf{h}_2\end{bmatrix}\right) = \log\left(1 + \frac{P_s}{\sigma^2}\left(\mathbf{h}_0^H\mathbf{h}_0 + \varphi^2\mathbf{h}_2^H\mathbf{h}_2 + \varphi^2\Delta_1\right)\right)$$

with $\mathbf{h}_0$ and $\mathbf{h}_2$ column vectors that contains the channel coefficients of the source-destination and relay-destination link, and Δ_1 given by,

$$\Delta_1 = \mathbf{h}_0^H\mathbf{h}_0\mathbf{h}_2^H\mathbf{h}_2 - \mathbf{h}_0^H\mathbf{h}_2\mathbf{h}_2^H\mathbf{h}_0 \tag{2.111}$$

However, the previous equation can also been defined in the following way,

$$\Delta_1 = \det\left(\begin{bmatrix}\mathbf{h}_0^H\mathbf{h}_0 & \mathbf{h}_0^H\mathbf{h}_2 \\ \mathbf{h}_2^H\mathbf{h}_0 & \mathbf{h}_2^H\mathbf{h}_2\end{bmatrix}\right) = \det\left(\Psi\right) \tag{2.112}$$

where the matrix Ψ is semi-definite positive by construction, so Δ_1 is always greater or equal to 0. Likewise, that means that protocol II (2.110) provides larger mutual information values than protocol I (2.109), $C_b^I \le C_b^{II}$, for such antenna configuration.

When n_d>1, it is more difficult to prove analytically the previous proposition. For that reason, in the following we will show experimental results that confirms the previous assert, investigating the values of

$$\phi = C_b^{II} - C_b^{I}$$

(2.113)

Figure 2.40 presents the cumulative density function (CDF) of ϕ (Pr(ϕ <x_0) with x_0 the value of the *x*-axis) defined in (2.113). It has assumed a large number of independent Rayleigh fading realizations for the channel, $P_s/\sigma^2 = 10$ and different antenna configurations {n_s=1, n_d=2} (crosses), {n_s=2, n_d=3} (circles) and {n_s=3, n_d=6} (diamonds). For all those configurations where n_s<n_d, ϕ is always greater than 0. For example for {n_s=2,n_d=3} the 90% of different channel realizations the variable ϕ>1 bps/Hz, while for {n_s=3, n_d=6} ϕ>4 bps/Hz.
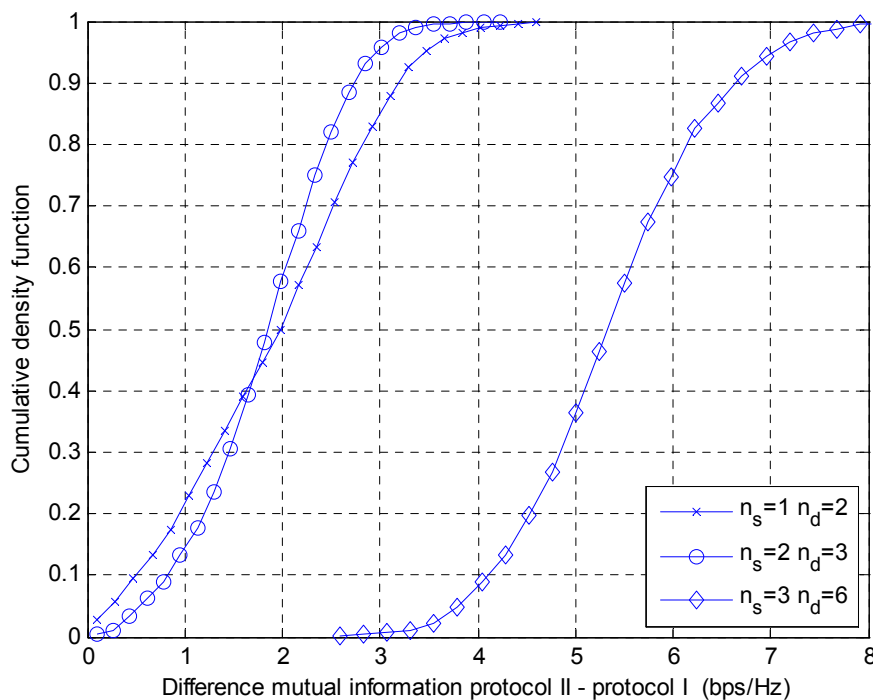
Figure 2.40.- CDF of the difference between protocol II and protocol I. {n_s=1,n_d=2}, {n_s=2, n_d=3} and {n_s=3, n_d=6}. $P_s/\sigma^2 = 10$.

◻ If n_s>n_d

For this antenna configuration, similar steps can be done as in the previous section, but now assuming that the mutual information of protocol I can be written as,

$$C_b^{I} = \log \det \left(\mathbf{I}_{2n_d} + \frac{P_s}{\sigma^2 n_s} \begin{bmatrix} \mathbf{H}_0 \mathbf{H}_0^H & \varphi \mathbf{H}_0 \mathbf{H}_2^H \\ \varphi \mathbf{H}_2 \mathbf{H}_0^H & \varphi^2 \mathbf{H}_2 \mathbf{H}_2^H \end{bmatrix} \right)$$

(2.114)

and this equation has to be compared with protocol II, C_b^{II} defined in (2.107).

For n_d=1 and n_s>1, the previous equation is given by,

$$C_b^I = \log\det\left(\mathbf{I}_2 + \frac{P_s}{\sigma^2 n_s}\begin{bmatrix} \mathbf{h}_0^H\mathbf{h}_0 & \varphi\mathbf{h}_0^H\mathbf{h}_2 \\ \varphi\mathbf{h}_2^H\mathbf{h}_0 & \varphi^2\mathbf{h}_2^H\mathbf{h}_2 \end{bmatrix}\right) = \log\left(1 + \frac{P_s}{\sigma^2 n_s}\left(\mathbf{h}_0^H\mathbf{h}_0 + \varphi^2\mathbf{h}_2^H\mathbf{h}_2 + \varphi^2\Delta_1\right)\right)$$

where $\mathbf{h}_0$ and $\mathbf{h}_2$ stand for column vectors that contains the channel coefficients of the source-destination and relay-destination link. In fact, that channel coefficients are in the row of matrix $\mathbf{H}_0$ and $\mathbf{H}_2$ of dimensions ($n_d \times n_s$) of (2.114). Additionally, Δ_1 given by,

$$\Delta_1 = \mathbf{h}_0^H\mathbf{h}_0\mathbf{h}_2^H\mathbf{h}_2 - \mathbf{h}_0^H\mathbf{h}_2\mathbf{h}_2^H\mathbf{h}_0 \tag{2.115}$$

which also can be obtained as a result of the determinant of a semi-definite positive matrix, as in (2.112). The previous equation has to be compared with C_b^{II},

$$C_b^{II} = \log\det\left(1 + \frac{P_s}{\sigma^2 n_s}\left(\mathbf{h}_0^H\mathbf{h}_0 + \varphi^2\mathbf{h}_2^H\mathbf{h}_2\right)\right)$$

Therefore, the comparison between C_b^I and C_b^{II} follow similar guidelines as in the previous case, although now for $n_s > n_d$, $C_b^I \geq C_b^{II}$.

2.9 References

[1] I.E.Telatar, "Capacity of multi-antenna Gaussian channels", *European Transactions on Telecommunications*, vol. 10, pp. 585-595, Nov/Dec 1999.

[2] G.Foschini, M.J.Gans, "On limits of wireless communications in a fading environment when using multiple antennas", *Wireless Personal Communications*, vol. 6, no. 3, pp. 311-335, 1998.

[3] L.Zheng, D.N.C.Tse, "Diversity and multiplexing: A fundamental tradeoff in multiple antenna channels", *IEEE Trans. on Information Theory*, vol. 49, no. 5, pp. 1073-1096, May 2003.

[4] A.Sendonaris, E.Erkip, B.Aazhang, "User cooperation diversity-part I: System description", *IEEE Trans. on Communications*, vol. 51, no. 11, pp. 1927-1938, Nov. 2003.

[5] J.Laneman, D.N.C.Tse, G.W.Wornell, *"*Cooperative diversity in wireless networks: Efficient protocols and outage behavior*"*, *IEEE Trans. Information Theory*, vol. 50 no. 12, pp. 3062 – 3080. Dec. 2004.

[6] A.Wittneben, B.Rankov, "Impact of cooperative relays on the capacity of rank deficient MIMO channels", in *Proc. IST Mobile & Wireless Communications Summit* (IST-2003), Aveiro (Portugal), June 2003.

[7] M.Dohler, "Virtual Antenna Arrays", PhD Thesis, King's College London, London, UK, 2003.

[8] M.Dohler, E. Lefranc, A.H. Aghvami, "Virtual Antenna Arrays for Future Wireless Mobile Communication Systems", ICT 2002, Conference CD-ROM, Beijing, China, June 2002.

[9] E.C. van der Meulen, "Three-terminal communication channels", *Adv. Appl. Prob.*, vol. 3, pp. 120-154, 1971.

[10] T.M.Cover, A.A. El Gamal, "Capacity theorems for the relay channel", *IEEE Trans. on Information Theory*, vol. 25, no. 5, pp. 474-584, Sept. 1979.

[11] T.M.Cover, J.A. Thomas. *Elements of Information Theory*. John Wiley & Sons, 1991.

[12] A.Host-Madsen, J.Zhang, "Capacity bounds and power allocation for wireless relay channels", *IEEE Trans. on Information Theory*, vol. 51, no. 6, pp. 2020-2040, June 2005.

[13] B.Wang, J.Zhang, A.Host-Madsen, "On the capacity of MIMO relay channels", *IEEE Trans. on Information Theory*, vol. 51, no. 1, pp 29-43, Jan. 2005.

[14] A.Host-Madsen, "Capacity bounds for cooperative diversity", *IEEE Trans. on Information Theory*, vol 52, no. 4, pp. 1522-1544, April 2006.

[15] N.Jindal, U.Mitra, A.Goldsmith, "Capacity of ad-hoc networks with node cooperation", in *Proc. IEEE International Symposium of Information Theory* (ISIT-2004), Chicago (USA), June 2004.

[16] A.Host-Madsen, A.Nosratinia, "The multiplexing gain of wireless networks", in *Proc. IEEE International Symposium of Information Theory* (ISIT-2005), Adelaide, Australia, pp. 2310-2314, Sep. 2005.

[17] A.Sendonaris, E.Erkip, B.Aazhang, "User cooperation diversity-part II: Implementation aspects and performance analysis", *IEEE Trans. on Communications*, vol. 51, no. 11, pp. 1939-1948, Nov. 2003.

[18] O.Muñoz, J.Vidal, A.Agustin, "Linear transceiver design in nonregenerative relays with channel state information", *IEEE Trans. on Signal Processing*, vol. 44, no. 6, pp. 2593-2604. June 2007.

[19] O.Muñoz, J.Vidal, A.Agustin, "Non-regenerative MIMO relaying with channel state information", in *Proc. IEEE International Conference on Acoustics, Speech and Signal Processing* (ICASSP-2005), Philadelphia, USA, March 2005.

[20] J.N.Laneman, G.W.Wornell, "Distributed Space-Time Coded protocols for exploiting Cooperative Diversity in Wireless Networks", *IEEE Trans. on Information Theory*, vol. 49, no. 10, pp. 2415-2425, Oct. 2003.

[21] M.C.Valenti, B.Zhao, "Distributed turbo codes: Towards the capacity of the relay channel", in *Proc. IEEE Vehicular Technology Conf. Fall* (VTC-Fall 2003), Orlando, FL, Oct. 2003.

[22] A.Agustin, J.Vidal, O.Muñoz, "Hybrid turbo FEC/ARQ systems and distributed space-time coding for cooperative transmission", *International Journal of Wireless Information Networks* (IJWIN), vol.12, no.4, pp. 263-280, Dec. 2005.

[23] T.E.Hunter, A.Nosratinia, "Cooperation diversity through coding", in *Proc. IEEE International Symposium of Information Theory*, (ISIT-2002), Laussane, Switzerland, 2002.

[24] T.E.Hunter, A.Nosratinia, A.Hedayat, M.Janani "Coded cooperation in wireless communications: space-time transmission and iterative decoding", *IEEE Trans. on Signal Processing*, vol.52, no.2, pp. 362-371, Feb. 2004.

[25] A.Nosratinia, T.E.Hunter, A.Hedayat, M.Janani, "Cooperative communications in wireless networks", *IEEE Communications Magazine*, vol. 42, no. 10, pp. 74-80, Oct.2004.

[26] A.Wyner, J.Ziv, "The rate-distortion function for source coding with side information at the decoder", *IEEE Trans. Information Theory*, vol. 22, no. 6, pp. 1986-1992, Nov. 1976.

[27] R.Nabar, H.Bölcskei, F.Kneubühler, "Fading relay channels: performance limits and space-time signal design", *IEEE Journal Selected Areas Communications* (JSAC), vol. 22, no. 6, pp. 1099-1109, Aug. 2004.

[28] H.Ochiani, P.Mitran, V.Tarokh, "Variable rate two phase collaborative communications protocols for wireless networks", *IEEE Trans. on Information Theory*, vol. 52, no. 9, pp. 4299-4313, Sep. 2006.

[29] M.Dohler, A.Gkelias, A.H.Aghvami, "Resource allocation for FDMA-based regenerative multihop liks*", IEEE Trans. on Wireless Communications*, vol. 3, no. 6, pp.1989-1993, Nov. 2004.

[30] D.P.Palomar, A.Agustín, O.Muñoz, J.Vidal, *"Decode and Forward Protocol for Cooperative Diversity in Multi-Antenna Wireless Networks"*, in *Proc. IEEE Annual Conference on Information Sciences and Systems* (CISS-2004), Princeton, NJ (USA), Feb. 17–19, 2004.

[31] J.Wofowitz, *Coding Theorems of Information Theory*, 3rd ed. Berlin, Germany. Springer-Verlag, 1978.

[32] A.Lapidoth, P.Narayan, "Reliable communication under channel uncertainty", *IEEE Trans. on Information Theory*, vol. 44, no.6, pp. 2148-2177, Oct.1998.

[33] D.P.Palomar, J.M.Cioffi and M.A. Lagunas, "Uniform power allocation in MIMO channels: A game-theoretic approach", *IEEE Trans. on Information Theory*, vol. 49, no. 7, pp. 1707-1727, July 2003.

[34] K.Azarian, H.El Gamal, P.Schniter, "On the achievable diversity-multiplexing tradeoff in half-duplex cooperative channels", *IEEE Trans. on Information Theory*, vol.51, no.12, pp. 4152-4172, Dec. 2005.

[35] B.Zhao, M.C.Valenti, "Some new adaptive protocols for the wireless relay channel", in *Proc. Allerton Conference on Communications, Control and Computing*, Monticello, IL, Oct. 2003.

[36] Y.Liang, V.V.Veeravalli, "Gaussian orthogonal relay channels: optimal resource allocation and capacity", *IEEE Trans. on Information Theory*, vol. 51, no. 9, pp. 3284-3289, Sep. 2005.

[37] M.N.Khormuji, E.G.Larsson, "Analytical results on block length optimization for decode-and-forward relaying with CSI feedback", in *Proc. 8th IEEE Workshop on Signal Processing Advances in Wireless Communications* (SPAWC-2007), Helsinki, Finland, June 2007.

[38] V.Tarokh, H.Jafarkhani, A.R.Calderbank, "Space-Time block codes from orthogonal designs", *IEEE Trans. on Information Theory*, vol. 45, pp. 1456-1467, July 1999.

[39] A.Agustin, J.Vidal, "Radio Resources optimization for the Half-duplex Relay-assisted Multiple Access Gaussian Channel", in *Proc. 8th IEEE Workshop on Signal Processing Advances in Wireless Communications* (SPAWC-2007), Helsinki, Finland, June 2007.

[40] D.N.C.Tse, S.V.Hanly, "Multiacces Fading channels part I: Polymatroid structure, optimal resource allocation and throughput capacities*", IEEE Trans. on Information Theory*, vol. 44, no. 7, pp. 2796-2815, Nov. 1998.

[41] S.Boyd,L.Vandenberghe, *Convex optimization*. Cambridge University Press, 2004.

[42] A.Agustin, J.Vidal, "TDMA amplifying and forward cooperation under interference-limited spatial reuse of the relay slot", *in Proc. IEEE International Conference on Acoustics, Speech and Signal Processing* (ICASSP-2006), Toulouse, France, May 2006.

[43] G.Kramer, M.Gastpar, P.Gupta, "Cooperative strategies and capacity theorems for relay networks", *IEEE Trans. on Information Theory*, vol. 51, no.9, pp. 3037-3063, Sept. 2005.

[44] A.Reznik, S.R.Kulkarni, S.Verdu, "Degraded Gaussian Multirelay channel: Capacity and Optimal Power allocation", *IEEE Trans. on Information Theory*, vol. 50, no. 12, pp. 3037-3046, Dec. 2004.

[45] B.Rankov, A.Wittneben, "Spectral efficient protocols for half-duplex fading relay channels", *IEEE Journal on Sel. Areas in Communications*, vol.25, no. 2, pp. 379-389, Feb. 2007.

[46] Y.Fan, C.Wang, J.Thompson, H.Vincent Poor, "Recovering multiplexing loss through successive relaying using repetition coding", *IEEE Trans. on Wireless Communications*, vol. 6, no.12, pp. 4484-4493, Dec. 2007.

[47] A.Agustin, J.Vidal, "Resource optimization in the decode-and-forward multiple relay-assisted channel", *submitted to Proc. 9th IEEE Workshop on Signal Processing Advances in Wireless Communications* (SPAWC-2008), Recife-Pernanbuco, Brazil, July 2008.

[48] H. Weingarten, Y. Steinberg, S. Shamai, "On the Capacity Region of the Multi-Antenna Broadcast Channel with Common Messages", in *Proc. IEEE International Symposium of Information Theory (*ISIT-2006), Seattle, USA, July 2006.

[49] S.Vishwanath, N.Jindal, A.Goldsmith, "On the duality of Gaussian Multiple-Access and Broadcast channels", *IEEE Trans. Information Theory*, vol. 50, no. 5, pp. 768-783, May 2004.

Chapter 3

Radio resource optimization for the synchronous/asynchronous half-duplex relay multiple access channel

RADIO resource allocation for the cooperative/relay-assisted transmission is investigated for the multiple access relay channel when the relays are half-duplex and all single-antenna terminals are power constrained. Protocol III with *decode and forward* (DF) is adopted for the relay-assisted transmission. Among the possible roles played by the source, relay and destination, three different scenarios are identified and compared: Relay-assisted Multiple Access Channel (RMAC), User Cooperation (UC) and Multiple Access Relay Channel (MARC). We define the problem by optimizing the mutual information obtained by *synchronous* and *asynchronous* networks with respect to the radio resources allocated to the *relay-receive* and *relay-transmit phase* of the relay-assisted transmission. The duplexing mode of the transmission can be TDD (Time Division Duplexing) or FDD (Frequency Division Duplexing), while the access scheme of each relay-assisted user might be based on TDMA (Time Division Multiple Access), FDMA (Frequency Division Multiple Access) or Superposition Coding multiple access (SC). We show under which conditions the radio resource allocation is a convex problem and evaluate the achievable rate regions for the two-user case in the different cooperative scenarios.

3.1 Introduction

Chapter 2 has shown that relay-assisted transmission is a promising solution capable of improving the mutual information or achievable rates of the wireless communication systems with a single source and single destination. In this chapter we address the problem of optimizing the radio resources allocation (*dynamic resource allocation relaying*) to obtain maximum achievable rates when multiple sources are transmitting to a single destination with the help of a relay terminal working in *decode and forward* (DF) mode. The assisting relay is assumed to work with the *half-duplex constraint*, i.e. its transmission and reception must be done in orthogonal domains, either time division duplexing (TDD) or frequency division duplexing (FDD). The half-duplex relay protocol used by each source is protocol III, defined in section 2.3.1.4 of chapter 2. In the single-user case depicted in Figure 3.1 protocol II is defined in this way: in the *relay-receive* period (named phase I) the source transmits to the assisting relay and the destination. The relay decodes, re-encodes and retransmits the message received in this phase. Afterwards, in the *relay-transmit* period (phase II) both relay and source transmit to the

destination. The destination is aware the transmissions received in both phases in order to decode the message. This protocol has been studied in chapter 2 for single-assisting relay in an *asynchronous* network, i.e. there is not full CSI (channel state information) of all the links.

This work analyses the relay-assisted transmission with multiple sources and a single destination, all equipped with a single antenna when *transmission power* and *transmission time*s are allocated to each relay phase. That setup is amenable to a centralized cellular system in the *uplink*, where the destination is the Base Station (BS), the sources are the terminals distributed around the cell and the assisting relays can be other terminals (*user relaying*) or specific terminals (*infrastructure relaying*) placed at selected positions of the cell. We have identified three relay-assisted scenarios which are able to describe the *user* and *infrastructure relaying* for the multiple user relay-assisted transmission:

- *Relay-assisted Multiple Access Channel* (RMAC), where each source is assisted by single/multiple relays associated only to that source (*user relaying*). This scenario can be found in systems with many idle terminals spread by the cell. In such a case the sources can select their assisting relays among their nearby terminals, see Figure 3.3 in section 3.4.1. The roles between sources and relays can be exchanged through time, allowing all the terminals of the cell make good use of the relaying transmission and thus motivating that idle terminals will be interested in working as assisting relays.

- *User cooperation* (UC) [2], where the multiple sources help one each other (*user relaying*), see Figure 3.6 in section 3.4.2. The work presented in [2] assumes full-duplex terminals. This scenario is very similar to RMAC and can be found when all sources are nearby or there are not idle terminals on the cell. As compared to RMAC, this scheme assumes that a peer agreement is reached between source and relay to cooperate in a communication to the destination.

- *Multiaccess Relay Channel* (MARC) [1], where there are multiple sources assisted by a single relay to transmit to a destination (*infrastructure relaying*), see Figure 3.7 in section 3.4.3. This scenario might correspond to cellular system where the density of relays is much lower than with the other two scenarios, like when lampposts are envisaged as relays and shared by a group the source terminals interested in the relay-assisted transmission. In [1] coding strategies are provided for full-duplex relays, although they are also valid for half-duplex relays. In this work we present the radio resource allocation.

The terminals are power constrained, hence in the time duplexing, the source transmits at its maximum power in both phases (*maximum power constraint*). However, when the relay-assisted transmission is done in FDD, the power transmitted by the source in each phase also needs to be optimized. In this later case there is an *individual average power constraint* at the terminals. Additionally, the access scheme of relay-assisted users must be indicated in each phase (I and II), which can be: time division multiple access (TDMA), frequency division multiple access (FDMA) or superposition-coding multiple access (SC). When the terminals have complete channel state information at the transmitter (CSIT), having all terminals complete channel state information at the receiver (CSIR), the network is defined as *synchronous*, following the definition of [6] where the carrier phases of the distributed transmitting nodes are also synchronized. In such a case, the nodes active in phase II (source and relay) can jointly transmit to the destination the same message using for example *eigenvector precoding* techniques. This is not possible in *asynchronous* networks, where there is incomplete CSIT.
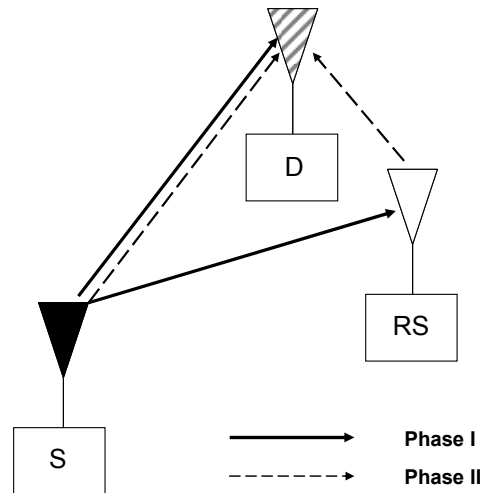
Figure 3.1.- In the relay-receive period (phase I) source transmit to relay and destination. In the relay-transmit period (phase II) both transmit to destination. Protocol III.

The novelty of this work with regard to other contributions is the design of the radio resource allocation for the multiple user relay-assisted transmission with *decode-and-forward* and *half-duplex relays*. With the goal of achieving highly spectral efficient systems, we consider the optimization of resources allocated to each phase of the communication. This optimization is shown to be strongly tied to the duplexing mode (time (TDD) / frequency (FDD)), the access scheme (orthogonal (TDMA or FDMA) /superposition coding) and network synchronization. It will be shown that the radio resource allocation of the three relay-assisted scenarios can be solved by algorithms based on convex optimization when relay-assisted transmission is done in FDD (*synchronous/asynchronous* networks) and in the TDD for *asynchronous* RMAC relay-assisted scenario. The following work has been presented in [3] and [4].

This remainder of this chapter is organized follows. In section 3.2 the system model is presented. Section 3.3 is devoted to introduce the single user relay-assisted transmission in TDD and FDD, where there are some differences to the transmission considered in chapter 2. The multiple user relay-assisted transmission is detailed in section 3.4, presenting the three relay-assisted scenarios assumed in this work, where the communication is done under different duplexing modes and access schemes. Section 3.5 depicts results for the two user case and section 3.6 concludes the chapter.

3.2   System model

All the terminals are equipped with a single antenna and are power constrained. The terminals may have complete channel state information (CSI) of the different links involved in each individual relay-assisted transmission, thus all terminals will transmit *synchronously*, or just an incomplete CSI, hence the terminals will transmit *asynchronously*. In the following $\rho_{S\text{-}D,k}$, $\rho_{S\text{-}R,k}$ and $\rho_{R\text{-}D,k}$ will denote the received signal power over noise power in the source-destination (measured with power $P_{s,k}$), source-relay and relay-destination (measured with power $P_{r,k}$) links related to the *k*-th source, respectively, for time domain relaying. For frequency domain transmissions, the variable ρ defines the received signal power over noise power spectral density. All the transmissions are performed in frames of length T_{frame} (*s*) with total bandwidth *W* (*Hz*), both parameters will be normalized to the unity.

For the sake of clarity let us define the following normalized capacities valid for single input and single output (SISO) links for the Gaussian channel and for the fixed channel realization, which will be used in the following sections,

$$C_{R-D,k}\left(\varepsilon,\delta\right)=\log_2\left(1+\frac{\delta\rho_{R-D,k}}{\varepsilon}\right) \quad C_{S-R,k}\left(\varepsilon,\delta\right)=\log_2\left(1+\frac{\delta\rho_{S-R,k}}{\varepsilon}\right)$$

$$C_{S-D,k}\left(\varepsilon,\delta\right)=\log_2\left(1+\frac{\delta\rho_{S-D,k}}{\varepsilon}\right) \tag{3.1}$$

$$C_{SR-D,k}\left(\varepsilon,\delta,\theta,\lambda\right)=\log_2\left(1+\frac{\delta\rho_{S-D,k}}{\varepsilon}+\frac{\lambda\rho_{R-D,k}}{\varepsilon}+\frac{2\sqrt{\theta\rho_{S-D,k}\rho_{R-D,k}}}{\varepsilon}\right)$$

where $C_{S-R,k}, C_{R-D,k}, C_{S-D,k}$ and $C_{SR-D,k}$ are the capacities (bits/channel use) of the source-relay, relay-destination, source-destination and joint (source,relay)-destination links connected with the k-th source, respectively. Finally, ε, δ, λ and θ are dummy variables related to the phase duration and the power allocation. The capacity of the joint (source,relay)-destination, $C_{SR-D,k}$, depicted in (3.1) assumes that there is a correlation between the simultaneous *synchronous* signals transmitted by the source and relay which depends on θ, thanks to the full knowledge of the CSI. For *asynchronous* terminals θ =0. These equations also provide a lower bound of the capacity for the ergodic Rayleigh fading channel (with a penalty in terms of the SNR, [5]).
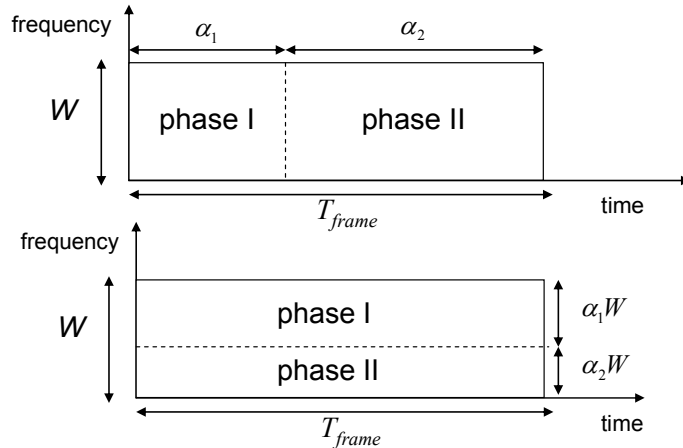
Figure 3.2.- a) (top) Relay-assisted transmission in TDD. In phase I the source transmits to the relay and destination at its maximum power. In phase II, the source transmits two independent signals, one signal with power $\beta_1 P_s$ transmits the same signal as the relay and the other signal with power $\beta_2 P_s$ will send new information b) (bottom) Relay-assisted transmission in FDD. In phase I, the source transmits with power $\beta_0 P_s$ to the relay and destination. In phase II, the source transmits two independent signals equally to the TDD. The relay transmits with power P_r.

3.3   Single user relay-assisted transmission

As an introductory and yet necessary case, let us derive the achievable rate regions for the single user (Figure 3.1), both in time (TDD) and frequency duplexing (FDD). It should be emphasized that both achievable rate regions will be in general different when the terminals are power limited as is the case in this work. Otherwise, when terminals are constrained by energy/bit or average transmitted power, the achievable rate regions in the time and frequency duplexing yields the same performance, as it is shown for the Broadcast channel under TDMA and FDMA in [7] and for the *virtual antenna array* in [8]. This section presents some differences

with respect section 2.3 of chapter 2, where only *asynchronous* network was assumed. Moreover, this section also differs from section 2.4 of chapter 2 where the relay-assisted transmission with multiple-assisting relays is investigated under a *sum average power* constraint for *asynchronous/synchronous* networks, where the single-assisting relay is subsumed. On the other hand, in this work the terminals are transmitting with its maximum power when they are active, which corresponds to a *maximum power* constraint and *individual average power* constraint for the relay-assisted transmission under TDD and FDD, respectively, following the definition of section 2.3 in chapter 2.

3.3.1 Time duplexing (TDD)

Figure 3.2a presents the frame structure of the relay-assisted transmission in the time duplexing, both phases are using all the bandwidth (W) but with variable time allocation, α_1(phase I) and α_2 (phase II), respectively. The source transmits with its maximum power in each phase. When the assisting relay works in the half-duplex constraint this scheme resembles to MAC channel with 2 virtual users. The first virtual user (named *source-relay virtual user*) is made up of the source in phase I and II and the relay in phase II, which transmits a virtual message with rate R_r. Basically, this virtual message is made of two messages (see Appendix A in section 3.7): in phase I the source transmits a message to be decoded at the relay (with power P_s), afterwards, in phase II the relay and the source jointly transmit a message with power $\left(\sqrt{\beta_1 P_s} + \sqrt{P_r} \right)^2$ (in *asynchronous* networks β_1=0). The other virtual user (*source-only virtual user*) is the source transmitting a new message in phase II at a rate R_s and power $\beta_2 P_s$. The power distribution at the source in phase II is constrained by,

$$\beta_1 + \beta_2 = 1 \tag{3.2}$$

Taking into account the definitions of (3.1) and (3.39)-(3.42) in Appendix A, the achievable rate region of the single-user relay-assisted transmission in terms of (R_s,R_r) in the time duplexing, named $B_{tdd}(\alpha,\beta)$, is characterized by

$$B_{tdd}(\boldsymbol{\alpha},\boldsymbol{\beta}) = \begin{cases} R_r \le \alpha_1 C_{S-D}(1,1) + \alpha_2 C_{SR-D}(1,\beta_1,\beta_1,1) \\ R_r \le \alpha_1 C_{S-R}(1,1) \\ R_s \le \alpha_2 C_{S-D}(1,\beta_2) \\ R_r + R_s \le \alpha_1 C_{S-D}(1,1) + \alpha_2 C_{SR-D}(1,1,\beta_1,1) \end{cases} \tag{3.3}$$

$$\boldsymbol{\alpha} = \begin{bmatrix} \alpha_1 & \alpha_2 \end{bmatrix}^T \qquad \boldsymbol{\alpha}^T \mathbf{1} = 1 \qquad \boldsymbol{\beta} = \begin{bmatrix} \beta_1 & \beta_2 \end{bmatrix} \qquad \boldsymbol{\beta}^T \mathbf{1} = 1$$

with C_{R-D}, C_{S-D}, C_{SR-D} and C_{S-R} being defined in (3.1). The rate region defined by $B_{tdd}(\alpha,\beta)$ for given vectors α and β results into a polyhedron with a rectangular or pentagonal shape, depending on the capacity of the links. This region satisfies the properties to be a *polymatroid* (*definition 3.1* in [9]), and hence any vertex of that region can be achieved by successive decoding. In such a case, the achievable rates are found as solution of (*lemma 3.2* of [9])

$$\max_{R_r, R_s} \mu_r R_r + \mu_s R_s \quad s.t. (R_r, R_s) \in B_{tdd}(\boldsymbol{\alpha}, \boldsymbol{\beta}) \tag{3.4}$$

for some positive μ_r, $\mu_s \in \Re_+$. However, the shape of the region depends on α and β, hence the achievable rate region will be given by the convex hull of the union of all the regions $B_{tdd}(\alpha,\beta)$. The boundary surface is achieved differently depending on the *network synchronization*.

For *asynchronous* networks (β_1=0 and β_2=1) the boundary of the convex hull of the union of the rate regions can be found as a solution of the following convex problem,

$$\max_{\boldsymbol{\alpha}, R_r, R_s} \mu_r R_r + \mu_s R_s \quad s.t. \left(R_r, R_s \right) \in B_{tdd}\left(\boldsymbol{\alpha}, \boldsymbol{\beta} \right) \quad \boldsymbol{\beta} = [0\,1]^T \tag{3.5}$$

for some positive μ_r, $\mu_s \in \Re_+$. The maximum is attained at some vertex of $B_{tdd}(\boldsymbol{\alpha},\boldsymbol{\beta})$ such that $\mu_r \geq \mu_s$. Equation (3.5) can be solved by convex optimization [10] because the rate region $B_{tdd}(\boldsymbol{\alpha},\boldsymbol{\beta})$ is concave over the variables $\boldsymbol{\alpha}$, R_s, R_r for a given $\boldsymbol{\beta}$. In this case we are interested in maximizing the sum rate, ($\mu_r = \mu_s$). This case was analyzed in section 2.3.1.4 of chapter 2, where there is a closed-form expression for $\boldsymbol{\alpha}$ (equation 2.65).

On the contrary, when the network is *synchronous*, $B_{tdd}(\boldsymbol{\alpha},\boldsymbol{\beta})$ is not concave over all the variables and convex optimization cannot be applied directly. The boundary of the achievable rate region is obtained by,

$$\max_{\boldsymbol{\beta}} \left(\max_{\boldsymbol{\alpha}, R_r, R_s} \mu_r R_r + \mu_s R_s \quad s.t. \left(R_r, R_s \right) \in B_{tdd}\left(\boldsymbol{\alpha}, \boldsymbol{\beta} \right) \right) \tag{3.6}$$

where for each possible vector $\boldsymbol{\beta}$ we maximize the sum rate for some positive $\mu_r, \mu_s \in \Re_+$. The most efficient optimization is obtained by using the Golden section search, [11].

3.3.2 Frequency duplexing (FDD)

When the relay-assisted transmission is carried out in the frequency domain (FDD), both source and assisting relay transmit continuously, (see Figure 3.2b) at maximum power, and hence spending more energy than the relay-assisted transmission duplexed in time (TDD). Now, the frequency band is split for the different relay phases. As a consequence the source may distribute the available power between the frequency bands allocated for phase I and II. That motivates some changes in the *source-relay virtual user* configuration defined for TDD (section 3.3.1): now during phase I, the source is transmitting to the relay with power $\beta_0 P_s$ (not with the maximum as in the TDD mode). The power constraint at the source is defined by,

$$\beta_0 + \beta_1 + \beta_2 = 1 \tag{3.7}$$

The achievable rate region in the frequency domain will be defined as,

$$B_{fdd}\left(\boldsymbol{\alpha}, \boldsymbol{\beta} \right) = \begin{cases} R_r \leq \alpha_1 C_{S-D}\left(\alpha_1, \beta_0 \right) + \alpha_2 C_{SR-D}\left(\alpha_2, \beta_1, \beta_1, 1 \right) \\ R_r \leq \alpha_1 C_{S-R}\left(\alpha_1, \beta_0 \right) \\ R_s \leq \alpha_2 C_{S-D}\left(\alpha_2, \beta_2 \right) \\ R_r + R_s \leq \alpha_1 C_{S-D}\left(\alpha_1, \beta_0 \right) + \alpha_2 C_{SR-D}\left(\alpha_2, \beta_1 + \beta_2, \beta_1, 1 \right) \end{cases} \tag{3.8}$$

$$\boldsymbol{\alpha} = \left[\alpha_1 \, \alpha_2 \right]^T \qquad \boldsymbol{\alpha}^T \mathbf{1} = 1 \qquad \boldsymbol{\beta} = \left[\beta_0 \, \beta_1 \, \beta_2 \right] \qquad \boldsymbol{\beta}^T \mathbf{1} = 1$$

with C_{R-D}, C_{S-D}, C_{SR-D} and C_{S-R} denoting the capacity of the relay-destination, source-destination, joint (source,relay)-destination and source-relay links. The selection of different values of $\boldsymbol{\alpha}$ and

β changes the SNR of the different links (see equation (3.1)). Consequently, the achievable rate region will be defined by the convex-hull of the union of the regions obtained $B_{fdd}(\alpha,\beta)$. In contrast to the time duplexing, the region $B_{fdd}(\alpha,\beta)$ is concave over all the variables under *synchronous* or *asynchronous* networks, hence convex optimization techniques can be used to get the boundary of the achievable rate region,

$$\max_{\boldsymbol{\alpha},\boldsymbol{\beta},R_r,R_s} \mu_r R_r + \mu_s R_s \quad s.t. (R_r, R_s) \in B_{fdd}(\boldsymbol{\alpha},\boldsymbol{\beta}) \tag{3.9}$$

for some positive μ_r, $\mu_s \in \Re_+$.

3.4 Multiple user relay-assisted transmission

Let us now turn to the case where multiple relay-assisted users transmit to a single destination. Three different relay scenarios will be considered: RMAC (Figure 3.3), UC (Figure 3.6), and MARC (Figure 3.7). The first two scenarios are quite similar and the differences are on the type of assisting relay: in the MARC scenario, all the sources share the same relay. All schemes are illustrated in the TDD and FDD modes for two relay-assisted sources (power limited terminals) although the generalization to more users is straightforward. A comparison between different access schemes is proposed: in each phase it can be *orthogonal* (TDMA or FDMA) or *superposition-coding* (SC). Table 3.1 summarizes the duplexing mode and access schemes considered in this work.

Scenario	Duplexing mode	Acces scheme in phase I	Access scheme in phase II	Achievable rate region (equation)
RMAC	TDD	TDMA	TDMA	(3.11)
	FDD	FDMA	FDMA	(3.14)
	TDD	TDMA	Superposition-coding (SC)	(3.16)
	FDD	FDMA	Superposition-coding (SC)	(3.19)
UC	TDD	TDMA	TDMA	(3.22)
	FDD	FDMA	FDMA	(3.24)
	TDD	TDMA	Superposition-coding (SC)	(3.26)
	FDD	FDMA	Superposition-coding (SC)	(3.28)
MARC	TDD	Superposition-coding (SC)	Superposition-coding (SC)	(3.32)
	FDD	Superposition-coding (SC)	Superposition-coding (SC)	(3.36)

Table 3.1.- Duplexing mode and access schemes considered for each multiple-user scenario.

Each relay-assisted source is made of up a *source-relay* and *source-only virtual user*, hence the analysis considers four virtual users transmitting at rates $(R_{r,1}, R_{s,1})$ and $(R_{r,2}, R_{s,2})$, although we are interested in the achievable rate region defined by $R_1 = R_{r,1} + R_{s,1}$ and $R_2 = R_{r,2} + R_{s,2}$.

Lets us define

$$\mathbf{R} = \begin{bmatrix} R_{r,1} & R_{s,1} & R_{r,2} & R_{s,2} \end{bmatrix}^T, \quad S_t = \{1,2,3,4\}, \quad S_r = \{1,3\} \quad S_s = \{2,4\}$$

$$\boldsymbol{\beta}_k = \begin{cases} \begin{bmatrix} \beta_{1,k} & \beta_{2,k} \end{bmatrix}^T & \text{time duplexing} \\ \begin{bmatrix} \beta_{0,k} & \beta_{1,k} & \beta_{2,k} \end{bmatrix}^T & \text{frequency duplexing} \end{cases} \tag{3.10}$$

where $\mathbf{R}$ is the vector containing the rates of the four virtual users, S_t stands for the set of all virtual users, S_r and S_s denote the subsets of *source-relay* and *source-only virtual users*, respectively. Finally, $\boldsymbol{\beta}_k$ is the vector associated to the *k*-th relay-assisted source: $\beta_{0,k}$ (only in FDD) and $\beta_{1,k}$ connected with a *source-relay virtual user* and $\beta_{2,k}$ connected a *source-only virtual user*.

As in the single-user case, the boundary of the achievable rate region is reached by convex optimization in the FDD (both in the *synchronous* and the *asynchronous* cases) for the three relay-assisted scenarios and only for the *asynchronous* case in the time duplexing of the RMAC. For the non-convex cases, optimization must include a search on power distribution in the terminals. In our variable definition, *asynchronous* networks imposes that the variable $\beta_{1,k}$=0.

3.4.1 Relay-assisted Multiple Access channel (RMAC)

In this scenario each source has its own assisting relay, see Figure 3.3. In phase I sources transmits orthogonally (TDMA or FDMA) to their assisting relays while the in the second phase it is possible to have orthogonal (TDMA or FDMA) or superposed transmission (SC).
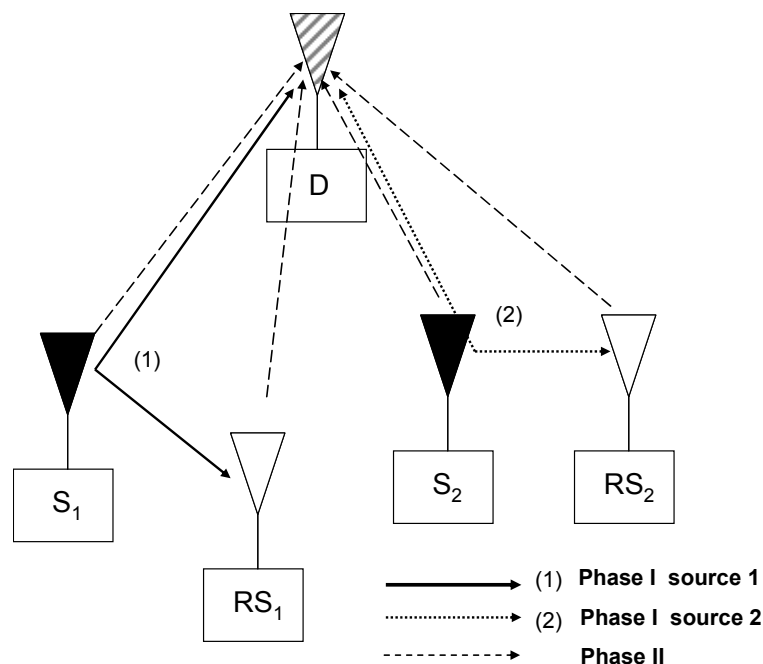

Figure 3.3.- In the relay-receive period (phase I) source users transmit to their associated relays and destinations. In the relay-transmit period (phase II) all nodes transmit to destination.

3.4.1.1 Orthogonal multiple access

The orthogonal multiple access assumes that each phase of the relay-assisted transmission associated to each source is allocated orthogonally. Figure 3.4a depicts the frame structure for the time duplexing (TDD), where the fraction of time devoted to the phase I is equal to $\alpha_{1,k}$ and $\alpha_{2,k}$ is the fraction of time for the phase II, both associated to the k-th source. Both sources access orthogonally in both phases by TDMA, (TDD-TDMA-TDMA). This case is a straightforward extension of the single user case of section 3.3.1. The achievable rate region is given by,

$$
M_{tdd\_ort}(\boldsymbol{\alpha},\boldsymbol{\beta}_1,\boldsymbol{\beta}_2) = \begin{cases}
R_{r,k} \le \alpha_{1,k}C_{S-D,k}(1,1) + \alpha_{2,k}C_{SR-D,k}(1,\beta_{1,k},\beta_{1,k},1) \\
R_{r,k} \le \alpha_{1,k}C_{S-R,k}(1,1) \\
R_{s,k} \le \alpha_{2,k}C_{S-D,k}(1,\beta_{2,k}) \\
R_{r,k} + R_{s,k} \le \alpha_{1,k}C_{S-D,k}(1,1) + \alpha_{2,k}C_{SR-D,k}(1,1,\beta_{1,k},1)
\end{cases}
\tag{3.11}
$$

$$
\boldsymbol{\alpha} = \begin{bmatrix} \alpha_{1,k} & \alpha_{2,k} \end{bmatrix}^T \qquad \boldsymbol{\alpha}^T\mathbf{1} = 1 \qquad \boldsymbol{\beta}_k = \begin{bmatrix} \beta_{1,k} & \beta_{2,k} \end{bmatrix}^T \qquad \boldsymbol{\beta}^T\mathbf{1} = 1
$$

where $C_{R-D,k}$, $C_{S-D,k}$, $C_{SR-D,k}$ and $C_{S-R,k}$ are the link capacities for the k-th user (3.1). As it was mentioned in the single-user case, (3.11) is neither concave nor convex over all the variables, so the boundary of the achievable rate region has to be obtained as,

$$
\max_{\boldsymbol{\beta}_1\boldsymbol{\beta}_2}\left(\max_{\boldsymbol{\alpha},\mathbf{R}} \boldsymbol{\mu}^T\mathbf{R} \quad s.t. \quad \mathbf{R} \in M_{tdd\_ort}(\boldsymbol{\alpha},\boldsymbol{\beta}_1,\boldsymbol{\beta}_2) \right)
\tag{3.12}
$$

with $\boldsymbol{\mu}=[\mu_{r,1},\mu_{s,1},\mu_{r,2},\mu_{s,2}]^T \in \Re^4_+$, $M_{tdd\_ort}(\boldsymbol{\alpha},\boldsymbol{\beta}_1,\boldsymbol{\beta}_2)$ defined in (3.11). However, for the *asynchronous* case ($\beta_{1,k}=0$ and $\beta_{2,k}=1$) the problem is convex because all the constraint on M_{tdd_ort} are concave over variables $\boldsymbol{\alpha}$ and $\mathbf{R}$. Therefore, this problem can be solved by interior point methods.
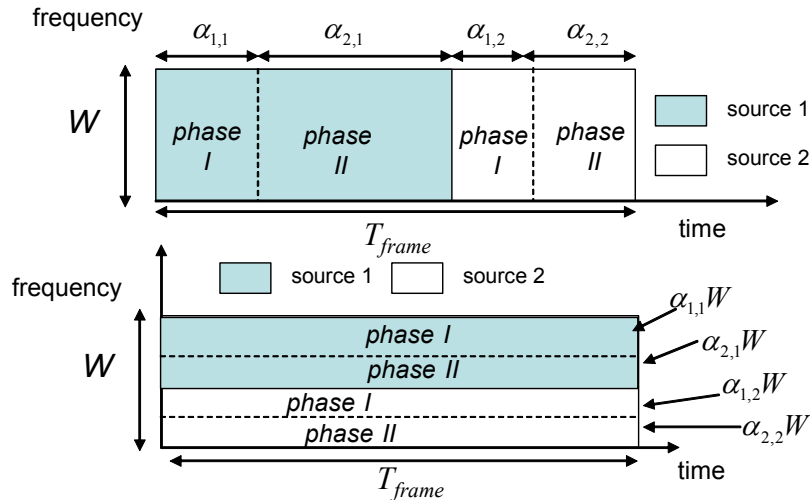

Figure 3.4.- Frame structure for a)(top) TDD-TDMA-TDMA, b)(bottom) FDD-FDMA-FDMA relay-assisted transmission.

The frequency duplexing (FDD) with FDMA in both phases (Figure 3.4b), FDD-FDMA-FDMA, the k-th source distributes its transmitted power among the phase I and II according to β_k defined in (3.10). The boundary of achievable rate region is given by,

$$\max_{\boldsymbol{\alpha},\boldsymbol{\beta}_1,\boldsymbol{\beta}_2,\mathbf{R}} \boldsymbol{\mu}^T \mathbf{R} \quad s.t. \quad \mathbf{R} \in M_{fdd\_ort}\left(\boldsymbol{\alpha},\boldsymbol{\beta}_1,\boldsymbol{\beta}_2\right) \tag{3.13}$$

with $\boldsymbol{\mu}=[\mu_{r,1},\mu_{s,1},\mu_{r,2},\mu_{s,2}]^T \in \mathfrak{R}^4_+$ and $M_{fdd\_ort}(\boldsymbol{\alpha},\boldsymbol{\beta}_1,\boldsymbol{\beta}_2)$ defined by

$$G_{fdd\_ort}(\boldsymbol{\alpha},\boldsymbol{\beta}_1,\boldsymbol{\beta}_2) = \begin{cases} R_{r,k} \le \alpha_{1,k} C_{S-D,k}\left(\alpha_{1,k},\beta_{0,k}\right) + \alpha_{2,k} C_{SR-D,k}\left(\alpha_{2,k},\beta_{1,k},\beta_{1,k},1\right) \\ R_{r,k} \le \alpha_{1,k} C_{S-R,k}\left(\alpha_{1,k},\beta_{0,k}\right) \\ R_{s,k} \le \alpha_{2,k} C_{S-D,k}\left(\alpha_{2,k},\beta_{2,k}\right) \\ R_{r,k} + R_{s,k} \le \alpha_{1,k} C_{S-D,k}\left(\alpha_{1,k},\beta_{0,k}\right) + \\ \qquad\qquad + \alpha_{2,k} C_{SR-D,k}\left(\alpha_{2,k},\beta_{1,k}+\beta_{2,k},\beta_{1,k},1\right) \end{cases} \tag{3.14}$$

$$\boldsymbol{\alpha} = \begin{bmatrix} \alpha_{1,k} & \alpha_{2,k} \end{bmatrix}^T \qquad \boldsymbol{\alpha}^T \mathbf{1} = 1 \qquad \boldsymbol{\beta}_k = \begin{bmatrix} \beta_{0,k} & \beta_{1,k} & \beta_{2,k} \end{bmatrix}^T \qquad \boldsymbol{\beta}^T \mathbf{1} = 1$$

3.4.1.2   Superposition-coding multiple access (SC)

We consider now that during phase II all source-relay pairs use the same time/frequency resources by superposition-coding multiple access (SC), while there is an orthogonal access in phase I. See Figure 3.5 for the time duplexing (TDD-TDMA-SC).

Figure 3.5.- Time domain superposition-coding multiple access (TDD-TDMA-SC).

Additionally, in the following, we will use the notation

$$v(S) = \sum_{i \in S} \mathbf{v}(i) \tag{3.15}$$

for denoting a linear combination of some subset S of elements of a vector.

When the relay-assisted transmission is duplexed in the time domain (Figure 3.5, TDD-TDMA-SC) the achievable rate region for four virtual users is characterized by (see (3.47) in Appendix B),

$$M_{tdd\_sup}\left(\boldsymbol{\alpha},\boldsymbol{\beta}_1,\boldsymbol{\beta}_2\right)=\begin{cases}R(S)\le\sum_{k=1}^{2}\alpha_{1,k}Z(k,1,1,S)+\alpha_2 f\left(P_{1,\beta_{1,1},\beta_{1,2},1,1,\beta_{2,1},\beta_{2,2}}(S)\right) & \forall S\subset S_t\\ R_{r,k}\le\alpha_{1,k}C_{S-R,k}(1,1) & \forall k\end{cases}$$

$$\boldsymbol{\alpha}=\begin{bmatrix}\alpha_{1,1} & \alpha_{1,2} & \alpha_2\end{bmatrix}^T \qquad \boldsymbol{\alpha}^T\mathbf{1}=1 \qquad \boldsymbol{\beta}_k=\begin{bmatrix}\beta_{1,k} & \beta_{2,k}\end{bmatrix}^T \qquad \boldsymbol{\beta}_k^{~T}\mathbf{1}=1$$

(3.16)

with S denoting all possible subsets of S_t (3.10), $R(S)$ and $P(S)$ use (3.15) and the next definitions,

$$f(x)=\log_2(1+x) \qquad Z(n,\varepsilon,\delta,\phi)=\begin{cases}C_{S-D,n}(\varepsilon,\delta) & if~n\in\phi\\ 0 & otherwise\end{cases}$$

$$\mathbf{P}_{\varepsilon,\delta_1,\delta_2,\delta_3,\delta_4,\delta_5,\delta_6}=\frac{1}{\varepsilon}\left[\left(\sqrt{\delta_3\rho_{R-D,1}}+\sqrt{\delta_1\rho_{S-D,1}}\right)^2 \quad \delta_5\rho_{S-D,1} \quad \left(\sqrt{\delta_4\rho_{R-D,2}}+\sqrt{\delta_2\rho_{S-D,2}}\right)^2 \quad \delta_6\rho_{S-D,2}\right]^T$$

(3.17)

where ε, δ_1, δ_2, δ_3, δ_4, δ_5 and δ_6 are dummy variables and $C_{S-D,k}$ is defined in (3.1). The odd elements of $\mathbf{P}$ are connected with the *source-relay virtual users*, while the even elements are connected with the *source-only virtual users*. $P(S)$ stands for a linear combinations of the elements of $\mathbf{P}$ according to S, (3.15). Finally, the boundary of the achievable rate region is obtained by

$$\max_{\boldsymbol{\beta}_1\boldsymbol{\beta}_2}\left(\max_{\boldsymbol{\alpha},\mathbf{R}}\boldsymbol{\mu}^T\mathbf{R} \quad s.t. \quad \mathbf{R}\in M_{tdd\_sup}\left(\boldsymbol{\alpha},\boldsymbol{\beta}_1,\boldsymbol{\beta}_2\right)\right)$$

(3.18)

with $\boldsymbol{\mu}=[\mu_{r,1},\mu_{s,1},\mu_{r,2},\mu_{s,2}]^T\in\Re^4_+$ and $M_{tdd\_sup}(\boldsymbol{\alpha},\boldsymbol{\beta}_1,\boldsymbol{\beta}_2)$ defined in (3.16). That rate region is concave over variables $\boldsymbol{\alpha}$ and $\mathbf{R}$.

When the relay-assisted transmission is duplexed in the frequency domain (FDD-FDMA-SC, counterpart of Figure 3.5) the power distribution at the source nodes must be considered,(3.10), leading to the following achievable rate region (concave for all the variables),

$$M_{fdd\_sup}\left(\boldsymbol{\alpha},\boldsymbol{\beta}_1,\boldsymbol{\beta}_2\right)=\begin{cases}R(S)\le\sum_{k=1}^{2}\alpha_{1,k}Z(k,\alpha_{1,k},\beta_{0,k},S)+\alpha_2 f\left(P_{\alpha_2,\beta_{1,1},\beta_{1,2},1,1,\beta_{2,1},\beta_{2,2}}(S)\right) & \forall S\subset S_t\\ R_{r,k}\le\alpha_{1,k}C_{S-R,k}(\alpha_{1,k},\beta_{0,k}) & \forall k\end{cases}$$

$$\boldsymbol{\alpha}=\begin{bmatrix}\alpha_{1,1} & \alpha_{1,2} & \alpha_2\end{bmatrix}^T \qquad \boldsymbol{\alpha}^T\mathbf{1}=1 \qquad \boldsymbol{\beta}_k=\begin{bmatrix}\beta_{0,k} & \beta_{1,k} & \beta_{2,k}\end{bmatrix}^T \qquad \boldsymbol{\beta}_k^{~T}\mathbf{1}=1$$

(3.19)

where $R(S)$, $P(S)$ use definition (3.15), f, Z and $\mathbf{P}$ are defined in (3.17) and $C_{S-R,k}$ is defined in (3.1). The boundary surface of the rate region can be obtained maximizing the following equation,

$$\max_{\boldsymbol{\alpha},\boldsymbol{\beta}_1,\boldsymbol{\beta}_2,\mathbf{R}}\boldsymbol{\mu}^T\mathbf{R} \quad s.t. \quad \mathbf{R}\in M_{fdd\_sup}\left(\boldsymbol{\alpha},\boldsymbol{\beta}_1,\boldsymbol{\beta}_2\right)$$

(3.20)

with $\boldsymbol{\mu}=[\mu_{r,1},\mu_{s,1},\mu_{r,2},\mu_{s,2}]^T\in\Re^4_+$.

3.4.2 User cooperation (UC)

User cooperation scenario is depicted in Figure 3.6. There are two sources and a single destination. The sources decide to cooperate in order to help one each other, that is, the other source will work as an assisting relay. Therefore, on the contrary to the RMAC scenario, here the maximum power transmitted by the relays will be constrained by the maximum power at the sources. In the time domain, each source transmits to the relay (the other source in Figure 3.6) with its maximum power in phase I. During phase II, both sources work also as relays. Let us assume that each relay associated to k-th user is transmitting with power $\psi_k P_{s,k}$ where ψ_k is the fraction of the total power devoted for relaying the message of its partner and

$$\rho_{R-D,1} = \rho_{S-D,2} \qquad \rho_{R-D,2} = \rho_{S-D,1} \tag{3.21}$$
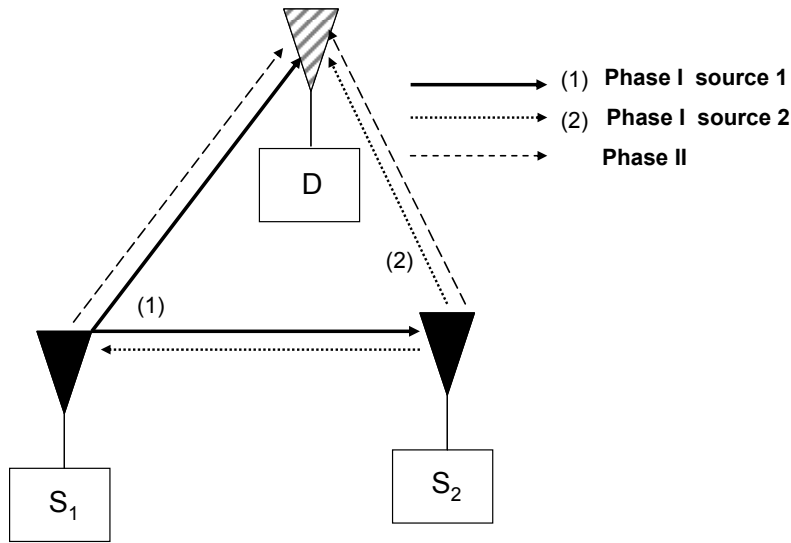
Figure 3.6.- In the relay-receive period (phase I) sources transmit to relays (other sources) and destination. In the relay-transmit period (phase II) both transmit to destination.

3.4.2.1   Orthogonal multiple access

When the user cooperation is duplexed in time, Figure 3.4a (TDD-TDMA-TDMA), the achievable rate region is constrained by,

$$G_{tdd\_ort}(\boldsymbol{\eta}) \atop \boldsymbol{\eta}=[\boldsymbol{\alpha},\boldsymbol{\beta}_1,\boldsymbol{\beta}_2,\psi_1,\psi_2] = \begin{cases} R_{r,k} \leq \alpha_{1,k} C_{S-D,k}(1,1) + \alpha_{2,k} C_{SR-D,k}\left(1,\beta_{1,k},\beta_{1,k}\psi_{m(k)},\psi_{m(k)}\right) \\ R_{r,k} \leq \alpha_{1,k} C_{S-R,k}(1,1) \\ R_{s,k} \leq \alpha_{2,k} C_{S-D,k}(1,\beta_{2,k}) \\ R_{r,k} + R_{s,k} \leq \alpha_{1,k} C_{S-D,k}(1,1) + \alpha_{2,k} C_{SR-D,k}\left(1,\beta_{1,k}+\beta_{2,k},\beta_{1,k}\psi_{m(k)},\psi_{m(k)}\right) \end{cases} \tag{3.22}$$

$$\boldsymbol{\alpha} = \begin{bmatrix} \alpha_{1,k} & \alpha_{2,k} \end{bmatrix}^T \quad \boldsymbol{\alpha}^T \mathbf{1} = 1 \quad \boldsymbol{\beta}_k = \begin{bmatrix} \beta_{1,k} & \beta_{2,k} \end{bmatrix}^T \quad \begin{bmatrix} \boldsymbol{\beta}_k^T & \psi_m \end{bmatrix} \mathbf{1} = 1 \quad m = \begin{cases} 1 & if \quad k=2 \\ 2 & if \quad k=1 \end{cases}$$

where the link capacities are defined in (3.1) and $\psi_{m(k)}$ stands for the fraction of the power used by k-th relay. Notice that the power used by the relay associated to the source 1 (actually the

source 2) has an impact on the available power of the source 2 to transmit its own message in phase II (*source-only virtual user*). The boundary of the achievable rate region is found by maximizing,

$$\max_{\beta_1,\beta_2,\psi_1,\psi_2} \left(\max_{\alpha,\mathbf{R}} \mu^T \mathbf{R} \quad s.t. \quad \mathbf{R} \in G_{tdd\_ort}\left(\alpha,\beta_1,\beta_2,\psi_1,\psi_2\right) \right) \tag{3.23}$$

where $\mu=[\mu_{r,1},\mu_{s,1},\mu_{r,2},\mu_{s,2}]^T \in \Re^4_+$ and $\mathbf{R}$ is defined in (3.10). Notice that the rate region defined by G_{tdd_ort} is concave over the variables α and $\mathbf{R}$.

Otherwise, when the user cooperation is performed under frequency duplexing (FDD-FDMA-FDMA) Figure 3.4b the achievable rate region is characterized by,

$$G_{fdd\_ort}(\eta) \underset{\eta=[\alpha,\beta_1,\beta_2,\psi_1,\psi_2]}{=} \begin{cases} R_{r,k} \leq \alpha_{1,k}C_{S-D,k}\left(\alpha_{1,k},\beta_{0,k}\right) + \alpha_{2,k}C_{SR-D,k}\left(\alpha_{2,k},\beta_{1,k},\beta_{1,k}\psi_{m(k)},\psi_{m(k)}\right) \\ R_{r,k} \leq \alpha_{1,k}C_{S-R,k}\left(\alpha_{1,k},\beta_{0,k}\right) \\ R_{s,k} \leq \alpha_{2,k}C_{S-D,k}\left(\alpha_{2,k},\beta_{2,k}\right) \\ R_{r,k} + R_{s,k} \leq \alpha_{1,k}C_{S-D,k}\left(\alpha_{1,k},\beta_{0,k}\right) \\ \qquad\qquad + \alpha_{2,k}C_{SR-D,k}\left(\alpha_{2,k},\beta_{1,k}+\beta_{2,k},\beta_{1,k}\psi_{m(k)},\psi_{m(k)}\right) \end{cases} \tag{3.24}$$

$$\alpha = \begin{bmatrix} \alpha_{1,k} & \alpha_{2,k} \end{bmatrix}^T \quad \alpha^T \mathbf{1} = 1 \quad \beta_k = \begin{bmatrix} \beta_{0,k} & \beta_{1,k} & \beta_{2,k} \end{bmatrix}^T \quad \begin{bmatrix} \beta_k^T & \psi_m \end{bmatrix}\mathbf{1} = 1 \quad m = \begin{cases} 1 & if \quad k=2 \\ 2 & if \quad k=1 \end{cases}$$

The rate region defined by G_{fdd_ort} is concave over all the variables, hence the boundary of the achievable rate region is found by maximizing,

$$\max_{\alpha,\beta_1,\beta_2,\psi_1,\psi_2,\mathbf{R}} \mu^T \mathbf{R} \quad s.t. \quad \mathbf{R} \in G_{fdd\_ort}\left(\alpha,\beta_1,\beta_2,\psi_1,\psi_2\right) \tag{3.25}$$

with $\mu=[\mu_{r,1},\mu_{s,1},\mu_{r,2},\mu_{s,2}]^T \in \Re^4_+$.

3.4.2.2   Superposition-coding multiple access (SC)

Following similar steps as in the RMAC (section 3.4.1.2) with superposition multiple access in phase II and taking into account the constraint on the maximum power transmitted by the source, the achievable rate region when the transmission is duplexed in the time domain (TDD-TDMA-SC) is given by,

$$G_{tdd\_sup}(\eta) \underset{\eta=[\alpha,\beta_1,\beta_2,\psi_1,\psi_2]}{=} \begin{cases} R(S) \leq \sum_{k=1}^{2} \alpha_{1,k}Z\left(k,1,1,S\right) + \alpha_2 f\left(P_{1,\beta_{1,1},\beta_{1,2},\psi_{m(1)},\psi_{m(2)},\beta_{2,1},\beta_{2,2}}(S)\right) & \forall S \subset S_t \\ R_{r,k} \leq \alpha_{1,k}C_{S-R,k}\left(1,1\right) & \forall k \end{cases} \tag{3.26}$$

$$\alpha = \begin{bmatrix} \alpha_{1,1} & \alpha_{1,2} & \alpha_2 \end{bmatrix}^T \quad \alpha^T \mathbf{1} = 1 \quad \beta_k = \begin{bmatrix} \beta_{1,k} & \beta_{2,k} \end{bmatrix}^T \quad \begin{bmatrix} \beta_k^T & \psi_m \end{bmatrix}\mathbf{1} = 1 \quad m = \begin{cases} 1 & if \quad k=2 \\ 2 & if \quad k=1 \end{cases}$$

where $R(S)$, $P(S)$ use definition of (3.15), Z, f and $\mathbf{P}$ are defined in (3.17). The boundary of the achievable rate region is attained by,

$$\max_{\beta_1,\beta_2,\psi_1,\psi_2} \left(\max_{\alpha,\mathbf{R}} \mu^T \mathbf{R} \quad s.t. \quad \mathbf{R} \in G_{tdd\_sup}\left(\alpha,\beta_1,\beta_2,\psi_1,\psi_2\right) \right) \tag{3.27}$$

with $\mu = [\mu_{r,1},\mu_{s,1},\mu_{r,2},\mu_{s,2}]^T \in \mathfrak{R}^4_+$.

Under frequency duplexing (FDD-FDMA-SC) the achievable rate region is described by,

$$G_{fdd\_sup}(\eta) = \begin{cases} R(S) \le \sum_{k=1}^{2} \alpha_{1,k} Z\left(k,\alpha_{1,k},\beta_{0,k},S\right) + \alpha_2 f\left(P_{\alpha_2,\beta_{1,1},\beta_{1,2},\psi_{m(1)},\psi_{m(2)},\beta_{2,1},\beta_{2,2}}(S)\right) \forall S \subset S_t \\ R_{r,k} \le \alpha_{1,k} C_{S-R,k}\left(\alpha_{1,k},\beta_{0,k}\right) \qquad\qquad \forall k \end{cases} \tag{3.28}$$

$$\alpha = \begin{bmatrix} \alpha_{1,1} & \alpha_{1,2} & \alpha_2 \end{bmatrix}^T \quad \alpha^T \mathbf{1} = 1 \quad \beta_k = \begin{bmatrix} \beta_{0,k} & \beta_{1,k} & \beta_{2,k} \end{bmatrix}^T \quad \begin{bmatrix} \beta_k^T & \psi_m \end{bmatrix}\mathbf{1} = 1 \quad m = \begin{cases} 1 & if \quad k=2 \\ 2 & if \quad k=1 \end{cases}$$

where $R(S)$, $P(S)$ use definition (3.15), Z, f and $\mathbf{P}$ are defined in (3.17). The boundary surface of the achievable region can be derived by,

$$\max_{\alpha,\beta_1,\beta_2,\psi_1,\psi_2} \mu^T \mathbf{R} \quad s.t. \quad \mathbf{R} = \begin{bmatrix} R_{r,1} & R_{s,1} & R_{r,2} & R_{s,2} \end{bmatrix}^T \in G_{fdd\_sup}\left(\alpha,\beta_1,\beta_2,\psi_1,\psi_2\right) \tag{3.29}$$

with $\mu = [\mu_{r,1},\mu_{s,1},\mu_{r,2},\mu_{s,2}]^T \in \mathfrak{R}^4_+$.

3.4.3 Multiple Access Relay channel (MARC)

The MARC channel assumes that there are two sources, a single destination and a single relay which will help both sources in transmitting their messages to the destination, see Figure 3.7. Both sources transmit simultaneously to the relay during phase I. Afterwards, both sources and the relay transmit to the destination, in phase II. Therefore superposition-coding multiple access (SC) is considered in both phases.
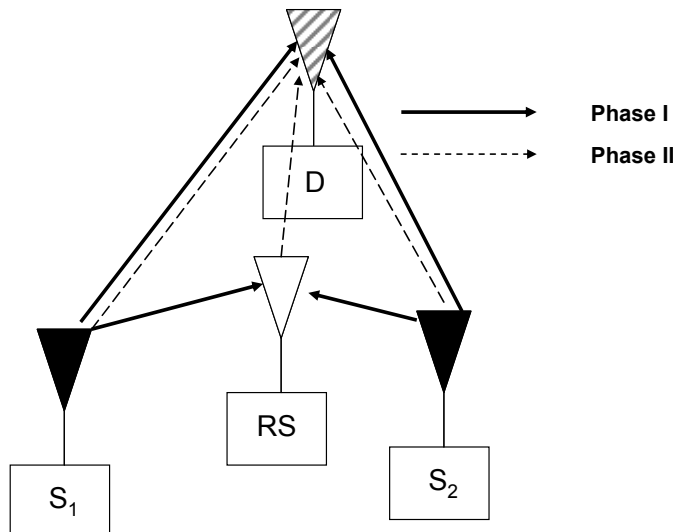

Figure 3.7.- In the relay-receive period (phase I) source users transmit to the relay and destination. In the relay-transmit period (phase II) all nodes transmit to destination.

This scenario can be analyzed assuming that there are four virtual users transmitting to a common destination and considering the following hints:

- A single relay distributes its power helping both sources at the same time. So the relay will transmit independent messages of power $\psi_k P_r$ each one to assist the k-th source.

- During phase I, the maximum achievable rates obtained at the relay and the destination are described by the conventional MAC channel of two users. Let us define the achievable rate vector at the relay as,

$$\mathbf{R}_r = \begin{bmatrix} R_{r,1} & R_{r,2} \end{bmatrix} \tag{3.30}$$

- We consider the following equation to make good use of definition of $\mathbf{P}$ in (3.17),

$$\rho_{R-D,1} = \rho_{R-D,2} = \rho_{R-D} \tag{3.31}$$

Taking into account these hints and following similar steps as in Appendix B (section 3.8), the achievable rate region obtained by the MARC scenario in the time duplexing (TDD-SC-SC) is characterized by,

$$U_{tdd}\left(\boldsymbol{\alpha}, \boldsymbol{\beta}_1, \boldsymbol{\beta}_2, \boldsymbol{\psi}\right) = \begin{cases} R(S) \le \alpha_1 f\left(Q_{1,1,1}\left(S \cap S_r\right)\right) + \alpha_2 f\left(P_{1,\beta_{1,1},\beta_{1,2},\psi_1,\psi_2,\beta_{2,1},\beta_{2,2}}\left(S\right)\right) \\ R_r(S) \le \alpha_1 f\left(T_{1,1,1}\left(S \cap S_r\right)\right) \qquad\qquad\qquad\qquad \forall S \subset S_t \end{cases} \tag{3.32}$$

$$\boldsymbol{\psi} = \begin{bmatrix} \psi_1 \ \psi_2 \end{bmatrix}^T \quad \boldsymbol{\psi}^T \mathbf{1} = 1 \quad \boldsymbol{\alpha} = \begin{bmatrix} \alpha_1 \ \alpha_2 \end{bmatrix}^T \quad \boldsymbol{\alpha}^T \mathbf{1} = 1 \quad \boldsymbol{\beta}_k = \begin{bmatrix} \beta_{1,k} \ \beta_{2,k} \end{bmatrix}^T \quad \boldsymbol{\beta}_k^T \mathbf{1} = 1$$

where f and $\mathbf{P}$ are defined in (3.17), S_r denotes the subset of the *source-relay virtual users* (3.10), $\boldsymbol{\psi}$ describes how the relay distributes its power to help the different sources and $\mathbf{T}$ and $\mathbf{Q}$ vectors are defined by,

$$\mathbf{Q}_{\varepsilon,\delta_1,\delta_2} = \frac{1}{\varepsilon}\begin{bmatrix} \delta_1 \rho_{S-D,1} & \delta_2 \rho_{S-D,2} \end{bmatrix}^T \quad \mathbf{T}_{\varepsilon,\delta_1,\delta_2} = \frac{1}{\varepsilon}\begin{bmatrix} \delta_1 \rho_{S-R,1} & \delta_2 \rho_{S-R,2} \end{bmatrix}^T \tag{3.33}$$

Additionally, $R(S)$, $R_r(S)$, $T(S \cap S_r)$ and $Q(S \cap S_r)$ stand for a linear combination of the elements of vectors $\mathbf{R}$, $\mathbf{R}_r$, $\mathbf{T}$ and $\mathbf{Q}$, following the definition of (3.15). The boundary of the achievable rate region is found by,

$$\max_{\boldsymbol{\beta}_1,\boldsymbol{\beta}_2,\boldsymbol{\psi}}\left(\max_{\boldsymbol{\alpha},\mathbf{R}} \boldsymbol{\mu}^T \mathbf{R} \quad s.t. \quad \mathbf{R} \in U_{tdd}\left(\boldsymbol{\alpha}, \boldsymbol{\beta}_1, \boldsymbol{\beta}_2, \boldsymbol{\psi}\right)\right) \tag{3.34}$$

When the transmission is duplexed in the frequency domain (FDD-SC-SC) the boundary of the achievable rate region is attained with the maximization of,

$$\max_{\boldsymbol{\alpha},\boldsymbol{\beta}_1,\boldsymbol{\beta}_2,\boldsymbol{\psi},\mathbf{R}} \boldsymbol{\mu}^T \mathbf{R} \quad s.t. \quad \mathbf{R} \in U_{fdd}\left(\boldsymbol{\alpha}, \boldsymbol{\beta}_1, \boldsymbol{\beta}_2, \boldsymbol{\psi}\right) \tag{3.35}$$

with $\boldsymbol{\mu} = [\mu_{r,1}, \mu_{s,1}, \mu_{r,2}, \mu_{s,2}]^T \in \Re^4_+$ and the achievable rate region U_{fdd} defined by,

$$U_{fdd}(\boldsymbol{\eta}) = \begin{cases} R(S) \le \alpha_1 f\left(Q_{\alpha_1,\beta_{0,1},\beta_{0,2}}\left(S \cap S_r\right)\right) + \alpha_2 f\left(P_{\alpha_2,\beta_{1,1},\beta_{1,2},\psi_1,\psi_2,\beta_{2,1},\beta_{2,2}}(S)\right) & \forall S \subset S_t \\ R_r(S) \le \alpha_1 f\left(T_{\alpha_1,\beta_{0,1},\beta_{0,2}}\left(S \cap S_r\right)\right) \end{cases} \qquad (3.36)$$

$$\boldsymbol{\psi} = \begin{bmatrix} \psi_1 & \psi_2 \end{bmatrix}^T \qquad \boldsymbol{\psi}^T \mathbf{1} = 1 \qquad \boldsymbol{\alpha} = \begin{bmatrix} \alpha_1 & \alpha_2 \end{bmatrix}^T \qquad \boldsymbol{\alpha}^T \mathbf{1} = 1 \qquad \boldsymbol{\beta}_k = \begin{bmatrix} \beta_{0,k} & \beta_{1,k} & \beta_{2,k} \end{bmatrix}^T \qquad \boldsymbol{\beta}_k^T \mathbf{1} = 1$$

with f and $\mathbf{P}$ and $\mathbf{T},\mathbf{Q}$ defined in (3.17) and (3.33), respectively.

3.5 Results

This section illustrates the achievable rate regions for the three relay-assisted scenarios considered in this chapter: *relay assisted multiple access channel* (RMAC), *user cooperation* (UC) and the *multiple access relay channel* (MARC).
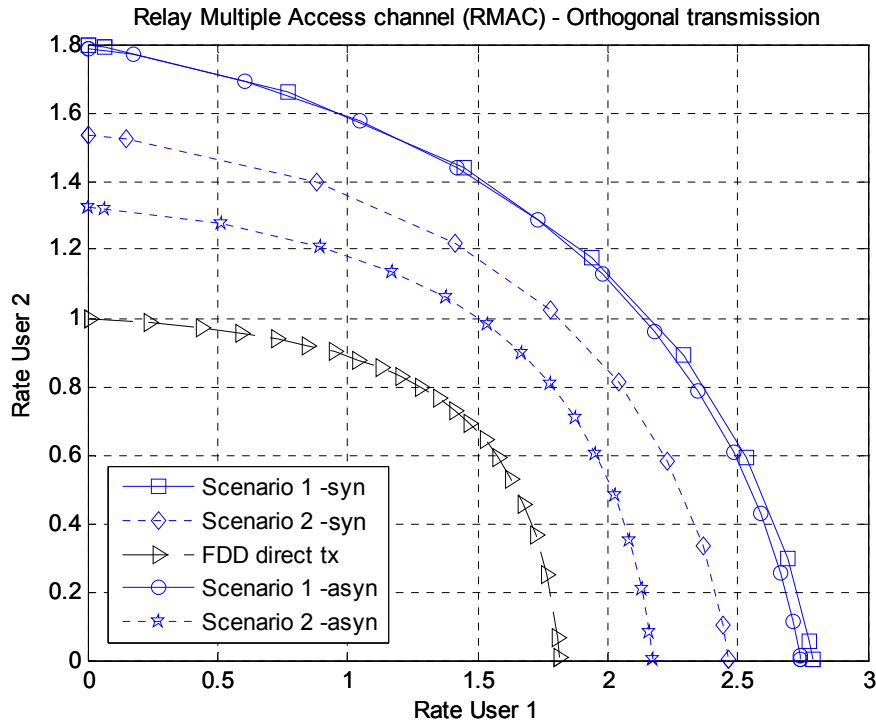
Figure 3.8.- Achievable rate regions for the direct transmission and RMAC scenario with configurations of sec. 3.5.1. Orthogonal multiple access and transmission done in the frequency domain (FDD-FDMA-FDMA). Synchronous and Asynchronous transmission.

A. Impact of the link quality and network synchronization in RMAC

In order to study the impact of the different link qualities and the network synchronization [6] we have assumed two scenario settings for the RMAC with the following configuration:

- *Scenario 1*: $\rho_{S-D,1}$= 4 dB, $\rho_{S-R,1}$=10 dB, $\rho_{R-D,1}$=6 dB (source 1) and $\rho_{S-D,2}$=0 dB, $\rho_{S-R,2}$=5 dB, $\rho_{R-D,2}$=4 dB (source 2)

- *Scenario 2*: $\rho_{S-D,1}$= 4 dB, $\rho_{S-R,1}$=10 dB, $\rho_{R-D,1}$=0 dB (source 1) and $\rho_{S-D,2}$=0 dB, $\rho_{S-R,2}$=5 dB, $\rho_{R-D,2}$= -3 dB (source 2)
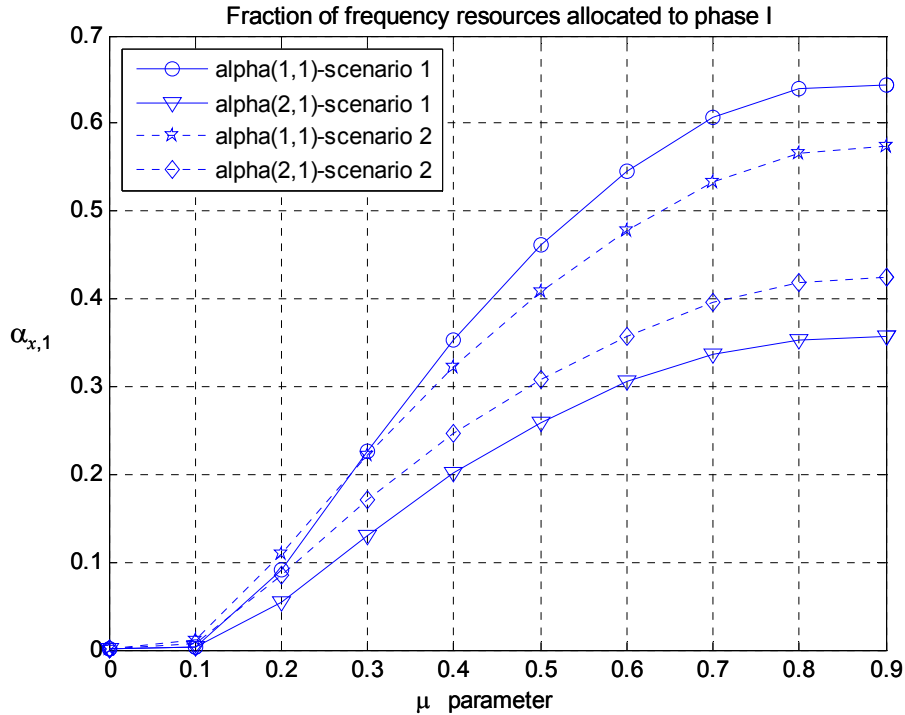
Figure 3.9.- Distribution of frequency resources for user 1 ($\alpha_{1,1}$ and $\alpha_{2,1}$) as a function of the μ parameter with $\mu_{s,1}=\mu_{r,1}=\mu$ and $\mu_{s,2}=\mu_{r,2}=1-\mu$. Two scenario configuration of the RMAC is considered. FDD-FDMA-FDMA.

The main difference between both scenarios is the relay-destination link quality. Figure 3.8 depicts the achievable rate region for the RMAC with orthogonal multiple access and transmitting with the frequency duplexing (FDD-FDMA-FDMA). Solid lines stand for the *synchronous/asynchronous* transmission at *scenario 1*. On the other hand, dotted lines are associated to the performance obtained at *scenario 2*. First, it can be observed that the use of the assisting relays enlarges the achievable rate region as compared to the direct transmission (dashed line). The assisting relays present good link qualities in the source-relay links, while in the relay-destination links qualities are similar to the source-destination links (scenario 1) and even worse (scenario 2). These gains are possible due to the radio resources optimization (frequency band allocation for each phase and transmitted power), see for example Figure 3.9 how the frequency allocation of user 1 for each phase ($\alpha_{1,1}$ and $\alpha_{2,1}$ are connected with phase I (*relay-receive*) and phase II (*relay-transmit*)) varies with the parameter μ (allows obtaining the boundary of the achievable rate region with $\mu_{s,1}=\mu_{r,1}=\mu$ and $\mu_{s,2}=\mu_{r,2}=1-\mu$, see (3.13)). For the scenario 2, where the relay-destination link quality is worse than for scenario 1, the band allocated for phase II ($\alpha_{2,1}$) is increased to combat the relay-destination link poor quality. Additionally, Figure 3.8 also allows comparing *synchronous* or *asynchronous* networks ($\beta_{1,1}=\beta_{1,2}=0$ in (3.14)). In such a case, when the relay-destination link is good (*scenario 1*), the source is not really helpful during the phase II, so the *synchronous* and *asynchronous* transmission exhibit a similar performance. Otherwise, when the relay-destination link is worse (*scenario 2*), the transmission of the source during phase II has an important influence.

B. Performance of cooperative/relay-assisted schemes

A direct comparison of the three cooperative schemes is a difficult task. While UC and RMAC seem more suitable for *user relaying*, the MARC is more appropriate for *infrastructure relaying*.

On the other hand, in UC relay terminals have their own traffic, whereas in RMAC and MARC relays are idle terminals. Hence, we have assumed different propagation scenarios in each case,

- *Scenario* RMAC: $\rho_{S-D,1}$= 4 dB, $\rho_{S-R,1}$=10 dB, $\rho_{R-D,1}$=6 dB (source 1) and $\rho_{S-D,2}$=0 dB, $\rho_{S-R,2}$=5 dB, $\rho_{R-D,2}$=4 dB (source 2)

- *Scenario* UC: $\rho_{S-D,1}$= 4 dB, $\rho_{S-R,1}$=10 dB, $\rho_{R-D,1}$=$\rho_{S-D,2}$ (source 1) and $\rho_{S-D,2}$=0 dB, $\rho_{S-R,2}$=10 dB, $\rho_{R-D,2}$= $\rho_{S-D,1}$ (source 2)

- *Scenario* MARC: $\rho_{S-D,1}$= 4 dB, $\rho_{S-R,1}$=10 dB, (source 1), $\rho_{S-D,2}$=0 dB, $\rho_{S-R,2}$=5 dB (source 2), and ρ_{R-D} =15 dB

The selection of parameters in each scenario has followed this rational: each source presents the same source-destination link quality in all scenarios, while the source-relay and relay-destination link quality is different. Note that in the UC, the relay-destination link SNR is the same for both sources. In the MARC configuration there is a single relay with a good relay-destination link quality, while for the RMAC scenario the relay-destination link quality is similar to the source-destination link quality
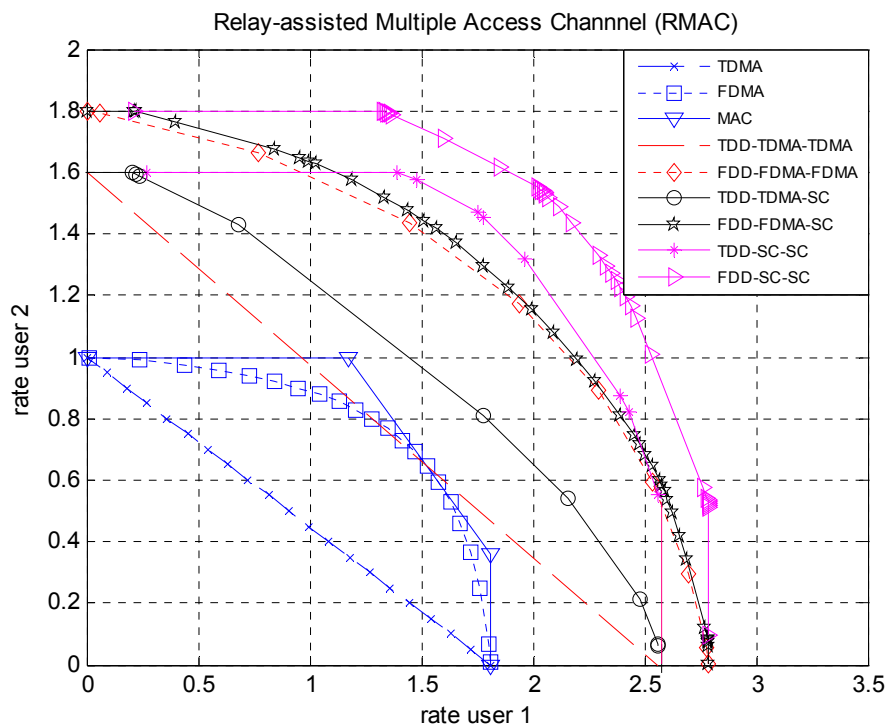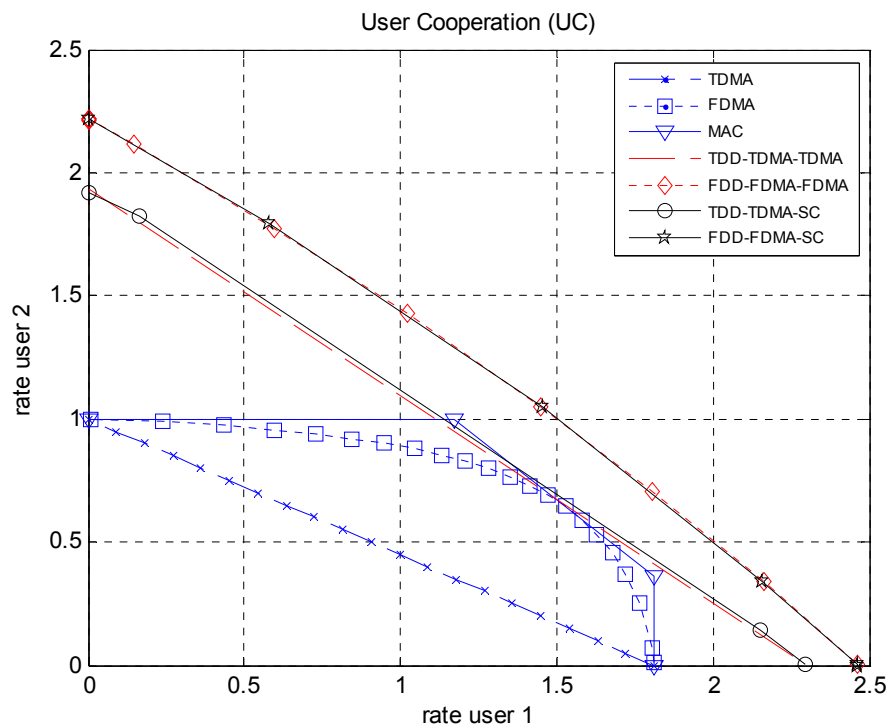

Figure 3.10.- Achievable rate regions for the direct transmission and RMAC scenarios. The relay-assisted transmission is duplexed in {TDD,FDD} and the access scheme on each phase can be {TDMA,FDMA,SC}. Synchronous transmission.

Figure 3.10 presents the achievable rate regions for the RMAC scenario when *synchronous transmission* is assumed under the different duplexing modes (TDD or FDD) and access schemes (TDMA, FDMA, SC) presented in section 3.4.1. Results are compared with a direct transmission scenario (where the sources do not use the assisting relays) under TDMA, FDMA

or superposition-coding transmission (conventional MAC channel). It can be seen the achievable rate region obtained with TDD-TDMA-SC is superior to the TDD-TDMA-TDMA, but FDD-FDMA-SC is just slightly better than FDD-FDMA-FDMA. Moreover we have extended the SC to phase I. Therefore, phase I becomes an *interference channel* because each relay is only interested in assisting its associated source (the signals transmitted from other sources are seen as interference). Figure 3.10 also shows the achievable rate region for the RMAC with TDD-SC-SC (stars) and FDD-SC-SC (right-triangle) when no-interference in phase I is assumed ($\alpha_{1,1}$= $\alpha_{1,2}$=α and α_2=(1-α) in (3.16) and destination observes a MAC channel in phase I, hence the constraints defined in the first row of (3.16) and (3.19) should be replaced by the ones in the first row of (3.32) and (3.36), respectively). In this manner, when the interference is high (but not enough to decode the interfering message at the assisting relays) the sources can transmit in phase I in orthogonal multiple access mode and when the interference is weak or much lower than the noise power, the sources can share the same resources for phase I. It is convenient to highlight that the difference between the TDD and FDD transmissions are due to the increased average power used by the sources and relays.

Figure 3.11.- Achievable rate regions for the direct transmission and UC scenarios. The cooperative transmission is duplexed in {TDD,FDD} and the access scheme on phase I and II can be {TDMA,FDMA} and {TDMA, FDMA, SC}, respectively. Synchronous transmission.

Figure 3.11 presents the achievable rate regions for the UC scenario (section 4.2) with *synchronous transmission*. The rate regions attained with TDD-TDMA-SC and FDD-FDMA-SC are just slightly better than using TDD-TDMA-TDMA and FDD-FDMA-FDMA, respectively. For this scenario it is not possible to adopt SC in phase I since relays operate in half-duplex mode.
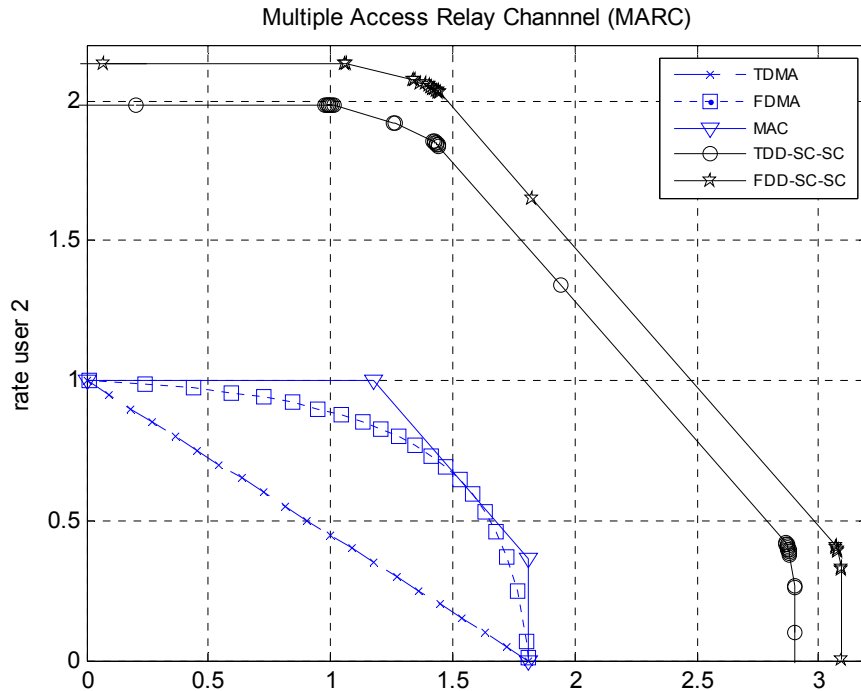
Figure 3.12.- Achievable rate regions for the direct transmission and MARC scenarios. The relay-assisted transmission is duplexed in {TDD, FDD} and superposition-coding multiple access (SC) is assumed for phase I and phase II. Synchronous transmission.

Figure 3.12 depicts the achievable rate regions for the MARC scenario (section 3.4.3) with *synchronous transmission*. The MARC scenario is able to enlarge the direct transmission achievable rate region thanks to the good relay-destination link quality. The differences of the regions obtained under TDD or FDD modes are due to increased average power used in the FDD transmission, as we have been assuming *power limited terminals.*

3.6 Conclusions

This work has shown that the radio resource allocation under optimization of the achievable rate region in the half-duplex relay multiple access channel with single-antenna terminals can be seen as a convex problem, under certain conditions. Three scenarios have been investigated: RMAC and UC (*user relaying*) and MARC (*infrastructure relaying*), where the terminals are assumed power constrained and relay duplexing is TDD or FDD. Basic access schemes can be considered under the same framework: orthogonal (TDMA or FDMA) or superposition coding (SC). The analysis also takes into account the *synchronous* (full CSIT at all transmitters) and *asynchronous* networks, and hence it is a general framework to compare performances and orient system design.

3.7 Appendix A. Achievable rate region of protocol III with synchronous transmission

The derivation of the achievable rate region defined in equation (3.3) and (3.8) for the single user relay-assisted transmission is similar to the one defined in section 2.6 of chapter 2 (Achievable rate region of protocol III) for the *asynchronous transmission*. The introduction of the *synchronous* transmission is straightforward as it will be shown in the following. Although the achievable sum-rate for the decode and forward relay channel is known [6], this derivation is needed for the multiple user case with half-duplex relays in Appendix B.

Let us assume the conventional MAC channel [7], two nodes transmitting independent messages of length *n* symbols in *n* channel uses, $X_{1,1}, X_{1,2}, \ldots X_{1,n}$ and $X_{2,1}, X_{2,2}, \ldots X_{2,n}$ with rate R_r and R_s, respectively. Both are transmitting to a common destination which is receiving the message $Y_1, Y_2, \ldots Y_n$, corrupted by Gaussian noise,

$$Y_k = X_{1,k} + X_{2,k} + N_k \qquad k = 1 \ldots n \tag{3.37}$$

This is the MAC channel with capacity region defined by [7],

$$\begin{cases} nR_r \leq \sum_{k=1}^{n} I\left(X_{1,k}; Y_k \mid X_{2,k}\right) \qquad nR_s \leq \sum_{k=1}^{n} I\left(X_{2,k}; Y_k \mid X_{1,k}\right) \\ n\left(R_s + R_r\right) \leq \sum_{k=1}^{n} I\left(X_{1,k}, X_{2,k}; Y_k\right) \end{cases} \tag{3.38}$$

In the following it will be shown that the half-duplex DF relay channel can be seen as a MAC channel with a proper modification of (3.38). The relay only is able to help the destination in phase II (Figure 3.2a). The destination is receiving data during both phases. In this scenario we can identify two *virtual* users transmitting independent messages: *source-relay virtual user* and *source-only virtual user*.

- *Source-relay virtual user*.- It is transmitting in two parallel channels from the source (in phase I with α*n* symbols) and the pair (source, relay) (in phase II with (1-α)*n* symbols). In the *asynchronous* mode, only the relay is considered in phase II. The relay must decode the message received in phase I. The message of the *source-relay virtual user* is given by

$$X_{1,k} = \begin{cases} X_{a,k} & k = 1 \ldots \lfloor \alpha n \rfloor \\ X_{b,k} & k = \lfloor \alpha n \rfloor + 1 \ldots n \end{cases} \tag{3.39}$$

with $X_{a,k}$ independent and identically distributed (i.i.d) according to a Gaussian distribution with power P_s (due to time domain) and $X_{b,k}$ i.i.d. Gaussian distributed simultaneously transmitted by the *synchronous* source and relay in phase II with power $\left(\sqrt{\beta_1 P_s} + \sqrt{P_r}\right)^2$. If the source and relay are *asynchronous* then β_1 is set 0. The achievable rate of the *source-relay virtual user* with is given by two constraints of the conventional *degraded relay channel* [7],

$$nR_r \leq \sum_{k=1}^{n} I\left(X_{a,k}; \tilde{Y}_k \mid X_{b,k}, X_{2,k}\right) = \sum_{k=1}^{\lfloor \alpha n \rfloor} I\left(X_{a,k}; \tilde{Y}_k \mid X_2\right)$$

$$nR_r \leq \sum_{k=1}^{n} I\left(X_{a,k}, X_{b,k}; Y_k \mid X_{2,k}\right) = \sum_{k=1}^{\lfloor \alpha n \rfloor} I\left(X_{a,k}; Y_k \mid X_{2,k}\right) + \sum_{k=\lfloor \alpha n \rfloor+1}^{n} I\left(X_{b,k}; Y_k \mid X_{2,k}\right)$$

(3.40)

where $\tilde{Y}_k$ denotes the signal received at the relay corrupted with Gaussian noise.

- *Source-only virtual user*.- Here, the source transmits in phase II $((1-\alpha)n$ symbols). It transmits an independent message using a Gaussian i.i.d. codeword $X_{2,k}$ with power $\beta_2 P_s$. Its achievable rate is given by,

$$nR_s \leq \sum_{k=1}^{n} I\left(X_{2,k}; Y_k \mid X_{1,k}\right) = \sum_{k=\lfloor \alpha n \rfloor+1}^{n} I\left(X_{2,k}; Y_k \mid X_{1,k}\right)$$

(3.41)

Finally, the constraint over the sum of the rates is given by

$$n\left(R_s + R_r\right) \leq \sum_{k=1}^{\lfloor \alpha n \rfloor} I\left(X_{a,k}; Y_k\right) + \sum_{k=\lfloor \alpha n \rfloor+1}^{n} I\left(X_{b,k}, X_{2,k}; Y_k\right)$$

(3.42)

The power distribution among the different messages during both phases at the source is constrained by,

$$\beta_1 + \beta_2 = 1$$

(3.43)

3.8   Appendix B. Achievable rate region for the RMAC

Based on the result of Appendix A, let us turn to the achievable rate region for *m* cooperative users in the RMAC channel, Figure 3.3, with TDMA in phase I and the superposition-coding multiple access in phase II (see Figure 3.5 for *m*=2). There are *m* phases I of length $\alpha_{1,k}n$ (*k*=1..*m*) channel uses and one phase II of $\alpha_2 n$ channel uses. The messages transmitted by the each cooperative user are defined in (3.39) for the *source-relay virtual* user and in (3.41) for the *source-only virtual user*. This scenario is in fact a MAC channel with $2m$ virtual users. Let us define the vector **R** with all the rates of the virtual users, defined by the set S_t and the operator $R(S)$ as a linear combination of some subset of those elements defined by S,

$$\mathbf{R} = \left[R_{r,1}\, R_{s,1}\, \ldots R_{r,m}\, R_{s,m} \right] \qquad R(S) = \sum_{i \in S} \mathbf{R}(i)$$

$$S_t = \{1 \ldots 2m\} \quad S_r = \{1, 3, \ldots 2m-1\} \quad S_s = \{2, 4, \ldots 2m\}$$

(3.44)

Notice that the odd elements of S_t define the position in vector **R** of the rates of the *source-relay virtual users* ($R_{r,k}$), subset S_r, while the even elements (subset S_s) are connected with the position of the rates of *source-only virtual users*, ($R_{s,k}$) in **R**.

The achievable rate region of the MAC channel [7] with $2m$ virtual users, a generalization of (3.38), is

$$nR(S) \le \sum_{k=1}^{n} I\left(X_k(S); Y_k \mid X_k(S^c)\right) \quad \forall S \subset S_t \tag{3.45}$$

with S^c denoting the complement of S and

$$X_k(S(u)) \begin{cases} X_{a,k}^{(l)} \text{ or } X_{b,k}^{(l)} & \text{if } S(u) \in S_r \\ X_{2,k}^{(t)} & \text{if } S(u) \in S_s \end{cases} \quad l = \frac{S(u)+1}{2}, \quad t = \frac{S(u)}{2} \tag{3.46}$$

where $S(u)$ is the u-th element of S, $X_{a,k}^{(l)}, X_{b,k}^{(l)}$ are the messages of the *source-relay virtual user* and $X_{2,k}^{(t)}$ stands for the message of the *source-only virtual user* connected with of the l-th and t-th cooperative user. S_r, S_s are the subset of *source-relay* and *source-only virtual users* defined in (3.44). In this sense the achievable rate region of the *2m* virtual users (*m* relay-assisted users) is defined by,

$$M_{tdd\_sup} = \begin{cases} nR(S) \le \eta(m,S) + \sum_{k=p(m)+1}^{n} I\left(X_k(S); Y_k \mid X(S^c)\right) \forall S \subset S_t \\ nR_{r,i} \le \sum_{k=p(i-1)+1}^{p(i)} I\left(X_{a,k}^{(i)}; \tilde{Y}_k \mid X_{b,k}^{(i)} = 0\right) \quad \forall i = 1 \ldots m \end{cases}$$

$$\eta(m,S) = \sum_{k=1}^{p(1)} Z(k,1,S) + \ldots + \sum_{k=p(m-1)+1}^{p(m)} Z(k,m,S) \tag{3.47}$$

$$Z(t,u,S) = \begin{cases} I\left(X_{a,t}^{(u)}; Y_t \mid X(S^c)\right) & \text{if } u \in S \\ 0 & \text{otherwise} \end{cases} \quad p(t) = \lfloor \alpha_{1,t} n \rfloor \quad \sum_{t}^{m} \alpha_{1,t} + \alpha_2 = 1$$

where $\tilde{Y}_k$ is the signal received at the k-th relay corrupted with Gaussian noise and the operator $R(S)$ is defined in (3.44). The function Z stands for the mutual information obtained by the message of the u-th *source-relay virtual user* during phase I ($\alpha_{1,u}$ channel uses) when that user is considered by the subset S. Moreover, the function η is due to the TDMA in phase I, while the $(m+1)$-th operator in (3.47) is because the SC of all *virtual* users in phase II. The message $X_k(S)$ is given by (3.46). The second constraint in (3.47) considers the achievable rates at the assisting relays for the *source-relay virtual users*.

3.9 References

[1] G.Kramer, M.Gastpar, P.Gupta, "Cooperative strategies and capacity theorems for relay networks", *IEEE Trans. on Information Theory*, vol. 51, no.9, pp. 3037-3046, Sept. 2005.

[2] A.Sendonaris, E.Erkip, B.Aazhang, "User cooperation diversity-Part I: system description", *IEEE Trans. on Communications*, vol. 51, no. 11, pp. 1927-1938, November 2003.

[3] A.Agustin, J.Vidal, "Radio resources optimization for the half-duplex relay-assisted multiple access gaussian channel", in *Proc. 8th IEEE Workshop on Signal Processing Advances in Wireless Communications* (SPAWC-2007), Helsinki, Finland, June 2007.

[4] A.Agustin, J.Vidal, "Radio resource optimization for the synchronous/asynchronous half-duplex relay multiple access channel", submitted to IEEE Trans. on Wireless Communications, December 2007 (TW-Dec-07-1454).

[5] E.Biglieri, G.Taricco, *Transmission and reception with multiple antennas: Theoretical Foundations*, Foundations and Trends™ in Communications and Information Theory Series, Now Publishers Inc., 2004.

[6] A.Host-Madsen, J.Zhang, "Capacity bounds and power allocation for wireless relay channel", *IEEE Trans. on Information Theory*, vol. 51, no.6, pp. 2020-2040, June 2005.

[7] T.M.Cover, J.A. Thomas, *Elements of Information Theory*, New York: Wiley 1991.

[8] M.Dohler, "Virtual Antenna Arrays", PhD Thesis, King's College London, London, UK, 2003.

[9] D.N.C.Tse, S.V.Hanly, "Multiaccess Fading channels-part I: Polymatroid structure, optimal resource allocation and throughput capacities", *IEEE Trans. on Information Theory*, vol. 44, no.7, pp. 2796-2815, November 1998.

[10] S.Boyd, L.Vandenberghe, *Convex optimization*, Cambridge University Press, 2004.

[11] J.Kiefer, "Sequential minimax search for a maximum", Proceedings of the America Mathematical Society, vol. 4, no. 3, pp.502-506, June 1953.

Chapter 4

TDD half-duplex relaying applied to TDMA systems with reuse of resources

THE relay-assisted transmission duplexed in time (TDD) is adapted to a cellular system based on TDMA in the *downlink* by using protocol I defined in chapter 2. Although there it was shown that in general the resources used in the relay-assisted transmission should be optimized (*relay-receive* and *relay-transmit phase*), here it is assumed a fixed and equal allocation of resources without requiring big modifications in the current cellular systems based on fixed-duration slot TDMA (*static resource allocation relaying*). However, this implies that the spectral efficiency of the relay transmission can be even lower than direct transmission case. In order to avoid such a case this chapter considers the cell-wide spatial reuse of the *relay-transmit phase* by multiple assisting relays associated to different destinations, which will transform the *relay-transmit phase* into an interference channel (IFC). Two possible solutions are envisaged to deal with the interference:

1. A distributed *power control*, where each relay must adjusts the transmitted power, and

2. A centralized *rate control*, based on the knowledge of the statistics of the interfering power. It is imposed a *target SNR* in the relay-destination link for all the simultaneous relay-assisted destinations. The source tunes the data rate based on the statistics of the interference.

In both cases, it is assumed that the relays are performed by idle terminals (*user relaying*). However it will be shown that *user relaying* is able to get similar gains as *infrastructure relaying*, where the relays (lampposts) are placed in positions with good source-relay and relay-destination channel conditions, which is beneficial for the relay-assisted transmission. Finally, cellular TDMA wireless networks can be enhanced with the *multiuser gain* by selecting those destinations with the best instantaneous channel realization. This aspect is analyzed for the relay-assisted transmission along with fairness between all destinations by proposing an adaptation of the *proportional fair* (PF) scheduler for the distributed power control solution.

4.1 Introduction

Chapter 2 has shown how the relay-assisted transmission is able to provide enhanced mutual information as compared to direct transmission in a three-terminal network. Henceforth, this chapter investigates the adoption of the relay-assisted transmission duplexed in time (TDD) for

cellular systems which are based on Time Division Multiple Access (TDMA) and there are a single source and multiple destinations. The principal objective is maximizing the spectral efficiency of the relay-assisted transmission, keeping the number of modifications in the cellular system as low as possible.

In the considered cellular system the source, a base station (BS), transmits the messages to destinations in equally sized time slots during a total time of T_{frame}. This type of communication is known as *downlink* transmissions. The relay-assisted transmission needs two time slots (*relay-receive* and *relay-transmit phase*). A loss in terms of spectral efficiency is expected because of the *static resource allocation relaying* (chapter 2).

Recently in [1], [2] a new strategy named *two-way relaying* is considered for improving the spectral efficiency in half-duplex relay transmissions. In a three-terminal network with two sources willing to transmit a message to each other, both assisted by a half-duplex relay, the transmission assumes that during the *relay-receive phase* both sources simultaneously transmit to the relay (as in the Multiple Access Channel, MAC). Afterwards, the relay transmits to both sources as in the broadcast channel (BC) during the *relay-transmit phase*. In this regard, two messages are transmitted in two time slots without requiring of extra resources. This strategy allows *uplink* and *downlink* transmissions in a cellular system in two phases, and hence the spectral efficiency loss is reduced. The relay must be selected to be good for both sources and because all the terminals operate in half-duplex mode (cannot receive and transmit simultaneously on the same frequency band) no cooperation is possible between source and relay.

An alternate way of dealing with the spectral efficiency loss is tackled in this chapter. We consider the cell-wide spatial reuse of a relay slot. Basically, it uses a single time slot to allocate all *relay-transmit phases* of the destinations served in the same frame. Therefore, having a frame of N_u+1 time slots only N_u destinations can be allocated in the same frame. If the number of allocated destinations grows, the increased utilization of resources is negligible. The spatial reuse will be investigated in the *downlink* and for *user relaying*.

In the *downlink* transmission the source transmits with full[1] power to each destination, allowing that other terminals (assisting relays) receive the same message. In this regard, protocol I, defined in chapter 2, has been considered to be applied in such scenario. Figure 4.1 depicts an example of the spatial reuse of a relay slot using protocol I. In this example there are two active destinations with two assisting relays (one per destination) and the communications will be carried out in a frame with three time slots. During the first time slot (*relay-receive phase* for destination-relay pair 1), the source transmits a signal which is received by the destination and the assisting relay. Afterwards, the source transmits a new signal that is received by the second destination and its associated relay (*relay-receive phase* for destination-relay pair 2). Finally, in the third time slot, both assisting relays transmit to its associated destinations (dashed lines in Figure 4.1). To this end, each destination is receiving in two time slots which can be seen as an increment of the *virtual receiving antennas*, [4].

As a consequence of the spatial reuse of the relay slot (third time slot in Figure 4.1) the common *relay-transmit phase* becomes an interference channel for which we will assume only *single-user receivers* at each destination. In this chapter, the achievable rate of the relay-

---

[1] As it happens in systems like HSDPA (High Speed Downlink Packet Access) systems [3].

assisted transmission will be investigated when the interfering power received during the *relay-transmit phase* is combated by means of,

- Distributed *power control* algorithm (section 4.3 and 4.4)

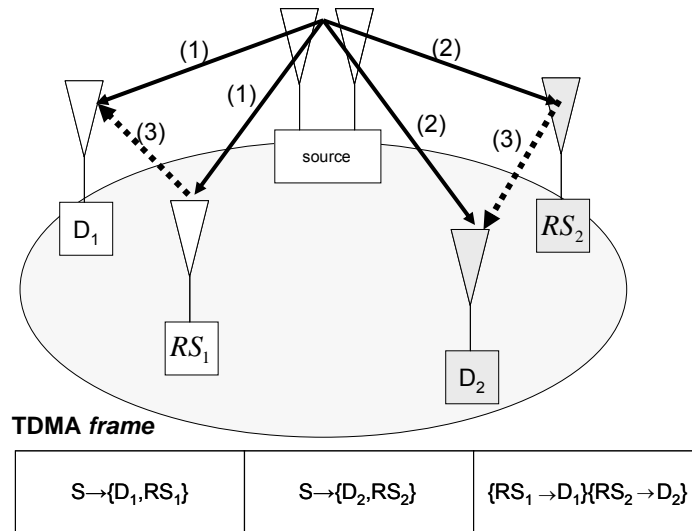- Centralized *rate control* based on the statistics of the interference (sections 4.5 and 4.6)

Figure 4.1.- Relay-assisted transmission for 2 destinations. Solid lines: transmissions during the *relay-receive phase* (in two orthogonal slots). Dashed lines: transmissions in the common *relay-transmit phase*.

The interfering power during the *relay-transmit phase* can be reduced by controlling those terminals which produce the larger interference to other destinations by a distributed power algorithm. For example in [5], a game theory framework is proposed for maximizing the rate between a source-relay pairs under simultaneous transmissions. It formulates a non-cooperative game in order to obtain the suitable power allocation strategy for each pair under OFDMA. In section 4.3 it will be presented an analysis of the cell-wide spatial reuse of the relay slot in the *downlink* also based on game theory [6]. The distributed power algorithm is applied to relay terminals which are idle terminals distributed around the cell (*user relaying*). The performance obtained under the assumption of *user relaying* is compared with *infrastructure relaying*, where the relays are lampposts with good link conditions with the source. It will be shown that *user relaying* is able to obtain similar performance as *infrastructure* relays when the terminal density is high enough. An additional aspect tackled for the relay-assisted transmission with spatial reuse of the relay slot is the definition of a practical scheme for medium access that is able to obtain some *multiuser gain* [7]. In non-relay-assisted networks, this gain is attained by allocating all the transmission resources to those destinations with the best instantaneous channels. Nevertheless, aspects related to the fairness among users also have to be considered. This task is performed by the scheduling algorithms. Section 4.4 presents redefinitions of the conventional scheduling algorithms for accommodating relay-assisted transmission *amplify-and-forward* (AF) and *decode-and-forward* (DF), [42][43].

On the other hand, when the interfering power statistics are known, the considered way for dealing with the interference is by tuning the rate of each transmission (*rate control*), [8], [9],[10]. In that case, the destinations served in the same frame are selected randomly over the cell in order to guarantee that the interference is a random process. For certain cases it is possible to

model the interfering power statistics, not the actual value of the interfering power. In such a case, the source may select a conservative rate to maximize the throughput of the system or keep a maximum outage probability. In order to provide a simple solution with low-complex terminals, only AF relay-assisted transmission is considered. However, this way does not allow exploiting the *multiuser gain*.

4.2   Scenario and signal model definition

The centralized cellular system (of area A m^2) is built upon a single source, the base station (BS), equipped with n_s antennas and N_{tot} terminals spatially distributed according to a *Poisson* distribution with parameter λ (average number of terminals per unit area) and having n_d antennas. Because of the assisting relays will be selected from those idle terminals (*user relaying*) the number of antennas at the relay will be the same as the active destinations, $n_r = n_d$.

Each destination interested in relay-assisted transmission selects the nearest idle terminal as its assisting relay. However, sometimes the nearest terminal might not be available. If all the idle terminals present the same probability to be successfully selected, named success probability, p_s, and the terminal have a *Poisson* distribution, then the distance, named r, between a destination and its assisting relay becomes a random variable modeled by a Rayleigh distribution with *pdf* given by [11] (see Appendix A in section 4.8),

$$f_r\left(r\right) = 2\pi\lambda_{relay}\,p_s\,r\,\exp\left(-\pi\lambda_{relay}\,p_s\,r^2\right) \tag{4.1}$$

where λ_{relay} denotes the idle terminal density of the cell, p_s is the success probability which accounts for a reduction in the density of the candidate relays. If $p_s = 1$, then the nearest terminal will always be the assisting relay. The success probability, p_s, may depend on several factors equal to all the terminals, for example the shadowing at the relay, the probability of having bad channel conditions in the source-relay link or the probability of this terminal being an active destination and hence not available as a relay. This last situation can be considered very unlikely if the number of terminals in the cell is much higher than the number of active terminals at each frame.
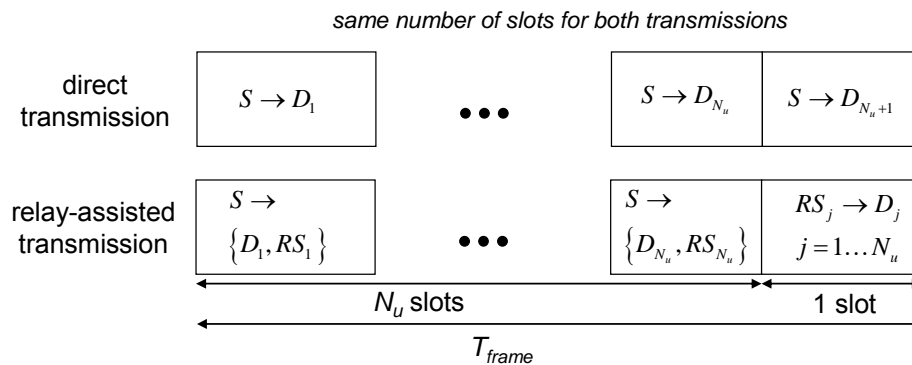

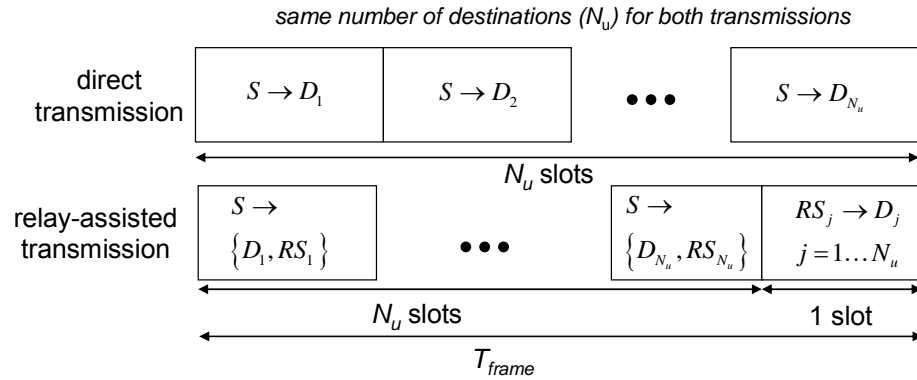**Figure 4.2.- Resource allocation for direct and relay-assisted transmission in TDMA with the same number of slots for both types of transmission.**

The source serves to N_u destinations selected among all terminals in TDMA-based transmission using a time frame length T_{frame}. The process described in Figure 4.1 for the relay-assisted transmission is extended for N_u destinations in Figure 4.2, where the frame is made up of N_u+1 time slots of length T_{slot}. Notice that with that frame definition it is possible to serve up to N_u+1 destinations using direct transmission. The ratio between the time slot and the frame duration is given by,

$$\frac{T_{slot}}{T_{frame}} = \frac{1}{N_u + 1}$$

(4.2)

However, when relay-assisted and direct transmission has to be compared with the same number of served destinations (N_u), then the frame structure under direct transmission must change keeping constant the T_{frame} (see Figure 4.3). In this regard the time slots considered in direct transmission must be larger than in the relay-assisted transmission, leading to define the following ratio

$$\frac{T_{slot}}{T_{frame}} = \begin{cases} \dfrac{1}{N_u} & \text{direct tx} \\ \dfrac{1}{N_u + 1} & \text{relay tx} \end{cases}$$

(4.3)

Figure 4.3.- Resource allocation for direct and relay-assisted transmission in TDMA with same number of served destinations for both types of transmission.

Taking into account the assumptions previously presented, for a given N_{tot} terminals in a region with area A, the different densities considered in this work are defined as,

$$\lambda = \frac{N_{tot}}{A} \quad \lambda_{active} = \frac{N_u}{A} \quad \lambda_{relay} = \frac{N_{tot} - N_u}{A}$$

(4.4)

with λ the terminal density, λ_{active} the density of the active destinations in the TDMA frame and λ_{relay} the idle terminal density.

In the following it will be defined the notation used for the channel matrices of the different relay links,

$$\begin{array}{lll} \mathbf{H}_0 & \left(n_d \times n_s\right) & \text{source-destination link} \\ \mathbf{H}_1 & \left(n_r \times n_s\right) & \text{source-relay link} \\ \mathbf{H}_2 & \left(n_d \times n_r\right) & \text{relay-destination link} \end{array} \tag{4.5}$$

Additional sub-indexes can be considered in order to specify the channel matrix for the different destinations. Moreover, it has been assumed that there is not channel state information at the transmitter (CSIT), so equal average transmitted power per antenna is adopted.

In direct transmission the source transmits orthogonally to each destination, so the normalized mutual information for each destination is defined as [12],

$$I^{DT} = \frac{T_{slot}}{T_{frame}} \log\det\left(\mathbf{I}_{n_d} + \frac{P_s}{n_s \sigma_{n_d}^2} \mathbf{H}_0 \mathbf{H}_0^H \right) \tag{4.6}$$

where $\sigma_{n_d}^2$ is the noise power at the destination, n_d and n_s denote the number of antennas at the destination and source, P_s is the power used by the source and T_{slot} and T_{frame} are defined by (4.2) or (4.3).

Protocol I is adopted for the relay-assisted transmission, see chapter 2, and relays works under *amplify-and-forward* (AF) or *decode-and-forward* (DF) mode. There is not any resource optimization because the *relay-receive* and *relay-transmit phase* are constrained to be of equal size T_{slot} (*static resource allocation relaying*). On the other hand, the signal model of the relay-assisted transmission should be modified in order to consider the interference received in the *relay-transmit* phase (relay slot).

For the AF approach, the signal received at the destination during both phases is modeled by,

$$\begin{bmatrix} \mathbf{y}^{(I)} \\ \mathbf{y}^{(II)} \end{bmatrix} = \begin{bmatrix} \mathbf{H}_0 \\ \mathbf{H}_2\mathbf{G} \ \mathbf{H}_1 \end{bmatrix} \mathbf{x} + \begin{bmatrix} \mathbf{I}_{n_d} & \mathbf{0}_{n_d} & \mathbf{0}_{n_d} \\ \mathbf{0}_{n_d} & \mathbf{H}_2\mathbf{G} & \mathbf{I}_{n_d} \end{bmatrix} \begin{bmatrix} \mathbf{n}_{n_d} \\ \mathbf{n}_{n_d} \\ \mathbf{n}_{n_r} \end{bmatrix} + \begin{bmatrix} \mathbf{0}_{n_d} \\ \mathbf{\upsilon} \end{bmatrix} = \mathbf{H}_{AF}\mathbf{x} + \mathbf{n}_b \tag{4.7}$$

where $\mathbf{y}^{(I)}$ and $\mathbf{y}^{(II)}$ are the received signal at the destination in each phase of the relay-assisted transmission, $\mathbf{x}$ is the signal transmitted by the source, $\mathbf{n}_{n_d}$ and $\mathbf{n}_{n_r}$ stand for the white Gaussian noise of zero-mean and covariance $\sigma_{n_d}^2$ and $\sigma_{n_r}^2$, $\mathbf{\upsilon}$ accounts for the interference received in the *relay-transmit phase* with interfering power σ_i^2. The interference is Gaussian when all the relays transmit Gaussian codewords. Finally, $\mathbf{G}$ is a linear combining matrix at the relay defined by,

$$\mathbf{G} = g\mathbf{I}_{n_r} \qquad g = \sqrt{\frac{P_r}{n_r} \bigg/ \left(trace\left(\mathbf{H}_1^H \mathbf{H}_1\right)\frac{P_s}{n_s} + n_r \sigma_{n_r}^2 \right)} \tag{4.8}$$

with P_r the power transmitted by the relay. The noise plus interference covariance matrix is given by,

$$\mathbf{R}_b = \begin{bmatrix} \sigma_{n_d}^2 \mathbf{I}_{n_d} & \mathbf{0} \\ \mathbf{0} & \sigma_{n_d}^2 \mathbf{H}_2 \mathbf{G}\mathbf{G}^H \mathbf{H}_2^H + \sigma_{n_d}^2 \mathbf{I}_{n_d} + \mathbf{v}\mathbf{v}^H \end{bmatrix} \qquad (4.9)$$

The normalized achievable rate of the AF relay-assisted transmission without CSIT is,

$$I^{AF} = \frac{T_{slot}}{T_{frame}} \log \det \left(\mathbf{I}_{2n_d} + \frac{P_s}{n_s} \mathbf{R}_b^{-1} \mathbf{H}_{AF} \mathbf{H}_{AF}^H \right) = \frac{1}{N_u + 1} \log \det \left(\mathbf{I}_{2n_d} + \frac{P_s}{n_s} \mathbf{R}_b^{-1} \mathbf{H}_{AF} \mathbf{H}_{AF}^H \right) \qquad (4.10)$$

Notice that the relay-assisted system resembles to a MIMO $2n_d \times n_s$ system for each destination in a TDMA system, except for the extra channel resources.

On the other hand, for the decode-and-forward approach the relay will be working under *unconstrained coding* (UC) (see section 2.2.1 equation (2.1)), hence the signal received at the destination is modeled as,

$$\begin{bmatrix} \mathbf{y}^{(I)} \\ \mathbf{y}^{(II)} \end{bmatrix} = \begin{bmatrix} \mathbf{H}_0 & \mathbf{0}_{n_d} \\ \mathbf{0}_{n_d} & \mathbf{H}_2 \end{bmatrix} \begin{bmatrix} \mathbf{x}_s \\ \mathbf{x}_r \end{bmatrix} + \begin{bmatrix} \mathbf{n}_{n_d} \\ \mathbf{n}_{n_d} \end{bmatrix} + \begin{bmatrix} \mathbf{0}_{n_d} \\ \mathbf{v} \end{bmatrix} = \mathbf{H}_{DF} \mathbf{x} + \mathbf{n}_b \qquad (4.11)$$

where $\mathbf{x}_s$ and $\mathbf{x}_r$ are the signals transmitted from the source and relay, respectively. The covariance matrices of the signal transmitted and the noise plus interference are,

$$\mathbf{Q}_x = \begin{bmatrix} \dfrac{P_s}{n_s} \mathbf{I}_{n_s} & \mathbf{0} \\ \mathbf{0} & \dfrac{P_r}{n_r} \mathbf{I}_{n_r} \end{bmatrix} \qquad \mathbf{R}_b = \begin{bmatrix} \sigma_{n_d}^2 \mathbf{I}_{n_d} & \mathbf{0} \\ \mathbf{0} & \sigma_{n_d}^2 \mathbf{I}_{n_d} + \mathbf{v}\mathbf{v}^H \end{bmatrix} \qquad (4.12)$$

The achievable rate of the DF approach taking into account the signal model of (4.11) and the source-relay transmission without CSIT, see section 2.2, is defined as

$$I^{DF} = \frac{1}{N_u + 1} \min \left(\log \det \left(\mathbf{I}_{n_r} + \frac{P_s}{n_s \sigma_{n_r}^2} \mathbf{H}_1 \mathbf{H}_1^H \right), \log \det \left(\mathbf{I}_{2n_d} + \mathbf{R}_b^{-1} \mathbf{H}_{DF} \mathbf{Q}_x \mathbf{H}_{DF}^H \right) \right) \qquad (4.13)$$

with $\mathbf{Q}_x$, $\mathbf{R}_b$ defined in (4.12) and $\mathbf{H}_{DF}$ defined in (4.11).

4.3 Distributed power control

Game theory is a tool for analyzing multi-person decision making. It has been used by the economists, but in recent years it has been considered also to analyze different problems in different areas of communications, like power control in CDMA wireless systems [15].

The objective is to apply the game theory framework in the scenario described in the previous section, the spatial reuse of the relay slot. In this regard, during the *relay-transmit phase* or relay

slot, see Figure 4.1, there are N_u assisting relays transmitting simultaneously to their associated destinations generating interference to the remaining terminals which will depend on the power transmitted by each relay. The TDMA frame is made up of N_u+1 slots and the ratio between slot and frame duration is given by (4.2) for direct and relay-assisted transmission. Game theory offers a framework to control in a distributed way the interference.

4.3.1 Game theory overview

In *non-cooperative*[2] games each player involved in the game pursues his own interests which may be partly conflicting with others [13],[14]. As the players do not always have complete control over the outcome of the game, conflicts with other players arise. The components of game are:

- The set of players named Ω with Q players. $\Omega = \{1, 2, 3, \ldots, Q\}$

- The set of pure strategies $X \subseteq \mathcal{R}^Q$ with $\mathbf{p} = \begin{bmatrix} p_1, \ldots p_Q \end{bmatrix}^T \in X$ where p_q represents the strategy of the *q*-th player. Additionally, $\mathbf{p}_{-q}$ will define the strategy of all the remaining Q-1 players.

- The set of utility (or payoff) functions that map the strategies of each user to real numbers. The function u_q will be the utility function for the *q*-th player which also depends on the strategy of all the players.

The *non-cooperative* game is defined by

$$G = \left\{ \Omega, X, \left\{ u_q \right\}_{q \in \Omega} \right\} \tag{4.14}$$

where all players always maximize their utility function rationally, i.e. they do not try to cheat. Each player modifies its strategy in order to maximize its utility function in each iteration of the game. The *readjustment scheme* is defined as how the players update their actions. For example in this work, all players update their actions simultaneously. Another possibility is that the players update their actions sequentially.

Two concepts are important in game theory, the *Nash equilibrium* and the *Pareto solution*. The Pareto solution is obtained when it is impossible to improve the utility of any player without degrading the utility of other player. We can get an optimal set $\mathbf{p}^*$ such as fulfills the following equation,

$$u_q \left(p_q^*, \mathbf{p}_{-q}^* \right) \geq u_q \left(p_q, \mathbf{p}_{-q} \right) \qquad \forall \, p_q \in \mathbf{x}_q, q \in \Omega \tag{4.15}$$

The *Nash equilibrium* (NE) is a strategy profile where no player may get better utility by unilaterally deviating, providing a stable operating point. Each player finds a solution p_q^* such as,

$$u_q \left(p_q^*, \mathbf{p}_{-q} \right) \geq u_q \left(p_q, \mathbf{p}_{-q} \right) \qquad \forall \, p_q \in \mathbf{x}_q, q \in \Omega \tag{4.16}$$

---

[2] It is a type of game and is not connected with cooperative/relay-assisted transmission.

The number of NE in a game, if it exists, can be more than one. Therefore if it desired that the game always converge to the same point for each possible strategy, we must prove its existence and uniqueness. The Pareto solution might not coincide with any of the NE points.

In [16] it is proved the existence and uniqueness of *Nash equilibrium* point when the utility functions used by the players are concave. Moreover, [17] defines the concept of *standard* utility functions which describe games with a unique *Nash equilibrium* point. A utility function is *standard* if for all $\mathbf{p} \geq 0$ the following properties are satisfied:

- *Positivity* $u_q(\mathbf{p}) > 0 \qquad \forall q \in \Omega, \quad \mathbf{p} \in \mathbf{X}$

- *Monotonicity³* *if* $\mathbf{p} \geq \mathbf{p}'$ $u_q(\mathbf{p}) \geq u_q(\mathbf{p}')$ $\forall q \in \Omega, \quad \mathbf{p}, \mathbf{p}' \in \mathbf{X}$ (4.17)

- *Scalability*   For all $\alpha > 1, \quad \alpha u_q(\mathbf{p}) > u_q(\alpha \mathbf{p}) \qquad \forall q \in \Omega, \quad \mathbf{p} \in \mathbf{X}$

Another way for deriving sufficient conditions for existence and uniqueness is the use of the called *potential games*, [18]. This type of game is produced when the incentive of all players to change their strategy can be expressed by a global utility function V. There is an *exact potential game* if it exist the function V such that,

$$u_q\left(p_q, \mathbf{p}_{-q}\right) - u_q\left(p_q^+, \mathbf{p}_{-q}\right) = V\left(p_q, \mathbf{p}_{-q}\right) - V\left(p_q^+, \mathbf{p}_{-q}\right) \qquad \forall \, p_q, p_q^+ \in \mathbf{x}_q, q \in \Omega \qquad (4.18)$$

An *ordinal potential game* is defined by,

$$u_q\left(p_q, \mathbf{p}_{-q}\right) - u_q\left(p_q^+, \mathbf{p}_{-q}\right) > 0 \Rightarrow V\left(p_q, \mathbf{p}_{-q}\right) - V\left(p_q^+, \mathbf{p}_{-q}\right) > 0 \quad \forall \, p_q, p_q^+ \in \mathbf{x}_q, q \in \Omega \qquad (4.19)$$

In such a case, the game defined by the utility function V present the same NE points as the original game, (4.14). See for example [19], where the different utility functions of the players can be reduced to a common utility function.

The efficiency of a NE point in *non-cooperative* games can be improved by *pricing* [20]. It consists in modifying the utility function of each player, sometimes incorporating some common value known by all the players. In that case, all the players should have access to that value.

4.3.2 Spatial reuse of the relay slot

The power control in the relay transmissions with spatial reuse can be defined as game

$$G = \left\{ \Omega, \mathrm{X}, \left\{ u_q \right\}_{q \in \Omega} \right\} \qquad (4.20)$$

where Ω is the set of players, in this case the destination-relay pairs active in the *relay-transmit phase* (or relay slot), X denotes the set of pure strategies, where the set of the values of power transmitted by the q-th relay is in the set X_q and u_q the utility of each player,

---

³ When two vector are defined as $\mathbf{p} \geq \mathbf{p}'$, the condition is satisfied in each element of the vector.

$$\Omega = \{1,2,3,\ldots,N_u\}$$
$$X_q = [0, P_{max}] \qquad \forall q \in \Omega \qquad (4.21)$$
$$X = X_1 \times X_2 \times \ldots X_Q$$

The proposed utility function for each user considered here is,

$$u_q(\mathbf{p}) = \frac{I(p_q, \mathbf{p}_{-q})}{P_s + p_q} \quad bits/Joule \qquad p_q \in \mathbf{x}_q \quad \forall q \in \Omega \qquad (4.22)$$

where $I()$ is the mutual information of the relay-assisted transmission (in AF, equation (4.10) or in DF, equation (4.13)), P_s is the power used at the source which transmits with fixed power, p_q is the selected transmission power of the q-th assisting relay and $\mathbf{p}_{-q}$ defines de power vector of the remaining relays. The proposed utility function gives the theoretical maximum number of bits/s/Hz[4] without error we can transmit per unit of employed energy. The consideration of the total required power, including the source power, P_s, allows a fair comparison of mutual information with respect to the direct transmission scheme in terms of equal transmitted power. Hence, it is possible to identify when the use of relay-assisted transmission does not improve mutual information, in that case the utility function presents a maximum for p_q equal to zero, and therefore that relay is automatically switched off.

The game will be played during several iterations for the destination-relay pairs in order to adjust the powers at the relays. This implies that the channel must keep constant if expressions defined in (4.10) for the AF and (4.13) for the DF are used. In order to avoid this limitation, the players will use approximations of the previous expressions assuming uncorrelated channels, large number of antennas and $n_s \geq n_r \geq n_d$,

$$\tilde{I}^{AF}(\mathbf{p}) = \frac{1}{N_u + 1}\left(n_d \log(1 + \gamma_0) + n_d \log\left(1 + \frac{\gamma_1 \gamma_2}{1 + \gamma_1 + \gamma_2}\right)\right)$$

$$\tilde{I}^{DF}(\mathbf{p}) = \frac{1}{N_u + 1}\min\left(n_r \log(1 + \gamma_1), n_d \log(1 + \gamma_0) + n_d \log(1 + \gamma_2)\right) \qquad (4.23)$$

with γ_0, γ_1, γ_2 denoting the signal to noise ratio (SNR) in the source-destination, source-relay and relay-destination link due to the path-loss. The definition for the q-th player is given by,

$$\gamma_{0,q} = \frac{P_s}{L_{0,q}\sigma_{n_d}^2} \qquad \gamma_{1,q} = \frac{P_s}{L_{1,q}\sigma_{n_r}^2} \qquad \gamma_{2,q} = \frac{p_q/L_{2,q}}{\sigma_{n_d}^2 + \sum_{k=1}^{Q}\frac{p_k}{L_{2,q-k}}} \qquad (4.24)$$

where $L_{0,q}$, $L_{1,q}$, $L_{2,q}$ stand for the path-loss in the source-destination, source-relay and relay-destination link. Additionally, $L_{2,q-k}$ defines the path-loss between the q-th relay and the k-th destination (which is interfered by the q-th relay).

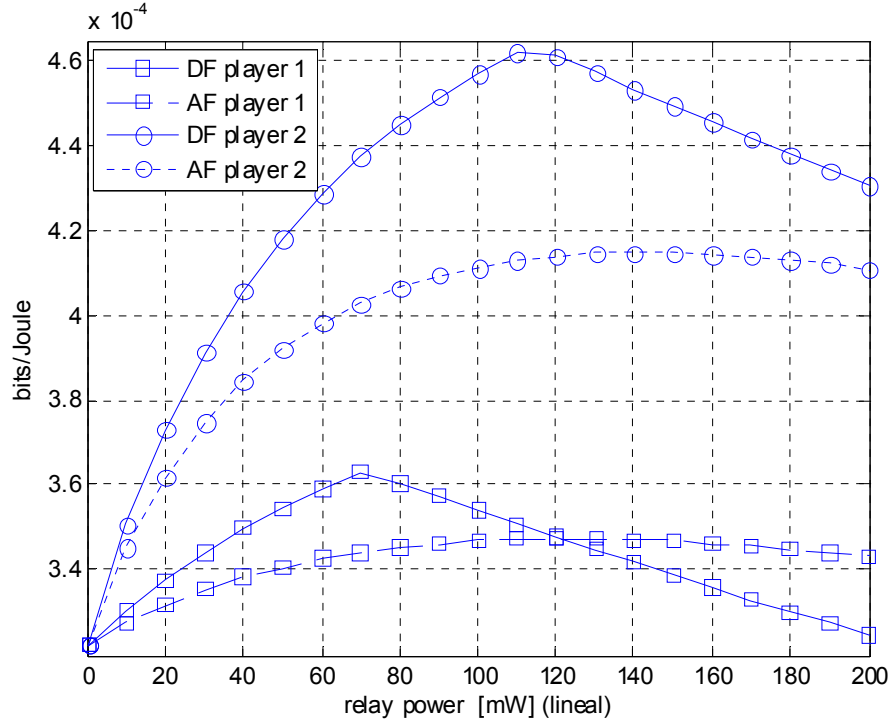[4] Assuming ideal sampling and filtering process, otherwise it is *bits/channel use.*

Figure 4.4.- Utility function of 2 players. Amplify and forward with n_s=2,n_r=n_d=1 (dotted lines), Decode and forward with n_s=n_r=2, n_d=1 (solid lines).

Figure 4.4 depicts the utility function defined in (4.22) for two different players using AF (dotted lines) or DF (solid lines) as a function of the transmitted power of the relay. The utility function considers the approximations of the mutual information defined in (4.23). The utility function depends on the mutual information, which increases with the power of the q-th relay p_q but at the same time the use of more power increases the denominator of (4.22) penalizing the utility function. That motivates that the utility function is zero when $p_q \rightarrow \infty$. For example, using the utility function with AF the players present the maximum values at p_1=120 and p_2=140 mW. For the DF case, it can be seen that $min()$ operator in (4.23) may produce discontinuities in the derivatives of the utility function (at p_1=110 and p_2=70 mW).

4.3.3 Existence and uniqueness of Nash Equilibrium

The proposed utility function in (4.22) is not concave. It is not a *standard* function (4.17), because it can not satisfy the monotonicity property. Additionally it can not be formulated as a *potential game* because there is not a function V valid for all the users satisfying the properties of (4.18) or (4.19). Therefore some additional results are needed to prove the existence and uniqueness of the Nash Equilibrium points of a game with the proposed utility function.

Existence of Nash Equilibrium

Proposition 1.-The game $G = \left\{ \Omega, \mathrm{X}, \left\{ u_q \right\}_{q \in \Omega} \right\}$ has a least one Nash equilibrium point if for all $q \in \Omega$:

    1) $\mathbf{x}_q$ is a non-empty, convex, and compact subset of a Euclidean space.
    2) $u_q(\mathbf{p})$ is continuous in $\mathbf{p}$ and quasi-concave in p_q.
Proof: See [21].

By definition the action sets $\mathbf{x}_q$ are non-empty and convex (4.21). Each $\mathbf{x}_q$ is closed so it is also compact, satisfying the first condition. Moreover, our proposed utility function in (4.22) is quasi-concave.

A function $y(x)$ is quasi-concave if and only if either [22]

- y is *non-increasing*
- y is *non-decreasing*
- there is a x^* such that $y(x)$ is *non-decreasing* for $x<x^*$ and *non-increasing* for $x>x^*$.

Therefore the first and second derivatives of the function u_q over the variable p_q have to be studied in order to know their properties. The function u_q (4.22) can be redefined as,

$$u(p) = f(p)g(p) \qquad f(p) = I(p) \quad g(p) = \frac{1}{P_s + p} \tag{4.25}$$

where $I()$ denotes the mutual information for the AF or DF defined in (4.23). The set of p values which set to zero the first derivative of u is given by,

$$\Psi = \left\{ p \mid f'(p)g(p) - f(p)g'(p) = 0 \right\} \tag{4.26}$$

The second derivative is defined by

$$u''(p) = \frac{f''(p)}{f(p)} - 2\left(\frac{g'(p)}{g(p)} \right)^2 + \frac{g''(p)}{g(p)} \qquad p \in \Psi \tag{4.27}$$

Taking into account the current value of the $g()$ function (4.25) and its derivatives, the second derivative of the utility simplifies to,

$$u''(p) = \frac{f''(p)}{f(p)} \qquad p \in \Psi \tag{4.28}$$

For the AF approach the equation (4.28) is always negative because the mutual information increases logarithmically with p. Hence, there is no minimum, or equivalently, the utility function is monotonic (*non-increasing* or *non-decreasing*) or it has a single maximum (conditions for quasi-concavity). On the other hand, for the DF the mutual information (4.23) depends on the minimum of two functions, so the evaluation of (4.28) is more elaborated. Assume that p_0 is the power which bounds that the mutual information is limited by the source-relay or the (source,relay)-destination link. When the power of the relay p goes from 0 to p_0 the mutual information is given by the expression of the (source,relay)-destination link and increases logarithmically with p. As a consequence for that interval of values the utility function is monotonic or it has a single maximum. When $p>p_0$ the mutual information is limited by the source-relay link which is constant and the utility function $u(p) = g(p)$ decreases with p (see equation (4.25)). Therefore, the utility function is also quasi concave.

Uniqueness of Nash Equilibrium

Unfortunately, the uniqueness of Nash Equilibrium only can be assessed by means of simulations. In this regard *definition 4.5* of [13] is adopted,

Definition 1.- In a game G (4.20), a Nash equilibrium p_q^* with $q \in \Omega$, is stable with respect to an *readjustment scheme S* if it can be obtained as the limit of the iteration,

$$p_q^* = \lim_{\tau \to \infty} p_q(\tau) \tag{4.29}$$

$$p_q(\tau+1) = \arg \max_{p_q \in \mathbf{x}_q} u_q\left(p_q, \mathbf{p}_{-q}^{S_\tau}\right), \qquad p_q(0) \in \mathbf{x}_q, \quad q \in \Omega \tag{4.30}$$

where equation (4.30) is also known as the *best response* of the q-th player, the superscript S_τ indicates that the precise choice of $\mathbf{p}_{-q}^{S_\tau}$ depends on the *readjustment scheme* selected, that is, how the players update their actions. If the iteration of *definition 1* converges, the Nash equilibrium is unique with respect to the scheme S. For example the scheme considered in this work is

$$\mathbf{p}_{-q}^{S_\tau} = \mathbf{p}_{-q}(\tau) \tag{4.31}$$

which describes the situation where the players update their actions simultaneously in response to the most recent actions of the other players.

4.3.4 Distributed power computation

The game will be played on each TDMA frame. The following procedure summarizes the distributed power computation,

1. Initialization (τ=0). Firstly, all the relays will transmit with some initial power $p_q \in \mathbf{x}_q$ (see equation (4.21)).

2. During the *relay-transmit phase* (relay slot) of the τ-th frame, each destination measures the interfering power received (which will be the denominator of $\gamma_{2,q}$ in (4.24)), and $\gamma_{1,q}$, $\gamma_{0,q}$ of the q-th player.

3. Decision of the power used at each relay for the next frame (τ+1). Each player independently obtains the *best response*,(4.30), i.e. selects that power which maximizes its own utility function u_q, (4.22) given the measured interfering power. Notice that the value of the interfering power depends on the actions taken by the other players in the previous frame.

4. The iterative procedure continues until all players find that the change in their power levels is less than a pre-defined bound, or an upper limit on the number of iterations is reached.

Results will show that the game describing the simultaneous relay transmissions in the *relay-transmit phase*, (4.20), converges to the same power values for different power initializations.

4.3.5 Results

For the simulations, the following scenario has been considered: a square area of 900x900 m^2, one source in the center of the cell using omni-directional antennas, terminals are uniformly distributed in the cell with Rayleigh flat fading channels. The distance loss model is the usual inverse law with propagation exponent to be 4. The source transmission power is 30 dBm (P_s=1000 mW) and the terminals have maximum transmission power of 23 dBm (P_{max}=200 mW). The thermal noise at the terminals is −115.2 dBm, [3]. We consider that each user has chosen a relay terminal around which is at a distance according to (4.1), (*user relaying*).

Convergence of the algorithm

Figure 4.5 shows the evolution in the transmitter power for the relays assigned to three destinations named 2, 3 and 6 for a specific scenario realization where the assisting relays create interference to the associated destinations to those relays. It has considered three different initializations of the iterative algorithm, considering the AF scheme. It is worth noticing that the power of the assisting relay 2 converges to zero, that it is destination 2 decides to do not use the relay-assisted transmission. The algorithm converges, after a few iterations, to the same stationary point for the relays power with independence of the initial power values. The same behaviour, not plotted in the figure for clarity, is observed over the remaining destinations served in the same frame.

Cellular capacity

Figure 4.6 shows the cumulative function of the cell capacity or sum-throughput[5] for n_s equal to two antennas at the source (BS) with and without relay-assisted transmission (cross solid line). Two different terminal densities are considered which will impact on the terminal selection as assisting relay, λ=10^{-3} terminals/m^2 (circles) and λ=10^{-4} terminals/m^2 (diamonds). Circle and diamond solid lines corresponds to the AF approach with n_r=1 antenna at the assisting relay while dotted lines corresponds to the DF approach with n_r=2 antennas. As in the *user relaying* the assisting relay will be nearby the destination, we will assume that the assisting relays are equipped with n_r=2 antennas in order to avoid the limitation of the source-relay link in the DF. In such a case, the source-relay links present a 2×2 MIMO configuration. It can be seen that the relay-assisted transmission improves the direct transmission (2×1 MISO). When DF is assumed, gains of 66% (λ=10^{-4}) and 90% (λ=10^{-3}) over the direct transmission are possible. On the other hand, using AF the gains are 45% (λ=10^{-4}) and 66% (λ=10^{-3}). Although the AF is inferior to the DF, it only requires of a single antenna and simple operation (*amplify-and-forward*) at the relay-assisting terminal.

Basically, these gains of the relay-assisting transmission depend on:

1.-The reuse of the relay slot (number of terminal using relay-assisted transmission in the same frame).

2.-Interference at the relay-transmit phase (relay slot).

3.-The position of the relay terminal.

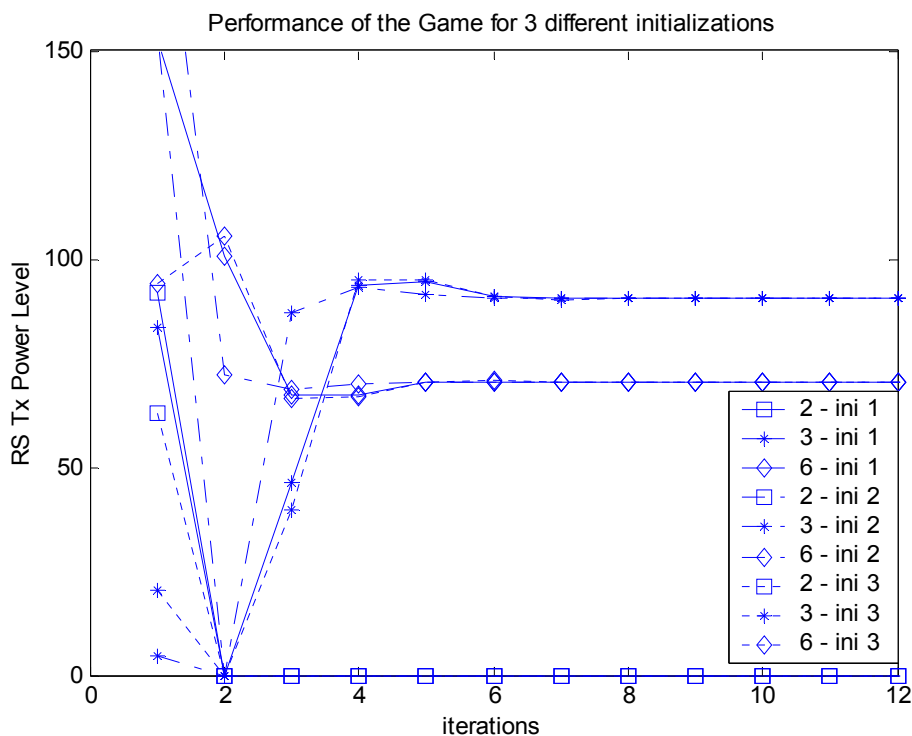[5] Total throughput delivered by the source in each frame.

Figure 4.5.- Convergence of the algorithm. The destination-relay pairs {2,3,6} describe a scenario where those destinations are receiving interference from the other relays.
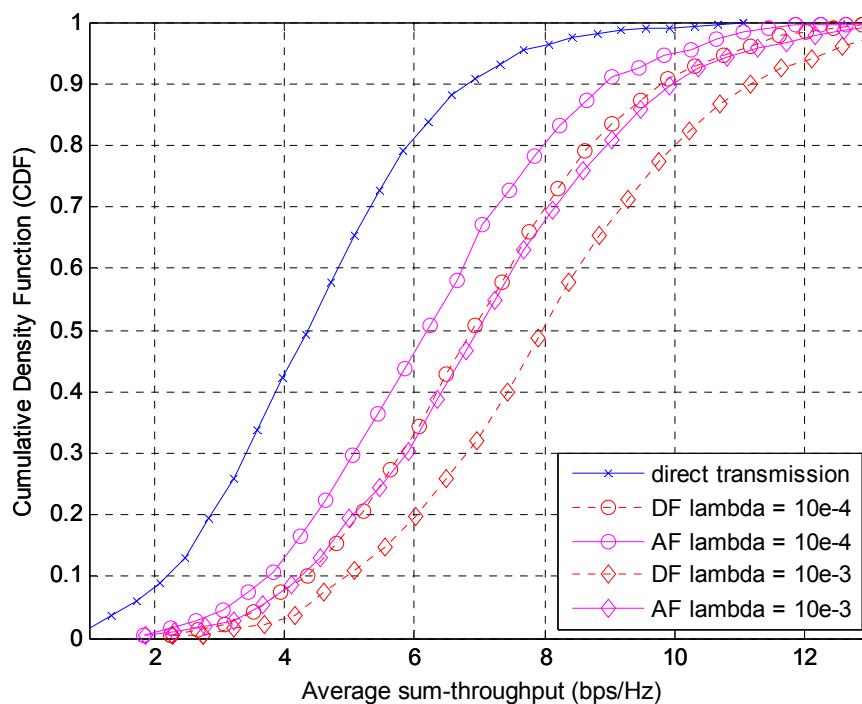

Figure 4.6.- CDF of the average sum-throughput for direct and relay-assisted transmission (AF- solid lines, DF- dotted lines) with different terminal densities ($\lambda=10^{-3}$ – circles, $\lambda=10^{-4}$ - diamonds). $n_s=2$, $n_d=1$, $n_r=1$ (AF) and $n_r=2$ (DF).

Figure 4.7 depicts the cumulative density function of the number of destinations that participate in the relay-assisted transmission for the AF $n_s=2$, $n_r=n_s=1$ (solid lines) and DF $n_s=2$, $n_r=n_s=1$ (dotted lines) modes. The frame contains 10 time slots (maximum 9 relay-assisted

destinations). Those destinations which select the direct transmission after playing the distribute power algorithm are allocated in the same frame. For example with DF during the 90% of the time only 3.2 terminals (in average) will use the relay-assisted transmission, while for the AF, up to 5.5 terminals ($\lambda=10^{-4}$) and 7.2 terminals ($\lambda=10^{-3}$) use this type of transmission.
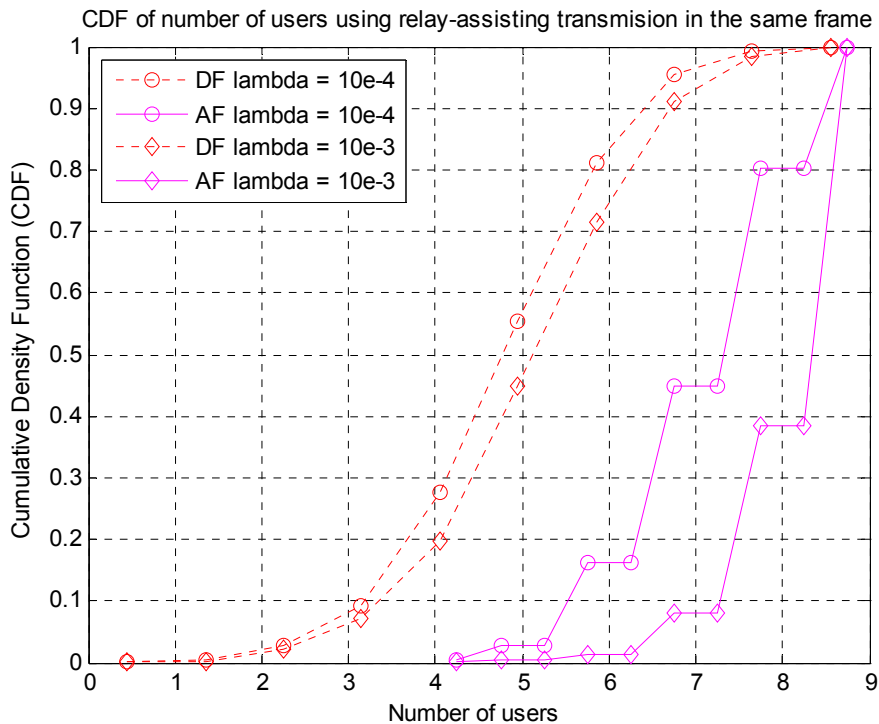
Figure 4.7.- CDF of the number of terminals using relay-assisting transmission in a frame with 10 time slots when using DF (dotted lines) or AF(solid lines). Different terminal densities: $\lambda=10^{-3}$ (circles) and $\lambda=10^{-4}$ (diamonds). n_s=2, n_d=1, n_r=1 (AF) and n_r=2 (DF).

Infrastructure vs user relaying

A comparison between the *infrastructure relaying*, where the relays are usually a lamppost in Line of Sight (LOS) with the source, and the *user relaying*, where the relays are idle terminals close to the destination is presented in [33]. Figure 4.8 depicts the *infrastructure relaying*, where the transmissions from the source and relay are duplexed in time and there is not spatial reuse of the *relay-transmit phase*, see Figure 4.8-bottom, so there are as many relay slots as destinations served in a frame. Although the efficiency of this scheme is 1/2 (two time slots are required) compared with direct transmissions (1 time slot), see Figure 4.2. It is expected that the factor 1/2 could be compensated by the *multipath gain* provided by the relay position (or *path-loss breaking*). On the other hand, for the *user relaying*, Figure 4.1, it is assumed that each destination has a partner (relay) nearby and there is only 1 relay slot spatially reused. In the relay slot, all the active assisting relays transmits simultaneously to its associated destination, producing an interference channel, as it has been described in section 4.2. The power control algorithm described in section 4.3 is adopted to combat the interference. In order to compare both types of relaying, the time slots for *infrastructure relaying* have the half-size of the time slots considered for *user relaying*. However, now, each destination is using two time slots.
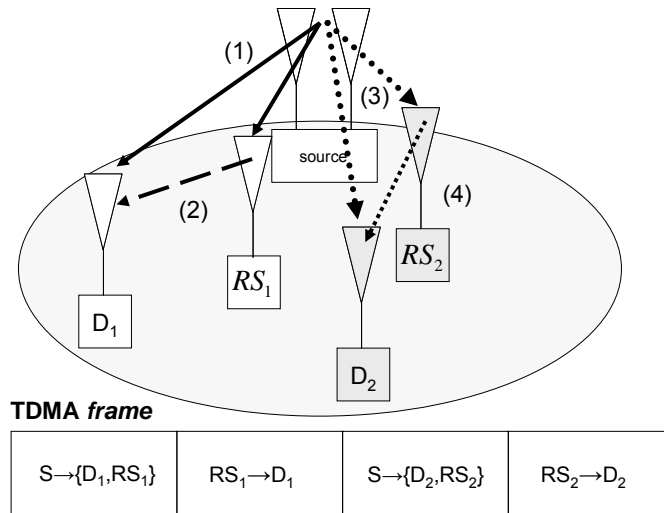
Figure 4.8.- Infrastructure relaying. The relay-assisted transmission is done using protocol I (or forwarding) in orthogonal time slots (no spatial reuse).
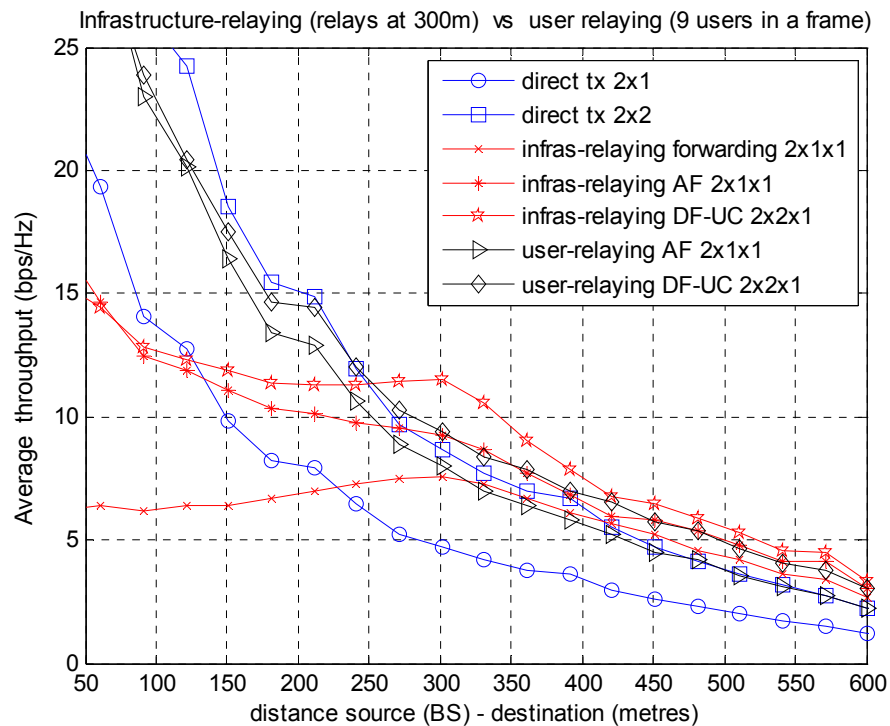

Figure 4.9.- Average throughput vs distance for the infrastructure relaying (RS placed at 300 meters) and for the user relaying, with a user density $\lambda=10^{-4}$ users/m^2.

Figure 4.9 shows the results in terms of average throughput as a function of the distance. The source, relay and destination have n_s=2, n_r=1(AF) or 2(DF), n_d=1 antennas, respectively. For the *infrastructure relaying* there are 8 relays (lampposts) placed at 300 meters from the source and each destination selects the nearest one. In the *user relaying* case, the assisting relay is nearby of the destination at a random distance depending on the terminal density (section 4.2). In Figure 4.9 several aspects can be observed. First, the AF forwarding, (destination only considers the data received in the *relay-transmit phase*), improves the total throughput for users in the border cell. This performance can be improved when the destination is allowed to combine the transmissions from the source and the relay. Note that for a destination close to the relay terminal (300 m) the throughput is improved. However, the nearest users to the source

(BS) are affected for the spectral efficiency loss and the distance from the relay (there is no optimization of the duration of the *relay-receive* and *relay-transmit* phase). See also Table 4.1 for results in terms of spectral efficiency. Figure 4.9 also shows the performance of the relay-assisted transmission under *user relaying*. Note that in this case the average throughput is improved for destinations in all the distances, achieving a similar performance as $n_s \times 2n_d$ direct TDMA system. Although the infrastructure scheme still offers better efficiency, see Table 4.2.

Transmission	Efficiency (bps/Hz/Km^2)	
	Average	*10% Outage*
Direct Tx $\quad n_s \times n_d$	3.5	2.8
Relaying AF	4.9	3.9
Relaying DF $\quad n_r=1$	5.0	4.0
Relaying DF $\quad n_r=2$	5.6	4.9
Cooperative AF $\quad n_r=1$	6.2	5.1
Cooperative DF $\quad n_r=1$	5.5	4.6
Cooperative DF $\quad n_r=2$	7.0	6.2

Table 4.1.- Efficiency for the infrastructure relaying.

Transmission	Efficiency (bps/Hz/Km^2)	
	Average	*10% Outage*
Direct Tx $n_s \times n_d$	3.5	2.8
Direct Tx $n_s \times 2n_d$	6.9	5.7
Cooperative AF $n_r=1$	5.3	4.1
Cooperative DF $n_r=2$	5.9	4.9

Table 4.2.- Efficiency for the user relaying. $\lambda=10^{-4}$ users/m^2.

However, when the terminal density increases up to $\lambda=5\times10^{-3}$ terminals/m^2, the *user relaying* provides similar performance than the infrastructure relaying, see Table 4.3.

Transmission	Efficiency (bps/Hz/Km^2)	
	Average	*10% Outage*
Direct Tx $n_s \times n_d$	3.5	2.8
Direct Tx $n_s \times 2n_d$	6.9	5.7
Cooperative DF $n_r=2$ $\quad(\lambda=10^{-4})$	5.9	4.9
Cooperative DF $n_r=2$ $\quad(\lambda=10^{-3})$	6.9	5.7
Cooperative DF $n_r=2$ $\quad(\lambda=5\times10^{-3})$	7.1	5.9

Table 4.3.- Efficiency for the user relaying for different terminal densities.

Summarizing, it has been shown how the relay-assisted transmission under *user relaying* is able to obtain similar results as $n_s \times 2n_d$ direct transmission and additionally it can achieve similar results as the infrastructure relaying considering 1-hop system.

4.4 Medium access for distributed power control

Scheduling algorithms are important components in the provision of guaranteed quality of service (QoS). The design of scheduling algorithms for a centralized wireless networks is

especially challenging given the variability of the scenario. The following features are the most important in a scheduling algorithm:

- **Efficient link utilization**.- In a multiple user scenario a new form of diversity arises: *multiuser diversity.* This gain can be exploited by tracking the channel fluctuations of the users and selecting those with the best instantaneous channels.

- **Fairness**.- The algorithm should redistribute the available resources fairly across the different users.

Mainly, there are three scheduling algorithms considered in the mobile communications: the *round robin* (RR), the *greedy* and the *proportion fair* (PF). The RR is the fairest algorithm. It serves all the users following a circular list without considering the current channel of the user. Therefore it does not achieve the *multiuser gain*. The greedy (also named *max C/I*) transmits to that user with the best instantaneous channel (*multiuser gain*), but it suffers from a poor level of fairness, because there are users never or rarely served. Finally, the PF has a performance in terms of *multiuser gain* and *fairness* which can be adjusted, [34]. The users are selected according to the following criterion:

$$ J_n = \arg \max_{i \in \{1,...,N_{users}\}} \frac{R_i(n)}{T_i(n)} $$

where $R_i(n)$ and $T_i(n)$ are the instantaneous rate (which is equal to the instantaneous mutual information) and the average throughput served of the *i-th* user respectively. The average throughput is measured using an exponentially decaying window given by,

$$ T_i(n+1) = \begin{cases} (1-\alpha)T_i(n) + \alpha R_i(n) & i = i^* \\ (1-\alpha)T_i(n) & i \neq i^* \end{cases} \qquad T_i(0) = 1 \qquad (4.32) $$

where i^* denotes the user selected by the scheduling algorithm to be served. Depending on the value of α, the PF performance is similar to the RR when $\alpha=1$ and to the *Greedy* scheduler when $\alpha=0$. A tradeoff solution between efficiency and fairness is obtained for intermediate values of α.

When the number of antennas at the source (without full CSI at the transmitter) is higher than the number of antennas at each destination, the *multiuser gain* decreases because these *additional* antennas dampen the variations of the channel, [7]. For example a scenario where the source is equipped with n_s antennas and destinations with $n_d=1$ is analyzed in [38]. When $n_s>n_d$, results for the *greedy* algorithm show worse performance than for the case $n_s=n_d$. However, if the scheduler considered is the RR when $n_s>n_d$, the obtained results are better than for $n_s=n_d$ (but worse than results obtained by the greedy algorithm).

The diversity-multiplexing tradeoff in multiple access channels is presented in [35]. A relevant example of scheduling algorithm which takes into account the *multiuser gain* and the fairness is presented in [34], this is the proportional fair (PF). It is proposed for a centralized system in the downlink and additionally introduces an opportunistic beamforming to induce fast and large fluctuations in the instantaneous channel of the users (necessary to exploit the multiuser diversity in scenarios with little scattering and/or slow fading). It is assumed that the scheduler

has perfect information about the instantaneous mutual information of all the users. The *multiuser diversity* has been studied for imperfect CSI at the scheduler in [36] and [37].

Additionally the scheduling algorithm could be beneficial to deal with the interference. For example, in [39], an ad-hoc scenario is considered and the interference is mitigated by means of the scheduling process, which selects the most suitable users, along with power control.

4.4.1 Scenario and assumptions

The scenario considered is a centralized wireless TDMA network as was defined in section 4.2. There is a single source, *base station*, which must serve to the terminals uniformly distributed around the cell. The relay protocol considered is protocol I (section 2.3) with spatial reuse of the relay slot, Figure 4.2. The TDMA frame format will be the same for direct and relay-assisted transmission. There are N_u+1 time slots, hence only N_u destinations can be served under relay-assisted transmission, while N_u+1 destinations can be served under direct transmission. Moreover in the same frame it is possible to allocate different types of destinations, using only direct transmission and/or relay-assisted transmission. The ratio between the duration of the time slot and the frame is defined by (4.2).

The following aspects have to be considered in order to enhance the relay-assisted transmission in combination with the *multiuser gain*,

- **Reuse factor**: In order to increase the spectral efficiency of the relay slot, a cell-wide high reuse of this link is desirable.

- **Relay selection**: The interference level of the relay needs to be minimized by means of a suitable relay selection and power control.

- **Channel State Information**: The CSI of every destination in terms of the mutual information of the transmission for that channel configuration (using relay-assisted transmission or not) should be known at the scheduler by the greedy or proportional fair algorithms for the *multiuser gain*.

4.4.2 Proposed solution

The search space between the powers and the suitable relay selection in function of the others selected destinations in the frame grows in an exponential manner with the total number of users in the cell. Therefore a suboptimal solution is proposed by dividing the problem in three phases: *neighbor search and relay selection*, *admission control* and *scheduling*.

A. Neighbor search and relay selection

It is assumed that an underlying probing protocol is present allowing the exchange of broadcast information among neighboring terminals, as in [40]. In this phase we consider that each destination chooses the nearest idle terminal as assisting relay, in order to mitigate the generated interference. The distance r_0 between destination and the closest selected relay is a *r.v.* depending on the idle terminal density, λ_{relay}, (4.1). Therefore, in the following phases of the algorithm the relay-destination pair can be considered as the same *entity*.

B. Relay power adjustment and admission control for relay transmission

The objective of the admission process is to create a group of relay-destination pairs that can transmit simultaneously in spite of the generated interfering power in the relay slot. First, the power of the simultaneous transmitting relays is adjusted using the game theory-based iterative distributed algorithm presented in section 4.3. Because of low amount of data needed to be exchanged between each relay-destination pair (only training sequence to estimate the current channel by the destination and optionally the source-relay channel condition) the admission process can performed over control channels implemented as mini-slots (i.e. grey box in Figure 4.10).
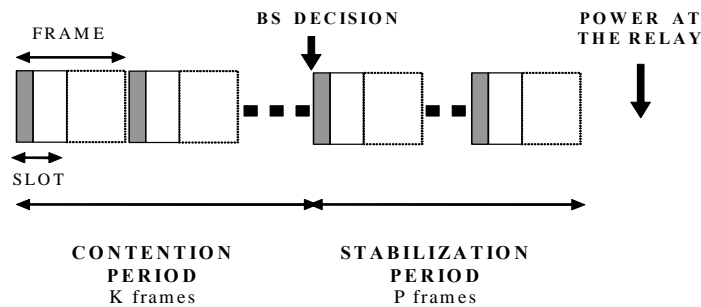
Figure 4.10.- Admission control.

Within the admission control process we consider three phases: the *contention* period, *selection* of active pairs by source (BS) and the *stabilization* period, as it is shown in Figure 4.10. In those phases we have assumed that all the destinations have obtained measures related to the source-destination and source-relay links during the reception of *downlink* control channels, i.e. pilots, and transferred to the source.

- **Contention period.**- All the relay-destination pairs play the power control game described in section 4.3.4. Specifically, the destination does the following tasks:

    - It estimates the relay-destination channel and the interfering power level of each relay terminal. This is possible by assigning different training sequences to the different assisting relays. For example, each destination may estimate the channel of each interfering relay. Another example could be the following. Let us assume that each destination has estimated the total received power. The interfering plus noise power at each destination can be obtained by subtracting the power of your intended signal, obtained thanks to the training sequence, to the estimated total received power.

    - It calculates the power level for its assisting relay that maximizes the utility function of the power control algorithm, (4.22).

    - It informs to the relay about the power level it should transmit in the next game iteration. This communication can be done in different ways with different Media Access Control Layer overheads:

        - Transmitting +/-Δ increments using another mini-slot in the same frame by circular shifts of the training sequence.
        - Through the source (assuming that there is another broadcast control channel between the source and the relay-destination pair). Moreover,

the destination can inform the new power at the relay by using +/-Δ increments or transmitting the exact value.

This process is done during K frames, the time required for the power game to converge. After that, some pairs will have selected a relay power level equal to zero if relay-assisted transmission is not useful due to the high interference of the relay slot. Therefore, the set of pairs candidate to share a given relay slot will have been obtained in a distributed way.

- **Centralized decision of pairs**.- Due to the limited number of downlink slots, only a fixed maximum number of users, N_{coop}, can be allocated in the same frame. The source selects the best pairs within the candidate set to *share* the relay slot based on the mutual information values obtained in the contention period. It will be selected those $N_i \leq N_{coop}$ terminals that maximizes the sum-mutual information. In [43] other possibilities are envisaged.

- **Stabilization period**.- After the source has selected the best pairs and has informed to everybody about its decision, the power control game is played again with the selected pairs during P frames. Note that the solution obtained at the end of this period will be different (or equal in some special cases) from the solution obtained at the end of the *contention period* because the number of relay-assisting users is lower due to the source selection. The power levels obtained at the end of this phase will remain fixed during the relay-assisted transmission of packets until the next admission control process. This process will use P frames, although this process might be faster than the contention period ($P \leq K$) because the current power values are initially adjusted to a stable situation.

Here it has been shown how to build one relay-assisted group using 1 mini-slot. However, this technique allows the construction of G disjoint relay-assisted groups (using G mini-slots and repeating the previous process in each one) extending the relay-assisted transmission to different users in the cell. The analysis of the total overhead will be discussed in section 4.4.3.

C. Scheduling using TDMA

The scheduling process is executed by the source (BS) and is performed in each frame. This phase of length S frames is much longer than the $K+1+P$ frames required for the admission control phase. The frame has the structure depicted in Figure 4.11. The frame has a control part, where some mini-slots are used for measuring the instantaneous values of the mutual information of the direct and relay-assisted transmission.
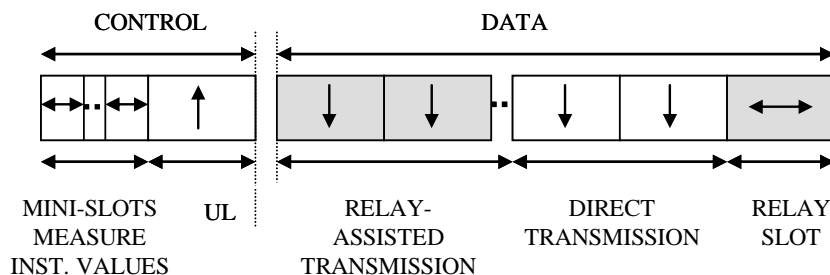
Figure 4.11.- Frame structure.

Once the *G* groups of simultaneous relay-destination pairs are made up, the scheduler decides the amount of temporal resources allocated to each group, according to classical criteria (proportional fair, round robin, etc.) but applied to the groups of relay-assisted destinations instead to applying to single users. The information needed by the scheduler is:

- The instantaneous mutual information of all the destinations in the downlink (direct transmission).

- The instantaneous mutual information of the relay-assisted transmission.

Moreover, those users which are not allowed to transmit in relay-assisted way, as a result of the admission control process, are scheduled in purely downlink slots. In these slots, the users from the relay-assisted groups which have not been selected are also considered, although only using direct transmission.

The scheduler decides which destinations are selected to be served in the traffic data part, Figure 4.11. This decision depends on the selected scheduling algorithm. For instance the PF which can subsume the round-robin (RR) and the greedy algorithm will be considered,

Relay-assisted PF

The best group of relay-destination pairs is selected taking into account as a metric the average PF metric per group,

$$J_n^{group} = \arg \max_{i \in \{1,\ldots,G\}} \frac{1}{N_i} \sum_{k \in \{1,\ldots,N_i\}} \frac{R_k^i(n)}{T_k^i(n)} \tag{4.33}$$

where $T_k^i(n)$ (given by equation (4.32)) is the average served throughput for the *k*-th user in the *i*-th group, *G* stands for the number groups and N_i denotes the number of relay-assisted terminals in each group.

4.4.3 Overhead of the relay-assisted transmission

The protocol for relay-assisted transmission is executed every ($K+P+1+S$) frames with *K*, *P* and *S* the number of frames devoted to *contention*, *stabilization* and *scheduling periods*. The flowchart of the relay-assisted transmission is presented in Figure 4.12. The extra resources for the relay-assisted transmission are due to the time slots in the different periods of time

- *Admission control.-* It is required at least 1 time slot (which can accommodate several mini-slots for different groups) for the *contention* and *stabilization* periods. As the terminal must inform to the relays about the increment/decrement of the power, it is needed an additional time slot. Therefore $2K+1+2P$ time slots are employed.

- *Scheduling period.-* When instantaneous values of the mutual information of the relay-assisted transmission are required, the relays must transmit during some mini-slots in order to measure that value. Therefore *S* slots are required. This overhead can be avoided if the metrics assumed at the scheduler are based on average values rather than instantaneous values [43].

Assuming that in a frame there are 10 time slots devoted for relay-assisted transmission, the overhead is measured as,

$$Overhead = \begin{cases} \dfrac{2K+1+2P+S}{(K+1+P+S)10} & \text{instantaneous values} \\[3mm] \dfrac{2K+1+2P}{(K+1+P+S)10} & \text{average values} \end{cases} \tag{4.34}$$

If $K=P=10$ and $S=100$ the overhead introduced by the relay-assisted transmission is around 11.6% and 3.3% with instantaneous and average values, respectively. It is worth mentioning that by increasing S when average values of the mutual information are assumed, the total overhead is reduced. Moreover, the overhead introduced by the probing protocol is lower than the 10% of the fast fading bandwidth (for slow fading scenarios its impact is minimum), [43].
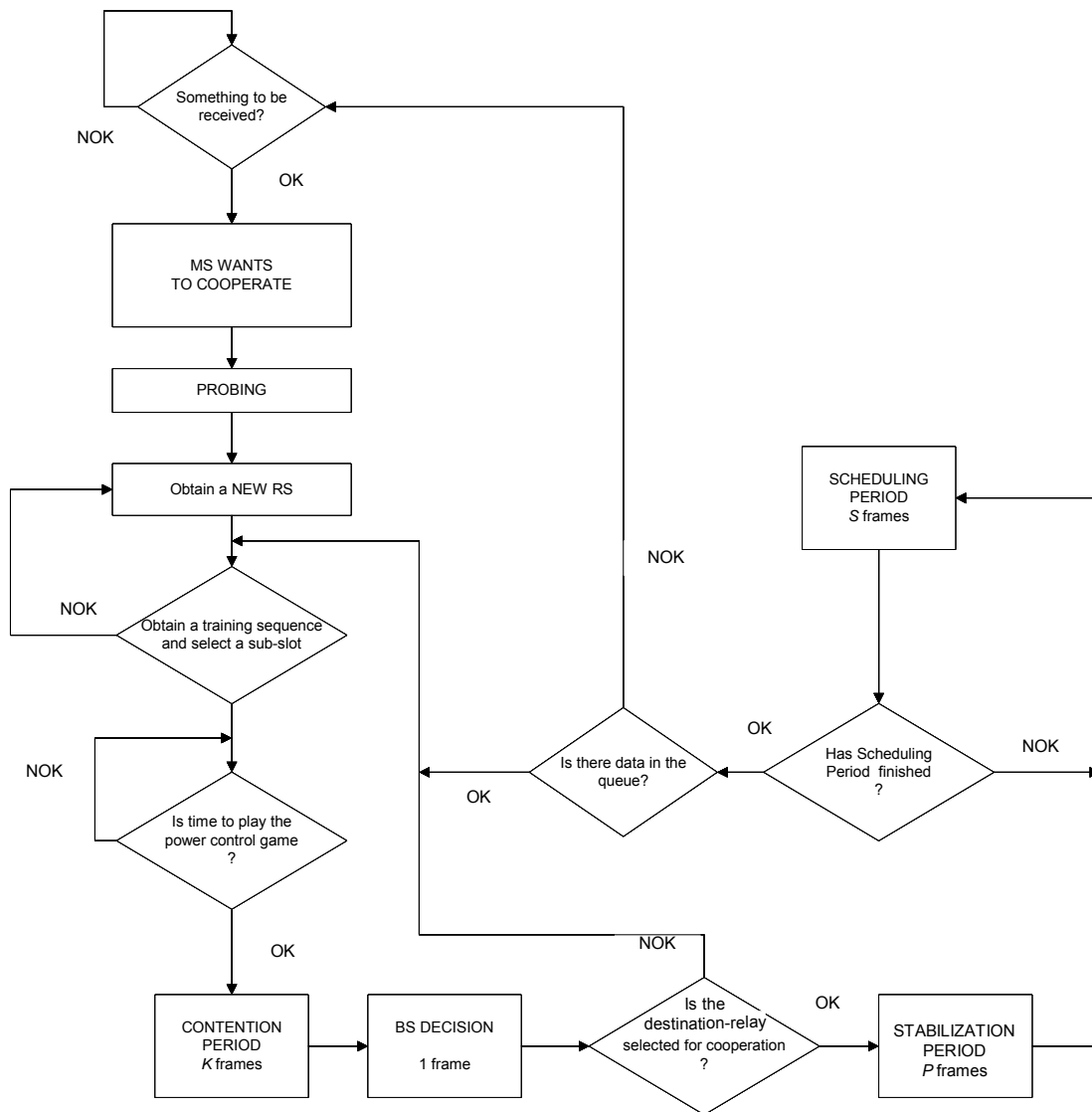
Figure 4.12.- Flowchart of the relay-assisted scheduling protocol, where the source, relays and destinations are denoted by BS, RS and MS, respectively.

4.4.4 Results

For the simulations a square area of 900x900 m^2 has been considered. The source is at the center of the cell using n_s=2 omni-directional antennas with transmission power of 29 dBm. Destinations are uniformly distributed in the cell with n_d=1 antenna each, although the cooperative transmission can double the virtual receiving antennas. The terminal density is λ=10^{-3} users/m^2. The assisting relays are around the destination according to (4.1) and they have n_r=2 antennas with a maximum transmission power equal to 23 dBm. The distance loss model has been obtained from [41], which takes into account the line of sight (LOS) and non-LOS (NLOS) events and the shadowing effect. A Rayleigh flat fading channel has been assumed (uncorrelated between consecutives frames). All the destinations have infinite loaded queues, so that in each frame all the destinations have data to be transmitted. The *decode and forward* protocol is adopted for relay-assisted transmissions. Results have been obtained from 200 independent scenarios of 60 users and using G$_{max}$=5 groups for relay-assisted transmissions. For simplicity of presentation one packet of information is transmitted in each time slot. There are 10 of 15 slots/frame devoted for direct and relay-assisted transmissions (9+1). The remaining ones are reserved for uplink and control data transmissions. The PF algorithm has been simulated for: α=0.9 (enhance the fairness), α=0.01 (*greedy performance*) and α=0.06. In [43] the *amplify-and-forward* is also considered along with different traffic models, effect on the selection of the maximum number of relay-assisting users per group (N_{coop}). In the following results the overhead effect has not been considered.

In Figure 4.13 the cellular throughput or sum-throughput is depicted for the direct transmission PF (DT-PF) and relay-PF for different values of α. It can be observed that for α=0.9 and 0.06 the relay-PF improves the total throughput. That performance is due to the increase of the *virtual* receiving antennas. However, for α=0.01, the relay-PF is not able to achieve a throughput better than DT-PF, because the relay-assisted groups are obtained from mean values of the channel and not from instantaneous values.
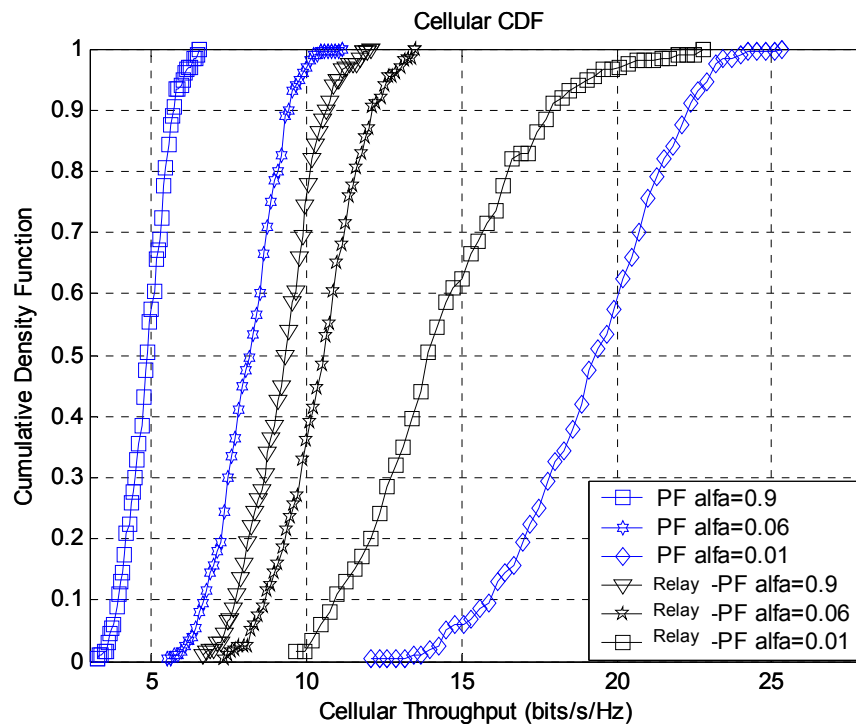
Figure 4.13.- Cellular Sum-Throughput. Maximum number of cooperating users N_{coop}=7.
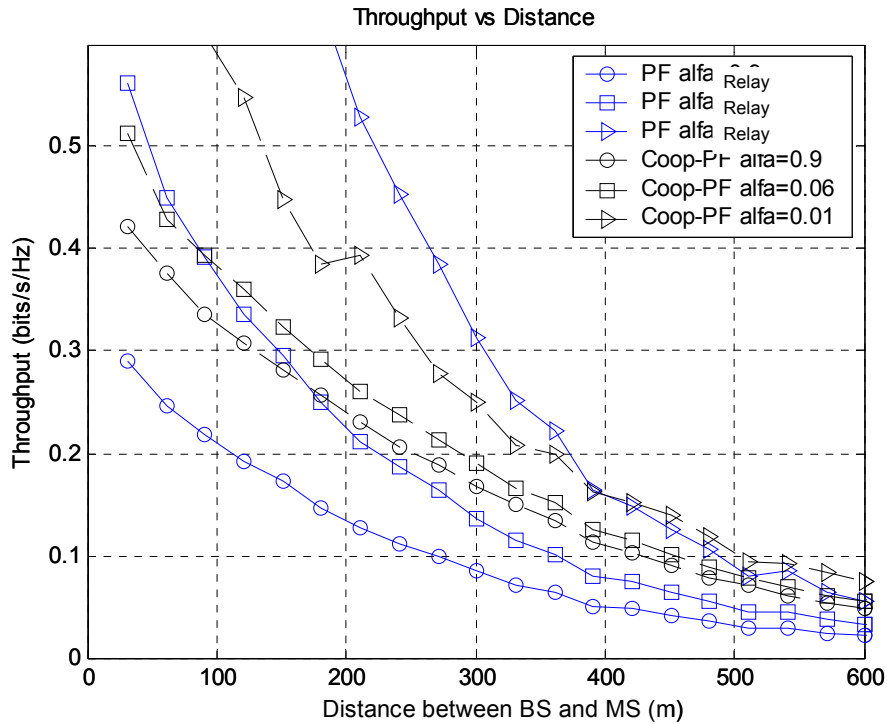
Figure 4.14.- Average individual throughput served vs Distance. Maximum number of relay-assisting terminals N_{coop}=7. No channel estimation error is assumed. Relay-assisted transmission (black dashed lines) and direct transmission (blue solid lines). Source and destination denoted by BS and MS, respectively.
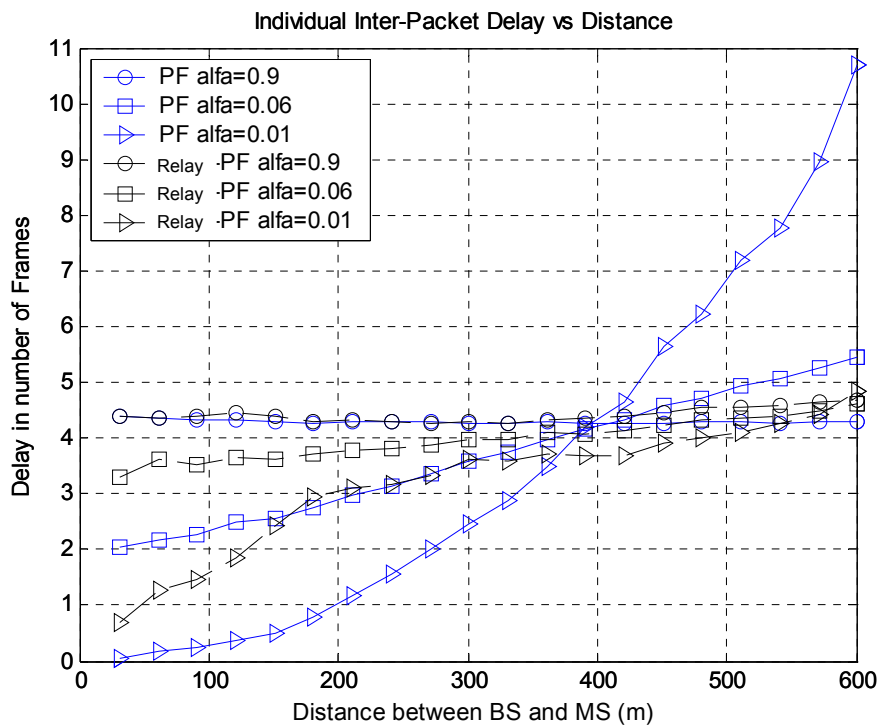

Figure 4.15.- Inter-packet Delay vs Distance. Maximum number of cooperating users N_{coop}=7. No channel estimation error is assumed. Relay-assisted transmission (black dashed lines) and direct transmission (blue solid lines). Source and destination denoted by BS and MS, respectively.

In Figure 4.14 some results are presented in terms of individual throughput *vs.* distance of the terminals to the source, for different values of α (controlling the *fairness* and the *multiuser gain*)

and for relay-assisted transmission (black dashed lines) and direct transmissions (blue solid lines). Relay-assisted transmission improves the throughput of destinations at all distances from the source for α=0.9 and 0.06. However, for α=0.01 the throughput of closer users to the source is worse than the DT-PF, Figure 4.15. Moreover, Figure 4.15 shows the inter-packet delay as a function of the distance between destinations and the source. In general, the fairness (in terms of delay) is improved for all users independent of the factor α. Therefore, the relay-assisted transmission could be a useful strategy for providing fairness and enhancing the throughput.

4.5 Rate control interference management for relay-assisted users with single relays

In this section (and also in section 4.6) the relay-assisted transmission is designed under interference limitation principles, where the *amplify-and-forward* (AF) deals with unknown fast changing interference patterns on the relay slot. To that end, we develop a model for the interfering power, by adapting some previous results from [23]. The interfering power received at the different destinations during the *relay-transmit phase* (see Figure 4.1) is modeled by an α-stable distribution, (see for example [24]), which depends on several aspects: the terminal density, the transmitted power at the relay, the distance between assisting relay-destination pairs and the spatial traffic pattern. The main difference with regard to the approach considered in sections 4.3 and 4.4 is that the relays are transmitting with a constant power (details in 4.5.1) rather than adjusting the power transmitted as has been done in previous sections. The source will adapt the data rate of each transmission (*rate control*) to combat the interference.

The main contribution of this section is a semi-analytical evaluation of the sum-throughput delivered by the source during a frame for a low complexity implementation of the relay-assisted transmission with *amplify-and-forward*. When the source knows the statistics of the interfering power at each destination it can:

- Selects the rate which maximizes the throughput. This situation is commonly found in *best effort* traffic services where retransmissions are allowed.

- Selects a conservative rate to keep the outage probability of the transmission below a certain value. This one is found in services where retransmissions are not permitted as in delay sensitive traffic services.

Significant throughput gains can be achieved without strictly controlling the power transmitted by the relays (power control is managed between relay and destination) neither which assisting relays are transmitting (only the number of simultaneously transmitting relays is fixed). It is important to emphasize that the analysis of the overhead of the cooperating transmission at the Media Access Control layer is out of the scope of this work (see for example [25] for the MIMO case. Relay association and channel reporting issues are not considered.

4.5.1 Assumptions

The scenario defined in section 4.2 applies here with the following system assumptions:

1. The assisting relays will be selected from those terminals in idle mode (*user relaying*). All the terminals present the same opportunity to be assisting relays.

2. Each destination is assisted by a single relay (nearest idle terminal). All terminals are equipped with a single antenna ($n_r = n_d = 1$) while the source has n_s antennas.

3. The source has perfect knowledge of the current SNR of the source-relay, source-destination and relay-destination (without interference) links, but not of the exact complex channel gain, i.e. there is not *perfect* CSI. The channel coefficients remain fixed during all the relay-assisted transmission. The source may know the source-relay and source-destination channel by reciprocity and the destination should report the quality of the relay-destination link. Otherwise, the destination and relay should inform about the quality of the different links.

4. There is a slow variation of the fading (large coherence time), hence the terminals may report the link quality of their channels to the source with a small overhead.

5. As a result of the unknown interference, outage events appear at the relay slot.

6. Each assisting relay adjusts the power level in order to set a *target* SNR (measured without interference) in the relay-destination link, SNR_t. Its value is the same for all the relay-assisted users in the cell, becoming a parameter of the system. The transmitted power depends on the quality of the relay-destination link.

7. The source selects randomly N_u active destinations to be served in each TDMA frame (*round robin* packet scheduling). In this regard, the transmitting relays will change in each frame, and each destination will observe a random interfering power.

8. All the terminals are equipped with simple receivers, i.e. the interfering signals are considered as additive noise and the receivers are not able to do multi-user decoding.

9. Relays operate in *amplify-and-forward* mode duplexed in TDD. The relay must be able to store the analog data into a memory and retransmit it. Each destination is assisted by a single relay.

According to *assumption 6* the target signal to noise ratio (SNR_t) in the relay-destination link (without interference and only due to the path-loss in the relay link) is established to be the same for all active relay-destination pairs around the cell. This implies that the power transmitted by a relay becomes a random variable because of the distance between each assisting relay-destination (named r) is also a random variable, (4.1). It is defined by,

$$P_r = \min\left(P_{MAX}, \frac{\sigma^2 \cdot SNR_t \cdot r^\gamma}{K_r} \right), \quad SNR_t = \frac{K_r P_r}{r^\gamma \sigma^2} \tag{4.35}$$

where P_{MAX} is the maximum power allowed at the relay, σ^2 denotes the noise power, K_r considers the effect of shadowing, r is the distance between the pair relay-destination, (4.1) and γ stands for the propagation exponent.

4.5.2 Interfering power modeling

Since all the assisting relays (associated to different destinations) transmit simultaneously during the relay slot (*relay-transmit phase),* they induce interference to all the destinations. Taking into account the assumptions of previous sections, the interfering power received at each destination during the relay slot becomes a random variable. A similar scenario is investigated in [23], where the statistics of the interference power are obtained in an adhoc network of *Poisson* distributed terminals, all transmitting the same power in a channel affected only by path-loss. Now we need to incorporate to that model the shadowing and the multipath fading, taking into account that in our case each relay transmits with power according to the *target* SNR (*assumption* 6).

We will assume that the interfering power received from a transmitter placed at distance r_i, $g(r_i)$, satisfies the following two conditions:

$$1.- \quad \lim_{r_i \to 0} g\left(r_i\right) = \infty, \quad \lim_{r \to \infty} g\left(r_i\right) = 0, \quad g\left(r_i\right) \text{ is monotonically decreasing}$$

$$2.- \quad \lim_{r_i \to \infty} r_i^2 g\left(r_i\right) = 0 \qquad \text{(finite interfering power in a network)}$$

(4.36)

Notice that the interfering power when r_i tends to zero will be very large but not necessarily ∞. However, we follow the same assumption as in [23] because the probability of having two terminals very close tends to zero for Poisson distributed users. Additionally, the assumption of ∞ interfering power when r_i tends to zero allows obtaining closed-form expressions for the interfering power model. The interfering power received at a destination from a single interfering relay due to the multipath and/or fading is,

$$\eta\left(K_i, r_i\right) = K_i g\left(r_i\right) = K_i \frac{P_r}{r_i^\gamma}$$

(4.37)

where P_r is the power transmitted by the interfering relay, r_i denotes the distance between the destination and the interfering relays, γ is the propagation exponent and K_i is a constant that takes into account the shadowing and fast fading effects in the interfering relay-destination link (with the same distribution for all the users). The power transmitted by each assisting relay is variable according to equation (4.35), so the interference power observed at each destination depends on r_i and also on r, distance between the interfering relay and its associated destination, see Figure 4.16. There, D_1 is receiving an interfering signal from the relay RS_2, which is transmitting with power according to SNR_t, (4.35), depending on the distance r to its associated destination, D_2.
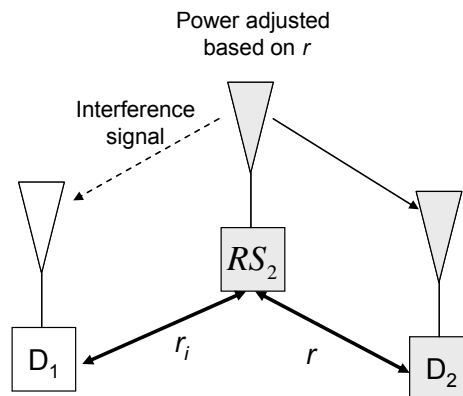

Figure 4.16.- Interfering power at a destination. D_1 is receiving interference when RS_2 is assisting to D_2. RS_2 adjusts its power to get the target SNR (4.35) in the RS_2-D_2 link.

Thus, the received interfering power only due to the distance is given by,

$$g\left(r_i,r\right)=\begin{cases}\dfrac{1}{K_r}N_0\cdot SNR_t\left(\dfrac{r}{r_i}\right)^{\gamma} & r\leq\Delta \\[3mm] \dfrac{P_{MAX}}{r_i^{\gamma}} & otherwise\end{cases}\qquad\Delta=\left(\dfrac{K_rP_{MAX}}{N_0SNR_t}\right)^{\frac{1}{\gamma}}\quad\gamma>2\qquad(4.38)$$

Let Y_a be the interfering power received from the active assisting relays in D_a, a disk of radius a,

$$Y_a=\sum_{r_i\leq a}\eta\left(K_i,r_i,r\right)=\sum_{r_i\leq a}K_i g\left(r_i,r\right)\qquad(4.39)$$

After some calculation, see Appendix B (section 4.9) for details, we obtain the interference power Y (Y_a when $a\rightarrow\infty$) as an α-stable variable [24] whose characteristic function depends on the α-th moment of the variable K_i:

$$\phi_Y\left(\omega\right)=\exp\left(-K\cos\left(\alpha\pi/2\right)\omega^{\alpha}\left(1-j\tan\left(\alpha\pi/2\right)\right)\right)\qquad(4.40)$$

where α and K are given by,

$$\alpha=\gamma\big/2\qquad\qquad K=\Upsilon\,\mu_{K_i,\alpha}\qquad(4.41)$$

$$\Upsilon=\Gamma\left(1-\alpha\right)\lambda_{active}\pi\left(\left(\frac{N_0SNR}{K_r}\right)^{\alpha}\frac{\left(1-\left(1+\pi\lambda_{relay}p_s\Delta^2\right)\Omega\right)}{\pi\lambda_{relay}p_s}+\Omega\,P_{MAX}^{\alpha}\right)\qquad(4.42)$$

$$\Omega=\exp\left(-\pi\lambda_{relay}p_s\Delta^2\right)\qquad\mu_{K_i,\alpha}=\int K_i^{\alpha}f_{K_i}\left(K_i\right)dK_i$$

where $\Gamma(\cdot)$ the Gamma function, λ_{active} depends on the number of active destinations in each frame, λ_{relays} depends on the probability of a neighbor terminal to become a relay, λ is the terminal density, (4.4), Δ is given by equation (4.38) and $\mu_{K_i,\alpha}$ is the αth-moment of the random variable K_i. When $\gamma=4$ it is possible to obtain closed-form expressions for its probability and cumulative density function (*pdf* and *cdf*) of the interfering power as,

$$f_y\left(y\right)=\frac{K}{2\sqrt{\pi}}y^{-3/2}\exp\left(-\frac{K^2}{4y}\right),\qquad F_y\left(y<x\right)=erfc\left(\frac{K}{2\sqrt{x}}\right)\qquad(4.43)$$

Notice that the final expression depends on the αth-moment of the random variable K_i (4.37), which accommodates the multipath fading and/or shadowing in the interfering relay-destination link. Table 4.4 presents the *K-factors* for different distributions considered to model the multipath fading or the shadowing. Figure 4.17 shows how this model fits with the experimental results for 75 destinations with a target SNR in the relay-destination link equal SNR_t=10 dB (4.35) and for 25 users under Rayleigh fading in the relay-destination link with a SNR_t=25 dB, (4.35).

Name	Probability Density Function	K-parameter of α-stable distribution (4.41)
Rayleigh	$p(x) = \dfrac{1}{2\sigma_{Ray}^2}\exp\left(-\dfrac{x}{2\sigma_{Ray}^2}\right)$	$K = \Upsilon\, 2^{\alpha}\, \sigma_{Ray}^{2\alpha}\, \Gamma\left(1+\dfrac{\alpha}{2}\right)$
Chi-Square (χ^2)	$p_{\chi^2}(x,n) = \dfrac{1}{2^{n/2}\Gamma(n/2)\sigma_{\chi^2}^{n/2}} x^{n/2-1}\exp\left(-\dfrac{x}{2\sigma_{\chi^2}^2}\right)$	$K = \Upsilon\, \dfrac{2^{\alpha}\sigma_{\chi^2}^{2\alpha}\Gamma(n/2+\alpha)}{\Gamma(n/2)}$
Log-Normal	$p(x) = \dfrac{10/\ln(10)}{x\sqrt{2\pi\sigma_{Shad}^2}}\exp\left(-\dfrac{\left(10\log_{10}(x)-\mu_{Shad}\right)^2}{2\sigma_{Shad}^2}\right)$	$K = \Upsilon\, 10^{\frac{\mu_{Shad}\alpha}{10}}\exp\left(\dfrac{\alpha^2\sigma_{Shad}^2\left(\ln(10)\right)^2}{200}\right)$

Table 4.4.- K-parameters for the interference model when K_i, (4.42), follows different distributions. Υ defined at (4.42).
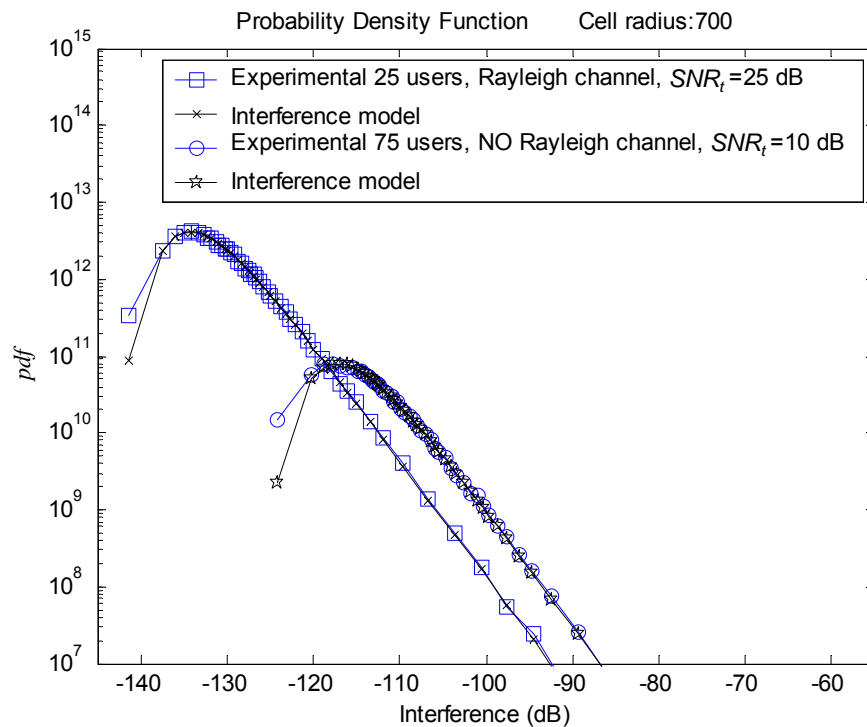
Figure 4.17.- Comparison between the interference obtained experimentally and the one generated with the model, (4.42). There are 75 simultaneous destinations with target SNR_t=10 dB and 25 destinations with target SNR$_t$=25 dB and Rayleigh fading (σ^2 =10).

4.5.3 Properties of AF relay-assisted transmission

This section analyzes the properties of the TDD *amplify and forward* (AF) transmission of a destination served in the TDMA frame, (4.3). First, it will be derived a simple expression for the mutual information when the source is equipped with possible multiple antennas and the relays and destinations feature a single antenna, $n_s \geq 1$, $n_r = n_d = 1$. The mutual information (4.10) is given by,

$$I^{AF} = \frac{T_{slot}}{T_{frame}}\log\det\left(\mathbf{I}_2 + \frac{P_s}{n_s}\mathbf{R}_b^{-1}\mathbf{H}_{AF}\mathbf{H}_{AF}^H\right) = \frac{1}{N_u+1}\log_2(\Psi) \qquad (4.44)$$

Assuming that the noise power at the different links is the same, i.e. $\sigma_{n_d}^2 = \sigma_{n_r}^2 = \sigma^2$ in (4.9) and the channel matrices are given by column vectors due to the antenna configuration, then the Ψ variable is defined by,

$$\Psi = \left(1 + \frac{\mathbf{h}_0^H \mathbf{h}_0 \frac{P_s}{n_s L_0}}{\sigma^2}\right)\left(1 + \frac{\frac{P_s}{n_s L_2 L_1} h_2 g \mathbf{h}_1^H \mathbf{h}_1 g^* h_2^*}{\frac{h_2 g g^* h_2^*}{L_2} \sigma^2 + \sigma^2 + Y}\right) - \frac{\frac{P_s \mathbf{h}_1^H \mathbf{h}_0}{n_s \sqrt{L_0 L_1}} \frac{g^* h_2^* h_2 g}{L_2} \frac{\mathbf{h}_0^H \mathbf{h}_1 P_s}{n_s \sqrt{L_0 L_1}}}{\sigma^2 \left(\frac{h_2 g g^* h_2^*}{L_2} \sigma^2 + \sigma^2 + Y\right)} \quad (4.45)$$

with Y being the interfering power received in the relay link, L_0, L_1 and L_2 denoting the path-loss terms in each link and $\mathbf{h}_0$, $\mathbf{h}_1$ and h_2 being the channel complex gains of dimensions $n_s \times 1$, $n_s \times 1$ and 1×1, respectively. After tedious transformations the mutual information becomes,

$$I^{AF} = \frac{1}{(N_u + 1)}(m_{DT} + m_{AF})$$

$$m_{DT} = \log(1 + SNR_0) \quad m_{AF} = \log\left(1 + \frac{SNR_1 \, SNR_2 \, \Theta}{SNR_2 + (1 + Y/\sigma^2)(SNR_1 + 1)}\right) \quad (4.46)$$

with the following variable definition,

$$\Theta = \frac{1 + SNR_0(1 - \xi)}{1 + SNR_0} \quad \xi = \frac{|\mathbf{h}_1^H \mathbf{h}_0|^2}{\mathbf{h}_0^H \mathbf{h}_0 \mathbf{h}_1^H \mathbf{h}_1} = \cos^2(\phi)$$

$$SNR_0 = \frac{P_s \mathbf{h}_0^H \mathbf{h}_0}{\sigma^2 L_0 n_s} \quad SNR_2 = \frac{P_{TX} h_2 h_2^*}{\sigma^2 L_2} \quad SNR_1 = \frac{P_s \mathbf{h}_1^H \mathbf{h}_1}{\sigma^2 L_1 n_s} \quad (4.47)$$

where SNR_0, SNR_1 and SNR_2 are the SNR in the source-destination, source-relay and relay-destination links, respectively. Finally, m_{DT} and m_{AF} stand for the mutual information in the source-destination and source-relay-destination link. Notice that benefits of the relay-assisted transmission depend on the m_{AF} value.

It is relevant to point out the importance of ξ and Θ in the mutual information for the *amplify and forward* scheme, (4.46). When $n_s = 1$, then $\xi = 1$ (channels $\mathbf{h}_0$ and $\mathbf{h}_1$ are vectors of dimension 1) and $\Theta = 1/(1 + SNR_0)$, penalizing the mutual information of m_{AF} (4.46). On the other hand, allowing $n_s > 1$ in Rayleigh fading channels, ξ becomes a random variable distributed as a Beta function [26] with parameters $(1, n_s - 1)$ and *pdf* given by,

$$f_\xi(x) = \frac{1}{B(a,b)} x^{a-1}(1-x)^{b-1} I_{(0,1)}(x) \quad a = 1, b = n_s - 1 \quad (4.48)$$

where $B()$ is the Beta function and $I_{(0,1)}(x)$ is the indicator function which ensures that only values of x in the range (0,1) have non-zero probability. Figure 4.18 presents the *pdf* for different values of n_s. When $n_s = 2$, ξ is uniformly distributed in (0,1). As n_s increases the distribution of ξ concentrates around zero and Θ around 1. Therefore, m_{AF} is defined in the following interval which also limits the mutual information of the AF scheme, I^{AF},

$$\log\left(1+\frac{SNR_1\,SNR_2\big/\left(1+SNR_0\right)}{SNR_2+\left(1+Y\big/\sigma^2\right)\left(SNR_1+1\right)}\right)\le m_{AF}\le\log\left(1+\frac{SNR_1\,SNR_2}{SNR_2+\left(1+Y\big/\sigma^2\right)\left(SNR_1+1\right)}\right)\quad(4.49)$$

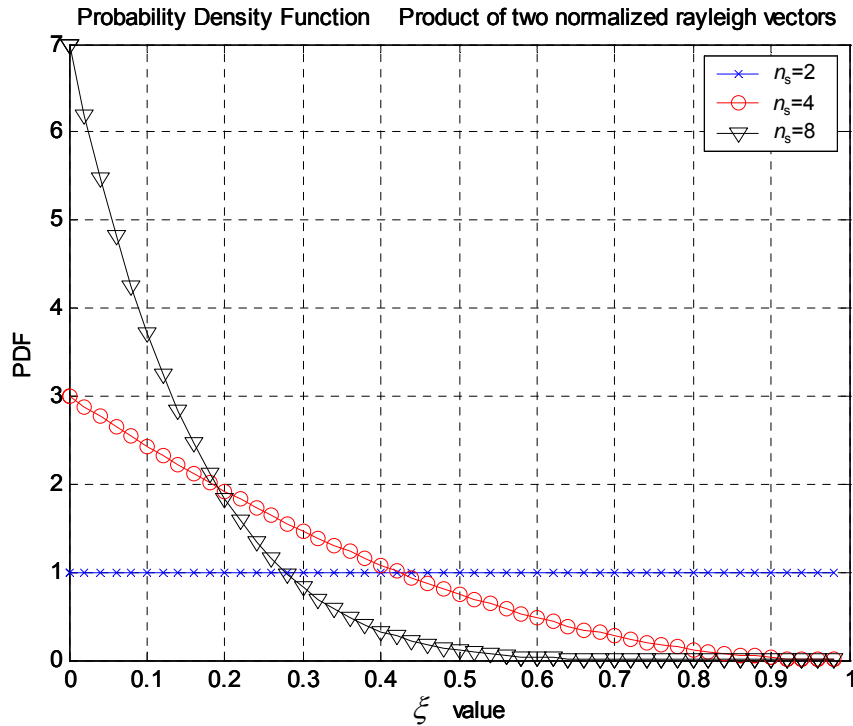where its actual value depends on the variable ξ.

Figure 4.18.- Beta probability density function with parameters {1,n_s-1} for ξ, (4.48).

The value ξ could be an additional criterion for selecting an assisting relay so as to enlarge m_{AF}. For example, each destination selects the nearest idle terminal such that $\xi\le\xi_0$ in order to have a high value on m_{AF}. However, this strategy will also impact on the relay selection by modifying the success probability of idle terminals, $p_s=P\left(\xi\le\xi_0\right)$. When the source-relay and source-destination links present a Rayleigh fading distribution, then the success probability, p_s, is given by,

$$p_s=P\left(\xi\le\xi_0,a,b\right)=\frac{1}{\mathrm{B}\left(a,b\right)}\int_0^{\xi_0}t^{a-1}\left(1-t\right)^{b-1}dt\qquad a=1,b=n_s-1\qquad(4.50)$$

In this regard the effective average density of relays λ_{relay} (4.1) is reduced according to the lines of Appendix A (section 4.8), thus increasing the transmitted power at the relays to satisfy the *target* SNR in the relay-destination link (SNR_t) and introducing more interfering power in the relay slot. Therefore, a tradeoff appears.

When comparing the direct transmission and the relay-assisted AF both systems must use the same average transmitted power in order to evaluate the efficiency of the communication. Because both transmission schemes use a different resource allocation, as defined by equation (4.3), the direct transmission should transmit with the following *cooperative power* (P_{coop}),

$$P_{coop} = \frac{N_u}{N_u + 1}\left(P_s + P_r\right) \tag{4.51}$$

with P_r denoting the current power transmitted by the assisting relay, (4.35).

4.5.3.1 Rate selection in the relay-assisted transmission

In section 4.5 it has been assumed so far that the outage events only come up in the *relay-transmit phase* due to the interference generated by the simultaneous transmissions of all assisting relays (*assumption 5* and *7* in section 4.5.1). To mitigate the outage the source has to select a conservative rate (*rate control*), R^{AF}. There are two possible options: fixing the probability that the transmission is not in outage (ζ) or maximizing the throughput.

The probability of the selected rate, R^{AF} is not in outage is defined as,

$$\zeta = 1 - P_{out}\left(T_{frame} I^{AF} < T_{slot} R^{AF}\right) = F_y\left(Y < \left(\sigma^2\left(\frac{SNR_2}{1 + SNR_1}\left(\frac{SNR_1 \Theta}{2^{R^{AF} - m_{DT}} - 1} - 1\right) - 1\right)\right)\right) \tag{4.52}$$

where m_{DT} is defined in (4.47), Y is the interfering power received and F_y denotes the *cdf* of the interference which is the *erfc* function when $\alpha = 1/2$, (4.43). Assuming that the following parameter ε_0 is connected with ζ through,

$$\zeta = erfc\left(\varepsilon_0\right) \qquad \varepsilon_0 = erfc^{-1}\left(\zeta\right) = \frac{K}{2\sqrt{\left(\sigma^2\left(\frac{SNR_2}{1 + SNR_1}\left(\frac{SNR_1 \Theta}{2^{R^{AF} - m_{DT}} - 1} - 1\right) - 1\right)\right)}} \tag{4.53}$$

The selected rate R^{AF} for a given probability ζ of not being in outage (using the variable ε_0 (4.53)) is,

$$R^{AF} = \log\left(1 + \frac{SNR_1 \Theta}{1 + \left(1 + \left(\frac{K}{2\sigma\varepsilon_0}\right)^2\right)\left(\frac{1 + SNR_1}{SNR_2}\right)}\right) + \log\left(1 + SNR_0\right) \tag{4.54}$$

with K modeling the interfering power in the relay slot defined in (4.41), which will vary with the number of destinations server in a TDMA frame (N_u). Notice that the consequence of the inference is the following penalty factor $1 + \left(K/2\sigma\varepsilon_0\right)^2$. The throughput for a TDMA destination using relay-assisted transmission for a given probability of not being in outage (ζ) is,

$$\mathcal{T}_{AF} = \frac{1}{N_u + 1} R^{AF} \zeta \tag{4.55}$$

Additionally, if the relay-assisted rate R^{AF} is selected to maximize the throughput then

$$\mathcal{T}_{AF}^{*} = \max_{\zeta}\left(\frac{1}{N_u+1}R^{AF}\zeta\right)$$

(4.56)

where R^{AF} is connected with ζ as equations (4.54) and (4.53) show.

4.5.4 Cellular results

This section present the results obtained by the relay-assisted and the direct transmission, showing under what configurations the relay-assisted transmission is beneficial. Our scenario is defined by a circular cell with radius 700m and the source placed at the center with the following terminal densities $\lambda=\{7\times10^{-5},\ 2\times10^{-4},\ 5\times10^{-4},\ 8\times10^{-4}\}$ terminals/m^2. These values may describe different population densities in rural and suburban regions, see Table 1 in [27]. The multipath fading is modeled by a complex Rayleigh random variable of zero mean and unitary variance and the path-loss at a distance d in the source-destination (L_0), source-relay (L_1) and relay-destination (L_2) is given by,

$$\begin{cases} L_0 = L_1 = 43.65 + 3\times10\times\log_{10}(d) & (dB) \\ L_2 = \quad\ 43.65 + \gamma\times10\times\log_{10}(d) & (dB) \qquad \gamma=4 \end{cases}$$

(4.57)

The power transmitted by the source in the direct transmissions is P_s=30 dBm and the maximum power transmitted by an assisting relay is P_{MAX}=20 dBm. The noise power is set to σ^2=-102 dBm. Considering only the path-loss effect, the received SNR at the border of the cell is 3 dB, while the received SNR is -1.65 dB when an assisting relay is at 100 meters and transmitting with P_{MAX} (relay-destination link). Finally, the interfering power in the relay slot is modeled by an α-stable random variable according to equations (4.41) and (4.42).

Results are obtained with Monte-Carlo simulations, measuring average *sum-throughput*, i.e. the total throughput delivered by the source to all the destinations served in each frame. The destinations are randomly selected each time (*assumption 7* in section 4.5.1). The AF *sum-throughput* is compared with the *sum-throughput* obtained by the direct transmission using cooperative power, (4.51) in the following way,

$$\Delta\mathcal{T}(\%) = \frac{E\left\{\sum_{n=1}^{N_u}\mathcal{T}_{AF}(n)\right\} - E\left\{\sum_{n=1}^{N_u}\mathcal{T}_{DT}(n)\Big|_{P_{coop}}\right\}}{E\left\{\sum_{n=1}^{N_u}\mathcal{T}_{DT}(n)\Big|_{P_{coop}}\right\}}\times100$$

(4.58)

when N_u=1 the conventional AF (under *user relaying*) protocol is compared with the direct transmission.

Results are presented as contour plots for different throughput gains (4.58) as a function of the number of destinations (N_u) and the target SNR (SNR_t) selected in the relay-destination link, (4.35). In the following the factors which influence the final throughput gain are analyzed separately: a) number of antennas at the source, b) gains obtained when the outage probability of the transmission is fixed by the service, c) effect of considering different values of p_s, d) variation of the terminal density and e) ratio between the power at the source and the relay.

A. Number of antennas at the source

Figure 4.19 depicts the {10%, 35% and 45%} gains of the average *sum-throughput* AF over the average *sum-throughput* of the direct transmission with cooperative power when the terminals present a *Poisson* terminal density of $\lambda=5\times10^{-4}$ terminals/m^2. The source maximizes the throughput for each destination according to equation (4.56). Increasing the number of antennas at the source allows minimizing the constraints in terms of target SNR at the relay-destination link and N_u in order to achieve some throughput gains. For example with $n_s=1$ it is required a target SNR$\geq$17 dB and $6\leq N_u\leq19$ to obtain $\Delta\mathcal{T}=10\%$ of throughput gain. The conventional AF ($N_u=1$) gets a lower throughput gain because of the position of the relay. Whereas with $n_s=2$ and $n_s=4$ that throughput gain ($\Delta\mathcal{T}$) can be obtained for a lower SNR_t. In such a case, AF without reuse gets $\Delta\mathcal{T}=10\%$ because in some cases it is required $N_u=1$. Additionally Table 4.5 shows the maximum throughput gains and which configuration achieve them. With $n_s=4$ and $\lambda=5\times10^{-4}$ terminals/m^2, a $\Delta\mathcal{T}=48\%$ is possible when $N_u=9$ destinations and $SNR_t=34$ dB (relays transmitting with full power). These gains are possible because the variable ξ (in equation (4.47)) decreases to zero as n_s increases, improving the m_{AF} factor, (4.46).
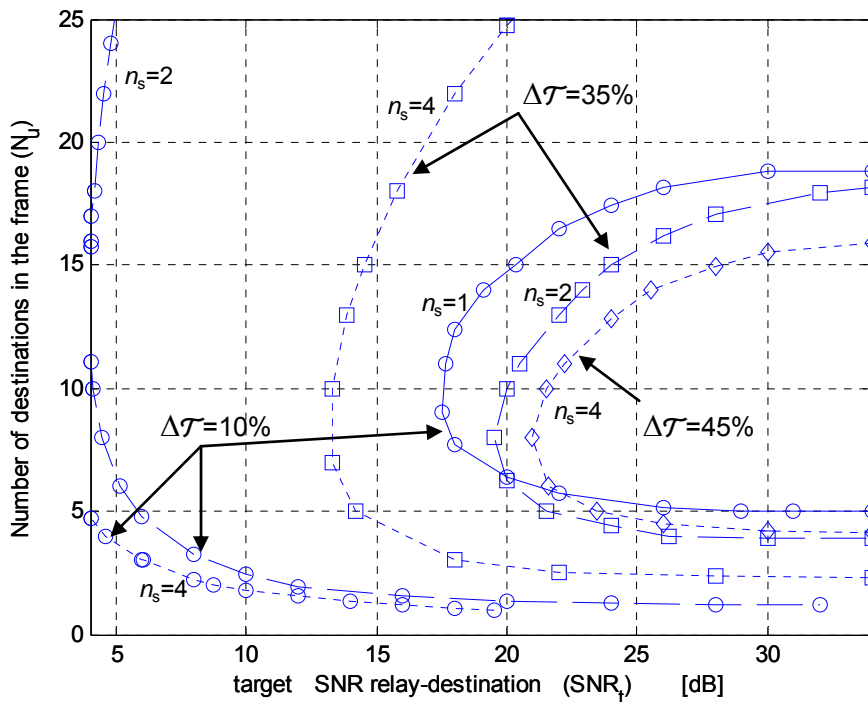
Figure 4.19.- {10%, 35%, 45%} gain plots of the average sum-throughput for the AF (under individual throughput maximization, (4.56)) over the direct transmission with cooperative power for different values as a function of the target SNR (4.35) and N_u. Terminal density $\lambda=5\times10^{-4}$ users/m^2. $n_s=\{1,2,4\}$. Propagation scenario defined by (4.57).

Maximum sum Throughput gain (%) AF	$\lambda=7\times10^{-5}$		$\lambda=2\times10^{-4}$			$\lambda=5\times10^{-4}$			$\lambda=8\times10^{-4}$		
	$n_s=2$	$n_s=4$	$n_s=1$	$n_s=2$	$n_s=4$	$n_s=1$	$n_s=2$	$n_s=4$	$n_s=1$	$n_s=2$	$n_s=4$
$\Delta\mathcal{T}$ (%)	7.2	12.2	4.2	24.6	32.2	12.3	39.2	48.4	16.1	45.6	55
Destinations	6	6	8	7	6	10	8	9	10	10	9

Table 4.5.- Maximum gain (%) of the AF average sum-throughput over the direct transmission with cooperative power for different terminal densities and antenna configuration.

B. Fixing the outage probability

In certain cases, as in sensitive services, the source must be able to select the suitable rate in order to keep a low probability of error of each transmission. Figure 4.20 shows that the relay-assisted transmission also achieves some throughput gains over the direct transmission when the source selects a rate to have an error probability (due to the interfering power at the relay slot) of 1% ($\zeta=0.99$) and 5% ($\zeta=0.95$), (4.55). The terminal density is $\lambda=5\times10^{-4}$ terminals/m² and there are $n_s=4$ antennas at the source. When the outage probability grows the throughput gains are improved, for example the throughput gain does not get the $\Delta\mathcal{T}=35\%$ for $P_{out}=1\%$. That gain is achieved when $P_{out}=5\%$ and even $\Delta\mathcal{T}=45\%$ is possible for that configuration. Additionally, we can see that working with $P_{out}=5\%$ needs more SNR_t and/or N_u to get the same gains as when we are working to maximize the throughput (see Figure 4.19 with $n_s=4$).
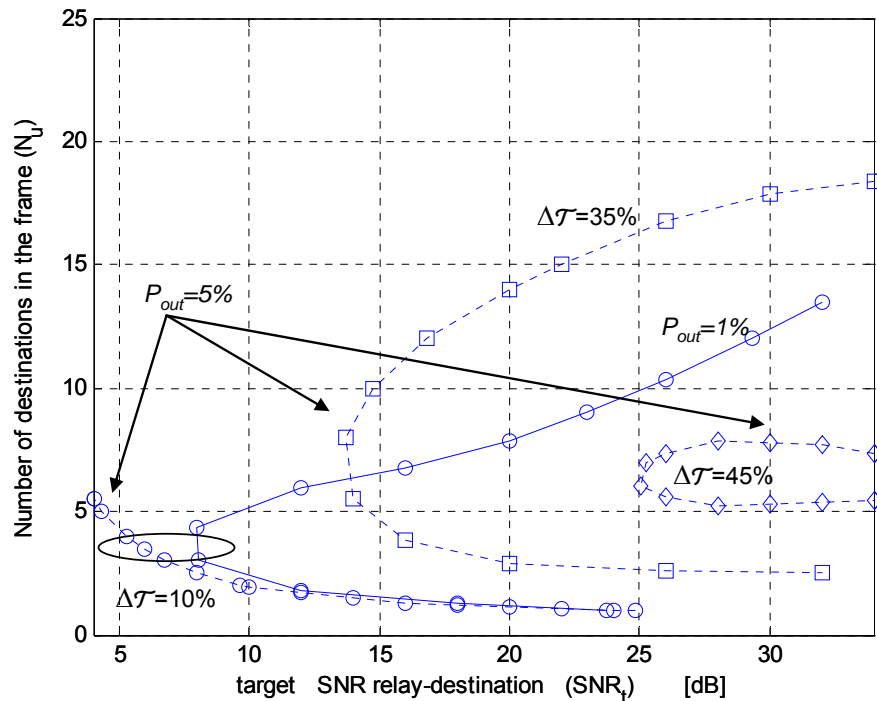
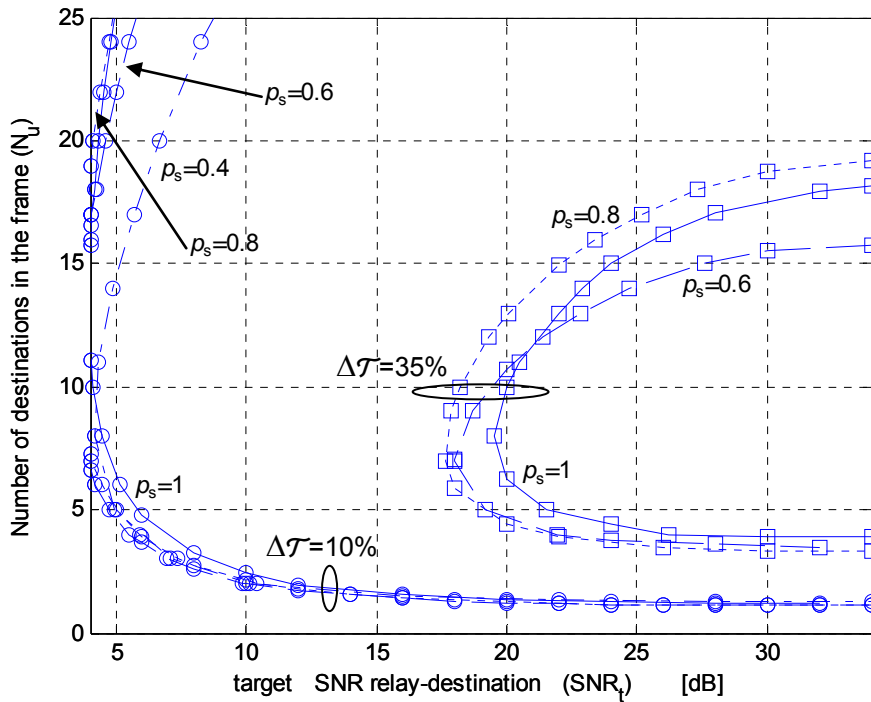**Figure 4.20.- {10%, 35%, 45%} gain plots of the average sum-throughput for the AF over the direct transmission with cooperative power when outage probability is fixed as a function of the target SNR and N_u. Terminal density $\lambda=5\times10^{-4}$ users/m², $n_s=4$, $P_{out}=\{1\%,5\%\}$. Propagation scenario defined by (4.57).**

C. Success probability

Section 4.5.3 has mentioned that the parameter ξ can be considered in the selection of the relay terminal for improving the throughput of the relays-assisted transmission, (4.46) and (4.47). But, the available idle terminals tend to decrease due to p_s. Hence, there is a tradeoff between selecting the relay terminal for a good value of ξ (thus increasing the mutual information) and the interference generated (decreasing p_s). Figure 4.21 shows this tradeoff for $n_s=2$ and $\lambda=5\times10^{-4}$ terminals/m^2 presenting the contour plots with $\Delta\mathcal{T}=\{10\%, 35\%\}$ for $\xi_0=\{1, 0.8, 0.6$ and $0.4\}$ which is equivalent for $n_s=2$ and Rayleigh fading, (4.48) to $p_s=\{1, 0.8, 0.6$ and $0.4\}$, (4.50). Selecting $p_s=0.8$ the same throughput gains are obtained but with less SNR_t in the relay-destination link or more destinations in the frame (N_u). The maximum throughput gain is 40.77% (not shown in that figure) obtained with target $SNR_t=34$ dB and $N_u=8$, better result that using $p_s=1$ (39.2%), Table 4.5. Decreasing p_s the same throughput gains needs more target SNR in the relay-destination link or less destinations in the frame in order to combat the generated interference. When we use $p_s=0.4$ the obtained throughput gain is always the worst, it does not achieve $\Delta\mathcal{T}=35\%$.

Figure 4.21.- {10%, 35%} gain plots of the average sum-throughput for the over the direct transmission with cooperative power as a function of the SNR_t and N_u. Terminal density $\lambda=5\times10^{-4}$ users/m^2, $n_s=2$, $p_s=\xi_0=\{1, 0.8, 0.6, 0.4\}$. Propagation scenario defined by(4.57).

D. Variation of terminal density

Figure 4.22 depicts the $\Delta\mathcal{T}=\{10, 35\%, 45\%\}$ for $n_s=4$ and $\lambda=\{2, 5, 8\}\times10^{-4}$ terminals/m^2. When increasing the terminal density, the assisting relays are closer to the destinations and the interfering power generated by the relays is lower, hence more destinations can be served in the same frame. It can be seen that when terminal density increases the constraints on the SNR_t and N_u are less restrictive to get the same throughput gains as lower terminal densities. Likewise, when $\lambda=8\times10^{-4}$ terminals/m^2 it is possible to get $\Delta\mathcal{T}=45\%$ with a similar configuration that the one needed for $\Delta\mathcal{T}=35\%$ with $\lambda=5\times10^{-4}$ terminals/m^2. Additionally, Table 4.5 shows that a maximum throughput gain of 55% (with $SNR_t=34$ dB and $N_u=9$) for $\lambda=8\times10^{-4}$ terminals/m^2

while with $\lambda=2\times10^{-4}$ terminals/m^2 the maximum throughput gain is 32.1% (with SNR_t=32 dB and N_u =6).
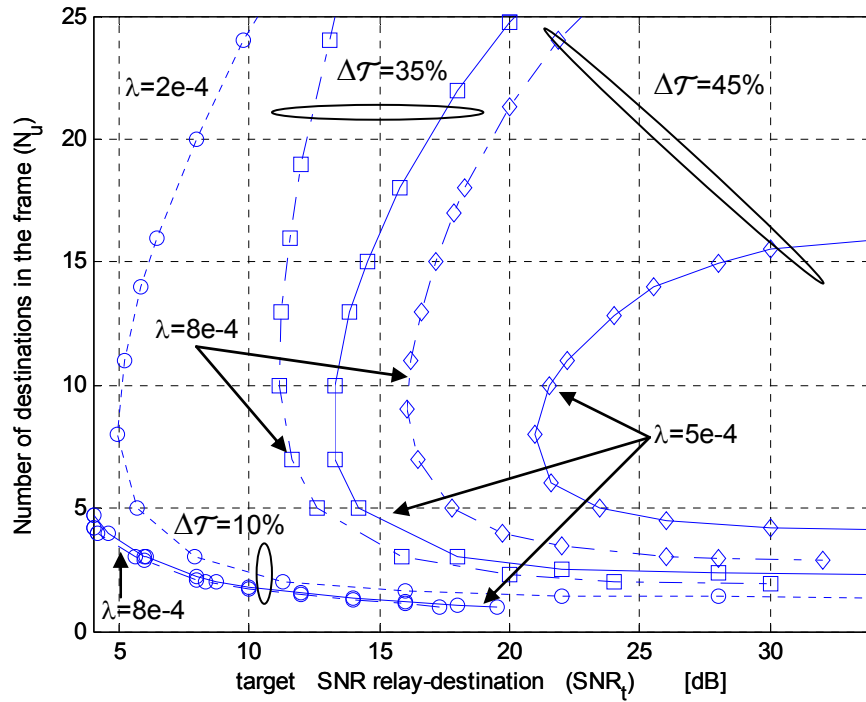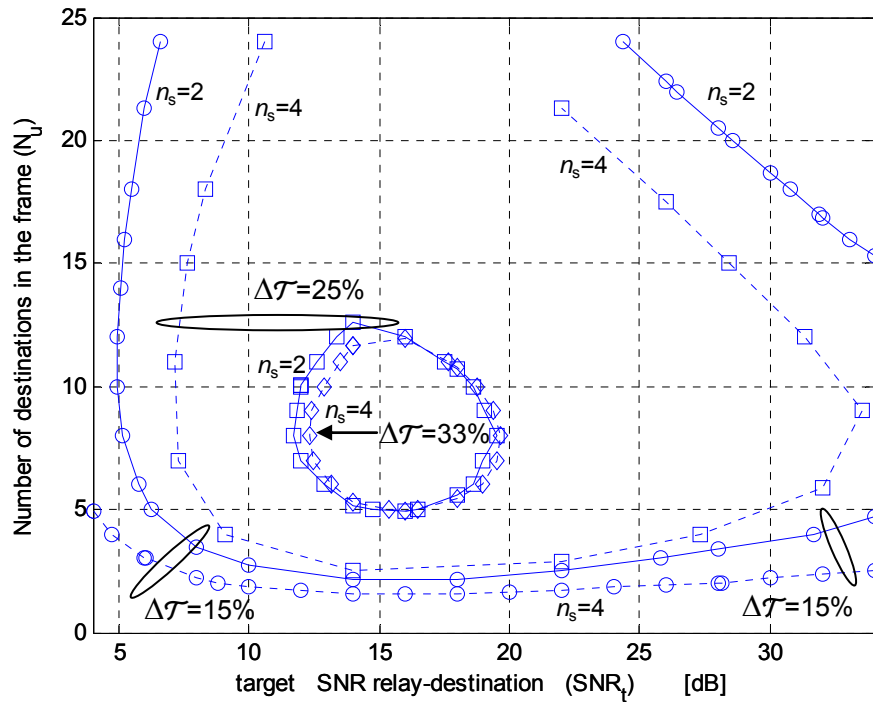

Figure 4.22.- {10%, 35% , 45%} gain plots of the average sum-throughput for the AF over the direct transmission with cooperative power as a function of the SNR_t and N_u. λ={2, 5, 8}×10^{-4} users/m^2. n_s=4. Propagation scenario defined by (4.57).

Figure 4.23.- {15%, 25%, 33%} gain plots of the average sum-throughput for the AF over the direct transmission with cooperative power as function of the target SNR and N_u. Terminal density λ=5×10^{-4} users/m^2. n_s={2,4}. Propagation scenario defined by (4.59).

E. Ratio power transmitted at source and the relay

All the previous results have shown that the best throughput gains over the *sum-throughput* of direct transmission with cooperative power are obtained for a high target SNR in the relay-destination link. This performance is because the power used by the relay is too low compared with the power used by the source, (4.51), so it has a low impact in the direct transmission with cooperative power. In the following it will be considered a different scenario with $P_s=P_{MAX}=20$ dBm and the path-loss given by,

$$\begin{cases} L_0 = L_1 = 62.09 + 2 \times 10 \times \log_{10}(d) & (dB) \\ L_2 = 43.65 + \gamma \times 10 \times \log_{10}(d) & (dB) \qquad \gamma = 4 \end{cases} \tag{4.59}$$

In this scenario a cell with radius 700m is also covered with a SNR=3 dB at the border of the cell (only with the pathloss). Figure 4.23 presents the $\Delta\mathcal{T}$ ={15%, 25%, 33%} for n_s={2, 4} and $\lambda=5\times10^{-4}$ terminals/m². The maximum throughput gains are 26.25% (attained at SNR_t=14 dB and N_u=8) and 34.28% (SNR_t=16 dB and N_u=7) for n_s=2 and n_s=4, respectively. In contrast to what happened in Figure 4.19, now it is not efficient transmitting with full power from the relay. In such a case, the direct transmission with cooperative power is able to get a better throughput. Now the maximum gains of the AF are reached for a target SNR close to 15 dB.

4.6 Rate control interference management for relay-assisted users with multiple relays

This section explores ways to boost the spectral efficiency of transmission schemes based on *amplify-and-forward* (AF) cooperation with multiple assisting relays in a multi-user scenario based on TDMA.

For single-user with multiple relays, there is a strategy transmission proposed in [28] that achieves diversity gains assuming simultaneous transmission from the multiple relays (in the *relay-transmit phase*). Each assisting relay does a phase rotation of the received signal, so that, the channel between the relays and the destination is transformed into a time-variant channel. On the other hand, in [29] and [30] the diversity-multiplexing tradeoff is investigated for different strategies where the assisting relays transmit in orthogonal time slots, increasing the transmission resources.

In multi-user environment based on TDMA it is possible to overcome the increased transmission resources by either spatially reusing the transmissions from different relay terminals or by using multiple relays similar to section 4.5. These two possibilities are not mutually exclusive and are studied below. It is shown that under mild assumptions the interference generated during the *relay-transmit phases* can be statistically modeled. The outage events generated by this interference are mitigated by an adaptive transmission rate scheme that maximizes the system throughput. This low complex implementation of multiple-relay AF provides significant throughput gains over a conventional TDMA scenario.

4.6.1 Scenario and signal model re-definition

The scenario is quite similar to the one described in section 4.2, where the centralized cellular system (of area A m^2) is built upon a single source and N_{tot} terminals spatially distributed according to a *Poisson* distribution with parameter λ (average number of terminals per unit area). All the terminals are served under TDMA and use simple receivers without any multi-user detection capability. The source serves packets randomly to all users in the cell. In each frame the source selects N_u terminals as destinations. The remaining terminals will be candidates to be assisting relays of those destinations. The role of the terminals will change through time, i.e. terminals that were destinations in some frame can be relays in other frames. The terminal density is also defined by (4.4). The antenna configuration is $n_s \geq 1$ antennas at the source and $n_r = n_d = 1$ antennas at the remaining terminals.

Multiple assisting relays

Now, each destination interested in relay transmission selects the nearest N_r idle terminals as assisting relays. Under this assumption, the joint probability density function (*pdf*) of the distance between the destination and the assisting relay (r_1 and r_2 in Figure 4.24 are statistically distributed) is given by [31],

$$f_{N_r}(r) = \frac{2\exp\left(-\lambda_{relay}\pi r^2\right)}{N_r} \sum_{x=1}^{N_r} \frac{\left(\lambda_{relay}\pi\right)^x}{(x-1)!} r^{(2x-1)} \tag{4.60}$$

where λ_{relay} is the idle terminal density (there are N_{tot}-N_u idle terminals in each frame). The density of idle terminals is assumed high enough so that the probability of two destinations selecting the same relay terminal is negligible. Appendix C (section 4.10) shows that this event can be approximated by a reduction of the total idle terminal density (also *Poisson*) when the number of terminals is roughly 4×N_r times greater than the active destinations.
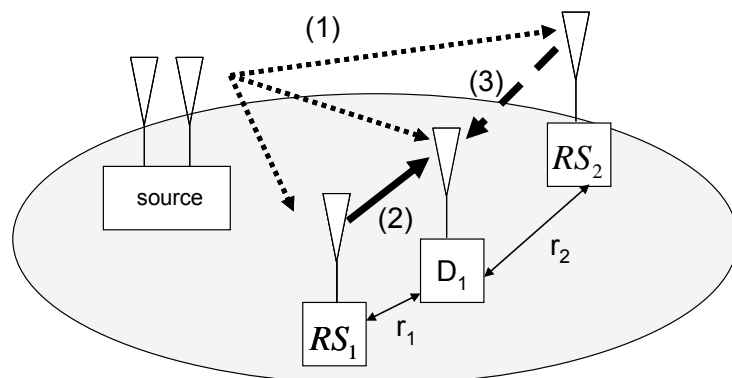
Figure 4.24.- Multiple relay-assisted transmission for a single destinations. Dotted lines: transmissions during the *relay-receive phase*. Solid and dashed lines: orthogonal transmissions (in two slots) in *relay-transmit phase*.

Relay-assisted transmission

The relay-assisted transmission will be done under protocol I and the multiple-assisting half-duplex relays work on *amplify and forward* mode duplexed in time (TDD), where the assisting relays transmits in orthogonal time slots. For example Figure 4.24 presents the relay-assisted transmission considered in this section. During the *relay-receive phase* the source transmits to

the destination in one time slot (dotted lines). That transmission is also received by the two assisting relays, which are spatial distributed around the destination. Now, the *relay-transmit phase* employs 2 time slots where each relay retransmits the signal received during the previous phase to the destination (solid and dashed lines).

In our approach we have considered that the relay slots are spatially reused by all the assisting relays active in that frame in order to improve the resources per user in spite of the interference generated. To illustrate this point, Figure 4.25 presents how the source distributes the resources among the destinations in each frame of duration T_{frame}. For direct transmission the source transmits to N_u destinations in equally sized slots (Figure 4.25-top). On the other hand for relay-assisted transmission (Figure 4.25-bottom) two phases can be observed. Firstly, the source transmits to each destination and its associated relays RS_j^i (*i*-th assisting relay associated to the *j*-th destination) in orthogonal time slots. Afterwards, each relay associated to the *j*-th destination (RS_j^i with $i=1..N_r$) transmits in N_r orthogonal time slots. However, each time slot is reused by all the assisting relays associated to other destinations, i.e in the *i*-th relay time slot there are N_u simultaneous and interfering transmissions from the assisting relays RS_j^i with $j=1..N_u$.
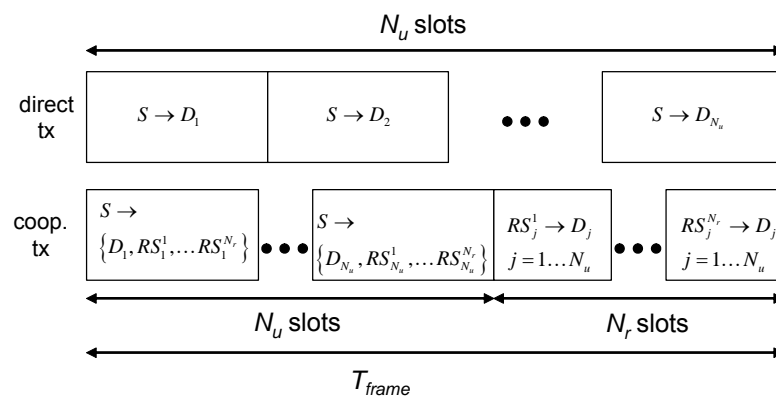
Figure 4.25.- Frame format for direct transmission (top) and relay transmission (bottom).

From Figure 4.25 it can be seen that the size of the time slots for the direct and relay transmission are different. The ratio between the time duration of the slot over the frame duration is defined as

$$\frac{T_{slot}}{T_{frame}} = \begin{cases} \dfrac{1}{N_u} & \text{direct tx} \\[2ex] \dfrac{1}{N_u + N_r} & \text{relay tx} \end{cases} \qquad (4.61)$$

Notice that with $N_r=1$ this equation is the same as (4.3).

Assumptions

In this new scenario each assisting relay will establish the target SNR (SNR_t) in the relay-destination link (in path-loss) in the same way as in the single-assisting relay, (4.35). It should be remarked that as the number of assisting relays grows, the distance between *j*-th relay to the

associated destination will also increase, hence it will require more power to adjust the target SNR (SNR_t) in that link. The assumptions considered in section 4.5.1 are still valid in this scenario, except for the type of events. Now, the outage events appear from the interference created at the relay slots and additionally from the channel variability. The channel coefficients remain constant for each transmission and change from frame to frame. Their current values are not known at the source.

Signal model for the amplify-and-forward transmission

The signal model for the multiple relay-assisted transmission under *amplify and forward* with the transmission defined by Figure 4.24 is given by ($n_s \geq 1$, $n_r = n_d = 1$),

$$\begin{bmatrix} y^{(I)} \\ y_1^{(II)} \\ \vdots \\ y_{N_r}^{(II)} \end{bmatrix} = \begin{bmatrix} \mathbf{h}_0^T \\ h_{2,1} g_1 \mathbf{h}_{1,1}^T \\ \vdots \\ h_{2,N_r} g_{N_r} \mathbf{h}_{1,N_r}^T \end{bmatrix} \mathbf{x} + \mathbf{B} \begin{bmatrix} n_{n_d} \\ n_{n_r} \\ \vdots \\ n_{n_r} \\ n_{n_d} \end{bmatrix} + \begin{bmatrix} 0 \\ \boldsymbol{\upsilon}_{N_r \times 1} \end{bmatrix} = \mathbf{H}_{AF} \mathbf{x} + \mathbf{n}_b \qquad (4.62)$$

where $h_{2,k}$ (1×1) is the channel between the k-th assisting relay to its associated destination, $\mathbf{h}_{1,k}$ ($n_s \times 1$) denotes the channel between the source to k-th assisting relay, $\mathbf{h}_0$ ($n_s \times 1$) is the channel of the source-destination link, $\mathbf{x}$ stands for the transmitted signal from the source, g_k is the gain introduced by each relay (there are N_r per destination) and is similar to (4.8) but considering the channels for the different relays, n_{n_d} and n_{n_r} are the white Gaussian noises received at the destination and relay and $\boldsymbol{\upsilon}$ vector is the interference measured at the relay slots with power distributed according to the model described in the following section. Matrix $\mathbf{B}$ is defined by,

$$\mathbf{B} = \begin{bmatrix} 1 & \mathbf{0}_{1 \times N_r} & 0 \\ \mathbf{0}_{N_r \times 1} & diag(\mathbf{F}) & \mathbf{1}_{N_r \times 1} \end{bmatrix} \quad \mathbf{F} = \begin{bmatrix} h_{2,1} g_1 & \cdots & h_{2,N_r} g_{N_r} \end{bmatrix} \qquad (4.63)$$

The $diag(\cdot)$ is an operator which transforms the vector $\mathbf{F}$ into a diagonal matrix whose non-zero elements are the components of $\mathbf{F}$.

The maximum normalized achievable rate of the relay-assisted transmission using AF without CSI at the transmitters (source and relay) is given by,

$$I^{AF} = \frac{T_{slot}}{T_{frame}} \log \det \left(\mathbf{I}_{(1+N_r)} + \frac{P_s}{n_s} \mathbf{R}_b^{-1} \mathbf{H}_{AF} \mathbf{H}_{AF}^H \right) \quad \text{bps/Hz} \qquad (4.64)$$

where $\mathbf{R}_b$ is the noise plus interference covariance matrix, (4.62), and T_{slot}/T_{frame} is the ratio between the slot and frame duration defined in (4.61). Notice that the relay-assisted system resembles to a $(1+N_r) \times n_s$ MIMO system, except for the extra channel resources because of orthogonal relay transmission.

Interfering power modeling

The interfering power received in each relay slot will be homogeneous and completely random and will depend on terminal density, activity in each slot and the *target* SNR, defined in (4.35). The interfering power, named Y, follows also an α-stable distribution as in the in the single-relay case (section 4.5.2) with the characteristic function (see details in Appendix D (section 4.11))

$$\phi_Y(\omega) = \exp\left(-K\cos(\alpha\pi/2)\omega^\alpha\left(1 - j\tan(\alpha\pi/2)\right)\right) \tag{4.65}$$

with α and *K*,

$$\alpha = \frac{\gamma}{2} \qquad K = \Upsilon\mu_{K_i,\alpha} \tag{4.66}$$

$$\Upsilon = \frac{\lambda_{active}\pi\,\Gamma(1-\alpha)(P_{MAX})^\alpha}{N_r}\Pi \qquad \mu_{K_i,\alpha} = \int K_i^\alpha f_{K_i}(K_i)\,dK_i$$

$$\Pi = \sum_{n=1}^{N_r}\left(\frac{\Gamma(n,\lambda_{relay}\pi\Delta^2)}{(n-1)!} + \left(\frac{N_0 SNR}{K_r P_{MAX}}\right)^\alpha\frac{\Gamma(n+1)-\Gamma(n+1,\lambda_{relay}\pi\Delta^2)}{\lambda_{relay}\pi(n-1)!}\right)$$

$$\Delta = \left(\frac{K_r P_{MAX}}{\sigma^2 SNR}\right)^{1/\gamma} \qquad \Gamma(a,z) = \int_z^\infty t^{a-1}\exp(-t)\,dt \qquad \Gamma(n+1) = n!$$

where λ_{active} is the active destination density. The main difference with the single-relay case is on the definition of the parameter Υ (compare (4.66) with (4.42)). Moreover, Table 4.4 is still valid for the K_i definition when the channel in relay-destination link presents those statistics.

4.6.2 Throughput

The source only has knowledge of the mean SNR of all links, so that the multipath fading channel and the interference in the relay slot become sources of outage. To mitigate those outage events, it is better to select a conservative rate, and to that end, the source has to maximize the throughput delivered to each destination,

$$\mathcal{T} = \max_{R'}\frac{1}{T_{frame}}R'\left(1 - P_{out}\left(T_{frame}I < R'\right)\right) \quad \text{bps/Hz} \tag{4.67}$$

where R' is the selected rate in bits/Hz in a time T_{slot}, I is the mutual information of the direct (4.6) or relay-assisted (4.64) transmission, and P_{out} denotes the outage probability. However, the P_{out} only present a closed-form expression for MISO (or SIMO) systems with Rayleigh fading, [32]. Additionally in our case, the channel state, the multiple assisting relays with different path-loss (different distances) and the interfering power from other relays are random variables to be considered for the outage probability, which makes difficult to find an analytical expression.

Let us assume the matrix Ω equal to the expression inside of the determinant in (4.64), the elements of its main diagonal are:

$$\Omega(1,1) = 1 + \frac{|\mathbf{h}_0|^2 P_s}{n_s \sigma^2} \qquad \Omega(k,k) = 1 + \frac{\dfrac{|h_{2,k}|^2 P_r}{\sigma^2} \dfrac{|\mathbf{h}_{1,k}|^2 P_s}{n_s \sigma^2}}{\dfrac{|h_{2,k}|^2 P_s}{\sigma^2} + \left(1 + \dfrac{|\mathbf{h}_{1,k}|^2 P_s}{n_s \sigma^2}\right)\left(\dfrac{Y}{\sigma^2} + 1\right)} \qquad (4.68)$$

where the channel coefficients $\mathbf{h}_0$, $\mathbf{h}_{1,k}$, $h_{2,k}$ incorporate the multipath fading and the path-loss (2 random variables per coefficient) due to the position of each terminal, P_r is a variable which also depends on the path-loss of the relay-destination link, (4.35) and Y is the interfering power at the destination which has been modeled by (4.65). Because of the difficulty of modeling (4.68) (there are 5 random variables) this work has used an experimental set of curves to evaluate the throughput obtained by a single relay-assisted destination (4.67) with relay nodes placed at a distance following (4.60) and the interfering power received during the relay slots are modeled by (4.65). As an example, Figure 4.26 presents some plots for the outage probability, taking into account all the known statistics, as a function of the normalized rate for a single destination with SNR_0=10 dB (source-destination link) and different number of assisting relays with distances distributed according to (4.60). Notice that the positions of the assisting relays to the source are also random variables. There is a terminal density of $\lambda = 2 \times 10^{-4}$ terminals/m^2, the source is equipped with n_s=2 antennas and there are 10 relay-assisted destinations served in the frame, i.e. in each relay slot there are 9 interfering relays. Moreover, the target SNR_t (in equation (4.35)) is fixed to 12 dB.
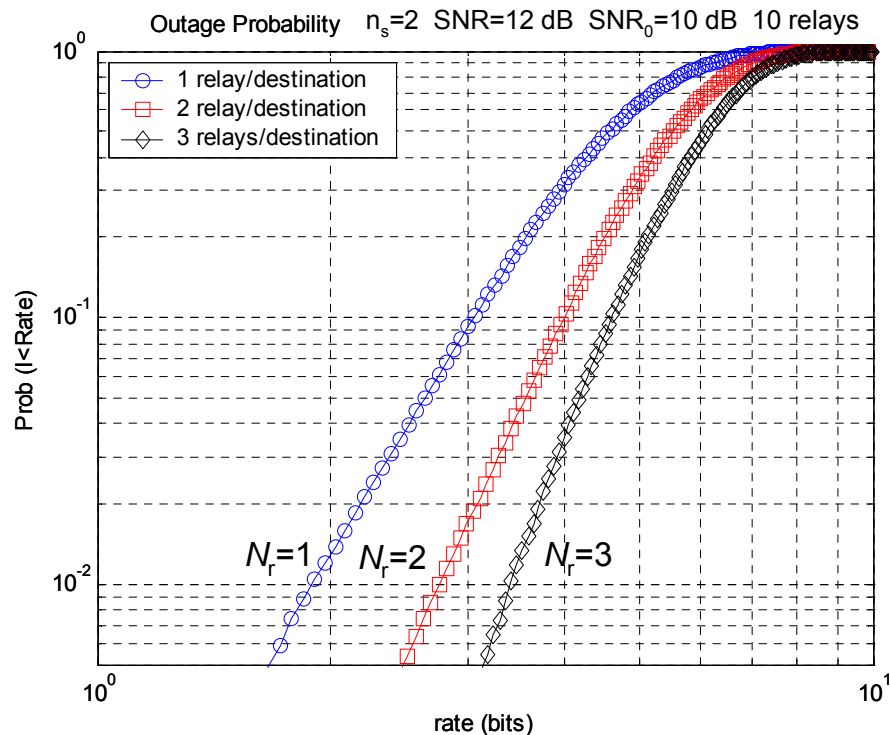
Figure 4.26.- Outage probability for the AF. n_s=2. SNR_t=12 dB. There are 10 simultaneous users in the relay slot.

The throughput thus obtained will be compared to the one obtained by direct transmission using all the transmitted power considered by the source and relays (named direct transmission with cooperative power in the sequel), which allows a fairly comparison of the gains obtained from cooperation over the direct transmission.

4.6.3 Results

Our results elaborate on a scenario built upon a cell with radius R_0=700 meters, one source with n_s={2,4} antennas and n_d=n_r=1 antennas at the destination and relays. The terminal density is λ=2×10^{-4} users/m^2. The path-loss at distance d between the source-destination and source-relay is proportional to d^3 whereas in the relay-destination link is proportional to d^4 (γ=4). The maximum power transmitted by each relay and by the source is 23 dBm and 30 dBm respectively. The source always transmits with its maximum power to each destination, except for direct transmission with cooperative power, where it also considers the power used by the assisting relays associated to that destination. The N_r assisting relays are distributed around the destination at a distance following (4.60). Notice that some relays can be in worse conditions than the direct link. The results shown are in terms of the individual throughput (4.64) of a TDMA destination with a signal to noise ratio from the source of SNR$_0$=10 dB (named SNR$_0$ because it is the source-destination link).

Individual throughput gains for a given target SNR

Figure 4.27 presents the throughput gain of the relay-assisted transmission (solid lines) and the direct transmission with the cooperative power (dotted lines) over the direct transmission, for n_s=2 and different number of the destinations in the frame (N_u) and assisting relays (N_r). A target value of *SNR*=12 dB has been arbitrarily selected. For example with N_r=1 (virtual MIMO 2×2 see (4.64)), the relay-assisted transmission is beneficial when there are more than 2 users to be served in the same frame. For N_u=3 users, almost the same gains are obtained by the relay-assisted and the direct transmission with cooperative power. Both are better than the direct transmission thanks to the extra power used at the relay. With N_r=1 and N_u=14 users in the frame, a gain up to 40% can be obtained over the direct transmission (37% over the direct transmission with cooperative power). If N_r=2 (*virtual* MIMO 2×3), gains up to 68% are possible (60% over direct transmission with cooperative power). Likewise, it has to be mentioned that the throughput of the direct transmission with cooperative power increases with the number of users in the frame. The reason is that the idle terminal density decreases with N_u, (see equation (4.4)) so the relays will be farther away from the destinations and more power will be required to attain the target SNR. Although due to the values considered in this work, this gain tends to saturate. Moreover, the case with N_u=1 corresponds to the conventional AF which can be improved by reusing the relay slots. The poor performance of the conventional AF in our scenario is because the assisting relay can be in worse conditions than the destination. If some criterion was considered for selecting the suitable assisting relays similar to the one used in (4.50) the performance of the relay-assisted transmission could be improved.
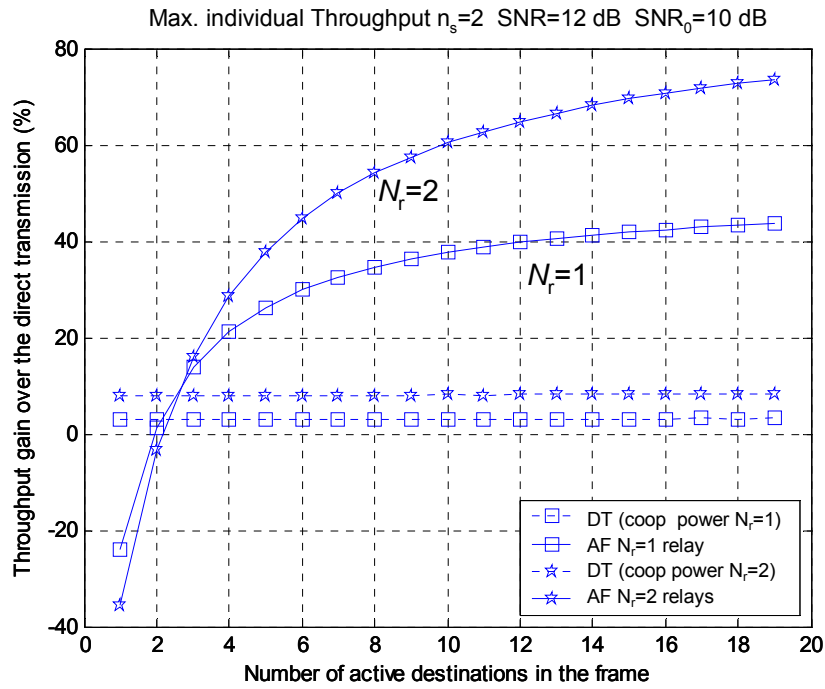
Figure 4.27.- Throughput gain (%) of the relay-assisted transmission and direct transmission with cooperative power over the direct transmission vs. N_u. SNR_t=12 dB, n_s=2, SNR_0=10 dB.
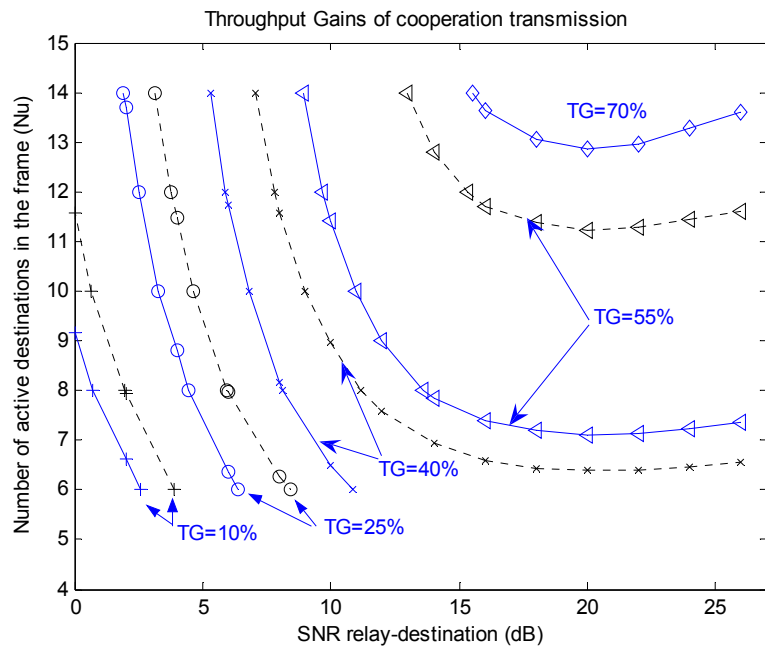

Figure 4.28.- Throughput relay gain (TG) in percentage over the direct transmission with cooperative power as a function of SNR_t and N_u. n_s=2 (dotted lines) and n_s=4 (solid lines). N_r=2 and λ=2×10^{-4} users/m^2.

Individual throughput gains

Clearly, the relay-assisted implementation presented in this work depends on several factors as the terminal density, the antennas at the source, the number of assisting relays per destination and the target SNR selected in the relay-destination link. Figure 4.28 presents the efficiency of this implementation, i.e. the regions where the throughput gains of relay-assisted transmission

over the direct transmission with cooperative power are constant for different values of target SNR (relay-destination link) and number of served users in the frame (N_u). The configuration selected is n_s=4 (solid lines) and n_s=2 (dotted lines), both with N_r=2 (virtual 4×3 and 2×3, see (4.64)). It can be seen how the target SNR and the number of served users (N_u) are connected for a given throughput gain (TG)[6]. For instance with n_s=4, the throughput gain due to the relay-assisted transmission obtained by a user with SNR_0=10 dB is 55% when there are N_u=14 destinations and SNR_t=9 dB or when N_u=8 and SNR_t=14 dB.
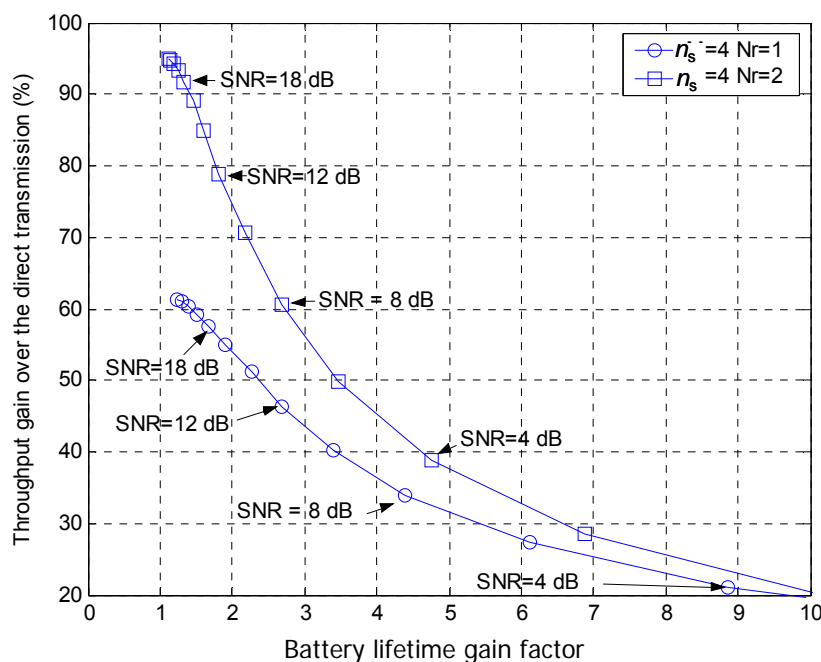
Figure 4.29.- Tradeoff between relay-assisted throughput gain (%-over the direct transmission) as a function of the battery lifetime gain factor for λ=2×10^{-4} users/m^2. n_s=4, N_r={1,2}.

Battery lifetime for user relaying

Previously the efficiency of the proposed implementation has been considered. On the other hand, if we are interested in the gains of the relay-assisted transmission over the direct transmission, i.e. considering the *extra-power* from the assisting relays as an additional benefit of the relay-assisted transmission, the relays should transmit always with maximum power. However, this work assumes that the assisting relays are in general idle terminals (*user relaying*) that spend the energy of its batteries to improve transmissions to destination users. Therefore, battery consumption is an important point to be considered. Assuming the simplification that the battery lifetime is connected with the transmitted energy through,

$$T_{lifetime} \propto \frac{1}{E\left\{E_{relay}\right\}} \propto \frac{1}{E\left\{P_{relay} \times \rho\right\}} \tag{4.69}$$

being ρ the activity of a terminal acting as relay. This value may be obtained as the ratio between the total assisting relays selected for cooperation and the terminals on the cell, that is, $N_u \times N_r/N_{tot}$. Therefore, from (4.69) it can be concluded that selecting low values of target SNR, the battery lifetime can be extended. Figure 4.29 presents the tradeoff between the relay-

---

[6] It considers the individual throughput and it is different from the one defined in (4.58).

assisted transmission gain over the direct transmission versus the battery lifetime gain factor for n_s=4 and N_r={1,2} assisting relays. For N_r=2 transmitting with maximum power a gain of 95% is possible. On the other hand, setting a SNR_t=12 dB (recall that the power used by each relay will depend on the distance to its associated destination, (4.35)), the gain is around 80%, but the battery lifetime has been increased 2 times compared to the case when the assisting relays transmits with full power, so that, the energy spent by the terminals for relaying decreases. Therefore, the value of the target SNR depends on desired gain for the relay-assisted transmission (*efficiency*) and battery lifetime of the terminals.

4.7   Chapter summary and conclusions

This chapter has shown the benefits of the relay-assisted transmission using protocol I in a centralized wireless system with TDD half-duplex relays. Basically it focuses in a scenario where the assisting relays are nearby the destination terminals. Because of the transmission resources in a TDMA system are fixed (all time slots present the same size) the spectral efficiency of the relay-assisted transmission is reduced (see section 2.2). The spatial reuse of the *relay-transmit phase* (relay slot) has been considered to enhance the spectral efficiency, where the assisting relays associated to different destinations simultaneously transmit in the same time slot, creating interference in that slot. With this method the destination obtains an additional *virtual* receiving antenna (transmission received in the relay slot).

One possible method investigated in this chapter to combat the interference is by a distributed power control algorithm based on game theory. It has been shown in section 4.3 that the algorithm converges after a few iterations. Moreover, the *sum-throughput* results obtained by the relay-assisted transmission with this power control algorithm improve the direct transmission results. When the reuse is high, the performance of the relay-assisted transmission approaches to the spectral efficiency obtained by direct transmission in a $n_s \times 2n_d$ MIMO system (also under TDMA). Additionally, when the terminal density of the cell is high the spectral efficiency of the relay-assisted transmission with *infrastructure* (with no spatial reuse of the relay slot) and *user relaying* becomes similar. Finally, the *multiuser diversity gain* has been investigated within a Media Access Control layer framework allowing a practical implementation of these concepts. Section 4.4 has shown that the proposed scheme for the relay-assisted transmission based on three phases (*neighbor search, admission control* and *scheduling*) obtains multiuser diversity gains and fairness among users. In fact, thanks to the relay slot is reused by multiple destinations distributed around the cell, their opportunities to be served by the source increase. Additionally, the overhead introduced is around 10% when instantaneous measures of the mutual information of each link are needed.

Another method to deal with the interference is by tuning the transmission rate (*rate control*), based on the knowledge of the interference statistics. Section 4.5 has shown that the interfering power received at the relay slot for the *user relaying* can be modeled as an α-stable process. With this information we are able to evaluate the outage event of the relay-assisted transmission (only due to the interference in the relay slot) under homogeneous distribution of the active destinations and a scheduling strategy producing spatially homogeneous interference (e.g. for *round-robin*). The performance of *amplify and forward* relay-assisted transmission has

been analyzed in terms of *sum-throughput* gain over the direct transmission presented as contour plots as a function of the number of destinations allocated in a frame (N_u) and the SNR selected in the relay-destination link. For $n_d=n_r=1$ antennas at the destination and relay, significant gains can be obtained depending on the terminal densities and the antennas at the source. Moreover, these gains depend on the type of traffic considered, *best effort* (maximization of the throughput) or *non-delay sensitive traffic* (upper bound in the outage probability). In section 4.6 the interference model has been extended to the case where each destination have multiple assisting relays (which will be transmitting in orthogonal time slots) and it has considered that the outage events come from the interference in the relay slot and the instantaneous channels. In spite of selecting more relays (the distance between relay and destination is larger) and using the simple amplify and forward technique, it is possible to get significant throughput gains. Additionally it has been shown that there is a tradeoff between the throughput gain and the battery lifetime of the terminal acting as assisting relay.

4.8 Appendix A. Reduction of the idle terminal density

Assume that at each active destination tries to find the nearest idle terminal as a relay and it succeeds with probability p_s. If it fails, it searches for the second nearest terminal and so on. Assuming a *Poisson* distribution of the terminals, then the probability of finding n_t relays in a circle of radius r is given by,

$$\Pr(n_t \ in \ r) = \frac{\left(\lambda\pi r^2\right)^{n_t}}{n_t!} \exp\left(-\lambda\pi r^2\right) \tag{4.70}$$

where λ is the user density and r denotes the radius of the circle. The probability of finding n_t-*th* closest node (the first node, the second node, etc.) in a cell area is given by,

$$\Pr(n_t, r) = 1 - \sum_{k=0}^{n_t-1} \Pr(k \ in \ r) \tag{4.71}$$

The probability density function becomes,

$$f_{n_t}(r) = \frac{d\Pr(n_t)}{dr} = \frac{2}{(n_t-1)!}(\lambda\pi)^{n_t} \ r^{(2n_t-1)} \exp\left(-\lambda\pi r^2\right) \tag{4.72}$$

Now if we assume that each closest node is successfully selected as a relay with probability p_s, the complete *pdf* can be written as,

$$f = p_s f_1 + \left(1-p_s\right) p_s f_2 + \dots + \left(1-p_s\right)^{n_t-1} p_s f_{n_t} \tag{4.73}$$

$$f = 2\lambda\pi r p_s \exp\left(-\lambda\pi r^2\right)\left(1 + \frac{z^2}{2!} + \frac{z^4}{3!} + \frac{z^6}{4!} + \dots\right) \quad where \quad z = r\sqrt{(1-p_s)\lambda\pi} \tag{4.74}$$

The expression depicted in (4.74) presents a finite sum,

$$f = 2\lambda\pi r p_s \exp\left(-\lambda\pi r^2\right)\exp\left((1-p_s)\lambda\pi r^2\right) = 2\lambda p_s \pi r \exp\left(-\lambda p_s \pi r^2\right) \tag{4.75}$$

The process of finding the closest terminal with probability p_s obtains the same *pdf* as finding the closest terminal when the user density is λp_s.

4.9 Appendix B. Interference power model when there is a single assisting relay per destination

Assuming the scenario defined in section 4.2 and the assumptions of sections 4.5.1 and 4.5.2, let Y_a be the interference power received from the active relays in D_a (a disk of radius a),

$$Y_a = \sum_{r_i \leq a} \eta\left(K_i, r_i, r\right) = K_i \sum_{r_i \leq a} g\left(r_i, r\right) \tag{4.76}$$

where K_i is a random variable modeling the multipath fading or shadowing channel gain that affects the interference and $g(.)$ (see equation (4.38)) is a function which models the relation between the interfering power and the distance between the destination and the interfering relay, r_i. The function η will be a piecewise function defined as,

$$\eta(K_i, r_i, r) = \begin{cases} \eta_1(K_i, r_i, r) = K_i g(r_i, r) = K_i \dfrac{N_0 SNR}{K_r r_i^\gamma} r^\gamma & r \le \Delta \\ \\ \eta_2(K_i, r_i) = K_i g(r_i) = K_i \dfrac{P_{MAX}}{r_i^\gamma} & otherwise \end{cases}$$
(4.77)

where Δ is defined in (4.38). The characteristic function of Y_a may be evaluated as,

$$\phi_{Y_a}(\omega) = \mathbf{E}\left\{\mathbf{E}\left\{e^{j\omega Y_a} \mid k \text{ in } D_a\right\}\right\} = \sum_{k=0}^{\infty} \frac{\left(\lambda_{active}\pi a^2\right)^k}{k!} \exp\left(-\lambda_{active}\pi a^2\right) \mathbf{E}\left\{e^{j\omega Y_a} \mid k \text{ in } D_a\right\}$$
(4.78)

with λ_{active} being the density of active relays in the relay link slot. Letting $a \to \infty$ then $Y_a = Y$, we will obtain the characteristic function of the total interference, Y. The k terminals are uniformly distributed in space thanks to the nature of the *Poisson* process. Therefore, the probability density function of the distance of each interfering terminal is given by,

$$f_{r_i}(r_i) = \begin{cases} \dfrac{2r_i}{a^2} & r_i \le a \\ \\ 0 & \text{otherwise} \end{cases}$$
(4.79)

Moreover, the sum of independent random contributions to interference is the product of their individual characteristic functions,

$$\mathbf{E}\left\{e^{j\omega Y_a} \mid k \text{ in } D_a\right\} = \left(\int_0^\infty \int_0^\infty \int_0^\infty \exp\left(j\omega\eta(K_i, r_i, r)\right) f_{r_i, r}(r_i, r) f_{K_i}(K_i) dr_i dr dK_i\right)^k$$
(4.80)

with $\eta(K_i, r_i, r)$ given by (4.77), $f_{K_i}(K_i)$ is the *pdf* of K_i which does not depend on r or r_i. Replacing (4.80) in (4.78) the characteristic function of Y_a is given by,

$$\phi_{Y_a}(\omega) = \exp\left(\int_0^\infty \lambda_{active}\pi a^2 \left(\int_0^\infty \int_0^\infty \exp\left(j\omega\eta(K_i, r_i, r)\right) f_{r_i, r}(r_i, r) dr_i dr - 1\right) f_{K_i}(K_i) dK_i\right)$$
(4.81)

By increasing the radius of the circle to infinity we will obtain the characteristic function of the complete interference Y,

$$\phi_Y(\omega) = \lim_{a \to \infty} \phi_{Y_a}(\omega) = \lim_{a \to \infty} \exp\left(\int_0^\infty \lambda_{active}\pi a^2 \left(A(K_i) + B(K_i) - 1\right) f_{K_i}(K_i) dK_i\right)$$
(4.82)

with A and B factors defined with the following equations related to the integration of the different parts of the piecewise function $\eta(.)$ in (4.77),

$$A(K_i) = \int_0^\Delta f_r(r) dr \int_0^\infty \exp\left(j\omega\eta_1(K_i, r_i, r)\right) f_{r_i}(r_i) dr_i =$$

$$= \int_0^\Delta f_r(r) dr \int_0^a \frac{2r_i}{a^2} \exp\left(j\omega\eta_2(K_i, r_i)\beta r^\gamma\right) dr_i$$
(4.83)

$$B(K_i) = \int_\Delta^\infty f_r(r)dr \int_0^a \exp\big(j\omega\eta_2(K_i,r_i)\big)\frac{2r_i}{a^2}dr_i = \frac{\Omega}{a^2}\int_0^a 2r_i \exp\big(j\omega\eta_2(K_i,r_i)\big)dr_i \qquad (4.84)$$

$$\beta = \frac{N_0 SNR}{K_r P_{MAX}} \qquad \Omega = \int_\Delta^\infty f_r(r)\,dr = \exp\big(-\pi\lambda_{relay}\Delta^2\big) \qquad (4.85)$$

where λ_{relay} is the parameter that models the distance between the destination and its associated *relay*, (4.1), and η_2 is defined in (4.77). Notice that the independence between random variables r_i (distance of interfering relay to a destination) and r (distance of each assisting relay to its associated destination) has been considered in (4.83) and (4.84) $f_{r_i,r}(r_i,r) = f_{r_i}(r_i)f_r(r)$. Firstly, we will obtain the integral of the second factor of (4.83) integrating by parts. Manipulating the expression,

$$X(K_i) = \int_0^a \frac{2r_i}{a^2}\exp\big(j\omega\eta_2(K_i,r_i)\beta r^\gamma\big)dr_i + 1 - 1 = \Sigma + 1 + H \qquad (4.86)$$

$$\Sigma = \frac{1}{a^2}r_i^2 \exp\big(j\omega\eta_2(K_i,r_i)\beta r^\gamma\big)\Big|_0^a - 1$$

$$H = -\frac{j\omega}{a^2}\int_0^a r_i^2 \exp\big(j\omega\eta_2(K_i,r_i)\beta r^\gamma\big)\beta r^\gamma \frac{\partial\eta_2(K_i,r_i)}{\partial r_i}dr_i = \{t = \eta_2(K_i,r_i)\beta r^\gamma\} = \quad (4.87)$$

$$= r^2\left(\frac{j\omega\big(K_i P_{MAX}\beta\big)^{2/\gamma}}{a^2}\int_0^\infty t^{-2/\gamma}\exp\big(j\omega t\big)dt\right) = r^2\frac{T_A(K_i)}{a^2}$$

Where the definition of $T_A(.)$ is straightforward from the last equality. Then $A(K_i)$ is,

$$A(K_i) = \int_0^\Delta X(K_i)f_r(r)dr = \Psi_A + (-\Omega + 1) + \frac{T_A(K_i)}{a^2}\left(\frac{1-\big(1+\pi\lambda_{relay}\Delta^2\big)\Omega}{\pi\lambda_{relay}}\right) \qquad (4.88)$$

$$\Psi_A = (1-\Omega)\Sigma$$

where Ω is defined in (4.85), $T_A(K_i)$ in (4.87) and Δ in (4.38). Additionally, following a similar procedure for $B(K_i)$, we get

$$B(K_i) = \Omega\left(\int_0^a \frac{2r_i}{a^2}\exp\big(j\omega\eta_2(K_i,r_i)\big)dr_i + 1 - 1\right) = \Psi_B + \Omega\left(1 + \frac{T_B(K_i)}{a^2}\right)$$

$$\Psi_B = \frac{\Omega}{a^2}\left(r_i^2 \exp\big(j\omega\eta_2(K_i,r_i)\big)\Big|_0^a - 1\right) \qquad (4.89)$$

$$T_B(K_i) = -j\omega\int_0^a r^2 \exp\big(j\omega\eta_2(K_i,r_i)\big)\frac{\partial\eta_2(K_i,r_i)}{\partial r_i}dr_i = j\omega\big(K_i P_{MAX}\big)^{2/\gamma}\int_0^\infty t^{-2/\gamma}\exp\big(j\omega t\big)dt$$

Let us define the following term when $a\to\infty$

$$\Pi(K_i) = \lim_{a\to\infty}\lambda_{active}\pi a^2\big(A(K_i) + B(K_i) - 1\big) =$$

$$= \lim_{a\to\infty}\lambda_{active}\pi a^2\big(\Psi_A + \Psi_B\big) + \lambda_{active}\pi T_B(K_i)\varphi \qquad (4.90)$$

$$T_A(K_i) = T_B(K_i)\beta^{2/\gamma} \qquad \varphi = \left(\frac{1-\big(1+\pi\lambda_{relay}\Delta^2\big)\Omega}{\pi\lambda_{relay}}\right)\beta^{2/\gamma} + \Omega$$

where term Ψ_A (which depends on Σ) (4.88) and Ψ_B can be neglected because of the assumption in (4.36) when $a \to \infty$,

$$\lim_{a \to \infty} \lambda_{active} \pi a^2 \Psi_A = \lim_{a \to \infty} \lambda_{active} \pi a^2 (1 - \Omega) \left(\exp\left(j\omega \eta_2 (K_i, a) \beta r^\gamma \right) - 1 \right) = 0$$

$$\lim_{a \to \infty} \lambda_{active} \pi a^2 \Psi_B = \lim_{a \to \infty} \lambda_{active} \pi a^2 \Omega \left(\exp\left(j\omega \eta_2 (K_i, a) \right) - 1 \right) = 0$$

(4.91)

Finally, equation (4.82) becomes,

$$\phi_Y(\omega) = \exp\left(\int_0^\infty \Pi(K_i) f_{K_i}(K_i) dK_i \right) =$$

$$= \exp\left(\lambda_{active} \pi \varphi P_{MAX}^\alpha \left(j\omega \int_0^\infty t^{-\alpha} \exp(j\omega t) dt \right) \int_0^\infty K_i^\alpha f(K_i) dK_i \right) =$$

(4.92)

$$= \exp\left(-K \exp\left(-j\frac{\pi}{2}\alpha \right) \omega^\alpha \right) = \exp\left(-K \cos\left(\frac{\pi}{2}\alpha \right) \omega^\alpha \left(1 - j\tan\left(\frac{\pi}{2}\alpha \right) \right) \right)$$

where α is equal to $2/\gamma$, φ is defined in (4.90), $\Gamma(.)$ denotes the Gamma function, K and $\mu_{K_i, \alpha}$ are given by

$$K = \lambda_{active} \pi \left(\left(\frac{N_0 SNR}{K_r} \right)^\alpha \frac{\left(1 - \left(1 + \pi \lambda_{relay} \Delta^2 \right) \Omega \right)}{\pi \lambda_{relay}} + \Omega P_{MAX}^\alpha \right) \Gamma(1 - \alpha) \mu_{K_i, \alpha}$$

$$\mu_{K_i, \alpha} = \int_0^\infty K_i^\alpha f_{K_i}(K_i) dK_i$$

The characteristic function belongs to the α-stable distributions where the K factor of the interfering power depends on the α-th moment of the random variable K_i.

4.10 Appendix C. Experimental model of the success probability

This section models experimentally the event that the nearest terminal cannot be selected because it has been selected by other destination. This event is modeled by the probability p_s of becoming an assisting relay at each idle terminal. This probability will be the same for all idle terminals. An experimental equation for estimating its value will be obtained, where p_s depends on the number of total terminals, active destinations and number of relays per destination. The accuracy of this approximation is enough for the purposes of this work.

Theoretical model

It is assumed that all idle terminals are uniformly distributed in a circular cell of radio R_0 following a *Poisson* distribution with density λ_t. Each destination tries to find the N_r nearest terminals, where each of them is selected with probability p_s. The probability of finding N_r terminals in a circle of radius r is given by,

$$\Pr\left(N_r \ in \ r\right) = \frac{\left(\lambda_t \pi r^2\right)^{N_r}}{N_r!}\exp\left(-\lambda_t \pi r^2\right) \tag{4.93}$$

where λ_t is the idle terminal density and r stands for the radius of the circle.

The probability of finding N_t-th closest node inside of a circle of radius r is,

$$\Pr\left(N_t, r\right) = 1 - \sum_{k=0}^{N_t-1}\Pr\left(k \ in \ r\right) \tag{4.94}$$

Accordingly, we have the following probability density function,

$$f_{N_t}\left(r\right) = \frac{d\Pr\left(N_t, r\right)}{dr} = \frac{2}{\left(N_t-1\right)!}\left(\lambda_t\pi\right)^{N_t} r^{\left(2N_t-1\right)}\exp\left(-\lambda_t\pi r^2\right) \tag{4.95}$$

However, because each terminal presents a success probability, p_s, to be selected, the N_r-th nearest selected terminal will not correspond with the N_r-th nearest terminal. So that, we have to consider the case that the N_r-th nearest relay will be in the set $N_t=[N_r, \ N_{r+1}, \ N_{r+2},..]$. In the following, an illustrative example where a destination tries to select N_r=2 relays will be explained. Afterwards, general case with N_r assisting relays will be presented. Assuming that each nearest terminal is selected with probability p_s (binomial distribution), the probability of selecting always the 2nd nearest terminal as the 2nd relay (hereinafter it will be named θ_2^2) is given by selecting always the first and second nearest terminals as relays, so that,

$$\theta_2^2\Big|_{Binomial} = p_s p_s \tag{4.96}$$

where sub-index stands for the number of relays to be selected and supra-index for the last terminal to be selected. The probability that the 3rd nearest terminal will be the 2nd relay will be obtained if (1st,3rd) or (2nd,3rd) terminals are selected, in that case that probability is,

$$\theta_2^3 = p_s\left(1-p_s\right)p_s + \left(1-p_s\right)p_s p_s = 2\left(1-p_s\right)p_s p_s \tag{4.97}$$

The probability that the 4th nearest terminal will be selected as the 2nd relay is given by the following possibilities: $\{(1^{st},4^{th}),(2^{nd},4^{th}),(3^{rd},4^{th})\}$. Therefore, it is given by,

$$\theta_2^4 = p_s\left(1-p_s\right)^2 p_s + \left(1-p_s\right)p_s\left(1-p_s\right)p_s + \left(1-p_s\right)^2 p_s p_s = 3\left(1-p_s\right)^2 p_s p_s \tag{4.98}$$

In general, the probability that the N_t-th nearest terminal will be the N_r-th selected relay becomes,

$$\theta_{N_r}^{N_t} = \left(\binom{N_t}{N_r}-\binom{N_t-1}{N_r}\right)\left(1-p_s\right)^{N_t-N_r}\left(p_s\right)^{N_r} = \binom{N_t}{N_r}\frac{N_r}{N_t}\left(1-p_s\right)^{N_t-N_r}\left(p_s\right)^{N_r} \tag{4.99}$$

Finally, the probability distribution function (pdf) of the N_r-th nearest relay is given by,

$$g_{N_r} = \sum_{N_t=N_r}^{\infty}\theta_{N_r}^{N_t}f_{N_t} \tag{4.100}$$

with $\theta_{N_r}^{N_t}, f_{N_r}$ given by (4.99) and (4.95) respectively. Notice that (4.100) is a sum with infinite operands. However, in the following we will show that it has a finite result. We can write the previous equation in the following way,

$$g_{N_r} = \exp\left(-\lambda_t \pi r^2\right) \left(\frac{2\left(\lambda_t \pi\right)^{N_r} r^{(2N_r-1)} \left(p_s\right)^{N_r}}{\left(N_r - 1\right)!}\right) \sum_{N_t=N_r}^{\infty} \frac{\left(\left(1-p_s\right)\lambda_t \pi\right)^{N_t-N_r} r^{2(N_r-N_t)}}{\left(N_t - N_r\right)!} \quad (4.101)$$

The last term of (4.101) presents a finite summation if the following variable is defined,

$$z = \lambda_t \pi \left(1 - p_s\right) r^2 \quad (4.102)$$

Therefore the last operand of (4.101) becomes,

$$\sum_{x=0}^{\infty} \frac{1}{x!}\left(1-p_s\right)^x \left(\lambda_t \pi\right)^x r^{(2x)} = \sum_{x=0}^{\infty} \frac{1}{x!} z^x = 1 + \frac{z}{1} + \frac{z^2}{2!} \ldots = \exp(z) \quad (4.103)$$

Combining (4.103) and (4.101), the probability density function is given by,

$$g_{N_r} = \exp\left(-\lambda_t \pi p_s r^2\right) \left(2\left(\lambda_t \pi p_s\right)^{N_r} r^{(2N_r-1)} \frac{1}{\left(N_r - 1\right)!}\right) \quad (4.104)$$

Notice that the difference between (4.104) and (4.95) is in the total terminal density, now is $\lambda_t p_s$. Therefore, the effect of p_s is a reduction of the total density of the available idle terminals. Finally, the joint *pdf* of the distance of the N_r nearest selected terminals is given by,

$$f_{1,\ldots N_r} = \frac{1}{N_r} \sum_{i=1}^{N_r} g_i = \frac{\exp\left(-\lambda_t p_s \pi r^2\right)}{N_r} \sum_{x=1}^{N_r} \left(\frac{2\left(\lambda_t p_s \pi\right)^x r^{(2x-1)}}{\left(x-1\right)!}\right) \quad (4.105)$$

Experimental model

In order to study this problem, it has considered an area of size A with N_{tot} terminals with *Poisson* distribution. Among those terminals, N_u active destinations are selected whereas the remaining ones will be idle terminals to possibly become assisting relays. Each destination will try to select the nearest N_r terminals in case they have not been selected previously.

After many realizations with different terminal positions, the probability that the N_t-th nearest terminal will be the N_r-th nearest relay has been measured and it will be referenced as $\theta_{N_r}^{N_t}$. This work proposes to approximate the previous probabilities distribution with a *Binomial* distribution of parameter p_s, (4.99). We have imposed,

$$\theta_{N_r}^{N_t}\Big|_{Binomial} = \binom{N_t}{N_r} \frac{N_r}{N_t}\left(1 - p_s\right)^{N_t-N_r} \left(p_s\right)^{N_r} \quad (4.106)$$

Moreover, in order to adjust the *Binomial* distribution to the true performance we can use the parameter p_s in (4.106). We have imposed,

$$\theta_{N_r}^{N_r}\Big|_{Binomial} = \theta_{N_r}^{N_r} \quad (4.107)$$

Therefore p_s will be given by

$$p_s = \left(\theta_{N_r}^{N_r} \right)^{1/N_r} \tag{4.108}$$
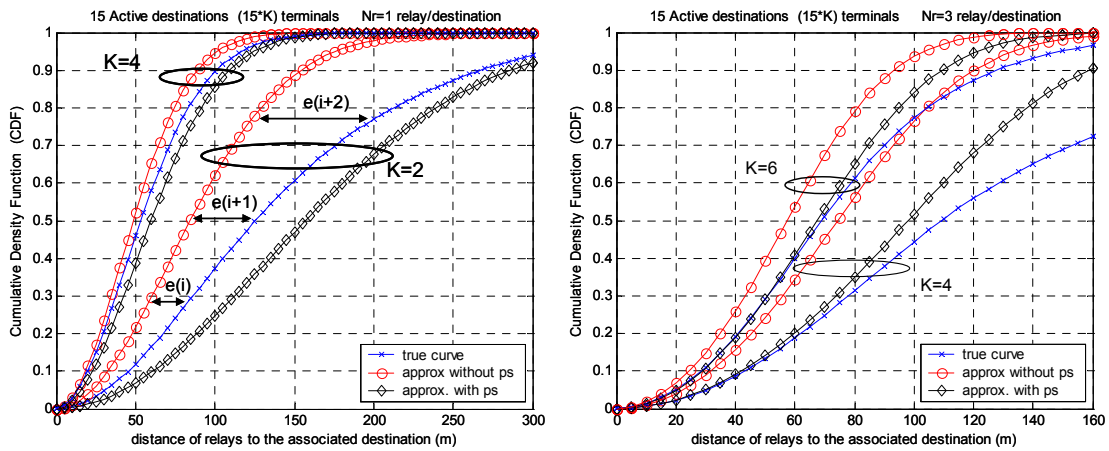
Figure 4.30.- CDF of the distance of the N_r=1 (left) and N_r=3(right) nearest relays taking into account the results obtained experimentally (cross), if the effect of a nearest terminal selected by other destination is not considered (circle) and binomial approximation (4.60) (diamond) (p_s given by (4.108)). There are 15 active destinations and terminals: 30 (K=2), 60(K=4) and 90(K=6).
$$K = N/N_u .$$
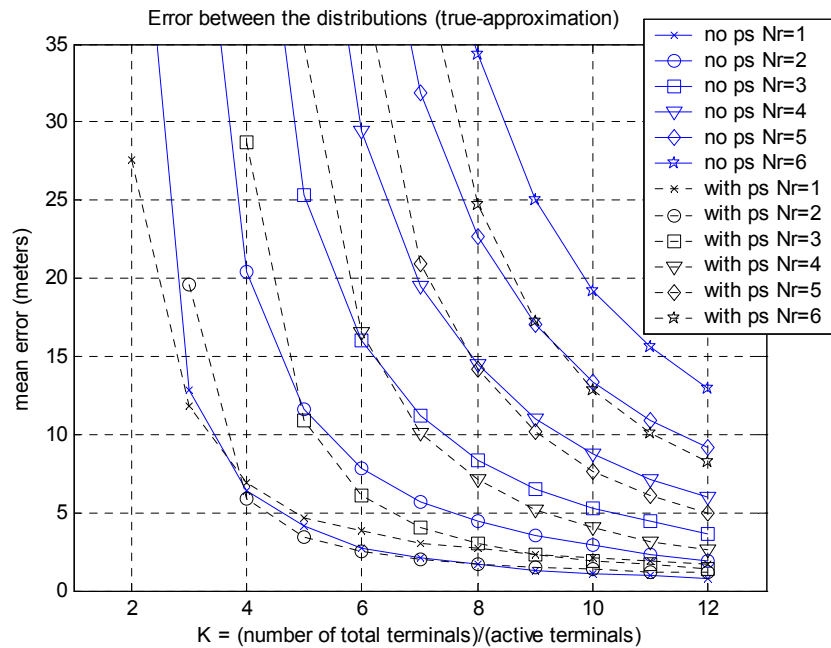
Figure 4.31.- Mean Error between the different approximations and the join CDF of the assisting relays. See Figure 4.30 for graphical example of how is defined the error, e(i), between two CDF.

Figure 4.30 presents the performance when there are N_u=15 destinations and each one looks for the N_r=1 (Figure 4.30-left) and N_r=3 nearest terminals (Figure 4.30-right) as assisting relays. It has been considered different number of terminals in the cell. For example, Figure 4.30-left shows that when there are N_{tot}=30 terminals, the obtained cumulative density function (*cdf*) of the distance between the relays to the associated destination is closer to true curve than not using it. On the contrary, when there are N=60 terminals in the cell, results with and without the approximation are close to the true performance. In Figure 4.30-right the results provided by the

approximation are always better than not using it. Consequently, in order to measure the *distance* of the approximation to the true performance, Figure 4.31 presents the mean error between the CDFs. This error has been measured for the same CDF-value of the different curves (see for example Figure 4.30-left).

Finally, Figure 4.32 depicts the success probability, (4.108) , for different terminals on the cell (N_{tot}) with different values of active destinations (N_u) searching for N_r assisting relays. The total number of terminals and the active destinations satisfy the following ratio $K = N/N_u$.
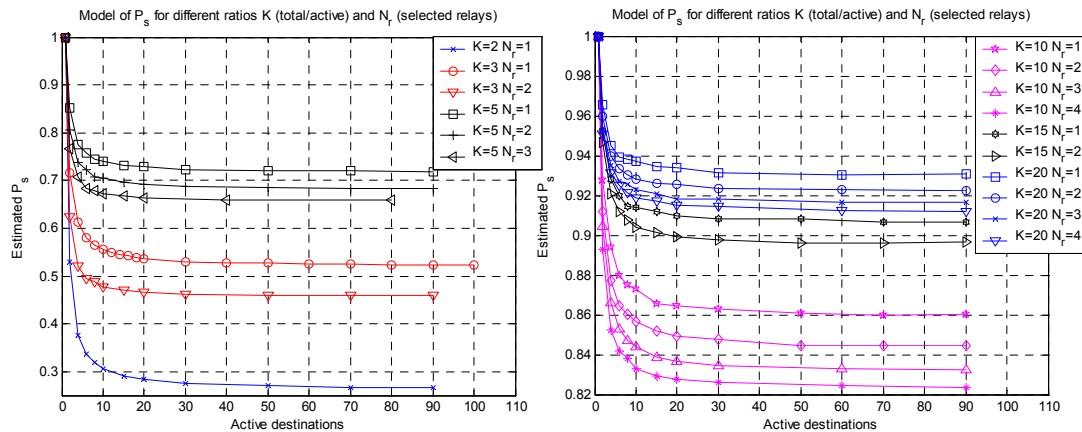
Figure 4.32.- Estimated p_s for different number of active destinations (N_u) with different number of total users (N) and selecting N_r relays. The following ratio is considered $K = N/N_u$.

Indeed, from the curves presented in Figure 4.32 we can give the following expression for the success probability, p_s, obtained by a curve fitting process based on least squares,

$$\hat{p}_s\left(N_u, K, N_r\right) = \left(1 - b\left(K, N_r\right)\right)\exp\left(-1.3203\left(N_u\right)^{\frac{1}{3}}\right) + b\left(K, N_r\right)$$

with

$$K = \frac{N_{tot}}{N_u} \quad b\left(K, N_r\right) = \left(\frac{0.998K^2 + 17.76K - 29.06}{K^2 + 19.09K - 2.055}\right) + \left(\frac{-0.1198K + 0.3116}{K^2 - 3.335K + 1.741}\right)\left(N_r - 1\right)$$

(4.109)

In conclusion, the event that the N_r-th nearest terminal has been selected by other destination, can be seen as reduction of the total idle terminal density (λ_t) by p_s, which is given by (4.109), and the resulting terminal density is also *Poisson* distributed. Although the approximation method is quite simple, (4.108), the obtained error is smaller that not using any one and enough for this work (Figure 4.31). If a better precision is required the estimation process could be enhanced.

4.11 Appendix D. Interference power model when there are multiple assisting relays per destination

This appendix derives the characteristic function of the interfering power received at each destination when there are multiple assisting relays. The steps are quite similar to the derivation of characteristic function for N_r=1 assisting relay done in Appendix B (see also section 4.5.2). However now the distance distribution between the assisting relays and destination is given by

$$f_{N_r}(r) = \frac{2\exp\left(-\lambda_{relay}\pi r^2\right)}{N_r}\sum_{x=1}^{N_r}\frac{\left(\lambda_{relay}\pi\right)^x}{(x-1)!}r^{(2x-1)} \tag{4.110}$$

In Appendix B it has been shown that the characteristic function of the interfering power Y can be defined as,

$$\phi_Y(\omega) = \lim_{a\to\infty}\phi_{Y_a}(\omega) = \lim_{a\to\infty}\exp\left(\int_0^\infty \lambda_{active}\pi a^2\left(A(K_i)+B(K_i)-1\right)f_{K_i}(K_i)dK_i\right) \tag{4.111}$$

where A and B factors are defined with the following equations,

$$A(K_i) = \int_0^\Delta f_r(r)dr\int_0^\infty \exp\left(j\omega\eta_1(K_i,r_i,r)\right)f_{r_i}(r_i)dr_i =$$

$$= \int_0^\Delta f_r(r)dr\int_0^\infty \exp\left(j\omega\eta_2(K_i,r_i)\beta r^\gamma\right)f_{r_i}(r_i)dr_i \tag{4.112}$$

$$B(K_i) = \int_\Delta^\infty f_r(r)dr\int_0^a \exp\left(j\omega\eta_2(K_i,r_i)\right)f_{r_i}(r_i)dr_i$$

with η_1, η_2 defined in (4.77), f_{r_i} the distance distribution of the interfering relays defined in (4.79) and defined in $(0,a)$ and β defined in (4.85). Additionally, now $f_r(r) = f_{N_r}(r)$ defined in (4.110). Therefore both factors can be written as,

$$A(K_i) = \frac{1}{N_r}\sum_{n=0}^{N_r}A_n = \frac{1}{N_r}\sum_{n=1}^{N_r}\int_0^\Delta p_n(r)dr\int_0^a \exp\left(j\omega\eta_2(K_i,r_i)\beta r^\gamma\right)\frac{2r_i}{a^2}dr_i \tag{4.113}$$

$$B(K_i) = \frac{1}{N_r}\sum_{n=0}^{N_r}B_n = \frac{1}{N_r}\sum_{n=1}^{N_r}\int_\Delta^\infty p_n(r)dr\int_0^a \exp\left(i\omega\eta_2(K_i,r_i,r)\right)\frac{2r_i}{a^2}dr_i \tag{4.114}$$

$$p_n(r) = \frac{2}{(n-1)!}\left(\lambda_{relays}\pi\right)^n r^{2n-1}\exp\left(-\lambda_{relays}\pi r^2\right) \tag{4.115}$$

Noticing that the integral of the second factor of (4.113) is the same as in (4.83). Therefore the equations used in (4.86)-(4.87) also are valid here to write the term A_n as,

$$A_n = \int_0^\Delta X(K_i)p_n(r)dr = \Psi_A + \Omega_n + \frac{T_A(K_i)}{a^2}\Phi_n = \Psi_A + \Omega_n + \frac{T_B(K_i)\beta^{2/\gamma}}{a^2}\Phi_n$$

$$\Psi_A = \left(\frac{1}{a^2}r_i^2\exp\left(j\omega\eta_2(K_i,r_i)\beta r^\gamma\right)\Big|_0^a - 1\right)\Omega_n \tag{4.116}$$

$$\Omega_n = 1 - \frac{\Gamma\left(n,\Delta^2\lambda_{relay}\pi\right)}{\Gamma(n)} \qquad \Phi_n = \frac{\Gamma(n+1)-\Gamma\left(n+1,\Delta^2\lambda_{relay}\pi\right)}{\lambda_{relay}\pi(n-1)!}$$

where $X(K_i)$ is defined in (4.86) and $T_A(K_i)$ and $T_B(K_i)$ are defined in (4.87) and (4.89), respectively. Repeating a similar procedure for the factor B_n, (4.114),

$$B_n = \Psi_B + (1 - \Omega_n)\left(1 + \frac{T_B(K_i)}{a^2}\right) \qquad \Psi_B = \frac{1 - \Omega_n}{a^2}\left(r_i^2 \exp\left(j\omega\eta_2(K_i, r_i)\right)\Big|_0^a - 1\right) \qquad (4.117)$$

where $T_B(K_i)$ is defined in (4.89).

Moreover, taking into account that the terms Ψ_A and Ψ_B can be neglected following the same arguments as in equation (4.91). Hence, the following term can be defined,

$$\Pi(K_i) = \lim_{a \to \infty} \lambda_{active} \pi a^2 \left(A(K_i) + B(K_i) - 1\right) = \frac{\lambda_{active} \pi T_B(K_i)}{N_r}\sum_{n=0}^{N_r}(1 - \Omega_n) + \beta^{2/\gamma}\Phi_n \qquad (4.118)$$

Therefore, equation (4.111) can be written as,

$$\phi_Y(\omega) = \exp\left(\int_0^\infty \Pi(K_i) f_{K_i}(K_i) dK_i\right) = \exp\left(-K\cos\left(\frac{\pi}{2}\alpha\right)\omega^\alpha\left(1 - j\tan\left(\frac{\pi}{2}\alpha\right)\right)\right) \qquad (4.119)$$

with $\alpha = \gamma/2$

$$K = \frac{\lambda_{active}\pi\,\Gamma(1-\alpha)}{N_r}\mu_{K_i,\alpha}\sum_{n=1}^{N_r}\vartheta(n)$$

$$\vartheta(n) = \left(\frac{N_0 SNR}{K_r}\right)^\alpha \frac{\Gamma(n+1) - \Gamma\left(n+1, \lambda_{relay}\pi\Delta^2\right)}{(n-1)!\lambda_{relay}\pi} + \frac{\Gamma\left(n, \lambda_{relay}\pi\Delta^2\right)P_{MAX}^\alpha}{(n-1)!}$$

$$\Gamma(a,z) = \int_z^\infty t^{a-1}\exp(-t)\,dt \quad \Gamma(n+1) = n! \quad \Delta = \left(\frac{K_r P_{MAX}}{\sigma^2 SNR}\right)^{1/\gamma}$$

$$\mu_{K_i,\alpha} = \int_0^\infty K_i^\alpha f_{K_i}(K_i)\,dK_i$$

$$(4.120)$$

The characteristic function belongs to the α-stable distributions where the K factor of the interfering power depends on the α-th moment of the random variable K_i. It can be seen that for $N_r = 1$ equation (4.120) is the same as (4.92).

4.12 References

[1]   B.Rankov, A.Wittneben, "Spectral efficient protocols for half-duplex fading relay channels", *IEEE Journal on Selected Areas in Communications*, vol. 25, no. 2, pp. 379-389, Feb. 2007.

[2]   T.J.Oechtering, H.Boche, "Optimal transmit strategies in multi-antenna bidirectional relaying", in *Proc. 8th IEEE Workshop on Signal Processing Advances in Wireless Communications* (SPAWC-2007), Helsinki, Finland, June 2007.

[3]   H. Holma, A. Toskala, *WCDMA for UMTS : Radio Access for Third Generation Mobile Communications*, John Wiley & Sons, 2004.

[4]   M.Dohler, "Virtual Antenna Arrays", PhD Thesis, King's College London, London, UK, 2003.

[5]   G.Scutari, S.Barbarossa, D.Ludovici, "Cooperation diversity in multihop wireless networks using opportunistic driven multiple access", in *Proc. IEEE 3th Workshop on Signal Processing Advances in Wireless Communications* (SPAWC-2003), Rome, Italy, June 2003.

[6]   A.Agustin, O.Muñoz, J.Vidal, "A game theoretic approach for cooperative MIMO systems with cellular reuse of the relay slot"*, in Proc. IEEE International Conference on Acoustics, Speech and Signal Processing* (ICASSP-2004), Montreal, Canada, May 2004.

[7]   S.Borst, P.Whiting, "The use of Diversity Antennas in High-Speed Wireless Systems: Capacity gains, fairness issues, multi-user scheduling*", Bell Laboratories Technical Memorandum 2001*, Available on: http://mars.bell-labs.com.

[8]   A.Agustin, J.Vidal, "TDMA amplifying and forward cooperation under interference-limited spatial reuse of the relay slot", *in Proc. IEEE International Conference on Acoustics, Speech and Signal Processing* (ICASSP-2006), Toulouse, France, May 2006.

[9]   A.Agustin, J.Vidal, "Amplify-and-forward cooperation under interference-limited spatial reuse of the relay slot", accepted to *IEEE Transactions on Wireless Communications* (TW-Aug-07-0973.R1), December 2007.

[10]   A.Agustin, J.Vidal, "High spectral efficiency of multiple-relays assisted amplify-and-forward cooperative transmissions under spatial reuse", *in Proc. IEEE Vehicular Technology Conference Fall* (VTC-Fall-2007), Baltimore, USA, Sept. 2007.

[11]   R.Haining, *Spatial Data Analysis: Theory and Practice*, Cambridge Press, 2003.

[12]   I.E.Telatar, "Capacity of multi-antenna Gaussian channels", European Trans. on Telecommunications, vol. 10, pp. 585-595, Nov/Dec 1999.

[13]   T.Basar, G.J.Olsder. *Dynamic Noncooperative Game Theory*. SIAMS Classics in Applied Mathematics. Second Edition. 1999.

[14] D.Fudenberg, J.Tirole, *Game Theory*, MIT Press, Cambridge, MA, 1992.

[15] A.B.MacKenzie, S.B.Wicker, "Game theory in communications: Motivation, explanation and application to power control", *in Proc. IEEE Global Communications Conference* (GLOBECOM-2001), San Antonio, TX, USA, Nov. 2001.

[16] J.B.Rosen, "Existence and uniqueness of equilibrium points for concave n-person games", Econometrica, vol. 33, no. 3, pp. 520-534, July 1965.

[17] R.D.Yates, "A framework for uplink power control in cellular radio systems", *IEEE Journal on Selected Areas in Communications*, vol. 13, no.7, pp.1341-1348, Sept. 1995.

[18] D.Monderer and L.S.Shapley, "Potential games", *Games and Economics Behaviour*, vol. 14, pp. 124-143, 1996.

[19] G.Scutari, S.Barbarossa, D.P.Palomar, "Potential games: A framework for vector power control problems with coupled constraints", *in Proc. IEEE International Conference on Acoustics, Speech and Signal Processing* (ICASSP-2006), Toulouse, France, May 2006.

[20] C.U.Saraydar, N.B.Mandayam, D.J.Goodman, "Efficient power control via pricing in wireless data networks", *IEEE Transactions on Communications*, vol. 50, no. 2, pp. 291-303, Feb. 2002.

[21] G. Debreu, "A Social Equilibrium Existence Theorem*", in Proceedings of the National Academy of Sciences*, pp. 886-893, 1952.

[22] M.J. Osborne, *Mathematical methods for economic theory: a tutorial*, 1997-2007. Available online: http://www.economics.utoronto.ca/osborne/MathTutorial/

[23] E.Sousa, J.Silvester, "Optimum transmission ranges in a direct sequence spread spectrum multihop packet radio network", *IEEE Journal on Selected Areas in Communications*, vol. 8, no. 5, pp.762-771, June 1990.

[24] M.Shao, C.L.Nikias, "Signal Processing with Fractional Lower Order Moments: Stable Processes and their applications", *in Proc. of the IEEE*, vol. 81, no. 7, pp. 986-1010, July 1993.

[25] D.J.Love, "Duplex Distortion Models for Limited Feedback MIMO communications", *IEEE Trans. on Signal Processing*, vol. 54, no. 2, pp. 766-774, Feb. 2006.

[26] Burke, Zeidler, "CDMA reverse link spatial combining gains: optimal vs. MRC in a faded voice-data system having a single dominant high data user", *in Proc. IEEE Global Communications Conference* (GLOBECOM-2001), San Antonio, TX, USA, Nov. 2001.

[27] "A comparative analysis of Mobile WIMAX Deployment alternative in the access networks", Wimax Forum website May 2007.

[28] I.Hammerström, M.Kuhn, A.Wittneben, "Cooperative diversity by relay phase rotations in block fading environments", *in Proc. IEEE Workshop on Signal Processing Advances in Wireless Communications* (SPAWC-2004), Lisbon, Portugal, July 2004.

[29] K.Azarian, H.El Gamal, P.Schniter, "On the achievable diversity-multiplexing tradeoff in half-duplex cooperative channels", *IEEE Trans. on Information Theory*, vol. 51, no.12, pp. 4152-4172, Dec. 2005.

[30] S.Yang, J.C.Belfiore, "On slotted amplify-and-forward cooperative diversity schemes", *in Proc. IEEE International Symposium on Information Theory,* (ISIT-2006), Seattle, USA, July 2006.

[31] N.A.C.Cressie, *Statistics for Spatial Data*, New York. John Wiley and Sons, 1993.

[32] J.Proakis, *Digital Communications.* New York: Mc-Graw Hill, 3rd edition, 1995.

[33] J.Vidal, S.Barbarossa, A.Agustin, Document IEEE 802.11-00/797r0 presented at the Wireless Next Generation Standing Committee de IEEE 802.11 about Cooperative Transmission, as a result of the research done in the ROMANTIK project, Portland, USA, July 13, 2004.

[34] P.Viswanath, D.N.C.Tse, R.Laroia, "Opportunistic beamforming using dumb antennas", *in IEEE Trans. on Information Theory*, vol.48, no.6, pp. 1277-1294, June 2002.

[35] D.N.C.Tse, P.Viswanath, L.Zheng, "Diversity-multiplexing tradeoff in multiple access channels", *in IEEE Trans. on Information Theory*, vol.50, no.9, pp. 1859-1874, Sept. 2004.

[36] M.Kobayashi, G.Caire, D.Gesbert, "Antenna diversity versus multiuser diversity: quantifying the tradeoffs", i*n Proc. of Wireless World Research Forum*, WWRF11 meeting, Oslo, June 2004.

[37] Kobayashi, G.Caire, D.Gesbert, "Antenna diversity versus multiuser diversity: quantifying the tradeoffs*", in Proc. of Int. Symposium on Information Theory and its Applications*, (ISITA-2004), Oct. 2004.

[38] R.Gozali, M.Buehrer, B.D.Woerner, "The impact of multiuser diversity on space-time block coding*", in IEEE Communications Letters*, vol.7, no.5, pp.213-215, May 2003.

[39] T.A. ElBatt, A.Ephremides, "Joint scheduling and power control for wireless adhoc networks", *in IEEE Trans. on Wireless Communications*, vol.3, no.1, pp.74-85, January 2004.

[40] M.Madueño, J.Vidal, "Joint physical-MAC layer design of the broadcast channel protocol in adhoc networks", *in IEEE Journal Selected Areas in Communications*, Special Issue on AdHoc Networking, vol.23, no.1, pp.65-75, January 2005.

[41] Z.Wang, E.Tameh, A.Nix, "Last mile channel models for multi-hop relaying in the 2 GHz and 5 GHz Band", Deliverable D-329, IST-ROMANTIK project. Dec. 2004.

[42] A.Agustin, J.Vidal, O.Muñoz, "Multi-user diversity in the cooperative transmissions", in *Proc. of IST Mobile and Wireless Communications Summit*, (IST-2005), Dresden, Germany, June 2005.

[43] A.Agustin et al, "Selection of cooperative techniques for the MAC layer", Deliverable D531-IST-2001-32549 Romantik. May 2005. Available on: www.ist-romantik.org.

Chapter 5

Dynamic Link Control

THE final benefits of the relay-assisted transmission reported in previous chapters depend greatly on the actual communication system design. The relay-assisted transmission can be seen as a *virtual* MIMO system with *distributed* antennas, therefore many techniques used for MIMO systems can be adopted for the relay-assisted transmission, although they should be re-defined to the new scenario due to the presence of assisting relays. The system design depends on the type and accuracy of channel state knowledge available at the transmitter or at the source for the relay-assisted transmission. If the transmitter has *statistical information about the channel model* (e.g. the average capacity), the relay-assisted transmission will suffer outage events when the selected data rate is not supported by the channel realization. In such a case, automatic repeat request (ARQ) protocols are able to deal with those events by retransmitting the message when it is wrongly received. The system design involves the definition of the type of retransmission when a packet is wrongly decoded at the destination/relay, the error correcting scheme, decoding mode at the relay (*amplify-and-forward* or *decode-and-forward*) and distributed space time codes to be used. Likewise, the type of receivers used at the terminals (*linear* or *near-optimum*) is also important.

On the other hand, if the transmitter has *actual information about the current channel state* it can design the data rate adapted to each channel realization. The errors of the transmission are usually due to the thermal noise. This type of channel knowledge has been investigated under a frequency selective channel using a *multi-carrier transmission* scheme. The Exponential-Effective SIR Mapping (Exp-ESM) method is able to provide the *effective SNR*, which describes the link quality and is able to provide an error prediction for a forward error correction (FEC) code. The modulation and coding scheme (MCS) can be selected according to that parameter. The Exp-ESM has been applied to the relay-assisted transmission and expressions for the error prediction for relaying systems are obtained. With those expressions, the MCS for the relay-assisted transmission can be designed for different types of services as the result of an optimization problem.

5.1   Introduction

Relay-assisted transmission has shown in previous chapters its capability to provide capacity gains by using an additional terminal as a *distributed* antenna for combating the channel impairments. In fact, the relay-assisted transmission can be seen as a *virtual* MIMO system [13],[14],[15]. In this regard, MIMO systems without channel state information (CSI) at the transmitter (CSIT) have been shown to provide achievable rates that scale linearly with the

minimum number of transmitting and receiving antennas [5],[6] for systems with uncorrelated channel coefficients at high SNR. Beyond MIMO systems, half-duplex relay-assisted transmissions are able to deal with shadowing, transmitting antenna correlation and pathloss attenuation, but at the expenses of an increased use of channel resources.

The transmission strategy in a MIMO system depends on the type and accuracy of knowledge about the current channel available at the transmitter, [8]. Figure 5.1 depicts an example of MIMO channel transmission where the receiver has perfect channel state information (CSIR) while the channel state information at the transmitter (CSIT)[1] is provided through a feedback link from the receiver. Depending on this knowledge the transmitter allocates the optimal power through the transmitting antennas (by means of the transmit covariance matrix) and selects the bit rate of the transmission.
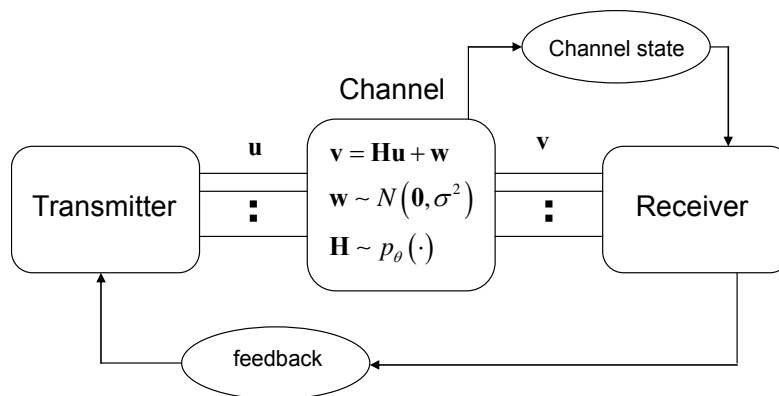
Figure 5.1.- MIMO channel.

In this work it will be assumed that the receiver always has a perfect CSIR. We classify the knowledge of the channel at the transmitter between *actual information about the current channel state* and *statistical information about the channel model*:

- **Actual information about the current channel state.** It corresponds to the case where the knowledge is about the current channel coefficients. There are several cases motivated by the imprecise channel estimation and the limited bandwidth allocated to the feedback channel:

  o *Perfect* CSIT. Exact knowledge of the channel coefficients is available. The fading channel changes slowly enough to be reliably measured by the receiver and feedback to the transmitter without significant delay. The transmitter designs the transmit covariance matrix by using statistics in a Bayesian framework, [9].

  o *Imperfect* CSIT. There is just an imperfect knowledge of the channel coefficients, commonly due to the noisy estimations and/or delays in the feedback link. In this case it is possible design of the transmit covariance matrix.

  o *Partial* CSIT. The transmitter does not know the channel coefficients but has information about some parameters of the link, for example the instantaneous

---

[1] The CSIT of each link also can be obtained by *reciprocity principle* when the transmissions are done in time division duplexing and previously, the receiver has sent a message to the transmitter.

SNR or the instantaneous capacity (assuming equal power distribution among the transmitting antennas). In such a case the error event in the transmission is dominated by the *thermal noise* present in the communication. It is motivated by the insufficient feedback bandwidth (which implies the transmission of a quantized version of the channel). It implies that the transmitter will allocate power uniformly (equal average power) through the antennas (*no CSIT*) [5][6]. The channel knowledge allows selecting the proper modulation and coding (FEC and space-time coding) scheme based on the current channel state.
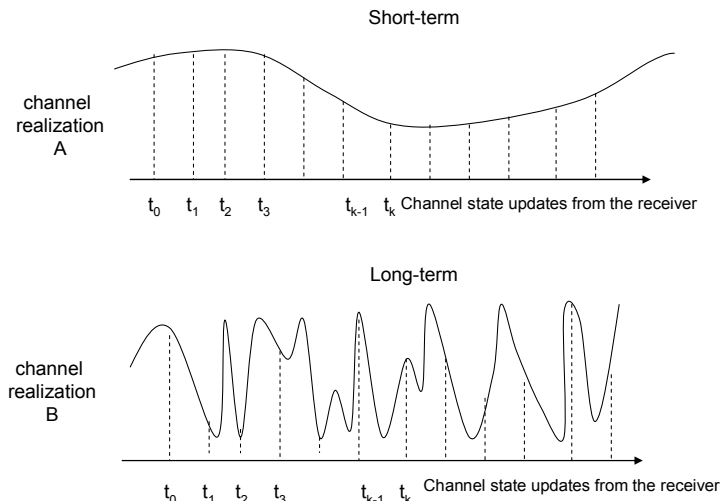
Figure 5.2.- Channel updates under short-term CDIT (top) and long-term CDIT (bottom). The variance of the error of the estimated CSI is smaller under short-term than for the long-term. In both cases the error event in the transmission is dominated by the outage probability due to the fading channel.

- **Statistical information about the channel state.** In this case the transmitter knows some Channel Distribution Information (CDI) feedback from the receiver (parameter θ shown in Figure 5.1). Depending on the scale of interest there are two types of models:

  o *Short-term* CDIT (CDI at Transmitter). When there are frequent updates of the CSI or the channel changes low enough, the transmitter can adapt its strategy to these short-term channel statistics, in such a case the variance of the error of the estimated CSI could be small[2]. See for example Figure 5.2-top, where the transmitter uses the CSI known at time t_{k-1} for transmitting at time t_k. The channel coefficients may have nonzero mean and a set of correlations reflecting the particular propagation environment. Sometimes it is referred to by many names including *mean* and *covariance feedback* or imperfect feedback [8]. The transmitter designs the transmit covariance matrix based on the known statistics.

  o *Long-term* CDIT. The channel variation is faster than the latency of the feedback channel, so the transmitter does not have any information about the current channel and the variance of the error of the estimated CSI is large. This situation is illustrated in Figure 5.2-bottom where the CSI known at time t_{k-1} is not longer valid in time t_k. A common assumption adopted is uncorrelated zero-

---

[2] Under the following notation short-term CDIT and partial CSIT coincides when the variance of the error of the estimated CSI is very small.

mean channel coefficients (Zero Mean Spatially White (ZMSW)). The receiver informs about the average capacity which define the rate that can be achieved by averaging all channel states. If the transmitter sends a rate that cannot be supported there is an outage event. When there is channel uncertainty (*no CSIT*) under ZMSW model, the transmitter transmits uniformly through all the antennas [5][6].

In the previous definition, we have abused the notation *no CSIT* for defining the cases where the transmitter transmits uniformly (equal average power) through all the antennas due to the uncertainty of the channel coefficients, see Figure 5.3. However, the selected data rate under *partial* CSIT or *long-term* CDIT will be different. For example, under *partial* CSIT some properties of the current channel are known so the rate selection will be done according to that knowledge. Under the *long-term* CDIT, the selected rate is based on the average channel state, so an outage is possible when the data rate is not supported by the current channel realization. Otherwise, under *perfect* CSIT, *imperfect* CSIT and *short-term* CSIT, the transmitter designs the transmit covariance matrix as a function of the type of knowledge over the channel coefficients along with the MCS.
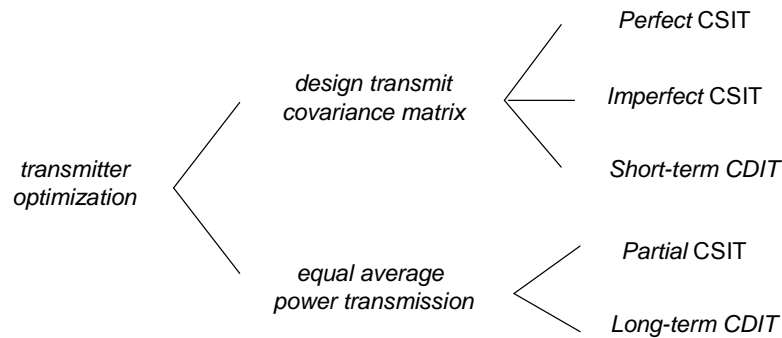
Figure 5.3.- Power transmitter optimization as a function of the channel state information.

The work presented in this chapter tackles the transmission strategy for both types of knowledge of the channel at the transmitter: *Actual information about the current channel state* and *statistical information about the channel state*. In our system it is assumed that the transmitter does not have any knowledge about the current channel coefficients (*no CSIT*), so that it transmits uniformly through all the antennas [5][6]. In such a case, the space-time codes (STC) are adopted to transmit the message through all the antennas. The transmission strategy will design the data rate (modulation and coding scheme) under *partial* CSIT and *long-term* CDIT. In this later case, the selected data rate might produce outage events at the receiver because the information is wrongly received. The automatic repeat request (ARQ and HARQ) protocols [31][32] help to combat those outage events by retransmitting the information.

The system design for the relay-assisted transmission will be based on the adaptation of the existing methods for MIMO systems because it can be seen as a distributed MIMO system. In the following the principal aspects to be considered in order to achieve or get near of the theoretical capacity of the system are given,

- *Distributed space-time codes* (DSTC)
- *Modulation and coding*
- *Automatic repeat request* (ARQ) *protocols*
- *Link error prediction methods for multi-carrier systems*

Distributed space time coding

The capacity gains predicted by [5][6] for MIMO channels depend on the CSI (and channel distribution information CDI) at the transmitter and/or at the receiver (i.e. [8] and references therein). In case of CSI only at the receiver, [5] shows that the best strategy that maximizes the ergodic capacity is achieved by dividing the transmit power equally among all the antennas. In this regard several orthogonal space-time codes (STC) are proposed in [10] and [18] in order to achieve the *diversity gain*. On the other hand, [11] presents a STC for achieving the *multiplexing gain*. Likewise, [43] presents a set of STCs (named Linear Dispersion Codes – LDC) able to get the *multiplexing*/*diversity gain,* handling any configuration of transmitting and receiving antennas. The codes are designed to optimize the mutual information between the transmitted and received signals. The scheme transmits data in linear combinations over space and time and subsumes the VBLAST (Vertical Bell Laboratories Space Time) code and orthogonal STCs.

However, in relay-assisted transmission there is not *multiplexing gain* when each terminal features a single antenna [7] but it has observed an *additive capacity gain* [12] (also studied in chapter 2). Furthermore, the encoding process at the source/relay should consider the distributed antennas of the whole system. When CSI is not available at the transmitting nodes the *distributed* space-time coding can be considered. The *diversity-multiplexing* tradeoff of DSTC is analyzed in [16] for relay-assisted transmission under protocol I (defined in section 2.2.1 of chapter 2). Moreover, the *diversity gain* in a relay-assisted system using protocol I is studied in [17], where there are one source and two single-antenna relays transmitting with the Alamouti ([18]) space-time code, providing approximate formulas of the average symbol error probability (ASEP) at the destination.

The major difference between DSTC and conventional STC performance consists in the decision errors at the relay node for *decode-and-forward* protocols. In the former case the conventional structure of the maximum likelihood (ML) has to be modified in order to introduce the vector error probabilities obtained at the assisting relay terminal [19], [20]. The optimal ML detector is derived for the BPSK transmission in [19]. An extension to the general multi-hop network is considered in [13][14], where throughput maximizing resource allocation strategies are derived when the system detects erroneous packets in each state (group of receiving relays which are in the same hop).

Modulation and coding

Forward error correction (FEC) codes have been considered for achieving the capacity in flat fading channels, see [21]. Mainly, in the low signal to noise ratio (SNR) regime binary codes are nearly optimal. Nevertheless, in middle and high SNR the constellation shaping is required. Currently, the re-discovery of low density parity check (LDPC) codes [24] and the invention of turbo codes (TC) [22],[23] provide results close to the capacity. In this later case, there are two possible implementations: *parallel* and *duo-binary-serial* (or convolutional turbo codes (CTC)), described in sections 5.2.1.2 and 5.3.1.1, respectively. The benefits obtained by the *duo-binary-serial* TC are better than with *binary* TC counterpart, see for example [25] and references therein. Additionally, the CTC have been adopted for the Digital Video Broadcasting (DVB) and the IEEE 802.16e[3] standard [26].

ARQ protocols

Communications in wireless channels are designed to be highly reliable. However when there is only *long-term* CDIT (*statistical information about the channel state*), the selected data rate

---

[3] CTC are defined as *optional* in the IEEE 802.16e standard.

might produce outage events with a negative impact on the *throughput* of the system (defined as the average information bits transmitted over an interval of time). The *throughput* can be improved by allowing a notification from the receiver about the successful or unsuccessful of the received message. This scheme is named automatic repeat request (ARQ) protocol [31],[32]. There are three basic request modes: *stop and wait* (SW-ARQ), *go back N* (GBN-ARQ) and *selective-repeat* (SR-ARQ). The SW-ARQ is the simplest one, where the transmitter sends a single packet and waits for the acknowledgment (ACK) in an idle state. Nevertheless, this mode has the worst *throughput* performance because during the idle state the transmitter does not transmit anything. GBN-ARQ assumes that the transmitter is capable of buffering *N* packets. When the transmitter is informed of an error in some packet, then the transmitter *goes back* to that packet and re-starts the transmission in that point. In this case the transmitter is always transmitting. Finally, the best scheme is the SR-ARQ because the transmitter only retransmits the specific packet for which the ACK is not received. Here the transmitter is also continuously transmitting and requires significant buffering in both the transmitter and the receiver.

Conventional ARQ protocols can be divided into two classes, pure ARQ and Hybrid ARQ protocols [31] depending on which information is retransmitted and how it is processed at the receiver. If a packet is wrongly decoded using pure ARQ, the received packet is discarded, a new transmission is performed and the decoder only considers the last received packet. In this work we define HARQ protocol when exist a combination between all the received packets. We define HARQ I (also named *chase combining*) if the packets are coherently combined. Furthermore, if the new transmissions are performed using different parts of the same codeword, the strategy is named H-ARQ II (also named *code combining*). In such a case, the codeword rate is decreased in each transmission, increasing the protection or *coding gain*. For instance, this can be done by using rate compatible punctured TC (RCPTC) with different orthogonal puncturing matrices. The benefits of the last protocol over the Pure ARQ, HARQ I and without retransmissions (only using FEC codes) over fading channels are shown in [33] and [34]. HARQ II can be considered as adaptive FEC that adapts to the instantaneous channel conditions thanks to the acknowledgment of the receiver.

Link error prediction methods

In multi-carrier systems, as OFDM/OFDMA in IEEE 802.16 standard [26], the transmission is done through several carriers. Because of the channel variation in the frequency domain it is desirable to have a predictor to model the coded OFDMA performance in terms of packet error rate (PER). The predictor based on the average SNR in single-carrier systems is no longer valid because two links with the same frequency average SNR may present different instantaneous PER values. This predictor can be also used in OFDMA system-level simulators to speed up the simulation time and/or for systems based on adaptive modulation/coding (AMC) when the transmitter has *partial* CSIT. In this later case, the predicted PER will be useful to select the suitable modulation and coding scheme (MCS). A similar situation comes up in MIMO architectures, where there are multiple parallel channels thanks to the multiple antennas.

Among all possible predictors those which are valid for a wide range of channel types are the most desirable because the calibration of the predictor is avoided. In [35] it is presented two prediction methods for multi-carrier communication schemes, the *PER-Indicator method* and the *Exponential-ESM* (Exp-ESM). Both predictors compare the estimated performance under the coded OFDMA transmission in the current channel conditions with the PER obtained in AWGN channel by the FEC code selected (in the following it will be called the reference curve). Basically, the *PER-Indicator* method assumes that all PER curves obtained for different channel conditions are nearly parallel. Therefore, there is a shift in terms of SNR between the current

performance and the reference curve. This predictor computes an *indicator* which is correlated with distance between the current and the reference PER curves. The second method is the Exp-ESM [36]. It computes an instantaneous effective SNR which depends on all SNR measured in the different carriers used by the OFDMA transmission.

Similar to the Exp-ESM predictor, [37] also describes other predictors as the *capacity effective SNIR* (CESM) and *logarithmic effective SINR* mapping (LESM) which use a compression function for mapping the received SNR vector to a single SNR value. In CESM the mutual information function is used where in the LESM the logarithm is considered. On the other hand, another predictor is described, the *mutual information effective SINR mapping* (MIESM) where the Bit-Interleaved Coded Modulation (BICM) capacity expression is considered. Results presented in [37] show that MIESM obtains the best performance closely followed by Exp-ESM. The Exp-ESM is adapted to MIMO architectures with space-time coding and zero-forcing (ZF) or minimum mean square error (MMSE) receivers at the destination in [38]. Additionally, this predictor should be modified in order to consider the effect of a retransmissions of a packet (*chase combining* or *incremental redundancy*), [39].

Organization of the chapter

All this aspects have to be reviewed for the relay-assisted transmission considering the half-duplex protocols (section 2.3 in chapter 2) and the strategy at the relay terminal (*amplify-and-forward*, *decode-and-forward*, persistent transmission, selective or incremental relaying, see section 2.1.3 in chapter 2). Among the plethora of possibilities in the system design, we have investigated the coded relay-assisted transmission from the following perspectives:

- **Statistical information about the channel (*long-term* CDIT) in section 5.2.** Because there is only a statistical knowledge of the channel, the Hybrid turbo FEC/ARQ protocol will be adopted to deal with the outage events produced by a data rate selection based on statistical knowledge. The receiver will request for a retransmission of the message when the channel realization does not support that selected rate. The scenario considered to evaluate this transmission strategy assumes a *single-carrier* system under the relay-assisted protocol I with *static resource allocation relaying* where *relay-receive* and *relay-transmit* phase present the same size. This type of scenario is similar to that one assumed in chapter 4.

- **Actual information about the current channel state (*partial* CSIT) in section 5.3.** The transmitter can design its data rate as a function of the current channel state. It is assumed that there is some parsimonious representation to describe the link quality. In this regard, when transmissions are done through multiple carriers, the Exp-ESM method is considered. That method provides an *effective SNR* as a function of the instantaneous SNR of all data carriers. The PER (Packet Error Rate) for a given MCS can be estimated from the effective SNR. Moreover, if the transmitter knows this parameter, it could design the suitable MCS for that channel realization.

Both perspectives have been presented in [1]-[4] and [52], respectively. Section 5.2 describes how the ARQ protocols can be used for the relay-assisted transmission, investigating the length of retransmissions, the space-time codes selected at the source and relay and the type of the receivers. Afterwards, section 5.3 derives the PER expressions to be used by the relay-assisted transmission in a multi-carrier system as a function of the *effective SNR* for a given MCS. When the transmitter knows the link quality, it can use those estimated error expressions for selecting the MCS under each protocol in order to guarantee a total PER or maximize the throughput.

5.2   Transmission strategy under *long-term* CDIT

It is assumed that the data rate is selected according to some statistical knowledge of the channel model, therefore for a given channel realization, that selected rate might produce an outage event at the receiver. The use of ARQ protocols are considered to avoid or minimize the impact of that outage event over the total *throughput* of the system. In this section, the utilization of hybrid retransmission in combination with FEC codes using DSTC will be developed for relay-assisted transmission using protocol I (see section 2.3) in a centralized TDMA system with a single source and multiple destinations. The transmission mode is *single-carrier*. With protocol I, the source transmits to the destination and its associated relay in one time slot (*relay-receive phase*) or downlink slot and the assisting relay transmits to the destination in other time slot (*relay-transmit phase*) or relay slot. Moreover, in order to improve the spectral efficiency it has been assumed that the time slot devoted for the *relay-transmit phase* will be spatially reused by all the relays associated to the destinations served in the same frame, similarly to the scenario detailed in chapter 4. Figure 5.4 shows an example of this type of communication. The size of the *relay-receive* and the *relay-transmit phase* is equal and fixed.

Results will be obtained assuming that in the same time frame there are many destinations to be served and the interference generated during the *relay-transmit* phase (relay slot) is negligible. These assumptions allow obtaining results for the single-user case, but those results should be scaled by $K/(K+1)$ with K the number of destinations (in Figure 5.4 $K=2$). It is worth noticing that there is always one time slot in the TDMA frame devoted for relay transmissions.

| $S \rightarrow \{D_1, RS_1\}$ | $S \rightarrow \{D_2, RS_2\}$ | $\{RS_1 \rightarrow D_1\}\{RS_2 \rightarrow D_2\}$ |
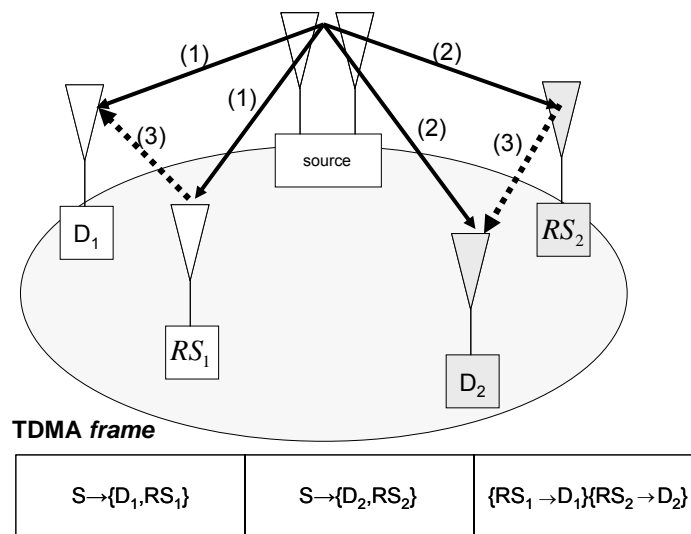
Figure 5.4.- Relay-assisted transmission for 2 destinations. Solid lines: transmissions during the *relay-receive phase* (in two orthogonal slots). Dashed lines: transmissions in the common *relay-transmit phase.*

5.2.1 Coded relay-assisted transmission

This section describes the different strategies proposed to achieve the capacity gains of the relay-assisted transmission over the direct transmission under TDMA. The relay-assisted transmission is done under *amplify-and-forward* (AF) or *decode-and-forward* (DF). In both cases, different distributed space-time block coding methods may be adopted. Additionally a

brief introduction to the Rate Punctured Turbo-Codes (RCPTC) will be done in section 5.2.1.2, necessary for a better understanding about the structure of the transmitted data, explained in section 5.2.1.3. Finally, section 5.2.1.4 describes the retransmission procedure.

5.2.1.1 Distributed space-time codes

Distributed space-time block codes are based on the space-time block codes applied to *distributed* antennas. We have considered space-time codes based on Linear Dispersion Codes (LDC) [43]. These codes disperse the energy of the transmitted symbols both in the spatial and temporal domain. A LDC builds a block of dimensions $T \times n_s$, $\mathbf{S}$, for each Q_s symbols as follows,

$$\mathbf{S} = \sum_{q=1}^{Q_s} \left(\mathbf{A}_q s_q^R + j\mathbf{B}_q s_q^I \right) \tag{5.1}$$

where s_q^R, s_q^I are the real and imaginary parts of the q-th symbol s and $\{\mathbf{A}_q, \mathbf{B}_q\}$ denote the dispersion matrices (DMs). DMs are a set of $T \times n_s$ matrices, where T is the number of channel uses per block and n_s is the number of transmitting antennas. Formulation of (5.1) also subsumes different space-time techniques as VBLAST and orthogonal codes, see Appendix A (section 5.5). In any case, the symbol rate transmission is $r_{STC} = Q_s/T$ symbols/s/Hz. The relation that allows working with a linear receiver is,

$$Q_s = \min(n_s, n_d) \cdot T \tag{5.2}$$

with n_d being the number of receiving antennas.

The received signal model can be written as,

$$\mathbf{y} = \mathbf{H}_{eq} \mathbf{\Theta} \mathbf{x} + \mathbf{n} \tag{5.3}$$

with the following signal definition,

$$\mathbf{y} = \begin{bmatrix} \mathbf{y}_R \\ \mathbf{y}_I \end{bmatrix} \quad \mathbf{x} = \begin{bmatrix} \mathbf{s}_R \\ \mathbf{s}_I \end{bmatrix} \quad \mathbf{H}_{eq} = \begin{bmatrix} \mathbf{H}_R \otimes \mathbf{I}_T & -\mathbf{H}_I \otimes \mathbf{I}_T \\ \mathbf{H}_I \otimes \mathbf{I}_T & \mathbf{H}_R \otimes \mathbf{I}_T \end{bmatrix} \quad \mathbf{\Theta} = \begin{bmatrix} \tilde{\mathbf{A}}_R & -\tilde{\mathbf{B}}_I \\ \tilde{\mathbf{A}}_I & \tilde{\mathbf{B}}_R \end{bmatrix} \quad \mathbf{n} = \begin{bmatrix} \mathbf{w}_R \\ \mathbf{w}_I \end{bmatrix} \tag{5.4}$$

where sub-indexes R and I stand for the real and imaginary part of a vector or matrix, $\mathbf{y}$ is the receiving data of dimensions ($2Tn_d \times 1$), $\mathbf{x}$ is the transmitted symbols (real and imaginary part) with dimension $2Q_s \times 1$, $\mathbf{H}$ is the current channel matrix of dimensions $n_d \times n_s$, $\mathbf{n}$ is the noise vector, the operator $\otimes$ is the kronecker product and finally,

$$\tilde{\mathbf{A}} = \begin{bmatrix} vec(\mathbf{A}_1) & \ldots & vec(\mathbf{A}_Q) \end{bmatrix} \qquad \tilde{\mathbf{B}} = \begin{bmatrix} vec(\mathbf{B}_1) & \ldots & vec(\mathbf{B}_Q) \end{bmatrix} \tag{5.5}$$

where the $vec()$ operator transforms a matrix of dimensions $n_s \times T$ into a vector of dimensions $n_s T \times 1$ (stacked by columns).

coefficients associated to one
transmitting antenna

$$\mathbf{A}_q = \begin{bmatrix} a_{1,1} & \cdots & a_{1,n_s} & a_{1,(n_s+1)} & \cdots & a_{1,(n_s+n_r)} \\ \vdots & & \vdots & \vdots & & \vdots \\ a_{T,1} & \cdots & a_{T,n_s} & a_{T,(n_s+1)} & \cdots & a_{T,(n_s+n_r)} \end{bmatrix}$$

coefficients associated to n_s coefficients associated to n_r
antennas at source   antennas at relay
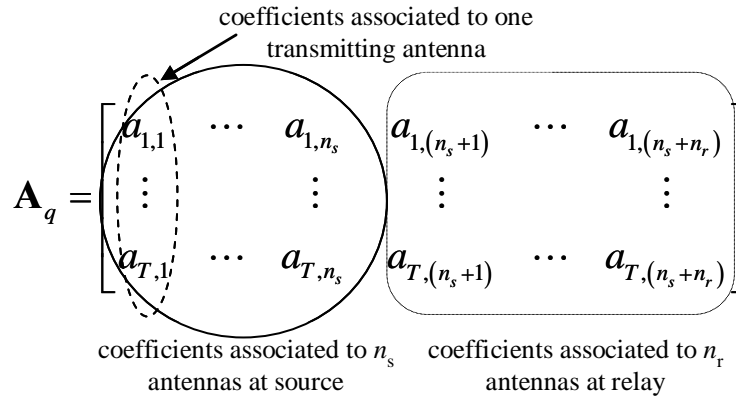
Figure 5.5.- Division of a Space-Time matrix between the source and relay for DF-UC. Some columns are associated to the source (n_s antennas) and others to the relay (n_r antennas).

Moreover, in the relay-assisted transmission where the source and the relay terminal are equipped with n_s and n_r antennas respectively, the *distributed* antennas use different parts of the dispersion matrices as is shown in Figure 5.5. The distributed space-time block coding transmission schemes considered for section 5.2 are detailed below. In each case, the rationale for adoption and the benefits that may be obtained are investigated. In all cases the destination is assumed to use a single antenna (n_d=1, despite of this it is possible to achieve high rate gains thanks to the relay-assisted transmission), while the assisting relay may feature one or two antennas (n_r=1 or 2). The source is equipped with n_s=2 antennas.

Direct transmission (DT)

This is a reference case to which we may compare the performance of the relay-assisted transmission scheme. The relay terminal is not operating and system can be considered as 2×1 MIMO system. All the destinations served in the same frame only use 1 time slot. For this case, the Alamouti STC [18] (1 symbol/channel use) is adopted.

Relay amplify-and-forward (relay-AF)

In the relay slot the relay transmits the received signal with an amplifying factor to the destination. The system can be approximated as a 2×2 *virtual* MIMO system using only n_r=1 antenna, (see equations 4.6 and 4.9 in section 4.2 of chapter 4). In order to make good use of the additional *virtual* receiving antenna two different STC are considered which will lead to the different gains provided by the MIMO systems.

- *Diversity gain*. This definition refers to the gain obtained by the relay scheme when the same STC as in the direct transmission is considered. Therefore, Alamouti STC (1 symbol/channel use) is considered.

- *STC rate gain*. In a 2×2 MIMO system the capacity can be achieved by selecting 2 symbols/channel use. In fact, the number of symbols depends on the MIMO configuration, as in equation (5.2). Hence in this case, we select the VBLAST STC (2 symbols/channel use).

For both cases the messages are only encoded at the source, as a conventional MIMO system, and the relay selects the proper amplifying factor for re-transmitting the same received message which includes noise.

Relay decode-and-forward (relay-DF)

Here the relay decodes the received signal, re-encodes the message and retransmits it to the destination. We have considered n_r=2 antennas at the relay (avoiding bad source-relay link quality in symmetric scenarios). The relay-assisted transmission can benefit from the additional *virtual* n_d receiving antennas at the destination and n_r transmitting antennas at the relay terminal. In the same way as in the previous scheme, the diversity and STC rate gain have been looked into,

- *Diversity Gain.* Also the Alamouti STC (code rate is 1 symbol/channel use) has been considered here, as in direct transmission. Additionally, the relay can select from two possible policies (see section 2.1.3):

  a) *Selective relaying.-* The relay transmits only when it decodes correctly the message. Otherwise, neither the relay nor the source transmits in the relay slot. The same approach as in section 2.1.3 cannot be considered here because the relay slot is spatially reused by multiple assisting relays associated to different destinations. If the source transmits for a given destination, it creates a high level of interference to all destinations served in that frame. For that reason the source remains silent in that time slot.

  b) *Persistent transmission.* The relay always retransmit (all bits are retransmitted even if they are decoded in error).

  The relay and source should transmit uncorrelated (and ideally Gaussian) symbols, although related to the same message, in order to maximize the mutual information see section 2.2.1 in chapter 2. This can be done by means of a convolutional or turbo code [41], [42] where source and relay are transmitting different *parity* data (or *redundancy*) relative to the same codeword. Further on, this process will be explained in more detail.

- *STC rate gain.* A different space-time code is selected due to the *virtual* MIMO configuration. In section 2.2.1 of chapter 2, it was also shown the two different options for the relay-DF with different achievable rates values.

  a) *Repetition Code (RC).* The source and relay transmit the same message using the same STC. In this case the VBLAST STC is considered (*virtual* 2×2 MIMO system).

  b) *Unconstrained Code (UC).* The whole system can be seen as a *virtual* $(n_s+n_r)×2n_d$ system, (see equation 4.10 in section 4.2). In this regard, a STC designed for 4×2 MIMO system has been considered, the Quasi-Orthogonal Design (QOD) codes introduced in [44]. The source uses the part of the STC related to the first n_s antennas and the relay uses the remaining data, see how the dispersion matrices of the STC are divided between distributed antennas in Figure 5.5.

The selected STCs allow a linear decoding of the transmitted symbols. Since the STCs are designed for MIMO systems with two receiving antennas and the destination only has n_d=1 antenna, it needs both transmissions (source to the destination and relay to the destination, therefore, 2 *virtual* receiving antennas) to be able to decode the message. For this reason the assisting relay must transmit the same message as the source, although it can use another part of the dispersion matrix (DM) of the STCs as in the UC, see Figure 5.5. In other words, *persistent transmission* from the relay is mandatory.

Mixed Coding relay DF (mixed relay-DF)

The relay terminal is equipped with n_r=2 antennas. This strategy tries to exploit the *diversity gain*, transmitting uncorrelated symbols from source and relay, and the *STC rate gain*, selecting a linear space-time code with higher code rate (2 symbols/channel use). Assuming that the message in previously encoded by a FEC code, here it is considered that the *systematic* data part of the message uses the VBLAST STC and the *parity* data uses the Alamouti STC. With this configuration the destination can linearly decode the parity information sent by the source and/or the relay independently (recall that n_d=1 antenna). The *parity* data transmitted by the source and by the relay is different in order to improve the *coding* gain. Finally, the destination needs the transmissions from both terminals for (linearly) estimating the *systematic* data and with the help of the *parity* data decode the whole message.

5.2.1.2 Rate compatible punctured turbo codes (RCPTC)

We are considering that the STC are fed by channel codes based on the turbo principle (*binary-serial*). Figure 5.7 shows the general structure of the parallel Punctured Turbo Codes [45]. These are parallel concatenated convolutional codes in which the information bits are first encoded by a RSC (Recursive Systematic Convolutional) encoder, Figure 5.6, and (after passing through an interleaver) encoded again by a second RSC. Finally, the codewords are composed by the raw bits sequence (*systematic* data) and the parity check sequences from the two RSC. The rate of this code is approximately 1/3 (if some tail bits are taken into account). The system can be generalized to achieve rate 1/n by adding more interleaver-plus-RSC blocks (see Figure 5.7).
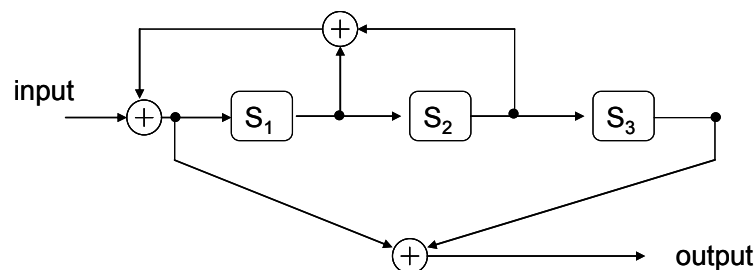
Figure 5.6.- Recursive Systematic Convolutional (RSC) encoder.

Additionally, a family of RCPTC [34] can be obtained by puncturing the coded bits of rate 1/3. Where each output bit stream is obtained using a puncturing pattern with period p, which is represented by the $3 \times p$ sized $\mathbf{P}$ matrix with ones and zeros. Ones represent the position of the bits to be transmitted and zeros correspond to erased bits. The first row is representative of the

systematic part, while the second and third correspond to the *parity* symbols. Note its applicability to incremental retransmission of the packets when different puncturing matrices are considered (each generated bit stream will contain some uncorrelated data).
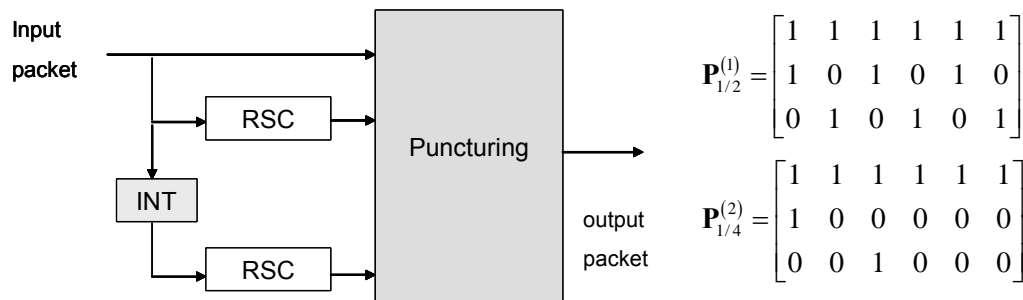
Figure 5.7.- Punctured turbo encoder.

We may associate the same or distinct puncturing matrices to the source and the relay, and to each of the retransmissions. For instance, in HARQ-I the initial transmission and all retransmissions use the same puncturing matrix, while these are different in HARQ-II. Figure 5.7 also shows an example of two different puncturing matrices of rate 1/2 and 1/4 $p=6$ (superscripts indicate the number of the retransmission). $\mathbf{P}^{(1)}$ transmits all the *systematic* data and different parity data, whereas $\mathbf{P}^{(2)}$ transmits less *parity* data (rows 2 and 3). The puncturing matrices are designed in such a way that all the symbols of a high rate punctured code are used by the lower rate codes, that is, the higher rate codes are embedded in the low rate codes. In this way, the transmitter needs only transmit supplementary code symbols to get a lower rate code.

5.2.1.3 Code structure for transmitted data

The use of the RCPT codes allows us to evaluate the different relay-assisted transmission schemes presented previously with different data rates and parity data transmitted from the source or relay, by a proper selection of the puncturing matrices. A description of how RCPT codes are combined with DSTC is given in the sequel assuming that the assisting relay decodes correctly the transmission from the source.

Direct transmission

The STC used is the Alamouti code, as it was mentioned in section 5.2.1.1. The source uses the message structure named type I and presented in Figure 5.8. For this case the amount of data of *systematic* and *parity* is the same, as it indicates the selected puncturing matrix, see Figure 5.8-right, providing rate 1/2. *Systematic* and *parity* symbols are concatenated.

Relay amplify-and-forward

For the relay-AF the encoding process is only performed at the source, because the relay retransmits the received signal with a proper amplifying factor to the destination (see for example equation 4.6 in section 4.2 of chapter 4). For this reason the structure of the transmitted data is similar to the direct transmission, message structure of type I, see Figure 5.8. When the *diversity gain* case is considered, the Alamouti code is applied to the *systematic*

and *parity* parts of the messages structure, while VBLAST code is used for the *STC rate gain* case. Let us recall that destination is able to linearly demodulate the symbols transmitted because of the transmissions received from the relay and the source.

Relay decode-and-forward

In this strategy the relay re-encodes the received signal before retransmission, for this reason the encoded process carried out at the source and relay could be different.

A) *Diversity gain.* In order to achieve this gain the objective is to work with a STC designed for a MISO system (Alamouti code) and transmit uncorrelated symbols from the source and relay which can be independently decoded by the destination (n_d=1). To accomplish this objective different puncturing matrices for the source and relay are considered. The source uses the message structure of type I and the relay selects the message structure of type II, both shown in Figure 5.8. In this case there are different parity bits transmitted from the relay to the destination. Additionally the amount of parity data in the relay transmission is larger than source transmission, (see the puncturing matrices depicted at the right of the frame structure in Figure 5.8).

B) *STC rate gain.* The difference from the previous case is the DSTC selected. Now we consider STC designed for MIMO systems with $2n_d$ receiving antennas. Additionally, in order to perform a linear detection of the transmitted symbols, the relay has to transmit exactly the same symbols as the source. For this reason, both terminals must have the same puncturing matrix and therefore the same message structure, (type I in this case, see Figure 5.8). Moreover, there are two different possibilities to achieve this gain (see section 2.2 in chapter 2), the repetition code (RC), where the source and relay use the same STC (designed for $n_s \times 2n_d$ MIMO system), or the unconstrained code (UC), where the source and relay selects different parts of a STC (designed for $(n_s+n_r) \times 2n_d$ MIMO system, see Figure 5.5).

Mixed coding relay decode-and-forward (mixed relay DF)

This strategy is considered to get both gains, *STC rate* and *diversity gain*. The main idea of this strategy is that the *systematic* data will use a STC designed for MIMO system with $2n_d$ receiving antennas, for instance the VBLAST code. The *systematic* data transmitted by the source and relay has to be the same for a linear decoding at the destination. For this reason the source transmits according to the message structure of type I and the relay selects the message structure of type III presented in Figure 5.8, note that the puncturing matrices transmit the same *systematic* data (see row 1). On the other hand, the *parity* data uses a STC designed for a MISO system (Alamouti STC) allowing to the destination decode independently the parity data sent from the source and relay. Hence the puncturing rows selected at the source and relay may be different (see in Figure 5.8-right the 2nd and 3rd rows of the puncturing matrices associated to the message structure of type I and III) and both terminals are transmitting uncorrelated symbols to the destination.
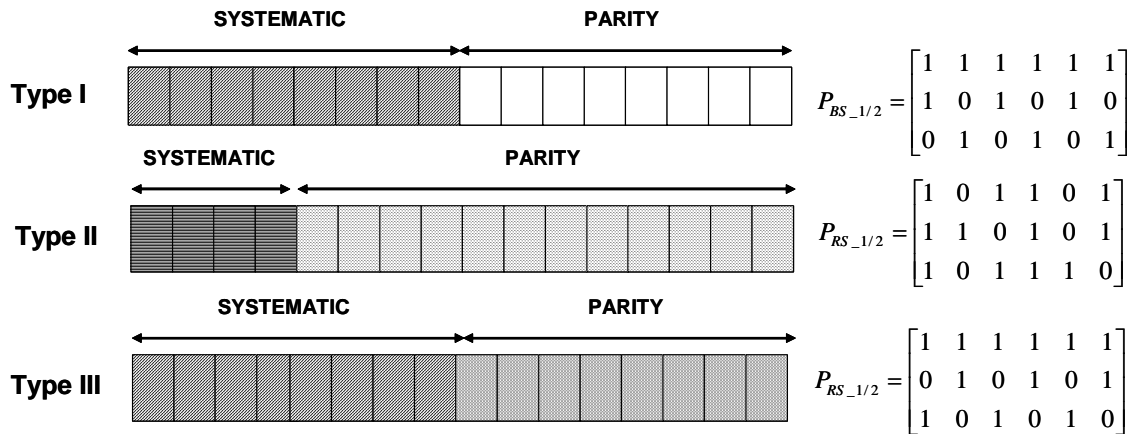
Figure 5.8.- Message structure and puncturing matrices associated to the source and relay transmissions. Different textures indicate different puncturing matrices.

5.2.1.4 ARQ protocols

The ARQ protocol considered here is based on the selective-repeat scheme [31]. Conventional ARQ protocols can be divided into two classes, Pure-ARQ and Hybrid ARQ protocols [31]. The difference between them is the task performed at the receiver and the type of the message transmitted. For the relay-assisted and direct transmission, only the destination informs to the source if it has decoded the packet correctly (ACK) or wrongly (NACK). In the sequel the process for the different ARQ methods is described:

- *Pure-ARQ.* If a packet is wrongly decoded, the destination requests a retransmission. The source transmits the same packet again. Then the destination discards the previous packet and tries to decode the new one.

- *HARQ-I.* This protocol considers all the received packets (the same packet) and combines them using the Maximal Ratio Combining (MRC) technique (*chase combining*). Therefore, the SNR of the packet to decode is increased in each retransmission.

- *HARQ-II.* When the source has to retransmit a packet, this protocol adds new *redundancy* (new *parity* bits) by changing the puncturing matrix (*code combining*) in each retransmission. The destination considers all the previous packets and builds a larger one with more *redundancy*. Then, the destination tries to decode this new packet. With this protocol the *coding gain* is increased in each retransmission. For example, let us assume that the source is transmitting a codeword of rate 1/2 (with N *systematic* bits and N *parity* bits). If the retransmission adds N new parity bits, the destination will try to decode a codeword of rate 1/3. In the case where some bits are transmitted again, then the MRC (Maximal Ratio Combining) technique has to be considered for those bits. In the previous example assume that the retransmission repeats $N/2$ *parity* bits and adds new $N/2$ *parity* bits. Therefore, the destination must perform the MRC of the $N/2$ repeated *parity* bits. Afterwards it will try to decode a codeword of rate 2/5.

5.2.2 Joint protocol and DSTC evaluation

Under the assumption that the re-use of the relay slot is high, only the relay-assisted transmission of one destination has been considered. This is a relevant assumption for a correct interpretation of the results presented below. If K users with the same configuration are transmitting simultaneously in the relay slot (without interfering between themselves), the throughput figures need to be scaled by $K/(K+1)$. Therefore, the throughput values shown below assume $K>>1$, (note that for 9 users, the total throughput has to be scaled by 0.9). A symmetric scenario has been fixed for simulations where each link has the same average SNR (*single-carrier* system).

The results analyzed in terms of throughput are divided in 7 subsections, in order to evaluate separately, the effect of the selected ARQ protocol for DF transmission, the performance of the direct transmission, the effect of relay DF and AF transmission, the results of the proposed cooperative mixed relay-DF and finally the comparison between linear vs. non-linear receivers.

5.2.2.1 Configuration

In Table 5.1 the main parameters of the simulation has been summarized. The channel coefficients include the zero-mean complex Gaussian component accounting for the Rayleigh fading. The zero-forcing receiver (for the Alamouti STC) and a non-linear Maximum Likelihood decode (list sphere decoder [46], [47]) followed by a max-log MAP turbo decoder [48] have been considered. Turbo Codes are considered as FEC codes using the interleaver named *S*-random [49].

Scenario	*Symmetric SNR configuration for all links involved in the cooperative transmission*
Channel	*Rayleigh flat fading channel*
STC	*Alamouti, VBLAST, QOD*
FEC codes	*Turbo Codes (1/3) with S-random interleaver*
Constellation	*4-QAM and 16-QAM*
Receiver	*Zero-Forcing, list-Sphere Decoder*
ARQ	*Pure-ARQ, HARQ-I, HARQ-II*
Length of Re-tx	*Full slot and Partial Slot (1/4)*
Max. tx per message	*10*

Table 5.1.- Configuration of the simulations.

The objective of this section is to show how the Hybrid turbo FEC/ARQ is able to improve the total throughput of the system by means of retransmissions and the distributed coding at the source and relay. To this end, the different strategies are compared in terms of throughput versus SNR, that is, expected number of correctly decoded information bits per channel use,

$$\eta = E\{\eta_{inst}\} = E\left\{\frac{N_b}{N_{tx}N_{ch}}\right\} \quad \text{bits/channel use} \tag{5.6}$$

with N_b the number of the transmitted information (*systematic*) bits, N_{tx} the number of transmissions from the source to destination required to receive the packet correctly and N_{ch} the number of channel uses. Only the channel uses in the source-destination link have been considered (downlink time-slot) the effect of the channel uses of the relay slot are considered in

the factor $K/(K+1)$. To evaluate the throughput, every packet is transmitted until it is correctly decoded or a maximum number of 10 re-transmissions are employed. After this, the packet is considered in error and produces an instantaneous throughput value η_{inst}=0. Notice that, we do not tackle the design of the modulation and coding scheme (MCS), we have just considered different configurations of MCS (in the different links) to be evaluated. The ARQ protocol will deal with the outage events produced by the current channel and the selected MCS. However, the work developed in section 5.3.3 for adapting the MCS to the current channel state could be used here. In that case, the MCS is selected as a function of the *effective SNR*[4] of each link, a parameter that describes the link quality. In our case, we should use the *average SNR*, the parameter of the channel we could know under *long-term* CDIT.

For the HARQ-II protocol up to three different puncturing matrices have been defined in the source and another three for the relay (for relay-DF and mixed relay-DF). As we have fixed the maximum number of re-transmissions to 10, the puncturing matrices have to be used several times. In that case, this protocol uses the MRC technique to combine the different packets. Additionally, because of the use of a simple turbo code of rate 1/3 sometimes it is not possible to send 10 retransmissions containing only *new parity* bits.

The distributed space-time codes are applied when the relay terminal decodes correctly the packet. If the message is received with error at the relay terminal and it has to transmit during the *relay-transmit* phase (*persistent transmission*) then the relay performs a hard decision of the received symbols and transmit them to the destination (with the proper space-time code), without applying the procedures defined in section 5.2.1.3 to add new parity bits to the sources' transmission (similar *to repetition coding*).

5.2.2.2 Effect of ARQ in relay-DF

In this subsection we present the throughput performance for the relay-DF strategy under different ARQ protocols. In Figure 5.9, the throughput obtained for the relay-DF (relay always transmit, *persistent transmission*) is depicted for the different ARQ protocols. Different codeword rate has been selected (from 1 (*uncoded*) to 1/3). It is shown that for a given codeword rate, see for instance 3/4 (*right-triangle*), the worst performance (at low SNR) is obtained for Pure-ARQ. The HARQ-I improves throughput and the best operation (though the gains are not really significant) is obtained for HARQ-II.

Additionally, for the HARQ-II protocol the throughput can be improved by decreasing the length of the retransmissions, because it can efficiently adapt to the channel state, see Figure 5.10. Note that for a SNR of 10 dB and code rate 1, there is an improvement of 0.9 bit/s/Hz between partial (Figure 5.10-right) and full slot retransmission (Figure 5.10-left), and for SNR=4 dB and code rate 3/4 the difference is about 0.3 bit/s/Hz. It is important to remark the effect obtained at low SNR, where the full-slot retransmission is better than partial slot option because of the fixed number of transmissions. The reason for this behavior is the following: given the same number of transmissions the full slot option can transmit more symbols (*systematic* or *parity*) than the partial slot mode.

---

[4] This parameter is defined in section 5.3.1.
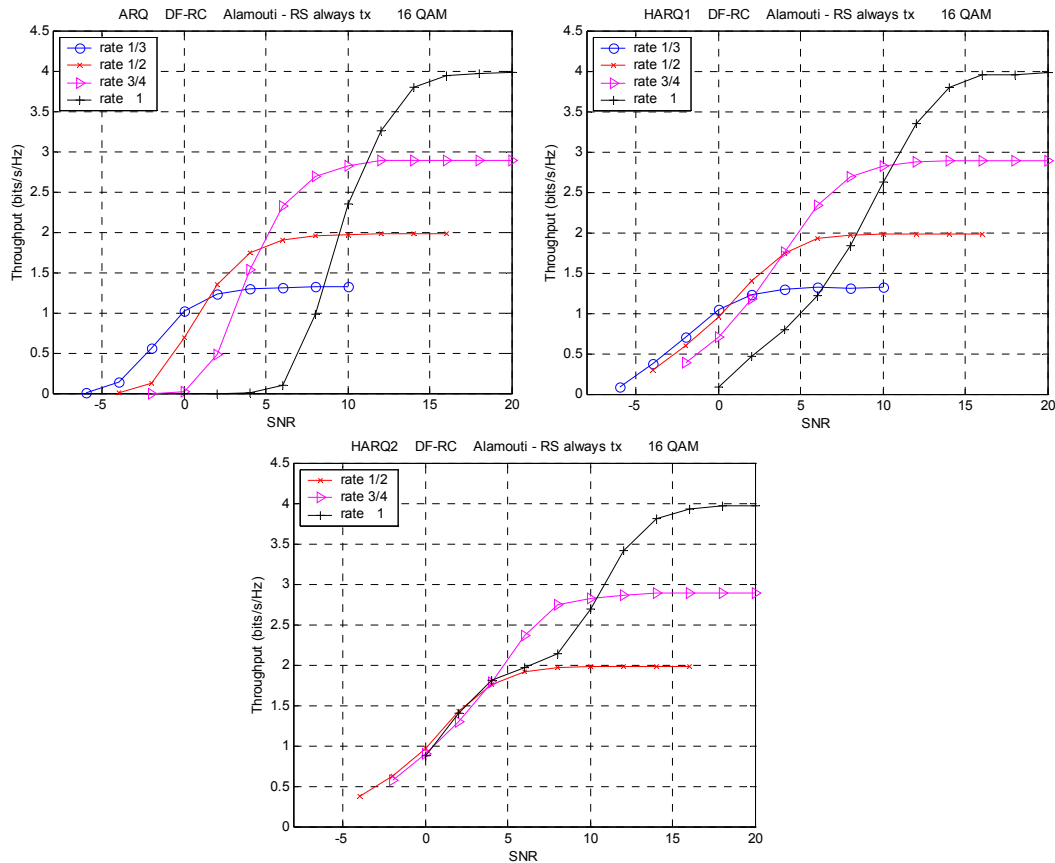
Figure 5.9.- Throughput performance for different Pure-ARQ (left-above), HARQ-I (right-above) and HARQ-II (below) for the relay-DF (diversity gain) with *persistent transmission*. 16-QAM. Alamouti STC. ZF-receiver.
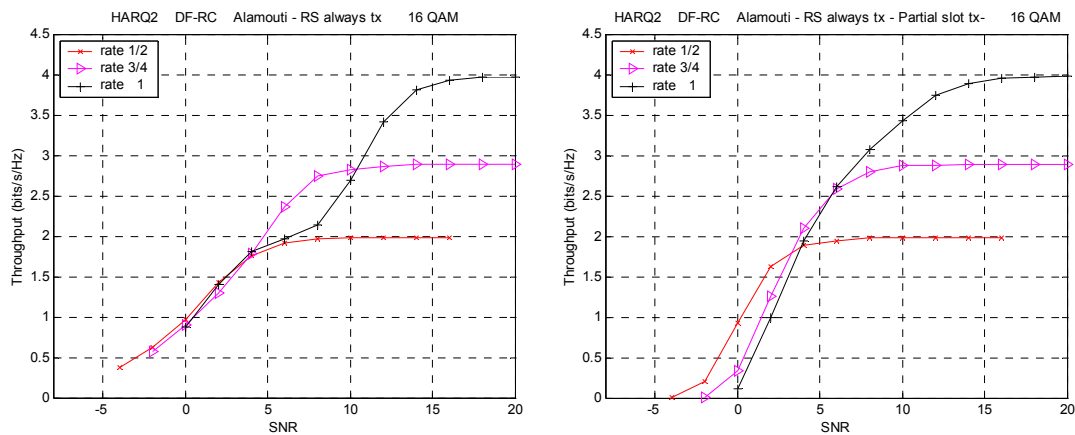
Figure 5.10.- Effect of the length of the transmissions for the HARQ-II, full slot (left) and partial slot retransmission (right). Relay-DF (diversity gain) with persistent transmission. ZF-receiver.

5.2.2.3 Direct MIMO transmission

Figure 5.11, shows the performance in terms of throughput and average number of transmissions (ANT) when the Alamouti ST code has been selected for the direct (MISO) transmission. The selected retransmission scheme is the HARQ-II, because it was shown in the previous sub-section to be the best one in terms of throughput. Direct transmission throughput results will be taken as relevant reference for the relay-assisted case presented in the following sections (let us recall that the source is using n_s=2 antennas and the destination is equipped with only n_d=1 antenna).
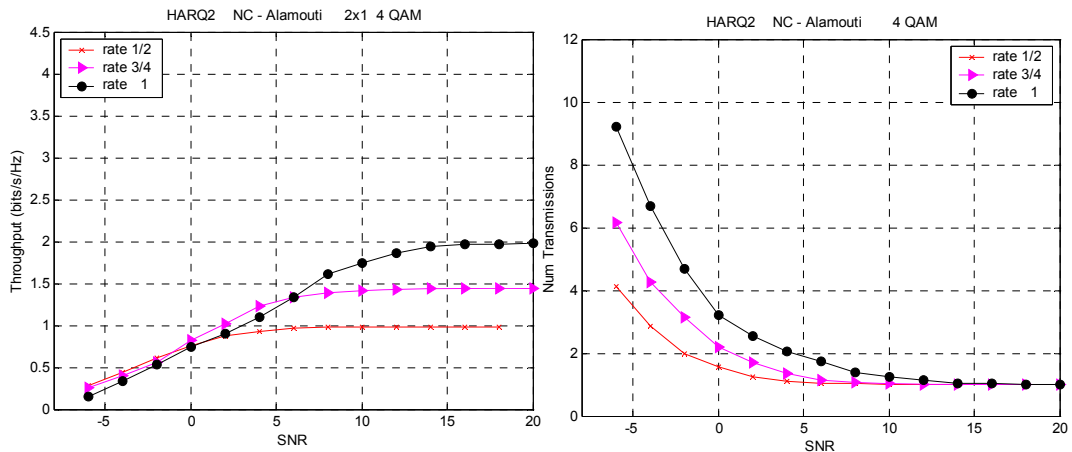
Figure 5.11.- Throughput (left) and average number of transmissions (right) for direct transmission using HARQ-II and RCPT codes with rates {1/2,3/4,1}, 4 QAM. ZF-receiver.

5.2.2.4 Performance of the relay transmission under DF

Diversity Gain

The average throughput of the relay-assisted transmission may be compared to the average capacity of an ideal 2×2 MIMO system (under no CSIT) using 4QAM. For full diversity gain, we use the Alamouti ST code and assume two possible policies for the relay: *selective relaying*[5], where the relay terminal transmits only if it decodes correctly the packet, Figure 5.12-left, and *persistent transmission*, where the relay always transmits, Figure 5.12-right. Additionally, it is shown how the relay may transmit regardless of erroneous reception without deteriorating the performance. That is because we are using the Alamouti code (optimum for 2×1 MIMO system) in the source-relay link (2×2 MIMO system), thus relay can decode correctly most of the time. Both strategies improve the throughput of the direct transmission scheme (around 2-3 dB, see Figure 5.11). The *selective relaying* will exhibit an improved performance with respect to the *persistent transmission* policy if the channel uses considered in this work will be different (in this work there is always a slot devoted for relay-assisted transmissions). However, the exact evaluation of this gain entails the definition of cell-wide radio resource management strategies which fully exploit this behavior.
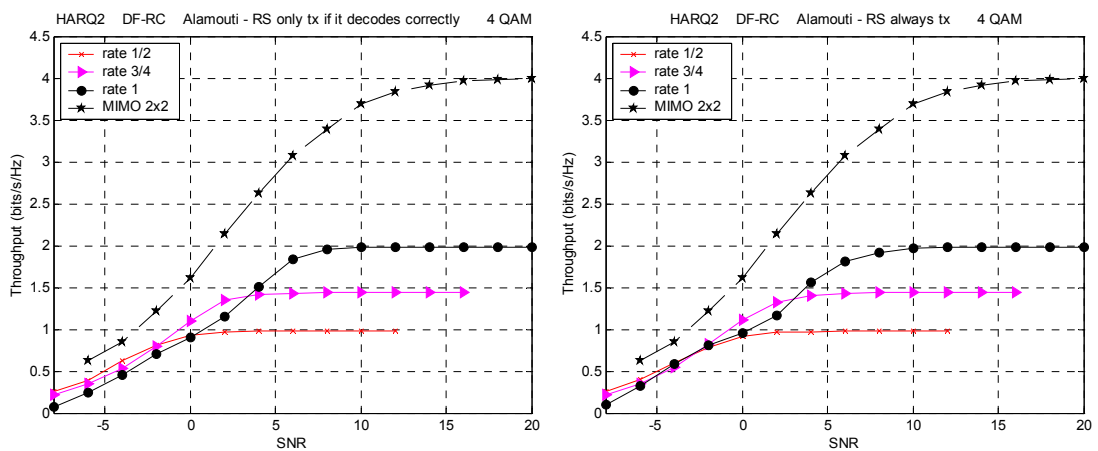
Figure 5.12.- Throughput for relay-DF scheme with HARQ-II with RCPTC of rates {1/2, 3/4,1}. *Selective transmission* (left) and *persistent transmission* (right). ZF-receiver.

---

[5] It is different from the *selective relaying* defined in section 2.1.3 because during the *relay-transmit phase* both the relay and source remain silent when the relay terminal is unable to decode the message.

STC rate gain

In the previous case, the selected STC (1 symbol/channel use) does not make good use of the *virtual* MIMO system where up to 2 symbols/channel use can be transmitted with a linear decoding. Therefore, two new STC are considered to test how much of this STC rate gain may be achieved, the VBLAST for *relay-DF-RC* and QOD [44] for *relay-DF-UC*, in Figure 5.13-left and Figure 5.13-right, respectively. It is shown that both codes achieve the mutual information of a 2×2 MIMO system with 4-QAM for high SNR values (QOD code presents a tighter performance) although for low SNR values the throughput is worse than in the previous cases, Figure 5.11 and Figure 5.12. This may be explained by the fact that we have traded STC rate gain by diversity gain. This effect could be used efficiently in the dynamic control of the link by selecting the rate of the STC according to the state of the cooperative link. Figure 5.13 also shows that at low values of SNR the DF-RC improves the DF-UC (in contrast to what happens at high SNR region). This is because of the split of the ST codes between the source and the relay. For DF-RC we use VBLAST code at the source, optimum for 2×2 MIMO system (source-relay link), whereas for the DF-UC the source uses some part of a QOD (designed for a 4×2 MIMO system, see Figure 5.5) and the resulting ST code for the source-relay link is not necessarily the optimum one.
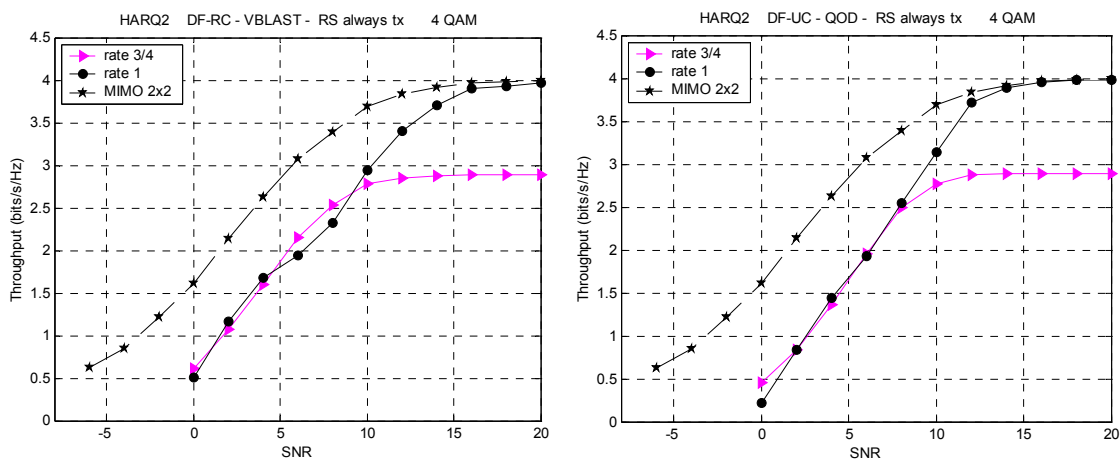
Figure 5.13.- Throughput for relay-DF scheme with HARQ-II with RCPTC of rates {3/4,1} using VBLAST (left) and QOD (right) STC. List-SD receiver.

5.2.2.5   Performance of the relay transmission under AF

In this section the AF case is considered using the Alamouti code (*diversity gain*) and VBLAST code (*STC rate gain*) as space-time codes (see results in Figure 5.14-right). In this case DSTC cannot be considered because the relay retransmits the received signal as it is received (including noise). This system is more similar to a conventional MIMO system because the space-time codes are only applied at the source. Notice that the performance is worse (around 1.5 dB) than DF-RC case (Figure 5.14-left) but it should be remarked that, in this situation, the relay works with only n_r=1 antenna. Moreover, the symmetric case is not the best scenario for the AF; it requires a good link source-relay or relay-destination so as not to amplify too much noise, see Figure 5.15 under AF and DF using Alamouti STC, where the SNR in the relay-destination link has been increased 3 and 6 dB over the SNR of the other links. Results show that relay-AF can improve the results obtained by the relay-DF. This system also outperforms the direct transmission system (see Figure 5.11).
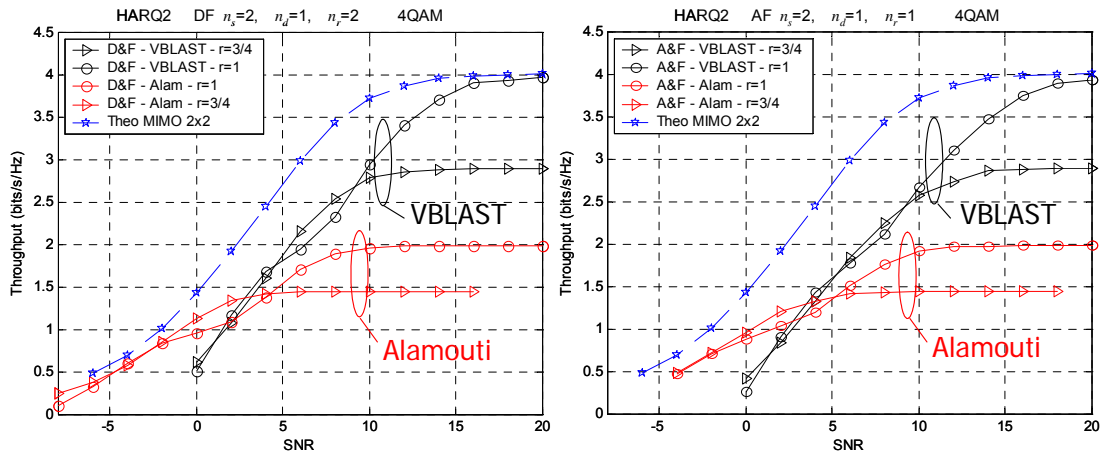
Figure 5.14.- Throughput for relay-DF (left) and relay-AF (right) schemes with HARQ-II with RCPTC of rates {3/4, 1} using VBLAST (list-SD) and Alamouti STC (ZF).

Figure 5.14 also presents the trade-off between diversity and STC rate gain for the DF and AF. For low SNR values the Alamouti STC is better, whereas for high SNR the VBLAST code is more useful. This is again suggesting that the rate of the STC should be a parameter to be used in link adaptation.
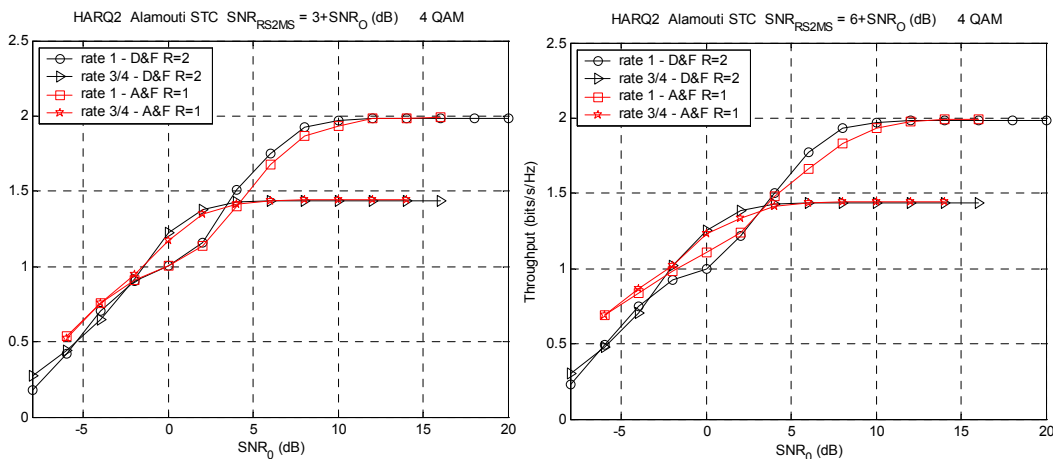

Figure 5.15.- Throughput for relay-DF and relay-AF with HARQ-II with RCPTC of rates {3/4, 1} using Alamouti STC (ZF), for $SNR_2=3+SNR_0$ (left) and $SNR_2=6+SNR_0$ (right). $SNR_1=SNR_0$. With SNR_0, SNR_1 and SNR_2 the SNR of the source-destination, source-relay and relay-destination link, respectively.

5.2.2.6 Performance under mixed relay-DF

The mixed coding relay DF combines the STC rate gain with the diversity gain, by transmitting the systematic data using the VBLAST and the parity data with Alamouti. Figure 5.16-right shows the obtained throughput using this strategy. Results show that mixed strategy obtains good throughput results for high SNR values, nevertheless for low SNR the results are worse than direct transmission, see Figure 5.9. Results are quite similar to the DF-RC (VBLAST) (see Figure 5.16-left). Additionally, it should be emphasized that the reason because the code rate 3/4 is saturated at 2.4 bits/s/Hz is due to the different number of channel used devoted for the *systematic* (VBLAST–2 symbols/channel use) and *parity* bits (Alamouti–1 symbol/channel use).
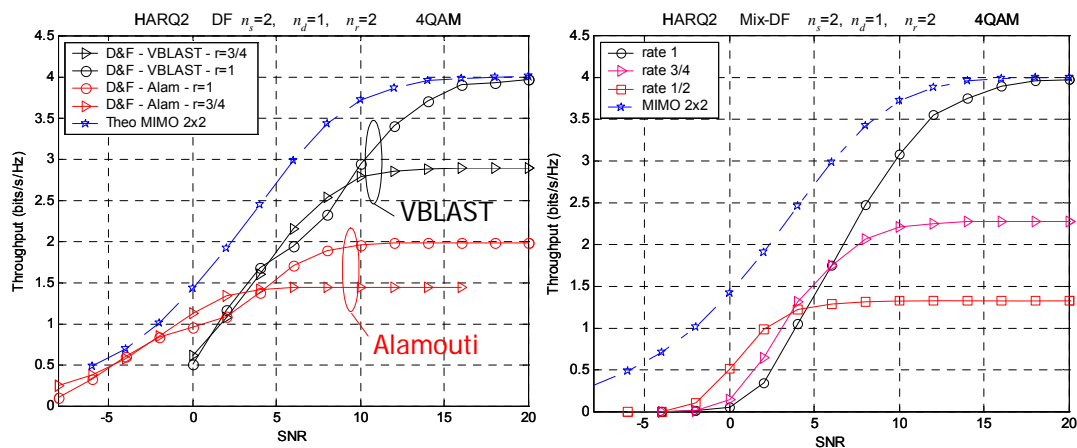
Figure 5.16.- Throughput for C-DF (left) and C-Mixed D&F (right) schemes with HARQ-II with RCPTC of rates {3/4, 1} using VBLAST and Alamouti STC.

5.2.2.7 Linear *vs* non-linear receivers

Finally, in this section a comparison between linear (zero forcing, ZF) and non-linear (list-SD) decoders is presented. Figure 5.17 shows the different performance of the receivers when a non-orthogonal STC (VBLAST in this case) is considered. It can be seen a difference around 4 dB at 2.5 bits/s/Hz. Therefore, the use of non-linear receivers is recommended for non-orthogonal STC.
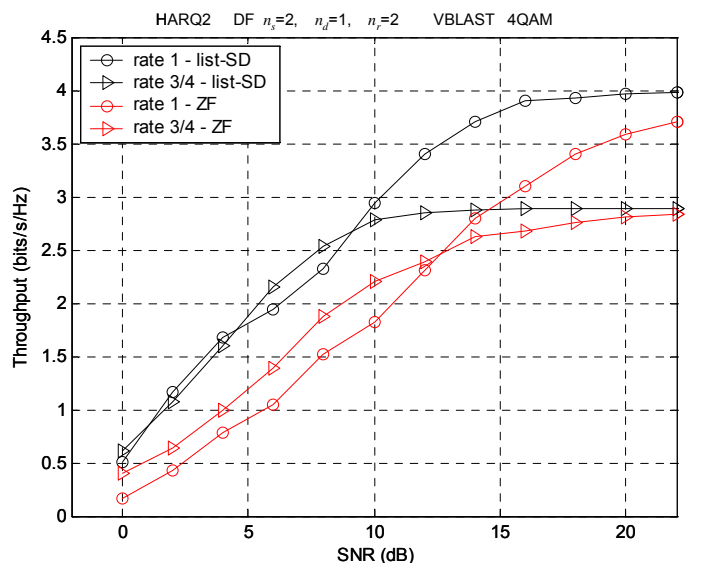
Figure 5.17.- Throughput for C-DF schemes with HARQ-II with RCPTC of rates {3/4,1} using VBLAST with the list-SD and the ZF receiver.

5.2.3 Conclusions

In section 5.2 the relay-assisted transmission applied in the downlink of a TDMA system has been investigated, using different schemes that combine ARQ, STC and turbo codes to achieve results close to the true capacity of the system. It has been shown that relay-assisted transmission outperforms the direct transmission in terms of throughput for a high reuse ($K \gg 1$) of the relay slot (assuming all the destinations with similar configuration). Additionally, different

ARQ protocols have been considered and hybrid protocols have shown better performance than Pure ARQ. For medium to high SNR values, the HARQ-II with partial slot retransmission seems to be needed to achieve better throughput results.

The following conclusions may be drawn:

- It has been shown that relay-DF (relay decodes the received data) is the best relay-assisted strategy in terms of throughput. For low SNR values a strategy exploiting the diversity gain (Alamouti) is the best, and hence, the selection of the rate for the STC seems to be a useful strategy.

- For the symmetric scenario (and since we have only considered the channel uses between source and destination) the use of *selective transmission* does not seem to offer significant gains, that is, transmissions from the relay always seem to be rewarding even when some errors are encountered.

- Whereas for medium and high SNR values, strategies using the *STC rate gain* with distributed space-time codes (RC, UC or Mixed relay-DF) are better in terms of throughput than the direct transmission, the relay-DF-UC is the best. It has shown that a suitable selection of the STC depending on the channel state is beneficial to improve the throughput.

- Additionally, the analysis for the AF also has been considered. Slight SNR losses are observed with respect to relay-DF, but there are two points to worth noticing, it only uses 1 antenna at the relay (in the DF n_r=2 are required) and the symmetric configuration (equal average SNR in all links) is slightly penalizing its performance. Moreover, if other scenarios are considered (asymmetric) the relay-AF can achieve better throughput results than the relay-DF, see Figure 5.14. Therefore, this strategy shows a good compromise between the performance and the complexity at relay.

- Finally, a comparison between linear (ZF) and non-linear (list-SD) receivers has analyzed. Differences around 4 dB have been found when non-orthogonal STC are considered. Therefore, the use of non-linear receivers seems to be required for the cases where the non-orthogonal STC are used.

- The extension for other antenna configuration requires the use of space-time codes designed for such configuration.

5.3 Transmission strategy under *partial* CSIT

The *partial CSIT* allows the transmitter to have *actual information about the current channel state*. The transmitter will transmit uniformly through the antennas because the channel coefficients are not known (no CSIT), but the decision on the data rate can be done over some parameter which describes the current channel realization. The data rate can be selected according to the current channel state, so the error event in the transmission will be dominated by the thermal noise. The suitable selection of the modulation and coding scheme (MCS) depends basically on the Packet Error Rate (PER) of the FEC code employed for the transmission under that channel realization.

The goal of this section is to determine the MCS for the relay-assisted transmission relaying on the IEEE 802.16e standard [26] using either PUSC (partial usage of sub-channels) or FUSC (full usage of sub-channels) mode in the downlink. It is assumed that there is not CSIT and space-time codes as Alamouti,[18], or Golden[6] code, [27][28][29], are considered. To this end, first in section 5.3.1 we will study one level of abstraction for predicting the link error performance of a relay-assisted transmission under the current channel realization given a FEC code and a MCS. It is based on the Exp-ESM [36] defined for point-to-point communications with multiple-carriers. This abstraction is considered for the relay-assisted transmissions for the different protocols in section 5.3.2. When this level of abstraction is known at the transmitter, it can design the MCS for a given channel realization (section 5.3.3).

5.3.1 Link error prediction

One level of abstraction considered in the past was the mean Signal to Noise ratio (SNR) for the single-carrier transmissions. However a different methodology must be adopted when transmitting through multiple carriers or in a MIMO system such as has been introduced in section 5.1. To this end we have considered an error prediction method based on the Exponential-Effective SIR Mapping (Exp-ESM) [36]. This section is organized as follows. First, the FEC code considered in 802.16e standard (convolutional turbo codes) is described. Afterwards, the Exp-ESM is detailed for the MIMO and STC configuration under a linear receiver (MMSE), providing the principal properties and dependences of its parameters. The actual values of those parameters are specific of the FEC code used, but the Exp-ESM is valid for all types of FEC codes. Section 5.3.1.3 describes how to combine two different metrics when the transmissions are *orthogonal* or *superposed*. This point of view will helpful for the extension of Exp-ESM to the relay-assisted transmission. Afterwards, the error prediction for the different relay-assisted protocols (forwarding, protocol I, II and III) is described for a given modulation and coding scheme (MCS).

5.3.1.1 Convolutional Turbo Codes (CTC)

The FEC codes considered in this section are the Convolutional Turbo Codes [30] (CTC) which are defined as optional for the IEEE 802.16e standard [26]. It consists of two circular recursive systematic convolutional codes used along with a log-MAP or max-log- MAP decoding. The main difference from the conventional parallel turbo codes (binary-serial) explained in section 5.2.1.2 is the type of encoders. In this regard, CTC use duo-binary constituent encoders (Figure 5.19) instead of the binary encoders considered in parallel TC (Figure 5.6). The encoding process in both cases is also different, compare Figure 5.7 with Figure 5.18. In the duo-binary case, two sub-packets (*A* and *B*) of length N_b are built given a packet of length $2N_b$ bits for the encoding process. Those sub-packets are fed to the constituent encoder simultaneously, producing the encoded sub-packets (parity) Y_1 and W_1. Afterwards, an interleaved version of the sub-packets *A* and *B* is encoded in order to generate additional parity bits (Y_2 and W_2). With this configuration, the encoded packet presents a codeword rate of 1/3.

---

[6] It is a linear STC defined for the IEEE 802.16e standard for $n_s=n_d=2$. Its dispersion matrices are given in Appendix A.
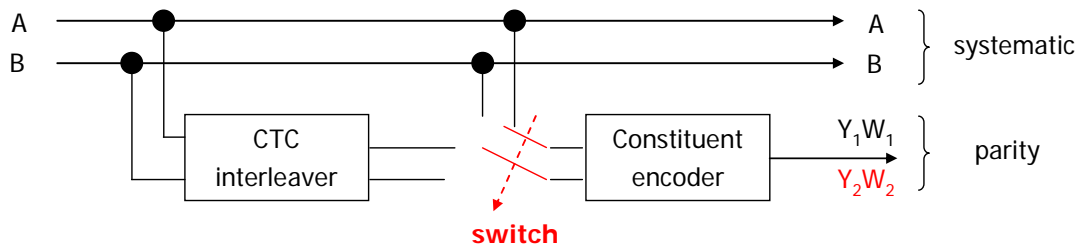
Figure 5.18.- CTC encoder.

It has to be emphasized that the *duo-binary* constituent encoder, Figure 5.19, uses a circular coding (tailbiting), hence the ending trellis state must be equal to the initial trellis state, called circular state $S_c=[S_1, S_2, S_3]$. In the classical parallel TC (section 5.2.1.2) some redundant tail bits are added to lead the trellis state to the zero state, but in the CTC these bits are not required, improving the spectral efficiency of the coding scheme. However, a pre-encoding operation (with encoder at state 0) is required to determine the ending state, S_{end}, of each of the constituent encoders because this state depends on the sequence to be transmitted (normal and interleaved). Based on S_{end} the circulation state S_c for each constituent encoder can be calculated by linear algebra, in section 8.4.9.2.3.3 of [26] it is given a lookup table. Afterwards, the sequence must be encoded initializing each encoder state to its calculated circular state. The interleaver and the puncturing process are described in section 8.4.9.2.3 of [26].

feedback branch: $1+D+D^3$ $(0xB)$

Y-parity branch: $1+D^2+D^3$ $(0xD)$

W-parity branch: $1+D^3$ $(0x9)$
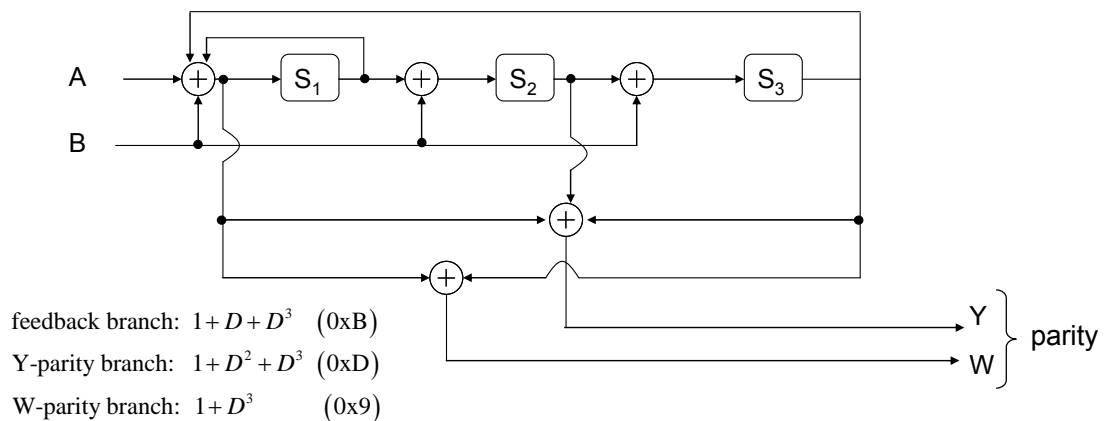
Figure 5.19.- CTC constituent encoder.

Although the use of *duo-binary* encoders (Figure 5.19) adds some complexity as the need of coding the data twice, there are also several benefits [25],

- The trellis of the circular recursive systematic convolutional code has fewer states than a binary code (one half).

- The suboptimal but efficient max-log-MAP algorithm can decode the *duo-binary* code at a cost of 0.1-0.2 dB relative to the optimal log-MAP algorithm. However, for binary codes that loss is around 0.3-0.4 dB.

- Perform better than its binary counterpart when the codes are punctured to higher rates.

The performance of the CTC in terms of packet[7] error rate (PER) depends on the packet size aside from the modulation and code rate (due to the puncturing process). Figure 5.20 illustrates some PER curves for different values of the packet size, using a codeword rate of 1/3 and modulation 4-QAM. In this regard, the packet size becomes an additional parameter to be considered when we select the MCS using CTCs (section 5.3.3).
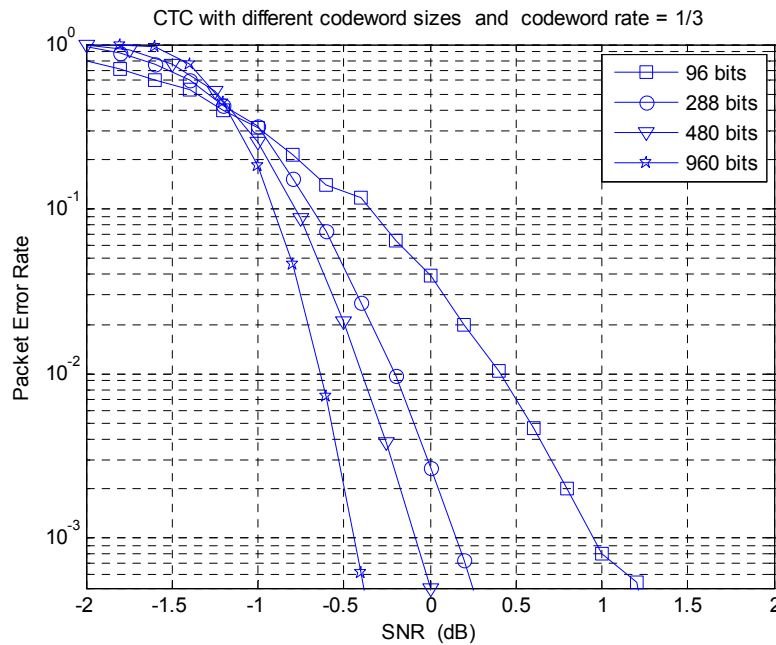
Figure 5.20.- PER of CT Codes of different sizes {96, 288, 480, 960} as a function of the SNR. Codeword rate 1/3, AWGN channel. 4-QAM.

5.3.1.2 The Exp-ESM link error prediction method

The Exp-ESM method is derived based on the Union-Chernoff bound for error probabilities for BPSK and QPSK modulations [36]. It assumes that the effect of transmitting a message with a given MCS through multiple carriers produces a multi-state channel, where the probability of each state is the same and corresponds to the SNR experienced at each carrier. The Exp-ESM provides an *effective SNR*, γ_{eff}, as a single parameter for describing the quality of the link. This parameter is considered for modeling the error probability of the transmission. For higher-order modulations the Exp-ESM degrades its accuracy. The Exp-ESM metric is briefly derived in Appendix B (section 5.6) and is defined as,

$$\gamma_{eff} = -\beta \ln\left(\frac{1}{N_{tot}} \sum_{i=1}^{N_{tot}} \exp\left(-\gamma_i \big/ \beta\right) \right) \tag{5.7}$$

where β is the parameter to adjust the performance for a given MCS, N_{tot} is the number of carriers used by the transmission and γ_i denotes the SNR for each carrier in a given channel realization. When the PER curves corresponding to the transmission of a message with a fixed MCS over different channel realizations are plotted as a function the *effective SNR* (calculated for each channel realization), those curves are closed to a reference PER curve obtained using the same MCS over an additive white Gaussian noise (AWGN) channel (the *effective SNR* is

---

[7] The codeword error rate also is referenced as block error rate (BLER), but in this work it will be used the term PER.

the mean SNR in that type of channel). Figure 5.21 depicts that performance where β is set to 1.2.
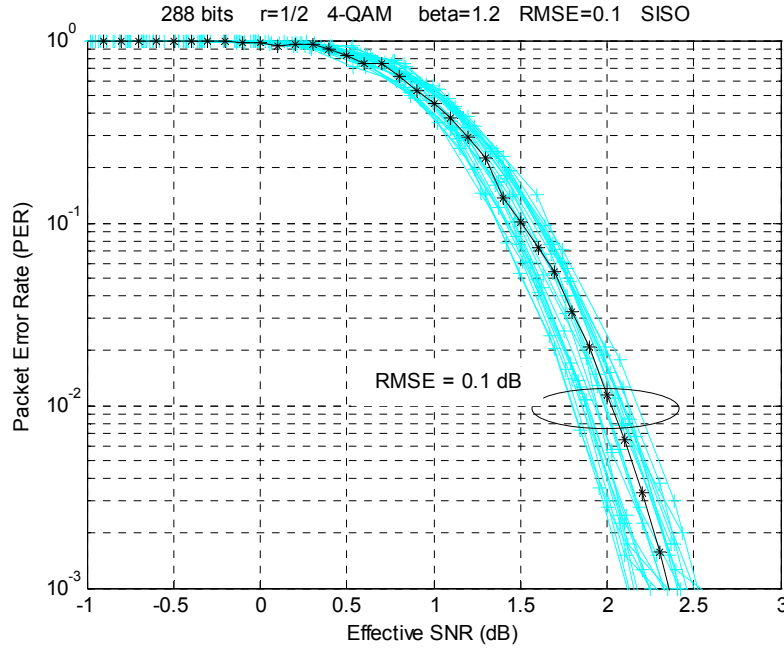
Figure 5.21.- Actual PER values for different channel realizations in terms of the effective SNR (cyan lines) and compared with the reference curve obtained in AWGN channel (black star lines). CTC with N_b=288 bits, code-rate 1/2 and 4-QAM. β=1.2.

When multiple antennas in combination with STC are used in the OFDMA transmission, the SNR of each estimated symbol in each carrier (at the output of the symbol estimator) have to be considered [38]. For linear STC as Alamouti and Golden STC, which transmits Q_s complex symbols during T channel uses, the signal model for a single-carrier can be written as (see (5.3)),

$$\mathbf{y} = \mathbf{H}_{eq}\mathbf{\Theta}\mathbf{x} + \mathbf{n} \tag{5.8}$$

where $\mathbf{y}$ is the received vector which incorporates the real and imaginary part of the received signal, $\mathbf{H}_{eq}$ contains the coefficients of the channel matrix, $\mathbf{\Theta}$ is a matrix with the STC defined in (5.4) and (5.5), $\mathbf{x}$ is the $2Q_s$-length complex vector of the symbols to be transmitted and $\mathbf{n}$ considers the noise. The linear minimum mean square error (MMSE) receiver is defined by,

$$\mathbf{W} = \mathbf{\Theta}^H\mathbf{H}_{eq}^H\left(\mathbf{H}_{eq}\mathbf{\Theta}\mathbf{\Theta}^H\mathbf{H}_{eq}^H + \frac{\sigma^2 n_s}{P_t}\mathbf{I}\right)^{-1} \tag{5.9}$$

with P_t the power transmitted by the source, n_s the number of transmitting antennas and σ^2 the noise power. The signal received at the output of the MMSE receiver is,

$$\mathbf{z} = \mathbf{W}\mathbf{H}_{eq}\mathbf{\Theta}\mathbf{s} + \mathbf{W}\mathbf{n} = diag\left(\mathbf{W}\mathbf{H}_{eq}\mathbf{\Theta}\right)\mathbf{s} + \left(\left(\mathbf{W}\mathbf{H}_{eq}\mathbf{\Theta} - diag\left(\mathbf{W}\mathbf{H}_{eq}\mathbf{\Theta}\right)\right)\mathbf{s} + \mathbf{W}\mathbf{n}\right) \tag{5.10}$$

where two terms can be distinguish in (5.10), the first connected to the signal and the second with a colored noise with the following covariance matrix,

$$\mathbf{R}_n = \frac{P_t}{n_s}\left(\mathbf{WH}_{eq}\mathbf{\Theta} - diag\left(\mathbf{WH}_{eq}\mathbf{\Theta}\right)\right)\left(\mathbf{WH}_{eq}\mathbf{\Theta} - diag\left(\mathbf{WH}_{eq}\mathbf{\Theta}\right)\right)^H + \sigma^2\mathbf{WW}^H \qquad (5.11)$$

Therefore, for each carrier we have to consider a $2Q_s$-length SNR vector which elements are,

$$\gamma_i = \frac{[\mathbf{S}]_{ii}}{[\mathbf{R}_n]_{ii}} \qquad with \quad \mathbf{S} = \frac{P_t}{n_s}diag\left(\mathbf{WH}_{eq}\mathbf{\Theta}\right)\left(diag\left(\mathbf{WH}_{eq}\mathbf{\Theta}\right)\right)^H \qquad (5.12)$$

where the operator $[\mathbf{A}]_{ii}$ stands for the i-th element of the diagonal of matrix $\mathbf{A}$ and $\mathbf{S}$ is a diagonal matrix with the power of the transmitted. Notice that now the metric defined in (5.7) is modified in the number of terms in the summation by the number of carriers and the symbols transmitted in each carrier, that is, length of the vector of (5.12).

5.3.1.2.1   Adjusting the parameters of Exp-ESM

The value of β is obtained by minimizing the error between the reference curve (PER-AWGN) and the obtained error curve for a given channel (PER-Exp-ESM). Figure 5.22 depicts two error curves for a given channel realization with different values of β (β_1 and β_2). The value of β impacts on the position of the PER-Exp-ESM curve. Those curves are nearly parallel placed at different distances from the reference curve depending on the value of β.
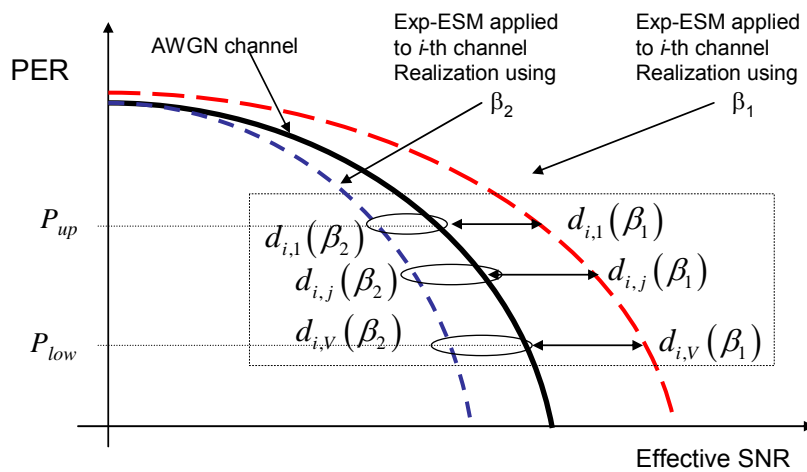
Figure 5.22.- For a given channel realization the Exp-ESM with different values of β produce different error curves plotted versus *effective* SNR. At given PER these curves are placed at distance *d* (dB) of the reference curve.

The optimization of the best β is done through L independent channel realizations minimizing the mean square error (MSE),

$$\hat{\beta}_{opt} = \arg\min_{\beta} e_m(\beta) \qquad (5.13)$$

where e_m is the mean square error (MSE) as a function of the selected β obtained along L channel realizations,

$$e_m(\beta) = \frac{1}{L}\sum_{i=1}^{L}\sum_{j=1}^{V}\left|d_{i,j}(\beta)\right|^2 \qquad (5.14)$$

where L denotes the number of channel realizations, $d_{i,j}(\beta)$ is the distance between the PER-Exp-ESM curve and the PER-AWGN performance at some PER$\in\{P_{up}, P_{low}\}$ for a given value of β. Finally, V is the number of PER values considered to measure $d_{i,j}(\beta)$. Likewise, the mean square error (MSE) obtained at the optimized value is given by $e_m\left(\beta_{opt}\right)$. Figure 5.21 shows the performance of the PER-Exp-ESM curves with the optimal β.

The root mean square error (RMSE) is defined as,

$$RMSE = \mu_{error} = \sqrt{e_m\left(\hat{\beta}_{opt}\right)} = \sqrt{\frac{1}{L}\sum_{i=1}^{L}\sum_{j=1}^{V}\left|d_{i,j}\left(\hat{\beta}_{opt}\right)\right|^2} \qquad (5.15)$$

In the following it will be shown how the optimum β, (5.13), and the RMSE (5.15), depend on the configuration of the transmission: number of data carriers, modulation, codeword rate, type of channel and space-time code selected. For comparison purposes we define the normalized number of carriers as the number of carriers used by each coded bit. This definition allows comparing codes with different packet size and codeword rate. It is given by,

$$N_c^{norm} = \frac{r}{N_b}N_{carriers} \qquad (5.16)$$

where $N_{carriers}$ is the number of carriers, N_b is the packet size and r the data codeword rate (N_b/r is the total coded bits). Moreover, the data region S for transmission will be defined by the time-frequency channel uses of size,

$$S = N_{carriers} \times N_{OFDM}$$
$$N_{OFDM} = \frac{1}{N_{carriers}}\frac{N_b}{r}\frac{1}{\left(\dfrac{Q_s}{T}\right)\log_2(M)} = \frac{1}{N_c^{Norm}\left(\dfrac{Q_s}{T}\right)\log_2(M)} \qquad (5.17)$$

where N_{OFDM} is the number of OFDM symbols transmitted, N_c^{norm} given by (5.16), Q_s the number of space-time symbols and T the channel uses required by the STC (see section 5.2.1.1), finally, M is the modulation considered. In the IEEE 802.16e standard [26], the PUSC transmission should contain at least 2 OFDM symbols, so that for 4-QAM and SISO transmission ($Q_s=T=1$) the $N_c^{norm}=0.25$. On the other hand, for 2×2 MIMO transmission with STC (using Golden Code, $Q_s=4$, $T=2$) and 4-QAM it is required $N_c^{norm}=0.125$. Table 5.2 depicts the maximum number of normalized carriers per coded bit under different STC and modulation configuration.

STC	Q_s	T	N_{OFDM}	M	N_c^{norm}
Alamouti	2	2	2	4	0.25
				16	0.125
				64	0.083
Golden	4	2	2	4	0.125
				16	0.0625
				64	0.0416

Table 5.2.- Maximum number of normalized number of carriers for coded bit.
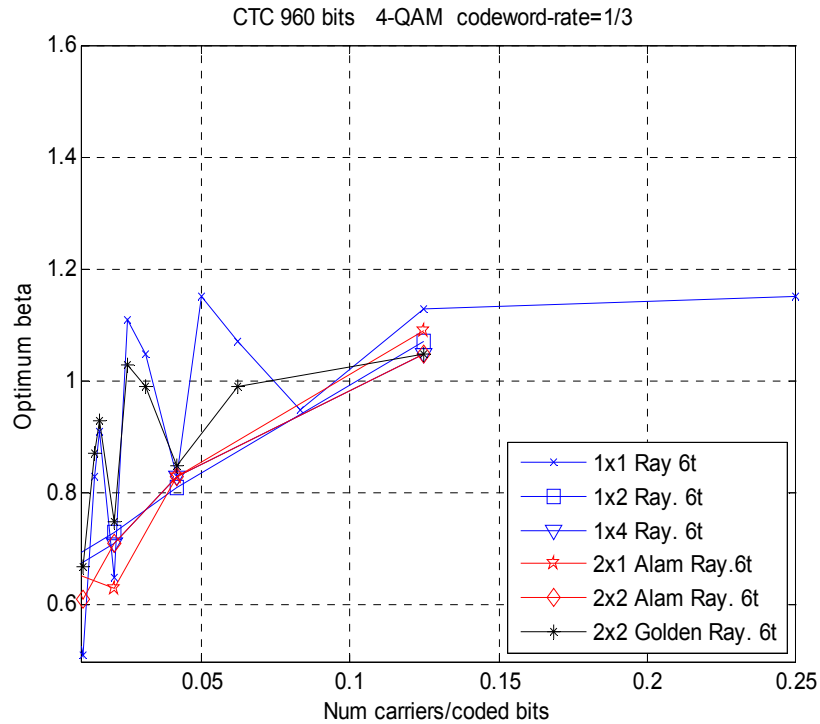
Figure 5.23.- Optimum β as a function of the normalized number of carriers, N_c^{norm}. CTC 960 bits, *r*=1/3, 4-QAM and Rayleigh channel with 6 taps (6 symbols length of equal average power).
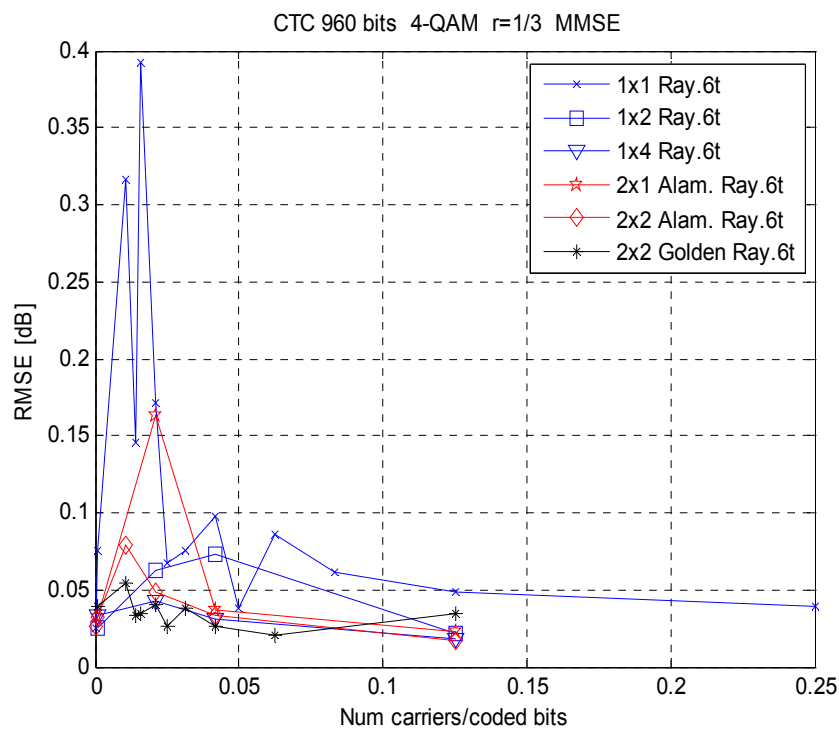

Figure 5.24.- RMSE as a function of the normalized number of carriers, N_c^{norm}. CTC 960 bits, *r*=1/3, 4-QAM and Rayleigh channel with 6 taps (6 symbols length of equal average power).

In Figure 5.23 and Figure 5.24 the optimum β and the RMSE are depicted against the normalized number of data carriers (5.16) for a CTC with N_b=960, codeword rate equal to 1/3

and 4-QAM. It has been considered different realizations of a Rayleigh channel with an impulse response of 6 taps (6 symbols length of equal average power) and different antenna configuration and STC: {1×1, 1×2, 1×4}, {2×1, 2×2} using Alamouti STC and {2×2} using the Golden STC. It can be observed that the optimum β present a similar performance for different configurations, but the RMSE is more reduced when the number of antennas is increased (at receive or transmitter side). In this case, the RMSE at $N_c^{norm} = 0.125$ is around 0.03 dB for all channel configurations except for the {1×1} case which gets a RMSE=0.05 dB. The SISO case also presents the worst RMSE values for low normalized number of carriers (except for single-carrier transmission in that case the RMSE is equal to zero[8]). Other configurations with different codeword rates and type of channel models are investigated in Appendix C (section 5.7).

5.3.1.2.2 Evaluation of the optimum β

Previously, Figure 5.23, Figure 5.24 and appendix C (section 5.7) have shown the dependence of β and RMSE with the number of data carriers, STC, codeword rate, modulation and type of channel model. When the number of carriers per coded bit increases the RMSE value tends to decrease. Thus, the Exp-ESM becomes more accurate when the number of carriers is high.

The goal of this section is to provide how do the optimal β and RMSE vary as a function of the codeword rate for a given modulation, packet size and STC when there is a high number of data carriers. More number of possible codeword rates than in the previous section has been taken into account. As a result, this section (and Appendix D in section 5.8) maps the optimum β and RMSE as a function of the codeword rate for a given configuration of modulation, packet size, STC and channel model.
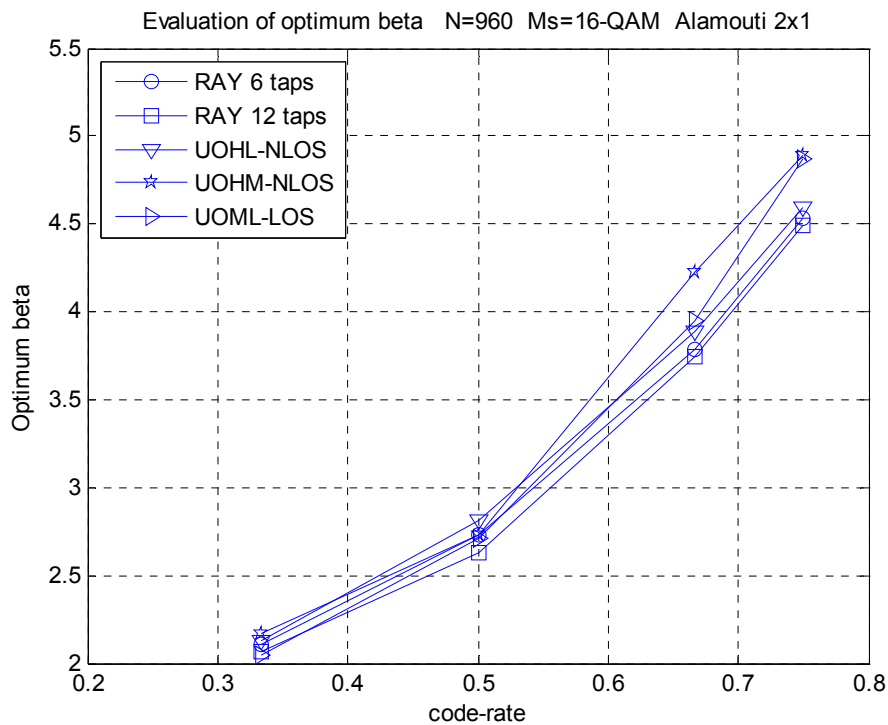
Figure 5.25.- Optimum β as a function of the code rate selected for different type of channels. 1×1 SISO. N_b=960 and 16-QAM.

---

[8] The performance is the same as the AWGN channel where the current SNR depends on the channel.

Evaluation of RMSE   N=960   Ms=16-QAM   Alamouti 2x1
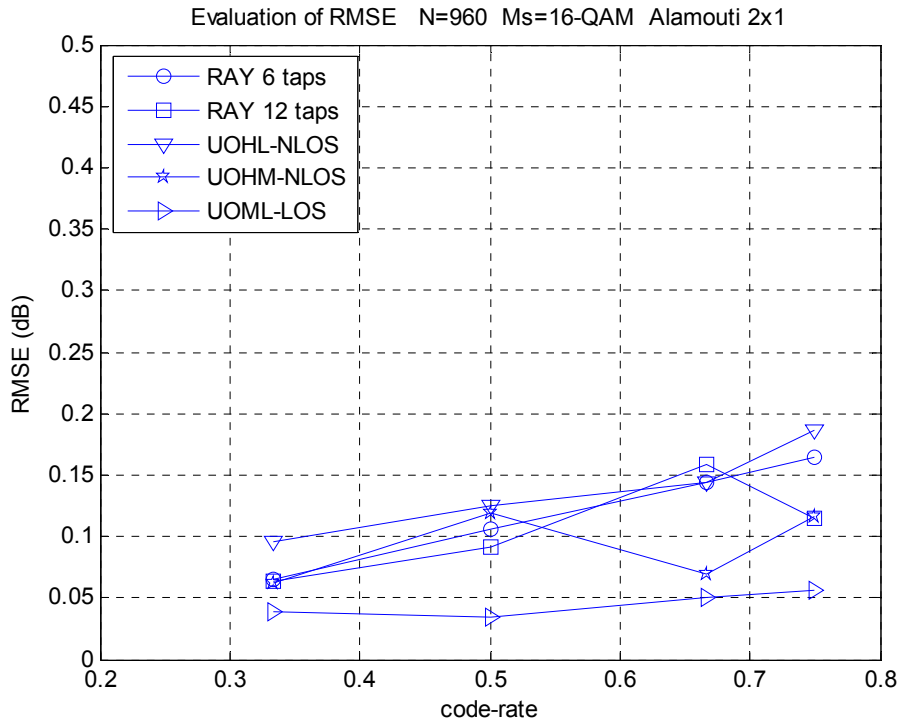
Figure 5.26.- RMSE as a function of the code rate selected for different type of channels. 1×1 SISO. N_b=960 and 16-QAM.

Figure 5.25 and Figure 5.26 illustrate the optimum β and RMSE as a function of the codeword rate. The considered transmission uses N_{OFDM} = 4 OFDM symbols with the maximum number of possible carriers for a CTC code being 960 bits and considering 16-QAM over a MISO channel with Alamouti STC. In those figures different types of channels are considered: Rayleigh (with 6 and 12 taps with 6 and 12 symbols length of equal average power, respectively) and three channels (UOHL-NLOS – Urban Outdoor High to low-NLOS, UOHM-NLOS – Urban Outdoor High to Medium -NLOS and UOML-LOS – Urban Outdoor Medium to Low-LOS) defined in [53] and introduced section 5.7.4 (Appendix C) that considers different types of channel impulse response lengths and antenna correlations. It can be seen that the optimum β seems independent of the channel model and the RMSE is always below of 0.2 dB.

More cases are studied in Appendix D (section 5.8) and [52] and the following conclusions can be drawn:

- The β_{opt} depends on the modulation, packet size, channel type and codeword rate. Although, in some circumstances this value is quasi-independent of the channel type.

- For 4-QAM (Appendix D) the RMSE is independent of the codeword rate and channel type.

- Using 16-QAM the RMSE is larger than using the 4-QAM, nevertheless it is bounded by RMSE<0.25 dB (N_b=960 bits) and RMSE<0.32 dB (N_b=288 bits).

- The RMSE reduces when the packet size increases.

5.3.1.2.3 Using the Exp-ESM for PER prediction

It has been shown that the Exp-ESM is able to get an *effective* SNR that maps the performance of a given MCS over a frequency selective channel with multi-carrier transmission close to the performance of that code over the AWGN channel for such SNR. However, this estimation requires the optimum β value and introduces an estimation error, quantified by the RMSE. Having both in mind, we describe the procedure for predicting the PER for some MCS (see the Figure 5.27):

1. Get the instantaneous SNR of the data carriers over which the message has to be sent. At the receiver this is possible through the pilot signals sent by the source.

2. Taking into account a given STC, build the vector of instantaneous SNR of length $N_{\text{carriers}} \times Q_s$ as defined in (5.12).

3. For a given MCS obtain the effective SNR (γ_{eff}) defined by (5.7) using the optimum β.

4. Get a conservative estimation of the effective SNR ($\hat{\gamma}_{eff}$) taking into account the RMSE. We consider the following modified *effective SNR*

$$\hat{\gamma}_{eff} = \gamma_{eff} - \eta \mu_{error} \quad (dB) \tag{5.18}$$

where μ_{error} is the RMSE defined in (5.15) and η is a parameter that ensures that the reference AWGN-PER is always a worst-case, i.e. the true PER will be lower that the one predicted by the $\hat{\gamma}_{eff}$ using the AWGN-PER curve. Usually $\eta = 2$ is enough.
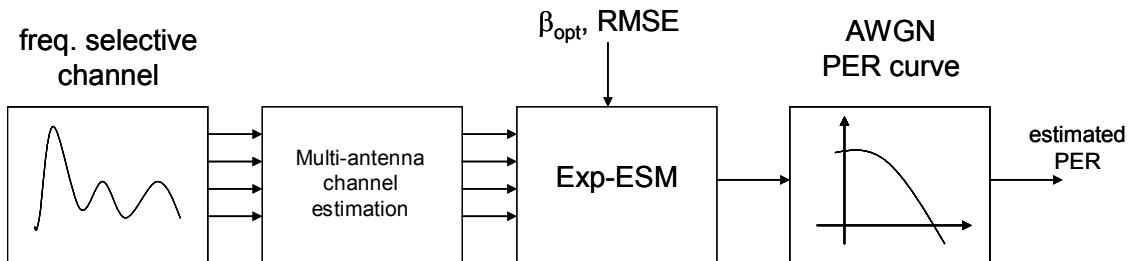
Figure 5.27.- PER estimation.

This process is done at the destination terminal, determining the proper MCS according to the channel realization. In [52] and Appendix D (section 5.8) it is given a list of RMSE and optimum β as a function of the codeword rate for different configurations of the CTC and high number of data carriers.

5.3.1.3 Combination of metrics

Coded transmission in relaying systems is carried out through different links. Two situations might happen: the channels are *orthogonal* or *superposed*. The former situation can be found in systems with retransmissions or relay-assisted transmission under protocol I, while the later situation can be found in systems with multiple transmitting antennas, from a single or multiple terminals, like in the relay-assisted protocols II and III.
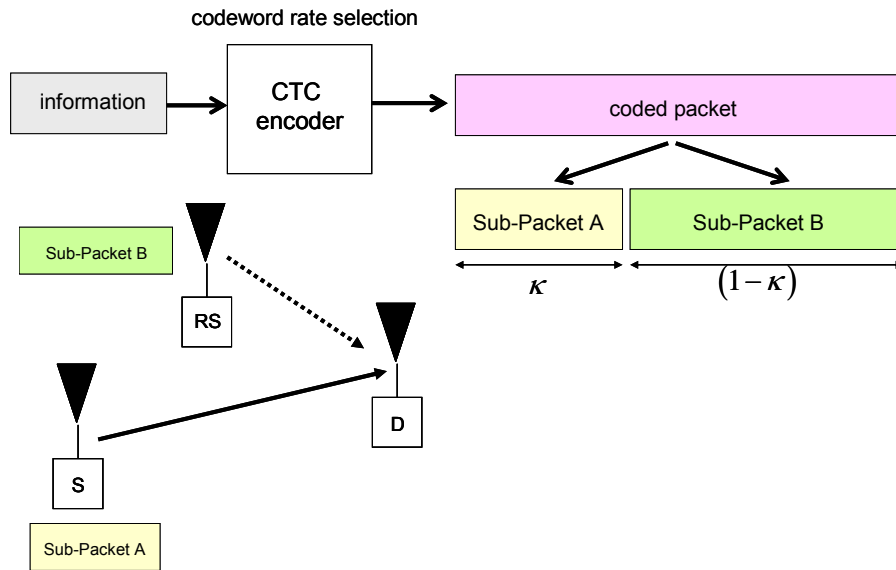
Figure 5.28.- Orthogonal transmission with incremental redundancy . Sub-packet A is transmitted through N_A data carriers and N_{OFDM}^A OFDM symbols, while sub-packet B is using N_B data carriers and N_{OFDM}^B OFDM symbols.

5.3.1.3.1   Orthogonal transmission

Transmitting a given message through orthogonal channels is the principle behind HARQ transmissions. In [39] it is defined how the Exp-ESM method has to be updated to cope with retransmissions. The HARQ can be considered as *chase combining* or *incremental redundancy* according to the data transmitted through the orthogonal channels. In order to easily show the main properties of the different types of transmissions we will assume two orthogonal transmissions. In Figure 5.28 the coded packet is divided into two sub-packets with different size, where the parameter κ defines the fraction of the coded packet allocated to each sub-packet. The transmission of each sub-packet is done orthogonally: there are two nodes that are transmitting to a common destination in orthogonal data regions. The destination uses both transmissions in order to decode the original packet.

Chase combining

In this case the signal transmitted in both orthogonal transmissions is the same: therefore the receiver can combine coherently the same symbols received orthogonally, i.e. with Maximal Ratio Combining (MRC). In Figure 5.28, sub-packet A and sub-packet B are copies of the coded packet. This combination produces an increment of the instantaneous SNR of each symbol, i.e. the final SNR to be considered is

$$\gamma_i = \gamma_i^{(1)} + \gamma_i^{(2)} \tag{5.19}$$

with $\gamma_i^{(j)}$ the SNR in the carrier *i*-th during the *j*-th transmission. The value of β remains unchanged.

Incremental redundancy – same MCS

For *incremental redundancy* the signals transmitted in the orthogonal transmissions are independent but connected to the same message through a FEC code as it is shown in Figure 5.28. The sub-packet A is using N_A data carriers and N_{OFDM}^A OFDM symbols, while sub-packet B employs N_B data carriers and N_{OFDM}^B symbols. A possible implementation would be

the following: assume that we encode a message with a CTC code of codeword rate 1/2, so the coded message can be divided in two parts: *systematic* and *parity*. If the first phase is used to transmit only the *systematic* part, then by receiving only the first transmission we will have the performance of the uncoded message. In the second phase the *parity* part is sent, considering both transmissions we will obtain the performance of a coded message with a CTC of codeword rate 1/2. The predictor must consider the whole transmission during both orthogonal transmissions through all the data carriers. However, the data regions allocated to each phase are in general different depending on the data carriers and OFDM symbols used by both sub-packets. Therefore, we cannot just consider the Exp-ESM defined in (5.7) with N_A+N_B data carriers. We propose to modify the Exp-ESM in the following way,

$$\gamma_{eff} = -\beta \ln \left(\frac{1}{N_A N_{OFDM}^A + N_B N_{OFDM}^B} \left(N_{OFDM}^A \sum_{i=1}^{N_A} \exp\left(-\frac{\gamma_i^{(1)}}{\beta}\right) + N_{OFDM}^B \sum_{i=1}^{N_B} \exp\left(-\frac{\gamma_i^{(2)}}{\beta}\right) \right) \right) \quad (5.20)$$

with $N_A \times N_{OFDM}^A$ and $N_B \times N_{OFDM}^B$ being the data region in terms of number of channel uses in both orthogonal transmissions (number of carriers times OFDM symbols). The total number of carriers is increased by a weighted sum depending on the OFDM symbols of the different data regions. If the number of OFDM symbols used by both sub-packets were equal, equation (5.20) would be the same as (5.7) by using $N_{tot}=N_A+N_B$. Additionally, equation (5.20) can be further described by the *effective SNR* of each orthogonal link,

$$\gamma_A = -\beta \ln \left(\frac{1}{N_A} \sum_{i=1}^{N_A} \exp\left(-\frac{\gamma_i^{(1)}}{\beta}\right) \right) \qquad \gamma_B = -\beta \ln \left(\frac{1}{N_B} \sum_{i=1}^{N_B} \exp\left(-\frac{\gamma_i^{(2)}}{\beta}\right) \right)$$

$$\gamma_{eff} = -\beta \ln \left(\frac{N_A N_{OFDM}^A}{N_A N_{OFDM}^A + N_B N_{OFDM}^B} \exp\left(-\frac{\gamma_A}{\beta}\right) + \frac{N_B N_{OFDM}^B}{N_A N_{OFDM}^A + N_B N_{OFDM}^B} \exp\left(-\frac{\gamma_B}{\beta}\right) \right) \quad (5.21)$$

where γ_A and γ_B denote the effective SNR in the 1st and 2nd transmission respectively. The *effective SNR* of the complete transmission is a weighted sum of the *effective SNR* measured in each link. In a more general way,

$$\gamma_{eff} = -\beta \ln \left(\alpha \exp\left(-\frac{\gamma_A}{\beta}\right) + (1-\alpha) \exp\left(-\frac{\gamma_B}{\beta}\right) \right) \quad \alpha = \frac{N_A N_{OFDM}^A}{N_A N_{OFDM}^A + N_B N_{OFDM}^B} \quad (5.22)$$

where the data regions defined by $N_A \times N_{OFDM}^A$ and $N_B \times N_{OFDM}^B$ depend[9] on α and the modulation selected in the following way,

$$S_A = N_A \cdot N_{OFDM}^A = \kappa \frac{N_b}{r \cdot r_{STC}^A \cdot \log(M)} \qquad S_B = N_B \cdot N_{OFDM}^B = (1-\kappa) \frac{N_b}{r \cdot r_{STC}^B \cdot \log(M)} \quad (5.23)$$

where r is the codeword rate, N_b stands for the packet size, M is the constellation selected in both transmissions, r_{STC}^I and r_{STC}^{II} are symbols/channel use (due to the space-time code (5.1)) in each phase and S_A and S_B are the channel uses allocated to both orthogonal transmissions.

---

[9] This definition is in general different from the one used in chapter 2. In that case α stands for the ratio of the channel uses allocated for the relay-receive and relay-transmit phase, both with the same bandwidth. When the number of data carriers allocated to each orthogonal transmission is the same in (5.22), then both variables are the same.

The symbol rate in each phase may vary because of considering different ST codes at the transmitters. Combining (5.22) and (5.23),

$$\kappa = \frac{\alpha r_{STC}^{A}}{\alpha r_{STC}^{B} + (1-\alpha) r_{STC}^{B}} \qquad (5.24)$$

It is worth noticing that the κ parameter is connected to the definition of the sub-packets (division of the coded packet), while α is relative to the number of channel uses allocated for each orthogonal transmission. Both parameters coincide when the modulation and symbol rate (r_{STC}^{A} and r_{STC}^{B}) selected for both sub-packets is the same.

Incremental redundancy – different MCS

In HARQ systems the retransmissions can be done with different MCS, so that the PER prediction method should also be able to combine metrics of the two orthogonal channels in that situation. In this sense, the transmitted signals in both phases use different modulations, M_A and M_B, respectively. One possible solution pointed out in [39] and defined in [50] is the use of a *demapping penalty.* It consists in applying a reduction to the *effective* SNR depending on the modulation selected and compare all the metrics with the same reference curve, for example 4-QAM. The penalty value is defined by the distance (in terms of dB) between PER curves (at the same PER value) using different modulations in the AWGN channel. All the curves are nearly parallel so the distance at different PER values remains almost constant. Figure 5.29 presents the penalty to be applied to a transmission due to the selected codeword rate and modulation. The difference when PER is equal to 10^{-2} has been measured. For example if the selected codeword rate is 1/3 and the constellation is 16-QAM, then a penalty of 5.65 dB has to be applied to the obtained *effective* SNR in order to use the same AWGN channel PER curve as the codeword rate 1/3 and constellation 4-QAM.
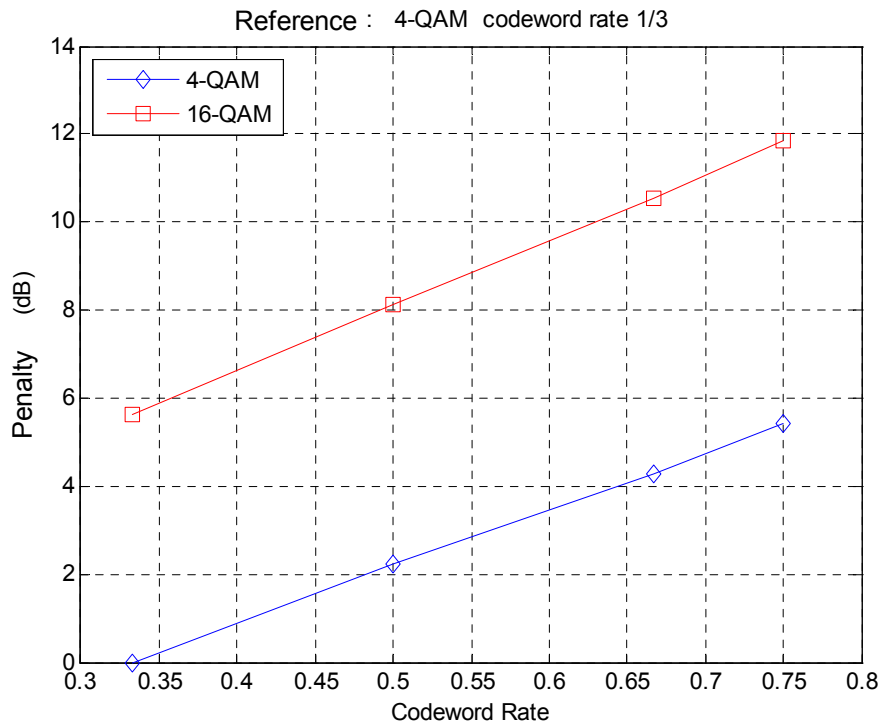
Figure 5.29.- SNR penalty ρ_{AB} as a function of the codeword rate and constellation. Measured at PER=10^{-2}.

The final *effective* SNR of the orthogonal transmission when different modulation is applied to both transmissions is defined as,

$$\gamma_{eff} = -\beta_A \ln\left(\alpha \exp\left(-\frac{\gamma_A}{\beta_A} \right) + (1-\alpha)\exp\left(-\frac{\gamma_B}{\beta_A} \right) \right)$$

$$\gamma_A = -\beta_A \ln\left(\frac{1}{N_A} \sum_{j=1}^{N_A} \exp\left(-\frac{\gamma_j^{(1)}}{\beta_A} \right) \right) \quad \gamma_B = -\frac{1}{\rho_{AB}} \beta_B \ln\left(\frac{1}{N_B} \sum_{j=1}^{N_B} \exp\left(-\frac{\gamma_j^{(2)}}{\beta_B} \right) \right)$$

(5.25)

where γ_A and γ_B are the *effective SNR* in the 1st and 2nd transmission respectively, β_A and β_B denote the parameters used to obtain the effective SNR in each link, N_A and N_B stand for the number of carriers, ρ_{AB} is the penalty to be applied to the effective SNR since two different constellations are used and α is defined in (5.22). The metrics can be readily extended to the combination of more than two transmissions. It has to be noticed that

$$S_A = N_A \cdot N_{OFDM}^A = \kappa \frac{N_b}{r \cdot r_{STC}^A \cdot \log(M_A)} \quad S_B = N_B \cdot N_{OFDM}^B = (1-\kappa)\frac{N_b}{r \cdot r_{STC}^B \cdot \log(M_B)}$$

(5.26)

where M_A, r_{STC}^A and M_B, r_{STC}^B denote the constellation and symbol rate (due to the space-time code (5.1)) selected on each link (orthogonal transmission) and S_A and S_B being the total channel uses. This expression differs from (5.23) because the orthogonal transmissions use different modulation. The parameters κ (ratio between the sub-packets, see Figure 5.28) and α (defined as the ratio between channel uses devoted for each orthogonal transmission (5.22)) are related through,

$$\alpha = \frac{\kappa \cdot r_{STC}^B \cdot \log(M_B)}{\kappa \cdot r_{STC}^B \cdot \log(M_B) + (1-\kappa) \cdot r_{STC}^A \cdot \log(M_A)}$$

(5.27)
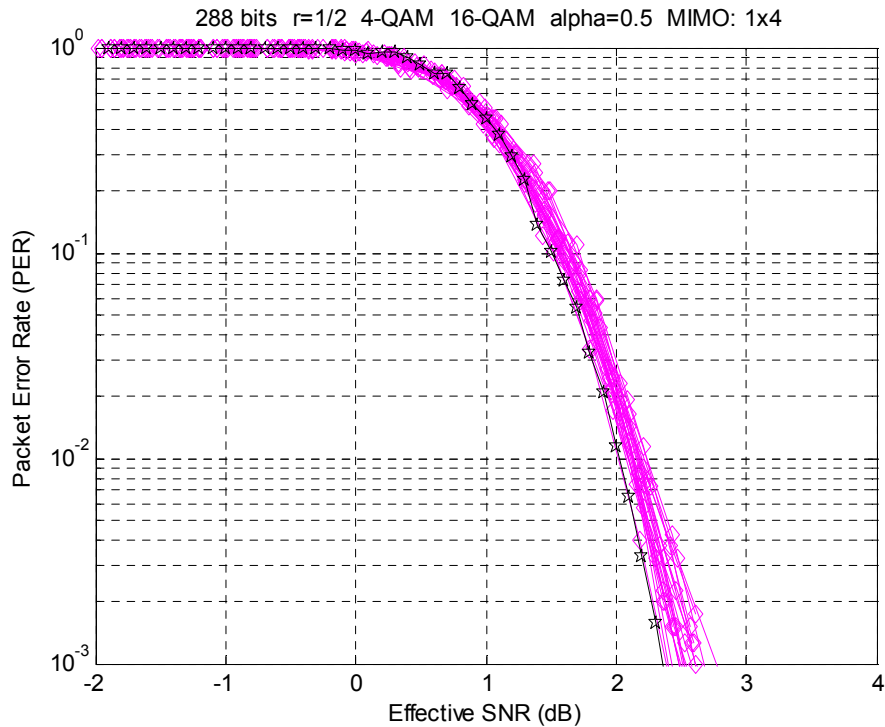
Figure 5.30.- Exp-ESM in orthogonal transmission for various frequency selective channels. α=0.5. M_A=4-QAM and M_B=16-QAM.CTC 288 bits,r=1/2 and MIMO 1×4. Rayleigh 6 taps (6 symbols length with equal average power). ω=10 dB. Reference curve in black stars.

Figure 5.30 presents PER performance of a codeword under different channel realizations as a function of the effective SNR of the Exp-ESM. The transmission scheme is depicted in Figure 5.28 and considers a CTC of 288 bits with codeword rate 1/2 (the total message has 576 coded bits), the source and relay are equipped with a single antenna and the destination has n_d=4 antennas and sub-packet A and B have 288 bits each one (κ=0.5). Different modulations are applied to different parts of the codeword. The modulation selected for the sub-packet A is 4-QAM, while for sub-packet B is 16-QAM. Additionally, those sub-packets are transmitted through independent channel realizations. In this case the channel B has an average SNR ω=10 dB higher than the channel A. The equivalent effective SNR is calculated as indicated by (5.25). When the actual PER values are plotted as a function of the effective SNR (diamond line), results are close to the reference curve (star line). Additional results are presented in Appendix C (section 5.9).
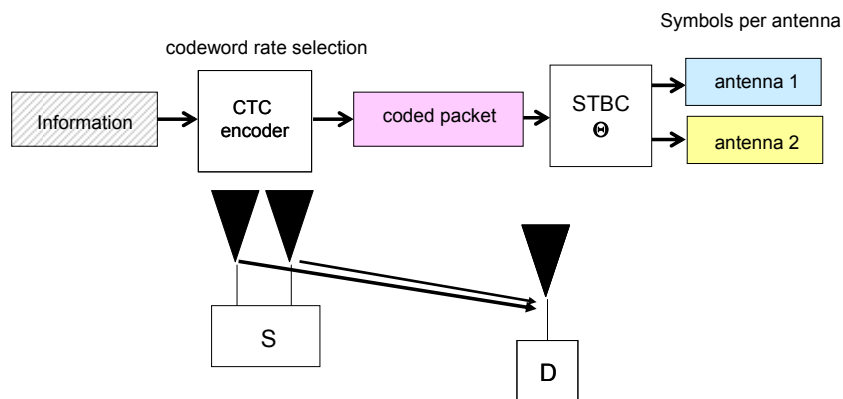
Figure 5.31.- Superposed transmission of the same message. MISO system with a STC.

5.3.1.3.2 Superposed transmission coding

Two options have to be considered when superposed transmission occurs: transmissions referencing the same message (not necessarily the same symbols) using a single CTC encoder or transmission involving independent messages encoded separately. Different reception techniques are considered in each case.

The former case is a situation that is typically found in MIMO systems with a STC distributing the symbols through all the antennas (see Figure 5.31). In such a case the receiver decodes simultaneously all the received symbols. In section 5.3.1.2 it has been shown that this scenario is transparent to the Exp-ESM. The predictor method already subsumes the SNR of the different symbols at the receiver, so that the signal model defined in (5.8) is still valid.

On the other hand, when the transmitted messages are independent as it happens in MIMO systems when each antenna transmits an independent stream or in a Multiple Access Channel (MAC), the receiver decodes the messages by *successive decoding*[10]. This scheme becomes asymptotically optimum as the error probability of intermediate decisions decreases with the codeword length of the messages [40]. Figure 5.32 depicts the simultaneous transmission of two coded packets. Packet A is transmitted through N_A data carriers and N_{OFDM}^A OFDM symbols, while packet B uses N_B data carriers and N_{OFDM}^B OFDM symbols. Some part of the data regions is superposed. We assume that the receiver decodes them in three steps. First, it decodes the *strongest* message considering the other one as additive noise. Afterwards, the

---

[10] This technique also can be used with superposed transmission of the same message (i.e. using non-orthogonal STC as VBLAST).We consider *successive decoding* when the messages are coded by independent CTC encoders.

contribution of that message into the incoming signal is subtracted using the estimated message. Finally, the receiver decodes the remaining message.
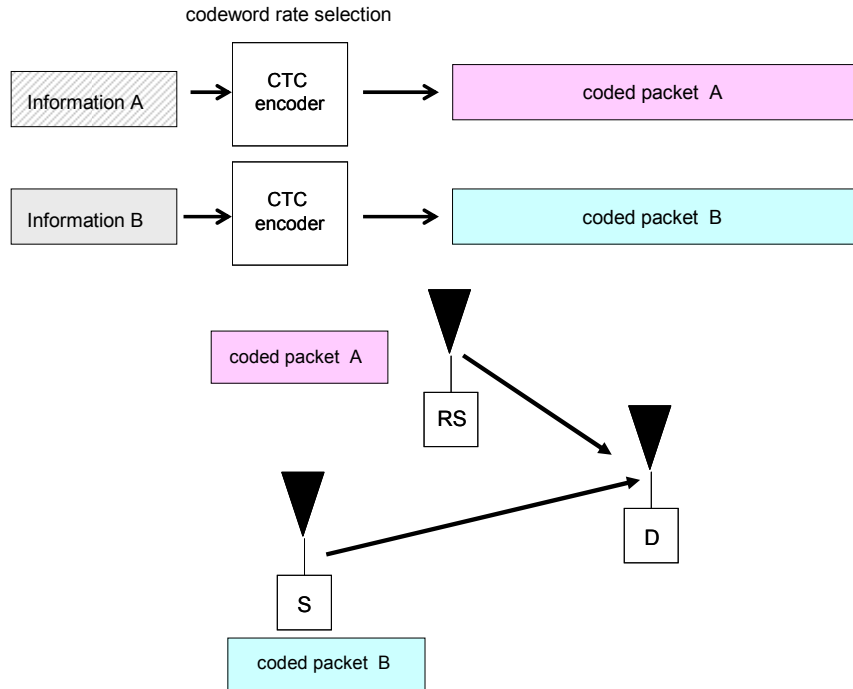

Figure 5.32.- Superposed transmission of two independent messages coded with different CTC encoders. Packet A is transmitted through N_A data carriers and N_{OFDM}^A OFDM symbols, while packet B uses N_B data carriers and N_{OFDM}^B OFDM symbols. Some part of the data regions allocated for both packets are superposed.

There are two issues to tackle in this type of transmission:

The decoding order

In order to establish which message has to be decoded first, we can make use both the *effective* SNR (associated to different channels) and the selected MCS of each message. If both messages have the same MCS then the one with the largest effective SNR will be the first. When the messages use different MCS then the message with the smallest estimated PER (using the *effective* SNR) will be the first.

Modification of the Exp-ESM for the first message to be decoded

The *strongest* message is decoded assuming that the other message is additive noise. Therefore, the exp-ESM has to be modified accordingly,

$$\tilde{\gamma}_{eff} = -\beta \log\left(\frac{1}{N_c}\sum_{i=1}^{N_c}\exp\left(-\frac{\tilde{\gamma}_i}{\beta}\right)\right) \qquad \tilde{\gamma}_i = \frac{\gamma_i^{(s)}}{1+\gamma_i^{(o)}} \tag{5.28}$$

where N_c is the number of carriers used the *strongest* message (N_A or N_B), $\gamma_i^{(s)}$ denotes the instantaneous SNR on the *i*-th carrier and $\gamma_i^{(0)}$ is the instantaneous SNR of the other message in those common carriers, otherwise $\gamma_i^{(0)}$ is set to zero. Notice that the decoding order is fixed for the whole coded packet because the first packet only can be only subtracted of the incoming signal after decoding.

The Packet Error Rate (PER)[11] of the *superposed transmission* of independent messages is evaluated taking into account that both messages have to be correctly decoded. This can be modeled by,

$$PER = \begin{cases} 1-\left(1-PER\left(\tilde{\gamma}_{eff}^{(A)}\right)\right)\left(1-PER(\gamma_B)\right) & \gamma_A \geq \gamma_B \\ 1-\left(1-PER\left(\tilde{\gamma}_{eff}^{(B)}\right)\right)\left(1-PER(\gamma_A)\right) & \gamma_A < \gamma_B \end{cases} \tag{5.29}$$

where γ_A, γ_B are the effective SNR of the links A y B (see Figure 5.32) and $\tilde{\gamma}_{eff}^{(x)}$ where $x=\{A,B\}$ stands for the equivalent *effective* SNR when the strongest message (x) is decoded first, as is indicated in (5.28).

Figure 5.33 presents the estimated and the actual PER of a packet made up of two independent messages (codewords) transmitted to a common destination through three different channel realizations, as it was shown in Figure 5.32. The average SNR of the channel B is ω=0 dB higher than channel A. The destination is receiving both packets simultaneously. In order to decode both packets the process described previously is applied, obtaining an estimated PER, as presented in (5.29). Notice that for estimating the total error performance we must consider the effective SNR of the channels A and B. Results are plotted against the effective SNR measured in channel A. Moreover, here, we do not have a single reference PER curve as happened in the previous sections. The estimated curve is built from the PER values under AWGN using the effective SNR measured in channel A and B and using (5.29). It can be observed that the prediction is close to the true performance. In order to measure the error due to the estimation,
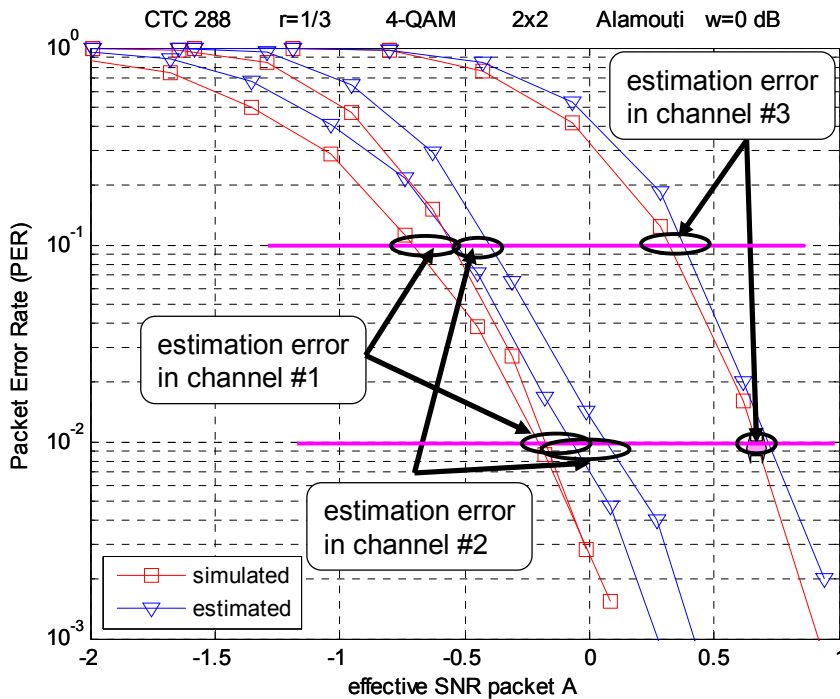
Figure 5.33.- PER of the superposed transmission vs. effective SNR of packet A. Two messages (A,B) where the mean SNR of the different links: SNR$_B$=SNR$_A$+0 (dB). Both with N_b=288, 4-QAM and r=1/3. Rayleigh channel with 6 taps with the same average power. Alamouti STC. n_s=n_r=2, n_d=2.

---

[11] In this case, the packet consists in the addition of two independent codewords
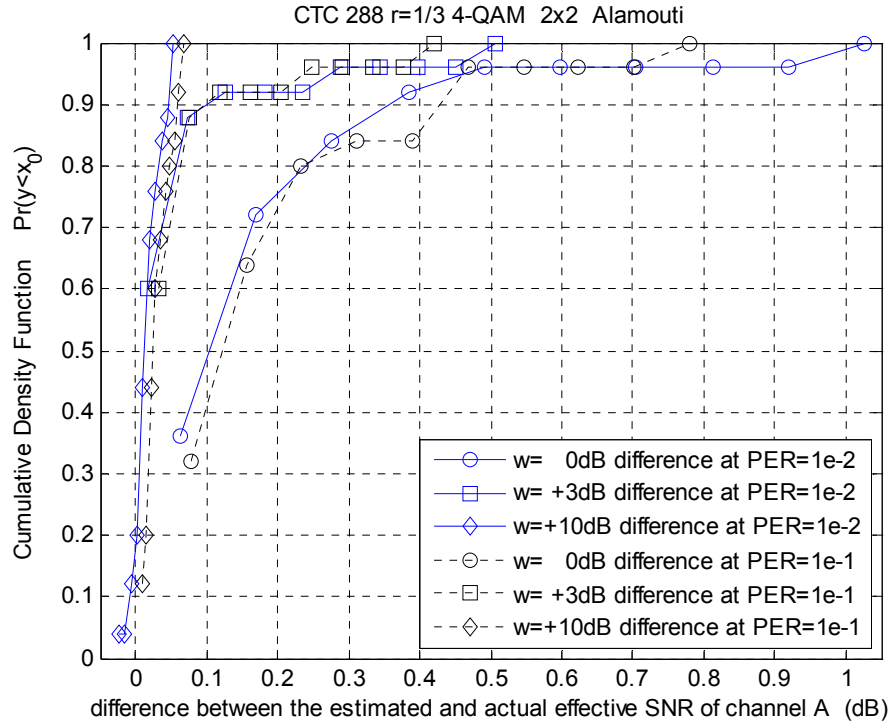
Figure 5.34.- CDF of the difference between the effective SNR of channel A required for getting the same PER values for the estimation and actual scenario (see Figure 5.33) in superposed transmission: $SNR_B=SNR_A+\omega$ (dB). $\omega=\{0,3,10\}$. Both with N_b=288, 4-QAM and r=1/3. Rayleigh channel with 6 taps with the same average power. Alamouti STC. $n_s=n_r$=2, n_d=2.

Figure 5.34 presents the cumulative density function (CDF) of the differences of required SNR to get a target PER between the estimation and the actual value (Figure 5.33) at values PER=$\{10^{-1}, 10^{-2}\}$. When the difference between the average SNR of the channels A and B is ω=0 dB, it can be seen that the error due to the estimation is less than 0.35 dB at PER=10^{-2} (solid lines with circles in Figure 5.34) and lower than 0.42 dB at PER=10^{-1} (dotted lines with circles in Figure 5.34) for the 90% of the channel realizations. Moreover, when the difference between the average SNR of the channels increases the estimation is closer to the true performance. For example, when ω=3 dB, for the 90% of channel realizations the error due to the estimation is less than 0.1 dB and for ω=10 dB the error lower than 0.05 dB.

5.3.2 Error prediction for relaying systems

The objective of this section is to characterize the overall PER of relay-assisted systems as a function of the individual PER of each link. Let us assume that the PER in each link is given by a function,

$$PER = f(MCS, \gamma, N_b) \tag{5.30}$$

that depends on the size of the block, the channel quality indicator γ (i.e. the *effective* SNR[12]) and the rate of the MCS defined by,

---

[12] Note that the derivation of PER is also valid for single-carrier systems. In that case, the instantaneous SNR should be considered, (effective SNR with a single carrier, N_c=1).

$$R = \left(\frac{Q_s}{T}\right) \cdot \log(M) \cdot r_c = r_{STC} \cdot \log(M) \cdot r_c = r \cdot \log(M) \tag{5.31}$$

where Q_s is the number of transmitted symbols by the STC, T is the channel uses per symbol, r_{STC} the symbol rate, M is the number of bits of the constellation and r_c is the FEC codeword rate. The symbol rate of the STC and the FEC codeword rate can be grouped in the variable r. The function defined in (5.30) will also depend on the number of antennas at each link, and the spatial correlation among them [51]. It has been shown in section 5.3.1.2 that the Exp-ESM method can cope with the effect of the number of antennas when STC is used because it considers the measured SNR at the output of the receiver (see equation (5.12)).

In the derivation of the equivalent PER of the different relay-assisted protocols (see chapter 2 for a description of protocols) it is assumed that the relay terminal is not generating any retransmission request, only the destination terminal, and the whole transmission is centralized at the source. In all cases we are considering that either a single message (in forwarding and protocol I) or a couple of messages (in protocols II-B and III) are to be delivered from the source to the destination. If a couple of messages are sent, both have to be correctly decoded at the destination. The selection of a certain MCS in every phase of the protocol, according to the channel state, allows detection with a certain probability of error or a maximization of the throughput.

5.3.2.1 Forwarding protocol

In the forwarding scheme, the source encodes a packet of size N_b bits with a FEC using a given MCS and transmits to the relay in the phase I (*relay-receive phase*) of the relay-assisted transmission as is indicated in Figure 5.35. Afterwards, the relay decodes the packet and re-encodes the N_b bits with possibly a different FEC code and MCS, transmitting it to the destination during phase II (*relay-transmit phase*). Therefore, the total Packet Error Rate (PER) for the forwarding transmission is given by

$$PER_F = f_{RD}(MCS_{RD}, \gamma_{RD}, N_b) + f_{SR}(MCS_{SR}, \gamma_{SR}, N_b)\left(1 - f_{RD}(MCS_{RD}, \gamma_{RD}, N_b)\right) \tag{5.32}$$

where $f_{SR}()$ and $f_{RD}()$ denote the PER for a given MCS and *effective* SNR (γ) of each link for a packet of size N_b bits. The PER curves depend on the length of the packet to be transmitted, so the calculation of (5.32) must be done for different packet sizes.
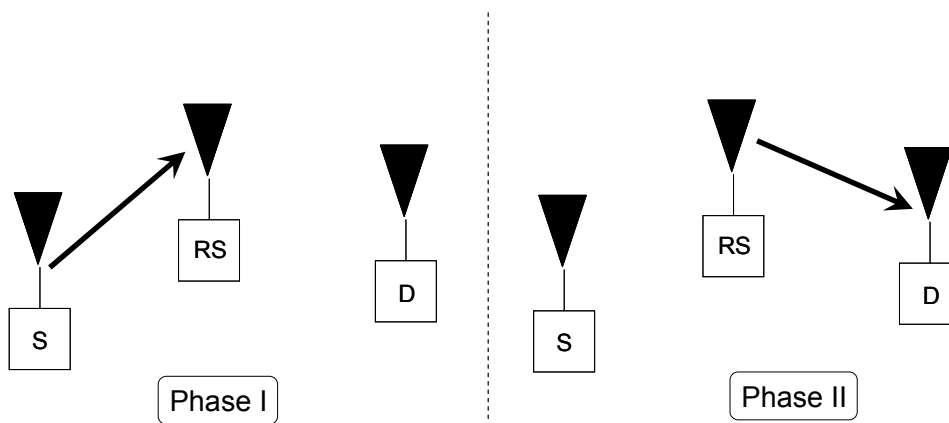

Figure 5.35.- Forwarding protocol of the relay-assisted transmission.

The channel uses consumed by this protocol in each orthogonal phase (φ_I and φ_{II}) depends on the codeword rate, modulations and packet size considered,

$$\varphi_I = \frac{N_b}{r_{SR}\log(M_{SR})} \qquad \varphi_{II} = \frac{N_b}{r_{RD}\log(M_{RD})} \tag{5.33}$$

where N_b is the information bits, r_{SR} and r_{RD} consider the FEC codeword rate and the STC symbol rate, (5.31), and M_{SR} and M_{RD} denote the modulations selected in each phase. The duration ratio between the channel uses allocated for phase I and phase II is given by,

$$\alpha = \frac{\varphi_I}{\varphi_I + \varphi_{II}} \tag{5.34}$$

5.3.2.2   Protocol I

Here, the source encodes a packet of size N_b bits with a FEC using a given MCS and transmits to the relay in phase I (*relay-receive phase*). That transmission is also received by the destination, see Figure 5.36. The relay decodes the packet and re-encodes the N_b bits with the same FEC and possibly with a different MCS, transmitting it to the destination during phase II (*relay-transmit phase*) of the relay-assisted transmission. The destination combines the signal received in both phases. Hence, the orthogonal transmission model (see Figure 5.28) is valid for this protocol because the destination receives a codeword transmitted by two terminals in orthogonal time slots. The duration of each phase is fixed beforehand. The PER for protocol I can be expressed as,

$$PER_{\mathrm{Prot\text{-}I}} = f_{SR}(MCS_{SR}, \gamma_{SR}, N_b)f_{SD}(MCS_{SR}, \gamma_{SD}, N_b) + {} $$
$$ {}+ f_{SR-D}(MCS_{SR}, MCS_{RD}, \gamma_{SR-D}, N_b)(1 - f_{SR}(MCS_{SR}, \gamma_{SR}, N_b)) \tag{5.35}$$

where $f_{SR}()$ denotes the PER for a given MCS and *effective* SNR of the source-relay link and $f_{SR\text{-}D}()$ stands for the PER after the combination of the source-relay to destination transmissions. It has to be emphasized that the source-relay to destination link (SR-D), see Figure 5.36, presents the same structure that the orthogonal transmission described in Figure 5.28. Therefore the Exp-ESM predictor for the SR-D link is described by (5.25).
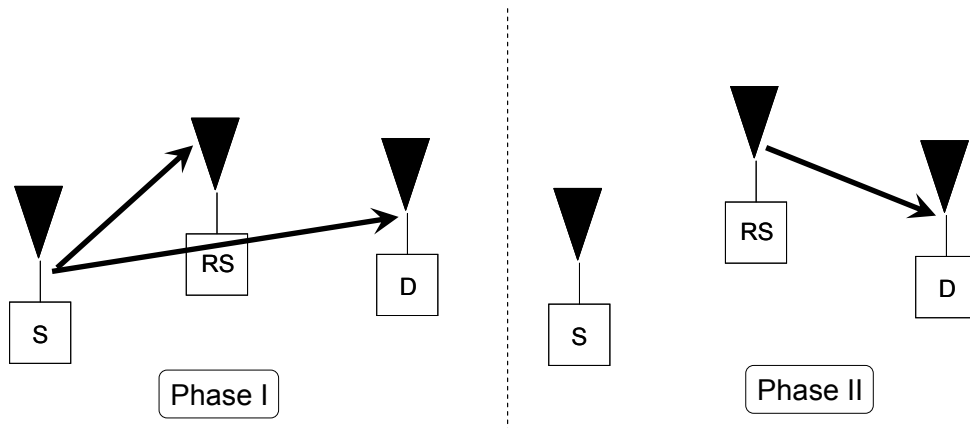

Figure 5.36.- Protocol I of the relay-assisted transmission.

The channel uses consumed by this protocol in each phase (φ_I and φ_{II}) depend on the codeword rate, modulations, the packet size considered and the ratio between each phase. In this protocol the codeword is transmitted in two orthogonal time slots, the FEC codeword rate r must be kept the same in both transmissions but the STC symbol rate may change,

$$\varphi_I = \kappa \frac{N_b}{r \cdot r_{STC}^{SR} \cdot \log(M_{SR})} \qquad \varphi_{II} = (1-\kappa) \frac{N_b}{r \cdot r_{STC}^{RD} \cdot \log(M_{RD})} \qquad (5.36)$$

where N_b is the information bits, r denotes the codeword rate, M_{SR}, r_{STC}^{SR} and M_{RD}, r_{STC}^{RD} stand for the modulations and STC symbol rate selected in each phase and κ the ratio between the message sent in the both phases as was shown in Figure 5.28. This parameter is connected with the ratio of the duration of each relay phase as (the inverse of (5.27)),

$$\kappa = \frac{\alpha \cdot r_{STC}^{SR} \cdot \log(M_{SR})}{\alpha \cdot r_{STC}^{SR} \cdot \log(M_{SR}) + (1-\alpha) \cdot r_{STC}^{RD} \cdot \log(M_{RD})} \qquad (5.37)$$

with α defined in (5.34). If both modulations are equal and $r_{STC}^{SR} = r_{STC}^{RD}$ then $\kappa = \alpha$. It is worth mentioning that the assisting relay must be able to decode the message sent by the source during phase I (*relay-receive phase*). Thus, if the aggregate message to be sent to the destination in both phases has codeword rate r, i.e. N_b/r coded bits, the selected α or κ must ensure that at least N_b bits will be transmitted in phase I. In fact the number of coded bits received by the assisting relay is $N_b \kappa / r$. The message sent only during phase I has the following codeword rate,

$$r_{phaseI} = \frac{N_b}{N_b \frac{1}{r} \kappa} = \frac{r}{\kappa} = r \left(1 + \left(\frac{1-\alpha}{\alpha}\right) \frac{r_{STC}^{RD} \cdot \log(M_{RD})}{r_{STC}^{SR} \cdot \log(M_{SR})}\right) < 1 \qquad (5.38)$$

The value of α establishes codeword rates allowed in our transmission. For example if M_{SR}=16 QAM, M_{RD}=4 QAM, $r_{STC}^{SR} = r_{STC}^{RD} = 1$ and α=0.1 the maximum codeword rate is r=0.1818, in such a case, the assisting relay receives a codeword that contains no redundancy.

5.3.2.3 Protocol II

In this protocol during phase I (*relay-receive* phase) the source transmits to the relay terminal and afterwards the source and relay transmit simultaneously to the destination, see Figure 5.37. The PER for protocol II can be expressed by,

$$\begin{aligned} PER_{P-II} &= f_{SR-D}(MCS_{RD}, MCS_{SD}, \gamma_{RD}, \gamma_{SD}) + \\ &+ f_{SR}(MCS_{SR}, \gamma_{SR})(1 - f_{SR-D}(MCS_{RD}, MCS_{SD}, \gamma_{RD}, \gamma_{SD})) \end{aligned} \qquad (5.39)$$

where $f_{SR}()$ is the PER for a given MCS and *effective* SNR of the source-relay link and $f_{SR-D}()$ stands for the PER during the source-relay transmission during phase II (*relay-transmit phase*). Nevertheless, depending on the type of messages transmitted by the source and the

relay during phase II the PER at the SR-D link ($f_{SR-D}()$) can be modeled by two different expressions associated to protocols IIA and IIB. Both possibilities have been considered in section 5.3.1.3, *superposed transmissions* with the same message, see Figure 5.31, or independent messages, see Figure 5.32.
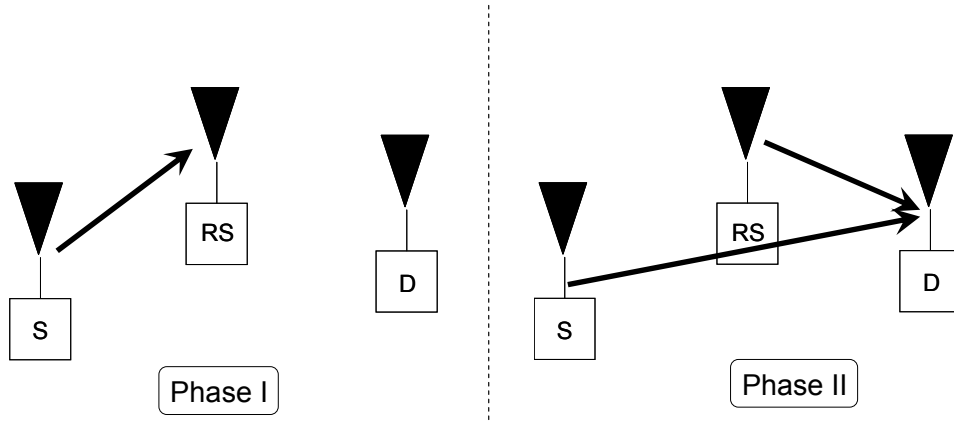

Figure 5.37.-Protocol II of the relay-assisted transmission.

Protocol IIA

This protocol is similar to the forwarding case since the relay must be able to decode all the data to be transmitted to the destination by the relay-assisted protocol. This is required because during phase II, both the source and relay transmits jointly the same message to the destination by using distributed space time codes, as was presented in Figure 5.31. In this regard, a single packet of size N_b bits is transmitted. Therefore, in this protocol the MCS selected by the relay and the source in phase II must be the same and the source-relay to destination link can be seen as a conventional MIMO system where STC is distributed between the source and relay, see Figure 5.5. Under these assumptions the Exp-ESM predictor can be applied without any modification as was shown in section 5.3.1.2 when the Exp-ESM is extended for STCs (at the receiver the different SNR of the distributed antennas is already considered).

$$\begin{cases} f_{SR}(MCS_{SR},\gamma_{SR}) = f_{SR}(MCS_{SR},\gamma_{SR},N_b) \\ f_{SR-D}\left(MCS_{SD},MCS_{RD},\gamma_{SD},\gamma_{RD}\right) = f_{SR-D}\left(MCS_{RD},\gamma_x,N_b\right) \end{cases}$$

$$\gamma_x = ExpESM\left(\gamma_{SD},\gamma_{RD}\right)$$

(5.40)

where γ_x stands for the *effective SNR* of the equivalent MIMO system with the distributed STC where the instantaneous SNR of the different data carriers has to be considered in order to get the instantaneous SNR of each symbol transmitted, see equation (5.12). The instantaneous channels of the source-destination and relay-destination link are included in the matrix $\mathbf{H}_{eq}$ (5.8).

The final expression of the PER is given by (5.39) using definitions of (5.40). The channel uses required for this protocol have the same expression as the forwarding protocol, (5.33).

Protocol IIB

In contrast to the previous case, now the source transmits a new and independent message to the destination in the *relay-transmit phase*, which will be receiving two independent messages

with different MCS and code length, as was depicted in Figure 5.32. Hence the packet sizes are N_{b1} and N_{b2}, for the message sent in the *relay-receive* and *relay-transmit phase* from the source. Both have to be decoded by *successive decoding*[13]. Following the same guidelines as in section 5.3.1.2.3, the *strongest* message has to be decoded first and the PER in the source-relay to destination link will be defined by,

$$\begin{cases} f_{SR}(MCS_{SR}, \gamma_{SR}) = f_{SR}(MCS_{SR}, \gamma_{SR}, N_{b1}) \\ f_{SR-D}(MCS_{SD}, MCS_{RD}, \gamma_{SD}, \gamma_{RD}) = \\ \qquad = \begin{cases} 1 - \left(1 - f_{RD}(MCS_{RD}, \tilde{\gamma}_{RD}, N_{b1})\right)\left(1 - f_{SD}(MCS_{SD}, \gamma_{SD}, N_{b2})\right) & \gamma_{RD} > \gamma_{SD} \\ 1 - \left(1 - f_{RD}(MCS_{RD}, \gamma_{RD}, N_{b1})\right)\left(1 - f_{SD}(MCS_{SD}, \tilde{\gamma}_{SD}, N_{b2})\right) & otherwise \end{cases} \end{cases} \tag{5.41}$$

where MCS_{RD}, MCS_{SD} stand for the MCS selected in the message transmitted in relay-destination and source-destination (in phase II) links, respectively, γ_x stands for the *effective* SNR in the x-th link and $\tilde{\gamma}_x$ is the *effective* SNR when the strongest message belongs to the x-th link and is calculated as is indicated in (5.28).

The total PER is given by (5.39) with the particularization of (5.41). Additionally, the channel uses required for this protocol are,

$$\varphi_I = \frac{N_{b1}}{r_{SR}\log(M_{SR})} \qquad \varphi_{II} = \max\left(\frac{N_{b1}}{r_{RD}\log(M_{RD})}, \frac{N_{b2}}{r_{SD}\log(M_{SD})}\right) \tag{5.42}$$

where r_{SR}, M_{SR} and r_{RD}, M_{RD} denote the configuration used for the packet of N_{b1} bits transmitted during each phase, r_{SD}, M_{SD} is relative to the packet of N_{b2} information bits transmitted by the source in phase II. The data rates r_{SR} and r_{SD} consider the FEC code and STC symbol rate, (5.31). Notice that in phase II there are two simultaneous transmissions, so that the channel uses are defined by that message which requires more number of channel uses. This protocol transmits $N_b = N_{b1} + N_{b2}$ bits.

5.3.2.4 Protocol III

This protocol (which corresponds to protocol IIIA defined in chapter 2) can be seen as a combination of protocol I and IIB. During phase I (*relay-receive phase*) the source transmits a message to the relay terminal, but this message is also received by the destination, see Figure 5.38. In phase II (*relay-transmit phase*), the relay decodes the message received in phase I, re-encodes and transmits to the destination. In phase II the source also transmits a new and independent message. In this case, the destination manages to decode two independent messages as in protocol II-B (by *successive decoding*), and it can also use the signal received during phase I (as in protocol I) for decoding the message that comes through the relay.

The total PER[14] depends on which packet is decoded first. For example, assuming that the *strongest* message is the one transmitted by the assisting relay in phase II the PER will be defined by,

---

[13] Both messages use independent CTC encoders.
[14] Both messages have to be decoded correctly.

$$PER_{\text{Prot-}III} = 1 - (1-\lambda_1)(1-\lambda_2)$$

$$\lambda_1 = f_{SR}(MCS_{SR}, \gamma_{SR}) f_{SD}(MCS_{SR}, \gamma_{SD}^{(1)}) +$$

$$+ f_{SR-D}(MCS_{SR}, MCS_{RD}, \gamma_{SR-D})(1 - f_{SR}(MCS_{SR}, \gamma_{SR})) \qquad (5.43)$$

$$\lambda_2 = f_{SD}(MCS_{SD}, \gamma_{SD}^{(2)})$$

$$\gamma_{SR-D} = -\beta_A \ln\left(\alpha \exp\left(\frac{-\gamma_{SD}^{(1)}}{\beta_A} \right) + (1-\alpha) \exp\left(\frac{-\tilde{\gamma}_{RD}/\rho_{AB}}{\beta_A} \right) \right)$$

where $\gamma_{SD}^{(1)}$ and $\gamma_{SD}^{(2)}$ are connected with the SNR in the source-destination link during phase I and II of the relay-assisted transmission, respectively, $\tilde{\gamma}_{RD}$ is the *effective* SNR when the message transmitted by the relay is decoded first and is calculated as shows (5.28). Moreover, now $f_{SR-D}()$ is used to model the PER of the message that comes from the source in phase I and from the assisting relay during phase II, as in protocol I with effective SNR γ_{SR-D}, following equation (5.25). Otherwise, if the message sent by the source in phase II is the first to be decoded then,

$$PER_{\text{Prot-}III} = 1 - (1-\lambda_1)(1-\lambda_2)$$

$$\lambda_1 = f_{SR}(MCS_{SR}, \gamma_{SR}) f_{SD}(MCS_{SR}, \gamma_{SD}^{(1)}) +$$

$$+ f_{SR-D}(MCS_{SR}, MCS_{RD}, \gamma_{SR-D})(1 - f_{SR}(MCS_{SR}, \gamma_{SR})) \qquad (5.44)$$

$$\lambda_2 = f_{SD}(MCS_{SD}, \tilde{\gamma}_{SD}^{(2)})$$

$$\gamma_{SR-D} = -\beta_A \ln\left(\alpha \exp\left(\frac{-\gamma_{SD}^{(1)}}{\beta_A} \right) + (1-\alpha) \exp\left(\frac{-\gamma_{RD}/\rho_{AB}}{\beta_A} \right) \right)$$

where $\tilde{\gamma}_{SD}^{(2)}$ is calculated assuming the signal from the relay adds noise to the message from the source, as in (5.28).
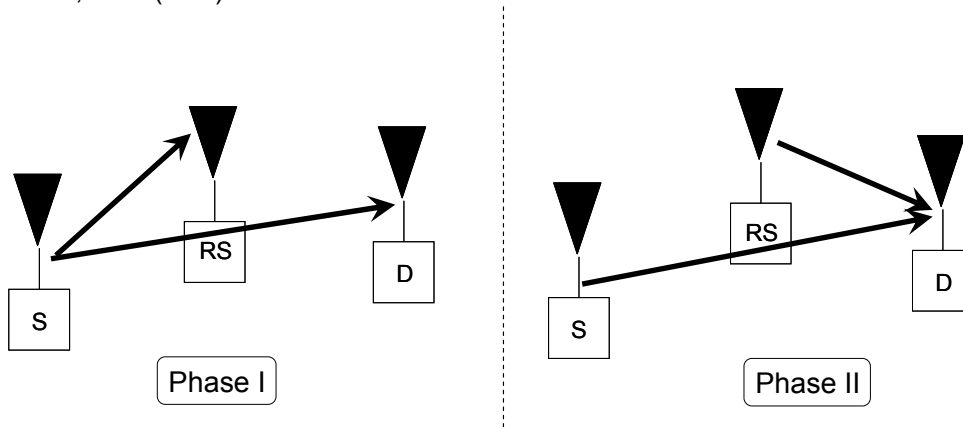

Figure 5.38.- Protocol III of the relay-assisted transmission.

The channel uses needed by this protocol will also be a combination of the ones required for protocol I and protocol II, as follows,

$$\varphi_I = \kappa \frac{N_{b1}}{r_1 \cdot r_{STC}^{SR} \cdot \log(M_{SR})} \qquad \varphi_{II} = \max\left(\frac{(1-\kappa)N_{b1}}{r_1 \cdot r_{STC}^{RD} \cdot \log(M_{RD})}, \frac{N_{b2}}{r_{SD} \log(M_{SD})} \right) \qquad (5.45)$$

where r_1, M_{SR} and M_{RD} denote the configuration used for the packet of N_{b1} information bits transmitted during phase I ($N_{b1}\kappa/r_1$ coded bits) and II (N_{b1}/r_1 coded bits in both phases in

total), r_{STC}^{SR} and r_{STC}^{RD} are the STC symbol rate considered in phase I and II, respectively. Finally, r_{SD} (which also considers the STC symbol rate employed for this transmission, (5.31)), M_{SD} are relative to the packet of N_{b2} information bits transmitted by the source in phase II (N_{b2}/r_{SD} coded bits) and κ is the ratio between data sent in both phases, see Figure 5.28. Its connection to the ratio between the channel uses in both phases (α) is defined by (5.37) as in protocol I when the channel uses due to the direct transmission in the phase II are less than the channel uses required by the transmission from the relay. In such a case, for a given α the maximum codeword rate for the message sent in both phases also depends on equation (5.38).

5.3.3 Dynamic link performance control

When the transmitter has some knowledge about the current channel state, it can adapt its transmission in function of that channel realization. The previous section has shown that it is possible to predict the PER for a given MCS as a function of the *effective* SNR (Exp-ESM). Departing from this point, this section proposes algorithms to control the link level parameters in function of the service requirements. Basically, they maximize the *transmission rate* or they maximize the *throughput*. However, in both cases, because of the discrete nature of the values of the modulation, codeword rate and packet size, a search over all possible combinations of MCS and packet lengths should be done. Additionally, the data region can be defined beforehand or become an additional variable to be designed. The optimization is based on *exhaustive search*.

Direct transmission

Let us define

N_b : Total number of encoded bits
r : Codeword rate (considering the FEC code rate and STC symbol rate)
M : number of symbols in the modulation
S : size of the data region in number of time-frequency channel uses
φ : channel uses employed by the selected configuration $\varphi = N_b /\left(r \cdot \log(M) \right)$
γ : the effective SNR of the channel
$PER\left(N_b, r, M, \gamma \right)$: The estimated PER which depends on the packet size, codeword rate, modulation and effective SNR.

There are two cases:

1. <u>Case 1</u>.- The size of the data region in terms of time-frequency channel uses (S) is not given a priori.

   Criterion 1. *Maximize the transmission rate*

   $$\max_{N_b,r,M,S} \frac{N_b}{S}$$
   $$\text{s.t.} \quad PER(N_b,r,M,\gamma) \le P_0 \qquad\qquad (5.46)$$
   $$\varphi \le S$$

   with P_0 the maximum PER. This is a meaningful goal for systems without retransmission capabilities.

Criterion 2. *Maximize the throughput*

$$\max_{N_b,r,M,S} \quad \frac{N_b}{S} \cdot \left(1 - PER(N_b,r,M,\gamma)\right)$$

$$\text{s.t.} \qquad \varphi \leq S$$

(5.47)

This goal is suitable for services allowing retransmissions.

2. <u>Case 2</u>.- The value of S is given beforehand. In that case the dimensionality of the search is reduced and the complexity decreases. Equations (5.46) and (5.47) are still to be used but the maximization is not carried out over variable S.

Moreover, if the quantization values are fine enough, low performance loss is expected if the channel uses S are set as $S = \lceil \varphi \rceil = \lceil N_b / (r \cdot \log(M)) \rceil$.

Relay-assisted transmission

Let us further elaborate on Case 2. For multihop transmissions, an independent resource allocation (and hence the size of the data regions S_{I} and S_{II}) may be obtained based on the results provided in chapter 2 for TDMA access, or as in [55] for multiuser OFDMA access. It is worth noticing that the optimization of the relay-transmit phases addressed in chapter 2 was done for a single-carrier Gaussian channel transmission and using the capacity of each link. In the following it is described how coded multi-carrier transmission and the use of ergodic achievable rates can be adopted under the same framework.

Let us assume a multi-carrier transmission through uncorrelated channels. If the rate in the information feedback for the channel state is insufficient, the transmission power is evenly allocated to every carrier and every codeword is transmitted through multiple carriers, after being interleaved across carriers[15]. Under this strategy, the channel capacity of the multi-carrier transmission is given by the ergodic (average) capacity,

$$C = W \cdot E_g \left\{ \log_2 \left(1 + |g|^2 \, SNR\right)\right\} \quad bps$$

(5.48)

with SNR being the average signal-to-noise ratio through the different carriers and g is the channel gain of any carrier. Assuming a unit power complex Gaussian circular random variable, this expression can be lower bounded by,

$$C = W \cdot \log_2 \left(1 + \varepsilon \cdot SNR\right)$$

(5.49)

where ε is the Euler-Marzeratti constant [57]. This expression can be used as a lower bound in space-time transmission in MIMO systems with the appropriate value of ε (see [56] for exact expressions for the ergodic capacity of MIMO systems).

---

[15] The PUSC mode of the standard 802.16e standard uses group of carriers which are far apart.

On the other hand, the channel capacity is not actually achieved by the existing FEC codes, although they are quite close. The achievable rate provided by FEC codes can be accurately determined by introducing a *degradation loss factor* named Γ in the received signal-to-noise ratio [54]. For example Figure 5.39 shows the SNR (in dB) required to obtaining a given value of bits/s/Hz for the CTC according to,
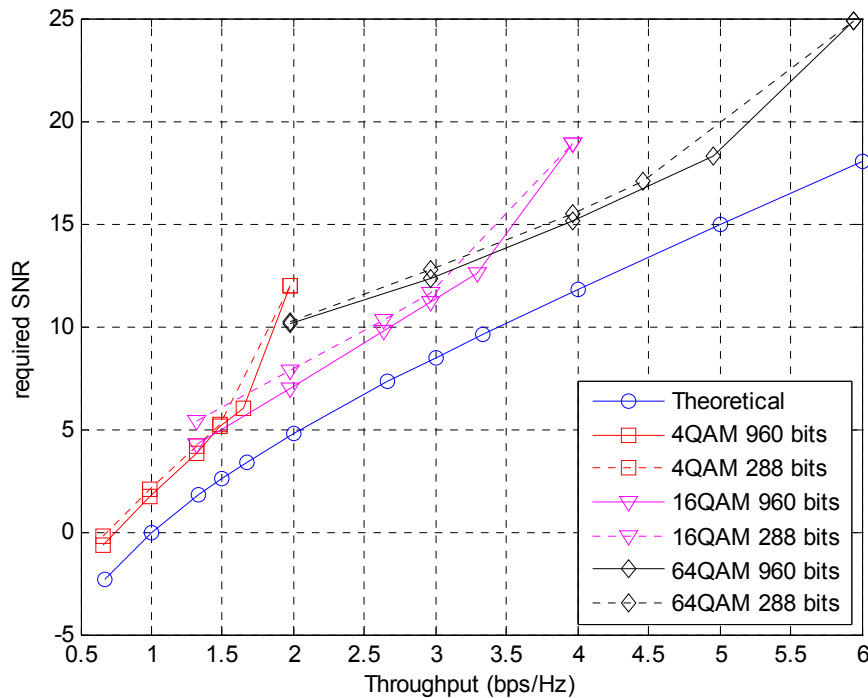
$$R = \log_2\left(1 + SNR_{req}\right) \rightarrow \quad SNR_{req} = 2^R - 1 \tag{5.50}$$

Figure 5.39.- Required SNR vs throughput using the CTC. {4, 16, 64}-QAM, codeword rates {1/3, 1/2, 2/3, 3/4, 5/6 and 1}. Packet sizes 288 (dotted lines) 960 (solid lines) bits. PER=10^-2. The MMSE receiver is used.

The blue-circles line shows the theoretical SNR. The remaining curves correspond to the required SNR for different combinations of modulation (4, 16 and 64-QAM), different codeword rates (1/3, 1/2, 2/3, 3/4, 5/6 and 1) for a CTC with packet size 960 bits (solid lines) and 288 bits (dotted lines). The throughput has been measured for a PER equal to 10^{-2} using the expression

$$\mathcal{T} = r \cdot \log(M) \cdot \left(1 - PER\left(N_b, r, M, \gamma\right)\right) \tag{5.51}$$

From the figure the degradation loss factor due to the CTC is around $\Gamma=3$ dB when the achievable rate is less than 5 bps (although for lower throughput regions this factor is somewhat smaller).

Therefore, the resource allocation techniques introduced in chapter 2 are able to design the data region assuming an equivalent SNR that considers the effect of coding across carriers, symbol constellation and imperfect FEC coding:

$$SNR_{eq} = \frac{\varepsilon}{\Gamma} SNR \qquad (5.52)$$

Observe that if Γ were 0 dB, the combined FEC and symbol constellation code would achieve the capacity. Using this approximation the scheduler may assign the data region and the duration of each relay phase for each relay-assisted destination, i.e. the value of α in an OFDM scenario.

The link level parameters for the relay-assisted transmission are found as the solution for the following optimization problems:

1. <u>Case 1</u>.- The size of the data region in terms of time-frequency channel uses (S) is not given a priori.

   Criterion 1. *Maximize the transmission rate*

$$\max_{\mathbf{z}_1, \mathbf{z}_2, S_I, S_{II}} \frac{N_{b1} + N_{b2}}{S_I + S_{II}}$$
$$\text{s.t.} \quad PER(\mathbf{z}_1, \mathbf{z}_2, \mathbf{\Psi}_1, \mathbf{\Psi}_2) \le P_0 \qquad (5.53)$$
$$\varphi_I \le S_I$$
$$\varphi_{II} \le S_{II}$$

   where P_0 is the maximum PER, S_I and S_{II} denote the data regions in terms of time-frequency channel uses, N_{b1} and N_{b2} stand for the packet sizes considered in each relay-assisted protocol, φ_I, φ_{II}, PER present the channel uses and the PER of each relay-assisted protocol (Table 5.3) and $\mathbf{z}_1, \mathbf{z}_2$, $\mathbf{\Psi}_1$, $\mathbf{\Psi}_2$ show the variables to be considered for each protocol (Table 5.4). Notice that, the forwarding, protocol I and protocol IIA only transmits one message, thus N_{b2}=0.

   Criterion 2. *Maximize the throughput*

$$\max_{\mathbf{z}_1, \mathbf{z}_2, S_I, S_{II}} \frac{N_{b1} + N_{b2}}{S_I + S_{II}} \cdot \left(1 - PER(\mathbf{z}_1, \mathbf{z}_2, \mathbf{\Psi}_1, \mathbf{\Psi}_2)\right)$$
$$\text{s.t.} \quad \varphi_I \le S_I \qquad (5.54)$$
$$\varphi_{II} \le S_{II}$$

2. <u>Case 2</u>.- The values of S_I and S_{II} are given beforehand. Equations presented in (5.46) and (5.47) are still to be used, but the maximization is not carried out over variables S_I and S_{II}. When the quantization values are fine enough, low performance loss is expected if the channel uses in each phase are set as $S_I = \lceil \varphi_I \rceil$ and $S_{II} = \lceil \varphi_{II} \rceil$.

	N_b	PER equation	φ_I	φ_{II}
Forwarding	N_{b1}	(5.32)	$\dfrac{N_{b1}}{r_{SR}\log(M_{SR})}$	$\dfrac{N_{b1}}{r_{RD}\log(M_{RD})}$
Protocol I	N_{b11}	(5.35)	$^{16}\kappa\dfrac{N_{b1}}{r\cdot r_{STC}^{SR}\cdot\log(M_{SR})}$	$(1-\kappa)\dfrac{N_{b1}}{r\cdot r_{STC}^{RD}\cdot\log(M_{RD})}$
Protocol IIA	N_{b1}	(5.39)	$\dfrac{N_{b1}}{r_{SR}\log(M_{SR})}$	$\dfrac{N_{b1}}{r_{RD}\log(M_{RD})}$
Protocol IIB	$N_{b1}+N_{b2}$	(5.41)	$\dfrac{N_{b1}}{r_{SR}\log(M_{SR})}$	$\max\left(\dfrac{N_{b1}}{r_{RD}\log(M_{RD})},\dfrac{N_{b2}}{r_{SD}\log(M_{SD})}\right)$
Protocol III	$N_{b1}+N_{b2}$	(5.43) or (5.44)	$\kappa\dfrac{N_{b1}}{r_1\cdot r_{STC}^{SR}\cdot\log(M_{SR})}$	$\max\left(\dfrac{(1-\kappa)N_{b1}}{r_1\cdot r_{STC}^{RD}\cdot\log(M_{RD})},\dfrac{N_{b2}}{r_{SD}\log(M_{SD})}\right)$

Table 5.3.- Parameters evaluated in this step for each possible combination of modulation, packet size and codeword rate.

	z_1	Ψ_1	z_2	Ψ_2
Forwarding	$[N_{b1},r_{SR},M_{SR},r_{RD},M_{RD}]$	$[\gamma_{SR},\gamma_{RD}]$	$[\,]$	$[\,]$
Protocol I	$[N_{b1},r,r_{STC}^{SR},M_{SR},r_{STC}^{RD},M_{RD},\kappa]$	$[\gamma_{SR},\gamma_{RD},\gamma_{SR-D}]$	$[\,]$	$[\,]$
Protocol IIA	$[N_{b1},r_{SR},M_{SR},r_{RD},M_{RD}]$	$[\gamma_{SR},ExpESM(\gamma_{RD},\gamma_{SD})]$	$[\,]$	$[\,]$
Protocol IIB	$[N_{b1},r_{SR},M_{SR},r_{RD},M_{RD}]$	$[\gamma_{SR},\gamma_{RD}]$	$[N_{b2},r_{SD},M_{SD}]$	$[\gamma_{SD}]$
Protocol III	$[N_{b1},r,r_{STC}^{SR},M_{SR},r_{STC}^{RD},M_{RD},\kappa]$	$[\gamma_{SR},\gamma_{RD},\gamma_{SR-D}]$	$[N_{b2},r_{SD},M_{SD}]$	$[\gamma_{SD}]$

Table 5.4.- Parameters evaluated in this step for each possible combination of modulation, packet size and codeword rate.

The previous optimization problems will obtain the parameters defined in vectors $\mathbf{z}_1$ and $\mathbf{z}_2$ in Table 5.4. It is worth noticing for protocol I and II, the variable r stands for the FEC codeword rate and variables $r_{STC}^{SR},r_{STC}^{RD}$ defines the STC symbol rate on each phase of the transmission for the packet of N_{b1} bits. For the other cases, the code rate (r_{SR}, r_{RD} or r_{SD}) considered subsumes two variables to be optimized: the FEC codeword and the STC symbol rate, (5.31).

5.3.3.1 Results

Figure 5.40 presents a simple scenario where the source and destination are separated with a normalized distance of 1 and the assisting relay is placed at distance d and (1-d) from the source and destination, respectively. By defining the parameter SNR_0, the SNR in the source-relay and relay-destination are established. The channels are AWGN.
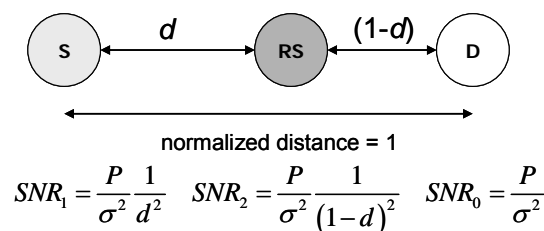
$$SNR_1=\frac{P}{\sigma^2}\frac{1}{d^2}\quad SNR_2=\frac{P}{\sigma^2}\frac{1}{(1-d)^2}\quad SNR_0=\frac{P}{\sigma^2}$$

Figure 5.40.- Considered scenario for the relay-assisted transmission.

---

[16] where κ is the ratio between the size of the sub-packets transmitted in each phase, (5.36).

Furthermore, it has assumed that the destination is served in a frame of 240 data carriers during 24 OFDM symbols. The relay-assisted transmission allocates the resources to each phase according to algorithms described in chapter 2, using the degradation loss factor to consider the effect of the CTC, (see equation (5.52)). Afterwards, the modulation, codeword rate and packet size are selected for that distribution of channel resources (case 2). Using this scenario the theoretical throughput of the relay-assisted transmission and the one obtained by using the discrete values of MCS will be depicted. We have the following discrete values in this work,

$$N_b = \begin{bmatrix} 288 & 480 & 960 \end{bmatrix} \text{ bits}$$
$$Mc = \begin{bmatrix} 4 & 16 & 64 \end{bmatrix}\text{-QAM}$$
$$r_c = \begin{bmatrix} \frac{1}{3} & \frac{1}{2} & \frac{2}{3} & \frac{3}{4} & \frac{5}{6} & 1 \end{bmatrix} \qquad Q_s = 1, T = 1 \tag{5.55}$$
$$MCS = \left(\frac{Q_s}{T} \right) \cdot r_c \cdot \log_2(M) = r \cdot \log_2(M)$$

Figure 5.41 presents the throughput of the relay-assisted transmission in terms of the position of the relay between the source and destination. Solid lines present the theoretical performance in a scenario with $SNR_0 = 0$ dB. However, the use of the CTC enforces a *degradation loss factor* of $\Gamma = 3$ dB, (see Figure 5.39), so that, with dotted lines are shown the predicted throughput of the different protocols. For example for protocol III when the assisting relay is placed at $d = 0.45$, the *degradation loss factor* leads to a loss of 33% of the ideal throughput in this scenario (low SNR, $SNR_0 = 0$ dB).
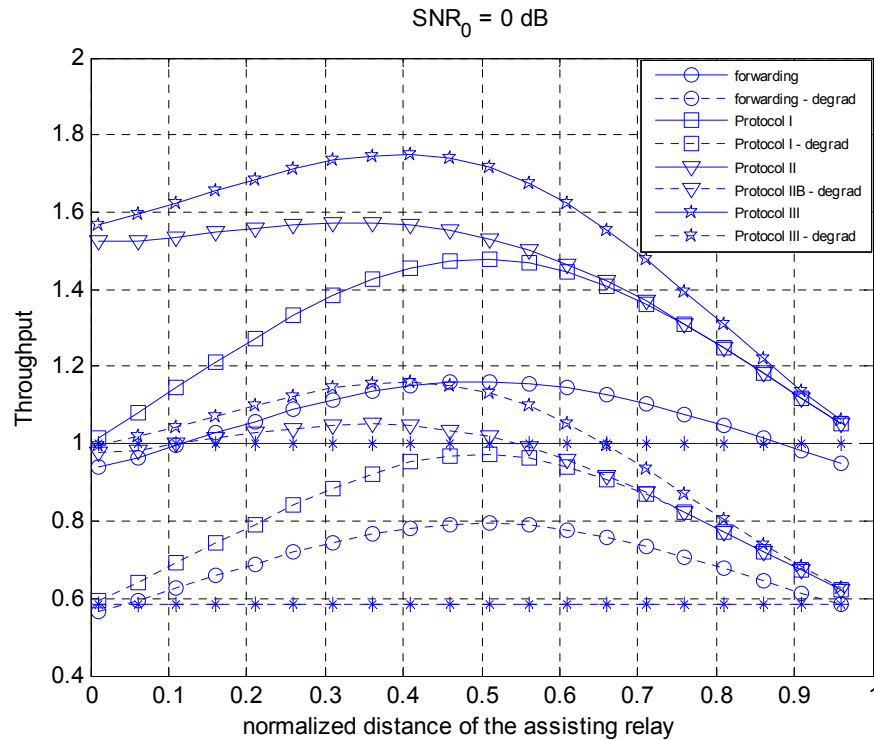
Figure 5.41.- Ideal throughput (solid lines) and predicted throughput (dotted lines) with the CTC (assuming the degradation loss factor Γ=3 dB).

SNR$_0$ = 0 dB low code-rate resolution
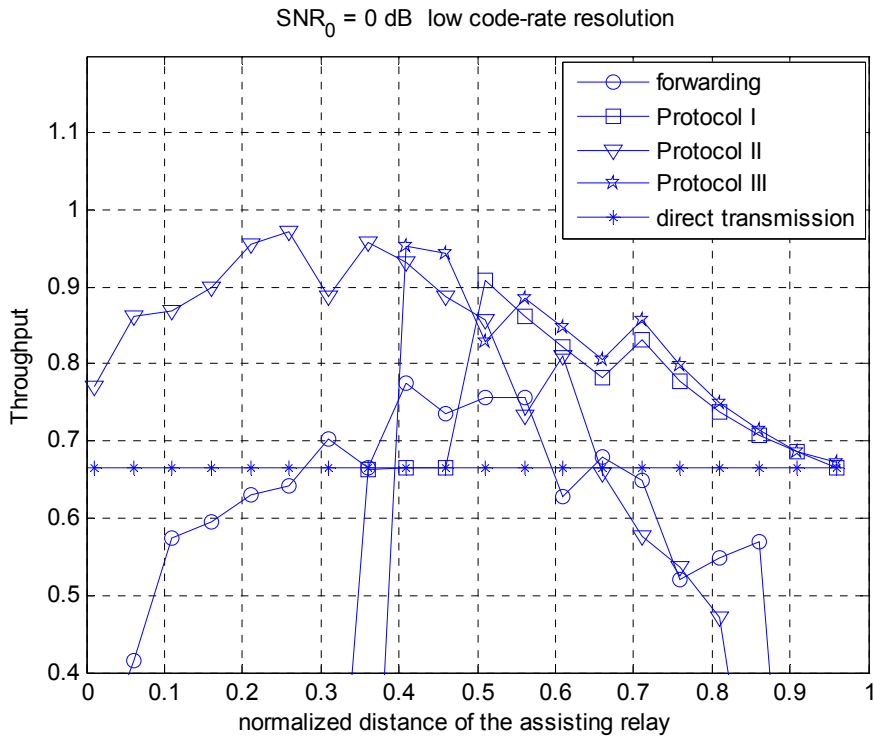
Figure 5.42.- Throughput of the different relay-assisted protocols as a function of the distance of the relay. Modulation and coding scheme defined in (5.55).
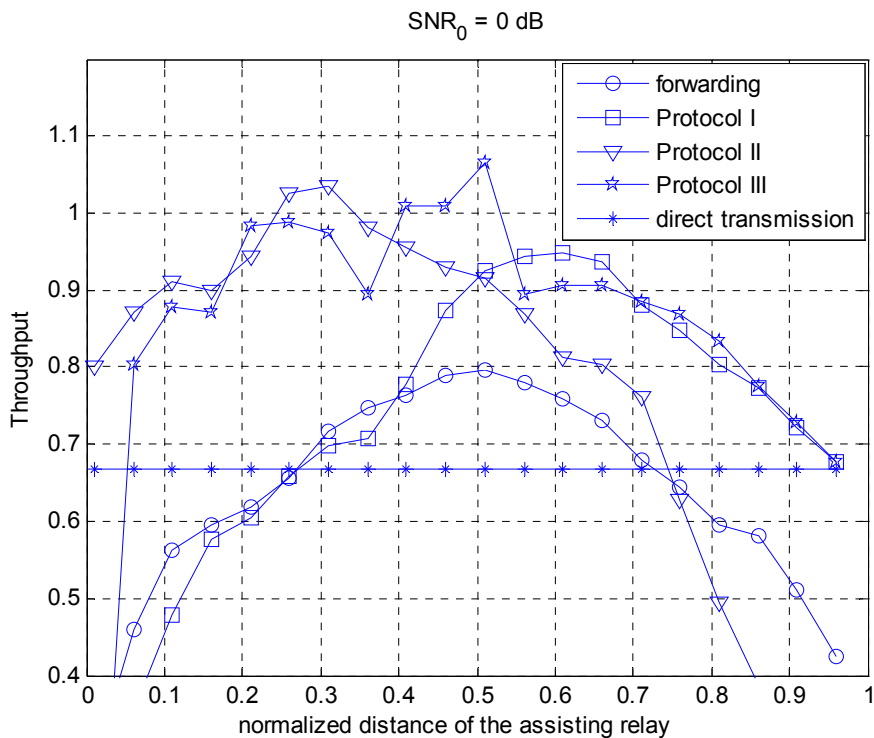
SNR$_0$ = 0 dB

Figure 5.43.- Throughput of the different relay-assisted protocols as a function of the distance of the relay. Modulation and coding scheme defined in (5.55) with a finer codeword rate resolution.

Figure 5.42 shows the obtained throughput when the modulation and coding scheme defined in (5.55) is considered. For the direct transmission a throughput of 0.68 bits/s/Hz is achieved, where the predicted throughput was 0.6 bits/s/Hz (see Figure 5.41). This performance is motivated by the *degradation loss factor*, Γ, which has assumed constant (3 dB) for all

throughput values, when its actual performance depends a little on the throughput value. For example, for low throughput values the Γ could be 2 dB (see Figure 5.39). Moreover, it can be seen that the forwarding protocol gets a throughput too different from the predicted one when the assisting relay is close to the source or the destination. In such a case, the source-relay and relay-destination link are so good that the capacity is high. However, our maximum achievable rate is limited by the maximum constellation (64-QAM – 6 bits). Protocol IIB obtains a similar throughput performance as the predicted one, there is around a 15% loss when the relay is placed at $0.15 \leq d \leq 0.5$ m. However, protocol I and III only get better results than the direct transmission for $0.4 \leq d \leq 1$ m. This is motivated by the predicted phase duration (α) when the relay is placed at $d \leq 0.4$, enforcing to the assisting relay to see a codeword that does not exist (5.38).

If the considered codeword rate presents a finer resolution and the minimum codeword rate is r=1/9, then throughput results of Figure 5.43 are obtained. It can be seen that total throughput is improved.

5.3.4 Conclusions

In this section a link error prediction method applied to the different protocols of relay-assisted transmission has been investigated. The Exp-ESM has been selected thanks to:

1. Good accuracy.

2. Simplicity of computation. It is required only the instantaneous SNR of each data carrier to compute the *effective SNR*.

3. Easy adaptability for relay-assisted schemes and when retransmissions are used.

It has been shown that this metric is defined by the parameters:

1. Optimum β (β_{opt}).

2. RMSE.

Those parameters depend on the packet size, codeword rate, modulation and number of carriers used by the transmission. However, when the number of normalized carriers N_c^{norm} (defined in (5.16)) is high, the RMSE value tends to stabilize. Moreover, those parameters present a remarkable low variability for different types of channel (channel impulse response, correlation at the antennas), so that, independent of the type of channel.

The error prediction of the relay-assisted protocols can be derived by looking into the combination of metrics of the *orthogonal* and *superposed transmission* (section 5.3.1.3). Additionally, an algorithm for the MCS selection has been described both for case where the data region is given beforehand or not and the type of service (*maximization the transmission rate* or *maximization the throughput*). Results show that the performance depends on the codeword resolution and the constellation considered. For example, in some cases higher order modulation of 64-QAM seems necessary. Although the performance of the half-duplex protocols is different from the predicted performance (based on capacity values and taking into account

the *degradation loss factor*) the relay-assisted transmission is able to provide throughput gains over the direct transmission.

5.4 Chapter summary and conclusions

This chapter has studied the dynamic link control for the relay-assisted transmission. It depends on a large number of parameters as the relay transmission mode, the resource allocation, *single* or *multi-carrier* transmission, number of antennas at the different nodes, selected space-time code, relay protocol, retransmission and length of retransmissions. The transmission strategy for the relay-assisted transmission depends on the type of knowledge about the current channel, which is classified as *statistical information about the state* and *actual information about the current channel*. In this chapter we have considered the transmission strategy under one scenario for each type of knowledge, *long-term* CDIT and *partial* CSIT, respectively. Both cases correspond to a situation where the transmitter does not have an exact knowledge of the channel coefficients, so it transmits uniformly through all the antennas. However the link control adopted in each case is different:

➢ *Long-term* CDIT. The rate of the transmission is selected according to some average measure as for example the average capacity or the average SNR. Therefore, the receiver might not receive correctly the message because the selected data rate is not supported by the channel state, generating an *outage event*. In this regard, the use of ARQ protocols alleviates those outage events and improves the throughput by informing the transmitter about the success of the transmission. If the message is wrongly decoded, the message is retransmitted, although the actual format depends on the type of ARQ protocol considered. We have studied a relay-assisted scenario similar to the one considered in chapter 4, where different destinations are served in a TDMA frame (with *single-carrier* transmission) using protocol I and there is one time-slot spatially reused by all the associated relays. We have also investigated the DSTC at the source and relay and the coding for the retransmissions. In this latter case, the RPCTC allows transmitting different parts of the same codeword by the source and relay.

➢ *Partial* CSIT. The transmitter knows some parameter related to the current link quality, but not the channel coefficients. In such a case, the transmitter can adapt its MCS to that scenario. In contrast to the *long-term* CDIT case, the accurate selection of the MCS does not produce any outage event, and packet error situations are only due to *thermal noise*. In this chapter we have considered that the transmission is carried out over a frequency selective channel through several parallel carriers. The selection of the MCS depends on the PER for each combination of packet size, modulation and codeword rate under a given link quality. In such scenario, we have considered the Exp-ESM method, which obtains the *effective SNR* for describing the link quality and estimating the PER. This method has been extended for the error prediction under different half-duplex protocols, and remarkable accuracy has been observed between actual and predicted PER. With that estimation, the suitable MCS can be selected as a function of the quality of the different links involved in the relay-assisted transmission. The conclusions of this work are presented in section 5.3.4.

5.5 Appendix A. Space-Time codes

In the following the Alamouti, VBLAST and Golden STC will be depicted as Linear Dispersion Codes (LDC):

Alamouti

This code [18] $Q_s=T=2$ is designed for $n_s=2$,

$$\mathbf{A}_1 = \begin{bmatrix} 1 & 0 \\ 0 & 1 \end{bmatrix} \quad \mathbf{A}_2 = \begin{bmatrix} 0 & 1 \\ -1 & 0 \end{bmatrix}$$
$$\mathbf{B}_1 = \begin{bmatrix} 1 & 0 \\ 0 & -1 \end{bmatrix} \quad \mathbf{B}_2 = \begin{bmatrix} 0 & 1 \\ 1 & 0 \end{bmatrix} \tag{5.56}$$

VBLAST

The VBLAST transmits $Q_s=4$ symbols during $T=2$ and assumes $n_s=2$. The original STC definition is given by,

$$\mathbf{A}_1 = \begin{bmatrix} 1 & 0 \\ 0 & 0 \end{bmatrix} \quad \mathbf{A}_2 = \begin{bmatrix} 0 & 1 \\ 0 & 0 \end{bmatrix} \quad \mathbf{A}_3 = \begin{bmatrix} 0 & 0 \\ 1 & 0 \end{bmatrix} \quad \mathbf{A}_4 = \begin{bmatrix} 0 & 0 \\ 0 & 1 \end{bmatrix}$$
$$\mathbf{B}_1 = \begin{bmatrix} 1 & 0 \\ 0 & 0 \end{bmatrix} \quad \mathbf{B}_2 = \begin{bmatrix} 0 & 1 \\ 0 & 0 \end{bmatrix} \quad \mathbf{B}_3 = \begin{bmatrix} 0 & 0 \\ 1 & 0 \end{bmatrix} \quad \mathbf{B}_4 = \begin{bmatrix} 0 & 0 \\ 0 & 1 \end{bmatrix} \tag{5.57}$$

Although the following definition (obtained by a rotation of the previous STC [43]) achieves the same mutual information and is able to get better results for linear receivers,

$$\mathbf{A}_1 = \begin{bmatrix} 1 & 0 \\ 0 & 1 \end{bmatrix} \quad \mathbf{A}_2 = \begin{bmatrix} 0 & 1 \\ -1 & 0 \end{bmatrix} \quad \mathbf{A}_3 = \begin{bmatrix} 1 & 0 \\ 0 & -1 \end{bmatrix} \quad \mathbf{A}_4 = \begin{bmatrix} 0 & 1 \\ 1 & 0 \end{bmatrix}$$
$$\mathbf{B}_1 = \begin{bmatrix} 1 & 0 \\ 0 & -1 \end{bmatrix} \quad \mathbf{B}_2 = \begin{bmatrix} 0 & 1 \\ 1 & 0 \end{bmatrix} \quad \mathbf{B}_3 = \begin{bmatrix} 1 & 0 \\ 0 & 1 \end{bmatrix} \quad \mathbf{B}_4 = \begin{bmatrix} 0 & 1 \\ -1 & 0 \end{bmatrix} \tag{5.58}$$

Golden Code

The Golden code [27][28][29] is defined for $Q_s=4$, $T=2$ and $n_s=2$,

$$\mathbf{A}_1 = \mathbf{B}_1 = \begin{bmatrix} 1 & 0 \\ 0 & jr \end{bmatrix} \mathbf{A}_2 = \mathbf{B}_2 = \begin{bmatrix} 0 & r \\ 1 & 0 \end{bmatrix} \mathbf{A}_3 = \mathbf{B}_3 = \begin{bmatrix} 0 & 1 \\ -r & 0 \end{bmatrix} \mathbf{A}_4 = \mathbf{B}_4 = \begin{bmatrix} jr & 0 \\ 0 & 1 \end{bmatrix}$$
$$j = \sqrt{-1} \qquad r = \frac{-1+\sqrt{5}}{2} \tag{5.59}$$

5.6 Appendix B. Derivation of the Exp-ESM

This appendix presents the derivation of the Exponential – Effective SIR Mapping (Exp-ESM) developed in [36]. First, it is assumed the case where the modulation uses a binary signaling. Afterwards, that model is generalized to include an MCS-dependent parameter that allows for fine-tuning of the Exp-ESM to different modulation and coding rates.

5.6.1 Basic Exp-ESM

The *Union-Chernoff* bound of error probabilities is considered as a basis of the Exp-ESM. The union bound for a coded binary transmission and maximum decoding is well known and given by

$$P_e(\gamma) \le \sum_{d=d_{\min}}^{\infty} \alpha_d P_2(d,\gamma) \tag{5.60}$$

where γ is the channel symbol SNR, d_{min} is the minimum distance of the binary code, α_d is the number of codewords with hamming weight d and $P_2(d,\gamma)$ is the pair-wise error probability (PEP) assuming a certain Hamming distance d and a certain symbol SNR, γ.

The PEP for a BPSK (binary phase shift keying) transmission under an AWGN channel can be upper bounded (Chernoff-bounded PEP)

$$P_2(d,\gamma) = Q\left(\sqrt{2\gamma d}\right) \le e^{-\gamma d} \triangleq P_{2,Chernoff}(d,\gamma) = \left[P_{2,Chernoff}(1,\gamma)\right]^d \tag{5.61}$$

It can be seen that the Chernoff-bounded PEP is directly given by the Chernoff-bounded (uncoded) symbol error probability.

$$P_e(\gamma) \le \sum_{d=d_{\min}}^{\infty} \alpha_d P_2(d,\gamma) \le \sum_{d=d_{\min}}^{\infty} \alpha_d \left[P_{2,Chernoff}(1,\gamma)\right]^d \triangleq P_{e,Chernoff}(\gamma) \tag{5.62}$$

Thus, the Chernoff-bounded error probability $P_{e,Chernoff}(\gamma)$ only depends on the weight distribution of the code ($P_{2,Chernoff}(1,\gamma)$).

Let us assume a 2-state channel for explaining the principles of the Union Chernoff bound. Those principles are straightforwardly extended to the general multi-state channel. In this regard, our 2-state channel is characterized by an SNR vector $\overline{\gamma} = [\gamma_1, \gamma_2]$ where the two states γ_1 and γ_2 occur with probability p_1 and p_2, respectively. Both SNR values are assumed to be independent from each other.

Let us now look at two arbitrary codewords with Hamming distance d. The SNR value, either γ_1 and γ_2, associated with each of the d differing symbols depends on the respective symbol position. We will consider the mean PER, averaged over all possible positions of the d differing symbols. In such a case, the Chernoff bounded PER can be expressed as,

$$P_{2,Chernoff}\left(d,[\gamma_1,\gamma_2]\right) = \sum_{i=0}^{d} \binom{d}{i} p_1^i p_2^{d-i} e^{-\left(i\gamma_1 + (d-i)\gamma_2\right)} = \left(p_1 e^{-\gamma_1} + p_2 e^{-\gamma_2}\right)^d \tag{5.63}$$

where the binomial theorem has been used to arrive at the final expression. The term $p_1^i p_2^{d-i}$ represents the probability that i of the d differing symbols are associated with SNR γ_1 and the residual (d-i) symbols are associated with SNR γ_2. Each event presents a Chernoff-bounded PEP equal to $e^{-\left(i\gamma_1 + (d-i)\gamma_2\right)}$.

It is worth noticing that the averaged Chernoff-bounded symbol error probability for the 2-state channel (5.63) is relative to the 1-state channel,

$$P_{2,Chernoff}\left(d,[\gamma_1,\gamma_2]\right) = \left[P_{2,Chernoff}\left(1,[\gamma_1,\gamma_2]\right)\right]^d \tag{5.64}$$

Moreover, from the polynomial theorem, it can be shown that the same is true for the general multi-state channel characterized by a vector $\bar{\gamma} = [\gamma_1,\gamma_2,...,\gamma_N]$, i.e.

$$P_{2,Chernoff}\left(d,\bar{\gamma}\right) = \left[P_{2,Chernoff}\left(1,\bar{\gamma}\right)\right]^d \tag{5.65}$$

This feature is now exploited to derive the Exp-ESM. The goal is to find an effective SNR value γ_{eff} of an equivalent 1-state channel such that the Chernoff-bounded error probability equals to the Chernoff-bounded error probability on the multi-state channel, i.e.

$$P_{e,Chernoff}\left(\gamma_{eff}\right) = P_{e,Chernoff}\left(\bar{\gamma}\right) \tag{5.66}$$

Due to the feature stated above, (5.65), this can be achieved by matching

$$P_{2,Chernoff}\left(1,\gamma_{eff}\right) = P_{2,Chernoff}\left(1,\bar{\gamma}\right) \tag{5.67}$$

The Exp-ESM is found as,

$$\gamma_{eff} = -\ln\left(\sum_{k=1}^{N} p_k e^{-\gamma_k}\right) \tag{5.68}$$

or, for the case of OFDM with N carriers and different SNR, γ_k, on each carrier

$$\gamma_{eff} = -\ln\left(\frac{1}{N}\sum_{k=1}^{N} e^{-\gamma_k}\right) \tag{5.69}$$

5.6.2 A generalized Exp-ESM

The derivations depicted in section 5.6.1 have assumed a binary transmission (BPSK). It is clear that, for QPSK (Quadrature Phase Shift Keying) or 4-QAM (Quadrature Amplitude Modulation), the Exp-ESM becomes,

$$\gamma_{eff} = -2 \cdot \ln\left(\frac{1}{N}\sum_{k=1}^{N} e^{-\frac{\gamma_k}{2}}\right) \tag{5.70}$$

For higher-order modulation, such as 16-QAM, it is not straightforward to determine the exact expression for the Exp-ESM. The reason is because the higher-order modulation can be seen itself as a multi-state channel from a binary-symbols transmission point of view. In this regard [36] proposes the use of the parameter β to match the Exp-ESM to a specific modulation and coding rate. The suitable value of parameter β is bound from link-level simulations. The generalized exponential ESM is defined as,

$$\gamma_{eff} = -\beta \ln\left(\frac{1}{N}\sum_{i=1}^{N} e^{-\frac{\gamma_i}{\beta}}\right) \tag{5.71}$$

5.7 Appendix C. Analysis of Exp-ESM parameters

This appendix explores the optimal β_{opt} (5.13) and the RMSE (5.15) obtained by the Exp-ESM for different configurations of antenna, space-time codes and type of channels. Results are depicted as a function of the normalized number of carriers introduced in (5.16), N_c^{norm}. It will be shown that the β_{opt} and the RMSE also depends on the packet size and the selected modulation.

5.7.1 Different space-time codes

A packet size of N_{b}=960 bits with codeword rate equal to r=1/3 has been assumed for a Rayleigh channel impulse response of 6 taps (6 symbols length with equal average power) and different antenna and STC configuration (Alamouti, Golden). Figure 5.23 and Figure 5.24 showed results when 4-QAM was adopted. Furthermore, Figure 5.44 presents results when 16-QAM is selected and SISO and 2×2 MIMO transmission (Golden STC) is used. It can be seen for 16-QAM that the RMSE is larger than for 4-QAM case. Moreover, the RMSE performance follows similar guidelines as the 4-QAM case, it also decreases by increasing the normalized number of carriers and the SISO performance is the worst.
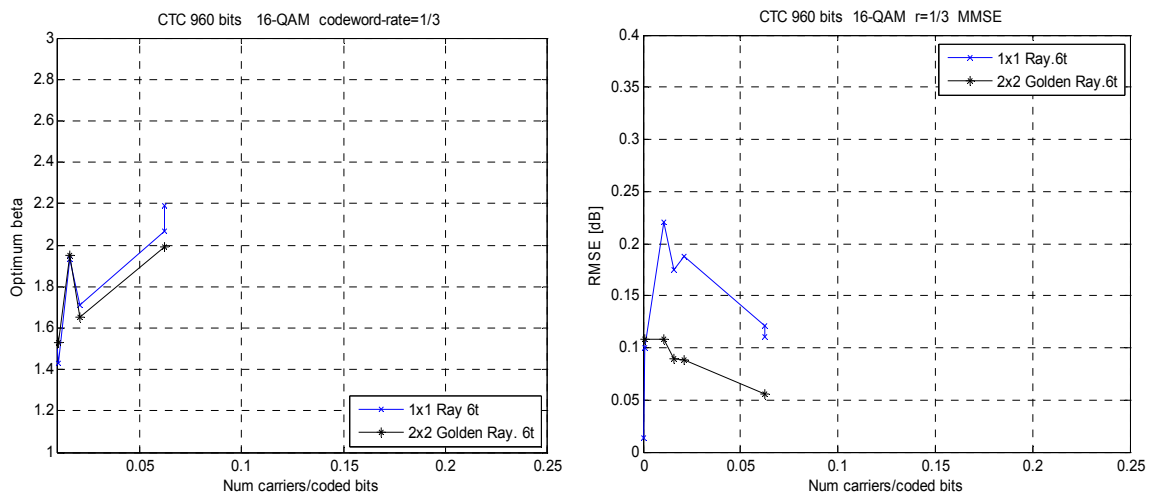
Figure 5.44.- (left plot) Optimum β and RMSE (right plot) as a function of the normalized number of carriers. CTC 960 bits, r=1/3, 16-QAM and Rayleigh channel with 6 taps.

5.7.2 Different packet size

This section present the performance of the β_{opt} (5.13) and the RMSE (5.15) when the packet size (N_b) of the CTC changes. Notice that the PER curve depends on the packet size as was shown in Figure 5.20, therefore the optimization of β parameter has to be done for each packet size. Figure 5.45, Figure 5.46 and Figure 5.47 present the results for N_b={960, 480, 288} bits, respectively, all using a codeword rate r=1/2 and 4-QAM. SISO and 2×2 MIMO transmission (Golden STC) is studied. When the packet size is small, the β_{opt} seems to be independent of the normalized number of carriers.
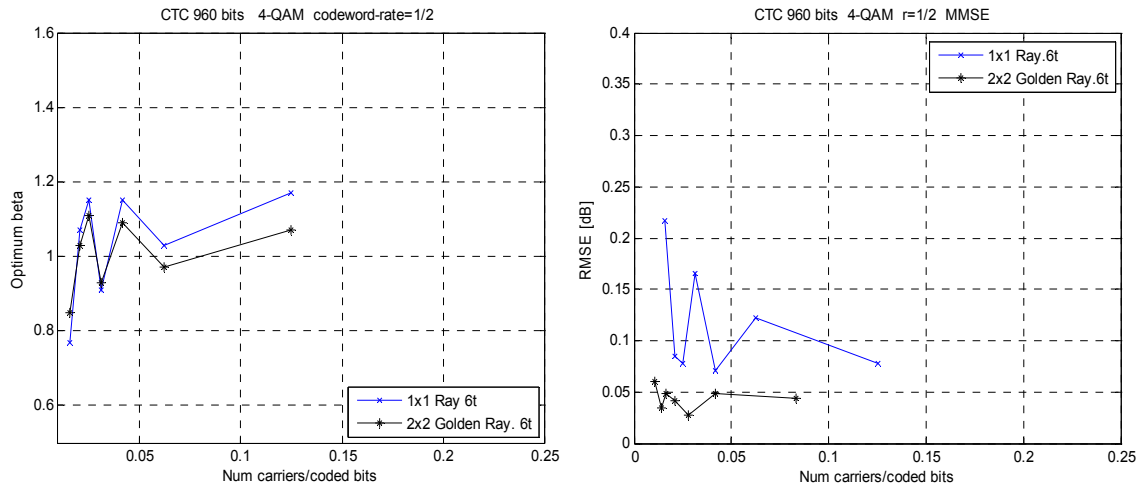
Figure 5.45.- left plot) Optimum β and RMSE (right plot) as a function of the normalized number of carriers. CTC 960 bits, r=1/2, 4-QAM and Rayleigh channel with 6 taps.
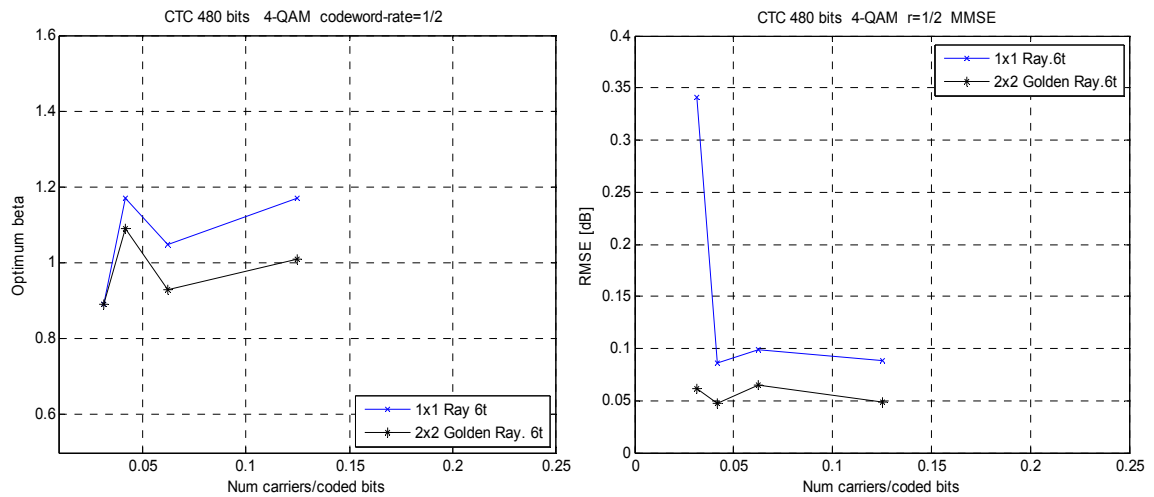
Figure 5.46.- (left plot) Optimum β and RMSE (right plot) as a function of the normalized number of carriers. CTC 480 bits, r=1/2, 4-QAM and Rayleigh channel with 6 taps.
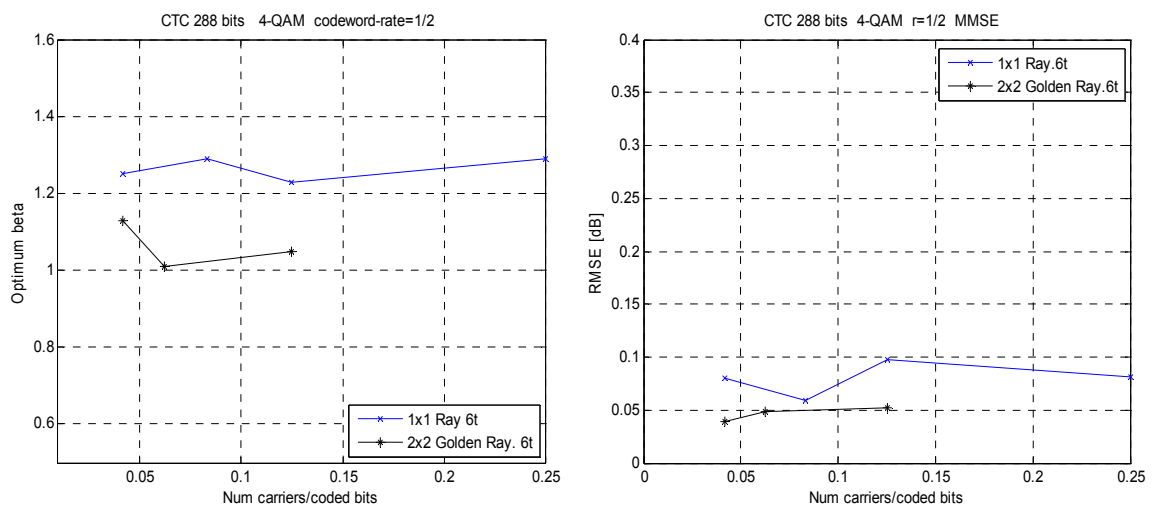
Figure 5.47.- (left plot) Optimum β and RMSE (right plot) as a function of the normalized number of carriers. CTC 288 bits, r=1/2, 4-QAM and Rayleigh channel with 6 taps.

5.7.3 Different frequency selective channel lengths

Figure 5.48 depicts the performance of β_{opt} (5.13) and the RMSE (5.15) when the channel impulse response for a Rayleigh channel varies. Results are obtained for Rayleigh channels with {3, 6, 9 and 12} taps (with equal average power and the same number of symbols length). The CTC code has N_b=288 bits, the codeword rate is r=1/2 and the modulation is 4-QAM. The transmission is done in a 2×2 MIMO system with Golden STC. Results of Figure 5.48 show that the β_{opt} and RMSE is independent of the channel impulse response.
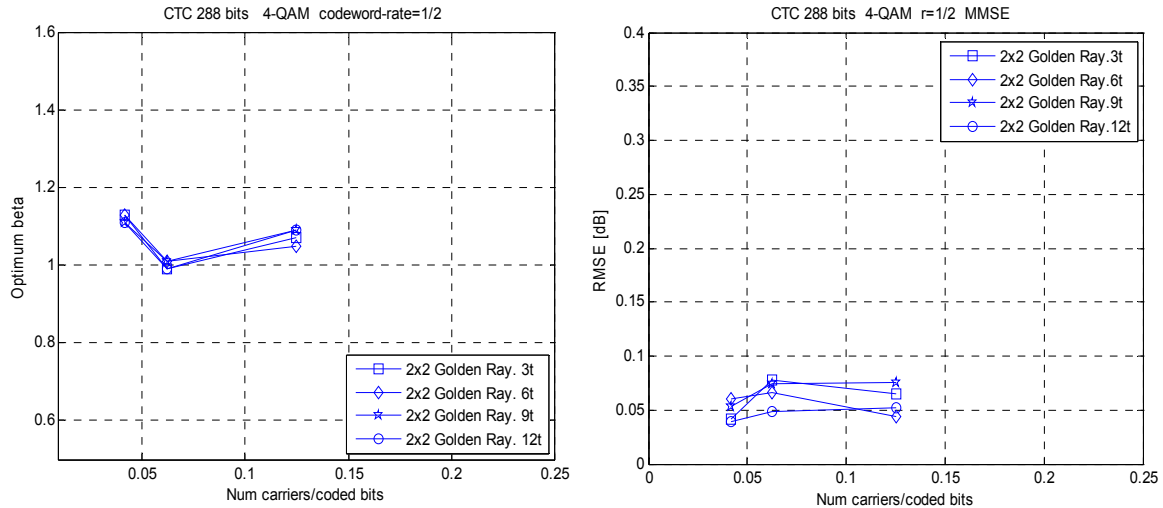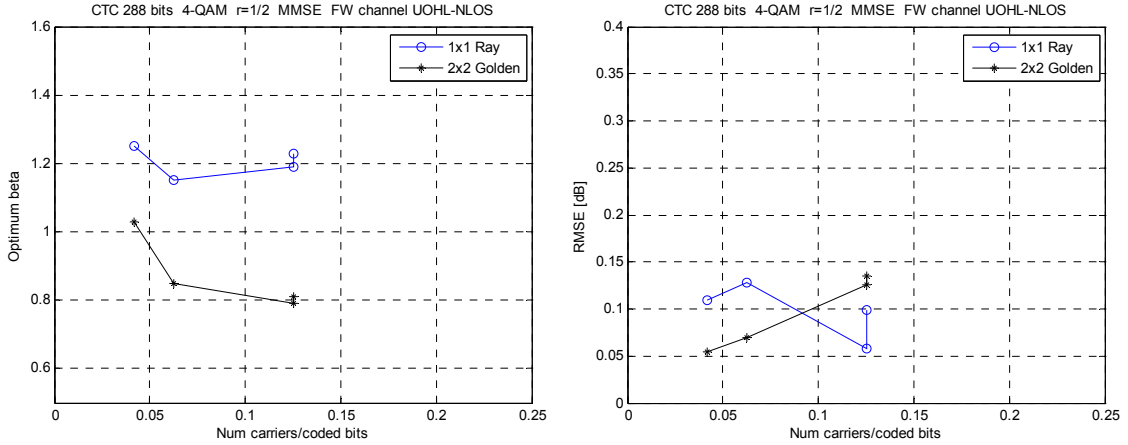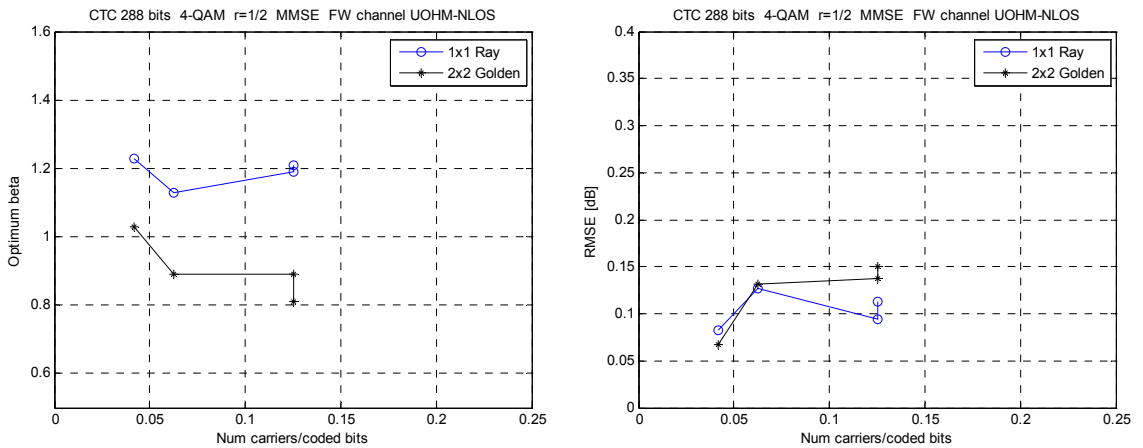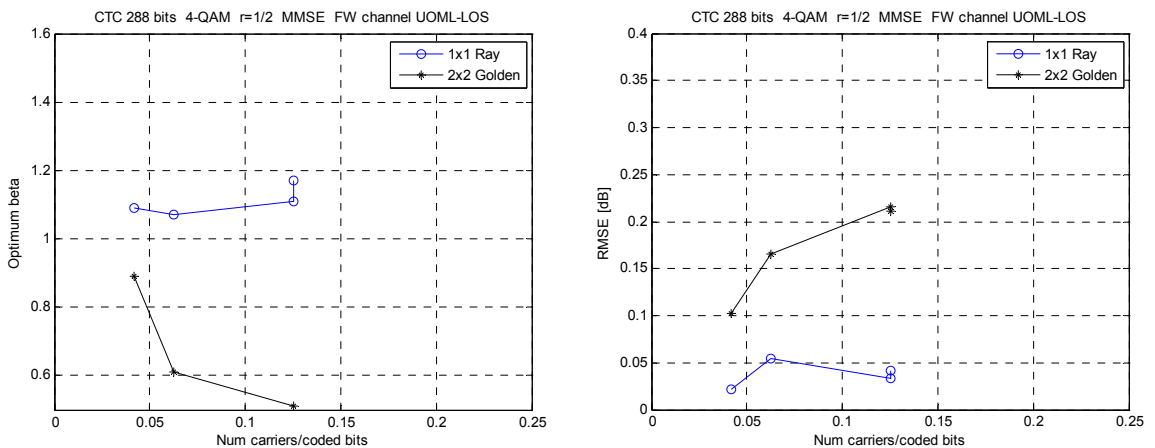

Figure 5.48.- (left plot) Optimum β and RMSE (right plot) as a function of the normalized number of carriers. CTC 288 bits, r=1/2, 4-QAM and Rayleigh channel with {3,6,9,12} taps, MIMO 2×2.

5.7.4 Results on Fireworks[17] scenarios

This section analyzes the performance of β_{opt} (5.13) and the RMSE (5.15) with different type of channels. For this purpose, it has been considered 3 channels defined in [53] named UOHL-NLOS (Urban Outdoor High to Low- NLOS), UOHM-NLOS (Urban Outdoor High to Medium – NLOS) and UOML-LOS (Urban Outdoor Medium to Low –LOS) which take into account different channel impulse responses and antenna correlations. Those results are presented in Figure 5.49, Figure 5.50 and Figure 5.51, respectively, using a CTC code N_b=288 bits with codeword rate r=1/2 and modulation 4-QAM. The transmission is done through a SISO channel (1×1) and (2×2) MIMO channel, with Golden codes as STC.

It can be seen that the SISO transmission obtains a similar performance for NLOS channels, Figure 5.49, Figure 5.50, where β_{opt}≈1.2 and the RMSE≈0.1. These values are similar to the ones obtained in the Rayleigh channel shown in Figure 5.47. For the channel with LOS (UOML scenario in Figure 5.51) β_{opt}≈1.1 and the RMSE≈0.05. This performance can be justified with the help of Figure 5.52, where the channel power delay profile of the different realizations of those channels is depicted. The UOHL-NLOS and UOHM-NLOS present a channel impulse response with more than 1 significant coefficient (3 and 4, respectively) and have similar performance as for the Rayleigh channel with different number of taps. When the channel impulse response has only 1 significant coefficient the SISO transmission is akin to the AWGN channel, all the carriers

---

[17] These are the scenarios considered in the FIREWORKS project (IST-4-027675-STP).

present the same instantaneous SNR. In such a case, the effective SNR is independent of the selected β. Nevertheless, the channel impulse response of the UOML-LOS has not exactly a single tap, producing that β_{opt} is equal to 1.1 (not too different from the results in other type of channels) and having the lowest RMSE.

Figure 5.49.- (left plot) Optimum β and RMSE (right plot) as a function of the normalized number of carriers. CTC 288 bits, r=1/2, 4-QAM and Fireworks channel UOHL-NLOS.

Figure 5.50.- (left plot) Optimum β and RMSE (right plot) as a function of the normalized number of carriers. CTC 288 bits, r=1/2, 4-QAM and Fireworks channel UOHM-NLOS.

Figure 5.51.- (left plot) Optimum β and RMSE (right plot) as a function of the normalized number of carriers. CTC 288 bits, r=1/2, 4-QAM and Fireworks channel UOLM-LOS.

For the 2×2 MIMO transmission with Golden code, the values of β_{opt} and RMSE for the UOHL-NLOS (Figure 5.49), UOHM-NLOS (Figure 5.50) and UOML-LOS (Figure 5.51) are quite different to the Rayleigh case shown in Figure 5.48. Notice that the RMSE is almost equal to 0.2 in Figure 5.51. This performance can be connected with the space-time code (STC), the MMSE receiver and the antenna (space) correlation. The Golden code transmits 4 symbols in two channel uses through 2 transmitting antennas. If there are 2 antennas at the receiver, a linear receiver (MMSE) can be considered at the destination. However the performance of the linear receiver will be degraded as the correlation between antennas (at transmitter and/or receiver side) increases. To illustrate it, assume a scenario where the channels between transmitting antennas to a common receiving antenna are highly correlated. The destination sees nearly the same channel from the multiple-antenna, i.e. a single transmitting antenna is enough to transmit to the destination (assuming no channel state information at the transmitter side).

In section 5.7.4.1 it has been measured the antenna correlation for the considered Fireworks channels. Table 5.5 depicts the ratio between the maximum over the minimum eigenvalue of the transmit (and receive) covariance matrix, (5.72). When the channel is Rayleigh, Figure 5.48, the antennas are uncorrelated. For channels UOHL-NLOS (Figure 5.50) and UOHM-NLOS (Figure 5.16), Table 5.5 shows that there is some correlation at the transmitter side, for those cases the β_{opt} is different from the uncorrelated case and the RMSE is worse. Finally, UOHL-LOS (as the name indicates) there is a high transmitter correlation, obtaining worse values of RMSE. In this case the Exp-ESM does not work properly.
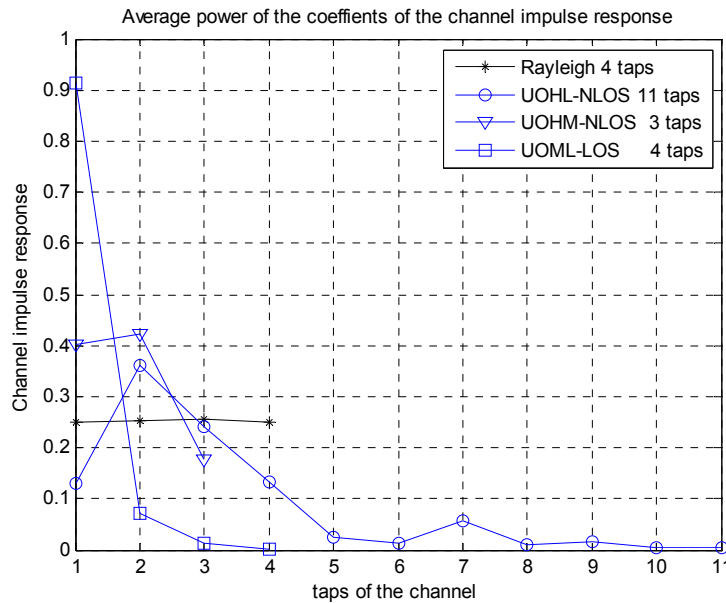

Figure 5.52.- Power delay profile of the coefficients of the channel impulse response for the channels: Rayleigh (4 taps), UOHL-NLOS (11 taps), UOHM-NLOS (3 taps) and UOML-LOS (4 taps).

5.7.4.1 Antenna correlation

The transmit and receive channel correlation matrix in a certain frequency is defined by,

$$\mathbf{R}_{TX} = E\left[\mathbf{h}_{TX}^{H}\mathbf{h}_{TX}\right] \qquad \mathbf{R}_{RX} = E\left[\mathbf{h}_{RX}\mathbf{h}_{RX}^{H}\right] \tag{5.72}$$

with $\mathbf{h}_{TX}$ ($\mathbf{h}_{RX}$) being the channel matrices between all transmitting (receiving) and one receiving (transmitting) antenna, of dimensions $1\times n_s$ ($n_d\times 1$), at a certain frequency. The $E[]$ function is the

expectation operator. The covariance matrices $\mathbf{R}_{TX}$ and $\mathbf{R}_{RX}$ have dimensions $n_s \times n_s$ and $n_d \times n_d$, respectively.

Table 5.5 presents the ratio between the maximum over the minimum eigenvalue of the covariance matrix. A value close to one implies that the channels at the transmission/reception are uncorrelated. On the other hand, a value larger than one implies some correlation between the antennas. The values depicted in Table 5.5 are for Rayleigh channels and Fireworks channels with antenna separation equal to $\lambda/2$, [53].

Type of channel	Ratio between max. and min. eigenvalue	
	Transmit correlation	*Receive correlation*
Rayleigh channel	1	1
UOHL-NLOS	14.3	2.19
UOHM-NLOS	1.17	1.13
UOML-LOS	90.9	4.20

Table 5.5.- Ratio of maximum and minimum eigenvalues of the covariance channel matrix of the transmitting and receiving antennas. n_s=2, n_d=2.

5.8 Appendix D. Optimal parameters of the Exp-ESM

This section is devoted to present the performance of the β_{opt} and RMSE as a function of the codeword selected, r for different antenna configuration and packet size. Here it has been assumed that the transmission is using 4 OFDM symbols with the maximum number of carriers. Results are obtained for Rayleigh channels (with 6 and 12 taps with equal average power) and UOHM-NLOS, UOHL-NLOS and UOML-LOS channels [53]. Two scenarios are assumed a 2×1 MIMO system where the Alamouti STC is used (Figure 5.53-Figure 5.55) and the 2×2 MIMO with Golden code (Figure 5.56-Figure 5.59). For each scenario a packet size of N_b={960, 288} bits and modulation M={4,16}-QAM are investigated.
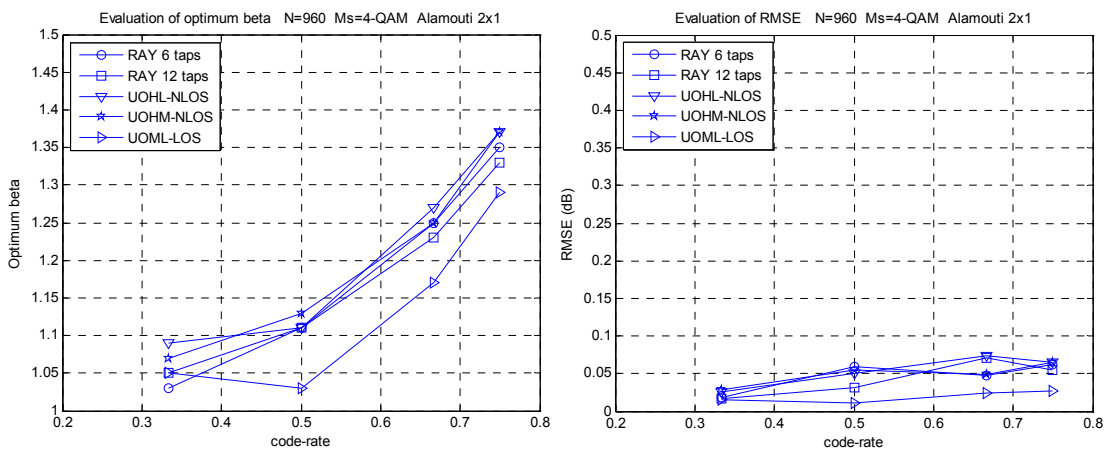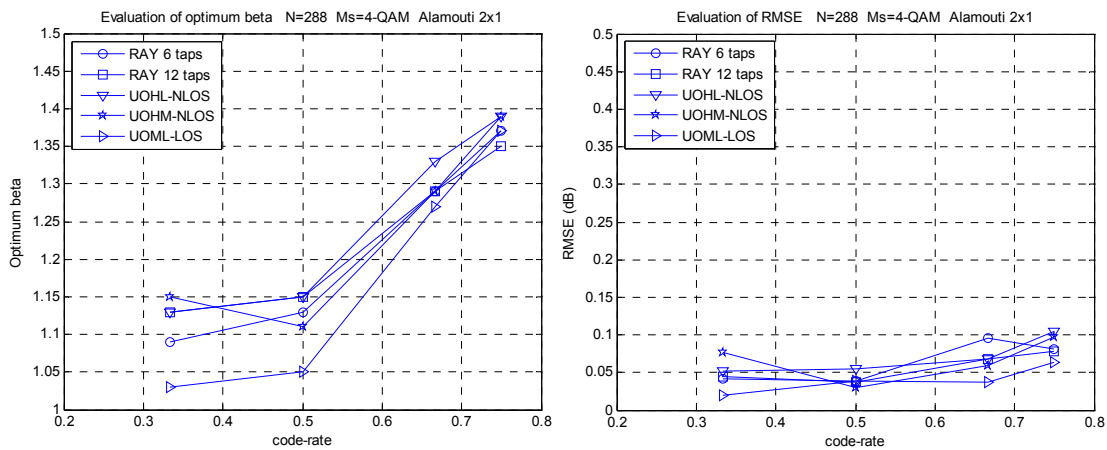
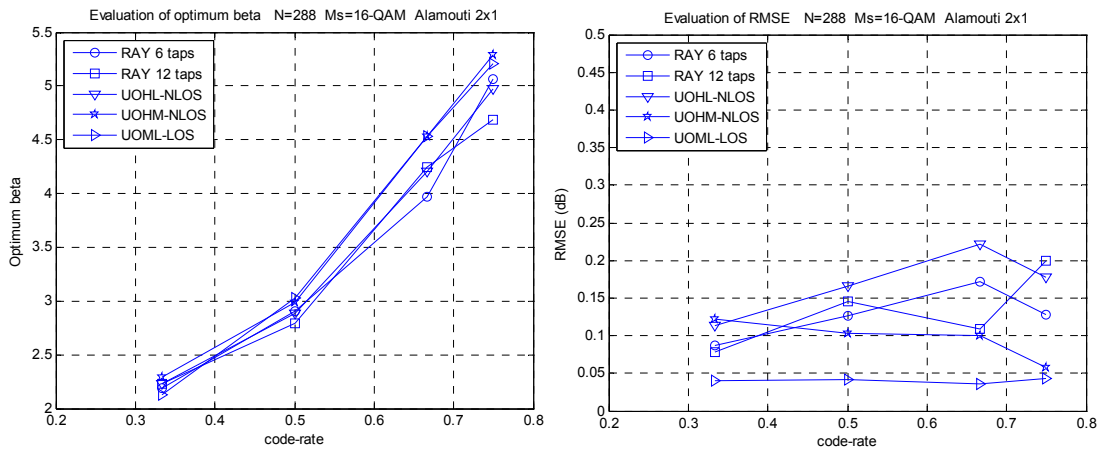**Alamouti STC (2×1 MIMO)**

Figure 5.53.- (left) Optimum β and (right) RMSE as a function of the code rate selected for different type of channels. 2×1 MIMO. Alamouti STC. N_b=960. M=4-QAM.

Figure 5.53-left depicts the β_{opt} as a function of the codeword rate for different type of channels when the Alamouti STC is considered in a 2×1 MIMO system using a modulation of 4-QAM with

a packet size of N_b=960 bits. It can be seen that β_{opt} is quite similar among the different channels. Likewise, the RMSE, Figure 5.53-right, shows a performance almost independent of the codeword selected, having a worst case performance of RMSE equal to 0.08 dB. If the modulation is increased up to 16-QAM (Figure 5.25 and Figure 5.26) the β_{opt} also present similar values for different types of channels, but the RMSE is increased for the NLOS channels.

When the packet size is reduced to N_b=288 bits, Figure 5.54 (4-QAM) and Figure 5.55 (16-QAM), the performance of the β_{opt} and RMSE follow similar steps, but the values of β_{opt} for a given codeword rate and RMSE are smaller than for larger packet sizes.

Figure 5.54.- (left) Optimum β and (right) RMSE as a function of the code rate selected for different type of channels. 2×1 MIMO. Alamouti STC. N_b=288. M=4-QAM.

Figure 5.55.- (left) Optimum β and (right) RMSE as a function of the code rate selected for different type of channels. 2×1 MIMO. Alamouti STC. N_b=288. M=16-QAM.

GOLDEN STC (2×2 MIMO)

Figure 5.56 and Figure 5.57 present the results of β_{opt} and RMSE when the transmission uses the Golden STC in a 2×2 MIMO scenario with a packet size of N_b=960 bits and modulation 4-QAM and 16-QAM, respectively. In contrast to the Alamouti STC with 4-QAM, now the UOHL-NLOS, UOHM-NLOS and UOML-LOS present a different β_{opt} compared with the Rayleigh case and the RMSE is dependant of the codeword rate. When 16-QAM is assumed,

see Figure 5.57, results in terms of obtained β_{opt} for the different channels are quite similar (as it happens with the Alamouti STC in Figure 5.25). However, the RMSE of the UOML-LOS is higher. This might be connected with the antenna correlation for this type of channel as has been discussed in section 5.7.4 in Appendix B.
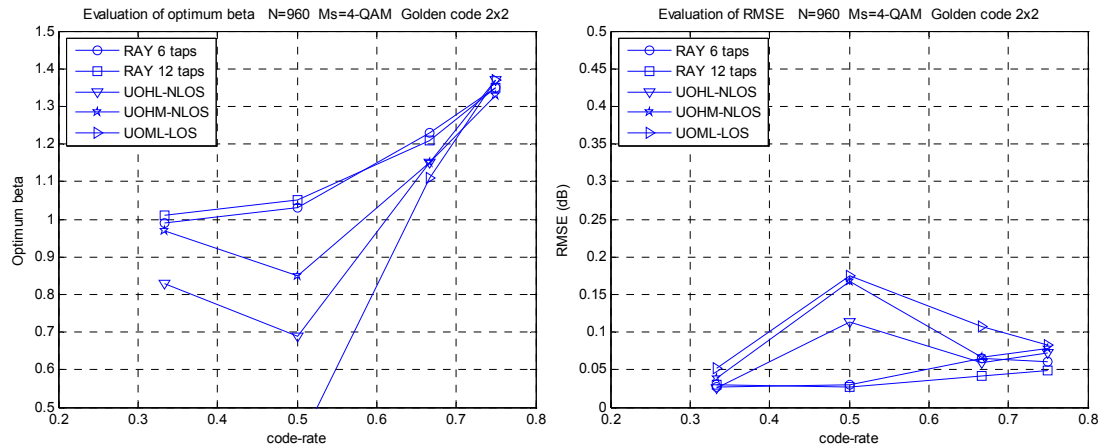

Figure 5.56.- (left) Optimum β and (right) RMSE as a function of the code rate selected for different type of channels. 2×2 MIMO. Golden STC. N_b=960. M=4-QAM.
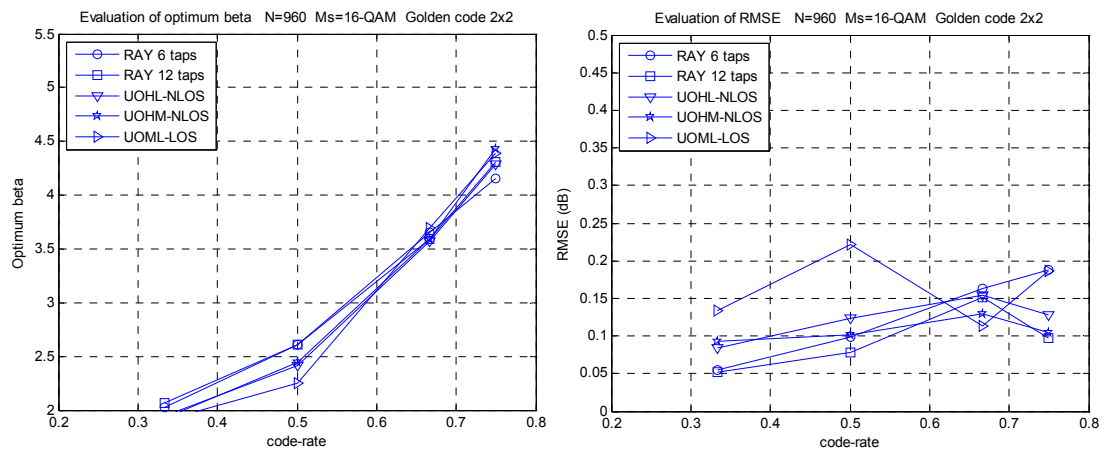

Figure 5.57.- (left) Optimum β and (right) RMSE as a function of the code rate selected for different type of channels. 2×2 MIMO. Golden STC. N_b=960. M=16-QAM.
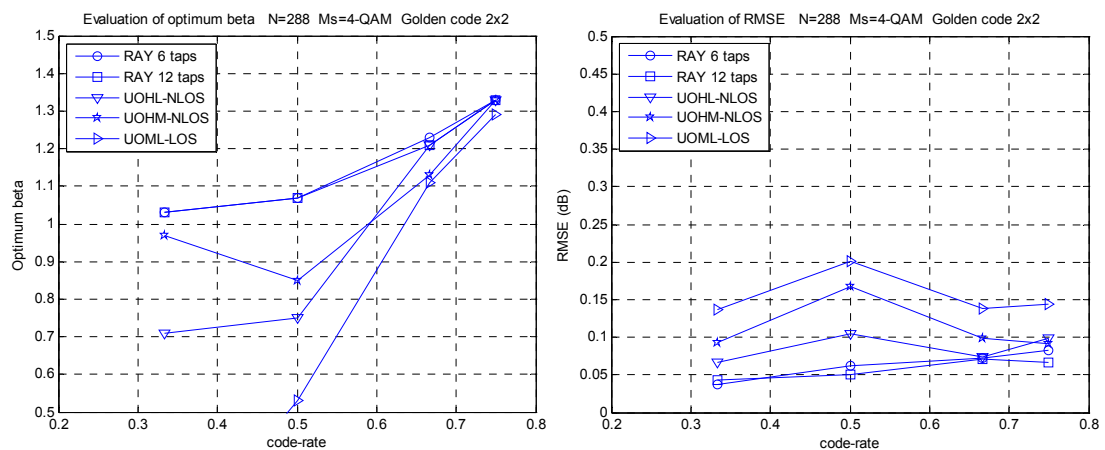

Figure 5.58.- (left) Optimum β and (right) RMSE as a function of the code rate selected for different type of channels. 2×2 MIMO. Golden STC. N_b=288. M=4-QAM.
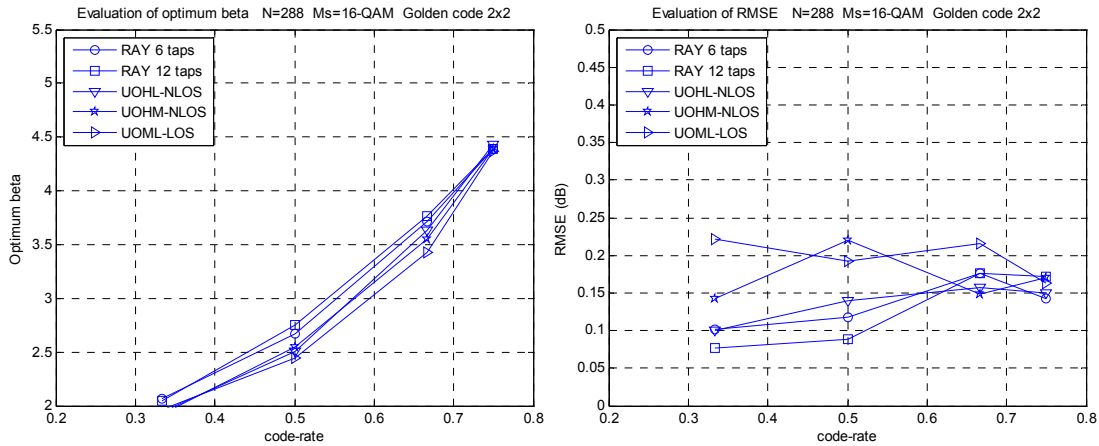
Figure 5.59.- (left) Optimum β and (right) RMSE as a function of the code rate selected for different type of channels. 2×2 MIMO. Golden STC. N_b=288. M=16-QAM.

When the packet size is reduced to N_b=288 bits (Figure 5.58 (4-QAM) and Figure 5.59 (16-QAM)) there are small changes in the β_{opt} but the RMSE is increased compared to the case with packet size N_b=960 bits.

5.9 Appendix E.   Metric performance for orthogonal transmission

In order to simulate the orthogonal transmission with incremental redundancy the scenario depicted in Figure 5.28 will be considered. In a nutshell, given a codeword of rate r, the coded bits are split in two sub-packets depending on the parameter κ (α). Those sub-packets are transmitted through orthogonal channels to a common destination using different data regions. Moreover, the orthogonal channels may present different average power levels, that is, channel B with a mean power level with ω dB higher than channel A, using ω={10, 5, 2.5, 0}. The destination must apply the Exp-ESM defined in (5.25) for estimated the *effective SNR*.

In Figure 5.60 and Figure 5.61 packets A and B use modulation 4 QAM and 16-QAM, respectively. Additionally, the mean power of the channels are the same (ω= 0 dB) and present a 1×4 MIMO configuration. It can be observed that the effective SNR estimated by (5.25) present results near of the reference curve (black stars) obtained for the AWGN channel.
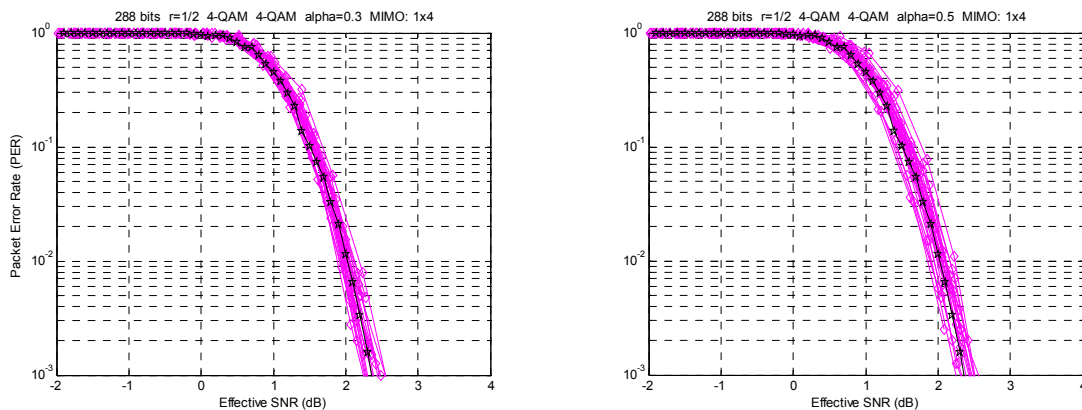

Figure 5.60.- Exp-ESM in orthogonal transmission for various frequency selective channels. (left) κ=0.3 and (right) κ=0.5, M_A=4-QAM and M_B=4-QAM. CTC 288 bits, r=1/2 and MIMO 1×4.Rayleigh 6 taps (6 symbols length with equal average power).ω=0 dB.
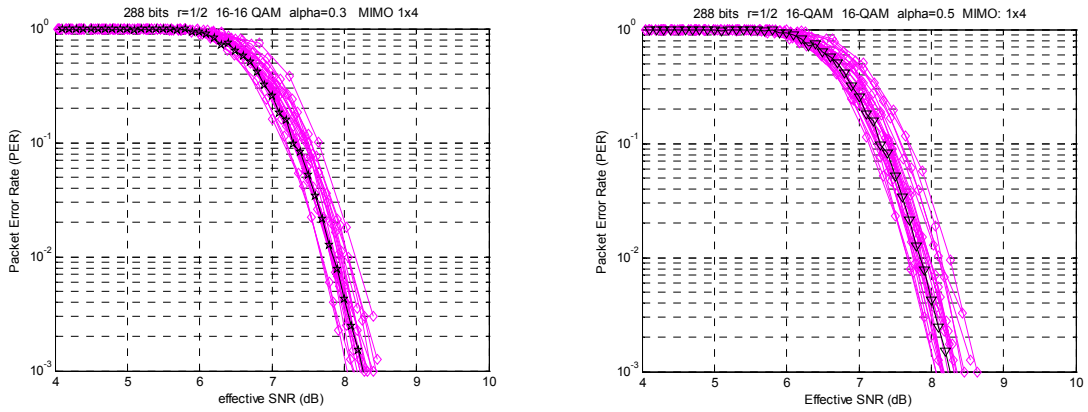
Figure 5.61.- Exp-ESM in orthogonal transmission for various frequency selective channels. (left) κ=0.3 and (right) κ=0.5, M_A=16-QAM and M_B=16-QAM.CTC 288 bits, r=1/2 and MIMO 1×4.Rayleigh 6 taps(6 symbols length with equal average power). ω=0 dB.

Figure 5.62, Figure 5.63 and Figure 5.64 are devoted to show the performance of the exp-ESM when the sub-packets use different modulation and the mean power of the channel is different. For the different cases considered ω= {10, 5, 2.5} dB, the metric described by (5.25) obtain results close to the reference.
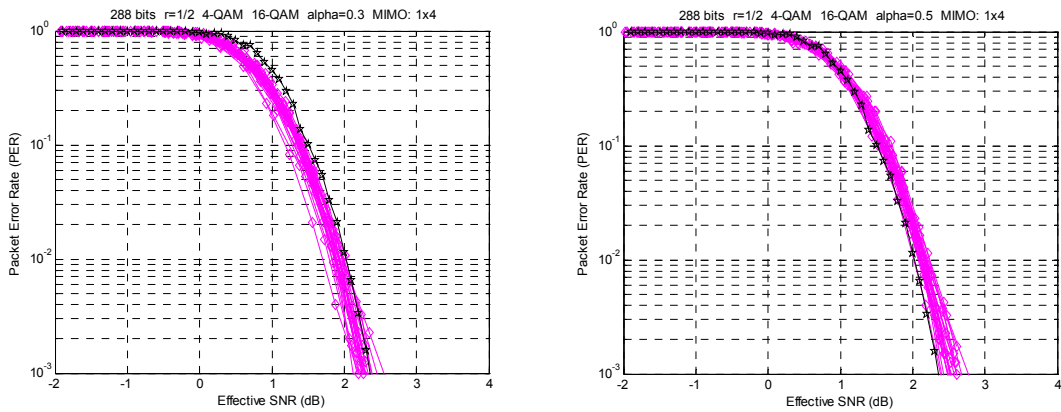

Figure 5.62.- Exp-ESM in orthogonal transmission for various frequency selective channels. (left) κ=0.3 and (right) κ=0.5.M_A=4-QAM and M_B=16-QAM.CTC 288 bits, r=1/2 and MIMO 1×4.Rayleigh 6 taps (6 symbols length with equal average power). ω=10 dB.

Figure 5.63.- Exp-ESM in orthogonal transmission for various frequency selective channels. (left) κ=0.3 and (right) κ=0.5,M_A=4-QAM and M_B=16-QAM. CTC 288 bits, r=1/2 and MIMO 1×4.Rayleigh 6 taps (6 symbols length with equal average power). ω=5 dB.
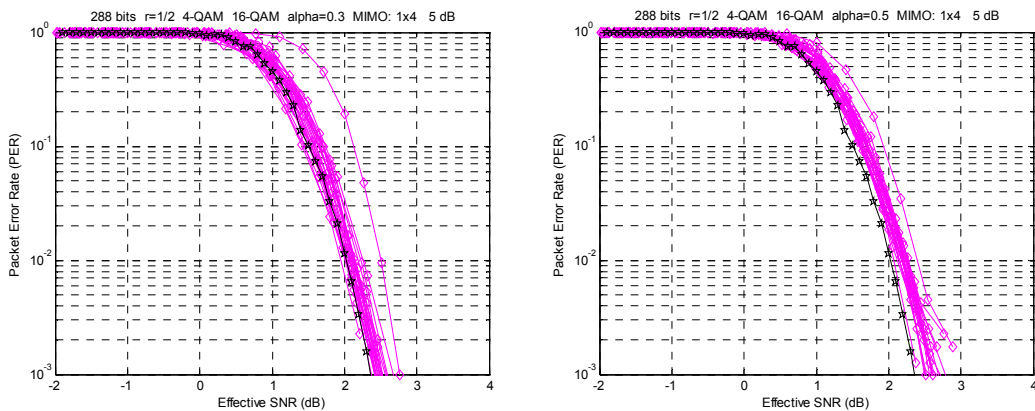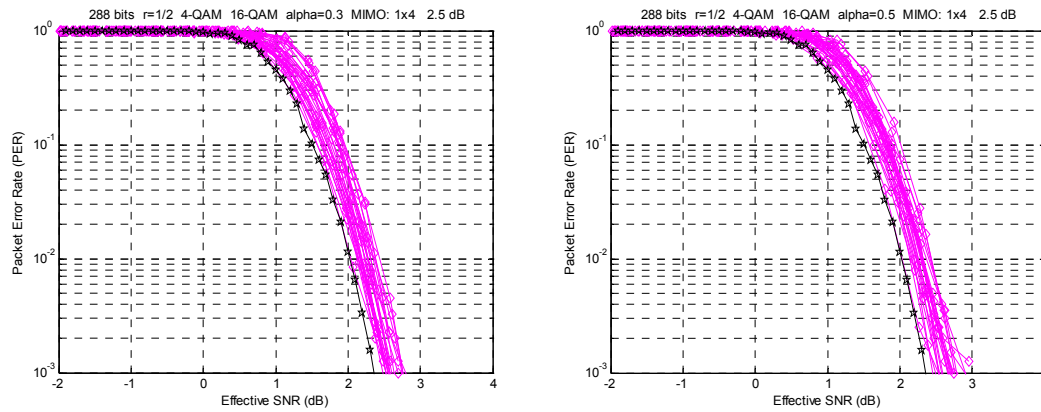
Figure 5.64.- Exp-ESM in orthogonal transmission for various frequency selective channels. (left) κ=0.3 and (right) κ=0,5, M_A=4-QAM and M_B=16-QAM.CTC 288 bits, r=1/2 and MIMO 1×4.Rayleigh 6 taps (6 symbols length with equal average power). ω=2.5 dB.

5.10 References

[1]   A.Agustin, J.Vidal, O.Muñoz, "Hybrid turbo FEC/ARQ systems and distributed space-time coding for cooperative transmission", *International Journal of Wireless Information Networks* (IJWIN), vol.12, no.4, pp. 263-280, Dec. 2005.

[2]   A.Agustín, J.Vidal, E. Calvo, O.Muñoz, "Evaluation of turbo H-ARQ schemes for cooperative MIMO transmission", *in Proc. IEEE International Workshop on Wireless Ad-Hoc Networks* (IWWAN-2004),Oulu, Finland, May 31-June 3, 2004.

[3]   A.Agustin, E.Calvo, J.Vidal, O.Muñoz, "Evaluation of turbo coded cooperative retransmission schemes", in *Proc. IST Mobile and Wireless Communication Summit*, Lyon, France, June 27-30, 2004.

[4]   A.Agustin, E.Calvo, J.Vidal, O.Muñoz, M.Lamarca, "Hybrid turbo FEC/ARQ systems and distributed space-time coding for cooperative transmission in the downlink", in *Proc. IEEE Personal Indoor Mobile Radio Communications* (PIMRC-2004), Barcelona, Spain, Sept. 5–8, 2004.

[5]   I.E.Telatar, "Capacity of multi-antenna Gaussian channels", *European Transactions on Telecommunications*, vol. 10, pp. 585-595, Nov/Dec 1999.

[6]   G.Foschini, M.J.Gans, "On limits of wireless communications in a fading environment when using multiple antennas", *Wireless Personal Communications*, vol. 6, no. 3, pp. 311-335, 1998.

[7]   L.Zheng, D.N.C.Tse, "Diversity and multiplexing: A fundamental tradeoff in multiple antenna channels", *IEEE Trans. on Information Theory*, vol. 49, no. 5, pp. 1073-1096, May 2003.

[8]   A.Goldsmith et al.,"Capacity Limits of MIMO channels", *in IEEE Journal on Selected Areas in Communications*, vol.21, no. 5, pp. 684-702, June 2003.

[9]   S.Barbarossa, *Multiantenna wireless communication systems*. Artech House mobile communications series. 2004.

[10]   V.Tarokh, H.Jafarkhani and A.R.Calderbank, "Space-Time block codes from orthogonal designs", *in IEEE Trans. on Information Theory*, vol.45, pp.456-1467, July 1999.

[11]   G.D.Golden, G.J.Foschini, R.Valenzuela, P.W. Wolniansky, "Detection algorithm and initial laboratory results using VBLAST space-time communication architecture", *in IEEE Electronic letters*, vol.35, pp.14-16, January 1999.

[12]   A.Host-Madsen, "Capacity bounds for cooperative diversity", *IEEE Trans. on Information Theory*, vol. 52, no. 4, pp. 1522-1544, April 2006.

[13]   M.Dohler, *Virtual Antenna Arrays*, PhD Thesis, King's College London, 2003.

[14]   M.Dohler, A.H.Aghvami, Y.Li, B.Vucetic, "Stage-by-Stage detection of distributed space-time block encoded relaying networks", in *Proc. IEEE Personal Indoor Mobile Radio Communications* (PIMRC-2004), vol. 4, pp. 2905-2909, Barcelona, Spain, Sept. 2004.

[15]   A.Wittneben, B.Rankov, "Impact of cooperative relays on the capacity of rank deficient MIMO channels", in *Proc. IST Mobile & Wireless Communications Summit* (IST-2003), Aveiro, Portugal, June 2003.

[16]   J.N.Laneman, G.W.Wornell, "Distributed Space-Time Coded protocols for exploiting Cooperative Diversity in Wireless Networks"*, IEEE Trans. on Information Theory*, vol. 49, no. 10, pp. 2415-2425, Oct. 2003.

[17]   P.A.Anghel, G.Leus, M.Kaveh, "Multi-user space-time coding in cooperative networks", in Proc. IEEE *International Conference on Acoustic, Speech and Signal Processing* (ICASSP-2003), vol 4, pp-IV:73-76, April 6-10, 2003.

[18]   S.Alamouti, "A simple transmit diversity technique for wireless communications", in *IEEE Journal Selected Areas Communications*, vol.16, no. 10, pp.1451-1458, Oct. 1998.

[19]   G.Scutari, S.Barbarossa, "Distributed space-time coding for regenerative relay networks", *in IEEE Trans. on Wireless Communications*, vol. 4, issue 5, pp. 2387-2399, Sept. 2005.

[20]   S.Barbarossa,G.Scutari, "Distributed space-time coding strategies for wideband multihop networks: regenerative vs non-regenerative relays", *in Proc. IEEE   International Conference on Acoustic, Speech and Signal Processing* (ICASSP-2004), May 17-21, Montreal, Canada.

[21]   G.D.Forney, G.Ungerboeck, "Modulation and coding for linear gaussian channels", in *IEEE Trans. on Information Theory*, vol.44, no.6, pp. 2384-2415, Oct. 1998.

[22]   C.Berrou, A.Glavieux, "Near optimum error correcting coding and decoding: Turbo codes", in *IEEE Trans. on Communications*, vol.44, no.10, pp. 1261-1271, October 1996.

[23]   S.Le Goff, A.Glavieux, C.Berrou, "Turbo-Codes and High Spectral Efficiency modulation", *in Proc. IEEE International Conference on Communications* (ICC- 1994), May 1994, New Orleans, USA.

[24]   R.G.Gallager, *Low-Density Parity-Check Codes*. Cambridge, MIT Press 1962.

[25]   M.C. Valenti, S.Cheng, R.I.Seshandri, "Turbo and LDPC Codes for Digital Video Broadcasting", Chapter 12 of *Turbo Code Applications: A journey form a paper to realization*, Springer, 2005.

[26]   IEEE Std 802.16e-2005, IEEE Standard for Local and metropolitan area networks, Part 16: Air Interface for Fixed and Mobile Broadband Wireless Access Systems, Amendment for Physical and Medium Access Layers for Combined Fixed and Mobile Operation in Licensed Bands, Feb. 2006.

[27]   J.C.Belfiore, G.Rekaya, E.Viterbo, "The golden code: a 2x2 full-rate space-time code with non-vanishing determinants", *IEEE Trans. on Information Theory*, vol. 51, no. 4, pp. 1432-1436, April 2005.

[28]   P.Dayal, M.K. Varanasi, "An optimal two transmit antenna space-time code and its stacked extensions", *Proc. of Asilomar Conf. on Signals, Systems and Computers* (ACSSC-2003), Monterey, CA, Nov. 2003.

[29]   H.Yao, G.W.Wornell, "Achieving the full mimo diversity-multiplexing frontier with roration-based space-time codes", Proc. of Allerton Conf. on Communication, Control and Computing (ACCCC-2003), October 2003.

[30]   S.Benedetto, D.Divsalar, G.Montorsi, F.Pollara, "Serial concatenation of interleaved codes: Performance analysis, design and iterative decoding", *IEEE Trans. Information Theory*, vol. 44, pp. 909-926, May 1998.

[31]   D.J.Costello, J.Hagenauer, H.Imai, S.B.Wicker, "Applications of error-control coding", *in IEEE Trans. Information Theory*, vol.44, no.6, pp.2531-2560, Oct.1998.

[32]   S. Lin, D.J.Costello, *Error Control Coding, Fundamentals and Applications*, Prentice Hall, Inc. Englewood Cliffs, New Jersey 07632, 1983.

[33]   E.Malkamäki, H.Leib, "Performance of truncated type-II hybrid ARQ schemes with noisy feedback over block fading channels", *in IEEE Trans. on Communications*, vol.48, no. 9, pp. 1477-1487, Sept. 2000.

[34]   D.N. Rowitch, L.B. Milstein, "On the performance of Hybrid FEC/ARQ systems using rate compatible Punctured Turbo (RCPT) Codes", *in IEEE Trans. on Communications*, vol.48, no.6, pp. 948-959, June 2000.

[35]   Y. Blankenship et al, "Link Error Prediction Methods for Multicarrier Systems", *in Proc. IEEE Vehicular Technology Conference* (VTC-2004-fall), Sept. 2004, Los Angeles (USA).

[36]   Ericsson, "System-level evaluation of OFDM – further considerations", TSG-RAN WG1#35, Nov. 2003.

[37] A.Alexiou et al., "Assessment of Advanced Beamforming and MIMO technologies", Deliverable D2.7, IST-2003-507581 WINNER, February 2005.

[38] S.Simoens et al., "Error Prediction for Adaptive Modulation and Coding in Multiple-Atenna OFDM systems", EURASIP Signal processing Journal, August 2006.

[39] B. Classon, et al, "Efficient OFDM-HARQ System Evaluation Using a Recursive EESM Link Error Prediction", *in Proc. IEEE Wireless Communications and Networking Conference* (WCNC-2006), April 2006.

[40] S.Verdu, S.Shamai, "Spectral efficiency of CDMA with random spreading", IEEE Trans. on Information Theory, vol. 45, no. 2, pp. 622-640, March 1999.

[41] M.C.Valenti, B.Zhao, "Distributed turbo codes: Towards the capacity of the relay channel", in *Proc. IEEE Vehicular Technology Conf. Fall* (VTC-Fall 2003), Orlando, FL, Oct. 2003.

[42] T.E.Hunter, A.Nosratinia, A.Hedayat, M.Janani, "Coded cooperation in wireless communications: space-time transmission and iterative decoding", *IEEE Trans. on Signal Processing*, vol.52, no.2, pp. 362-371, Feb. 2004.

[43] B.Hassibi, B.M.Hochwald, "High-rate codes that are linear in space and time", in *IEEE Trans. on Information Theory*, vol.48, pp.1804-1824, July 2002.

[44] A.Agustín, J.Vidal, A.Pagès, "Linear Dispersion Codes Construction with a defined structure", in *Proc. IEEE Vehicular Technology Conference Fall* (VTC-Fall 2003), Orlando, FL, Oct. 2003.

[45] J. P.Woodard, L. Hanzo, "Comparative study of turbo decoding techniques: An overview", *in IEEE Trans. Vehicular Technology*, vol.49, no.6, pp. 2208-2233, Nov. 2000.

[46] B.M.Hochwald, S.ten Brink, "Achieving near-capacity on a multiple antenna channel", *in IEEE Trans. on Communications*, vol.51, no.3, pp. 389-399, March 2003.

[47] A.M. Chan, I. Lee, "A new reduced-complexity sphere decoder for multiple antenna system", *in Proc. IEEE International Conference on Communications* (ICC-2002), May 2002, pp 460-464, New York, USA.

[48] J.Vogt, A.Finger, "Improving the max-log-MAP turbo decoder", *in IEEE Electronics Letters*, vol.36 no. 23, pp. 1937-1939, 2000.

[49] S.Dolinar and D. Divsalar, "Weight distributions for turbo codes using random and nonrandom permutations," TDA Progress Report 42-122, August 15, 1995.

[50] R.Ratasuk, A.Ghosh, B.Classon, "Quasi-Static Method for Predicting Link-Level Performance", in *Proc. IEEE Vehicular Technology Conference* (VTC-2002-Spring), 2002.

[51] P. Sartori et al., "Impact of Spatial Correlation on the Spectral Efficiency of Wireless OFDM Systems Using Multiple Antenna Techniques", in *Proc. IEEE Vehicular Technology Conference* (VTC-2002-Spring), 2002.

[52] A.Agustin, J.Vidal, O.Muñoz, "Link error prediction and MCS selection in relaying links under PUSC mode", Technical Note WP4- IST-27675 STP FIREWORKS, November 2007.

[53] A.Drettas, FlexIble RElay Wireless OFDM-based networks (FIREWORKS) consortium, "Channel Model Software Configuration for Link-level Simulations", Technical Note (Fireworks 4N-066a), June 2007.

[54] T.Starr, J.M.Cioffi, P.J. Silverman, *Understanding digital subscriber line technology*, Prentice Hall PTR, Upper Saddle River, NJ, USA, 1999.

[55] E.Calvo, J.Vidal, J.R. Fonollosa, "Resource allocation in multihop OFDMA Broadcast Networks", *in Proc. 8th IEEE Workshop on Signal Processing Advances in Wireless Communications* (SPAWC-2007), Helsinki, Finland, June 2007.

[56] M.Kiessling, "Unifying analysis of ergodic MIMO capacity in correlated Rayleigh fading environments", *European Transactions on Telecommunications*, vol. 1, no. 1, January 2005.

[57] E.Biglieri, G. Taricco, *Transmission and Reception with Multiple Antennas: Theoretical Foundations*, Foundations and Trends^{TM} in Communications and Information Theory, now Publishers, Hannover MA, 2004.

Chapter 6

Conclusions and Future Work

THIS dissertation has considered the design of half-duplex relay-assisted communication system, studying different algorithms and proposing solutions to enhance the *spectral efficiency* of this type of transmission. Some of these algorithms placed at the *physical layer* entail the definition of how the assisting relay may operate (AF or DF), when it has to be used (*persistent transmission*, *selective* or *incremental relaying*) and what type of message is transmitted by the relay (*repetition* or *unconstrained coding*). Other algorithms placed at the *data link layer* are responsible for defining the proper resource allocation for each orthogonal phase of the transmission (there is a *relay-receive* and *relay-transmit phase*) for single-user with single-assisting and multiple-assisting relays and multiple-user communication systems (RMAC, UC, MARC). The relay-assisted transmission has been applied to a centralized TDMA-based network where two solutions are proposed for homogenizing the service. Both are based on the spatial reuse of a relay slot (*relay-transmit phase*), that is all the assisting relays associated to different destinations transmit simultaneously, generating interference. A *power control* algorithm, based on game theory, and a *rate control* algorithm are the proposed solutions. In the first case, the conventional scheduling algorithms are also adapted to the relay-assisted transmission. It selects those destinations to be served in the same frame. In the latter case, it is assumed that the destinations served in each frame are selected randomly and under the assumptions considered in chapter 4 it is possible to model the interfering power statistics received at each destination in the relay slot (α-stable distribution). Finally the dynamic link control of the relay-assisted transmission has been investigated for different types of channel information state at the transmitter: *statistical information about the channel state* or *actual information about the current channel state*. In the first case we have specified the ARQ procedure to be used at the source and relay, the STC and length of retransmissions. In the second case, the MCS can be selected according the current channel realization.

6.1 Conclusions

A motivation of the Ph.D. dissertation has been given in chapter 1, presenting also the outline of the work and the research contributions in terms of publications.

Chapter 2 has presented and overview of the relay-assisted and cooperative transmission, describing the different protocols that can be defined when half-duplex relays are considered (forwarding, protocol I, II and III), the strategy at the relay (decoding mode) and under what conditions the relay should transmit. The protocol definition is connected with the activity of the

terminals in each phase of the transmission (*relay-receive* and *relay-transmit phase*). The resource allocation for each phase can be fixed (*static resource allocation relaying*) or adjusted in function of the channel quality of the links (*dynamic resource allocation relaying*). For *static resource allocation relaying* and protocol I, it has been studied the type of message transmitted by the relay, which can be *repetition* or *unconstrained coding*. The *unconstrained coding* is able to obtain the best gains in terms of *outage* and *average mutual information*. Additionally, the achievable rates of the different protocols have been derived for *dynamic resource allocation relaying*, presenting the performance under different constraints on the average transmitted power. Protocol III is the one that obtain best results. When the source and relay present an individual average power constraint (i.e. frequency duplexing), protocol I gets a similar performance than protocol III. The benefits of the relay-assisted transmission are significant in the *low* and *medium SNR* values. Moreover, it has been shown that the relay-assisted transmission is able to provide an *additive capacity gain* compared with the direct transmission. The mutual information of the direct transmission grows with the increase of the SNR, but the *additive capacity gain* becomes steady for high SNR values. Therefore, for *low* and *medium* SNR values the relay-assisted transmission enhances significantly the direct transmission, while for *high* SNR that improvement tends to be negligible when the mutual information of the direct transmission is larger than the *additive capacity gain*.

Two transmission techniques have been evaluated when a destination is assisted by multiple DF relays under different conditions of CSI. If assisting relays and source have perfect CSI they are able to transmit *synchronously*[1] (*eigenvector precoding techniques*) the same message. Otherwise they transmit *asynchronously*. When the relay-destination has a good link quality, *synchronous* and *asynchronous* transmissions get a similar performance. The transmission techniques define the type of messages transmitted to the relays during the relay-receive phase (i*ndependent* or *common messaging*). The resource allocation for those transmission techniques is formulated as a convex problem and the optimal solution has been evaluated. The use of *independent messaging* provides the best performance in terms of achievable rate. In a Gaussian channel, when one of the relays is placed near the source, *independent messaging* with *synchronous* transmission allows a quasi constant achievable rate irrespective of the position of the other relay. If one of the relays is placed half way between the source and destination, then *asynchronous* transmission get a performance not dependant of the position of the second relay.

Chapter 3 has formulated and solved the resource allocation for the half-duplex relay-assisted transmission applied to different multi-user scenario, where there are multiple sources (power limited) willing to transmit to a single destination. Three scenarios has been considered: RMAC (relay-assisted multiple access channel), where each source is assisted by a single relay, UC (user cooperation), where the sources cooperate between them, and MARC (multiple access relay channel), where all the sources are assisted by a single relay for transmitting to the destination. As duplexing modes, the TDD (time division duplexing) and FDD (frequency division duplexing) are considered. The multiple sources (and relay/s) access in each phase of the relay-assisted transmission by means of TDMA (time division multiple access), FDMA (frequency division multiple access) or SC (superposition coding multiple access).The problem is formulated as convex problem under some circumstances and solved efficiently.

---

[1] Assuming also the carrier phase of the distributed terminals.

Chapter 4 has applied the TDD relay-assisted transmission using protocol I to a centralized TDMA-based system assuming *user relaying*. The destinations are served in equally time slots. In order to improve the spectral efficiency, one time slot is devoted for the simultaneous transmission of the assisting relays associated to different destinations. Two solutions are proposed for combating the interference: *power control* and *rate control*. The first solution uses a *distributed power control* algorithm based on game theory. It has been shown that the algorithm converges after few iterations and results in terms of *sum-throughput* are close to the obtained by the direct transmission with a $n_s \times 2n_d$ MIMO system (also in TDMA) when the reuse of the slot (number of destination-relay pairs active) is high. Additionally, spectral efficiency obtained by this solution when the terminal density is high is similar to the *infrastructure relaying* (without spatial reuse of the relay slot). It is proposed an extension of the proportional fair (PF) algorithm to the relay-assisted transmission that shows that some *multiuser gain* can be obtained and additionally, the fairness in terms of average delay in transmitting a packet is highly improved. The *overhead* of the proposed scheme is around 10%. The second solution for dealing with the interference of the relay slot is by tuning the transmission rate (*rate control*). Under the assumptions defined in chapter 4, the interfering power received by each destination in the relay slot can be modeled by an α-stable process. It has been shown that using the *amplify and forward* (AF) technique, significant gains in terms of *sum-throughput* are possible, which depends on the number of destinations allocated in a frame and the *target* SNR in the relay-destination link. Moreover, this has been extended to the case where each destination present multiple-assisting relays, showing that the throughput gains also depend on the number of assisting relays. Finally, a tradeoff between the throughput gain and the battery lifetime of the assisting relay has been presented.

Chapter 5 has presented different algorithms for designing the dynamic link control of the relay-assisted transmission under different types of channel knowledge. First, when there is *statistical information about the channel state* based on *long-term* CDIT (usually the variance of the estimated error about the CSI is large) the errors in the transmission are dominated by the outage events due to the channel fading. The retransmission scheme ARQ is redefined for accommodating the relay-assisted transmission under the same scenario as in chapter 4. Different schemes for obtaining a *diversity* or *STC gain* are defined, which imply the definition of DSTC (distributed space-time codes) and the coding done at the relay (RCPTC). The best results are obtained by protocol HARQ-II, showing the superiority of DF versus AF, although for some configurations the performance can be similar, thus providing a good compromise between performance and complexity at the relay.

Otherwise, when the source has *actual information about the current channel state* based on *partial* CSIT the errors in the transmission are due to the *thermal noise*. A scenario where the relay-assisted transmission is done through multiple-carriers in a frequency selective channel has been investigated. The Exp-ESM obtains the effective SNR which describes the quality of each link and allows predicting the error rate for a given FEC and MCS. Following the same principles of Exp-ESM, the link error prediction can be obtained for the different half-duplex protocols of the relay-assisted transmission. The optimal MCS for the relay-assisted transmission is found by maximizing two different criteria: either the information rate for a given probability of packet loss or to maximize the throughput.

6.2 Future Work

There are several lines for future research having as a basis the work developed in this dissertation.

Chapter 2

- ➢ The extension of *dynamic resource allocation relaying* to multiple-assisting relays, investigating for which conditions is beneficial.

- ➢ Take into account when the channel state information is known perfectly when there are multiple antennas at the different terminals. The covariance transmit matrices can be designed accordingly.

- ➢ Investigate the *two-path relaying*, as an alternative way to reduce the loss in *spectral efficiency* inherent to half-duplex relaying. A destination is served by two relays transmitting orthogonally, but the *relay-receive* and *relay-transmit phase* of each assisting relays is superposed. When one relay is transmitting, the other one is receiving.

Chapter 3

- ➢ In the RMAC scenario, two sources are assisted by two different assisting relays, the source-relay transmission (*relay-receive phase*) is done orthogonally (i.e. in TDMA or FDMA). The resource allocation should also consider what happens when both sources transmit simultaneously, creating an *interfering channel*. Similar to the scenario considered in chapter 4, where a slot is reused for the *relay-transmit phase* of all the active destinations.

- ➢ The dual scheme of the RMAC scenario should be analyzed, a single source and multiple destinations with some assisting half-duplex relays. The assisting relays could exploit some knowledge of the messages to be transmitted to other destinations. Then some techniques using *dirty paper coding* could be considered.

Chapter 4

- ➢ In the relay slot, only the assisting relays transmit to their destinations active in that frame. In such a case, in a frame of N time slots N-1 destinations are served. However, the reuse of the relay slot can be improved by allowing an additional direct transmission from the source (with low amount of power) to some other destination nearby the source. In such a case, in a frame of N time slots N destinations are served (N-1 by relay-assisted transmission and 1 by direct transmission with interference).

- ➢ Further investigation in power control algorithms based on game theory, trying to improve the equilibrium points by means of *pricing techniques*.

- ➢ Extension of the results obtained when a *rate control* is considered under the DF.

➤   Investigate the allocation of resources for the *two-way relaying* as a way to reduce the loss in terms of *spectral efficiency* inherent to half-duplex relaying in a multiuser environment.

Chapter 5

➤   Further investigation in retransmission schemes for other relay-assisted protocols. In this dissertation only protocol I has been considered for the ARQ procedures.

➤   Look into the relay-assisted transmission when both the relay and destination are able to request retransmissions. In this dissertation only the destination is allowed.

➤   Investigation of efficient search algorithms for the modulation and coding selection.